TE
662
.A3
no.
FHWA-
RD-
73-13

rt No. FHWA-RD-73-13

NVESTIGATION OF THE EFFECTIVENESS OF EXISTING GE DESIGN METHODOLOGY IN PROVIDING ADEQUATE CTURAL RESISTANCE TO SEISMIC DISTURBANCES.

Phase I: Literature Survey

T. Iwasaki, J. Penzien, and R. Clough

DEPARTMENT OF
TRANSPORTATION
FEB 04 1974
LIBRARY

November 1972
Final Report

This document is available through
the National Technical Information
Service, Springfield, Virginia 22151.

Prepared for
FEDERAL HIGHWAY ADMINISTRATION
Offices of Research & Development
Washington, D.C. 20590

NOTICE

This document is disseminated under the sponsorship of the Department of Transportation in the interest of information exchange. The United States Government assumes no liability for its contents or use thereof.

The contents of this report reflect the views of the contracting organization, which is responsible for the facts and the accuracy of the data presented herein. The contents do not necessarily reflect the official views or policy of the Department of Transportation. This report does not constitute a standard, specification, or regulation.

TECHNICAL REPORT STANDARD TITLE PAGE

1. Report No. FHWA-RD-73-13	2. Government Accession No.	3. Recipient's Catalog No.
4. Title and Subtitle AN INVESTIGATION OF THE EFFECTIVENESS OF EXISTING BRIDGE DESIGN METHODOLOGY IN PROVIDING ADEQUATE STRUCTURAL RESISTANCE TO SEISMIC DISTURBANCES. Phase I: Literature Survey.		5. Report Date November 1972
		6. Performing Organization Code
7. Author(s) T. Iwasaki, J. Penzien, R. Clough		8. Performing Organization Report No. EERC 72-11
9. Performing Organization Name and Address University of California Campus Research Office 118 California Hall Berkeley, California 94720		10. Work Unit No. 35A2-012
		11. Contract or Grant No. DOT-FH-11-7798
12. Sponsoring Agency Name and Address Federal Highway Administration Office of Research Washington, D. C. 20590		13. Type of Report and Period Covered Phase I-Final Report June 30, 1971 to Nov.30, 1972
		14. Sponsoring Agency Code S0176

15. Supplementary Notes

Contract Manager for this report was James D. Cooper, HRS-11.

16. Abstract

This report is the first in a series to result from the investigation, "An Investigation of the Effectiveness of Existing Design Methodology in Providing Adequate Structural Persistance to Seismic Disturbances", sponsored by the U. S. Department of Transportation, Federal Highway Administration. Descriptions of the damages sustained by bridge structures during moderate to severe earthquakes in many countries of the world are given. Particular emphasis is placed on the damages occurring in Japan where the incidence of damage has been considerable. Surveys of important research investigations on seismic effects on bridges are presented. These investigations are classified into the following categories: (1) Seismicity, (2) characteristics of strong ground motions, (3) bearing capacity and stability of soils, (4) earth pressures, (5) hydraulic pressures, (6) dynamic properties of bridges, (8) dynamic analyses of bridges, and (9) laboratory experiments. Specifications for the earthquake-resistant design of bridges as used by many organizations are also included.

17. Key Words State-of-the-art: Earthquake, Bridges, Damaged Bridges, Structures, Seismic Design Criteria, Japanese Design Specifications.	18. Distribution Statement No restrictions. This document is available through the National Technical Information Service, Springfield, Virginia 22151

19. Security Classif. (of this report)	20. Security Classif. (of this page)	21. No. of Pages	22. Price
UNCLASSIFIED	UNCLASSIFIED	433 plus cover	

Form DOT F 1700.7 (8-69)

PREFACE

The literature survey with interpretation as described in this report was sponsored by the U. S. Department of Transportation, Federal Highway Administration, under Contract No. DOT-FH-11-7798 covering the period June 30, 1971 through June 30, 1974.

The general investigation called for in this contract is under the supervision and technical responsibility of Professors R. W. Clough, W. G. Godden, and J. Penzien. Professor Penzien acts as principal investigator.

TE
662
.A3
no.
FHWA-
RD-
74-14

DEPARTMENT OF
TRANSPORTATION
FEB 04 1974

ACKNOWLEDGEMENT

The authors wish to express their appreciation and sincere thanks to the many organizations and individuals who furnished information useful to the preparation of this report. Special thanks are extended to the Ministry of Construction, Public Works Research Institute of Japan, for its cooperation and support of the overall program and for allowing Mr. Toshio Iwasaki to work on the project both in Japan and the United States. Without this support, the literature survey could not have been successful.

TABLE OF CONTENTS

DISCLAIMER i

PREFACE ii

ACKNOWLEDGEMENT iii

TABLE OF CONTENTS iv

LIST OF TABLES vii

LIST OF FIGURES x

LIST OF PHOTOGRAPHS xvii

I. INTRODUCTION 1

II. SEISMIC DAMAGE TO BRIDGE STRUCTURES 4

A. General 4

B. Kanto Earthquake of 1923 4

C. Nankai Earthquake of 1946 13

D. Fukui Earthquake of 1948 15

E. Imaichi Earthquake of 1949 21

F. Tokachi-oki Earthquake of 1952 22

G. Northern Miyagi Earthquake of 1962 22

H. Niigata Earthquake of 1964 23

I. Ebino Earthquake of 1968 31

J. Tokachi-oki Earthquake of 1968 33

K. General Features of Seismic Damage to Japanese Bridges 34

L. Alaska Earthquake of 1964 35

M. Madang Earthquake of 1970 36

N. Chilean Earthquake of 1971 36

O. San Fernando Earthquake of 1971 37

P. Design Recommendations Based on San Fernando Earthquake Experience 47

Tables in Chapter II 52

Figures in Chapter II 60

Photographs in Chapter II 103

III. RESEARCH ACTIVITIES ON SEISMIC EFFECTS ON BRIDGES . . . 176

A. Seismicity 176

B. Characteristics of Strong Ground Motions 177

C. Subsoil Failures 179

D. Earth Pressures on Abutments 179

E. Hydrodynamic Pressure on Substructures 183

F. Dynamic Properties of Highway Bridges 184

G. Measured Dynamic Response of Bridges to Strong Motion Earthquakes 192

H. Dynamic Analyses 199

I. Model Experiments 209

Tables in Chapter III 212

Figures in Chapter III 227

IV. EARTHQUAKE-RESISTANT DESIGN CRITERIA 278

A. History of Earthquake-Resistant Design Criteria in Japan 278

B. Earthquake-Resistant Design Criteria JRA-1971 279

C. Earthquake-Resistant Design Criteria JHPC-1970 282

D. Seismic Design Standards TEPC-1967 283

E. Seismic Design Standards HEPC-1968 284

F. Specifications for Honshu-Shikoku Bridges JSCE-1967 285

G. Seismic Design Criteria for Railway Bridges JSCE-1968 287

H. Seismic Design Forces - California State Division of Highways 288

I. Seismic Resistances of New Zealand Bridges 290

J. Summary of World's Earthquake Regulations 294

Tables in Chapter IV 295

Figures in Chapter IV 305

V. CONCLUSIONS AND RECOMMENDATIONS 308

APPENDIX A BIBLIOGRAPHY ON SEISMIC EFFECTS ON BRIDGES

APPENDIX B BRIEF SUMMARY OF SEISMIC DESIGN CODES IN VARIOUS COUNTRIES

APPENDIX C SPECIFICATIONS FOR EARTHQUAKE-RESISTANT DESIGN OF HIGHWAY BRIDGES, JAPAN ROAD ASSOCIATION (JANUARY, 1971)

LIST OF TABLES

Table 2.1 Definitions of JMA Seismic Intensity Scale

Table 2.2 Statistics on Highway Bridge Damage due to the Kanto Earthquake of 1923

Table 2.3 Statistics on Damage to Highway Bridges due to the Nankai Earthquake of 1946

Table 2.4 Statistics on Damage to Highway Bridges due to the Fukui Earthquake of 1948

Table 2.5 Statistics on Damage to Highway Bridges (except Wooden Bridges) due to the Niigata Earthquake of 1964

Table 2.6 Results of Bearing Power Tests at the Bandai Bridge Site

Table 2.7 Numbers of Damaged Bridges with Various Kinds of Foundations due to the Niigata Earthquake of 1964 -For Highway Bridges within 60km from the Center of Niigata City-

Table 2.8 Damage Percentages of Individual Portions of Highway Bridges within 60km from the Center of Niigata City

Table 2.9 Statistics on Damage to Highways and Highway Bridges due to the Tokachi-oki Earthquake of 1968

Table 3.1 Results of Vibration Test for Pier 4 of the Shinkatsushika Bridge

Table 3.2 Results of Vibration Test for Pier 5 of the Shinkatsushika Bridge

Table 3.3 Results of Vibration Test for the Overall Structure of the Shinkatsushika Bridge

Table 3.4 Tests Results for Pier 3 at the Sokozawa Bridge

Table 3.5 Numbers of Strong-Motion Accelerographs

Table 3.6 Outline of Twenty-Eight Bridges where Seismic Records are Available.

Table 3.7 Comparison of Ground Accelerations (a_G) and Response Accelerations (a_R) at Bridges from Measurements during Earthquakes.

Table 3.8 Observed Accelerations and Analyzed Responses at the Ochiai Bridge (Longitudinal Direction)

Table 3.9 Results of Earthquake Observation at the Shinkatsushika Bridge

Table 3.10 Some Examples of Highway Bridges on Which Dynamic Analyses were Conducted

Table 3.11 Dimensions of Girders and Pier Columns of the Yoneyama Bridge

Table 3.12 Six Cases Considered in the Analysis of the Sokozawa Bridge

Table 3.13 Natural Frequencies Analyzed and Resonant Frequencies from the Field Experiment

Table 3.14 Preliminary Design of the Proposed Honshu-Shikoku Suspension Bridge Analyzed

Table 3.15 Natural Frequencies in Hertz from Test and Analysis for the Otani Interchange Bridge (After S. Yamaguchi, et al. [115]).

Table 3.16 Results of Dynamic Analysis for the Otani Interchange Bridge (After S. Yamaguchi, et al. [115])

Table 4.1 History of Design Loads for Highway Bridges in Japan (Primarily Seismic Loads)

Table 4.2 Highway Administration in Japan (Technical Field)

Table 4.3 Horizontal Design Seismic Coefficient (Out of Date)

Table 4.4 Seismic Zone Factor ν_1 for General Highway Bridges

Table 4.5 Ground Condition Factor ν_2 for General Highway Bridges

Table 4.6 Importance Factor ν_3 for General Highway Bridges

Table 4.7 Design Seismic Coefficient for Tokyo Expressways

Table 4.8 Classification of Ground Conditions for Tokyo Expressways

Table 4.9 Combination of Loads and Allowable Stresses in the Earthquake-Resistant Design of Tokyo Expressways

Table 4.10 Values of Factor m for Hanshin Expressways

Table 4.11 Value of Factor S for Honshu-Shikoku Suspension Bridges

Table 4.12 Design Horizontal Seismic Coefficient ($k_h = m_S \cdot m_I \cdot k_o$) for JNR Bridges

Table 4.13 Design Seismic Coefficients in Various Countries

LIST OF FIGURES

Fig. 2.1 Epicenters of Nine Earthquakes Which Caused Comparatively Severe Damage to Modern Engineering Structures in Japan

Fig. 2.2 The Kanto Earthquake of 1923

Fig. 2.3 Damage to the Tsuruno-bashi Bridge

Fig. 2.4 Damage to the Shinminato Bridge

Fig. 2.5 Damage to the Abutments of the Shinminato Bridge

Fig. 2.6 Damage to the Northern Abutment of the Bankoku Bridge

Fig. 2.7 Damage to the Hanazono Bridge

Fig. 2.8 Damage to the Toyokuni Bridge

Fig. 2.9 Drawings of the Sakawa Bridge

Fig. 2.10 Damage to the Banyu Bridge

Fig. 2.11 Damage to the Hayakawa Bridge

Fig. 2.12 Damage to the Takahata Bridge

Fig. 2.13 The Nankai Earthquake of 1946

Fig. 2.14 The Fukui Earthquake of 1948

Fig. 2.15 Damage to the Nakazuno Bridge

Fig. 2.16 Detailed Drawings of the Pier of the Nakazuno Bridge

Fig. 2.17 Damage to the Nagaya Bridge

Fig. 2.18 Damage to the Nagaya Bridge

Fig. 2.19 General Drawings of the Itagaki Bridge

Fig. 2.20 Damage to the Itagaki Bridge

Fig. 2.21 Damage to the Koroba Bridge

Fig. 2.22 The Niigata Earthquake of 1964

Fig. 2.23 Locations of the Seven Bridges Which Sustained Severe Damage.

Fig. 2.24 General View of the Bandai Bridge

Fig. 2.25 Boring Logs at the Bandai Bridge

Fig. 2.26 Soil Profile at the Bandai Bridge

Fig. 2.27 Damage to the Bandai Bridge

Fig. 2.28 Damage to the Side Spans of the Bandai Bridge

Fig. 2.29 General View of the Showa Bridge

Fig. 2.30 Boring Logs at the Showa Bridge

Fig. 2.31 Characteristics of Soil Grain Size at the Showa Bridge

Fig. 2.32 Soil Profile at the Showa Bridge

Fig. 2.33 Damage to the Showa Bridge

Fig. 2.34 Permanent Deformation of a Pile Pulled Out at the Showa Bridge

Fig. 2.35 General View of the Yachiyo Bridge

Fig. 2.36 Boring Logs at the Yachiyo Bridge

Fig. 2.37 Soil Profile at the Yachiyo Bridge

Fig. 2.38 Damage to the Yachiyo Bridge

Fig. 2.39 Deformation of the Side Spans of the Yachiyo Bridge

Fig. 2.40 General View of the Higashi-Kosenkyo Bridge

Fig. 2.41 Boring Logs at the Higashi-Kosenkyo Bridge

Fig. 2.42 Soil Profile at the Higashi-Kosenkyo Bridge

Fig. 2.43 Damage to the Higashi-Kosenkyo Bridge

Fig. 2.44 Deformations of Some Piles at the Higashi-Kosenkyo Bridge

Fig. 2.45 General View of the Matsuhama Bridge

Fig. 2.46 Boring Logs at the Matsuhama Bridge

Fig. 2.47 Damage to the Matsuhama Bridge

Fig. 2.48 General View of the Kosudo Bridge

Fig. 2.49 Boring Logs at the Kosudo Bridge

Fig. 2.50 Damage to the Kosudo Bridge

Fig. 2.51 Schematic Sketch of a Typical Highway Bridge

Fig. 2.52 Locations of Main and Larger Aftershocks - Allen et al.

Fig. 2.53 Ground Acceleration Time History at Pacoima Dam

Fig. 2.54 General Arrangement of Bridges and Overcrossings.

Fig. 3.1 Distribution of Epicenter and Magnitude of Major Historical Earthquakes in Japan (After H. Kawasumi [80])

Fig. 3.2 Contours of Maximum Earthquake Accelerations Expected in Japan Within Periods of (A) 75, (B) 100, and (C) 200 Years (After H. Kawasumi [80])

Fig. 3.3 Contours of Maximum Seismic Accelerations Expected Within A Period of 75 Years (After H. Goto and H. Kameda [82])

Fig. 3.4 Contours of Maximum Seismic Velocities Expected Within a Period of 75 Years (After H. Goto and H. Kameda [82])

Fig. 3.5 Seismic Risk Map (After T. Okubo and T. Terashima [85])

Fig. 3.6 (A) Average Acceleration Spectrum (After G. W. Housner [88])

Fig. 3.6 (B) Amplification Factor Spectrum Obtained From Fig. 3.6(A)

Fig. 3.7 Amplification Factor Spectrum (After T. Takata, T. Okubo, E. Kuribayashi [89])

Fig. 3.8 Amplification Factor Spectrum for Four Kinds of Ground Condition (After E. Kuribayashi, T. Iwasaki, K. Tuji [92])

Fig. 3.9 Earth Pressure Acting on Wall

Fig. 3.10 Coefficient of Active Earth Pressure

Fig. 3.11 Coefficient of Passive Earth Pressure

Fig. 3.12 Resultant Seismic Coefficient

Fig. 3.13 k and θ_o Values for Various k_h and k_v

Fig. 3.14 Coefficient of Active Earth Pressure During Earthquakes

Fig. 3.15 Coefficient of Passive Earth Pressure during Earthquakes

Fig. 3.16 Experimental Results of Earth Pressure during Harmonic Excitation (After N. Mononobe [206])

Fig. 3.17 Hydrodynamic Pressure on Vertical Wall

Fig. 3.18 Hydrodynamic Pressure on Column

Fig. 3.19 General View of the Shinkatsushika Bridge

Fig. 3.20 General View of Pier 4 of the Shinkatushika Bridge

Fig. 3.21 General View of Pier 5 of the Shinkatsushika Bridge

Fig. 3.22 Vibration Test Results for Pier 4 of the Shinkatsushika Bridge

Fig. 3.23 Vibration Test Results for Pier 5 of the Shinkatsushika Bridge

Fig. 3.24 Vibration Test Results for the Whole Bridge Structure of the Shinkatsushika Bridge

Fig. 3.25 General View of the Torii Bridge

Fig. 3.26 Open Caisson Foundation of Pier 1 of the Torii Bridge

Fig. 3.27 Test Results for the Foundation of Pier 1 of the Torii Bridge (Longitudinal Direction)

Fig. 3.28 Test Results for the Foundation of Pier 1 of the Torii Bridge (Transverse Direction)

Fig. 3.29 Test Results for the Whole Bridge Structure of the Torii Bridge (Transverse Direction)

Fig. 3.30 General View of the Sokozawa Bridge

Fig. 3.31 Pier 3 at the Sokozawa Bridge

Fig. 3.32 Locations of Exciter and Pick-Ups

Fig. 3.33 Test Results for the Whole Bridge Structure of the Sokozawa Bridge (Transverse Direction)

Fig. 3.34 Relationship Between Natural Period and Damping Ratio for Bridge Structures

Fig. 3.35 Relationship Between Natural Period and Damping Ratio for Bridges with Highrise Piers

Fig. 3.36 Relationship Between Height of Pier and Fundamental Natural Period

Fig. 3.37 Network of Strong-Motion Accelerographs at Highway Bridges

Fig. 3.38 Results of Earthquake Measurements at Twenty Seven Bridges

Fig. 3.39 Relation Between Ground Acceleration and Response Acceleration at the Crest of Bridge Structures in the Vertical Direction

Fig. 3.40 Results of Earthquake Measurements at Eight Bridges with Highrise Piers (Over 10 m above Ground Surface)

Fig. 3.41 Magnification Factors Measureed vs. Height of Bridge Structures

Fig. 3.42 General View of the Ochiai Bridge

Fig. 3.43 Outline of Pier 11 of the Ochiai Bridge

Fig. 3.44 Examples of Acceleration Records Observed at the Ochiai Bridge Station

Fig. 3.45 Relation Between Ground Acceleration and Response Acceleration Observed at the Ochiai Bridge in the Longitudinal Direction

Fig. 3.46 General View of the Itajima Bridge

Fig. 3.47 Acceleration Records at the Itajima Bridge During the Hyuganada Earthquake of April 1, 1968 [64]

Fig. 3.48 Acceleration Records at the Itajima Bridge During the Bungosuido Earthquake of August 6, 1968 [64]

Fig. 3.49 Results of Measurements and Dynamic Analyses at the Itajima Bridge

Fig. 3.50 Results of Earthquake Measurements at the Shinkatsushika Bridge

Fig. 3.51 Acceleration Records at the Shinkatsushika Bridge During the Higashi-Matsuyama Earthquake of July 1, 1968 (Recorded by Strong-Motion Accelerographs on the Ground Surface and at the Crest of Pier 5)

Fig. 3.52 Earthquake Records at the Shinkatsushika Bridge during the Higashi-Matsuyama Earthquake of July 1, 1968 (Records of Accelerations and Earth Pressures at the Foundation of Pier 5)

Fig. 3.53 Results of Earthquake Measurements at the Shinkatsushika Bridge during the Higashi-Matsuyama Earthquake of July 1, 1968

Fig. 3.54 Results of Earthquake Measurements at the Chiyoda Bridge

Fig. 3.55 Results of Earthquake Measurements at the Hirai Bridge

Fig. 3.56 Results of Earthquake Measurements at the Soka Viaduct

Fig. 3.57 General Bridge Substructure with Pile Foundation

Fig. 3.58 Analytical Model for Bridge Substructure With Pile Foundation

Fig. 3.59 General View of the Yoneyama Bridge

Fig. 3.60 Analytical Model for the Yoneyama Bridge

Fig. 3.61 Results of Dynamic Analysis - 1st to 4th Mode Shapes of the Yoneyama Bridge in the Transverse Direction

Fig. 3.62 Results of Dynamic Analysis - Displacement

Fig. 3.63 Results of Dynamic Analysis - Bending Moment

Fig. 3.64 Results of Dynamic Analysis - Shearing Force

Fig. 3.65 Analytical Model for the Sokozawa Bridge (T. Suruga, et al. [114])

Fig. 3.66 Comparison of Mode Shapes by Analysis and by Experiment for the Sokozawa Bridge (After T. Suruga, et al. [114])

Fig. 3.67 Coordinates of a Suspension Bridge

Fig. 3.68 An Analytical Model for Dynamic Analysis

Fig. 3.69 Maximum Bending Moments for the Main Tower Including Pier in the Longitudinal Direction

Fig. 3.70 General View of the Otani Interchange Bridge (After S. Yamaguchi, et al [115])

Fig. 3.71 Resonance Curve for Pier 7 of the Otani Interchange Bridge (After S. Yamaguchi, et al [115])

Fig. 3.72 Resonance Curves for the Overall Bridge Structure of the Otani Interchange Bridge (After S. Yamaguchi, et al [115])

Fig. 3.73 1st to 3rd Modes of the Otani Interchange Bridge - Observed and Computed (After S. Yamaguchi, et al [115])

Fig. 3.74 Results of Dynamic Analysis for the Otani Interchange Bridge (After S. Yamaguchi, et al [115])

Fig. 3.75 Model I for Dynamic Tests of a Viaduct (After E. Kuribayashi, et al [128])

Fig. 3.76 Model II for Dynamic Tests of a Viaduct (After E. Kuribayashi, et al [128])

Fig. 3.77 Setup of a Dynamic Test for Seismic Effects of Pile Foundation. (N. Ogata, S. Kotsubo [129])

Fig. 3.78 A Model of Tower-Pier System for Suspension Bridges (I. Konishi, et al [130])

Fig. 3.79 Sketch of a Model Structure Supported on Piles for Dynamic Tests (After K. Kubo [131])

Fig. 3.80 General View of a Model for a Suspension Bridge Subjected to Earthquake Excitation (E. Kuribayashi, et al [132])

Fig. 3.81 Records of Model Response to the Kushiro Earthquake Ground Motion, E-W Component (After E. Kuribayashi, et al. [132])

Fig. 4.1 Magnification Factor (β) for General Highway Bridges

Fig. 4.2 Seismic Coefficient for Higher Parts of Structures

Fig. 4.3 Magnification Factor β

Fig. 4.4 Distribution of Design Seismic Loads and value of m_2

Fig. 4.5 Value of m_2 for underground layers.

LIST OF PHOTOGRAPHS

Photo. 2.1 Damage to the East Support at the Southern Abutment of the Shinminato Bridge

Photo. 2.2 Damage to the West Support at the Northern Abutment of the Shinminato Bridge

Photo. 2.3 Damage to the Bankoku Bridge (Note Heavy Cracks at the Abutment)

Photo. 2.4 Damage to the East Support at the Northern Abutment of the Bankoku Bridge (Note the Large Dislocation).

Photo. 2.5 Damage to the East Support at the Southern Abutment of the Bankoku Bridge (Note Anchor Bolts Sheared off).

Photo. 2.6 Damage to the Right-Bank Abutment of the Yamashita Bridge

Photo. 2.7 Damage to the Toyokuni Bridge

Photo. 2.8 Damage to the Pier and the Truss of the Toyokuni Bridge

Photo. 2.9 Damage to the Sakawa Bridge

Photo. 2.10 Damaged Piers and Girders of the Sakawa Bridge

Photo. 2.11 Damage to the Left Abutment of the Sakawa Bridge

Photo. 2.12 Damage to the Piers of the Banyu Bridge While Under Construction.

Photo. 2.13 Damage to the Caisson Foundations of the Banyu Bridge While Under Construction.

Photo. 2.14 Damage to the Hayakawa Bridge

Photo. 2.15 Damage to the Hayakawa Bridge

Photo. 2.16 Damage to a Pier of the Takahata Bridge

Photo. 2.17 Damage to the Fifth Pier of the Takahata Bridge.

Photo. 2.18 Damage to the Right Abutment of the Takahata Bridge.

Photo. 2.19 Damage to the Support Shoes of the Kumano Bridge

Photo. 2.20 Damage to the Shimantogawa Bridge

Photo. 2.21 Damage to the Nakazuno Bridge

Photo. 2.22 Damage to the Nakazuno Bridge at the Column-To-Foundation Connection.

Photo. 2.23 Damage to the Column and Foundation of the Nakazuno Bridge.

Photo. 2.24 Damage to the Girders of the Nakazuno Bridge.

Photo. 2.25 Damage to the Left Abutment of the Nakazuno Bridge.

Photo. 2.26 Damage to the Girders of the Nakazuno Bridge.

Photo. 2.27 Damage to the Nagaya Bridge

Photo. 2.28 Damage to the Piers of the Nagaya Bridge.

Photo. 2.29 Damage to the Shioya Bridge.

Photo. 2.30 Damage to the Segoshi Bridge.

Photo. 2.31 Damage to the Itagaki Bridge.

Photo. 2.32 Damage to the Benten Bridge.

Photo. 2.33 Damage to the Benten Bridge.

Photo. 2.34 Damage to the Piers of the Koroba Bridge.

Photo. 2.35 Damage to a Column of the Koroba Bridge.

Photo. 2.36 Damage to the Third Pier of the Monbetsu Bridge.

Photo. 2.37 Damage to the Support Shoe at a Pier of the Shizunai Bridge.

Photo. 2.38 Damage to a Hinge Joint of the Horoman Bridge.

Photo. 2.39 Damage to the Girders of the Eai Bridge at a Supporting Pier

Photo. 2.40 Damage to the Abutment of the Bandai Bridge

Photo. 2.41 Damage to the Bandai Bridge

Photo. 2.42 Damage to the Showa Bridge

Photo. 2.43 Damage to the Showa Bridge (Settlement of the Approach Road at the Left-Bank Abutment).

Photo. 2.44 Damage to the Left-Bank Abutment of the Showa Bridge

Photo. 2.45 Damage to the Girders at the Seventh Pier of the Showa Bridge

Photo. 2.46 Damage to the Third Girder at the Second Pier of the Showa Bridge.

Photo. 2.47 Damage to a Pulled-Out Pile at the Fourth Pier of the Showa Bridge.

Photo. 2.48 Buckling Feature of the Pile Shown in Photo 2.47.

Photo. 2.49 Damage to the Yachiyo Bridge.

Photo. 2.50 Damage to the Second Pier of the Yachiyo Bridge.

Photo. 2.51 Damage to the Second Pier of the Yachiyo Bridge.

Photo. 2.52 Damage to the End of the Tenth Girder at the Ninth Pier of the Yachiyo Bridge.

Photo. 2.53 Damage to the End of the Tenth Girder at the Ninth Pier of the Yachiyo Bridge.

Photo. 2.54 Damage to the Higashi-Kosenkyo Bridge.

Photo. 2.55 Damage to the Pier Cap at the Ninth Pier of the Higashi-Kosenkyo Bridge

Photo. 2.56 Damaged Piles Pulled Out From the Ninth Pier of the Higashi-Kosenkyo Bridge.

Photo. 2.57 Damaged Piles Pulled Out From the Ninth Pier of the Higashi-Kosenkyo Bridge.

Photo. 2.58 Damage to the Matsuhama Bridge.

Photo. 2.59 Damage to the Support Shoe on the Thirteenth Pier of the Matsuhama Bridge.

Photo. 2.60 Damage to the PC Girder and the Abutment of the Kamezawa Bridge.

Photo. 2.61 Damage to the Kamimasaki Bridge.

Photo. 2.62 Damage to the Ikejima Bridge (Pier Settled Due to Soil Liquefaction)

Photo. 2.63 Damage to the Pile-Bent Pier of the Kaimei Bridge.

Photo. 2.64 Settlement of Pier at the Shiriuchi Bridge.

Photo. 2.65 Damage to the Abutment of the Noushi Bridge.

Photo. 2.66 Damage to the Abutment of the Deto Bridge.

Photo. 2.67 Crack of Abutment of the Komagome Bridge.

Photo. 2.68 Damage to the Support Shoe of the Kaimei Bridge.

Photo. 2.69 Failure of the Concrete Girders of the Komoto Bridge.

Photo. 2.70 North Abutment of Overcrossing at Golden State Freeway and Foothill Freeway Interchange.

Photo. 2.71 South Abutment of Overcrossing at Golden State Freeway and Foothill Freeway Interchange.

Photo. 2.72 Damaged San Fernando Road Overhead

Photo. 2.73 Steel Girders Taken From San Fernando Road Overhead

Photo. 2.74 Damaged San Fernando Road Overhead

Photo. 2.75 Southern Portion San Fernando Road Overhead

Photo. 2.76 Shear Failure in Column of San Fernando Road Overhead

Photo. 2.77 Shear Failure in Column of San Fernando Road Overhead

Photo. 2.78 Flexural Damage in Column of San Fernando Road Overhead

Photo. 2.79 Flexural Damage in Column of San Fernando Road Overhead

Photo. 2.80 Flexural Damage in Column of San Fernando Road Overhead

Photo. 2.81 View showing Horizontal Displacement of Bridge Deck on its Support - San Fernando Road Overhead

Photo. 2.82 Dislodged Rocker Support - San Fernando Road Overhead

Photo. 2.83 Settlement of Backfill - San Fernando Road Overhead

Photo. 2.84 Damaged Overcrossing at Golden State Freeway and Foothill Freeway Interchange

Photo. 2.85 Damaged Overcrossing at Golden State Freeway and Foothill Freeway Interchange

Photo. 2.86 Damaged Overcrossing at Golden State Freeway and Foothill Freeway Interchange

Photo. 2.87 Damaged Overcrossing at Golden State Freeway and Foothill Freeway Interchange

Photo. 2.88 Damaged Overcrossing at Golden State Freeway and Foothill Freeway Interchange

Photo. 2.89 Damaged Overcrossing at Golden State Freeway and Foothill Freeway Interchange

Photo. 2.90 Damaged Overcrossing at Golden State Freeway and Foothill Freeway Interchange

Photo. 2.91 Damaged Overcrossing at Golden State Freeway and Foothill Freeway Interchange

Photo. 2.92 Damaged Overcrossing at Golden State Freeway and Foothill Freeway Interchange

Photo. 2.93 Abutment of Overcrossing at Golden State Freeway and Foothill Freeway Interchange

Photo. 2.94 Column of Overcrossing at Golden State Freeway and Foothill Freeway Interchange

Photo. 2.95 Column of Overcrossing at Golden State Freeway and Foothill Freeway Interchange

Photo. 2.96 Failure at Base of Column Supported on a Single 6 Foot Diameter Cast-In-Drilled-Hole Pile - Golden State Freeway and Foothill Freeway Interchange

Photo. 2.97 Failure at Base of Column Supported on a Single 6 Foot Diameter Cast-In-Drilled-Hole Pile - Golden State Freeway and Foothill Freeway Interchange

Photo. 2.98 Failure at Base of Column Supported on Spread Footing - Golden State Freeway and Foothill Freeway Interchange

Photo. 2.99 Concentrated Ground Deformation Having Appearance of Fault Trace

Photo. 2.100 Damaged Railroad Tracks Near Golden State Freeway and Foothill Freeway Interchange

Photo. 2.101 Freeway Structures at Golden State Freeway and State Highway 14 Interchange

Photo. 2.102 Overcrossing at Golden State Freeway and State Highway 14 Interchange

Photo. 2.103 Overcrossing at Golden State Freeway and State Highway 14 Interchange

Photo. 2.104 Overcrossing at Golden State Freeway and State Highway 14 Interchange

Photo. 2.105 Overcrossing at Golden State Freeway and State Highway 14 Interchange

Photo. 2.106 Collapsed Span of Overcrossing at Golden State Freeway and State Highway 14 Interchange

Photo. 2.107 Crane Truck Crushed by Column - Golden State Freeway and State Highway 14 Interchange

Photo. 2.108 Collapsed Column of Overcrossing at Golden State Freeway and State Highway 14 Interchange

Photo. 2.109 Top End of Collapsed Column of Overcrossing at Golden State Freeway and State Highway 14 Interchange

Photo. 2.110 Top End of Collapsed Column of Overcrossing at Golden State Freeway and State Highway 14 Interchange

Photo. 2.111 Settlement of Backfill at Abutment of Overcrossing - Golden State Freeway and State Highway 14 Interchange

Photo. 2.112 Timber Falsework - Golden State Freeway and State Highway 14 Interchange

Photo. 2.113 Foothill Boulevard Undercrossing at Foothill Freeway Looking in a Westerly Direction

Photo. 2.114 Shear Failure of Column - Foothill Boulevard Undercrossing at Foothill Freeway

Photo. 2.115 Shear Failure of Column - Foothill Boulevard Undercrossing at Foothill Freeway

Photo. 2.116 Foothill Boulevard Undercrossing at Foothill Freeway Looking in an Easterly Direction

Photo. 2.117 Damaged Wing Wall of Abutment - Roxford Street Undercrossing at Foothill Freeway

Photo. 2.118 Damaged Concrete Apron on Abutment Slope - Roxford Street Undercrossing at Foothill Freeway

Photo. 2.119 Damaged Concrete Apron on Abutment Slope - Roxford Street Undercrossing at Foothill Freeway

Photo. 2.120 Damaged Concrete Apron on Abutment Slope - Roxford Street Undercrossing at Foothill Freeway

Photo. 2.121 Differential Settlement of Backfill at Abutment - Roxford Street Undercrossing at Foothill Boulevard

Photo. 2.122 Differential Settlement of Backfill at Abutment - Roxford Street Undercrossing at Foothill Boulevard

Photo. 2.123 Differential Settlement of Backfill at Abutment - Polk Street Undercrossing at Foothill Freeway

Photo. 2.124 Differential Settlement of Backfill at Abutment - Polk Street Undercrossing at Foothill Freeway

Photo. 2.125 Differential Settlement of Backfill at Abutment - Polk Street Undercrossing at Foothill Freeway

Photo. 2.126 Differential Settlement of Backfill at Abutment - Polk Street Undercrossing at Foothill Freeway

Photo. 2.127 Differential Settlement of Backfill at Abutment - Polk Street Undercrossing at Foothill Freeway

Photo. 2.128 Buckled Asphalt Pavement Caused by Large Compressive Ground Deformations

Photo. 2.129 Differential Settlement of Backfill at Abutment - Hubbard Street Undercrossing at Foothill Freeway

Photo. 2.130 Buckled Asphalt Pavement Caused by Large Compressive Ground Deformations

Photo. 2.131 View Showing Crushed Rock Forced Out of Weep Hole - Bledsol Street Undercrossing at Foothill Freeway

Photo. 2.132 View Showing Crushed Rock Forced Out of Weep Hole - Bledsol Street Undercrossing at Foothill Freeway

Photo. 2.133 Tyler Street Pedestrian Overcrossing at Foothill Freeway

Photo. 2.134 Tyler Street Pedestrian Overcrossing at Foothill Freeway

Photo. 2.135 Tyler Street Pedestrian Overcrossing at Foothill Freeway

Photo. 2.136 View of Permanent Support Displacement - Tyler Street Pedestrian Overcrossing at Foothill Freeway

Photo. 2.137 View of Permanent Support Displacement - Tyler Street Pedestrian Overcrossing at Foothill Freeway

Photo. 2.138 Flexural Damage at Top of Column - Tyler Street Pedestrian Overcrossing at Foothill Freeway

Photo. 2.139 Flexural Damage at Top of Column - Tyler Street Pedestrian Overcrossing at Foothill Freeway

Photo. 2.140 Base of Column - Tyler Street Pedestrian Overcrossing at Foothill Freeway

Photo. 2.141 Base of Column - Tyler Street Pedestrian Overcrossing at Foothill Freeway

Photo. 2.142 Damaged Wing Wall of Culvert Which Passes Under Foothill Freeway

Photo. 2.143 Via Princessa Undercrossing on State Highway 14

Photo. 2.144 Flexure Cracking in Diaphragm Abutment - Via Princessa Undercrossing on State Highway 14

Photo. 2.145 Pounding Damage at Expansion Joint - Santa Clara Overhead Crossing on State Highway 14

Photo. 2.146 Buckled Flexible Splice in Steel Conduit - Santa Clara Overhead Crossing on State Highway 14

I INTRODUCTION

The damages caused to bridge structures during the San Fernando Earthquake of February 9, 1971, pointed out the urgent need for both theoretical and experimental research related directly to seismic effects on bridge structures.

As a direct result, a three-year research investigation entitled "An Investigation of the Effectiveness of Existing Design Methodology in Providing Adequate Structural Resistance to Seismic Disturbances" was initiated in 1971 within the Earthquake Engineering Research Center, University of California, Berkeley, under the sponsorship of the U. S. Department of Transportation, Federal Highway Administration. This investigation is to consist of the following:

1) A search of the world literature on earthquake resistant design of bridges with specific attention to those publications documenting the experience of and investigations by bridge engineers in Japan where the incidence of damage to bridge structures due to earthquakes has been considerable.

2) A review of the damage to highway structures during the February 9, 1971, earthquake in Los Angeles and, based on this review, the establishment of priorities for the subsequent investigation of specific structural types.

3) A critical examination of advanced practices in seismic design used for buildings in order to determine which techniques are applicable to seismic design of bridge structures. In particular, those specific types of highway structures which differ so radically in dynamic behavior from buildings that new seismic design techniques must be developed, will be identified.

4) An analytical investigation of specific highway structures of the type identified in 3) above as requiring special consideration, including the development of appropriate response spectra to both horizontal and vertical components of typical seismic disturbances.

5) Detailed model experiments of three structures investigated under 4) above, using simulation scales large enough to permit realistic assessment of local as well as gross structural behavior. The models will be subjected to simulated seismic disturbances using the new University of California, Berkeley, shaking table.

6) A comparison of dynamic response indicated by model experiments and by analytical investigations will be made. Comparisons will also be made between model and analytical response and the apparent response of corresponding prototype structures during the San Fernando earthquake.

7) Prepare recommendations for changes in design specifications and methodology to provide more adequate protection against future earthquakes.

This report is the first in a series to result from the investigation. Chapter II describes the damages sustained by bridge structures during (1) the Kanto earthquake of 1923 (Richter Magnitude M = 7.9), (2) the Nankai earthquake of 1946 (M = 8.1), (3) the Fukui earthquake of 1948 (M = 7.3), (4) the Imaichi earthquake of 1949 (M = 6.7), (5) the Tokachi-oki earthquake of 1952 (M = 8.1), (6) the northern Miyagi earthquake of 1962 (M = 6.5), (7) the Niigata earthquake of 1964 (M = 7.5), (8) the Ebino earthquake of 1968 (M = 6.1), (9) the Tokachi-oki earthquake of 1968 (M = 7.9), (10) the Alaska earthquake of 1964 (M = 8.4), (11) the Madang earthquake of 1970 (M = 7.1), (12) the Chilean earthquake of 1971 (M = 7.5), and (13) the San Fernando earthquake of 1971. These descriptions provide considerable insight into the types and causes of damages to

bridge structures.

Chapter III describes many of the more important research investigations carried out to date on seismic effects on bridges. These investigations may be classified into the following categories: (1) seismicity, (2) characteristics of strong ground motions, (3) bearing capacity and stability of soils, (4) earth pressures, (5) hydraulic pressures, (6) dynamic properties of bridges, (7) field measurements of earthquake response of bridges, (8) dynamic analyses of bridges, and (9) laboratory experiments.

Chapter IV presents specifications for the earthquake-resistant design of bridges as currently used by many organizations. Emphasis is placed on Japanese specifications as they are judged by the authors of this report to be the most comprehensive and modern of any seismic design regulations used throughout the world. In addition, Chapter IV presents a summary of seismic regulations for 21 countries of the world. This summary indicates magnitudes of seismic coefficients being used and makes note of certain factors which affect these magnitudes.

Chapter V gives a brief summary of the conclusions deduced from the damage surveys given in Chapter II, the research investigations described in Chapter III, and the current code provisions outlined in Chapter IV.

II SEISMIC DAMAGE TO BRIDGE STRUCTURES

A. GENERAL

To develop a better understanding of seismic effects on structures, it is important to investigate seismic damages to similar existing structures during previous damaging earthquakes. Such studies are invaluable in developing rational and economical design procedures.

This chapter reviews the characteristics of damages to bridge structures, including superstructures, substructures and surrounding soils, caused by past earthquakes in Japan, the United States, and several other countries. Figure 2.1 provides brief information on nine major earthquakes which occurred in Japan since 1923 causing severe damage to many modern structures [51] [210]*.

B. KANTO EARTHQUAKE OF 1923 [23]

A severe earthquake occurred on September 1, 1923, in Sagami Bay off the southern coast of the Kanto area of Japan which includes Tokyo, Yokohama, and other major cities. It was the first such attack on modern facilities in Japan. The earthquake was recorded as magnitude 7.9 on the Richter scale. Its epicenter location was 35.2°N, 139.3°E and its hypocenter depth was estimated to be in the range 0 - 20 km. The epicenter location is shown in Figs. 2.1 and 2.2. Figure 2.2 shows the intensity distribution as determined by the Japan Meteorological Agency (JMA). The definitions of the JMA Intensity Scale are tabulated in Table 2.1. In this same table, corresponding magnitudes of accelerations at ground surface as suggested by H. Kawasumi [80] are also shown.

---

*Numerals in brackets refer to bibliography numbers

Substantial damage to bridge structures as well as other engineering structures was caused throughout the southern Kanto area, especially in Tokyo, Yokohama, and in the vicinity of the epicenter [23]. Although a great amount of damage was caused by fire in the larger cities, vibrational effects of the earthquake also caused extensive damage.

The Kanto earthquake was certainly one of the most significant earthquakes in Japan as it greatly influenced seismic design procedures in that country. Before the earthquake, no distinct regulations existed which required designing against seismic forces. Therefore, few structures had been designed with adequate lateral strength. After the earthquake, however, seismic design specifications were quickly introduced which required designing for seismic forces.

During the Kanto earthquake nearly two thousand bridges suffered light to heavy damage (see Table 2.2). While damage was severe in Tokyo, most damage to bridges was caused by fire rather than by ground vibration effects. Hundreds of bridges suffered damage by fire in that city; however, only 18 bridges were damaged by ground vibration. Damage caused by ground vibration was severest in Kanagawa Prefecture located near the epicenter. In the city of Yokohama, the percentage of bridges damaged by vibrational effects was very high.

The following sections describe the characteristics of damage caused by ground vibration effects on a number of bridges which suffered relatively heavy damage during the Kanto earthquake.

1. Tsuruno-bashi Bridge (Fig. 2.3) - Construction of this bridge which spanned the Shinyoshida River on the Bandaicho-Horaicho Road in Yokohama, Kanagawa Prefecture, about 40 km northeast of the epicenter was completed in 1914. The ground at the site of the bridge was very soft alluvial material. Both abutments were constructed of brick masonry with concrete foundations. Each of two piers was made of four spiral single-row cast-iron-pipe piles with added bracing as shown in Fig. 2.3. The superstructure consisted of 3 simple span plate girders. The total length of the bridge was 33.6 m (10.5 m + 12.6 m + 10.5 m) and the effective width of the pavement was 7.3 m.

The earthquake caused moderate damages to this bridge. Both abutments moved and tilted toward the center of the river and the two piers tilted considerably toward the left bank. The 3 spans of the superstructure moved primarily toward the left bank (left when looking from the upstream side).

The anchor bolts at the support on the left bank were broken off. As a result of this failure, the connection between the left end of the superstructure and the crest of the abutment was removed. Thus, the abutment could move freely towards the center of the river. The other portions of the bridge (right abutment, two piers, and superstructure) moved toward the left bank in accordance with the inward movement of the right abutment. Although this bridge suffered considerable permanent distortion, it was capable of carrying traffic immediately following the earthquake.

2. Shinminato Bridge (Figs. 2.4, 2.5; Photos 2.1, 2.2) - This bridge, completed in 1910, was located about 40 km northeast of the epicenter between Kaigandori and Shinminato-machi, Yokohama, Kanagawa Prefecture. It spanned across a waterway in Yokohama Harbor. Both abutments were of brick masonry with concrete spread footings resting on mudstone. A single span Petit steel truss weighing 365 tons, of length 36.6 m, and of width 13.4 m was erected on the abutments. This particular bridge carried both highway and railway traffic.

Due to the earthquake, this bridge sustained heavy damage at both abutments as shown in Figs. 2.4 and 2.5. The northern abutment tilted and moved considerably toward the center of the waterway. The maximum movement observed was 36 cm. Also observed were heavy cracks in the masonry abutments and a dislocation at the joint between the brick masonry and the footing (Fig. 2.5). The southern abutment suffered cracks having widths as large as 8 cm. The parapet walls at both abutments, supported separately by the back fills, were forced backwards considerably, probably due to collisions with the truss girders. No serious settlements were observed at the abutments themselves.

The bridge truss did not sustain any significant damage. However, due to the displaced abutments, a large relative dislocation was observed between the truss support and the substructure. The relative dislocation between support points was approximately 35 cm. This large dislocation caused the supporting shoes to fail at both the movable and the fixed supports (see Photos 2.1, 2.2).

3. Bankoku Bridge (Fig. 2.6; Photos 2.3, 2.4, 2.5) - This bridge, completed in 1903, was located very close to the Shinminato Bridge and across the same waterway. The abutments were constructed of brick masonry with concrete block foundations resting on mudstone. A single span pony steel truss weighing 314 tons, of length 36.6 m, and of width 12.2 m, was constructed on the abutments (Photo 2.3).

The earthquake caused severe damage to both abutments. The northern abutment slid horizontally toward the center of the waterway. The amount of sliding was 1.2 m at its maximum point. This drastic sliding was accommodated by a relative movement between the upper and lower blocks of the foundation (Fig. 2.6). Also observed was a huge vertical crack 2.7 cm wide in the abutment near the centerline of the bridge axis. Excessive earthpressures forced the two wing walls to separate from the abutment. The upper portion of the southern abutment also slid toward the center of the waterway. The amount of sliding at this location totalled about 30 cm. Both wing walls at this abutment also separated.

The bridge truss girder suffered no significant damage. However, several lattice beams attached to the lower chords buckled. The movable roller support on the northern abutment moved considerably (40 cm on the east side; 30 cm on the west side) towards the south, together with the abutment. At the east side of this support, the sole plate attached to the end of the truss was completely dislodged from the rollers (Photo 2.4). The fixed support on the southern abutment moved to the north (22 cm at the east side; 34 cm at the west side) along with the abutment, and all anchor bolts on both sides were sheared off (Photo 2.5).

It is clear from the damage experienced by this bridge that severe damage due to sliding between blocks in the abutments can be expected.

4. Yamashita Bridge (Photo 2.6) - This bridge, completed in September 1922, was located about 40 km northeast from the epicenter across the Horikawa River in Kaigandori, Yokohama, Kanagawa Prefecture. The northern abutment (left bank looking from upstream side) was constructed, from top to bottom, of poured-in-place concrete, 2-step concrete blocks, reinforced concrete placed in water, and a wooden pile foundation in the soft soil layer below. The southern abutment (right bank) was made, from top to bottom, of poured-in-place reinforced concrete, 3-step concrete blocks, and sacked concrete placed on top of the mudstone foundation.

A single span Pratt steel truss of length 52 m and width 14 m spanned the abutments.

During the earthquake, the southern abutment having no pile foundation sustained heavy damage. Severe cracking and tilting of the abutment was observed (Photo 2.6). No major structural damage was observed to other portions of the bridge. However, most lattice beams of the truss had buckled.

It was reported that the earth pressures which developed during the earthquake had significant effects on the southern abutment.

5. Hanazono Bridge (Fig. 2.7) - This bridge was located across the Ooka River about 40 km northeast of the epicenter between Ogi-machi and Yamashita Park, Yokohama, Kanagawa Prefecture. The two abutments were constructed of brick masonry and were placed on very soft soil. A single pony steel truss of length 50 m and width 7.6 m spanned the abutments.

During the earthquake, the abutments sustained moderate damage (Fig. 2.7). The right abutment having a fixed support, moved towards the center of the river. A horizontal crack of 3 cm width developed near the top of this abutment and the anchor bolts at the fixed support sheared off. It has been estimated that the crack occurred mainly due to the resistance of the superstructure against movement of the abutment toward the center of the river.

The left abutment having a roller support, also moved toward the center of the river. The parapet wall collapsed due to collision with the end of the truss girder. The bolts attaching the shoes were broken

off and the shoes moved 24 cm to the left relative to the abutment. The sole plates attached to the end of the truss moved 42 cm to the left relative to the shoes. Consequently, the truss moved 66 cm to the left relative to the abutment.

No significant damage was observed to the superstructure; however, the camber of the truss girder had been removed completely as a result of the large displacements of the abutments. The bridge experienced a fire as a result of the earthquake, which might have had an effect on the disappearance of camber.

It was quite apparent that large earth pressures had developed against both abutments.

6. Toyokuni Bridge (Fig. 2.8; Photos 2.7, 2.8) - This bridge spanning the Ooka River was located between Horai-cho and Masago-cho, Yokohama, Kanagawa Prefecture, about 40 km northeast of the epicenter. The original superstructure used light wood-steel Pratt trusses. However, at a later date (about 1897) these trusses were replaced by all steel pony trusses which were placed on the original substructure without modification. The abutments and two piers were built of masonry construction with concrete fill in their interior and were placed on top of very soft soils. No detailed information is available regarding the foundations. The superstructure consisted of 3 single spans of pony trusses having a total length of 48.5 m (15.5 m + 16.5 m + 15.5 m) and having a width of 6.7 m. This bridge was skewed at an angle of some 20° as shown in the plan view of Fig. 2.8.

During the earthquake, the substructures moved considerably causing one end of a superstructure span to fall into the river (Photos 2.7, 2.8). Both abutments moved toward the center of the river and tilted in the direction of their backfill. No serious cracks were observed.

The two piers tilted considerably toward the center of the river with angles of inclination of 8°41' at the northern pier, and 2° at the southern pier. The southern pier suffered serious breakage between the base of the shaft and the top of the foundation. It is believed that soil failures were the primary cause of tilting.

The superstructures moved drastically due to the movements of the substructures. On the northern pier having a fixed support made of a set of steel channels, the two truss girders moved to the south along with the support. Although this support was nearly dislodged from the top of the pier (see Fig. 2.8), the superstructure was prevented from falling off the pier.

On the southern pier having a roller support, the two truss girders also moved to the south and the southernmost girder fell from its support into the river. No significant damage was observed to the truss girders which did not fall from their supports.

It is understood that since the substructures were designed and constructed for the original lighter superstructures, they were not sufficient to support the later constructed heavier superstructures during the earthquake.

7. Sakawa Bridge (Fig. 2.9; Photos 2.9, 2.10) - This bridge, located in Odawara, Kanagawa Prefecture, was erected across the Sakawa River on National Highway No. 1. It was completed in July 1923, only two months prior to the occurrence of the earthquake. Located near the mouth of the river, it was one of those bridges situated very close to the epicenter - (about 13 km northwest of the epicenter).

The abutments were of gravity-type reinforced concrete construction placed on soft soils. The thirty-two piers were reinforced concrete rigid frame structures with concrete caisson foundations covered by wooden frames. These piers were also located on soft soils.

The superstructure consisted of 33 single spans built with reinforced concrete T-type girders. Its total length was 363 m (33 x 11) and its width was 6.7 m (Fig. 2.9).

During the earthquake, the bridge sustained very severe damage. The right abutment developed a huge crack between the main structure and one wing wall. The left abutment tilted slightly and the parapet wall broke off (Photo 2.11). All piers completely collapsed and as a result all 33 simple spans fell into the river (Photos 2.9, 2.10). The authors believe that falling of the superstructures was initiated at

the extreme left span and progressed to the right over the entire length of the bridge.

Based on the fact that a heavily damaged pier remained between the two sections of fallen girder, the authors believe that the girders moved extensively in a horizontal direction before falling. The maximum distance between one end of a fallen girder and the nearest pier was about 1.7 m.

It is understood that the severe damages caused to this bridge were due to the following: (1) the location was very close to the epicenter (about 13 km), (2) the soils at the site were very soft, and (3) the substructures were inadequate to resist the large seismic forces which developed in the rather heavy reinforced concrete girders.

8. Banyu Bridge (Fig. 2.10; Photos 2.12, 2.13) - This bridge was located across the Banyu River (presently the Sagami River) on National Highway No. 1 about 15 m northeast of the epicenter between Chigasaki and Hiratsuka, Kanagawa Prefecture. The bridge substructures were under construction at the time of the earthquake.

Both abutments of gravity-type reinforced concrete with pile foundations were completed at the time of the earthquake. The piers were reinforced concrete rigid frames with concrete caisson foundations. Among the total of 56 piers, only 6 had been completed near the left bank of the river. The caisson foundations of the remaining 42 piers had either just been completed, or were under construction at the time of the earthquake.

The superstructures, consisting of 57 simple span reinforced concrete T-shape girders of total length 620 m (57 x 10.9) and width 7.3 m, had not been erected at the time of the earthquake.

During the earthquake, the substructure sustained extensive damage (Fig. 2.10). The right and left abutments tilted about 12° and 4°, respectively, towards the center of the river. Major failures occurred in the horizontal beams of the piers (Photo 2.12). Insufficient curing of the concrete could have been an important factor causing this damage.

Large displacements and floating of several caisson foundations were

observed (Photo 2.13). In view of this type behavior of the foundations, it appears that liquefaction of soils took place at this site.

9. Hayakawa Bridge (Fig. 2.11; Photos 2.14, 2.15) - This bridge, completed in 1917, crossed the Hayakawa River on the Odawara-Yugawara Route of the Kanagawa Prefecture roads. It was located in Odawara, Kanagawa Prefecture, about 15 km west of the epicenter. The abutments and piers were constructed of plain gravel concrete with quoin stones and were supported by caisson foundations placed in gravel layers. The superstructures consisted of 6 simple span reinforced concrete T-shape girders having a total length of 82 m (6 x 13.6 m) and a width of 5 m. The three southern spans had been deformed permanently prior to the earthquake due to flow of heavy traffic immediately after completion of the bridge. Some repair of this damage had been performed by injecting cement paste into the cracks.

During the earthquake, serious damage occurred including the dislodging of girders entirely from their supports (Fig. 2.11; Photos 2.14, 2.15). The northern abutment developed cracks in the masonry and some cornerstones fell from their supports. No significant damage was observed to the southern abutment. All piers except the central one developed cracks on their down-stream side. The southernmost pier was pushed northward and tilted by a falling girder which caused heavy cracks to develop in the masonry.

All girders were displaced downstream (eastward) and towards the right bank (southward). The maximum displacement was about 50 cm. The three southern girders which had previously been damaged by traffic, suffered major cracks along their webs causing them to drop. The southernmost span eventually fell into the river as a result of this type failure.

This bridge which had a clear span of 13.6 m, was one of the longest concrete bridges of its time. It was reported that the bridge experienced high amplitude vertical oscillations during the earthquake.

10. Takahata Bridge (Fig. 2.12; Photos 2.16, 2.18) - This bridge was located across the Asakawa River on a Tokyo prefectural road in Hino,

Tokyo, about 53 km north of the epicenter. The maximum ground acceleration near the site was estimated to be about 0.2 g which is much less than that experienced at the other sites described previously. At the bridge location, a 3 m layer of gravel overlay a hard clayey soil. Near the right bank of this site, soft soils were present.

Both abutments were of gravity-type concrete construction. The right abutment was supported on a pile foundation. The piers were reinforced concrete rigid frames (3 columns and 1 beam). The superstructures consisted of 13 simple span I-shape steel plate girders having a total length of 115 m (7.5 m + 11 @ 9.1 m + 7.5 m) and a width of 5.5 m.

During the earthquake, the right abutment and two piers suffered severe damage (Fig. 2.12; Photos 2.16, 2.18). The right abutment moved towards the center of the river by the action of the earth pressures and sustained serious damage due to collisions with the superstructure (Photo 2.18). No significant damage was observed to the left abutment.

Only two piers, the fourth and fifth piers from the right bank suffered severe damage. This damage was located near the upper joint of the central column (3 columns total) probably due to large bending moments exerted by the superstructure. Photograph 2.17 shows this failure in the fifth pier.

No significant damage was observed in the superstructures.

C. NANKAI EARTHQUAKE OF 1946 [24]

One of the greatest earthquakes experienced in or near Japan occurred on December 21, 1946, about 60 km off Shionomisaki (coast of Kii Peninsula), Wakayama Prefecture of Honshu Island (Figs. 2.1, 2.13). Its magnitude was recorded at 8.1 on the Richter scale. The epicenter location was 33.0°N, 135.6°E and the hypocenter depth was 30 km. The JMA seismic intensity distribution is shown in Fig. 2.13.

Since this earthquake occurred within one year after the end of World War II, difficulties were encountered in assessing and repairing

the damages promptly. Nevertheless, engineers and seismologists made a great effort to survey the damage characteristics and to reconstruct heavily damaged structures. Several reports describing the damage have been published and are available [24] [210].

Over 300 highway bridges were damaged by the earthquake as tabulated in Table 2.3. Damaged bridges were observed throughout southern Japan. The most heavily damaged ones were located in Kochi Prefecture of Shikoku Island and Wakayama Prefecture on Honshu Island.

The following sections describe the severe damages caused to two important bridges during this earthquake.

1. Kumano Bridge (Photo 2.19) - This bridge, completed in March 1935, was located on National Highway No. 41 in Shingu, Wakayama Prefecture. It crossed the Kumano River about 90 km north of the epicenter. The JMA intensity at the site was 6 and the maximum acceleration was estimated to be 0.2 g or more. The surface ground layer at this site was gravel with cobble stones.

The abutments were U-shape gravity-type concrete construction having the dimensions 15 m in the transverse direction, 5 m and 2.3 m in the longitudinal direction at the base and crest, respectively, and 10 m in height. The piers were elliptical reinforced concrete columns with caisson foundations. The dimensions of the caissons were 11 m by 4 m in section and 13 m (main spans) or 8 m (side spans) in height.

The superstructures having a total length of 418.5 m consisted of three main spans (3 @ 54 m) plus six side spans (6 @ 41.4 m). All spans used simple Warren trusses and were 6 m wide.

During the earthquake, the bridge sustained moderate damage to bearing supports and appurtenant structures. Photograph 2.19 shows damage to the 4th pier from the left-bank side, which indicates movement of the movable shoe (right side of photo), and failure of the fixed shoe (left side of photo). No significant damages were observed to the substructures (abutments and piers). The wing walls on the right-bank (Wakayama) side separated about 20 cm letting the approaching backfill settle about 30 cm maximum.

Five trusses (4th to 9th span from right bank) moved about 4 cm towards the right bank. As a result of this movement, the mortar and concrete near the fixed bearing supports on the substructures were crushed. No lateral movements perpendicular to the bridge axis were observed.

2. Shimantogawa Bridge (Photo 2.20) - This bridge crossed the Shimanto River connecting Gudo and Nakamura, Hatata Country, Kochi Prefecture, about 250 km west of the epicenter.

The abutments were of gravity-type reinforced concrete construction and the piers were reinforced concrete columns having caisson foundations. The superstructures having a total length of 438 m and a width of 5.5 m, consisted of eight main spans (steel Warren trusses, 8 @ 46.05 m) and six side spans (reinforced concrete girders, 6 @ 11.6 m).

During the earthquake, the bridge sustained severe damage. The right abutment developed a serious crack at the parapet wall and its wing wall on the downstream side failed. The piers which supported steel trusses suffered heavy damage due to falling trusses. None of this particular damage was a direct result of the earthquake. The piers supporting the reinforced concrete girders did, however, develop cracks as a direct result of the earthquake. A total of six steel trusses (2nd to 7th spans from left) fell into the river (Photo 2.20). Although no detailed descriptions are available as to the causes of fall, it has been reported that the 4th span from the left fell down first, followed by the 3rd span, and finally by the 2nd, 5th and 6th spans which fell almost simultaneously.

D. FUKUI EARTHQUAKE OF 1948 [25]

A severe earthquake occurred inside the Fukui Plain, Fukui Prefecture, located in the midwestern part of Honshu Island, on June 28, 1948. This earthquake registered 7.3 on the Richter scale. Its epicenter (36.1°N, 136.2°E) was very close to several cities and towns in Fukui

and Ishikawa Prefectures; thus causing a tremendous amount of damage in each prefecture. The hypocenter depth was estimated to be 20 km.

The Fukui earthquake was one of the most damaging earthquakes ever to have occurred in Japan. An extensive survey of the damages inflicted on engineering structures was carried out. Certain statistics on damages caused to highway bridges are summarized in Table 2.4.

1. Nakazuno Bridge (Figs. 2.15, 2.16; Photos 2.21, 2.26) - This bridge, completed in 1932, crossed the Kuzuryu River on the Fukui- Kaga-Yoshizaki Route, one of the Fukui prefectural roads located between Kawai and Nakafujishima, Yoshida County, Fukui Prefecture. It was located about 8 km south of the epicenter where maximum ground acceleration was estimated at about 0.6g based on evidence of overturned tomb stones nearby.

The abutments were of gravity-type reinforced concrete construction with pile foundations. Thirteen piers present were reinforced concrete columns having either pile or caisson foundations. A general view of a typical pier shows in Fig. 2.16. The superstructures having a total length of 257 m and a width of 5.5 m, consisted of 14 simple span steel plate girders (14 @ 18.4 m).

During the earthquake, both the superstructures and the substructures sustained severe damage. The left abutment suffered cracking in its parapet walls (Photo 2.25), and the right abutment inclined toward the center of the river. The 1st and 2nd piers from the left bank did not suffer any damage. However, the 3rd to the 7th, the 9th and 10th piers tilted toward the left bank suffering heavy cracking at the connections between columns and caisson foundations (Photo 2.22) exposing the reinforcing bars. Extensive cracking was also observed at the connections between columns and beams at the pier caps. The 12th and 13th piers tilted toward the right bank and suffered cracking at the connections between columns and beams.

Ten of the 14 spans fell into the river (Fig. 2.15; Photos 2.21, 2.24, 2.26). Because they fell on the soft sand layer below, the girders and their lateral members suffered no significant damage and were easily re-

paired for later use. Failure of the substructures was the main cause of this behavior of the superstructures.

2. Nagaya Bridge (Figs. 2.17, 2.18; Photos 2.27, 2.28) - This bridge crossed the Jugo Irrigation Canal on the Katsuyama-Mikuniminato Route, one of the Fukui prefectural roads located in Higashijugo, Fukui Prefecture. The bridge site was about 20 km north of the epicenter where the maximum ground acceleration was estimated to be in the range 0.5 - 0.6 g.

The abutments were of concrete construction and the seven piers were reinforced concrete rigid frames (2 columns and 1 beam). The superstructures having a total length of 58.5 m and a width of 4 m consisted of 8 simple span I-shaped steel girders (4 @ 6 m + 3 @ 9.5 m + 6 m). The bearing plates were slide-type with two steel plates. Although the left abutment suffered no significant damage, the right abutment tilted toward the center of the canal. The 1st to 3rd piers from the left bank settled considerably while the 4th to 7th piers not only settled but tilted considerably as well. Large cracks were observed at the column to beam connections of the 4th to 7th piers (Fig. 2.18; Photo 2.28). Every span moved downward drastically due to settlement of the piers as shown in Fig. 2.17 and Photo 2.27.

3. Shioya Bridge (Photo 2.29) - This bridge was located near the mouth of the Daishoji River, Shioya, Ishikawa Prefecture, about 15 km north from the epicenter. The maximum ground acceleration at the site was estimated to be 0.5 g.

The abutments were of concrete construction and the seven piers were reinforced concrete rigid frames (3 columns and 1 beam). The superstructures having a total length of 86 m and a width of 4.5 m consisted of 8 simple span I-shaped steel girders (8 @ 10.75 m).

During the earthquake, this bridge sustained moderate damage to the substructure. The left abutment tilted slightly and developed a crack along the construction joint which was located 2 m below the crest of the abutment. As a result of this tilting, the anchor bolts

moved about 40 cm toward the left bank and about 5 cm in the upstream direction. The right abutment also tilted slightly. Every pier tilted toward the left bank and settled. Maximum settlement occurred at the 2nd pier from the right bank where it measured 25 cm (Photo 2.29). No significant damage of superstructure was observed.

4. Segoshi Bridge (Photo 2.30) - This bridge crossed the Daishoji River on one of the municipal roads at Segoshi, Ishikawa Prefecture about 15 km north of the epicenter. The maximum ground acceleration was estimated to be about 0.5 g.

The abutments were of concrete construction and the seven piers were of reinforced concrete solid-slab-type construction. The superstructures having a total length of 87.2 m and a width of 3.3 m consisted of 8 spans of I-shape steel girders (8.5 m + 4@ 11.4 m + 10.3 m).

During the earthquake, moderate damage was sustained by the substructures and superstructures. Both abutments tilted toward the center of the river due to sliding of the back fill. Several cracks developed in the main wall and the wing walls. All piers settled as shown in Photo 2.30. Maximum settlement was 50 cm at the 4th pier. All piers suffered tilting toward the left bank as well. The concrete deck slab moved generally in an upstream direction. The main I-shape steel girders were deformed due to twisting and bending forces.

5. Itagaki Bridge (Figs. 2.19, 2.20; Photo 2.31) - This bridge, completed in 1933, crossed the Ashiba River on the Hashidate-Fukui Route, one of the Fukui prefectural roads in Fukui. Maximum ground acceleration at this location was estimated to be about 0.6 g based on evidence of overturned tomb stones and other damage. The surface ground layer at the bridge site consisted of gravel.

The abutments were of gravity-type reinforced concrete construction and the twelve piers were reinforced concrete rigid frames (2 columns and 1 beam) with caisson foundations (Fig. 2.19). The superstructures having a total length of 156 m and a width of 4.5 m consisted of 13

reinforced concrete T-shape girders (13 @ 12 m). Tar paper was placed in the bearing support interfaces.

During the earthquake, both the substructures and the superstructures sustained extensive damage. Both abutments developed wide cracks in the parapet walls and in the masonry wing walls. The wing wall masonry at the left abutment collapsed. The 3rd, 4th, 5th, 6th, 7th and 8th piers tilted about 10°, 4°, 12°, 3°, 1° and 1°, respectively, toward the left bank. This tilting was caused by failures at the connections between the columns and the caisson foundations and also by tilting of the foundations. No permanent displacements were observed in the transverse direction of the bridge. Eight of the thirteen deck spans fell into the river due to pier failures (Fig. 2.20; Photo 2.31). Those spans which did not fall moved considerably and sustained severe damage to the main beams and the deck slabs.

6. Benten Bridge (Photo 2.32, 2.33) - This bridge crossed a tributary of the Daishoji River on one of the municipal roads in Daishoji, Ishikawa Prefecture, about 18 km north of the epicenter. The maximum ground acceleration of this site was estimated to be 0.4 g.

The abutments were of concrete construction and the five piers were reinforced concrete rigid frames (4 columns and 3 beams). The superstructures having a total length of 50.3 m and a width of 3.3 m consisted of 6 I-shape steel girders (2 @ 6 m + 3 @ 10 m + 8.3 m).

During the earthquake, the bridge sustained severe damage. The right abutment tilted toward the center of the river and the parapet walls at both abutments collapsed. The 2nd pier from the left bank was greatly deformed due to falling of the 3rd span. The 3rd pier overturned completely into the river. The 4th and 5th piers tilted toward the left bank about 20° and 3°, respectively. The ends of the 3rd and 4th spans located at the 3rd pier dropped into the river (Photos 2.32 and 2.33). The bearing support of the 6th span on the right abutment was moved out of position.

7. Koroba Bridge (Fig. 2.21; Photos 2.34, 2.35) - This bridge

crossed a tributary of the Daishoji River on one of the municipal roads in Daishoji, Ishikawa Prefecture, about 18 km north of the epicenter. The maximum ground acceleration at this site was estimated to be about 0.4 g.

The abutments were of concrete construction and the two piers were reinforced concrete rigid frames (3 columns and 2 beams at top and bottom) as shown in Fig. 2.21. The superstructures having a total length of 36 m and a width of 3.65 m consisted of 3 reinforced concrete T-shape girders (3 @ 12 m).

During the earthquake, the bridge sustained severe damage. The wing walls of both abutments suffered large cracking. The 1st pier from the left bank developed a large crack (15 cm wide) in its lower beam. Major compressive failures exposing the reinforcing bars occurred in the central and downstream columns 1 m below the pier crest. The upstream column of this same pier tilted in the upstream direction about 5°. The 2nd pier also suffered a crack in its lower beam and tilted in the upstream direction about 7°. The upstream column failed near midheight exposing the reinforcing bars. The superstructure suffered large cracking near midspan of the main girders in the 1st and 2nd spans. This damage to girders was the severest of all damages caused directly by vibrational effects of the earthquake.

8. Summary of Bridge Damages - Based on the above discussion of bridge damages caused by the Fukui earthquake of 1948, two general characteristics should be noted. Firstly, the damages to superstructures were primarily caused by overturning and failures within the substructures and secondly, the degree of damage sustained by superstructures was not severe. Only one bridge (Koroba Bridge) apparently sustained superstructure damage as a direct result of vibration caused by the earthquake.

Observations of damages to individual portions of bridge structures reveal the following general patterns:

(a) Damages to abutments included settlement, tilting (usually toward the center of the river), sliding, failure of parapet walls,

settlement of approaches, failure of wing walls, and cracking (usually horizontal cracking of wing walls and front walls).

(b) Damages to piers included settlement, tilting, overturning, and cracking.

(c) Damages to superstructures included failures at bearing supports, deformation of anchor bolts, dislodging of anchor bolts from abutments and piers, and movement of girders due to the failure of roller supports.

(d) Damages to main girders included cracking and compressive failures at the ends of main girders (usually in reinforced concrete girders) due to collisions with parapet walls on abutments.

(e) Other significant damages included cracking or complete failure at construction joints in concrete bridges, failures due to lack of reinforcement in concrete bridges, and failures due to inferior quality of concrete material.

E. IMAICHI EARTHQUAKE OF 1949 [27]

Two shallow focus earthquakes occurred about 8:17 am and 8:25 am on December 26, 1949, near Imaichi, Tochigi Prefecture about 110 km north of Tokyo (Fig. 2.1) which registered 6.4 and 6.7, respectively, on the Richter scale. The epicenter locations were at 36.7°N, 139.7°E.

During the earthquake, various engineering structures such as buildings (mostly residential houses), water supply plants, railways, and highways (within a radius of about 8 km) sustained severe damage and landslides were observed at several locations.

Based on aftershock data, it was estimated that the ground motion near the epicenter contained large accelerations and short period oscillations. The ground conditions near the epicenter were generally rocky layers or diluvial plateaus with loams.

No significant damage to bridge structures was observed. One railway bridge had failure at its bearing supports and one highway bridge overcrossing a railway sustained very light damage to an abutment.

F. TOKACHI-OKI EARTHQUAKE OF 1952 [28, 46]

A major earthquake occurred under the sea off Tokachi about 50 km east of Erimo Cape, Hokkaido, on March 4, 1952, registering 8.1 on the Richter scale. The epicenter location was 42.2°N and 143.9°E and the hypocenter depth was 45 km.

During the earthquake many engineering structures such as public works, transportation facilities, buildings, and houses in the southeast part of Hokkaido sustained heavy damage. The total loss in engineering structures was estimated to be about 15 billion yen which included about 410 million yen for highway damages (184 locations) and about 200 million yen for bridge damages (128 bridges); 360 yen = 1 U. S. dollar.

While some temporary wooden bridges collapsed, no significant damage was sustained by permanent concrete and steel bridges. However, bearing supports, substructure caps near supports, and hinge elements for suspended girders experienced slight damage for some bridges (Monbetsu Bridge, Photo 2.36; Shizunai Bridge, Photo 2.37; Horoman Bridge, Photo 2.38, and the Otanoshike Bridge).

G. NORTHERN MIYAGI EARTHQUAKE OF 1962 [30, 46]

A moderate earthquake occurred on April 30, 1962 (Fig. 2.1) in an inland area near the northern part of Miyagi Prefecture, Honshu Island, about 50 km north of Sendai which registered 6.5 on the Richter scale. Its epicenter location was 38.7°N, 14.1°E and its hypocenter depth was 10 km.

During the earthquake, many engineering structures such as public works, water supply systems, agricultural facilities, industrial facilities

and houses sustained moderate damage in a very limited area. The total loss was estimated to be about 4 billion yen. The loss to highways and highway bridges was about 102 million and 43 million yen, respectively. A total of 187 bridges sustained light damages. Only two bridges (Eai Bridge, Photo. 2.39; Kinoh Bridge) sustained moderate damage. These damages were primarily at bearing supports and the caps of the substructures. Slight collision damage between adjoining girders was observed at the Eai Bridge.

H. NIIGATA EARTHQUAKE OF 1964 [32, 42]

The Niigata Earthquake which occurred in the northwestern part of Honshu Island on June 16, 1964, registered 7.5 on the Richter scale (51). Its epicenter (38.4°N, 139.2°E) was under the sea near Awashima Island about 55 km north of Niigata City (Figs. 2.1, 2.22) and its hypocenter depth was estimated to be in the range 20 - 30 km.

Severe damage was caused on the alluvial plain near the mouths of the Shinano River and the Agano River in Niigata City, especially in the area near the mouth of the Shinano River where loose sand layers with a high water table existed. In this area, reinforced concrete buildings, highway bridges, and other structures sustained considerable damage due to liquefaction of the ground soils.

Two strong motion accelerographs, installed in the basement floor and the roof of a damaged apartment building located along the Shinano River, recorded time histories of acceleration during the earthquake. The maximum acceleration recorded at the basement level was about 0.15 g (predominant period 2 seconds) horizontally and about 0.05 g (predominant period 0.3 seconds) vertically.

In the following sections, the damages sustained by seven bridges are described.

1. <u>Bandai Bridge (Figs. 2.24 - 2.28; Photos 2.40, 2.41; Table 2.6)</u> - This bridge, completed in 1929, crossed the Shinano River on National

Highway No. 7 in Niigata City about 54 km south of the epicenter. The JMA intensity at this site was 5 and the maximum ground accelerations recorded nearby were 0.15 g horizontally and 0.05 g vertically. The ground consisted of sandy soils (Figs. 2.25, 2.26).

The abutments were of gravity-type reinforced concrete construction supported on wooden piles and the piers were solid slab-type reinforced concrete construction having caisson foundations. The superstructures having a total length of 309 m and a width of 21.8 m consisted of a reinforced concrete arch structure over 8 spans using 2-hinge arches for the side spans and continuous fixed arches for the six center spans (Fig. 2.24). Span lengths were (17.1 m + 43.6 m + 46.0 m + 46.9 m) x (2).

Table 2.6 indicates the results of bearing tests to determine ground bearing capacities at the bottom of the caissons.

During the earthquake, the bridge sustained severe damage (Figs. 2.27, 2.28; Photos 2.40, 2.41). The left abutment settled 1.4 m while the right abutment settled 0.4 m. Both abutments tilted slightly toward the center of the river. The back fills also settled considerably. The left and right parapet wall separated about 1 m and 2 m, respectively, from their abutments.

Two piers also settled moderately (30 cm at P1 and 15 cm at P6). Excessive deformations and large cracks were observed at the two extreme side spans due to substructure settlements (Fig. 2.28). Slight lengthening of the right side span was measured (Fig. 2.28). The six continuous spans sustained small permanent deflections (less than 10 cm at midspan locations) and slight cracking of the stone masonry near the piers (Photo 2.41). At the arch rib of the 7th span, small cracks appeared. The change in length of this span was found to be only a few centimeters. After the earthquake the tilting of abutments and piers, the change in span lengths, and the change in arch deflections were measured intermittently over a period of several months.

Although the bridge was capable of carrying traffic after minor repair which took only a couple of days, major repair was required over a much longer period of time. The total final cost of repair was about 330 million yen. Of all bridges in Niigata, this cost of repair was greatest.

2. Showa Bridge (Figs. 2.29 - 2.34; Photos 2.42 - 2.48) - This bridge crossed the Shinano River about 1.2 km up the river from the Bandai Bridge which was approximately 55 km south of the epicenter. Construction was completed in May 1964 just one month prior to the earthquake.

The ground at this site consisted of sandy soils which were comparatively soft near the left bank and comparatively hard near the right bank (Figs. 2.30 - 2.32). The abutments were pile bents (nine single-row piles of diameter 609 mm and of length 22 m) and so were the piers (nine single-row piles of diameter 609 mm and of length 25 m). These bents had collar braces and cap beams (Fig. 2.30). The seismic design coefficient for the substructures was 0.2. The superstructures having a total length of 303.9 m and a width of 24 m consisted of 12 composite steel simple span girders (13.75 + 10@ 27.64 + 13.75).

During the earthquake, the bridge sustained severe damage (Fig. 2.33). The left abutment moved about 1 m toward the center of the river and its approach road settled considerably. In contrast with this behavior, the right abutment and its approach road sustained no significant damage. The first to fourth piers from the left bank tilted toward the right bank. The magnitudes of permanent deformation were 13 to 42 cm at their caps. The fifth and sixth piers collapsed completely into the river while the seventh through the eleventh piers suffered only slight damage. Five girders (third through seventh from left bank) out of twelve fell into the river (Photo 2.42). Only the sixth span fell at both ends which was due to failure of the fifth and sixth piers.

Damage characteristics of the bridge are shown in Fig. 2.33. These reveal the following main causes of damage 1) the substructures consisting of single-row steel piles were too flexible, 2) liquefaction of the soils occurred (except near the right bank), 3) both bearing supports of the sixth span were movable, 4) the superstructures consisted of simple girders which were not connected together, and 5) catastrophic sliding of the ground occurred near the left bank.

After the earthquake extensive surveys and studies were made of this bridge including soils investigations, measurements of the dynamic properties of the less damaged portions, measurements of

deformation in the whole structure, pile investigations by pulling (Fig. 2.34; Photos 2.47, 2.48), and dynamic analyses of the bridge system subjected to strong earthquake motions.

3. Yachiyo Bridge (Figs. 2.35 - 2.39; Photos 2.49 - 2.53) - This bridge, completed in 1962, crossed the Shinano River at a location between the Bandai and Showa bridges along a Niigata municipal road about 55 km south of the epicenter.

The ground at this site consisted of sandy soils (Figs. 2.36, 2.37). The abutments were gravity-type reinforced concrete construction with reinforced concrete pile foundations. The piers were of solid-slab type reinforced concrete construction also with reinforced concrete pile foundations. The superstructures having a total length of 307.4 m with a width of 8 m consisted of 4 prestressed concrete simple girders for 4 site spans and 10 composite steel girders for 10 midspans (2 @ 7.48 m + 10 @ 27.5 m + 2 @ 8.72 m), (Fig. 2.35).

During the earthquake, the bridge sustained serious damage (Figs. 2.38, 2.39; Photos 2.49 - 2.53). Both abutments moved toward the center of the river but tilted in the opposite directions. The 1st, 2nd, 12th, and 13th piers from the left bank, which supported the prestressed concrete side spans, moved toward the center of the river (1.1 m maximum at 2nd pier) and also tilted in the opposite directions due to the resistance provided by the girders. The 2nd and 12th piers cracked severely. The 3rd through the 11th piers moved (40 cm maximum at 9th pier) moderately. The 4th and 9th piers suffered heavy cracking at their supports. It was understood that sliding of the grounds toward the center of the river at both abutments seriously affected the bridge damage.

The total length of the bridge superstructures shortened by 40 cm due to sliding of ground soils toward the center of the river. The girders supported by the 2nd, 4th, 9th, and 12th piers moved extensively and suffered serious damage. Since no girders fell into the river, the bridge was usable by pedestrians immediately following the earthquake.

4. Higashi-kosenkyo Bridge (Figs. 2.40 - 2.44; Photos 2.54 - 2.57)- This bridge, completed in 1963, is on a Niigata municipal road overpassing the Shinetsu Line of the Japanese National Railways. The bridge is located in Niigata Prefecture about 54 km south of the epicenter.

The ground at this site consists of sandy soils and has a water table about 2 to 3 m below the surface.

The abutments are of solid-slab-type reinforced concrete construction with wooden pile foundations and the two piers for the main span are also of similar construction using reinforced concrete or pile foundations. Thirteen piers are rigid frame structures using three columns with wooden pile foundations. The horizontal seismic coefficient used to design the substructures was 0.2. The superstructures having a total length of 229.5 m and a width of 8 m consisted of 15 prestressed concrete simple girders and a single composite steel girder (8 @ 13.5 m + 26.5 m + 7 @ 13.5 m), (Fig. 2.40).

During the earthquake, the bridge sustained severe damage to the main-span girder (Figs. 2.43 - 2.44; Photos 2.54 - 2.57). No significant damage to the abutment and first to seventh piers on the Niitsu-side was observed. The eighth and ninth piers tilted about 2° toward the Niitsu-side and 4° toward the Niigata-side, respectively. Furthermore, the ninth pier settled about 2.5 cm. The tenth to fifteenth piers and the Niigata-side abutment moved horizontally about 5 cm and settled considerably (about 40 cm maximum). After the earthquake, all reinforced concrete piles at the ninth pier were pulled out and examined for damage. Their maximum deformation was about 20 cm (Fig. 2.44; Photos 2.56, 2.57).

The eight girders on the Niitsu-side suffered no significant damage. The ninth girder (main girder) however fell down on the railroad at its movable end on the Niigata side. This collapse was due to a separation of the supports by about 67 cm which was caused by a large separation of the eighth and ninth piers. The seven girders on the Niigata-side moved both horizontally and vertically and the asphalt pavement cracked. In addition, failures of bearing supports and collision damage to girders were observed.

5. Fujimura Bridge - This Bridge, completed in 1933, crosses the Ochibori River on the Niigata prefectural road No. 503 located in Shiunji, Kita-Kambara County, about 28 km southeast of the epicenter.

Both abutments are of semi-gravity-type reinforced concrete construction with spread footings. The three piers are reinforced concrete rigid frames with caisson foundations. The superstructures having a total length of 33 m and a width of 3.7 m consists of 4 T-shape reinforced concrete simple girders.

During the earthquake, the bridge sustained serious damage. The abutments slid, settled, tilted, and suffered severe cracking. The main girders also cracked seriously and required major repairs.

6. Matsuhama Bridge (Figs. 2.45 - 2.46 Photos 2.58, 2.59) - This bridge crossing the Agano River, was located on prefectural road No. 503 in Matsuhama, Niigata, about 49 km south of the epicenter.

The ground consisted of sandy soils as shown in Fig. 2.46. The left abutment is of gravity-type reinforced concrete construction with a wooden pile foundation (4 x 7 = 28 piles; 20 cm diameter; 4.5 m length). The right abutment is of similar construction but has a caisson foundation (3.4 m by 10.6 m in plan; 7.5 m depth). The third piers are of reinforced concrete solid-slab-type construction with caisson foundations (4.6 m by 12.2 m in plan; 18-23 m depth). The superstructures having a total length of 921 m and a width of 6 m consists of 14 simple steel trusses of the Warren type (14 @ 65.8 m). The supports of each span are a pin support and a roller support (Fig. 2.45).

At the time of the earthquake, the bridge was still under construction. All substructures and the first and second spans from the left bank had been completed and the concrete slabs for these two spans had already been poured. The tenth and eleventh spans were at the stage of erection of the steel trusses and no upper chord members of the eleventh span had yet been connected. The erection of trusses in all other spans had been completed but the concrete slabs had not yet been poured.

During the earthquake, the bridge sustained damage to both the substructures and the superstructures (Fig. 2.48). The right abutment moved considerably toward the center of the river (about 1 m) and

several piers moved both horizontally and vertically. The ninth pier moved 23 cm on the downstream direction. The movements of other piers were less than several centimeters.

The eleventh span fell into the river at its roller support end due to failure of supporting timbers (Photo 2.58). This fall was permitted due to the fact the upper chord members had not yet been connected at the time of the earthquake. Moderate damage such as failure of anchor bolts (Photo 2.59), failure of mortar near supports, slight failures at expansion joints due to impact were observed in other spans.

7. Kosudo Bridge (Figs. 2.47 - 2.50) - This bridge, completed in December 1963, crosses the Shinano River on Prefectural road No. 538 in Kosudo, Nakakanhara County, Niigata prefecture about 72 km south of the epicenter.

The ground at this site consists of clayey silts and silty clays (Fig. 2.47) which are finer than the sands in Niigata.

The abutments and piers are of reinforced concrete solid-slab-type construction with caisson foundations (4.6 m by 12.2 m in plan; 13 m depth). The superstructures having a total length of 189 m and a width of 4 m consisted of 3 simple spans using Warren steel trusses (3 @ 62.9 m), (Fig. 2.49).

During the earthquake, the bridge sustained moderate damage (Fig. 2.50). All substructures settled without horizontal movements. Amounts of settlement at the left abutment, the first pier, the second pier, and the right abutment were 25 cm, 75 cm, 10 cm, and 7 cm, respectively. Slight cracks were observed in the right abutment.

While the superstructures sustained slight damage to the railings, the expansion joints, and the supports due to substructure settlements, no significant structural damage was sustained by the primary structure.

8. Summary of Bridge Damages - Following the Niigata earthquake, extensive field surveys of the damages were conducted. Experimental and analytical investigations were also carried out and correlated with

damages to structures and ground soils. In the dynamic analyses of highway bridges, acceleration records obtained during the earthquake were employed as inputs.

Table 2.5 indicates the number of bridges damaged during the Niigata earthquake. The total loss to highway bridges and to highways was approximately 1.47 billion yen and 2.34 billion yen, respectively. Most of this loss was in or near Niigata City.

After the earthquake, all bridges in or near Niigata City, whether apparently damaged or not, were inspected. As shown in Table 2.7, there were 86 bridges within a radius of about 60 km from the center of the City. Fifty-two of these bridges (60%) were damaged, among which seven bridges suffered severe damage. Thirty-four bridges (40%) sustained no significant damage. All of the seven severely damaged bridges experienced damage to the substructures. Four of these bridges sustained damage to the superstructures; however, this damage was caused by substructure failures.

Table 2.8 indicates numbers and percentages of damage to the separate components of highway bridges. Based on extensive damage surveys, it was observed that a) although damage to bridge structures was observed in Akita, Fukushima, Niigata, and Yamagata Prefectures, major damage was concentrated near the mouths of the Shinano and Agano Rivers in Niigata City where soil conditions were bad, b) the degree of damage to bridges was roughly proportional to the JMA seismic intensity; however, in some areas with the same intensity, different ground conditions considerably affected the degree of damage, c) superstructure damage was similar for the various types of structures, except for wooden girders which generally suffered more severe damage, d) abutments generally suffered more damage than did piers, due to the pressures developed by backfills, e) the degree of substructure damage appeared to be independent of foundation type, f) the soft saturated sandy soils near ground surface liquefied; thus reducing bearing capacities, which allowed substructures to slide, settle, and tilt, g) bridges having deep foundations resting on hard sandy layers with standard penetration values (N) greater than 25 sustained only minor damage, h) in addition to fallen girders, superstructures were

damaged primarily by failures of bearing supports, expansion joints, and handrails, and i) superstructure damage was indirectly caused by failures of the substructures.

The more important lessons to be learned from the Niigata earthquake regarding the behavior of bridge structures are a) liquefaction of foundation soils greatly affects the stability and safety of these structures, and b) particular attention should be given to details of design such as details of connections and methods of preventing girders from falling.

I. EBINO EARTHQUAKE OF 1968 [43]

An earthquake occurred near Ebino, Nishimorokata County, Miyazaki Prefecture, in the southern part of Kyushu Island on February 21, 1968, registering 6.1 on the Richter scale. Its epicenter was 32.0°N, 130.8°E and its hypocenter depth was judged to be very shallow.

About 2 hours prior to the main shock, a foreshock occurred having a magnitude 5.6. Many aftershocks also occurred including three major ones, one on February 22 (magnitude 5.5) and two on March 25.

Within a radius of about 5 km in the area of Ebino, Miyazaki Prefecture, and Yoshimatsu, Kagoshima Prefecture, where the ground is made up of volcanic sandy soils, several major landslides occurred on steep slopes. Many engineering structures sustained moderate damage and hundreds of wooden houses suffered severe damage.

In the following sections, the damages sustained by highway bridges during the earthquake will be described.

1. Kamezawa Bridge (Photo 2.60) - This bridge completed in 1964, crosses the Sendai River on a municipal road in Ebino, Miyazaki, Prefecture.

The abutments are of gravity-type reinforced concrete construction with reinforced concrete caisson foundations. The four piers are of solid-slab-type reinforced concrete construction with

wooden pile foundations. The superstructures, having a total length of 133 m and a width of 3.5 m consisted of prestressed concrete simple girders over 5 spans.

During the earthquake, the left abutment suffered heavy horizontal cracking near the ground surface and tilted towards the backfill (Photo 2.60). The fourth pier suffered slight breakage to the pier cap near a girder support. The end of the concrete girder supported by the left abutment suffered heavy damage and the support itself also failed (Photo 2.60). The earth fills of the approaches settled about 20 cm at both ends of the bridge.

2. Kamimasaki Bridge (Photo 2.61) - This bridge, completed in 1965, crosses the Sendai River on another municipal road in Ebino.

The abutments are reinforced concrete gravity-type construction with pile foundations. The four piers are of reinforced concrete solid-slab-type construction with caisson foundations. The superstructures, having a total length of 140.5 m and a width of 3.6 m consist of prestressed concrete girders over 5 spans.

During the earthquake, the second girder from the left bank moved about 20 cm downstream and about 5 cm toward the right bank. Due to the aftershocks on March 25, the downstream movement increased to about 26 cm (Photo 2.61). The concrete caps of the first and second piers failed slightly near the girder supports. Settlements of approach roads were also observed.

3. Ikejima Bridge (Photo 2.62) - This bridge, completed in 1964, crosses the Ikejima River on a municipal road in Ebino. The ground contains layers of volcanic sandy soils.

The abutments and the two piers are of reinforced concrete solid-slab-type construction with spread footings and pile foundations. The superstructures, having a total length of 49.6 m and a width of 6 m consist of steel H-shape simple girders over 3 spans.

The first pier from the left bank settled about 25 cm during the earthquake (Photo 2.62). No significant damage was observed to other

portions of the bridge. Near the bridge, the river bed surface cracked, settled considerably, and some sandy materials from the deeper layers boiled out through cracks. Therefore, it is believed that liquefaction occurred at this site.

4. Other Bridges - Several bridges, other than those described above, suffered failures at bearing supports, movements of girders, and settlements (5 - 20 cm) of the approach roads. A reinforced concrete Gerber bridge (Kakuto Bridge) sustained slight damage at the hinge.

J. TOKACHI-OKI EARTHQUAKE OF 1968 [46, 50]

The Tokachi-oki earthquake, measuring 7.9 on the Richter scale, occurred off Takachi on May 16, 1968. The epicenter was under the sea about 140 km south from Erimo Cape of Hokkaido and about 170 km east from the northeast coast of Honshu Island (Fig. 2.1). Its epicenter was 40.7°N, 143.6°E and its hypocenter depth was about 20 km.

During the earthquake various engineering structures such as buildings, highways, river and coastal enbankments sustained severe damage. However, no major damage was caused to bridge structures. Only minor damage was observed to bridges in Hokkaido and Aomori prefectures (Table 2.9). Therefore, the losses to bridge structures were very low in comparison with losses to other structures.

The damages to bridge structures had characteristics very much like those previously described for similar bridges during other earthquakes. Pile bent piers sustained moderate damage due to lack of stiffness (Photo 2.63) and one pier settled about 20 cm due to lack of bearing capacity in the foundation which had been scoured by the river stream (Photo 2.64). Several abutments were pushed toward the center of the river (Photo 2.65) and some abutments developed cracks in the concrete near the bearing supports (Photo 2.66, 2.67). Girders were

shifted slightly, and bearing supports sustained moderate damage including failure of the concrete (Photo 2.68). The ends of the girders of one reinforced concrete bridge collided causing significant crushing (Photo 2.69). Settlements of the approach roads amounting to a few decimeters were observed. These settlements were apparently caused by compaction of the fill during the earthquake.

K. GENERAL FEATURES OF SEISMIC DAMAGE TO JAPANESE BRIDGES

Seismic damages of bridge structures has occurred to abutments, piers, girders, and supports (Fig. 2.51). Most of these damages can be classified into three categories as follows [29]:

a) Due to weakness of supports - Because of the nature of seismic forces, the various elements of a complete bridge structure do not move in the same direction. Thus, the differential movements between superstructure and substructure can cause failures at the supports when they become sufficiently large. Such relative movements can even cause girders to fall off their supports. When this happens, both superstructure and substructure can suffer major damage due to the strong shock of the fall.

b) Due to weakness of substructure - When a substructure is not sufficiently strong to resist its own inertia forces as well as those developed in the girders, it will deform considerably, sometimes causing complete failure or overturning. Should this happen, the superstructure will, of course, sustain substantial damage.

c) Due to weakness of surrounding soils - When the soils surrounding the substructure settles or moves horizontally a large amount, the substructure will also move and very likely tilt sufficiently to cause substantial damage or even collapse of the superstructure.

Failures for individual components of bridges most often observed are a) tilting, settlement, sliding, cracking, and overturning of sub-

structures b) displacements, cracking, and complete dislodging of girders at supports, c) shearing or pulling-out of anchor bolts and crushing of concrete at supports, and d) settlement of approach roads, settlement and sliding of wing walls, separation of wing walls from abutments, and failure of parapet walls at abutments. It should be noted that a relatively small amount of damage to bridges in Japan has been caused directly by vibration effects.

In view of the above experiences, it seems reasonable that most bridge structures which have been properly designed and constructed in accordance with Specification for Design of Steel Highway Bridges, Japan Road Association, 1956 (Revised in 1964) can resist major earthquakes without sustaining major damage, provided they have been designed with special attention given to (1) geological considerations to avoid large ground failures, (2) soil considerations to avoid the problems associated with liquefaction, and (3) design details to avoid joint and support failures and the falling of girders.

The new specifications for seismic design of highway bridges as stipulated by the Japan Road Association in January 1971 will be mentioned subsequently in this report (Chapter 4, Appendices B, C).

L. ALASKA EARTHQUAKE OF 1964 [216 - 222]

During the great Alaskan earthquake of March 27, 1964, numerous bridges sustained light to heavy damage. Most damages occurred in south central Alaska along the Glenn, Richardson, Seward, Sterling, and Copper River Highways. Nearly all damages were caused by substructure failures resulting from large ground displacements, settlements, and loss of bearing capacity. Types of bridge damages included a) displaced and tilted piers, b) broken piers and abutment walls, c) displaced, tilted, and split piles, d) settlement of backfills, e) sheared and bent anchor bolts, f) deck slabs torn loose from stringers, g) broken connections and soleplate welds, and h) tilted rocker supports. Damages to superstructures were almost entirely caused by substructure failures.

Very little damage, if any, was caused directly by vibration effects. It is very significant to note that the causes and types of damages to bridge structures during the Alaskan earthquake followed very closely the patterns previously described for Japanese earthquakes.

Since excellent, and extensive detailed descriptions of bridge damages sustained during the Alaskan earthquake of March 27, 1964, are presented in the above referenced reports, no further discussion of this subject will be presented herein.

M. MADANG EARTHQUAKE OF 1970 [223]

An earthquake of magnitude 7.1 occurred on November 1, 1970, in Madang, Territory of Papua and New Guinea, causing damage to all but two of the forty-seven bridges located in the area. The damages to sixteen of these bridges was slight, however, twenty-nine were damaged to the point of needing extensive repairs. Only three multispan bridges existed in the area, all simple spans. Two of these, the Gogol and Sumerang bridges, sustained extensive damage, while the third, the Gilagil bridge, suffered minor support failures. All other bridges are single span, single lane truss or composite girder and concrete deck slab bridges.

As experienced in the Japanese earthquakes and the Alaskan earthquake of 1964, bridge damages were caused primarily by foundation failure, due to ground effects. Many failures were sustained by abutments due to high earth pressures. The abutments generally moved towards the center of the rivers causing failures in bearing supports, and closing expansion joints. Damage caused by vibration effects were negligible.

N. CHILEAN EARTHQUAKE OF 1971 [224]

A major earthquake occurred in central nothern Chile on July 8, 1971 which registered 7.5 on the Richter scale. Its epicenter location was

32.45°S, 71.58°W and its hypocenter depth was 60 km.

During the earthquake three simple spans of the Pullali bridge on the main highway running generally north and south fell from their supports. This bridge, consisting of a composite beam deck also suffered damage during the 1965 earthquake. The new bridge on the route from Tejas Verdes to Santo Domingo and the two-section steel bridge between Laguna and Penuelas also sustained damage. The former suffered horizontal displacements of the deck while the latter suffered failures in the central supporting pier. Nearly all bridges showed settlement of the abutment backfills of the order of 20 - 30 cm. Again ground effects rather than vibration effects are believed to be the basic causes of damage.

O. SAN FERNANDO EARTHQUAKE OF 1971 [225]

The San Fernando, California, earthquake which occurred at approximately 6:00 a.m. on February 9, 1971, had a magnitude of 6.5 on the Richter scale (Seismographic Station, University of California, Berkeley). The epicenter location has been given as 34° 24.0'N., 118° 23.7'W. (Fig. 2.52). The focal depth is reported to be 13.0 km. [226]

Although this earthquake was of moderate magnitude, accelerograph measurements and observed damages to engineered structures indicate the intensity of surface ground shaking in the immediate vicinity of the epicenter area was probably near the upper bound level, i.e., peak accelerations of the order of 0.6 g.

One component of ground acceleration recorded near the abutment of the Pacoima Dam (Fig. 2.53) showed a peak acceleration slightly over 1 g. This unusually high acceleration may not be of major significance, however, as it is believed to have been caused by very localized effects such as rock fracturing which is known to have occurred near the instrument location and by interaction of the dam with its foundation.

Since intensity of ground shaking decreased rapidly with distance from the epicenter, it is difficult to assess the intensities at the

locations of the damaged highway structures. Some appropriate assessments of these intensities can most likely be made as soon as all recorded strong motion accelerograms have been processed and analyzed.

In the following sections, the damaged to highway bridge structures as observed on 12-13 February 1971 are described.

1. Golden State Freeway (Interstate 5) and Foothill Freeway (Interstate 210) Interchange - The general arrangement of bridges and overcrossings at this interchange is shown in Fig. 2.54. Approaching this interchange from the east along the Southern Pacific Railroad, one first reaches the collapsed overcrossing {3}* which carried northbound traffic from the Golden State Freeway onto Foothill Freeway. Photograph 70 shows the north abutment of this overcrossing and the remaining debris of the adjacent box girder span. The south abutment and further debris are shown in Photograph 71. It should be noted that a demolition crew had cleared nearly all of the collapsed structure prior to 12 February 1971; thus, explaining the source of the fine debris showing in Photos 70 and 71.

The two principle causes of collapse of this particular overcrossing, as well as others, were (1) the large vibratory motions induced in the super-structure by the high intensity vertical and horizontal ground accelerations, and (2) the relative ground displacements which occurred between abutment and column supports. Unfortunately, in most cases, it was very difficult to assess the relative importance of these two causes.

The debris near the north abutment of the above mentioned overcrossing can also be seen in the right foreground of Photo 72. In the background of this same figure, one can see the damaged San Fernando Road Overhead {2} which is located at the intersection of the Golden State Freeway and the Southern Pacific Railroad. The central section of this bridge (original freeway) was built with steel girders and a reinforced concrete deck, while the two outside sections (widened freeway)

---

*Numbers in braces refer to identification numbers in Fig. 2.54.

were built entirely of reinforced concrete. During the earthquake the central section fell off one of its supports and was badly damaged. The outside steel sections remained in position but had to be removed after the earthquake to provide full access along the railroad. Some of the steel girders taken from this location can be seen in Photo 73.

Photograph 74 presents a close-up view of this bridge at the same location where the simple span crossing the railroad (front foreground) had been removed. In the background of this figure looking in a northerly direction, one can see the reinforced concrete structures which continue north along the Golden State Freeway. It is significant to note the very narrow ledges which provided bearing support surfaces for the simple span. The advisability of using such narrow support surfaces in seismic areas should be seriously questioned.

A close-up view of the reinforced concrete bridge system to the left (south) of the railroad is shown again in Photo 75. It is of particular interest to note the type of damages which occurred to the columns of this system. Many of the stiffer columns suffered shear failures (Photos 76, 77), while the more flexible columns suffered flexural damages at their tops (Photo 78).

Photograph 79 shows a close-up view of the flexural damages at the top of the column appearing in Photo 78, while Photo 80 shows a close-up view of similar damages in another column located nearby in the same structure. In each case, it is significant to note that the main reinforcing bars on both sides of the columns have been buckled by the flexural compressive forces. Once the concrete coverage spalls off the bars, the ties are inadequate to provide the needed lateral constraint to the main reinforcing bars and to provide containment for the concrete. Such damages reduce the flexural energy absorption capacities of these columns.

An inspection of the bearing and rocker supports of this same bridge reveals that large relative displacements occurred between the box girders and their abutment supports. For example, Photo 81 shows how one end of a box girder deck moved to the left on its bearing support approximately one foot with respect to the abutment.

Photograph 82 shows a rocker support where the relative displacement was sufficiently large to completely dislodge the steel rocker bar from its support assembly.

Observing these same bridge structures from the top rather than the bottom, one could easily see the large settlements caused by vibration-induced compaction of the soil fills leading up to the bridge abutments. Photograph 83 shows the large vertical offset which could be seen looking in a northerly direction at one of the south abutments.

Let us now review the damages which were produced to the highest overcrossing {4} at the Golden State Freeway and Foothill Freeway interchange. This particular overcrossing was designed to carry south-bound traffic entering the Golden State Freeway from Foothill Freeway.

Starting at the south abutment of this overcrossing (Photo 84), one can observe the first span of the box girder deck in its fallen positing on the side slope. Shown in the foreground of this same figure is the San Fernando Road Overhead previously described with its missing span located along the Southern Pacific Railroad.

The box girder deck of this overcrossing (approximately 770 feet in length) was supported on six central piers in addition to the end abutments. The two central piers located at the south end of the overcrossing were supported on spread footings which were in turn supported on driven concrete piles. Each of the four central piers located at the north end of the overcrossing were supported directly on a single round pile cast directly in a 6 foot diameter drilled hole. The box girder deck had one expansion joint near mid-crossing in addition to those at the abutments.

A little farther north from the view shown in Photo 84, but still south of the Southern Pacific Railroad, a portion of the box girder deck and its supporting column could be observed where they had fallen in a westerly direction (Photo 85). Again in evidence was the debris caused by the demolition crew in clearing damaged structures from the railroad tracks.

Looking still farther north and just across the railroad tracks (Photo 86), one could observe several broken sections of deck in their respective fallen positions where they had crashed through the San Fernando Road Overhead bridge. These broken sections can also be seen immediately above the road surface of the San Fernando Road Overhead bridge in Photo 83.

Continuing on north along this same overcrossing, one could observe sections of the collapsed structure in their fallen positions (Photos 87, 88). Note that this portion of the overcrossing also fell in a westerly direction.

Considering the location and orientation of abutments and the expansion joint and considering the general curvature of the deck in a plan view, it is quite apparent that the deck was highly constrained against large displacements in all directions except in a westerly direction. Therefore, it is easily understood why the structure collapsed in a westerly direction.

Photograph 89 shows the last deck span as it crashed through an overcrossing {5} of the Golden State Freeway which directs traffic coming from the north along the Golden State Freeway onto Foothill Freeway going east. Close-up views at this same location are shown in Photos 90 and 91.

Finally, the last deck span at the north abutment can be seen in Photo 92. A close-up view of this abutment is shown in Photo 93. Note the heavy damages to the abutment bearing supports and to the key side walls.

A close look at the columns of this overcrossing indicates that they generally failed at their bottoms due to the superposition of high flexure forces onto the axial forces. The column shown in Photos 94 and 95 also experienced flexural cracking at intermediate points where it crashed through the San Fernando Road Overcrossing. Quite obviously such cracks should be expected under such severe impact conditions.

Of much greater significance, however, are the characteristics of failure which were observed at the bases of these columns. Photographs 96 and 97 show almost identical failure characteristics which were typical of the columns supported on the 6 foot diameter cast-in-drilled-hole piles. It is quite apparent in each case that the anchorage of the main reinforcing bars (No. 18 bars) where they extended into the supporting pile was inadequate. Bond failures along the main reinforcing bars were quite evident at these locations.

Photograph 98 shows the base of one of the two columns which were supported on spread footings. The main reinforcing bars in this case entered the footing and were bent outward to provide added anchorage.

Obviously, this anchorage was inadequate.

Further, it is quite apparent that the relatively small ties (No. 4 bars) shown in Photo 98 could not possibly provide the required containment of main reinforcing bars and the enclosed concrete. Lateral forces which developed in the main reinforcing bars caused spalling of the concrete coverage; thus causing complete loss of bond with the concrete.

The principle causes of collapse of this particular overcrossing were the same as those previously mentioned, namely, (1) the large vibratory motions induced in the super-structure by the high intensity vertical and horizontal ground accelerations, and (2) the relative ground displacements which occurred between abutment and column supports. It is believed that the former was the major cause of collapse in this particular case.

Both of the above effects can, of course, combine to produce relative support movements at abutments and expansion joints. In this case, it appears quite certain that these relative displacements were sufficiently large to cause the deck spans to drop off their supports; thus, initiating complete collapse of the structure.

Photographs 99 and 100 are presented to show clear evidence of high local ground deformations in the vicinity of the Golden State Freeway and Foothill Freeway interchange. Photograph 99 is a view looking in a northerly direction across foothill freeway at a location very near the interchange. One can easily observe a concentrated ground deformation which looks like a fault trace running across the freeway and up the bank on the far side. Photograph 100 is a view looking east from the interchange along the Southern Pacific Railroad. The serious misalignment of the railroad tracks is further evidence of similar localized ground deformations.

2. Golden State Freeway and State Highway 14 Interchange - The location of this interchange can be seen on the upper left hand side of the map in Fig. 2.54. Several of the overcrossings in this interchange were still under construction at the time of the earthquake, as seen in Photo 101 looking in a northerly direction. In the foreground of this figure, one can see a row of newly constructed columns for an overcrossing.

Immediately behind these columns, steel formwork can be seen supporting a newly constructed box girder deck of another overcrossing.

Behind the latter overcrossing, one can see the highest overcrossing {7} in the interchange terminating at one of its expansion joints. From this point on to the right (east), a long section (approximately 400 feet) of the overcrossing collapsed during the earthquake. This long prestressed concrete section of bridge deck was supported at each end of bearing supports at expansion joints and by a single central column standing approximately 160 feet high. This column can be seen laying in its fallen positing on the side hill directly behind the steel formwork shown in Photo 101.

Continuation of this overcrossing at the right hand end (looking north) of the fallen section can be seen in the upper right hand side of Photo 102. Photograph 103 is another view of this same continuing section looking eastward while Photograph 104 is a similar view of the opposite continuing section west of the collapsed span. A close-up view of this latter section is given in Photo 105 to show the width (approximately 15 inches) of bearing support provided at the expansion joint.

The initial cause of collapse of this structure appears to have been the large relative deck displacements produced in the west expansion joint (Photo 105), which allowed the box girder to fall off its bearing supports. The falling cantilevered portion of the deck span pulled the deck system to the west permitting the east end of the span to fall off its supports in a similar manner. Both cantilevered portions of the deck span broke off at the top of the central column allowing them to fall almost directly down from their original positions. The central column fell to the west (Photo 106), landing nearly on top of the west portion of the deck span. Note that the top of the central column landed directly on a new truck crane. This totally damaged vehicle can be seen in a close-up view in Photo 107.

The east portion of the deck slid down the central column as indicated by the dark abrasive markings shown in Photo 106. These markings can also be seen in Photo 108, which gives a view of the central column looking from its top end towards its bottom end.

Unfortunately, the bottom end of this column was still covered with debris on 12 February and could not be inspected. Good close-up views of its top end could be seen, however, as shown in Photos 109 and 110. Note the very smooth manner in which the column cap sheared through the bridge deck and the lack of reinforcing bars tieing the cap onto the box girder deck.

Settlement of the fill leading up to the abutments of this overcrossing was observed as shown in Photo 111.

An additional point of interest noted at this particular interchange was the apparent stability of the timber falsework shown in Photo 112 which supports a sizeable load of lumber.

3. Foothill Boulevard Undercrossing at Foothill Freeway - The location of this intersection can be seen on the map in Fig. 2.54 {9}. Two similar reinforced concrete box girder bridges carry the Foothill Freeway traffic over Foothill Boulevard at this point. These two parallel bridges can be observed from below in Photo 113 as viewed from Foothill Boulevard looking in a westerly direction.

The central span columns of the east bridge suffered heavy shear damage followed by vertical crushing of the broken concrete causing the main reinforcing bars to buckle outwards. Clearly, the ties (No. 4 bars) provided were inadequate to contain the concrete and provide stability for the main reinforcing steel. Close-up views of the most easterly column in Photo 113 can be seen in Photos 114 and 115.

The progressively heavier damages observed (Photo 113), from the innermost column towards the outermost column would suggest that significant torsional displacements were produced by the earthquake.

Photograph 116 is a view of these same two bridges looking in an easterly direction with the above mentioned damaged columns of the east bridge showing in the background. In the foreground one can observe the most westerly central span column of the west bridge which is undamaged. The other central span columns of this same bridge had little damage.

While the central column of both bridges were similar in design, their foundation conditions were somewhat different. The central columns of the east bridge rested on spread footings having no piles, while the central columns of the west bridge rested on spread footings supported by cast-in-drilled holes concrete piles. In addition, fill had been placed under the west bridge. Differential settlement of this fill due to compaction may have caused the cracking of asphalt pavement as seen in Photo 116.

4. Roxford Street Undercrossing at Foothill Freeway - This bridge, {35} was a simple span prestressed concrete bridge. No damages to the deck and abutments were observed at this undercrossing. However, one wing wall had been totally broken away from its abutment, as shown in Photo 117. Further, it has been learned that recent excavations reveal heavy damages to the piles supporting the abutments. Damages such as these indicate that very high earth pressures were applied to the abutments during the earthquake.

Ground vibration at this overcrossing caused compaction of all fill placed around the abutments producing further damage due to differential settlement. Evidence of this type of damage to concrete aprons placed on fill slopes next to the abutments can be seen in Photos 118, 119, and 120. Photograph 117 shows breakage of an apron along the side of an abutment while Photos 118 and 119 show the extent to which this particular apron slid down its supporting slope.

Photographs 121 and 122 show the amount of differential settlement which occurred next to the abutments at one end of the bridge. The tire skid marks on the pavement in Photo 122 is a vivid reminder of the hazard to moving vehicles caused by such settlement.

5. Polk Street Undercrossing at Foothill Freeway - The damages observed at this undercrossing {38} were similar to those previously described for the Roxford Street Undercrossing, i.e., damages caused by backfill settlement near the abutments and damages to the wing walls were observed. Photographs 123, 124, and 125 show the differential settlement which occurred at the upper road surface level near the abutments, while Photos 126 and 127 show the settlement which occurred

below the bridge causing breakage and downward slippage of a concrete apron.

Large compressive ground deformations caused the asphalt pavement to buckle upwards in one location near this undercrossing, as shown in Photo 128.

6. Hubbard Street Undercrossing at Foothill Freeway - While this undercrossing suffered no structural damage, settlement of the fill caused differential vertical displacement to occur at the abutments, as shown in Photo 129. Near this bridge, excessive compressive ground deformations caused upward buckling of the asphalt pavement, as seen in Photo 130.

7. Bledsol Street Undercrossing at Foothill Freeway - The only point of interest at this undercrossing {36} in addition to the commonly observed settlement of fill, was the fact that the longitudinal oscillations of the bridge were apparently strong enough to force crushed rock to be thrown out of a weep hole, as shown in Photos 131 and 132. There was no evidence that water had forced the rock out of the hole. This same point of interest could be observed at several other bridges.

8. Tyler Street Pedestrian Overcrossing at Foothill Freeway - Photographs 133, 134, and 135 show the Tyler Street Pedestrian Overcrossing {37} at Foothill Freeway, which experienced fairly heavy damage due to vibration mainly along its longitudinal axis. The amount of permanent longitudinal displacement which occurred could be most readily seen at the far right hand support, as shown in Photos 136 and 137. This deformation was sufficient to cause serious flexural damage at the tops of the columns, as shown in Photos 138 and 139. Although only minor damage could be observed at the bases of these columns (Photos 140, 141), considerable flexural damage should be expected at the level of the footings.

9. Culvert under Foothill Freeway - Photograph 142 shows heavy damage at the connection of a wing wall with a reinforced concrete drainage culvert which passes under Foothill Freeway. No damage to the culvert itself could be observed.

10. Via Princessa Undercrossing on State Highway 14 - This simple span bridge {50}, as shown in Photo 143 has a bearing support at one abutment and a pinned support at the other. The longitudinal forces developed in the bridge deck during the earthquake were sufficient to cause severe flexure cracking in the diaphragm abutment at the pinned end, as shown in Photo 144.

11. Santa Clara Overhead Crossing on State Highway 14 - Considerable pounding damage was observed (Photo 145) along the expansion joints of the Santa Clara Overhead Crossing on State Highway 14. Also observed at this site was the buckled flexible splice (Photo 146) of a steel conduit to be located within the bridge concrete curbing which had not yet been poured.

P. DESIGN RECOMMENDATIONS BASED ON SAN FERNANDO EARTHQUAKE EXPERIENCE

1. Ground Motions - While it is difficult to assess quantitatively the intensities of vertical and horizontal ground shaking at the locations of the highway structures damaged by the San Fernando earthquake, it is reasonable to expect that similar intensities of shaking will occur during future earthquakes of moderate to large magnitudes. Full consideration should therefore be given to this possibility in the design of all highway structures located in seismically active regions.

2. Seismic Forces - The maximum base shears, occurring in linear elastic structures responding as single degree of freedom systems to horizontal ground motions, can be evaluated using response spectrum

curves. For example, extrapolating G. Housner's design response spectrum curves (see "Earthquake Engineering", R. L. Wiegel, coordinating editor, Prentice Hall, 1970, page 94) to a period of vibration T equal to 4.9 seconds, and using a damping coefficient of 5 percent of critical, one obtains a base shear coefficient approximately equal to 0.085 g for the El Centro, California, earthquake of 1940. A period of 4.9 seconds is assumed in this example, as it corresponds to the transverse period of vibration given by the code formula $T = 0.32 \sqrt{D/P}$ ("Bridge Planning and Design Manual", California State Division of Highway, Vol. 1 - Design Specifications, March 1968, pg. 2-24) for the high overcrossing which collapsed at the Golden State Freeway---State Highway 14 interchange [227].

3. Design Base Shear - It is extremely significant to note that the above mentioned base shear coefficient (0.085 g) is much greater than the design base shear coefficient of 0.030 g given by the empirical code formula $C = 0.05/\sqrt[3]{T}$. This simple comparison alone indicates these code seismic forces are too low for design purposes. Therefore, use of this code formula in the design of highway bridge structures should be seriously questioned and reconsidered for several reasons:

(a) It was originally developed and adopted for use in the design of buildings which are not equivalent to bridges in their earthquake behavior. Specifically, it is known that non-structural components, such as interior walls and exterior cladding, contribute significantly to the earthquake response of buildings.

(b) The seismic coefficient prescribed for the design of buildings does not represent the full force expected to be developed by a major earthquake; it is expected that inelastic deformations will result from a major earthquake, and the designer is expected to insure adequate ductile deformability of the structure.

(c) The formula for evaluation of the period of vibration of the

structure is grossly over-simplified. In many cases, the bridge deck will be subject to lateral flexure during the earthquake, and this mechanism must be recognized in evaluating the vibration period.

4. Causes of Collapse - The two principle causes of collapse of the high overcrossing {3,4,7} are considered to be: (1) the large vibratory motions induced in the super-structure by the high intensity vertical and horizontal ground accelerations, and (2) relative ground displacements which may have occurred between the abutment and column supports. It is the opinion of the authors that the former was the major cause of collapse in these particular cases; there is no evidence that relative ground displacements were a contributing factor. This observation is very significant as vibrational effects had caused relatively little damage to bridges during previous earthquakes.

5. Design Considerations - Based on the San Fernando earthquake experience, it is quite apparent that the following design considerations should be given careful study:

(a) Expansion Joints - Collapse of the high overcrossings were initiated by bridge spans falling off their supports at abutments and expansion joints due to excessive displacements of the spans relative to their supports. This type of behavior should be carefully examined and corrective measures should be taken as soon as possible. Full consideration should be given to eliminating expansion joints wherever feasible, to widening bearing supports, and to providing more effective ties across expansion joints.

(b) Columns - The failures in the central portion of the shorter stiff columns were caused by transverse shear forces, while the end failures in the larger more flexible columns were caused by flexural forces. In each case, there was a noticeable lack of transverse ties which contributed to these failures. Clearly, the design details of columns should be carefully examined, particularly with

regard to size and placement of reinforcing bars and ties, and corrective measures should be taken to improve their performance under ultimate loading conditions involving reverse deformation cycles such as occur during major earthquakes.

(c) Column Caps - There appears to be a serious lack of reinforcing bars tieing column caps onto their respective box girder bridge decks. Corrective measures should be taken to improve this design detail.

(d) Column Foundations - Failures at the base of columns for both types of support, i.e., single cast-in-place pile and spread footings with driven piles, showed inadequate anchorage of the main reinforcing bars. Corrective measures should be taken in each case so that sufficient anchorage is provided to develop the full strength of the main reinforcing bars.

(e) Abutments and Wing Walls - Failures in abutments and wing walls were caused by large dynamic forces transmitted by backfill earth pressures and by seismic forces developed in the bridge decks. The design details of these structures should be re-examined and appropriate corrective measures should be taken to improve their performance characteristics.

6. Design Philosophy - The present elastic design philosophy using equivalent static loading to represent seismic effects should be reviewed and appropriate code changes should be made to better reflect: (a) the dynamic character and intensities of seismic loading, (b) the desired structural characteristics under ultimate loading conditions, particularly with regard to strength and ductility, and (c) better behavior when deformed beyond the elastic limit.

7. Needed Research - The damages caused to bridge structures during the San Fernando earthquake point up the urgent need for both theoretical and experimental research which is related directly to seismic effects on bridge structures.

Recognizing this need, the three-year research investigation entitled "An Investigation of the Effectiveness of Existing Design Methodology in Providing Adequate Structural Resistance to Seismic Disturbances" was initiated at the University of California, Berkeley.

Table 2.1 Definitions of JMA Seismic Intensity Scale

Scale	Definitions	Corresponding Magnitude of Accelerations*
0	No Feeling: Too weak to cause human feeling, to be registered only by seismographs.	0 - 0.8 gals
1	Slight : To be felt only feebly by persons at rest or by those who are observant to an earthquake.	0.8 - 2.5 gals
2	Weak : To be felt by most persons, causing slight shaking doors and Japanese latticed sliding doors (Shoji).	2.5 - 8 gals
3	Rather strong : To cause shaking of houses and buildings, heavy rattling of windows and Shoji, swinging of hanging objects, stopping sometimes pendulum clocks and moving liquid in vessels. Some persons are so freightened as to run out of doors.	8 - 25 gals
4	Strong : To cause strong shaking of houses and buildings, overturning of unstable objects, and spilling of liquid out of vessels.	25 - 80 gals
5	Very strong : To cause cracks in the brick and plaster walls, overturning of stone lanterns and grave stones etc. and damaging of chimneys and mud-and-pluster warehouses. Landslides in steep mountains are to be observed.	80 - 250 gals
6	Disastrous : To cause demolition of Japanese wooden houses less than 30%, intense landslides, fissures on the flat ground accompanied sometimes by spouting of mud and water in low fields.	250- 400 gals
7	Ruinous : To cause demolition of houses more than 30%, large fissures and faults are to be observed.	400 gals or more

* After H.Kawasumi[80]

Table 2.2 Statistics on Highway Bridge Damage Due to the Kanto Earthquake of 1923

(A) TOTAL NUMBER OF BRIDGES DAMAGED

Prefectures or Cities	Total Number of Bridges Surveyed	Number of Bridges Damaged Due to Vibration and/or Fires	Percentages of Damage	Remarks
Tokyo	3,338	230	6.9%	Except City of Tokyo
City of Tokyo	675	358	53.0%	
Kanagawa	1,253	893	71.3%	Except City of Yokohama
City of Yokohama	108	91	84.2%	
Shizuoka	358	100	27.9%	Inside the affected area (Numazu or northern area)
Saitama	1,313	27	2.1%	
Yamanashi	245	21	8.6%	Only wooden bridges suffered inside the affected area
Chiba	690	65	9.4%	
TOTAL	7,980	1,785	22.4%	

(B) DAMAGE CHARACTERISTICS IN THE CITY OF TOKYO

Type of Bridges	Total Number of Bridges Surveyed	Number of Bridges Damaged and Percentages		
		Caused by Vibration	Caused by Fires	Total
Wooden	420	6 (1.4%)	276 (65.7%)	282 (67.1%)
Steel	60	6 (10.0%)	49 (81.7%)	55 (91.7%)
Masonry	144	2 (1.4%)	5 (3.5%)	7 (4.9%)
Plain Concrete	4	4 (100.0%)	0 (0.0%)	4 (100.0%)
Reinforced Concrete	47	0 (0.0%)	10 (21.3%)	10 (21.3%)
TOTAL	675	18 (2.7%)	340 (50.3%)	358 (53.0%)

(C) DAMAGE CHARACTERISTICS IN THE CITY OF YOKOHAMA

Type of Bridges	Total Number of Bridges Surveyed	Number of Bridges Damaged and Percentages			
		Caused by			Total
		Vibration & Fires	Vibration Only	Fires Only	
Wooden	75	26 (34.6%)	25 (33.4%)	8 (10.7%)	59 (78.7%)
Steel	31	11 (35.5%)	16 (51.6%)	3 (9.7%)	30 (96.8%)
Reinforced Concrete	2	0 (0.0%)	2 (100.0%)	0 (0.0%)	2 (100.0%)
TOTAL	108	37 (35.2%)	43 (39.8%)	11 (10.2%)	91 (84.2%)

Table 2.3 Statistics on Damage to Highway Bridges due to the Nankai Earthquake of 1946

Prefectures	Number of Bridges Damaged	Amount of Loss in Bridges	Amount of Loss in Highways Except Bridges
		Thousand Yen	Thousand Yen
Honshu Island	(179)	(25,365)	(80,626)
Aichi	26	806	432
Mie	73	1,578	4,230
Gifu	13	2,778	43
Nara	21	71	6,717
Wakayama	29	19,769	64,887
Okayama	14	346	4,174
Hiroshima	2	17	143
Shimane	1	small	small
Shikoku Island	(163)	(70,240)	(275,511)
Kagawa	7	478	1,033
Tokushima	19	3,687	8,243
Ehime	16	3,273	7,399
Kochi	121	62,802	258,826
Kyushu Island	(4)	(small)	(small)
Oita	1	small	small
Miyazaki	3	small	small
Total	346	95,605	356,137

(Note) Amount of loss was evaluated at the value at the time of the earthquake.

Table 2.4 Statistics on Damage to Highway Bridges due to the Fukui Earthquake of 1948

Prefectures	Bridge Damage		Highway Damage Except Bridges	
	Number of Bridges	Repairing Cost	Number of Sites	Repairing Cost
		Thousand Yen		Thousand Yen
Fukui	180	189,869	475	205,945
Ishikawa	63	17,782	155	41,463
Total	243	207,651	630	247,408

(Note) Amount of loss was evaluated at the value at the time of the earthquake.

Table 2.5 Statistics on Damage to Highway Bridges (except Wooden Bridges) due to the Niigata Earthquake of 1964

Prefectures	Number of Damaged Bridges	Number of Severely Bridges	Number of Fallen Bridges	Approximate Epicentral Distance
Akita	7	0	0	140 - 160^{km}
Fukushima	5	0	0	120 - 150^{km}
Niigata	74	8	3	30 - 90^{km}
Yamagata	12	0	0	60 - 100^{km}
Total	98	8	3	

Table 2.6 Results of Bearing Power Tests at the Bandai Bridge Site

Caisson No.	Date of Tests	Elevation of Bearing Surface at Tests	Soils	Area of Bearing Surface at Tests	Ultimate Bearing Powers	Elevation of Base of Caisson Completed
1	Oct., 1927	-12.4^{m}	Brown Coarse Sands	0.097^{m^2}	$75.35^{t/m^2}$	-12.4^{m}
2	Oct., 1927	-14.3^{m}	Gray Fine Sands	0.196^{m^2}	$118.14^{t/m^2}$	-15.2^{m}
3	Nov., 1927	-14.6^{m}	Gray Fine Sands	0.196^{m^2}	$133.69^{t/m^2}$	-15.2^{m}
4	Nov., 1927	-15.2^{m}	Gray Fine Sands	0.196^{m^2}	$131.61^{t/m^2}$	-15.2^{m}
5	Dec., 1927	-14.9^{m}	Gray Fine Sands	0.196^{m^2}	$131.86^{t/m^2}$	-15.2^{m}
6	Dec., 1927	-14.0^{m}	Gray Fine Sands	0.196^{m^2}	$133.43^{t/m^2}$	-15.2^{m}
7	Feb., 1928	-12.4^{m}	Brown Coarse Sands	0.196^{m^2}	$111.97^{t/m^2}$	-13.6^{m}

A sketch of the tests is shown on the figure.

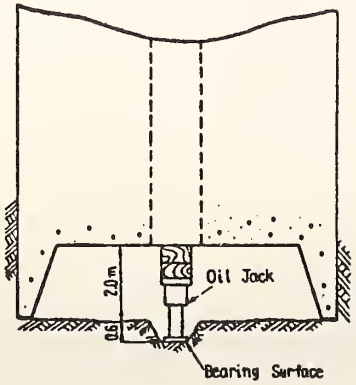

Table 2.7 Numbers of Damaged Bridges with various kinds of foundations due to the Niigata Earthquake of 1964

— For Highway Bridges within 60km from the center of Niigata City —

VARIETIES OF FOUNDATIONS	TOTAL NUMBER OF BRIDGES SURVEYED	NUMBER OF BRIDGES DAMAGED (INCLUDING SLIGHT DAMAGE)	NUMBER OF BRIDGES DAMAGED SEVERELY			
			AT SUBSTRUCTURE	AT SUPERSTRUCTVRE	IN VIEW OF TRAFFIC CAPACITY	OVERALL EVALUATION
BRIDGES WITH SPREAD FOOTINGS	18.5	10	1.5	0.5	0.5	0.5
BRIDGES WITH CAISSON FOUNDATIONS	21	13	1	1	0.5	0.5
BRIDGES WITH PILE FOUNDATIONS	46.5	29	4.5	2.5	4	2
TOTAL	86	52	7	4	5	3

Note) When there are two kinds of foundations for one bridge, the number of the bridge was accounted such as half for one foundation and half for the other foundation.

Table 2.8 Damage Percentages of Individual Portions of Highway Bridges within 60km from the Center of Niigata City

Structural classification	Type of structures		Number of structures Surveyed	Damaged structures	
				Number of structures	Percentages
Superstructures	Steel Girders		168 spans	19 spans	11.3 %
	Reinforced Concrete Girders		222 spans	33 spans	14.9 %
	Prestressed Concrete Girders		132 spans	11 spans	8.3 %
	Wooden Girders		8 spans	8 spans	100 %
	Total		530 spans	71 spans	13.4 %
Substructures	Abutments	WITH SPREAD FOOTINGS	24	4	16.7 %
		WITH PILE FOUNDATIONS	99	19	19.2 %
		WITH CAISSON FOUNDATIONS	29	7	24.0 %
		SUB-TOTAL	152	30	19.7 %
	Piers	WITH SPREAD FOOTINGS	40	0	0 %
		WITH PILE FOUNDATIONS	214	21	9.8 %
		WITH CAISSON FOUNDATIONS	180	15	8.3 %
		SUB-TOTAL	444	36	8.1 %
	TOTAL		596	66	11.1 %

Table 2.9 Stastistics on Damage to Highways and Highway Bridges due to the Tokachi-oki Earthquake of 1968

Administrative Agency		Highways		Highway Bridges		Total		Remarks
		Number of Sites	Loss	Number of Bridges	Loss	Number	Loss	
Ministry of Construction		111	Thousand Yen 969,604	—	—	111	Thousand Yen 969,604	Mostly to National Highways in Aomori Prefecture
Prefectural Governments	Hokkaido	63	319,359	30	Thousand Yen 206,176	93	525,535	
	Aomori	818	1,167,060	64	187,770	882	1,354,830	
	Iwate	41	34,178	3	19,000	44	53,178	
	Miyagi	—	—	3	5,100	3	5,100	
	Akita	4	4,600	1	3,000	5	7,600	
Total		1,037	2,494,801	101	421,046	1,138	2,915,847	

Note) Amounts of loss were estimated at the value as of June, 1968.

NO	Date	Name	M*
1	Sept 1, 1923	Kanta	7.9
2	Dec. 21, 1946	Nankai	8.1
3	Jun. 28, 1948	Fukui	7.3
4	Dec. 26, 1949	Imoichi	6.4
5	Mar. 4, 1952	Tokachi-oki	8.1
6	Apr. 30, 1962	Northern Miyagi	6.5
7	Jun. 16, 1964	Niigato	7.5
8	Feb. 21, 1968	Ebino	6.1
9	May 16, 1968	Tokochi-oki	7.9

(*) Magnitudes are on the Richter scale, after Rika Nenpya (Annual Report of Science) (1971).[31]

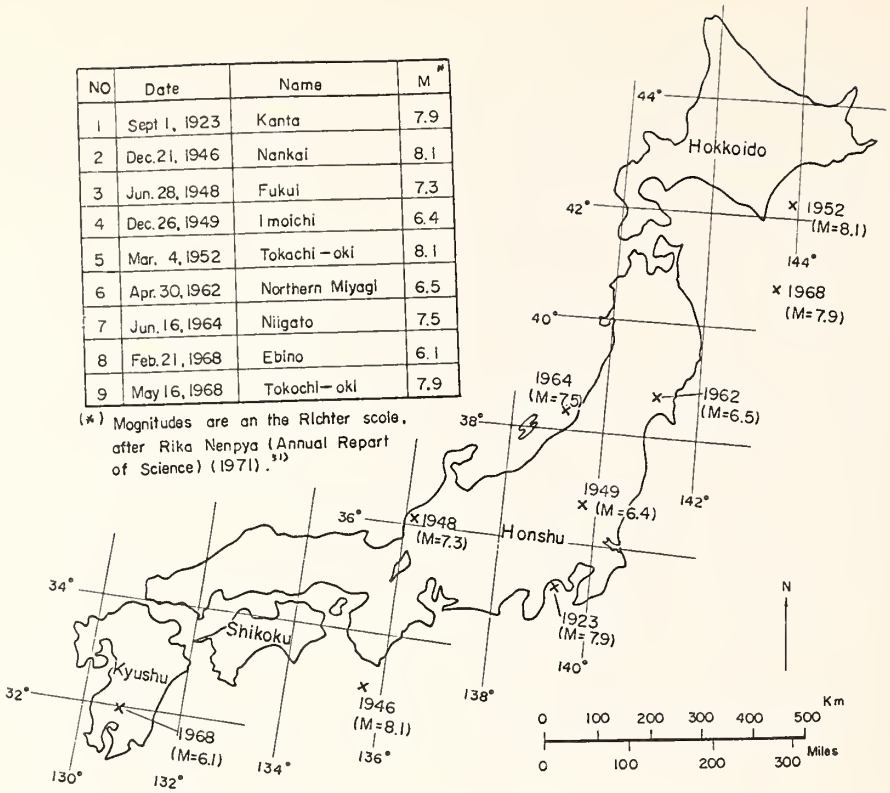

Fig. 2.1 Epicenters of nine earthquakes which caused comparatively severe damage to modern engineering structures in Japan

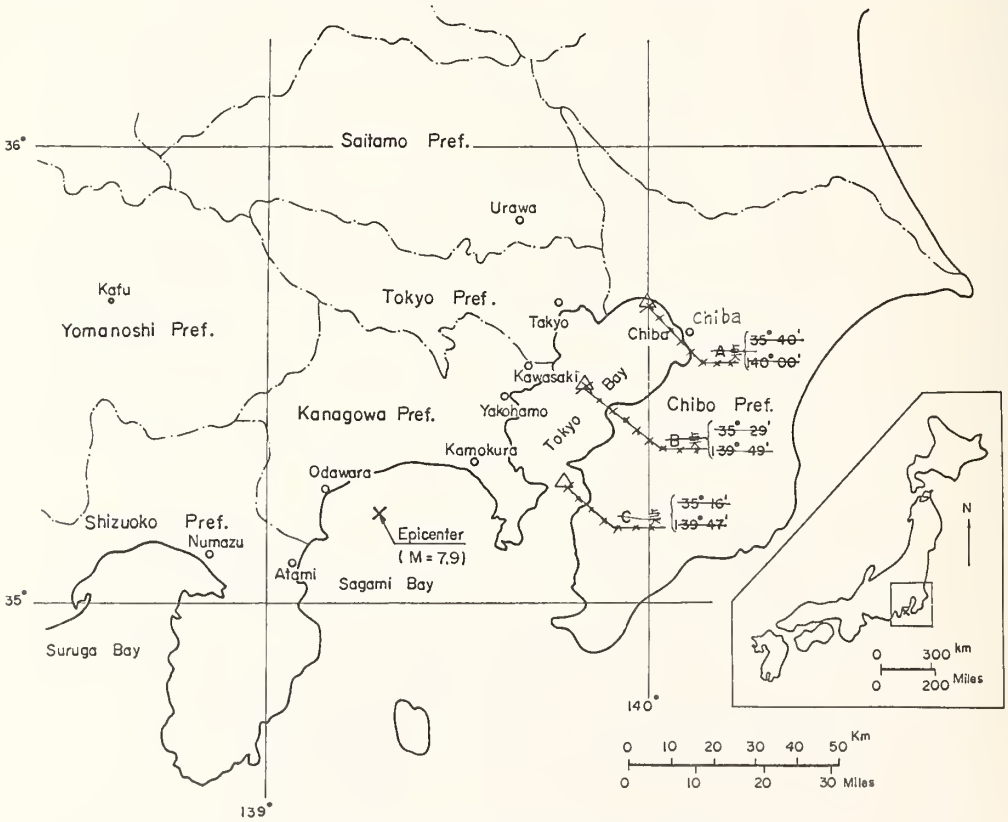

Fig. 2.2 The Kanto Earthquake of 1923

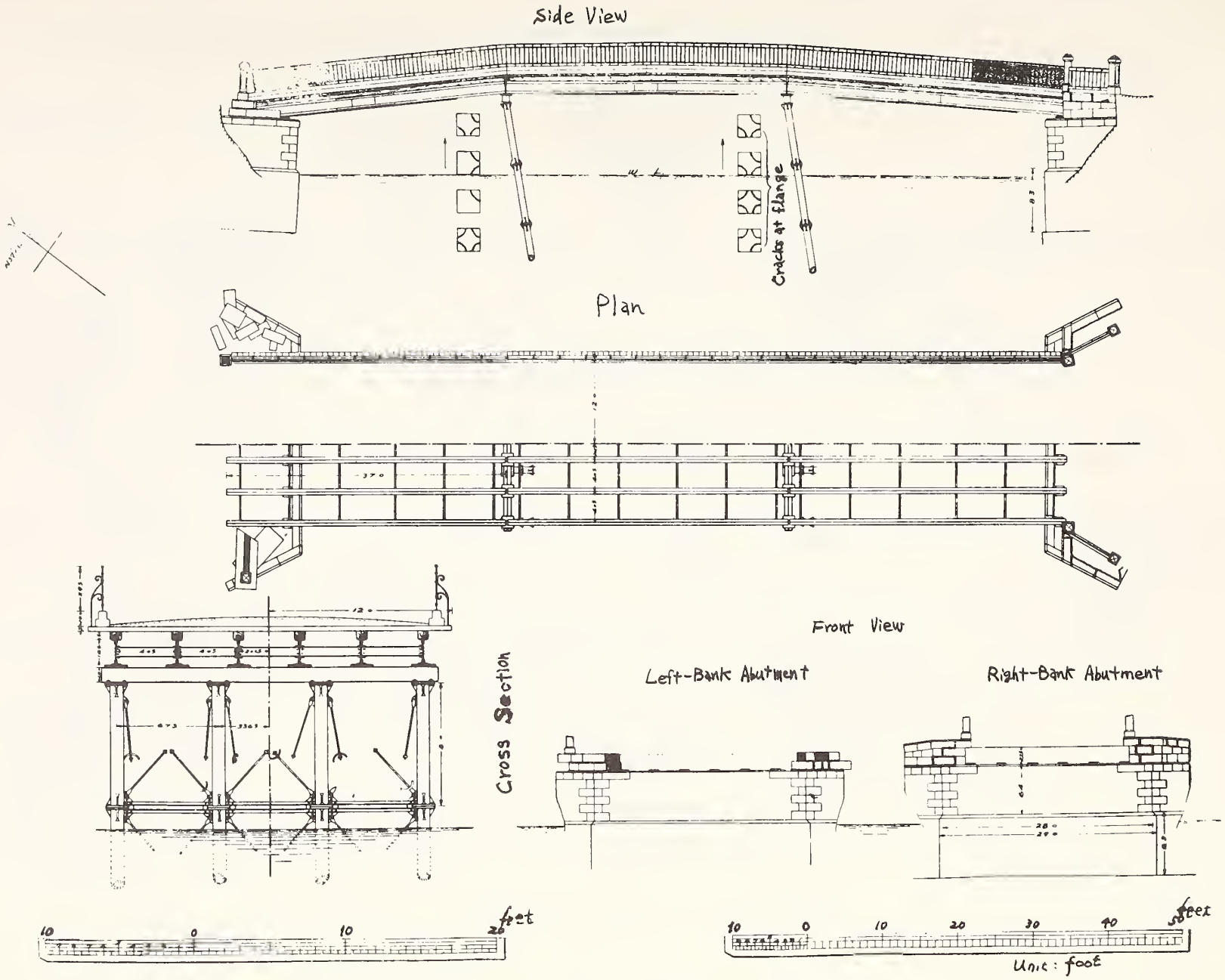

Fig. 2.3 Damage to the Tsuruno-bashi bridge

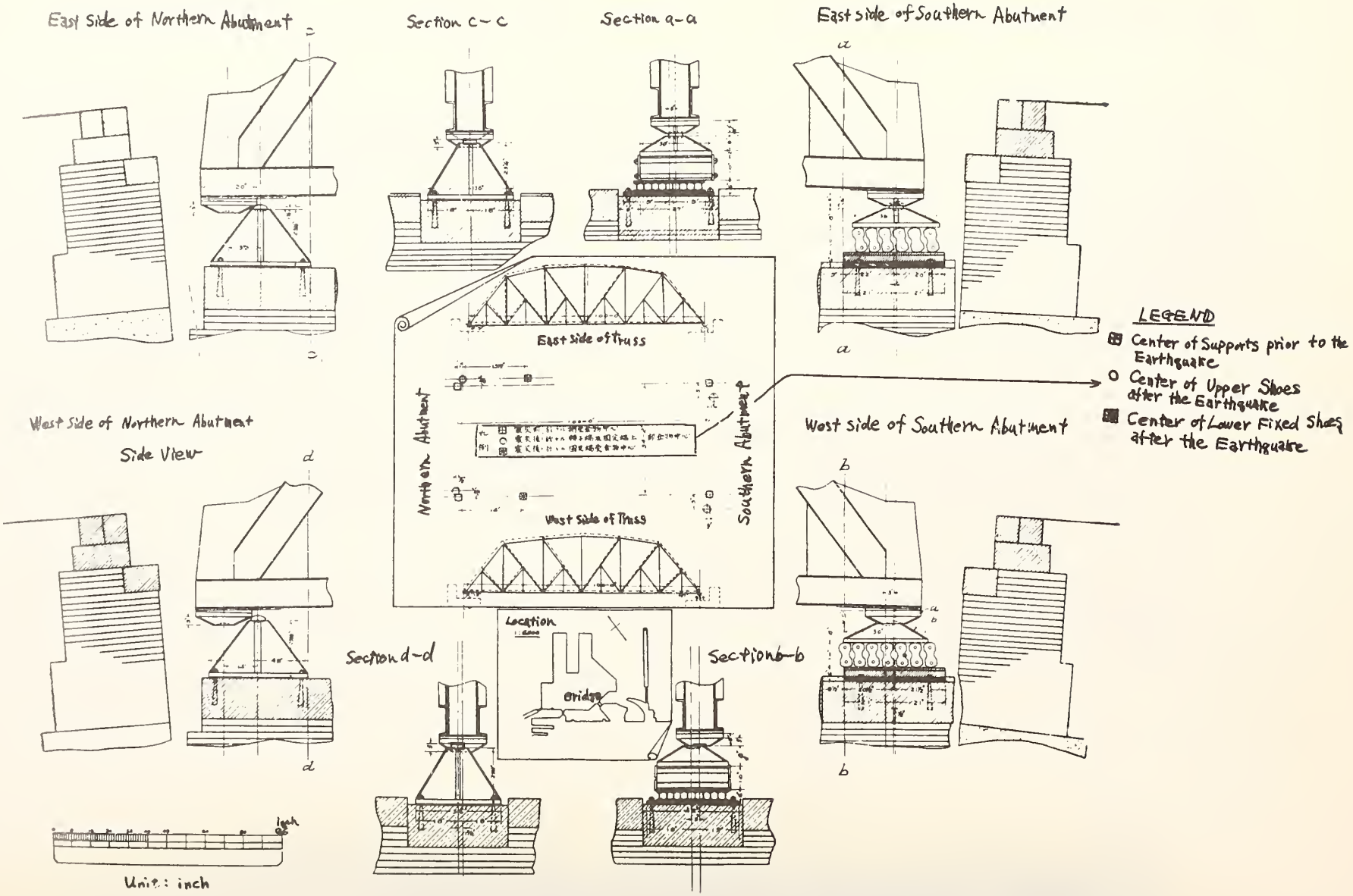

Fig. 2.4 Damage to the Shinminato bridge

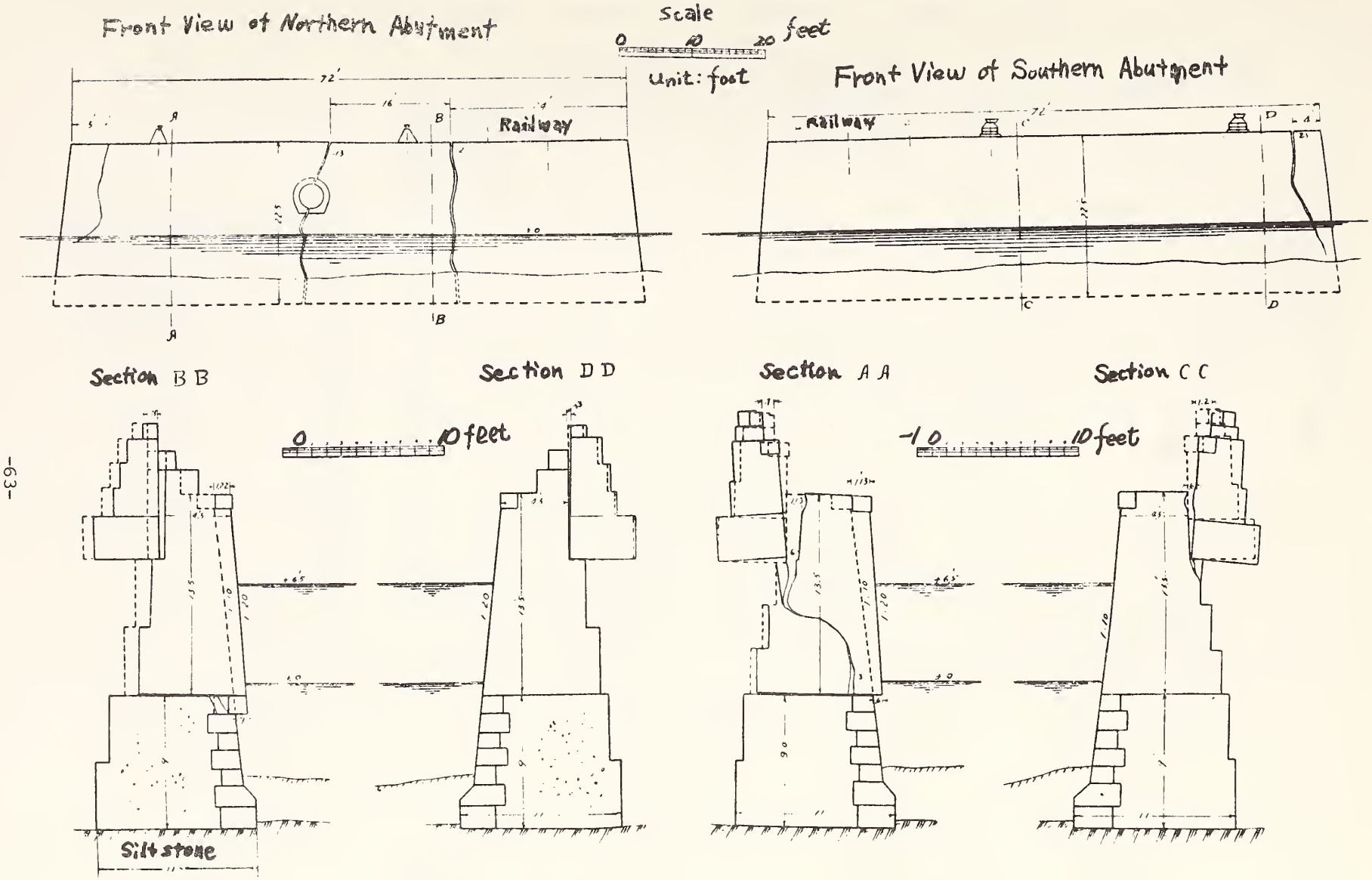

Fig. 2.5 Damage to the abutments of the Shinminato bridge

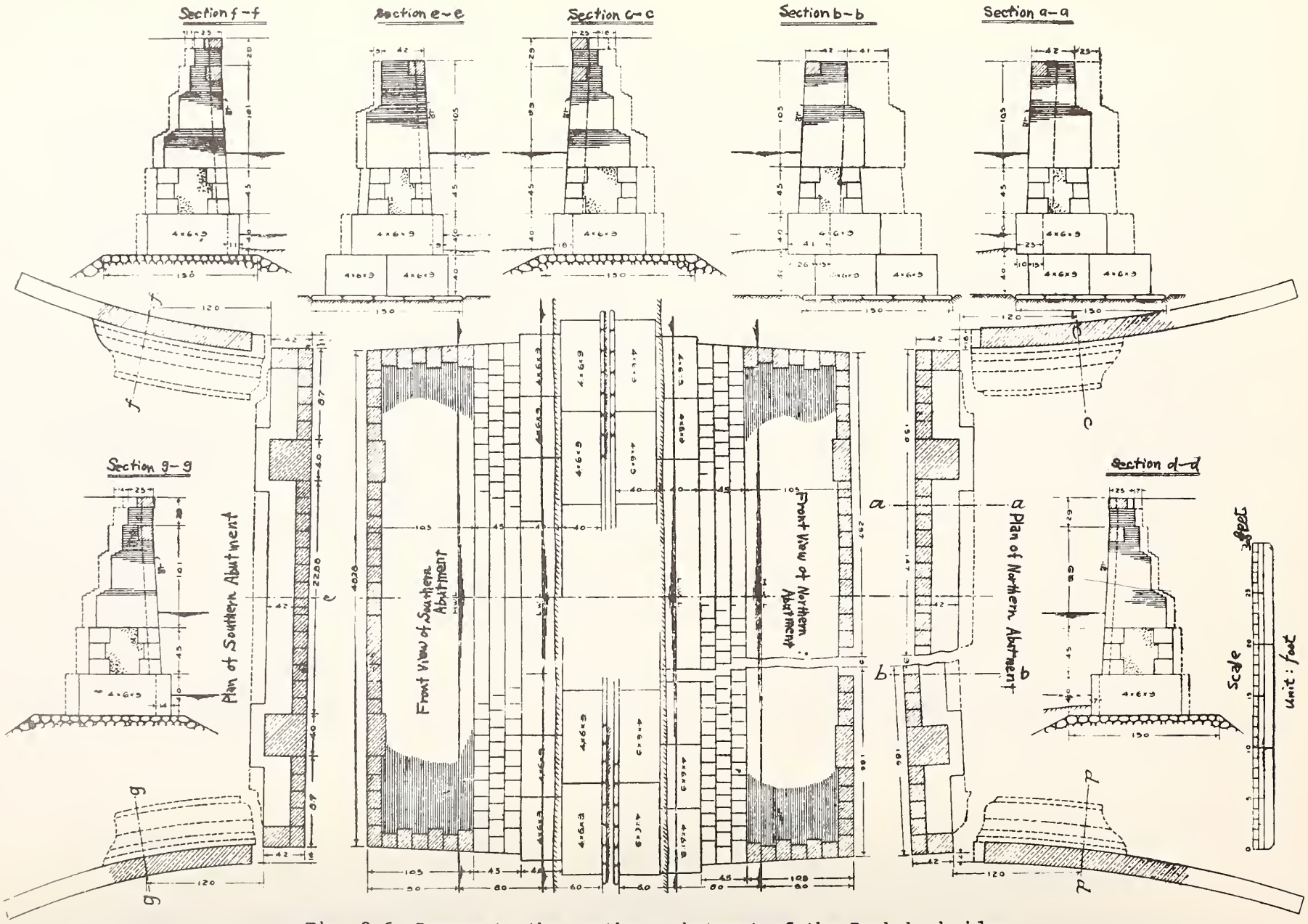

Fig. 2.6 Damage to the northern abutment of the Bankoku bridge

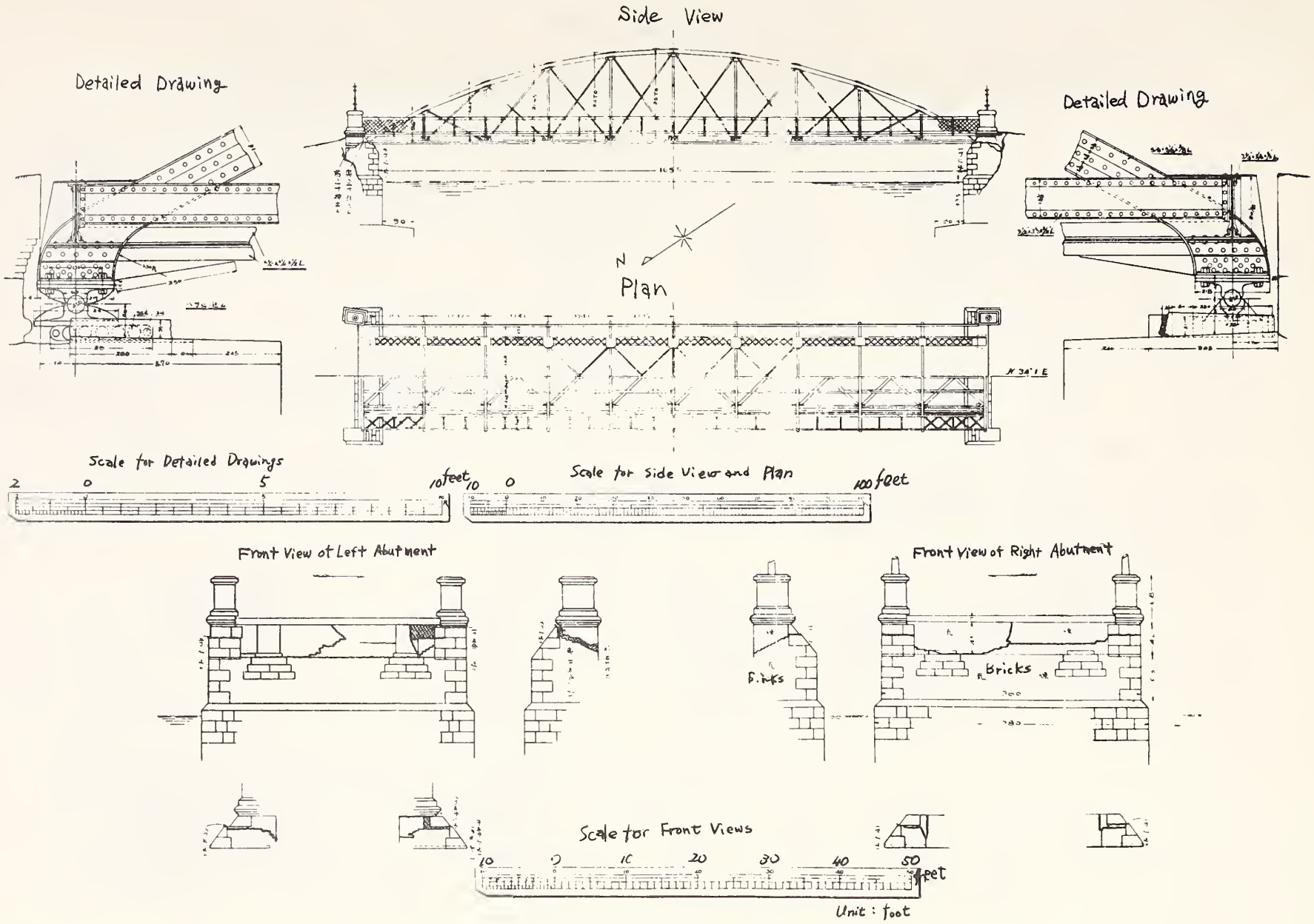

Fig. 2.7 Damage to the Hanazono bridge

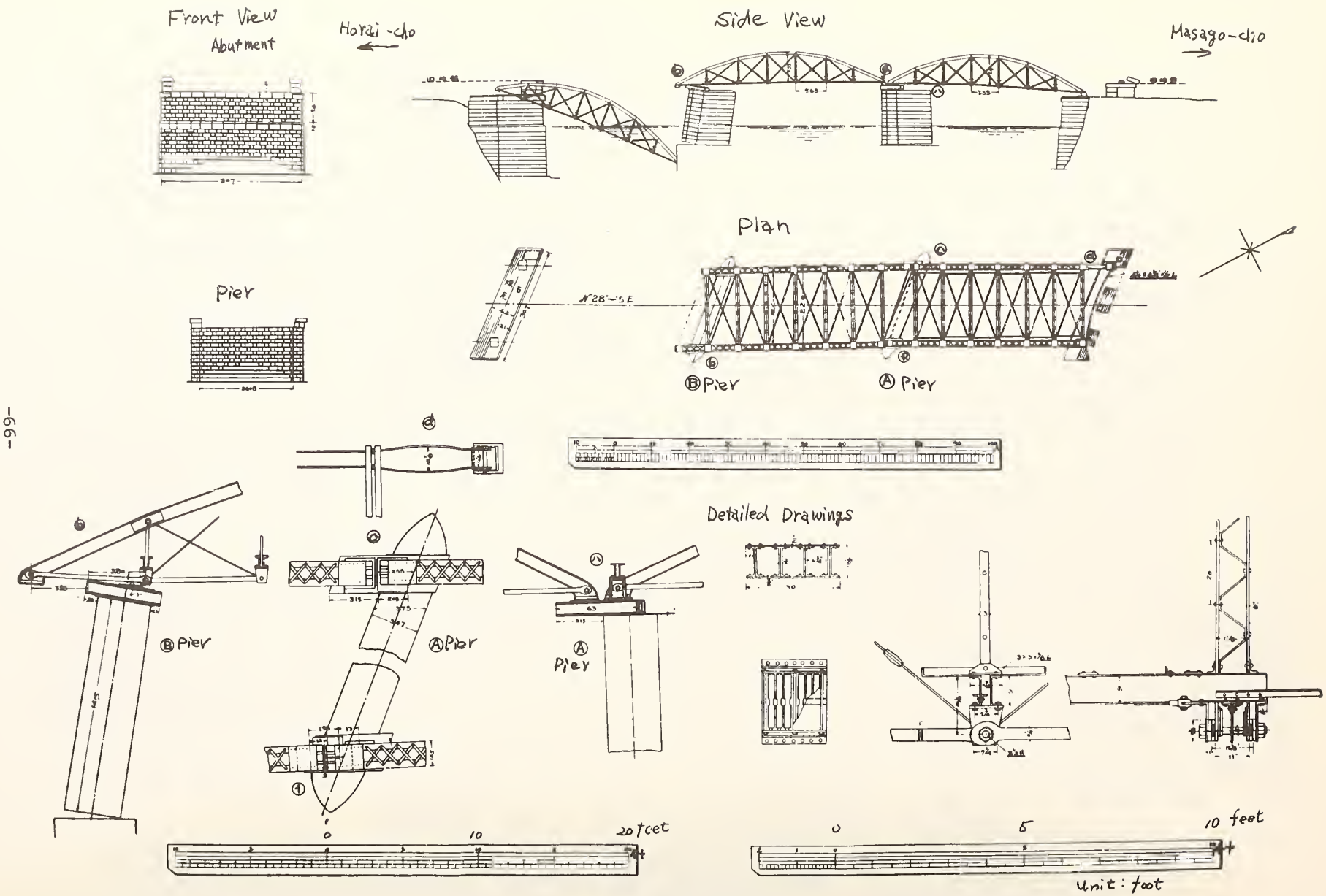

Fig. 2.8 Damage to the Toyokuni bridge

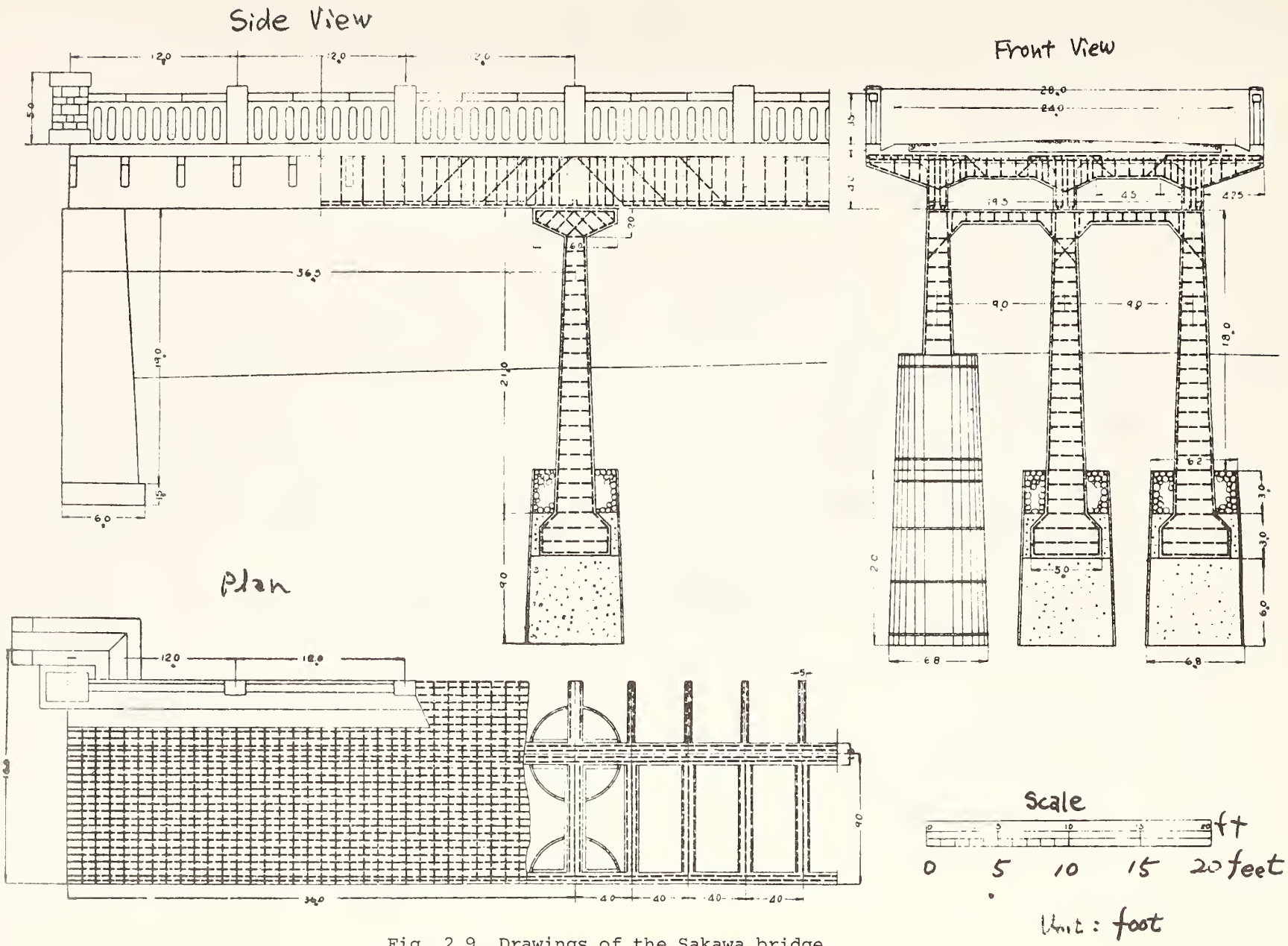

Fig. 2.9 Drawings of the Sakawa bridge

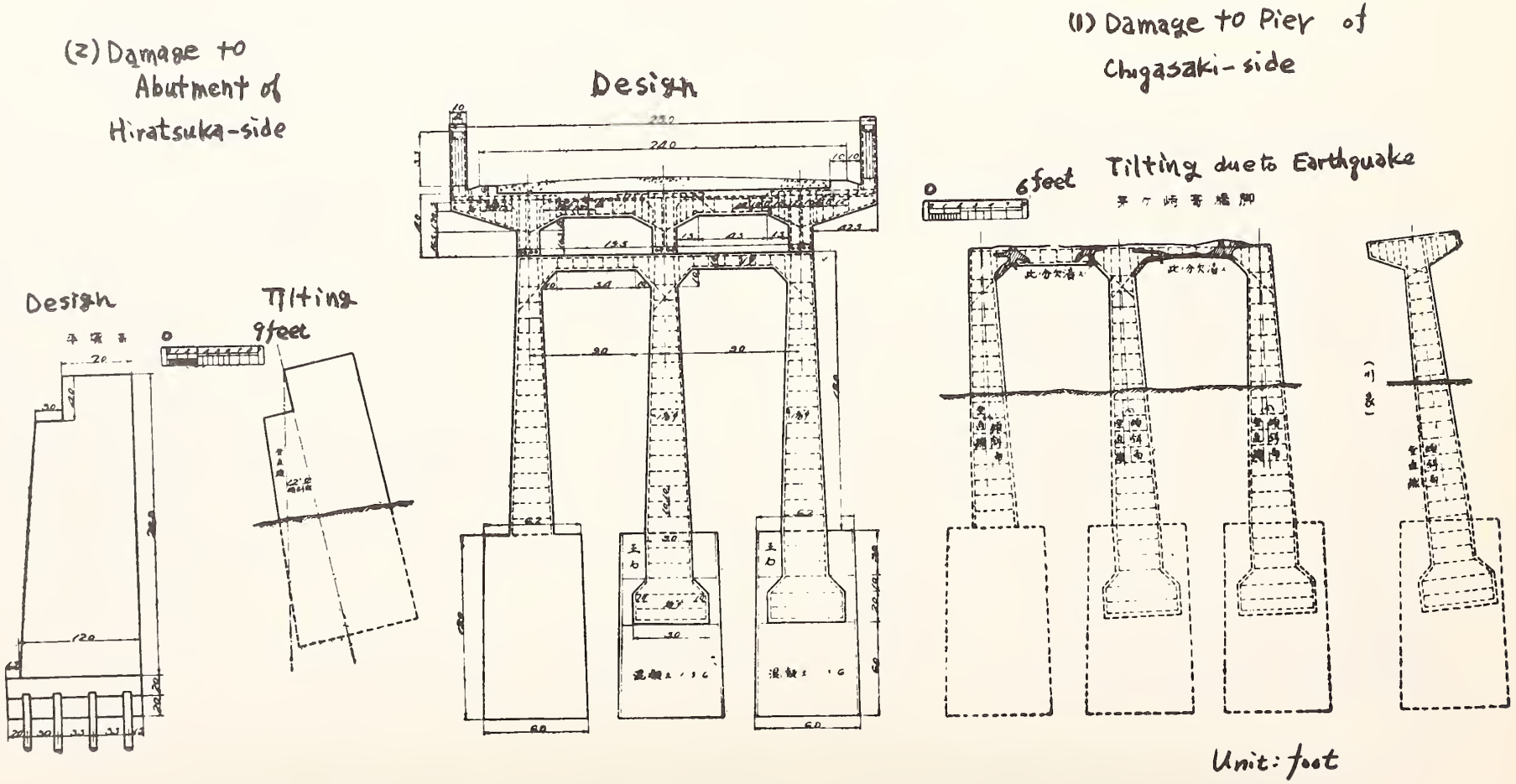

Fig. 2.10 Damage to the Banyu bridge

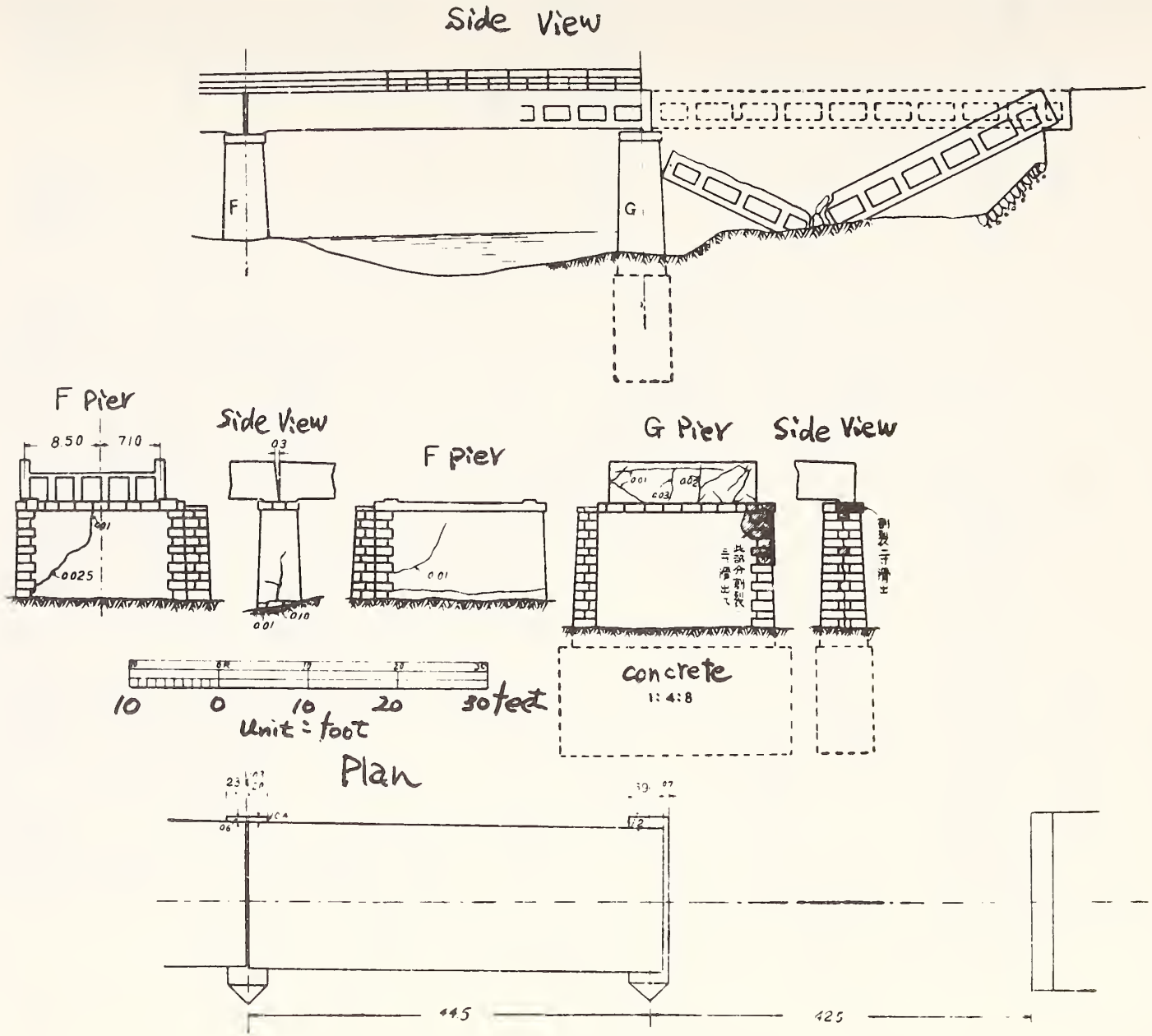

Fig. 2.11 Damage to the Hayakawa bridge

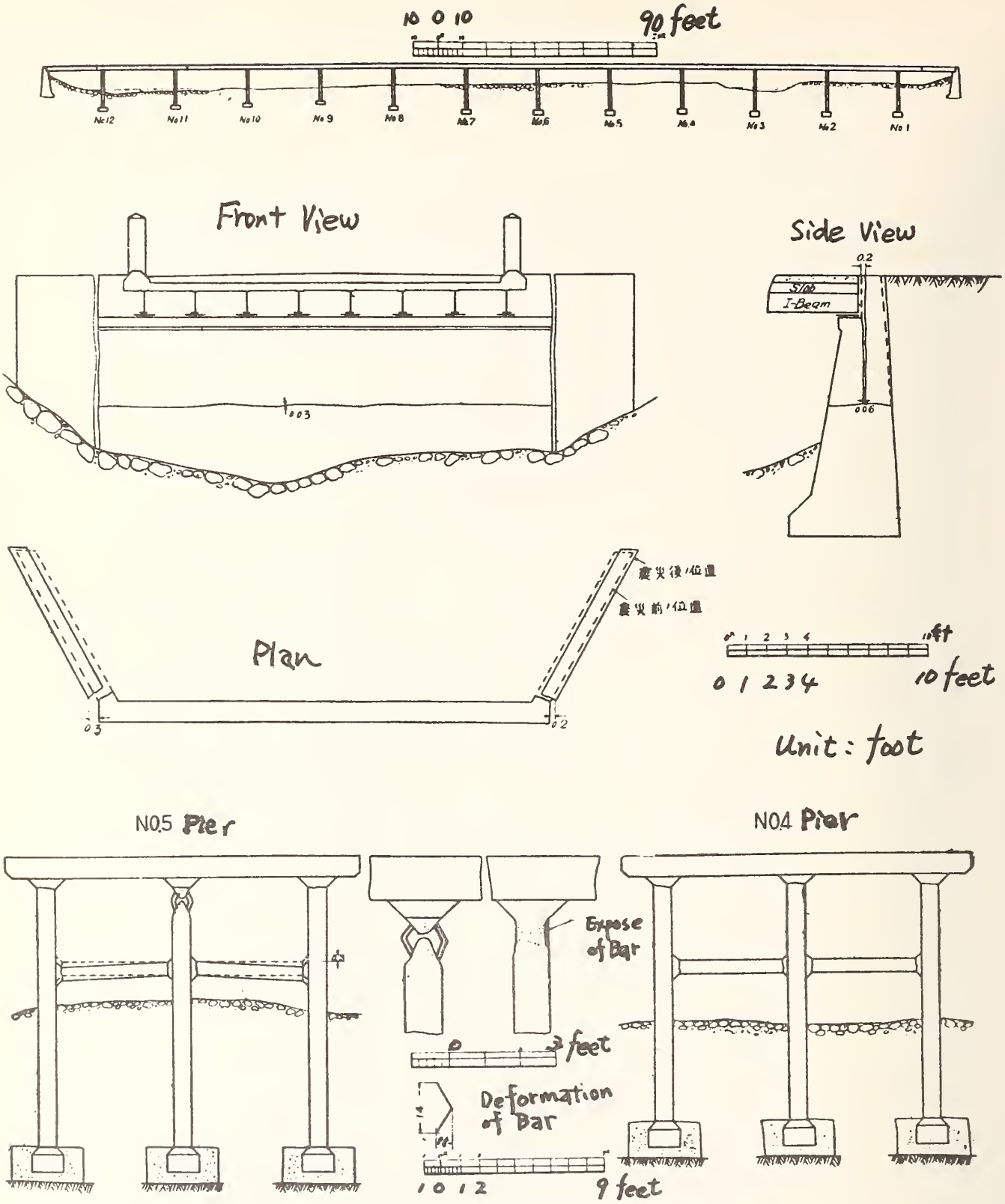

Fig. 2.12 Damage to the Takahata bridge

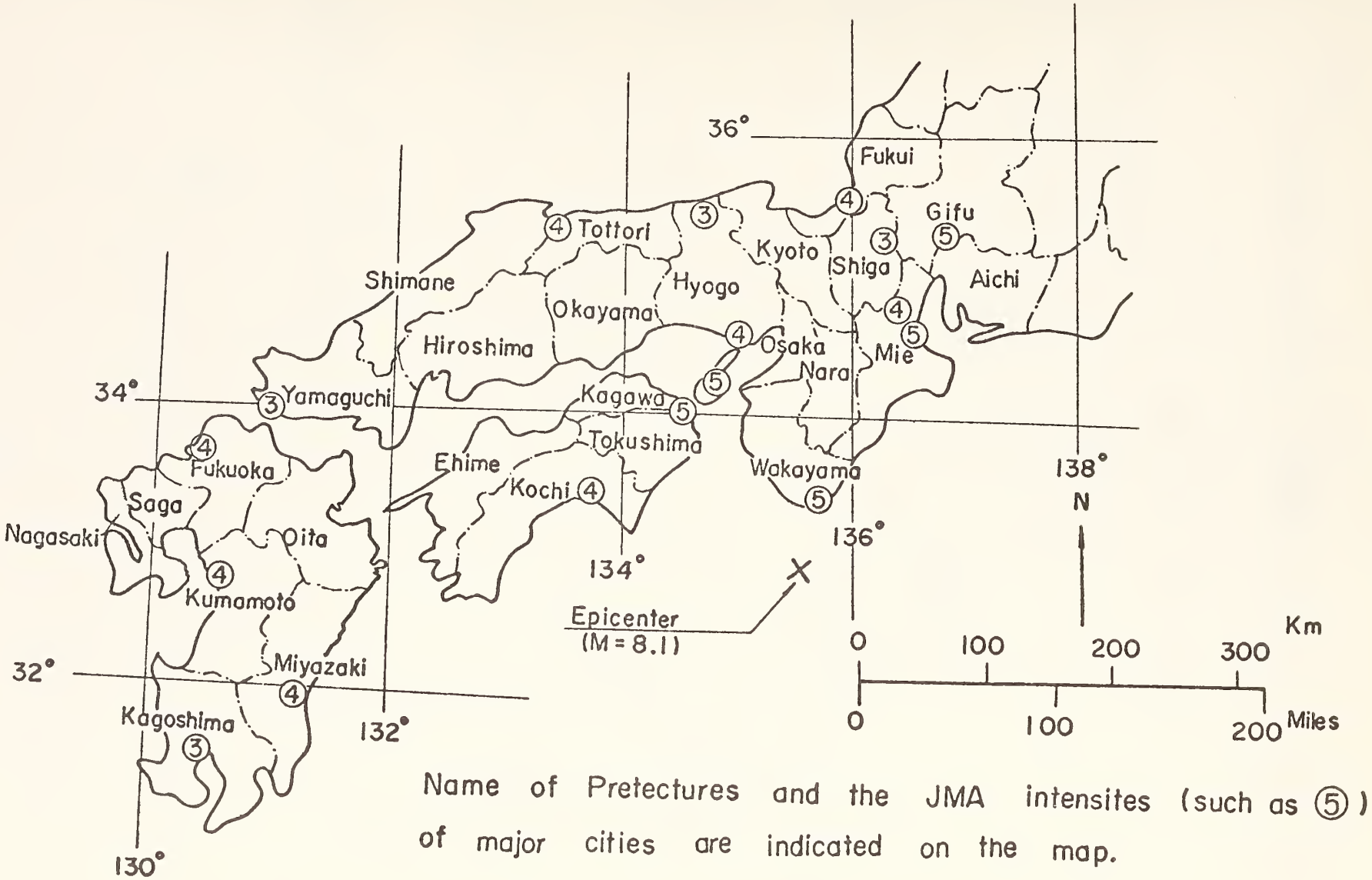

Name of Pretectures and the JMA intensites (such as ⑤) of major cities are indicated on the map.

Fig. 2.13 The Nankai Earthquake of 1946

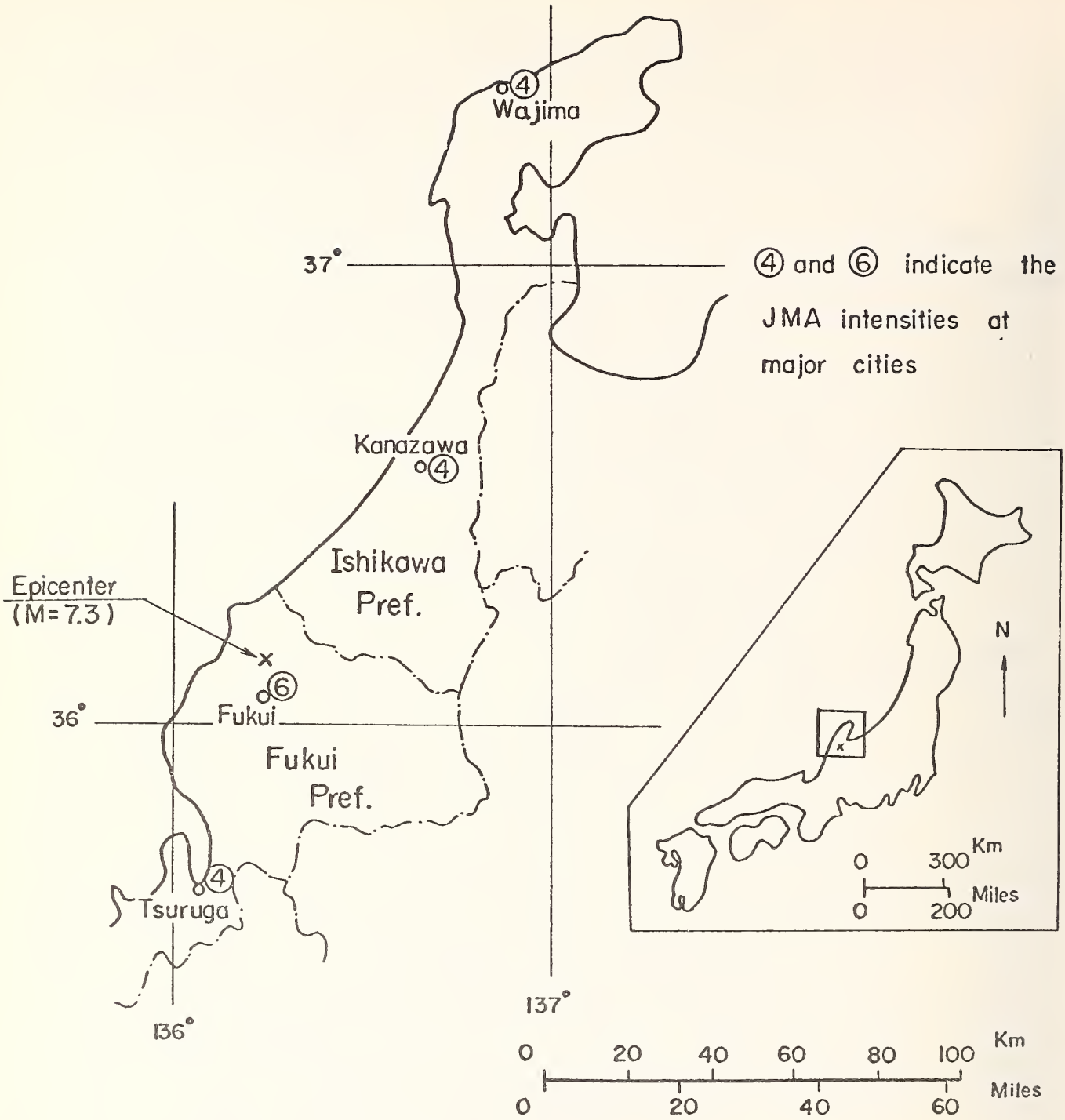

Fig. 2.14 The Fukui Earthquake of 1948

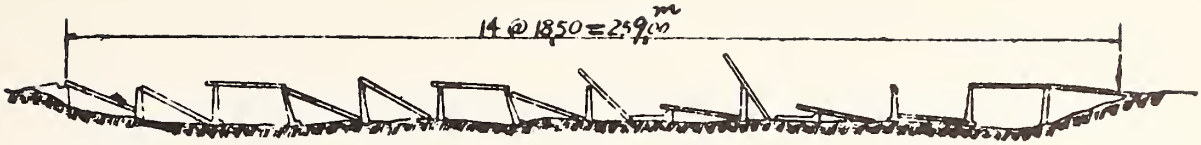

Fig. 2.15 Damage to the Nakazuno bridge

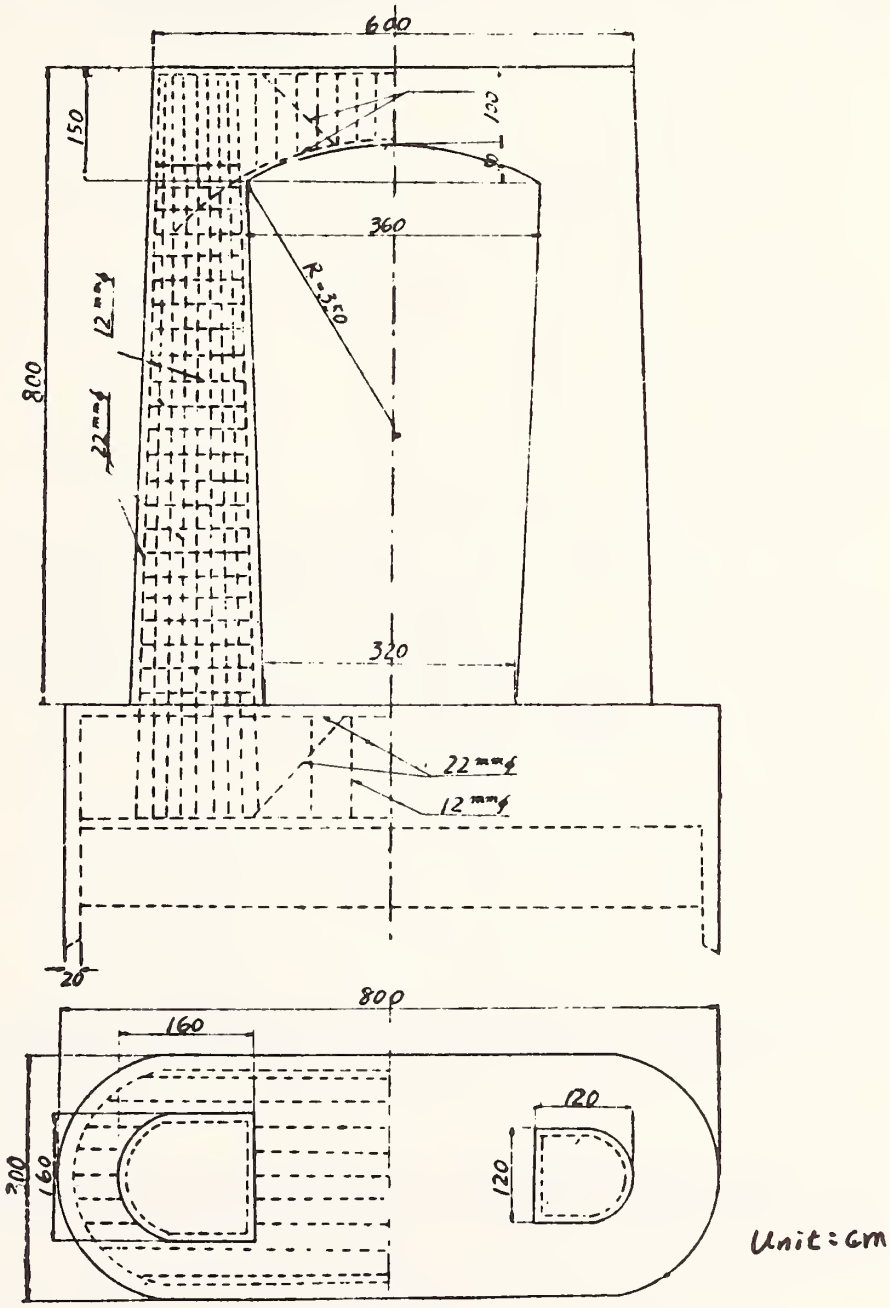

Fig. 2.16 Detailed drawings of the pier of the Nakazuno bridge

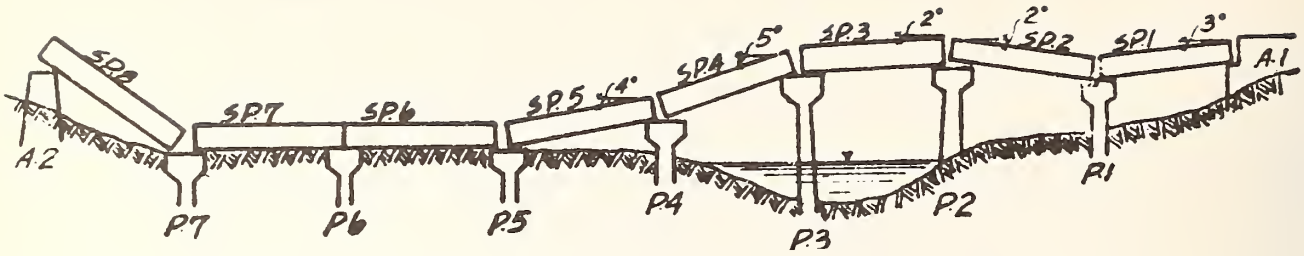

Fig. 2.17 Damage to the Nagaya bridge

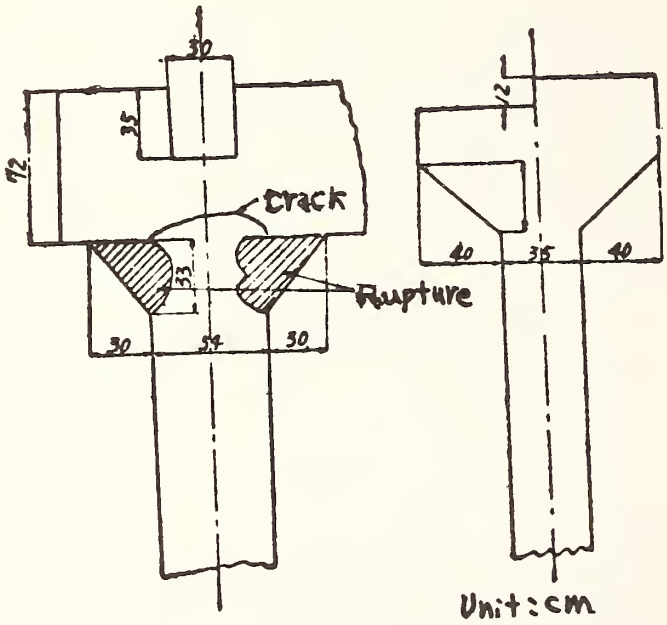

Fig. 2.18 Damage to the Nagaya bridge

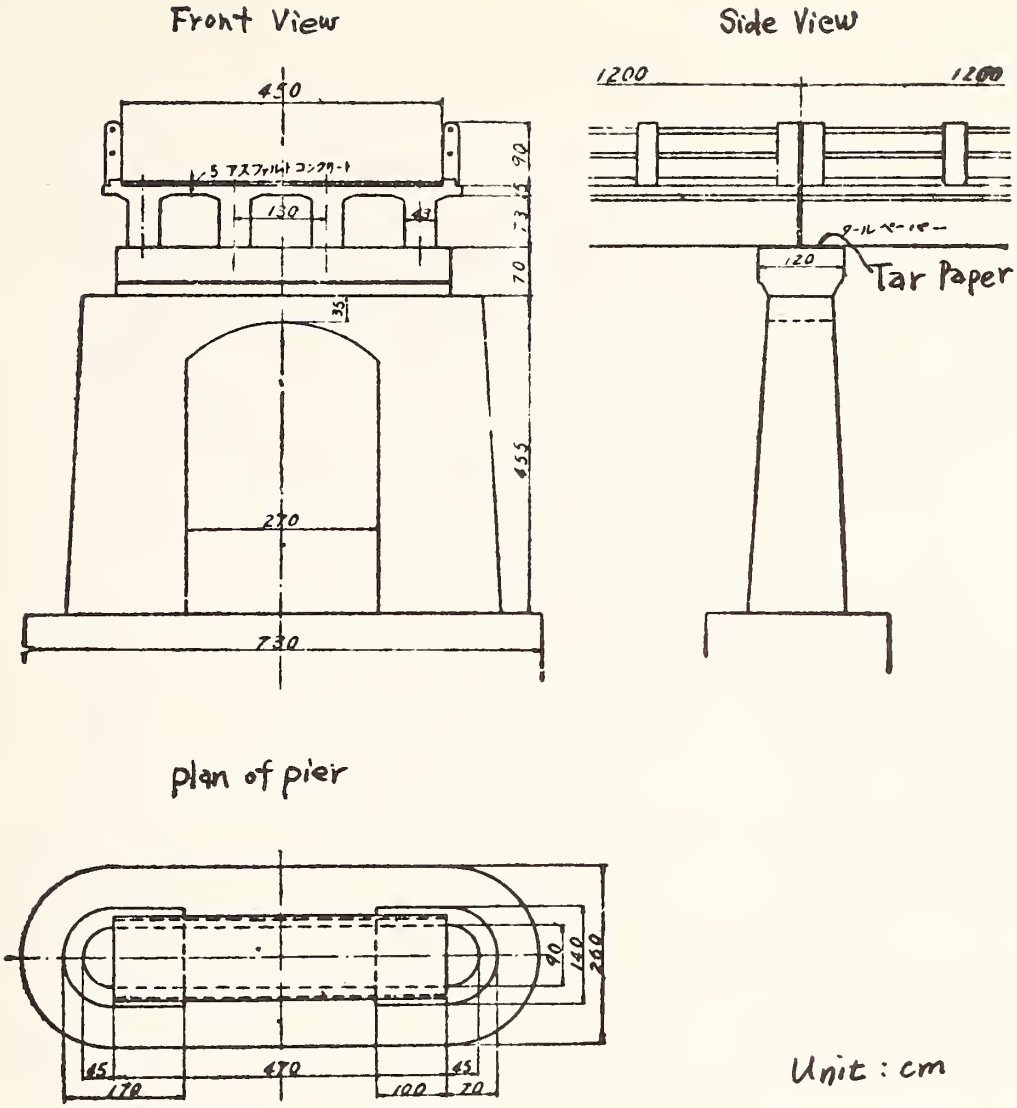

Fig. 2.19 General drawings of the Itagaki bridge

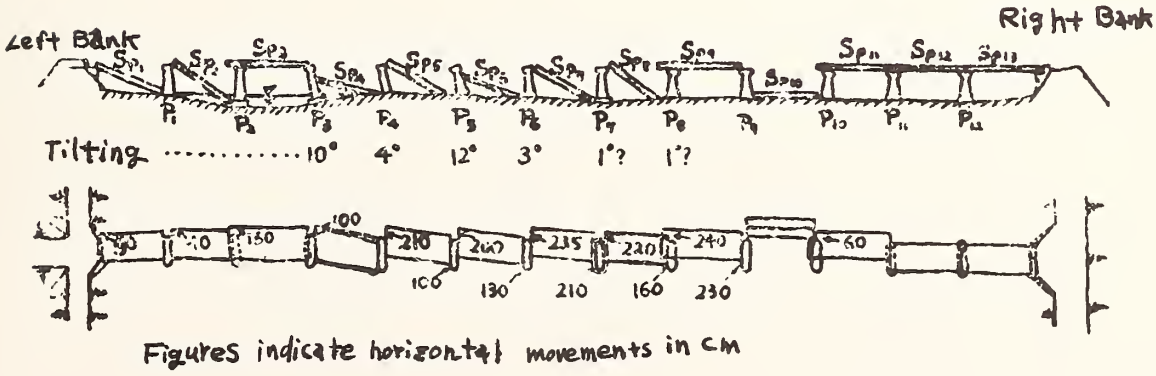

Fig. 2.20 Damage to the Itagaki bridge

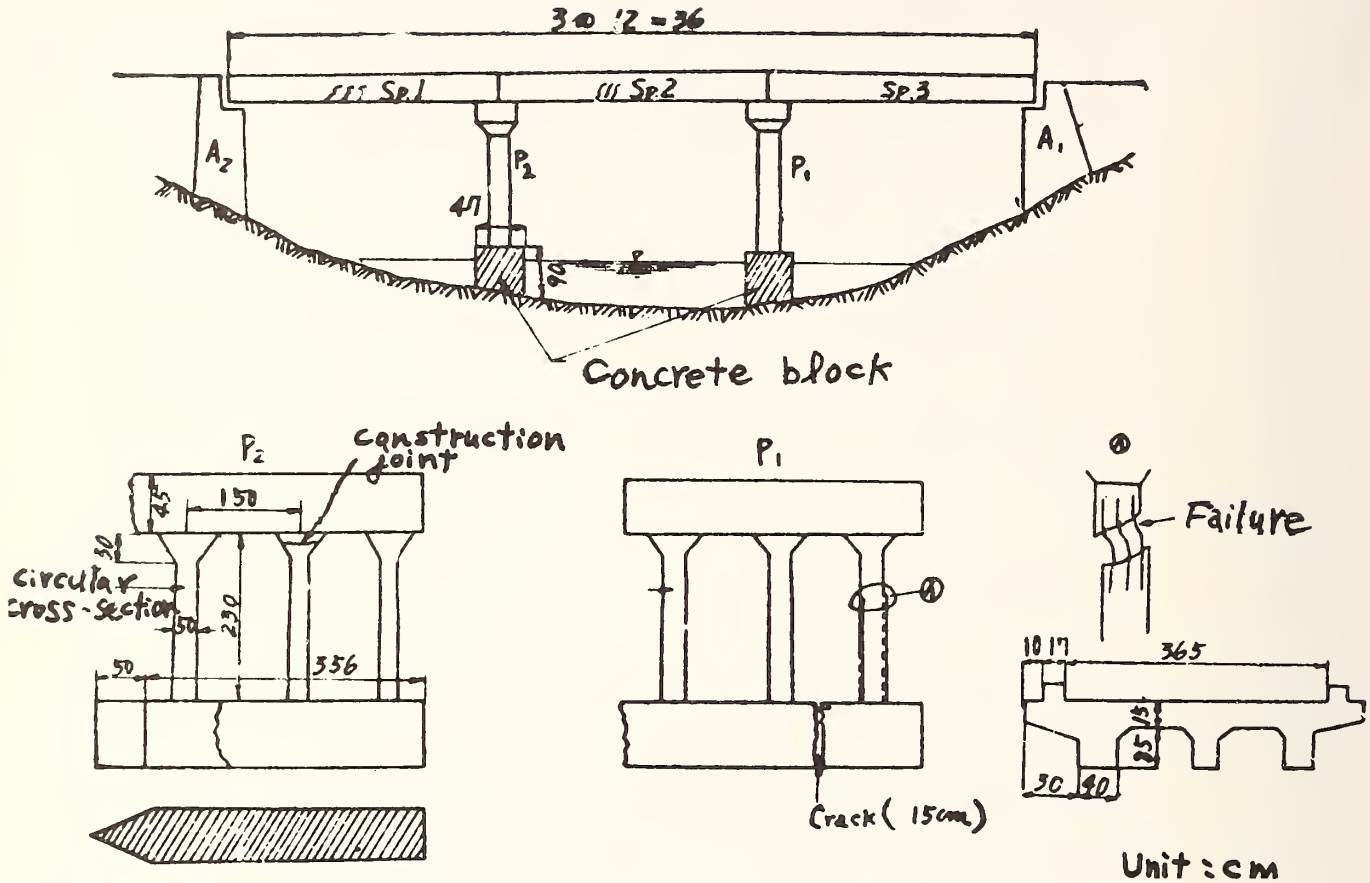

Fig. 2.21 Damage to the Koroba bridge

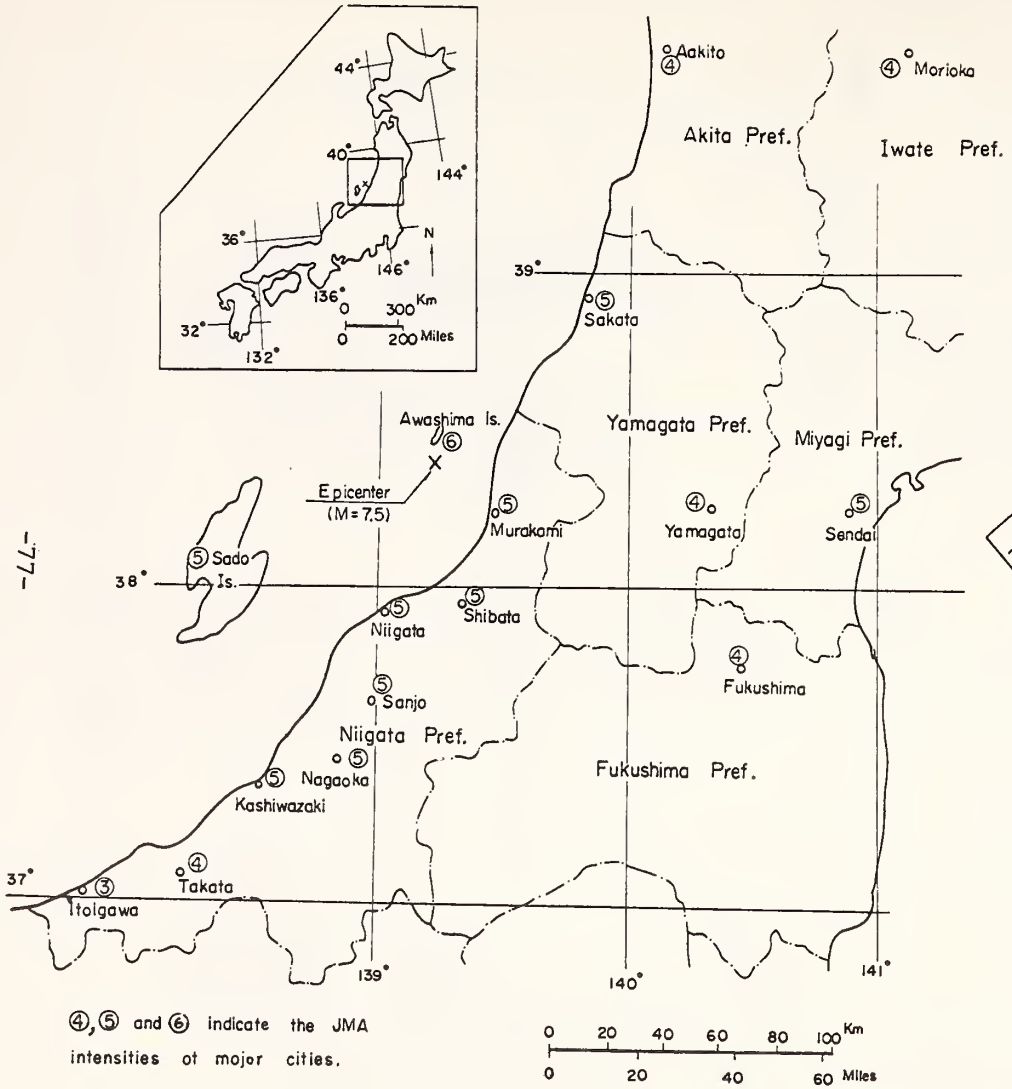

Fig. 2.22 The Niigata Earthquake of 1964

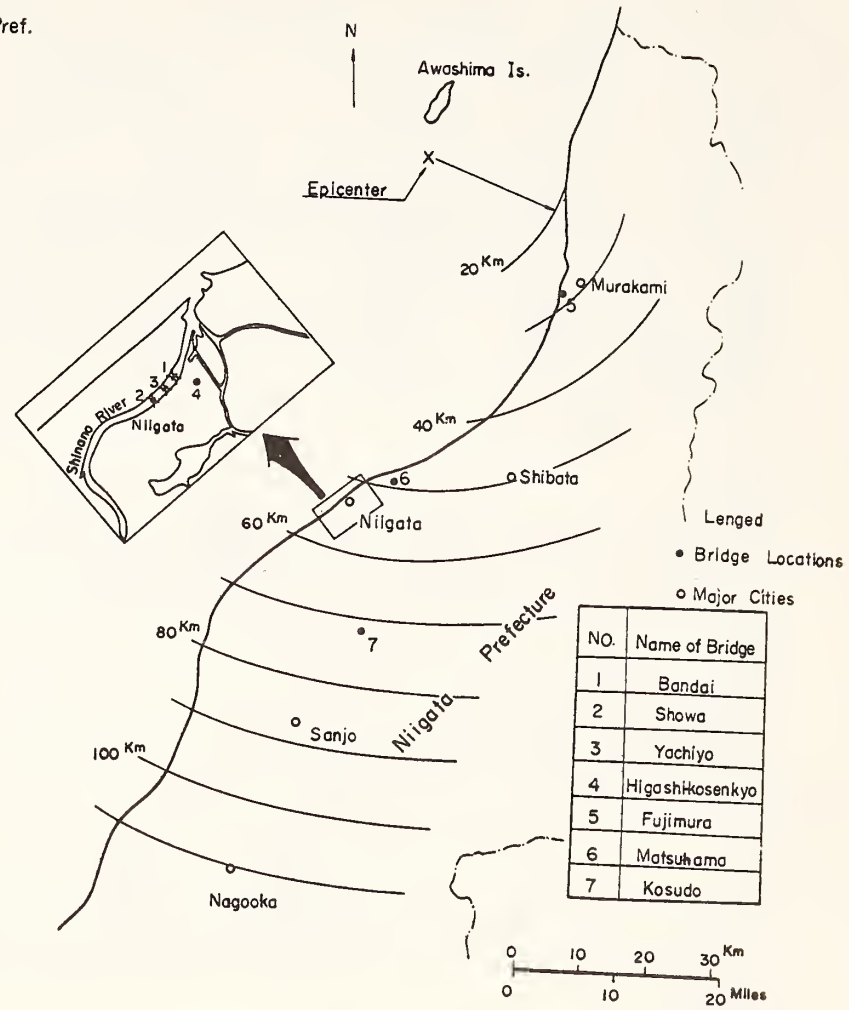

NO.	Name of Bridge
1	Bandai
2	Showa
3	Yachiyo
4	Higashikosenkyo
5	Fujimura
6	Matsuhama
7	Kosudo

Fig. 2.23 Locations of the seven bridges which sustained severe damage.

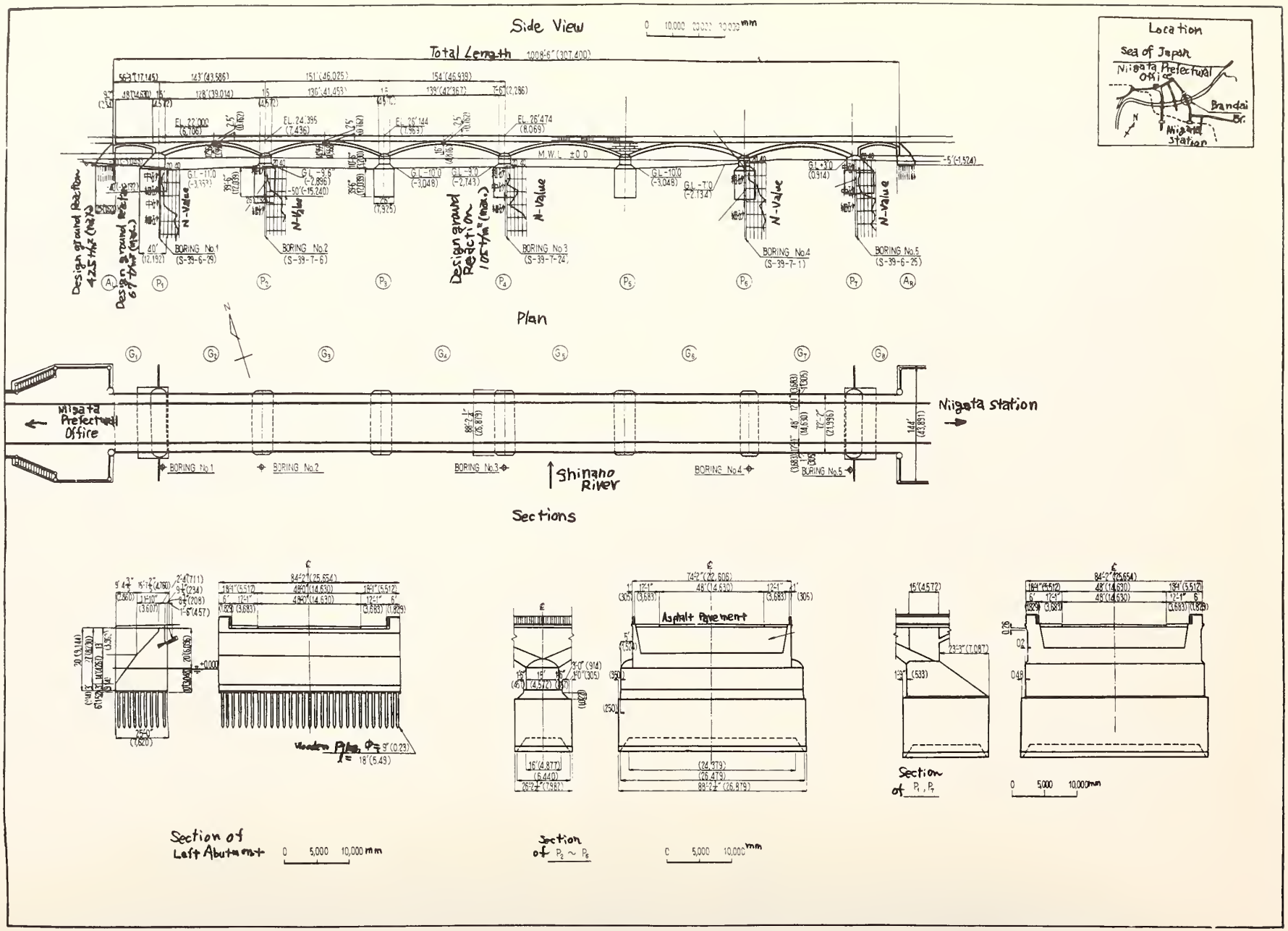

Fig. 2.24 General view of the Bandai bridge

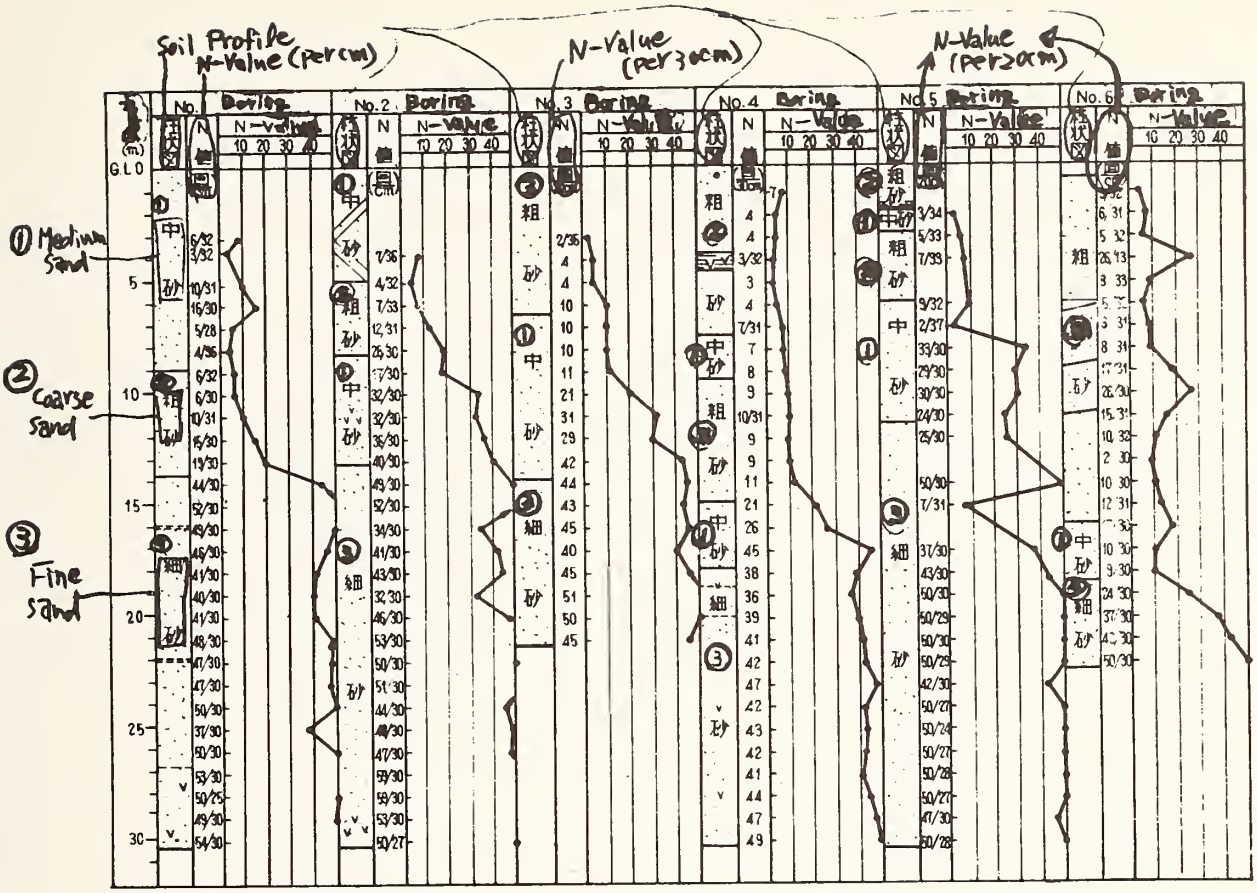

Fig. 2.25 Boring logs at the Bandai bridge

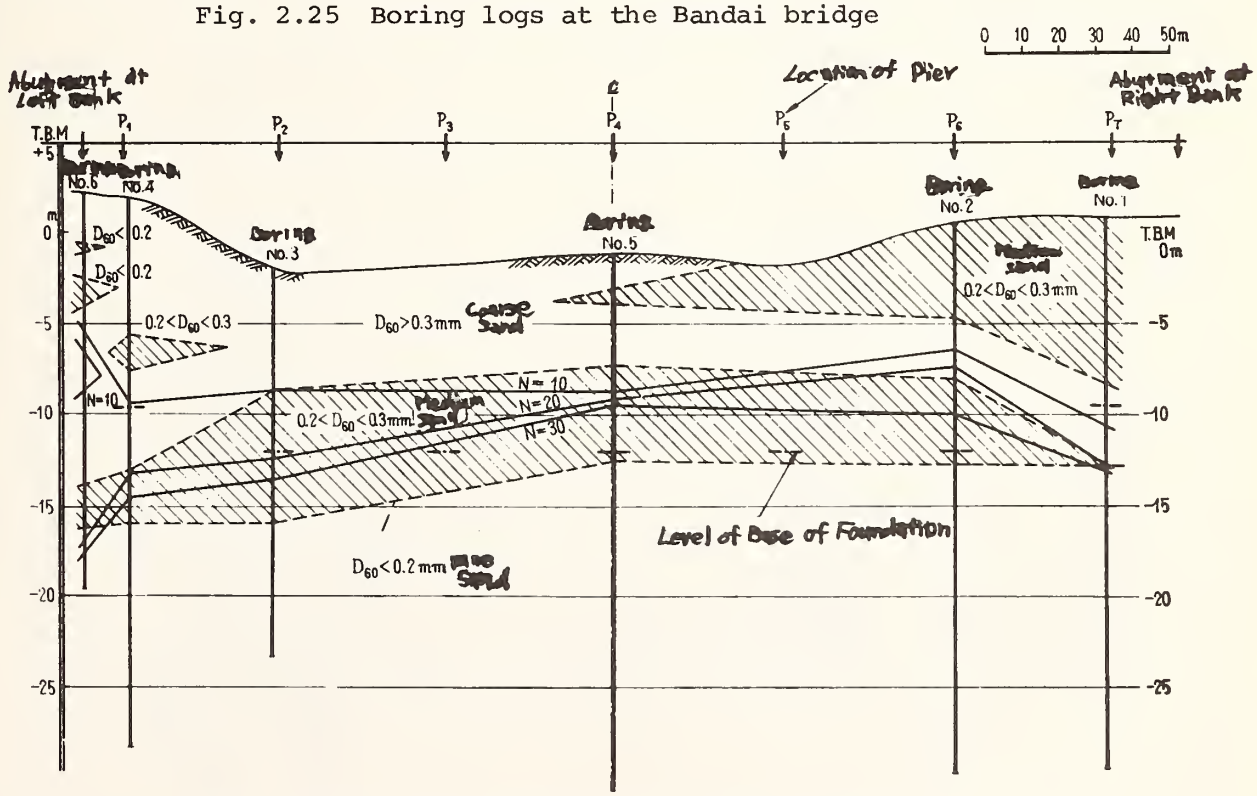

Fig. 2.26 Soil Profile at the Bandai bridge

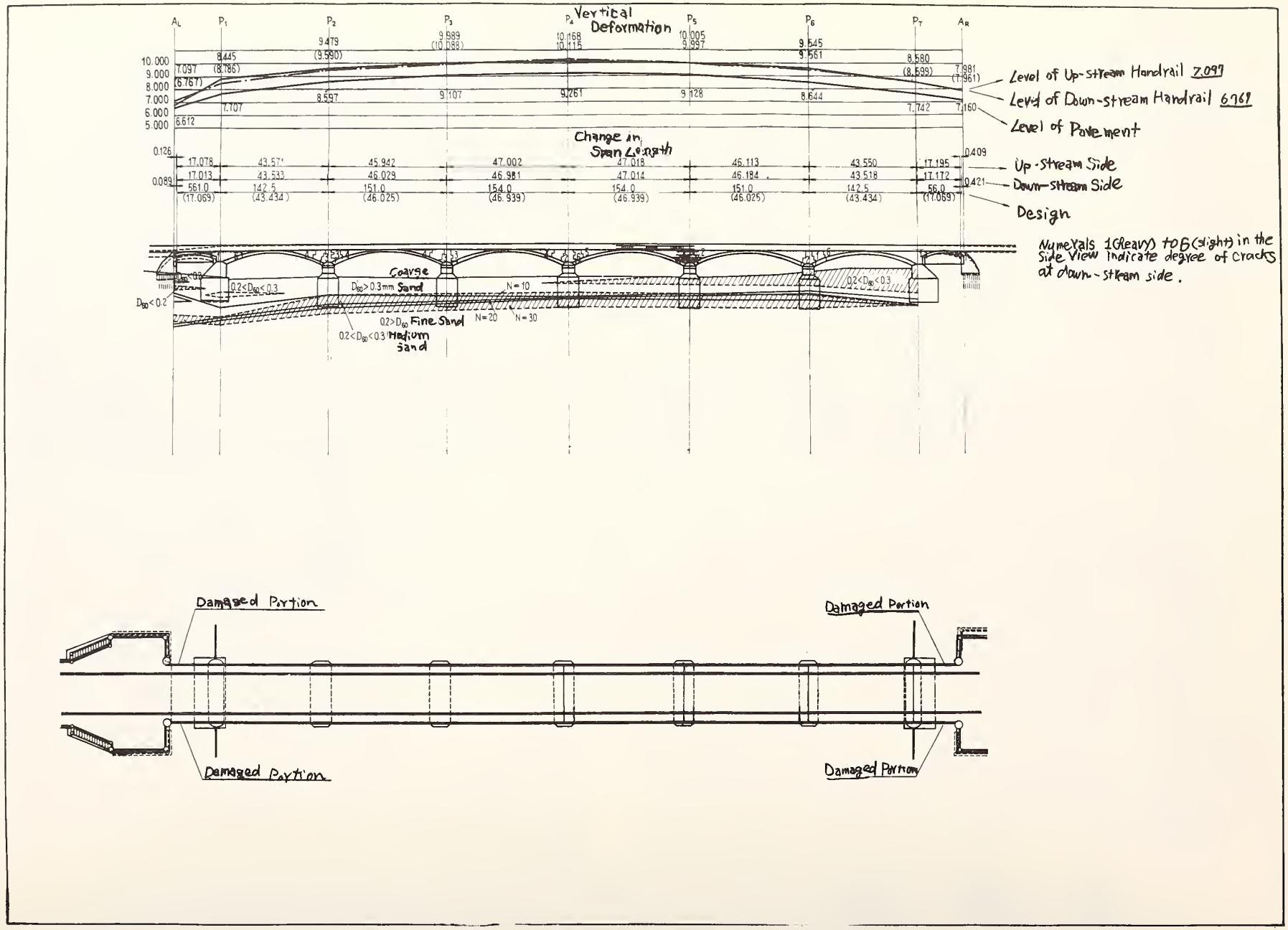

Fig. 2.27 Damage to the Bandai bridge

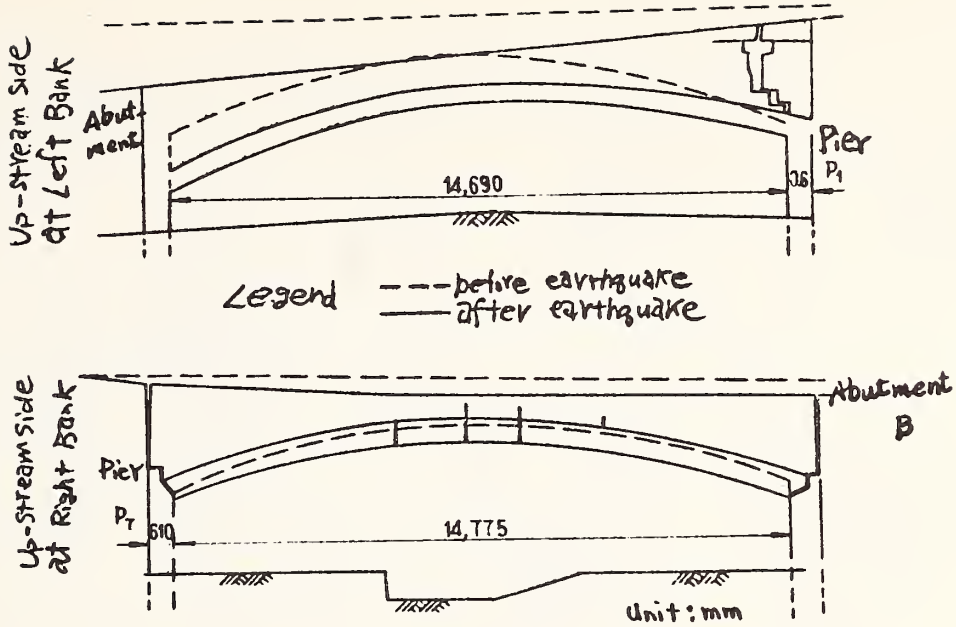

Fig. 2.28 Damage to the side spans of the Bandai bridge

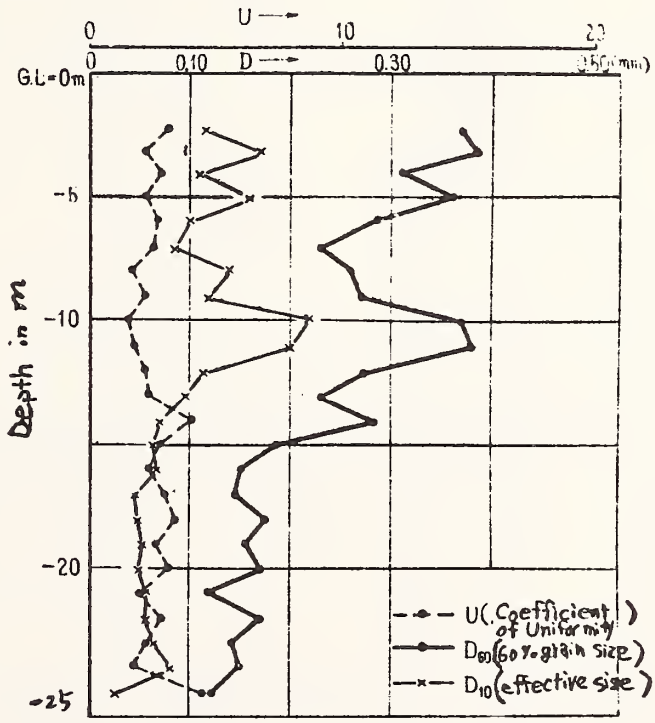

Fig. 2.29 Characteristics of soil grain size at the Showa bridge

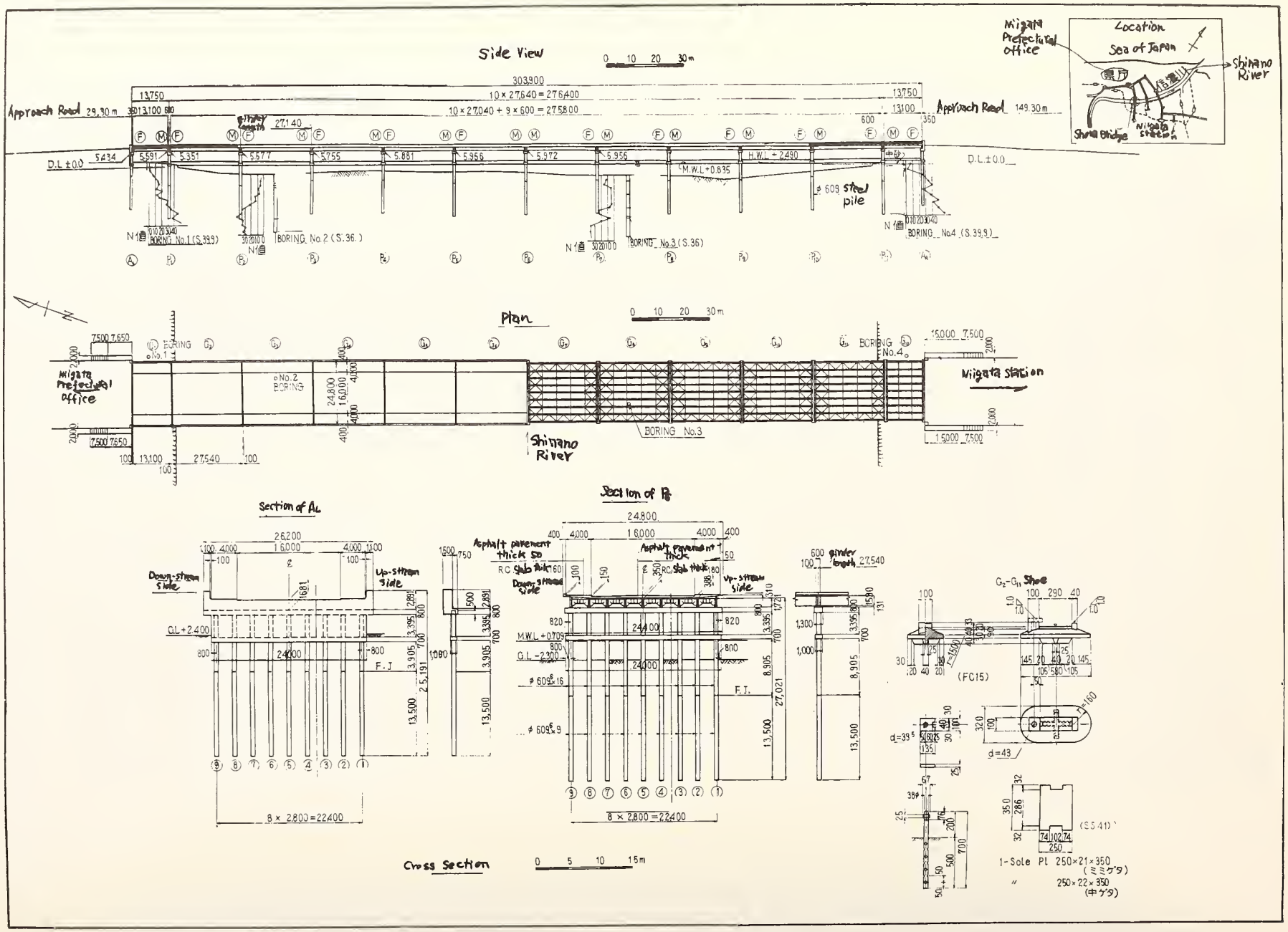

Fig. 2.30 General view of the Showa bridge

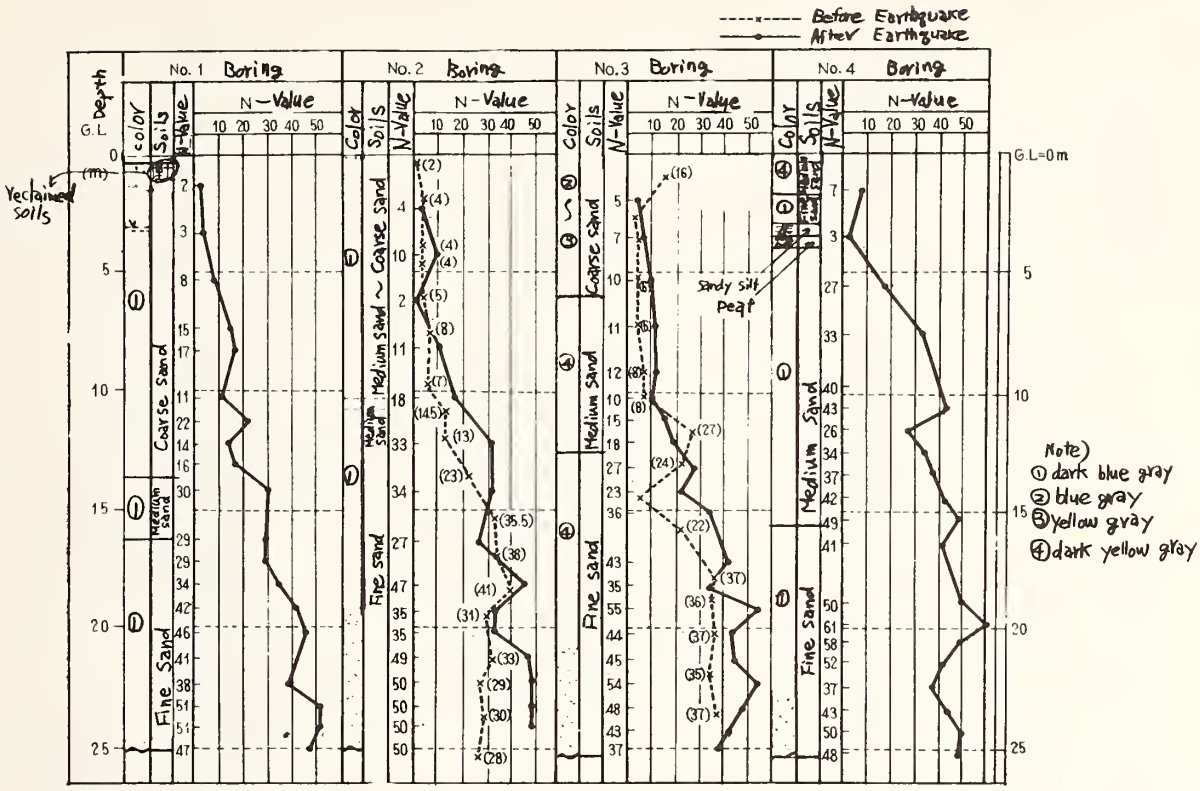

Fig. 2.31 Boring logs at the Showa bridge

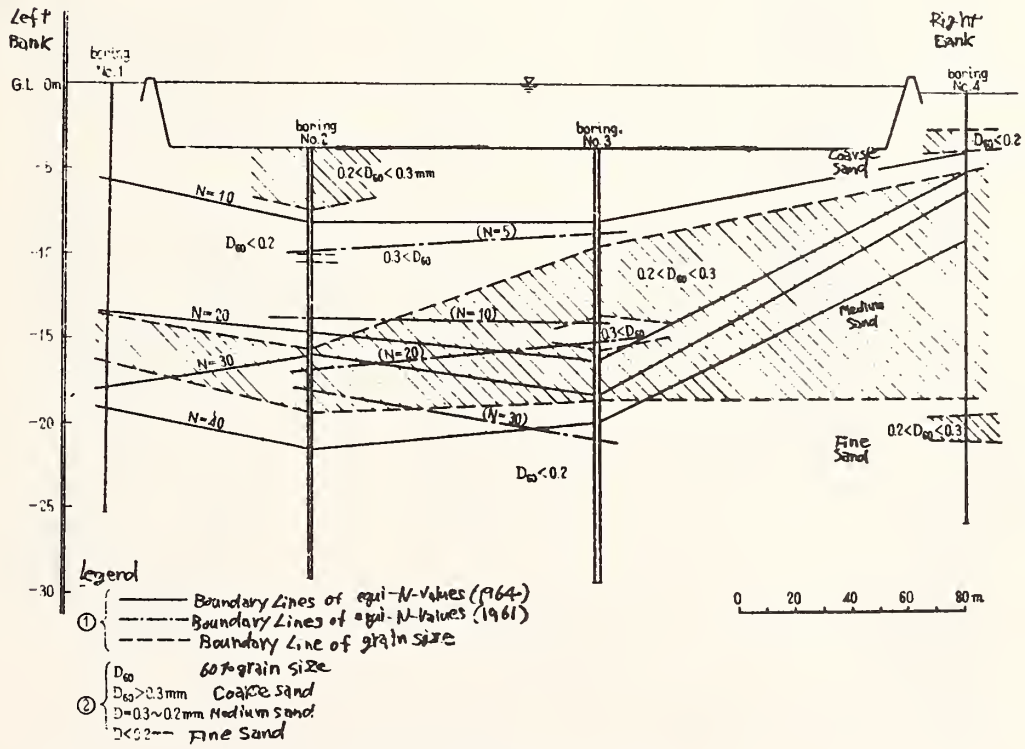

Fig. 2.32 Soil profile at the Showa bridge

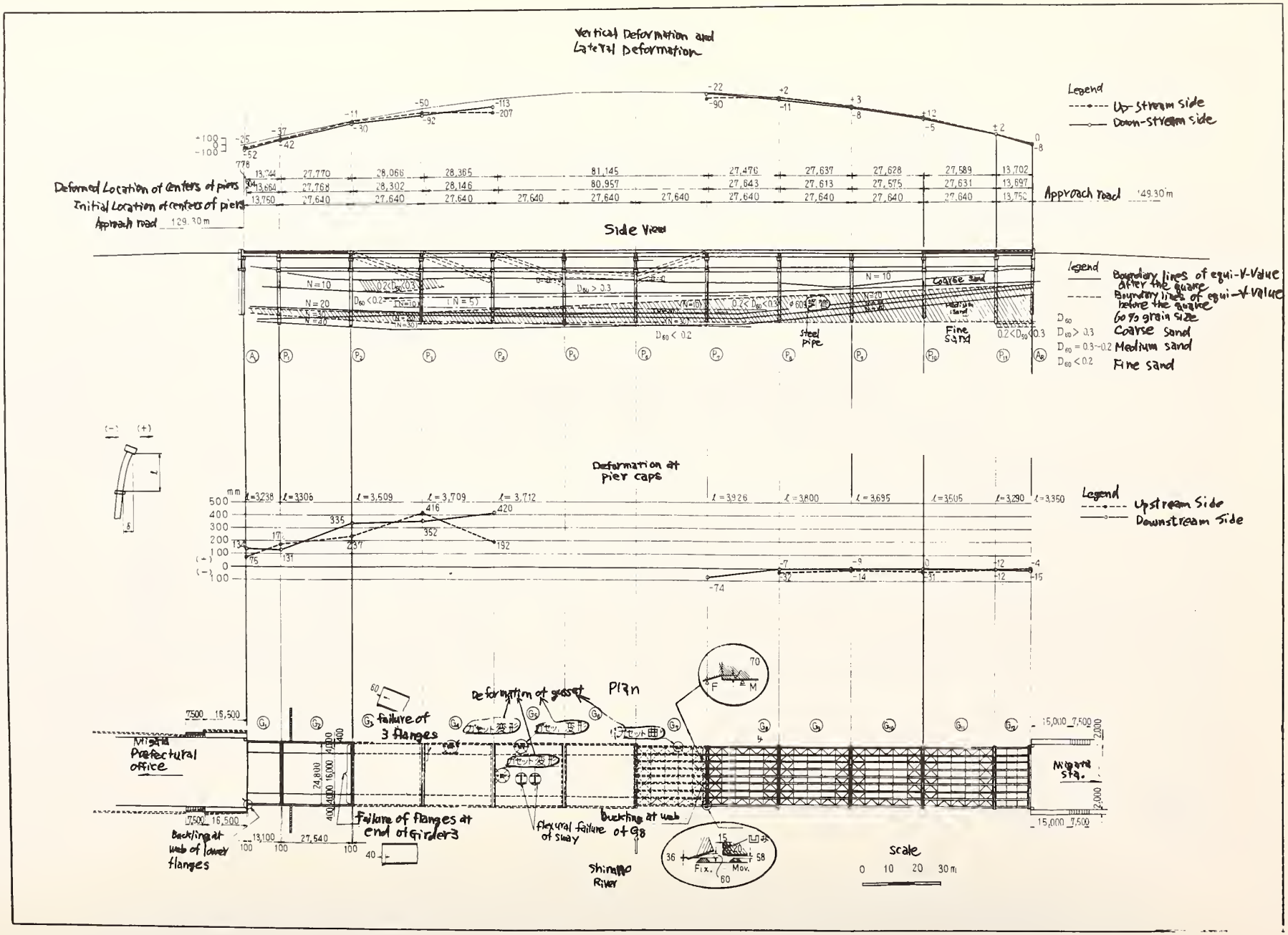

Fig. 2.33 Damage to the Showa bridge

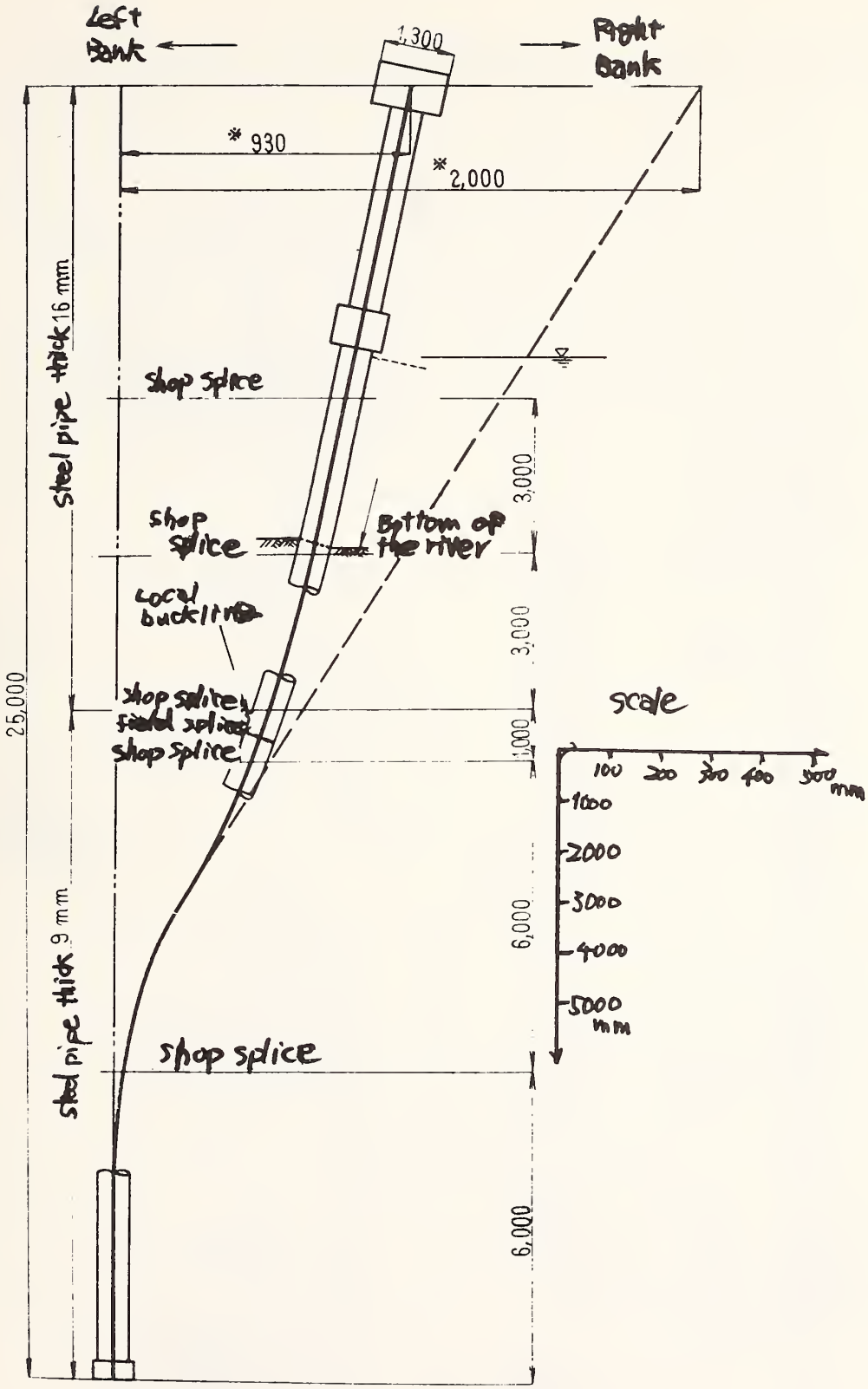

Fig. 2.34 Permanent deformation of a pile pulled out at the Showa bridge

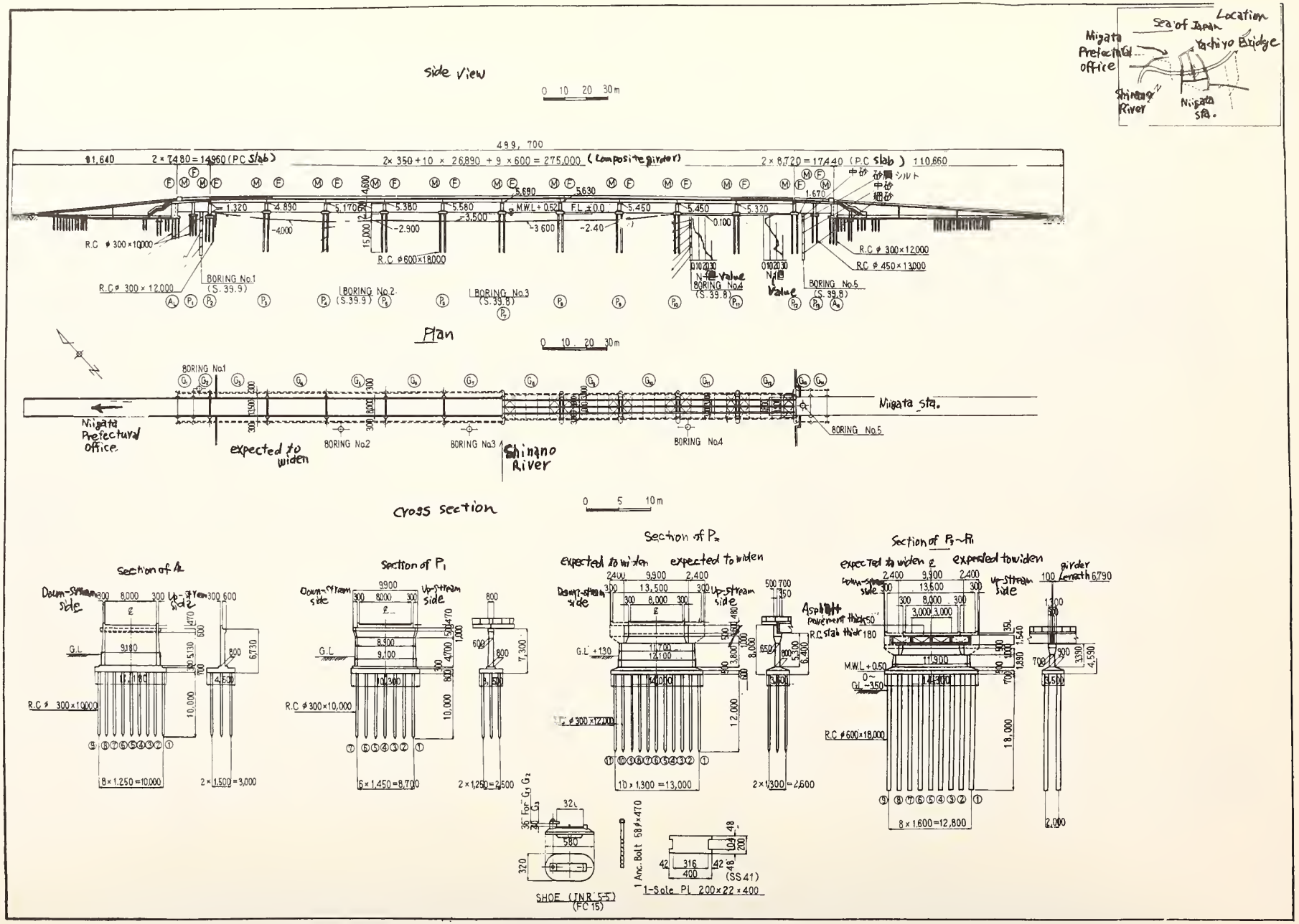

Fig. 2.35 General view of the Yachiyo bridge

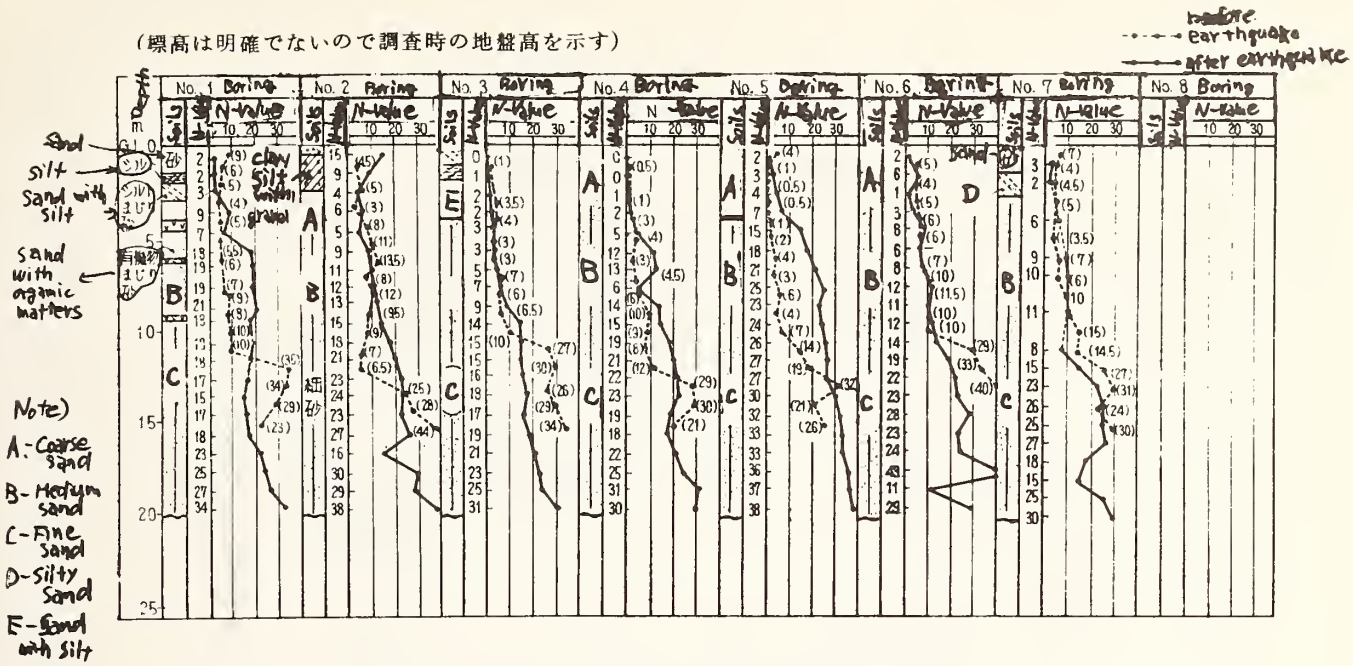

Fig. 2.36 Boring logs at the Yachiyo bridge

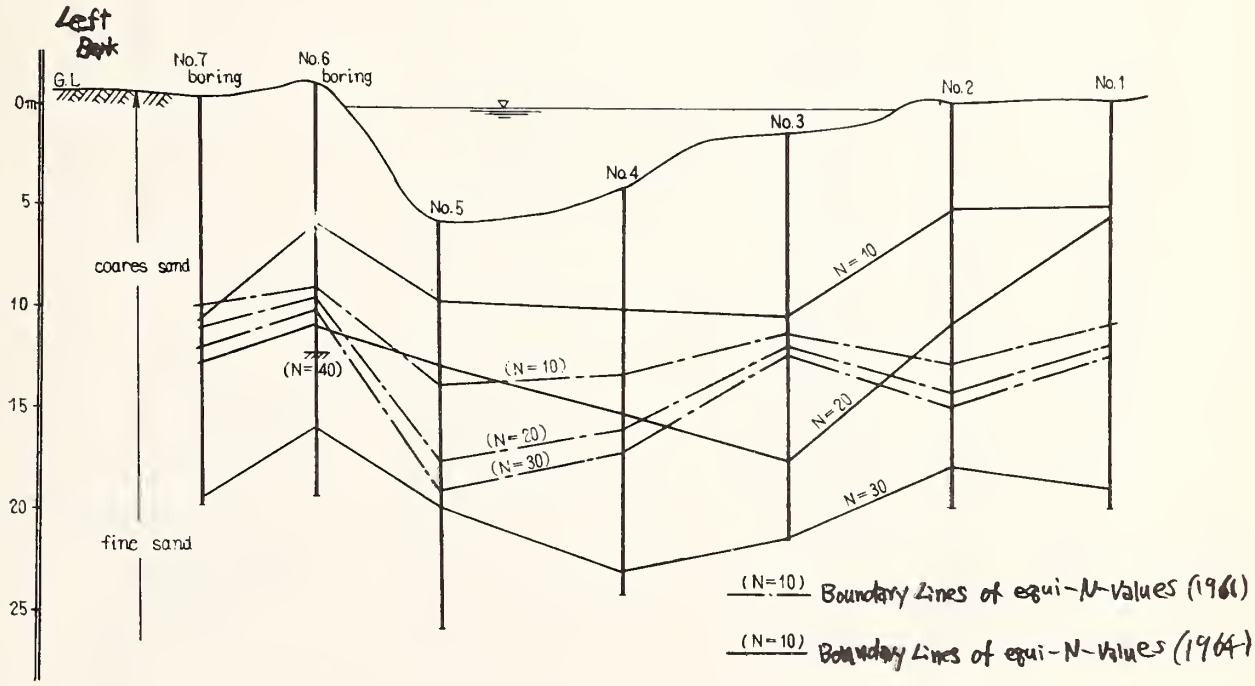

Fig. 2.37 Soil profile at the Yachiyo bridge

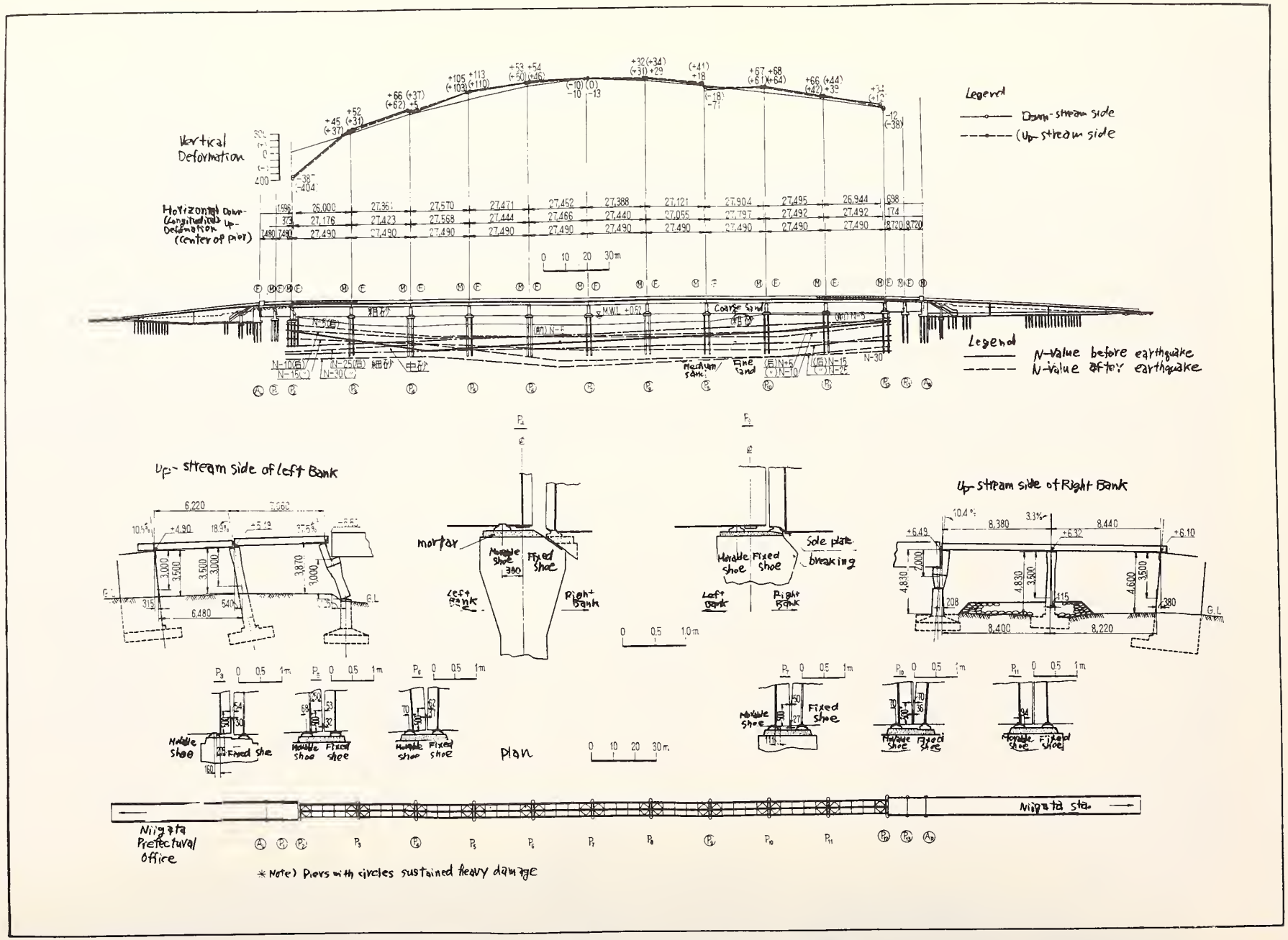

Fig. 2.38 Damage to the Yachiyo bridge

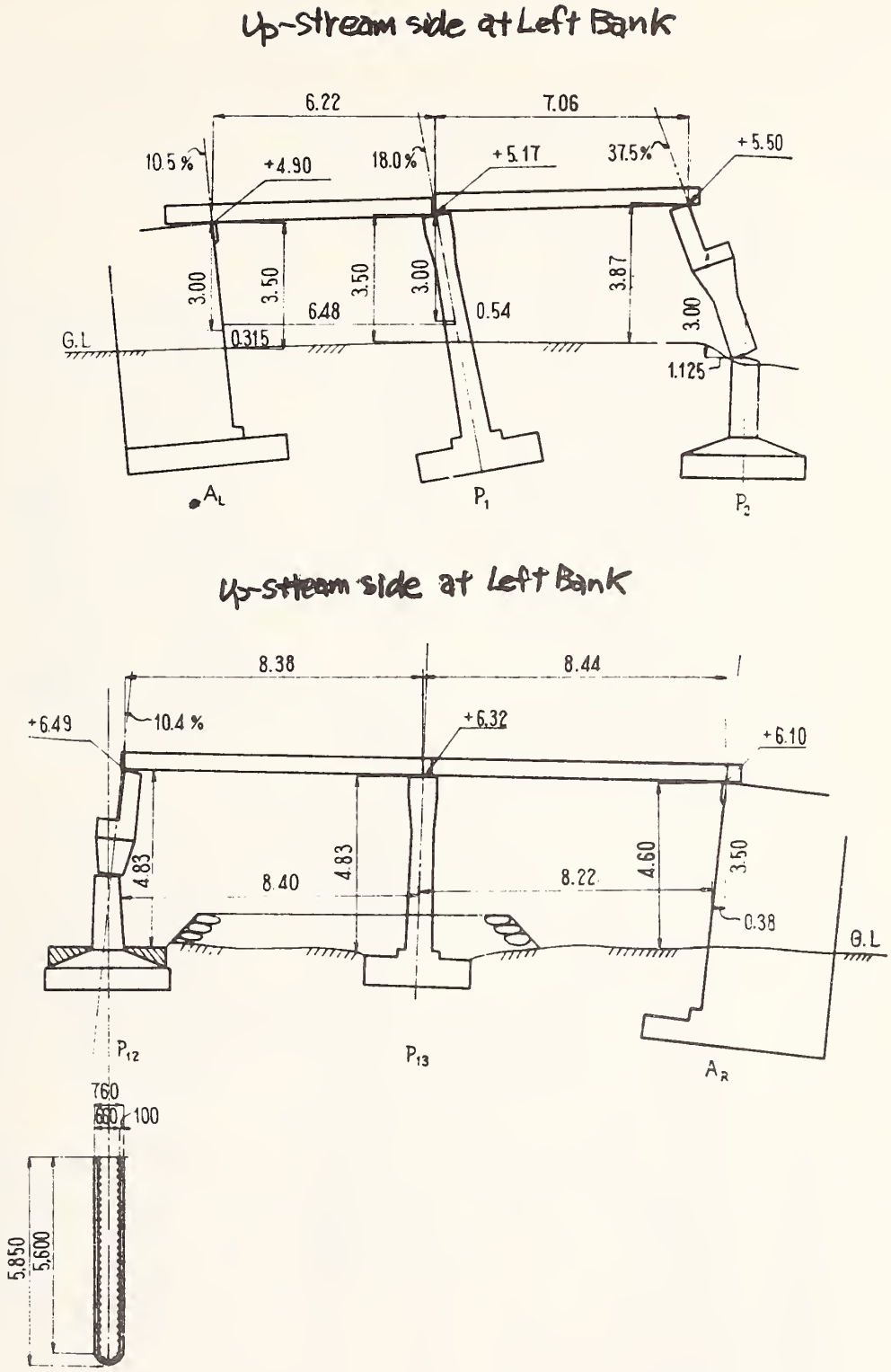

Fig. 2.39 Deformation of the side spans of the Yachiyo bridge

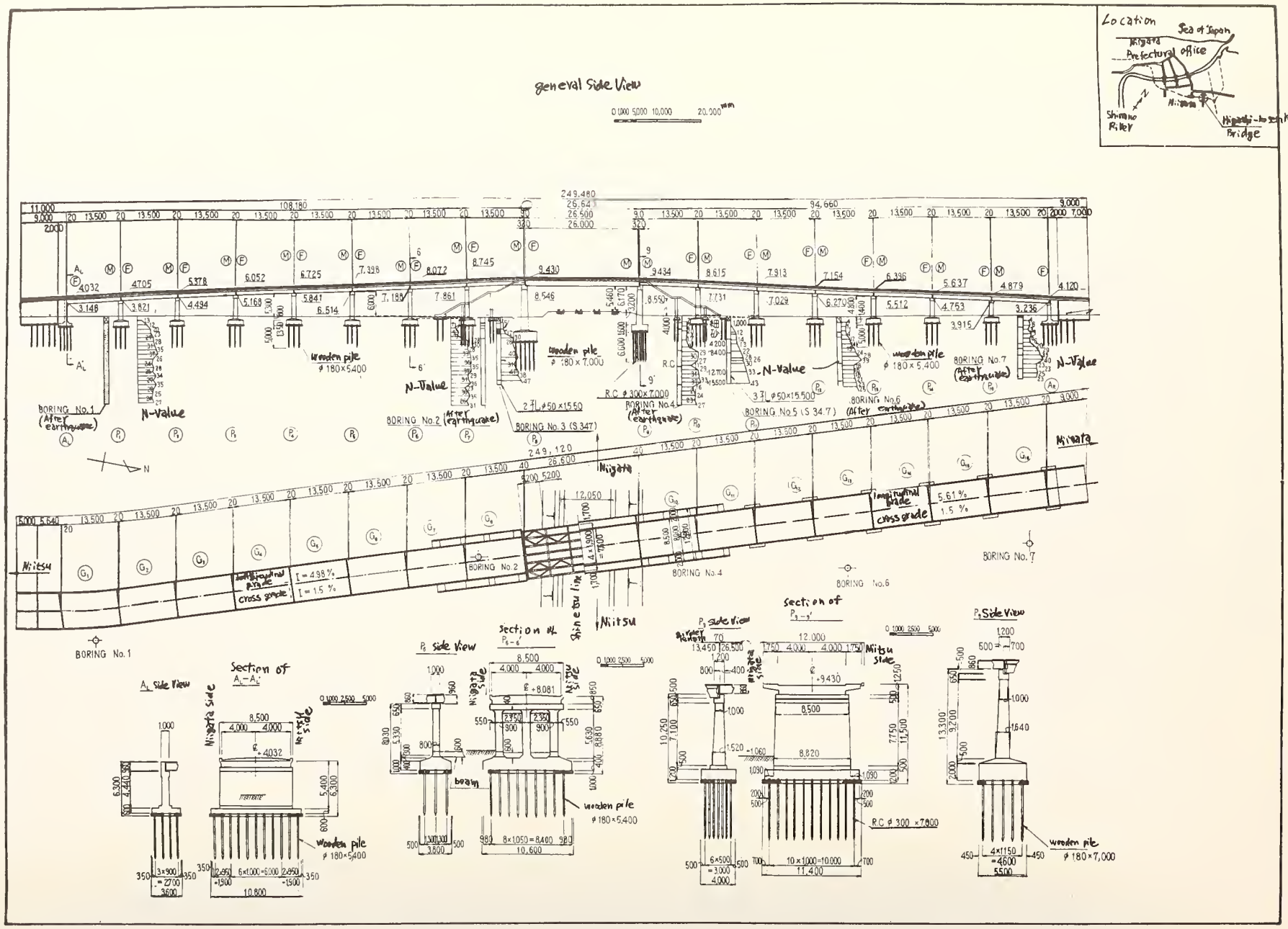

Fig. 2.40 General view of the Higashi-Kosenkyo bridge

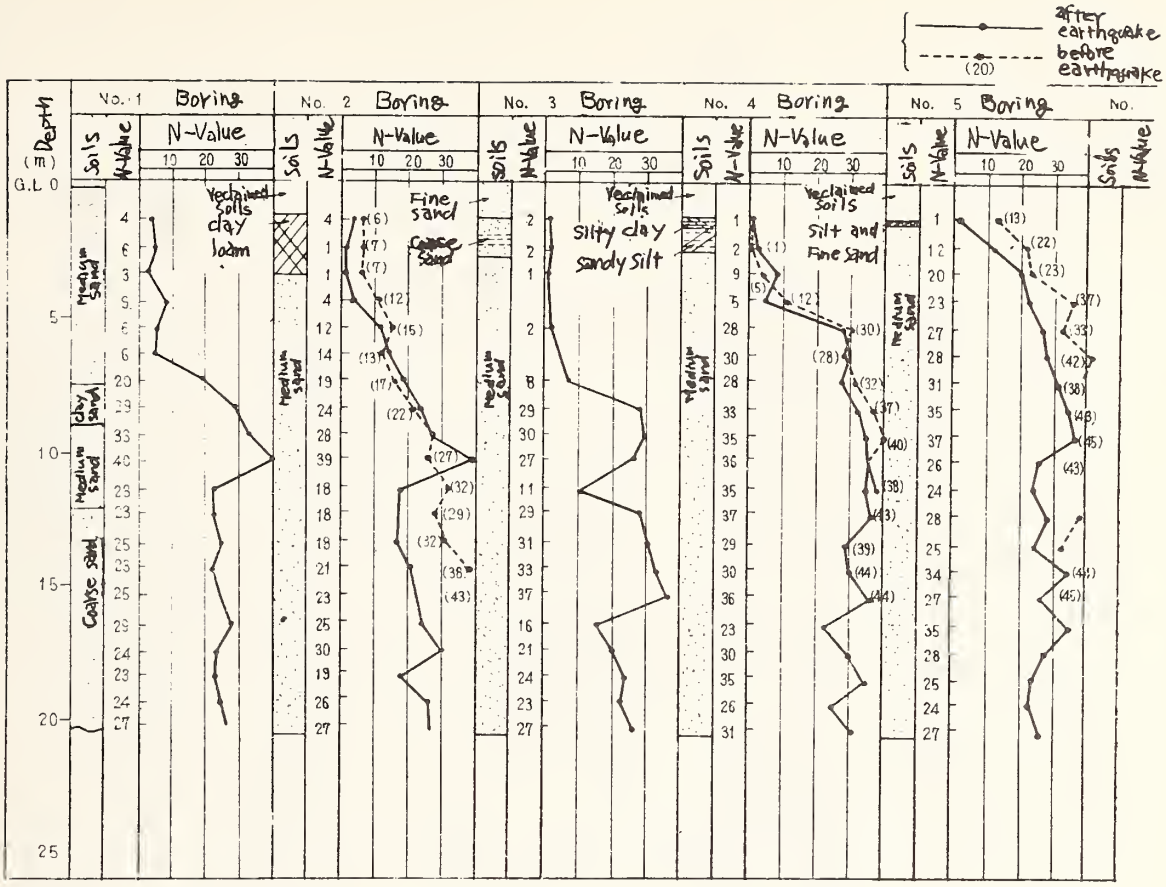

Fig. 2.41 Boring logs at the Higashi-Kosenkyo bridge

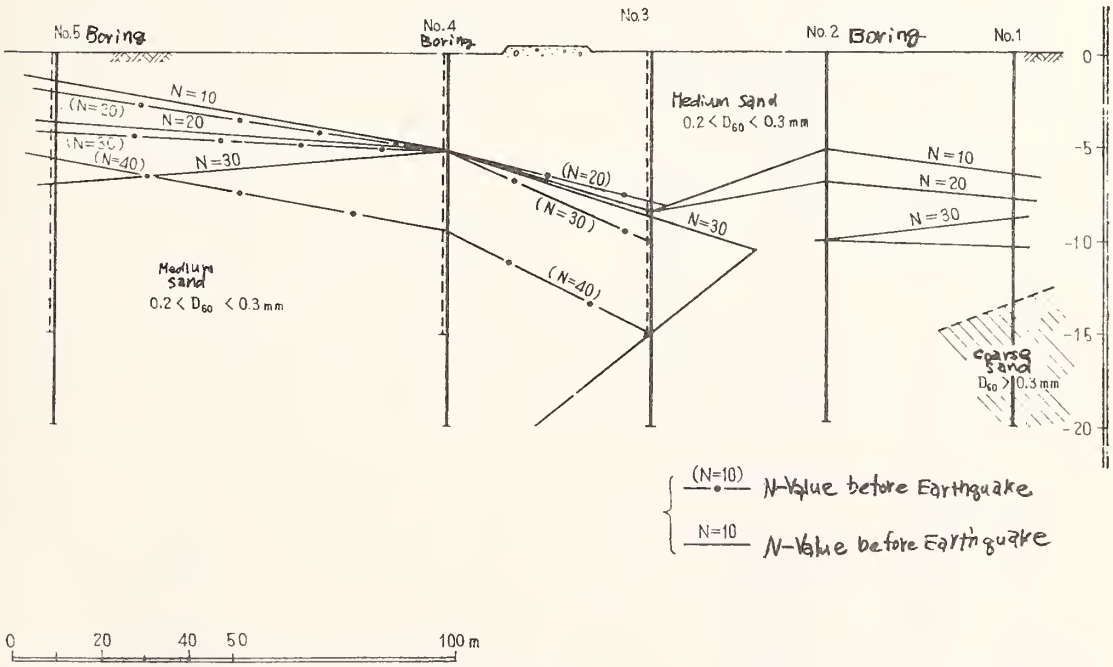

Fig. 2.42 Soil profile at the Higashi-Kosenkyo bridge

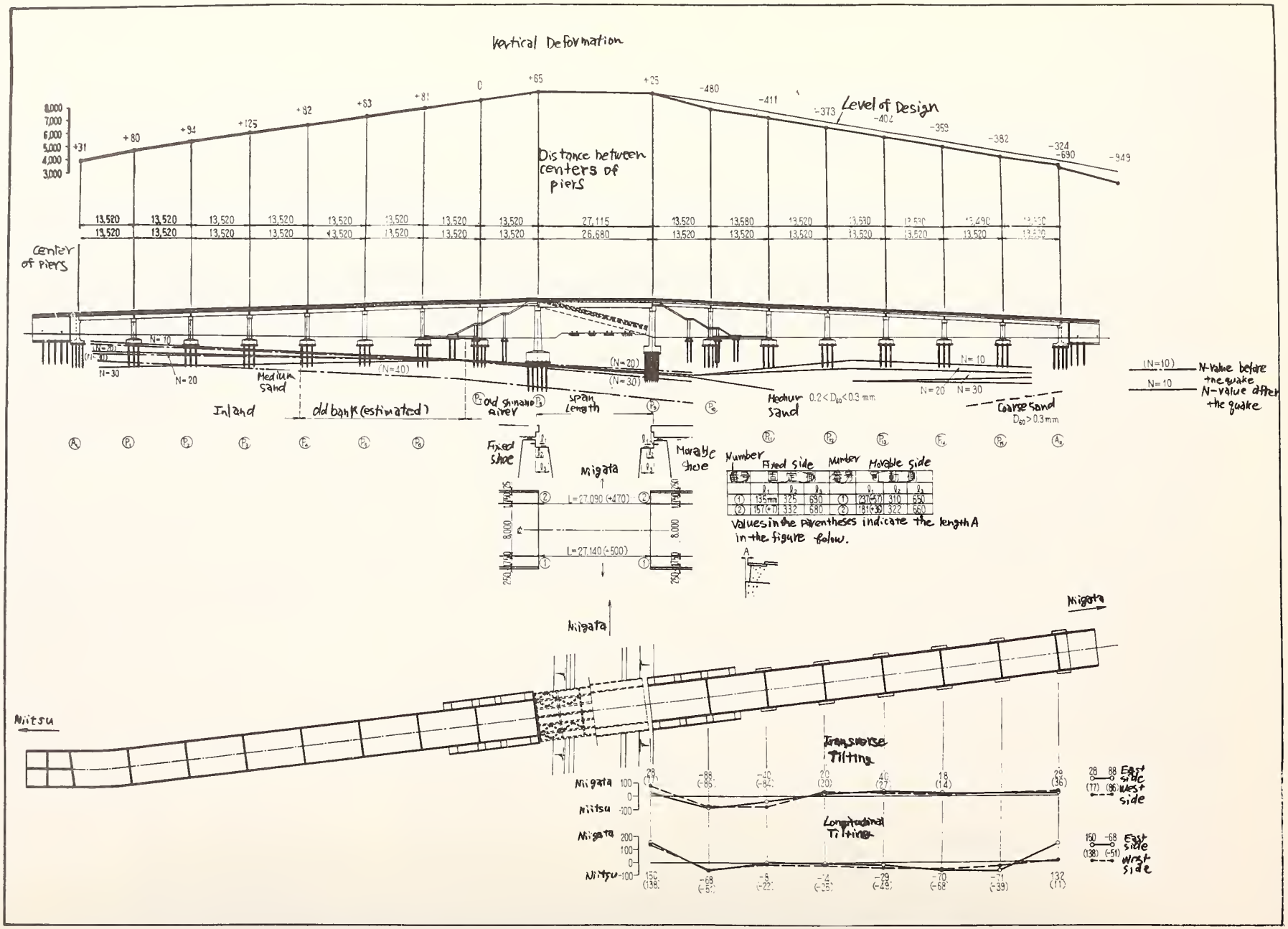

Fig. 2.43 Damage to the Higashi-Kosenkyo bridge

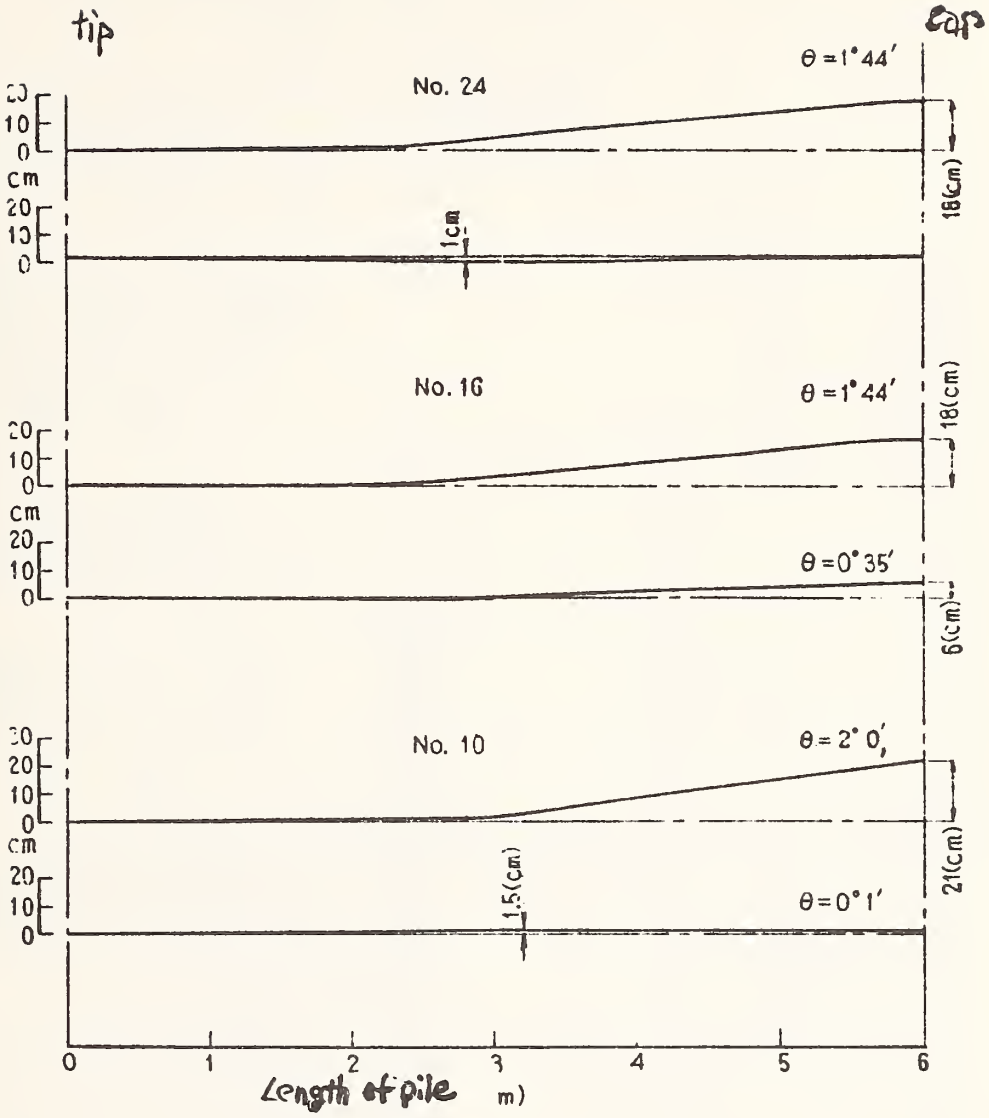

Fig. 2.44 Deformations of some piles at the Higashi-Kosenkyo bridge

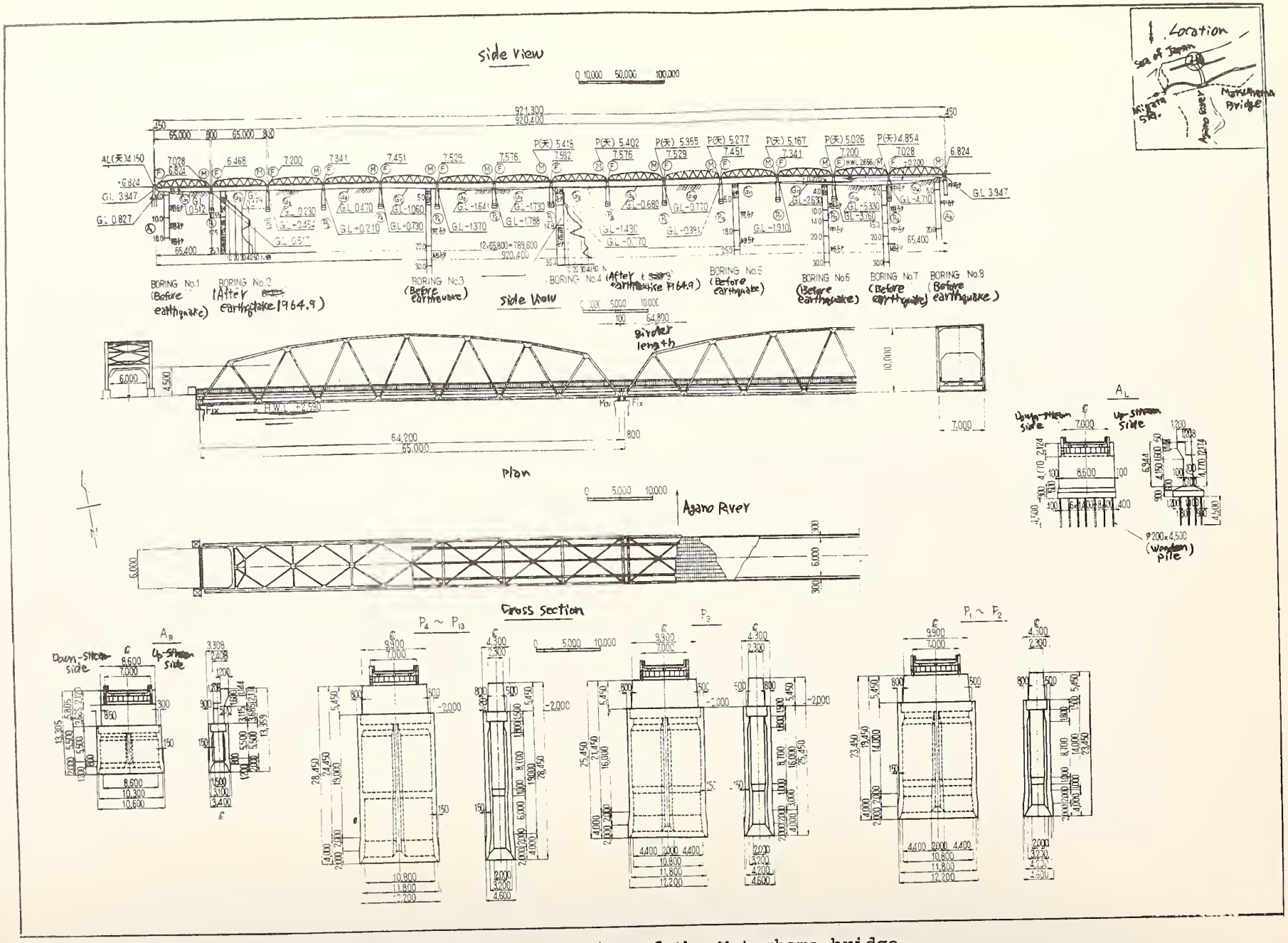

Fig. 2.45 General view of the Matsuhama bridge

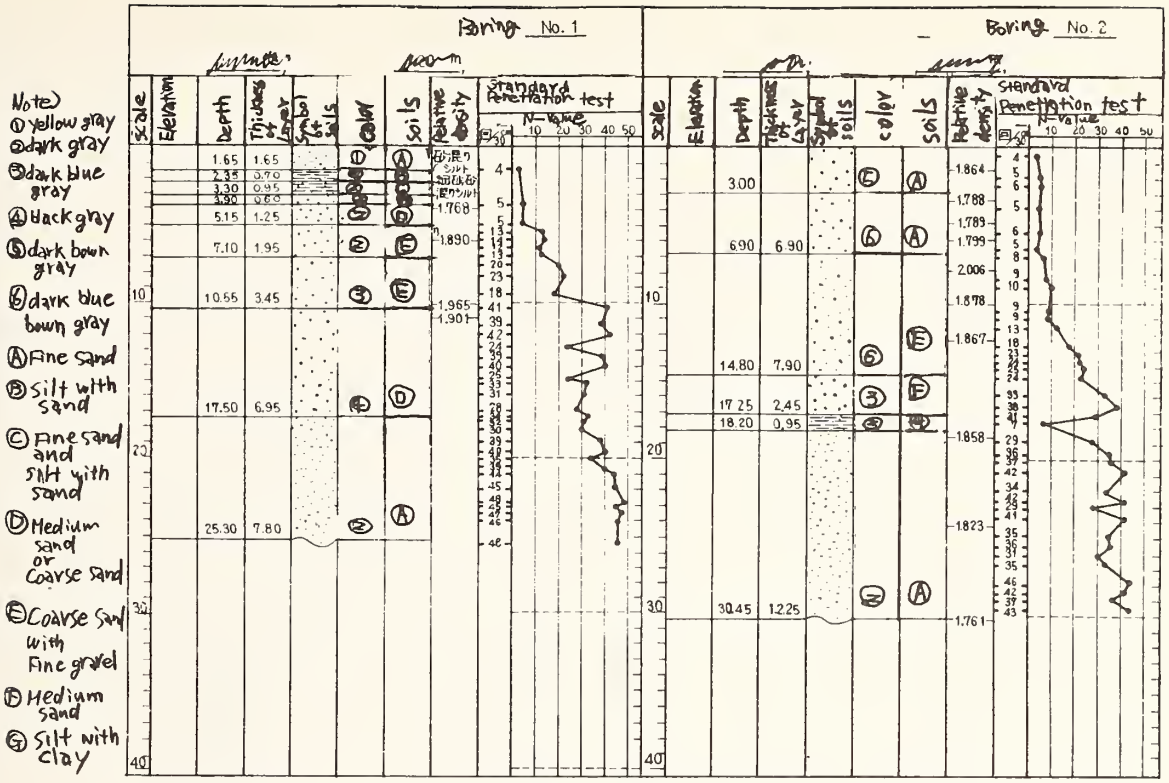

Fig. 2.46 Boring logs at the Matsuhama bridge

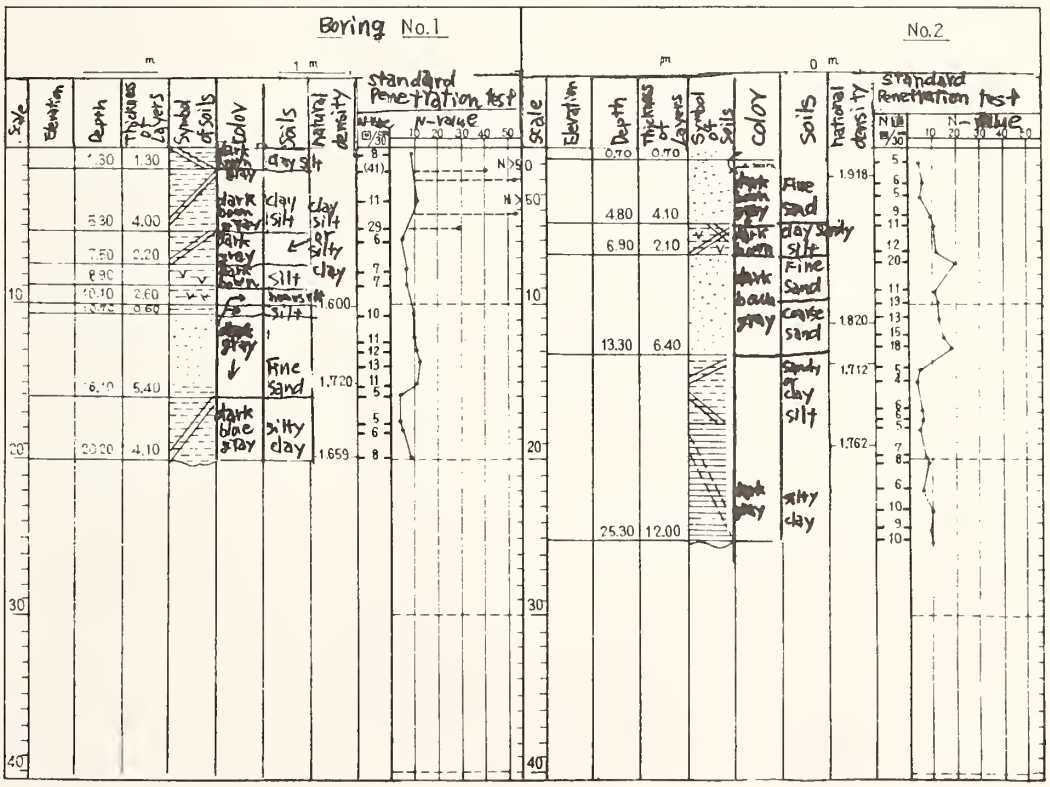

Fig. 2.47 Boring logs at the Kosudo bridge

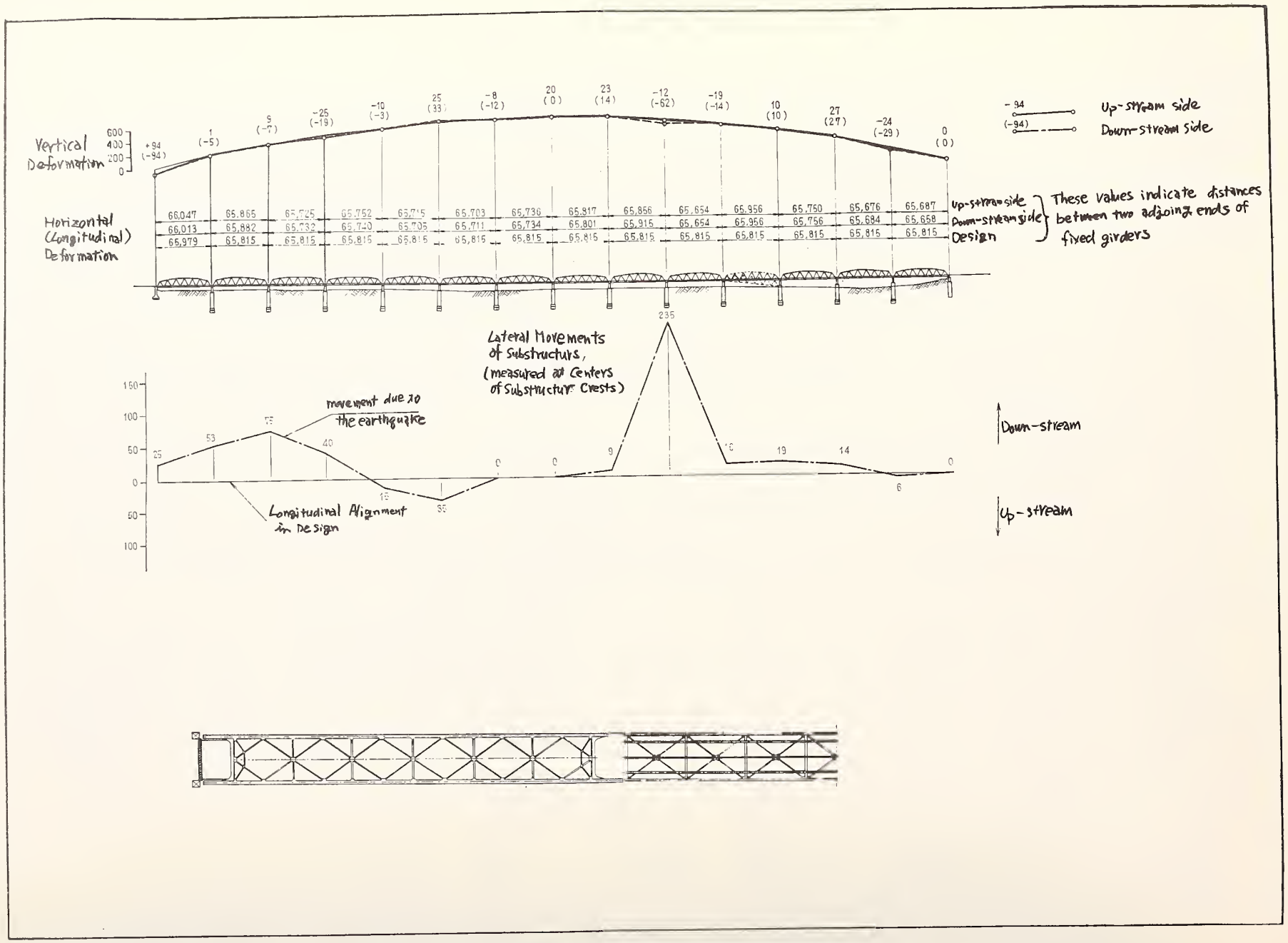

Fig. 2.48 Damage to the Matsuhama bridge

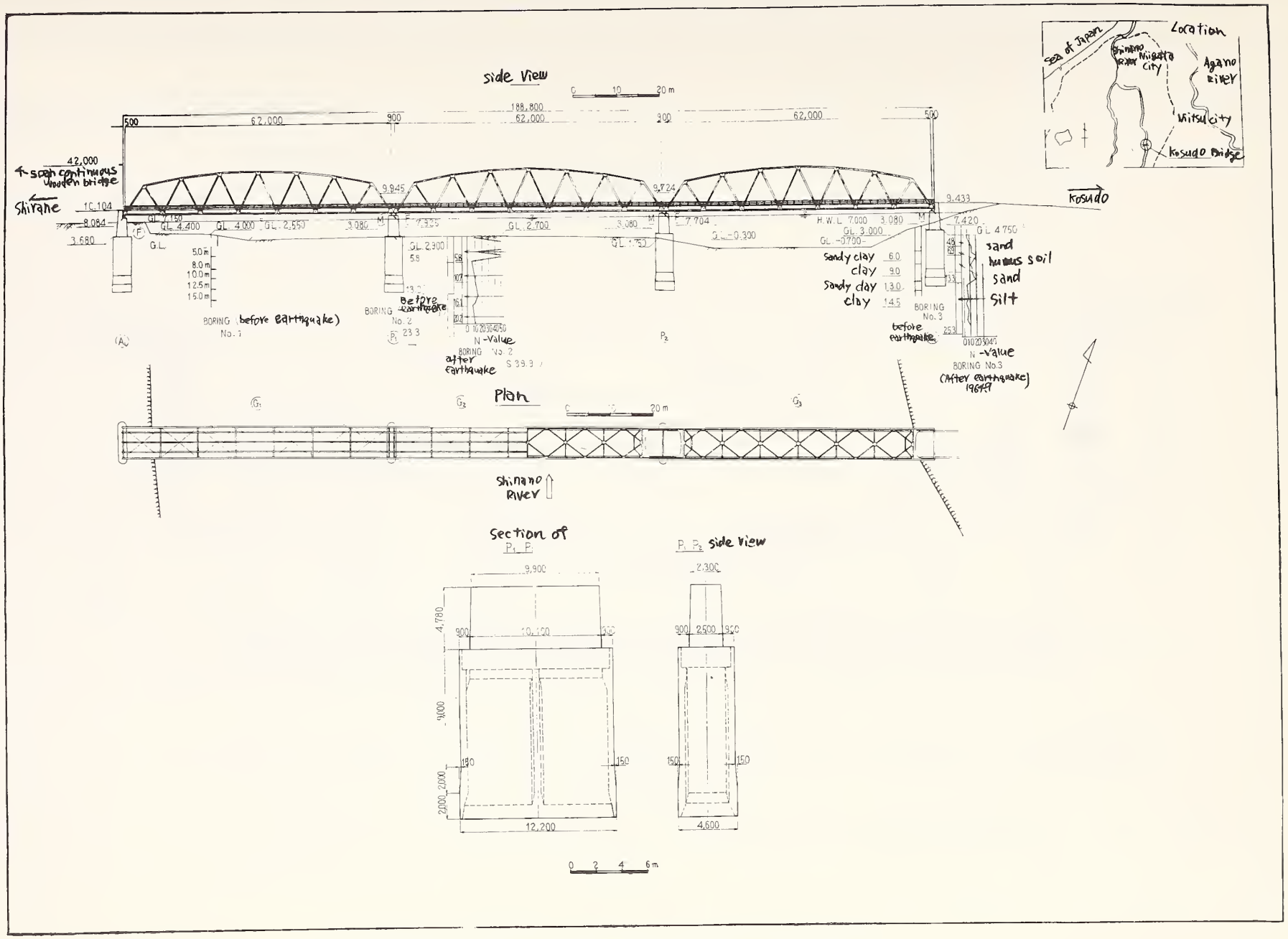

Fig. 2.49 General view of the Kosudo bridge

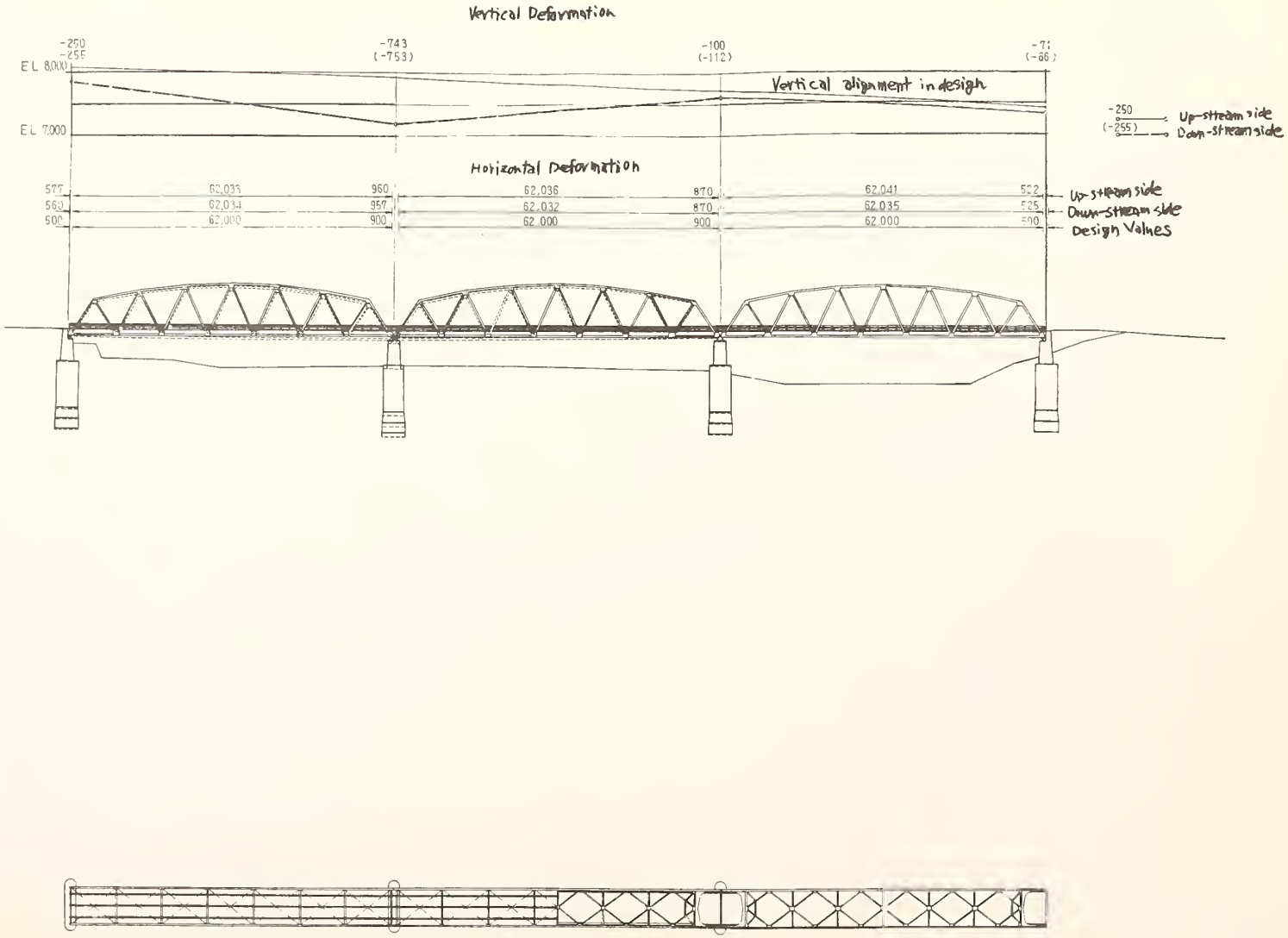

Fig. 2.50 Damage to the Kosudo bridge

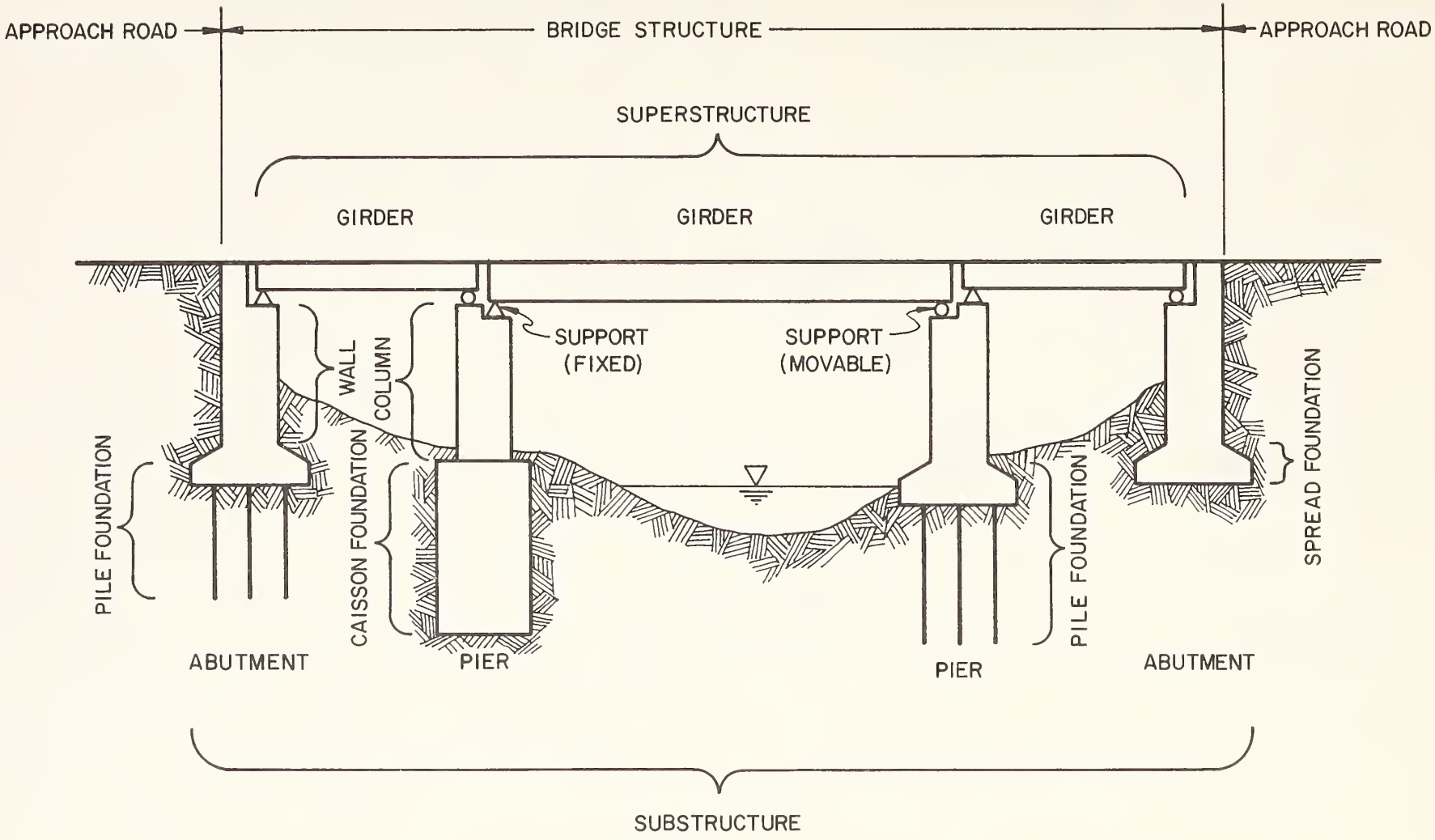

Fig. 2.51 Schematic sketch of a typical highway bridge

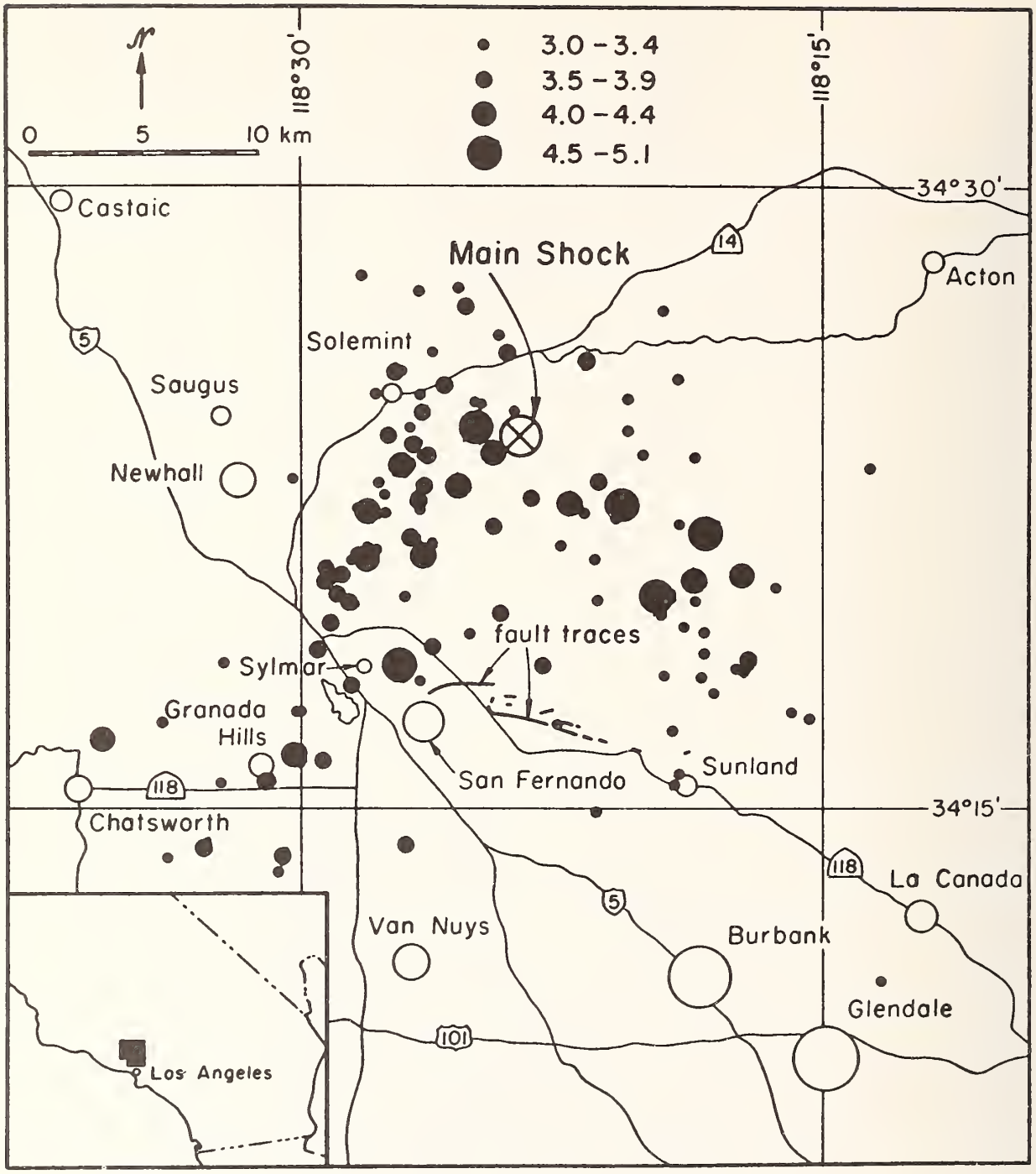

Fig. 2.52 Locations of main and larger aftershocks - Allen et al.

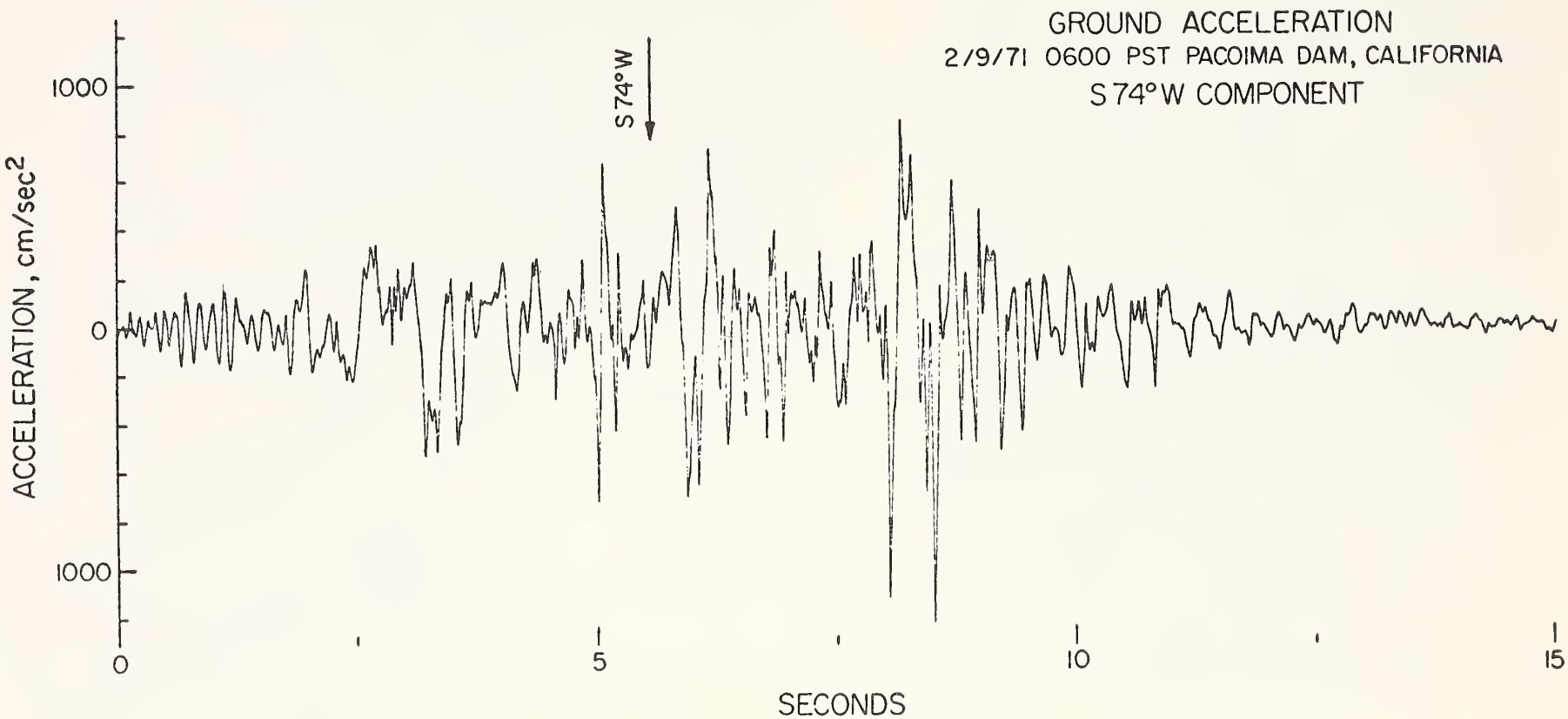

NOAA STRONG-MOTION ACCELEOGRAPH NETWORK AND
THE EARTHQUAKE ENGINEERING RESEARCH LABORATORY
CALIFORNIA INSTITUTE OF TECHNOLOGY

Fig. 2.53 Ground acceleration time history at Pacoima Dam

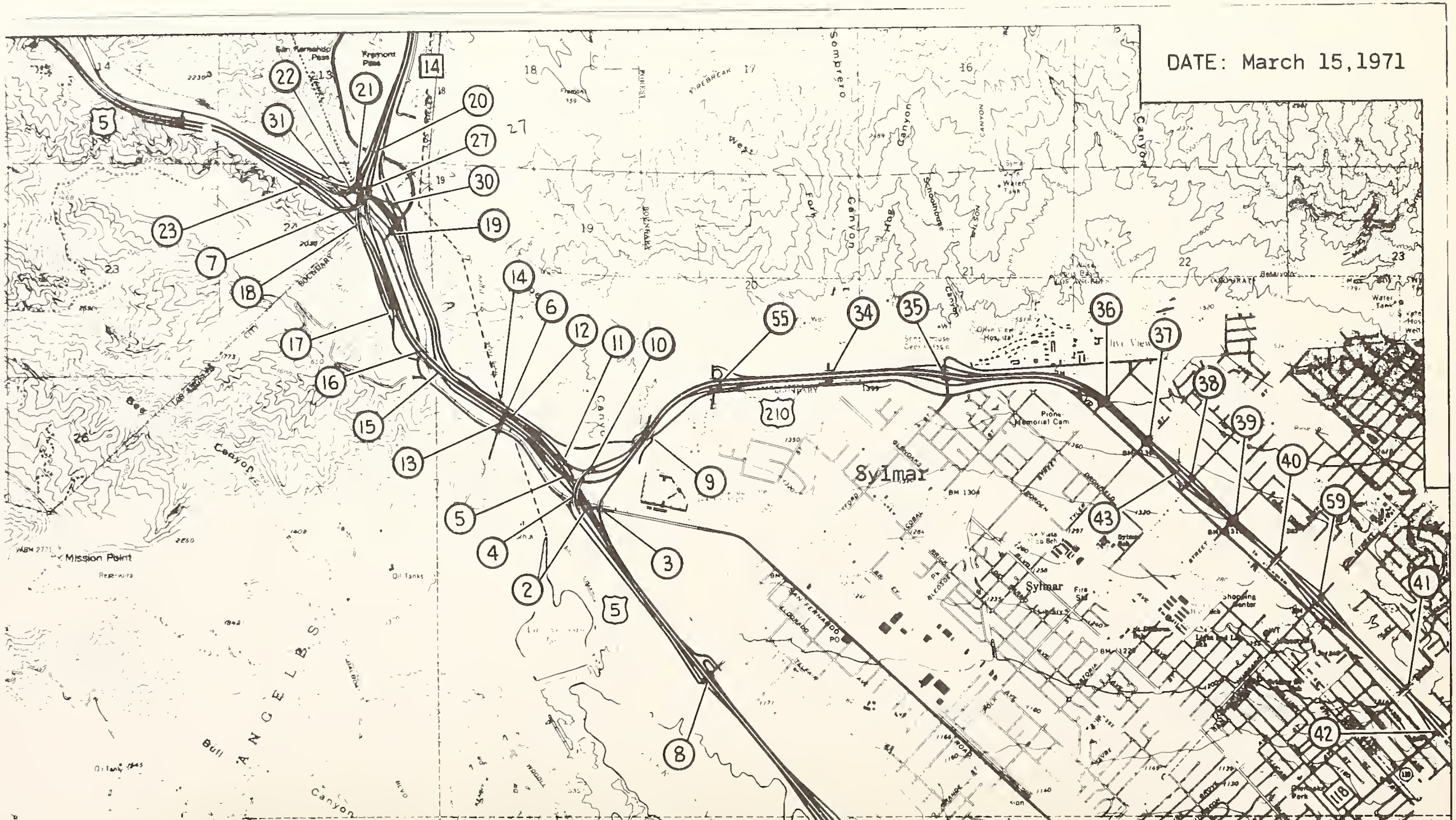

Fig. 2.54 General arrangement of bridges and overcrossings.

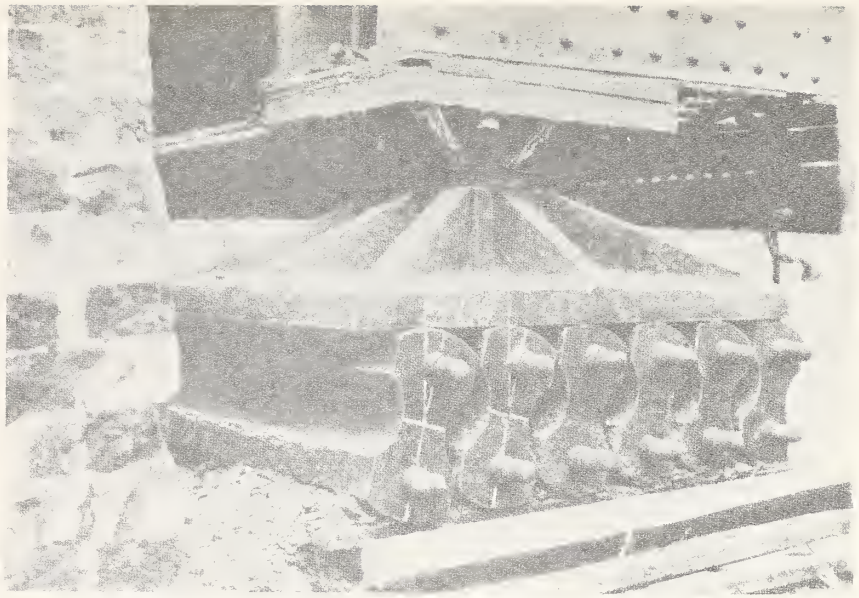

Photo. 2.1 Damage to the east support at the southern abutment of the Shinminato bridge.

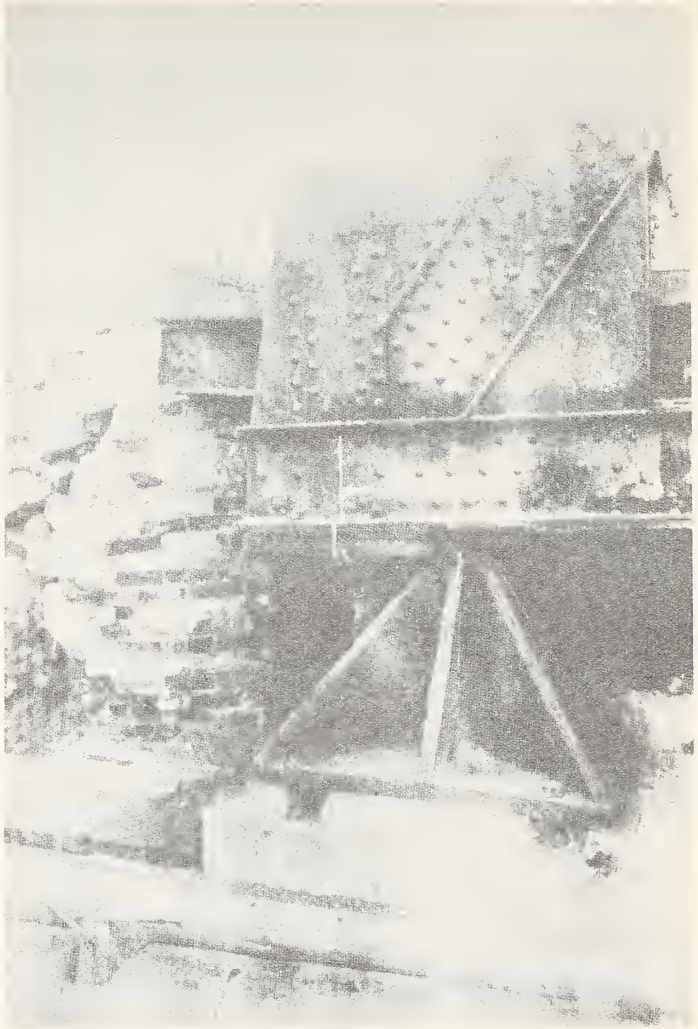

Photo. 2.2 Damage to the west support at the northern abutment of the Shinminato bridge.

Photo. 2.3 Damage to the Bankoku bridge
(note heavy cracks at the abutment)

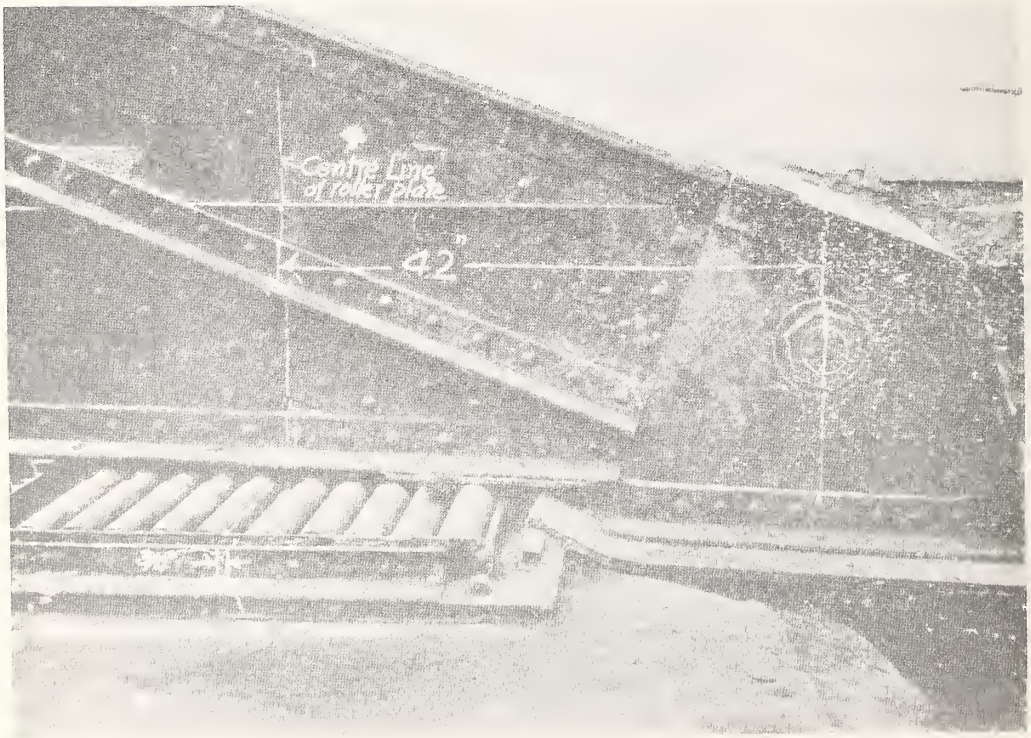

Photo. 2.4 Damage to the east support at the northern abutment of the Bankoku bridge (note the large dislocation).

Photo. 2.5 Damage to the east support at the southern abutment of the Bankoku bridge (note anchor bolts sheared off).

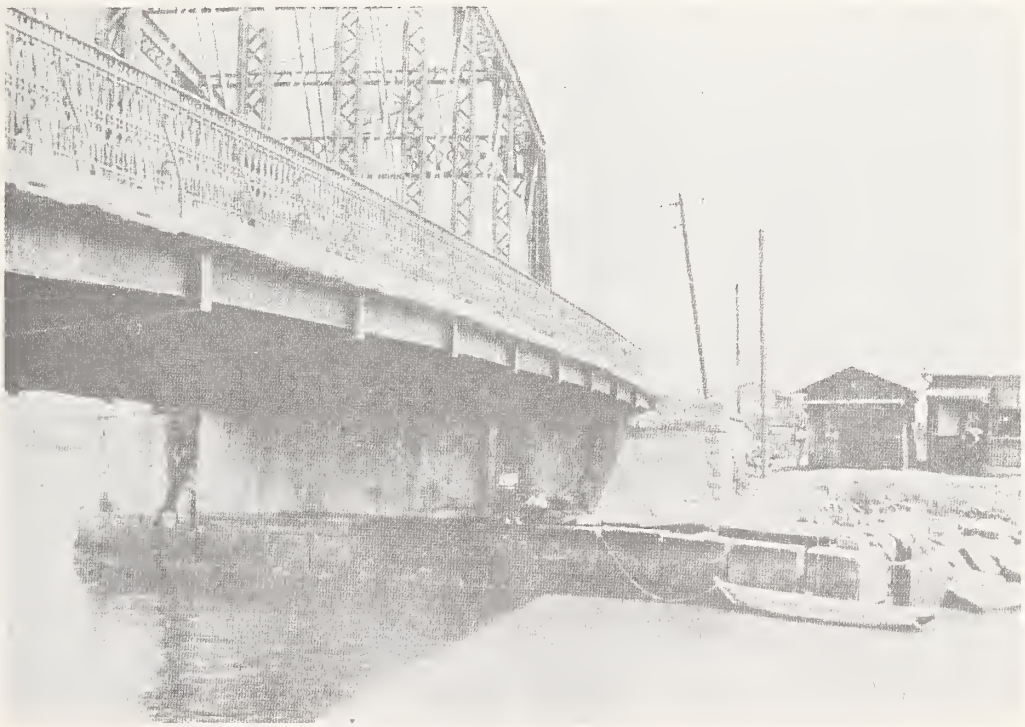

Photo. 2.6 Damage to the right-bank abutment of the Yamashita bridge.

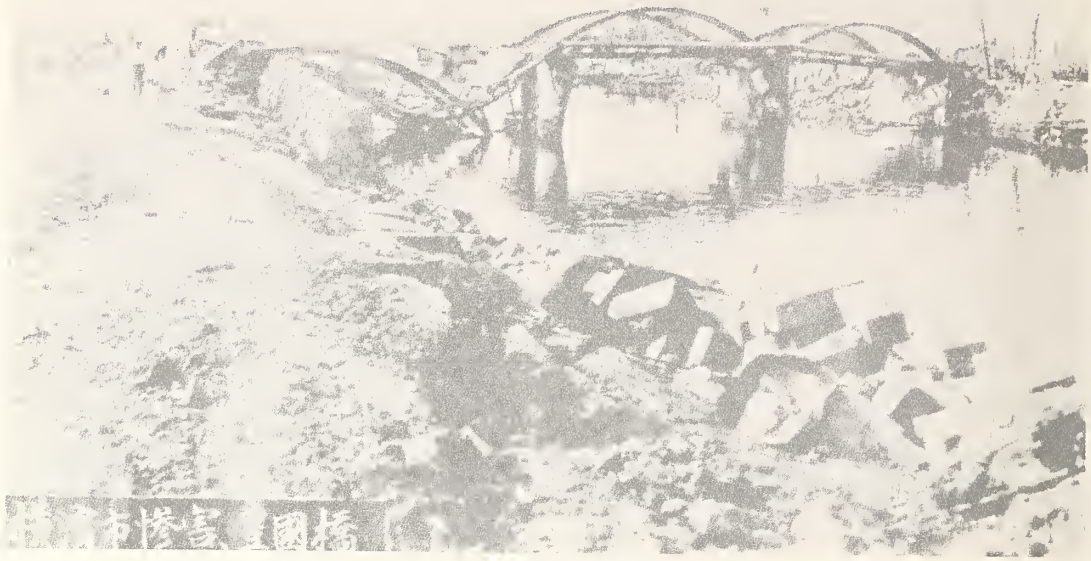

Photo. 2.7 Damage to the Toyokuni bridge

Photo. 2.8 Damage to the pier and the truss of the Toyokuni bridge

Photo. 2.9 Damage to the Sakawa bridge

Photo. 2.10 Damaged piers and girders of the Sakawa bridge

Photo. 2.11 Damage to the left abutment of the Sakawa bridge

Photo. 2.12 Damage to the piers of the Banyu bridge while under construction.

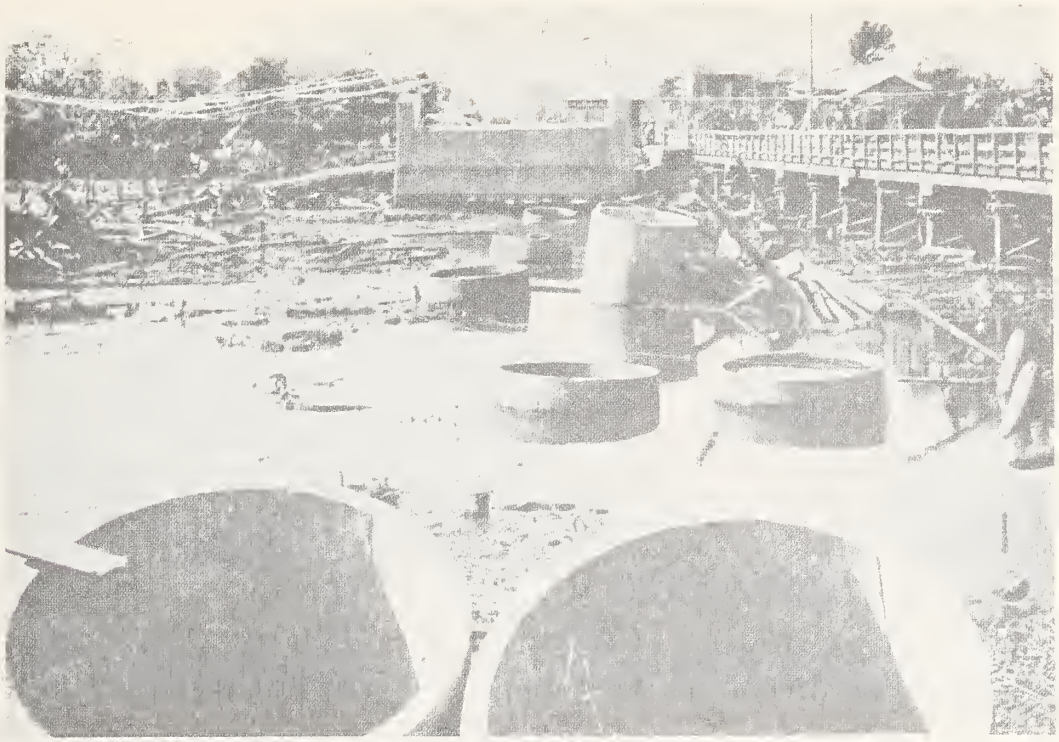

Photo. 2.13 Damage to the caisson foundations of the Banyu bridge while under construction.

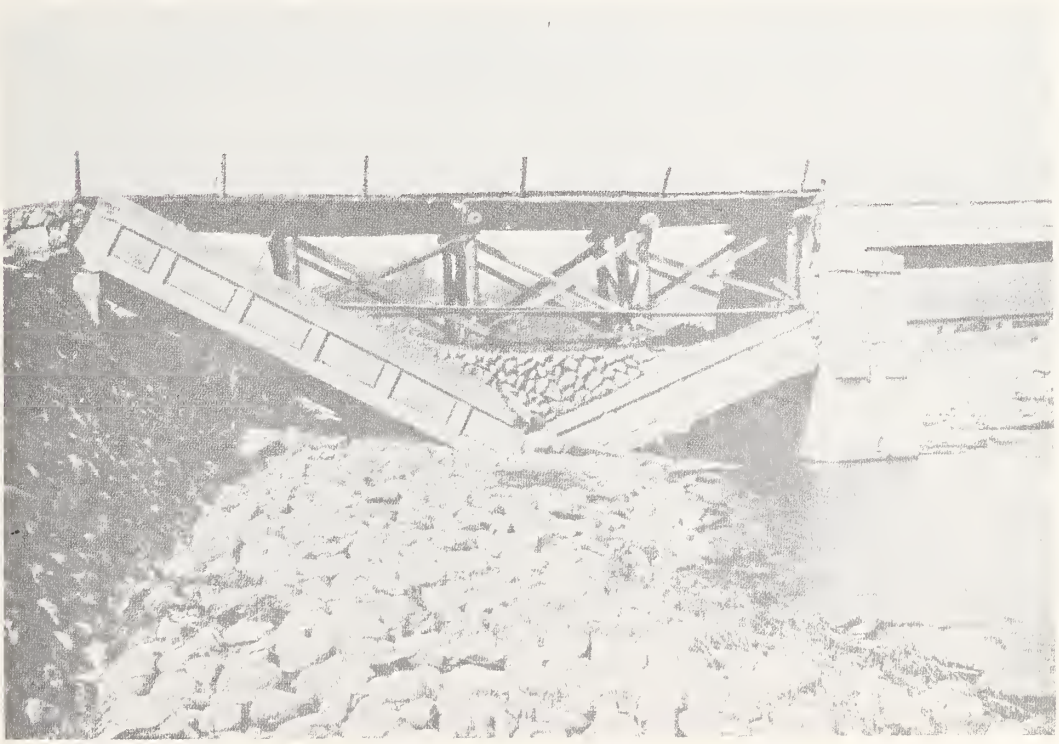

Photo. 2.14 Damage to the Hayakawa bridge

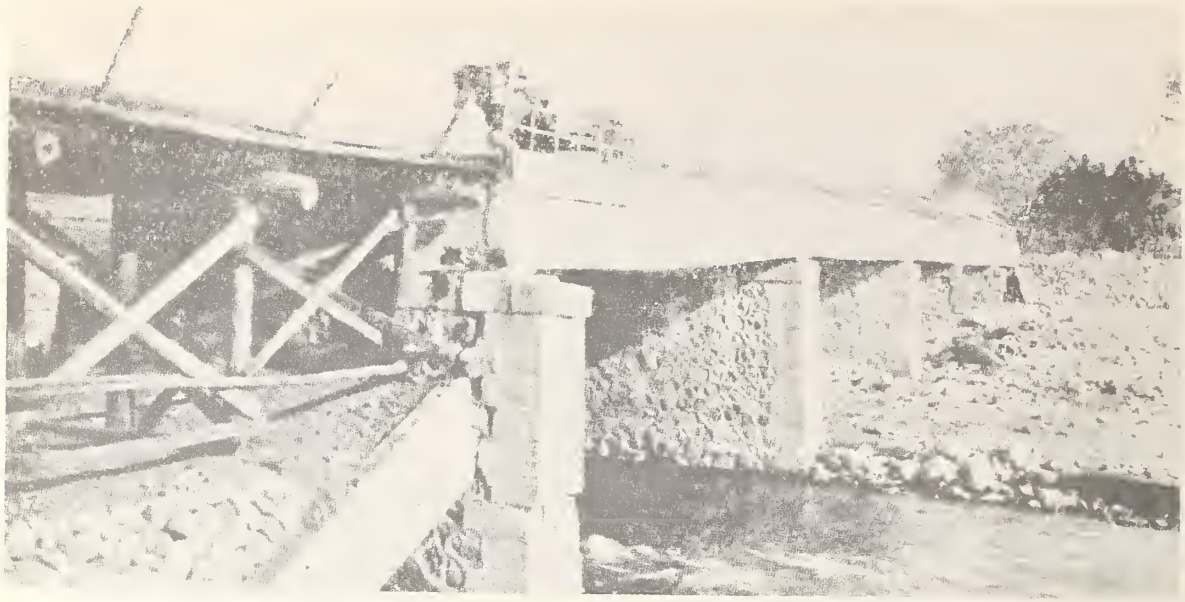

Photo. 2.15 Damage to the Hayakawa bridge

Photo. 2.16 Damage to a pier of the Takahata bridge

Photo. 2.17 Damage to the fifth pier of the Takahata bridge.

Photo. 2.18 Damage to the right abutment of the Takahata bridge.

Photo. 2.19 Damage to the support shoes of the Kumano bridge

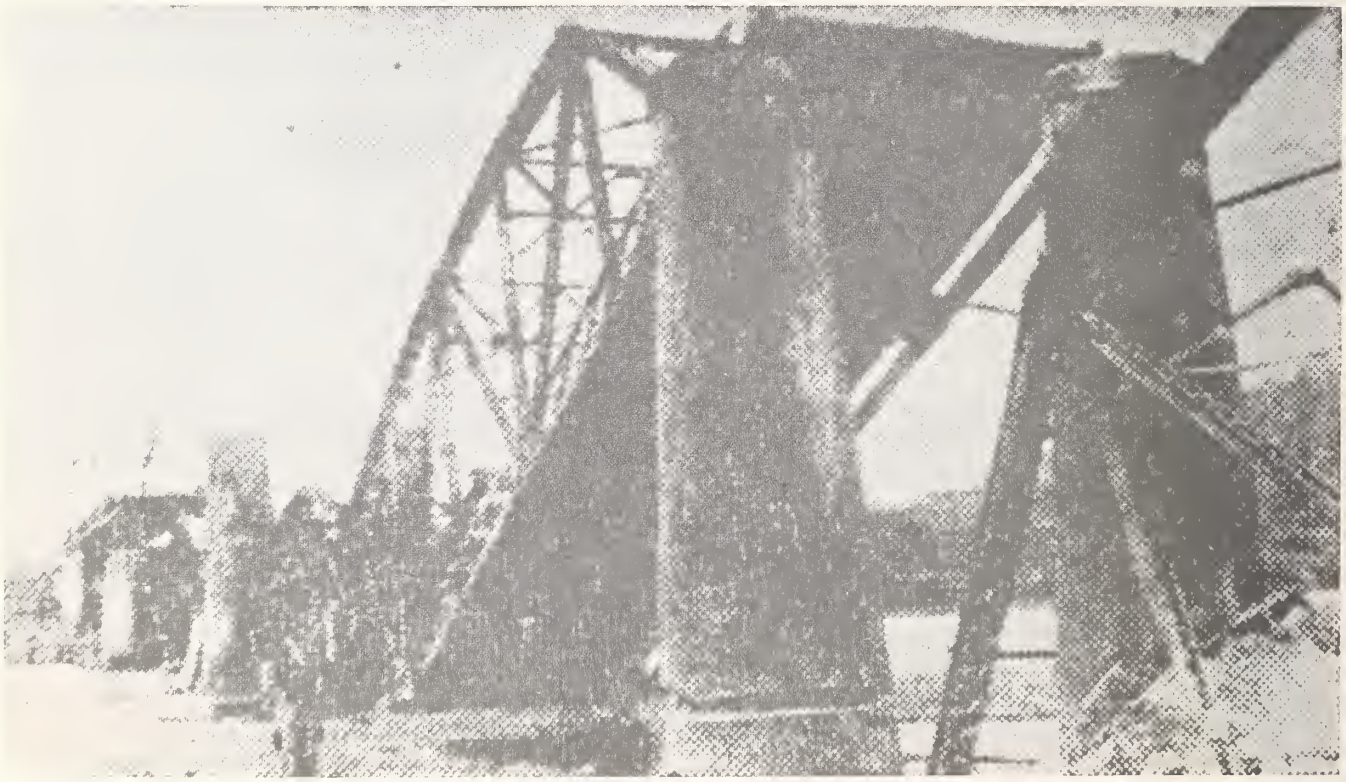

Photo. 2.20 Damage to the Shimantogawa bridge

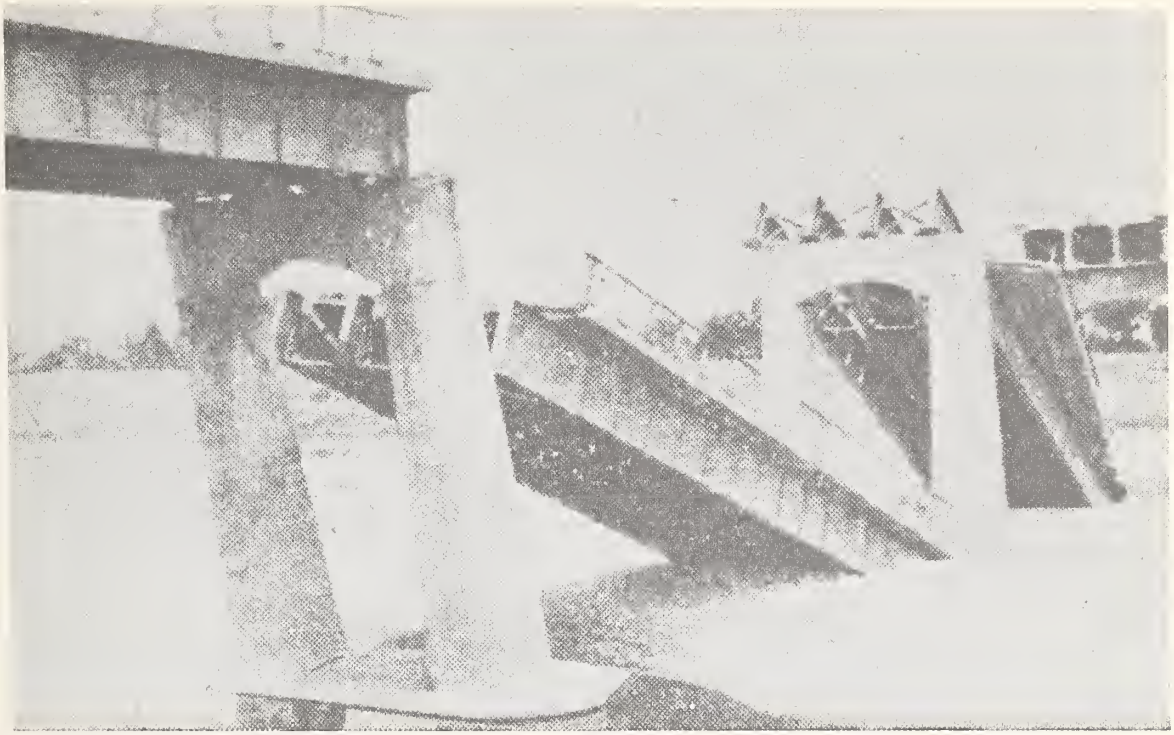

Photo. 2.21 Damage to the Nakazuno bridge

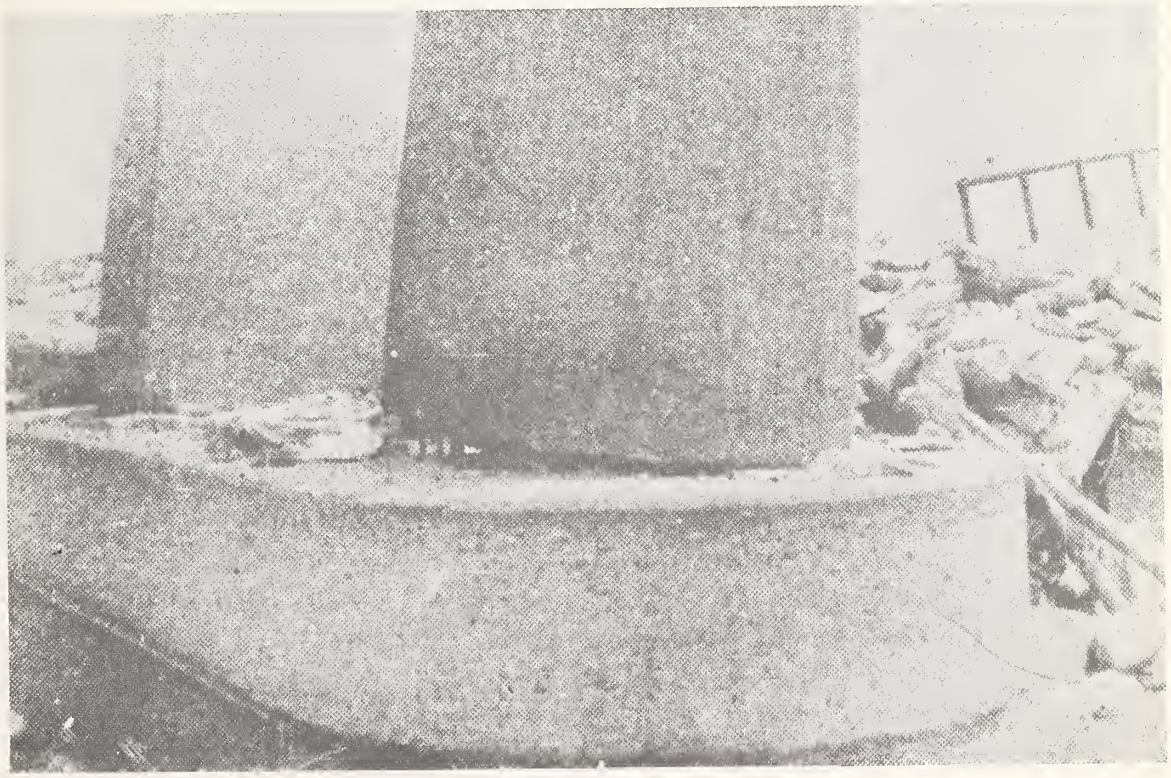

Photo. 2.22 Damage to the Nakazuno bridge at the column-to-foundation connection.

Photo. 2.23 Damage to the column and foundation of the Nakazuno bridge.

Photo. 2.24 Damage to the girders of the Nakazuno bridge

Photo. 2.25 Damage to the left abutment of the Nakazuno bridge

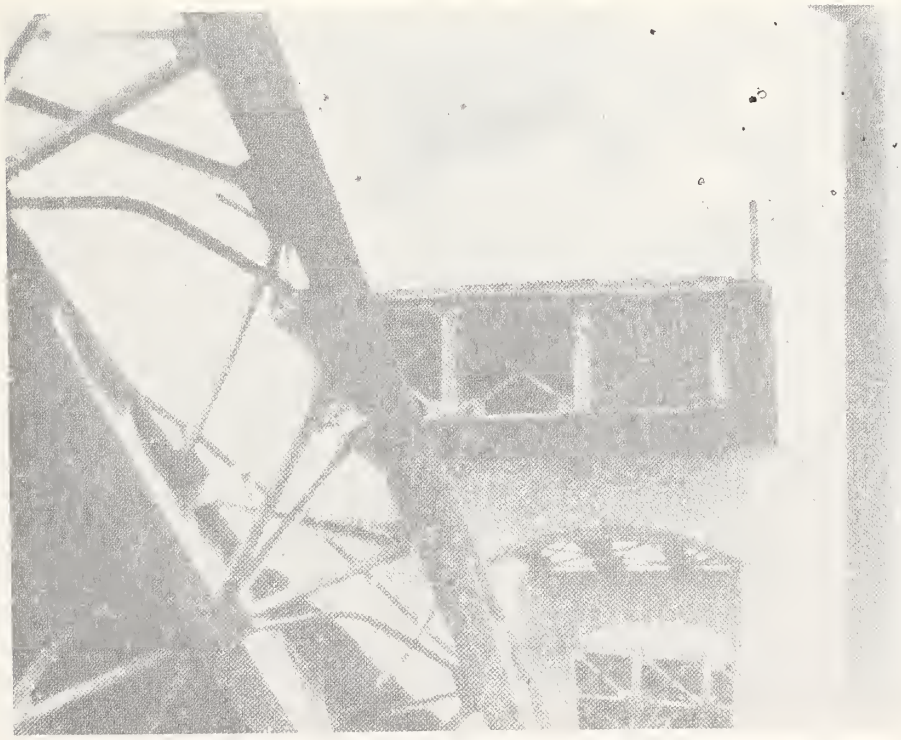

Photo. 2.26 Damage to the girders of the Nakazuno bridge

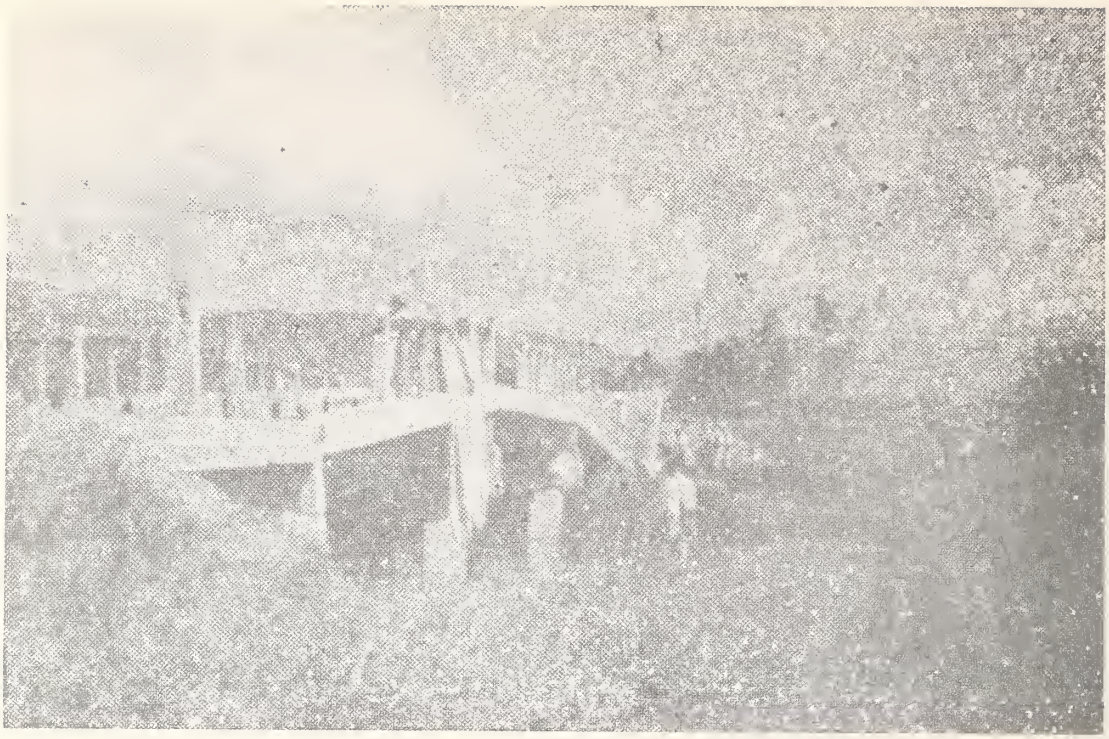

Photo.2.27 Damage to the Nagaya bridge

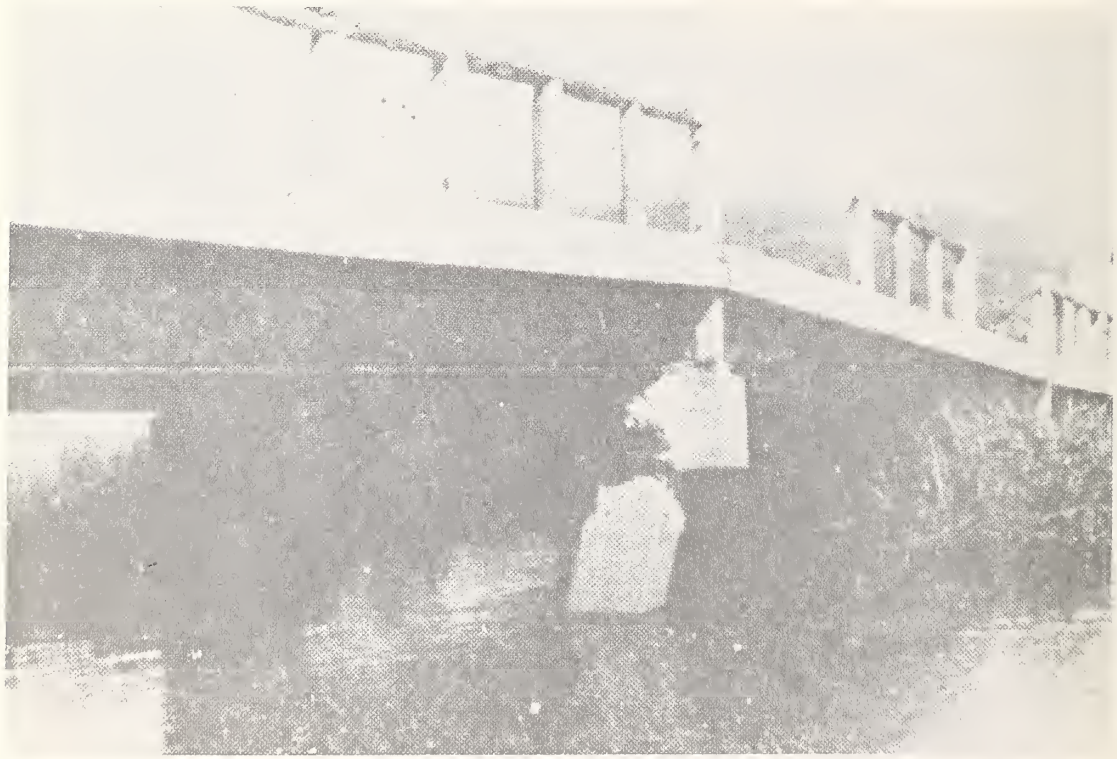

Photo.2.28 Damage to the piers of the Nagaya bridge

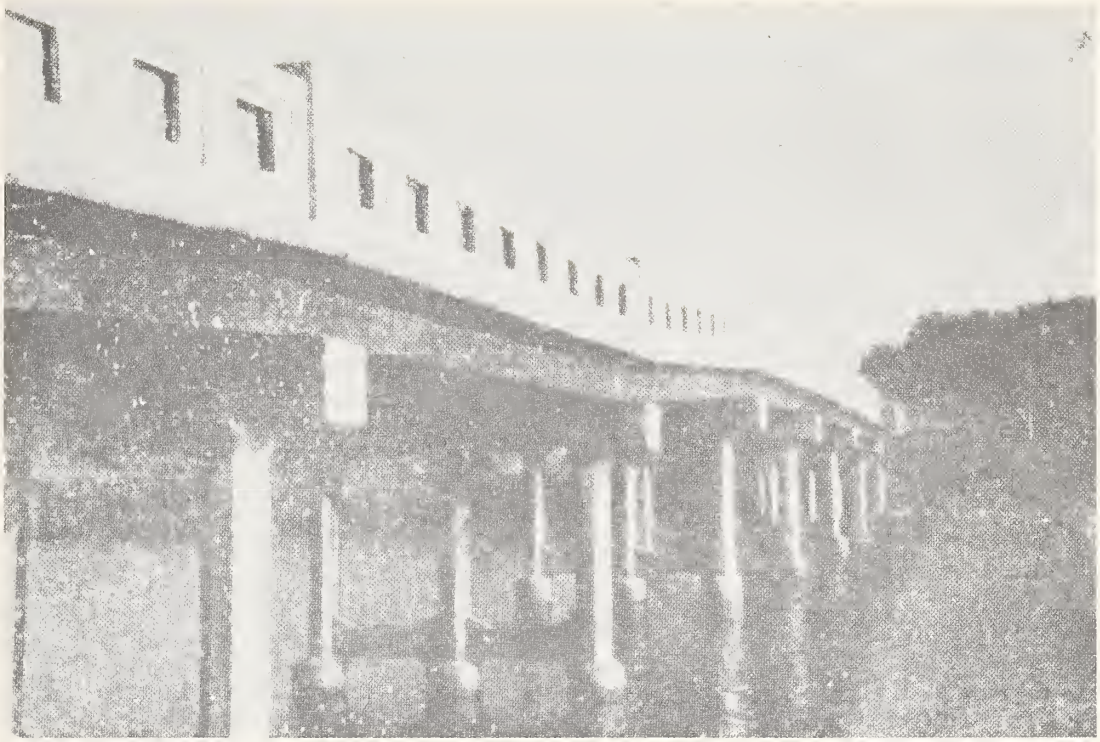

Photo. 2.29 Damage to the Shioya bridge

Photo. 2.30 Damage to the Segoshi bridge

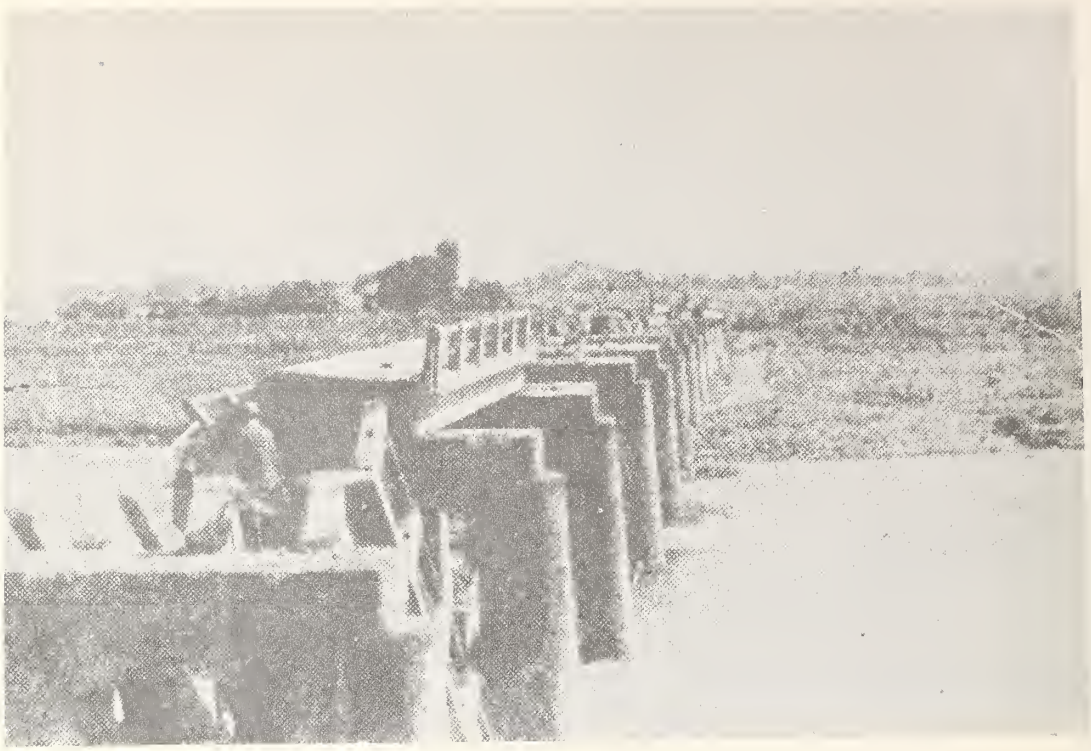

Photo. 2.31 Damage to the Itagaki bridge

Photo. 2.32 Damage to the Benten bridge

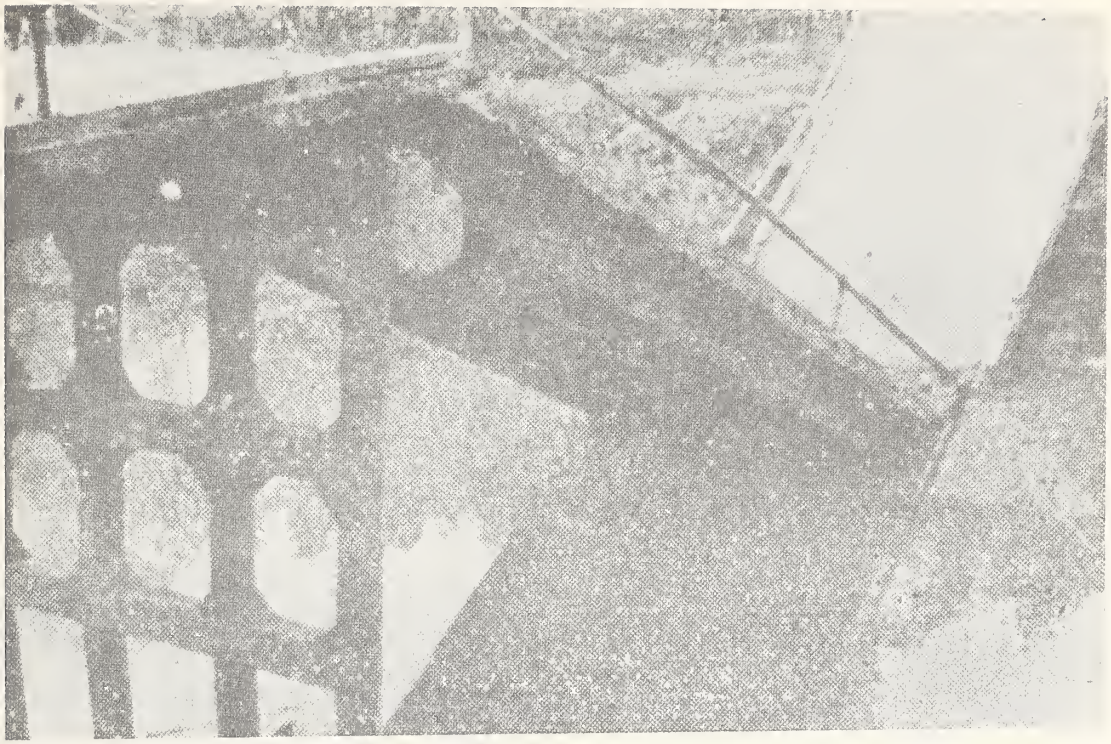

Photo. 2.33 Damage to the Benten bridge

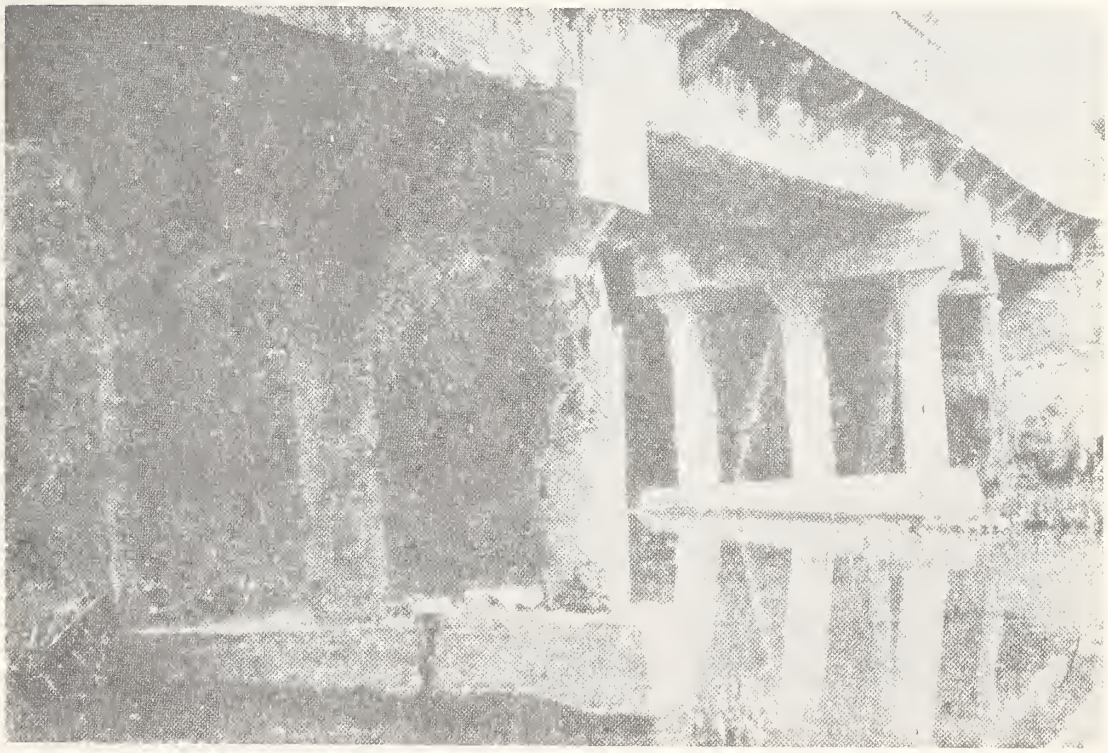

Photo. 2.34 Damage to the piers of the Koroba bridge

Photo. 2.35 Damage to a column of the Koroba bridge

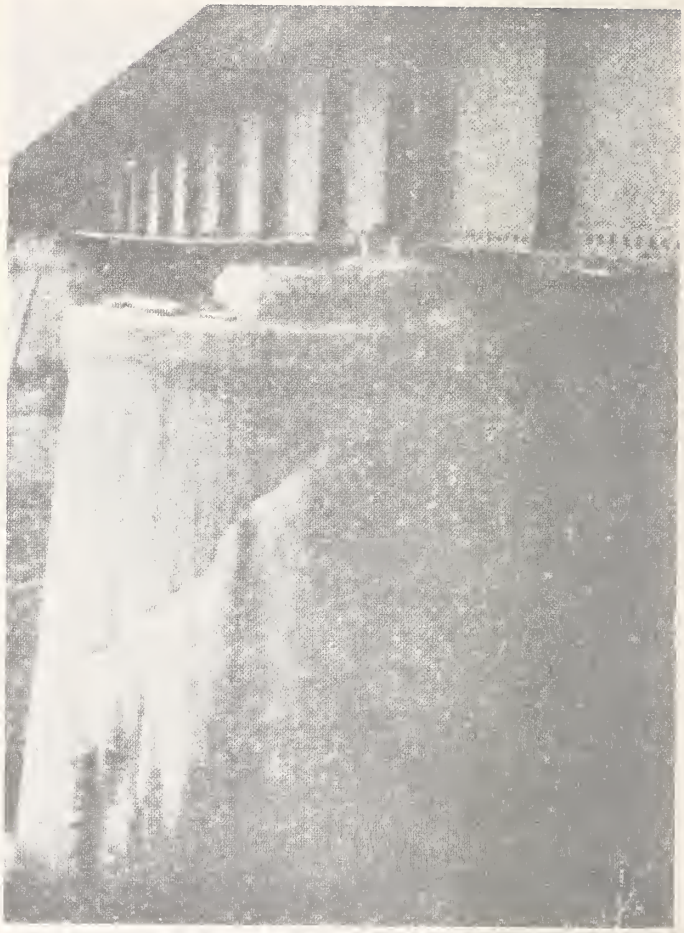

Photo. 2.36 Damage to the third pier of the Monbetsu bridge

Photo. 2.37 Damage to the support shoe at a pier of the Shizunai bridge

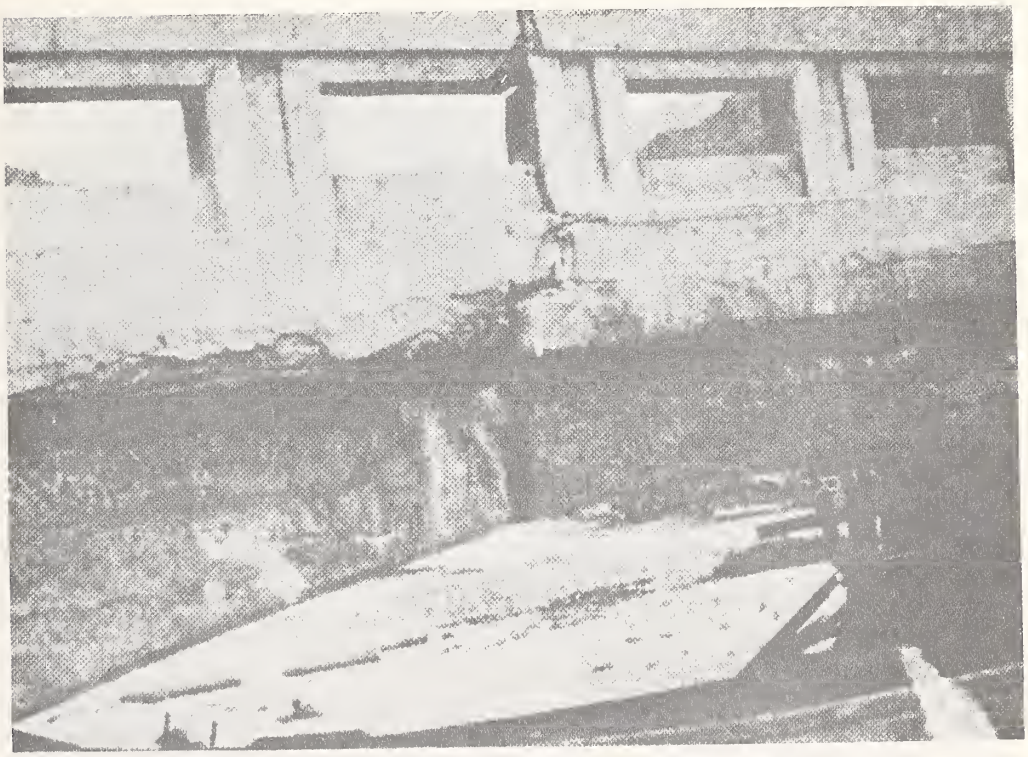

Photo. 2.38 Damage to a hinge joint of the Horoman bridge

Photo. 2.39 Damage to the girders of the Eai bridge at a supporting pier

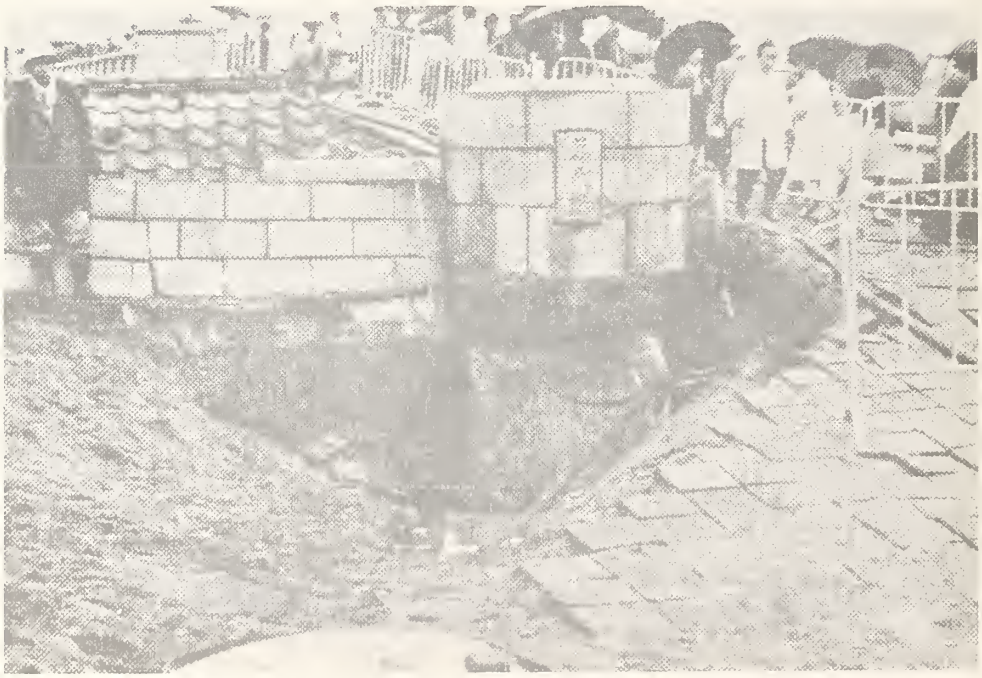

Photo. 2.40 Damage to the abutment of the Bandai bridge

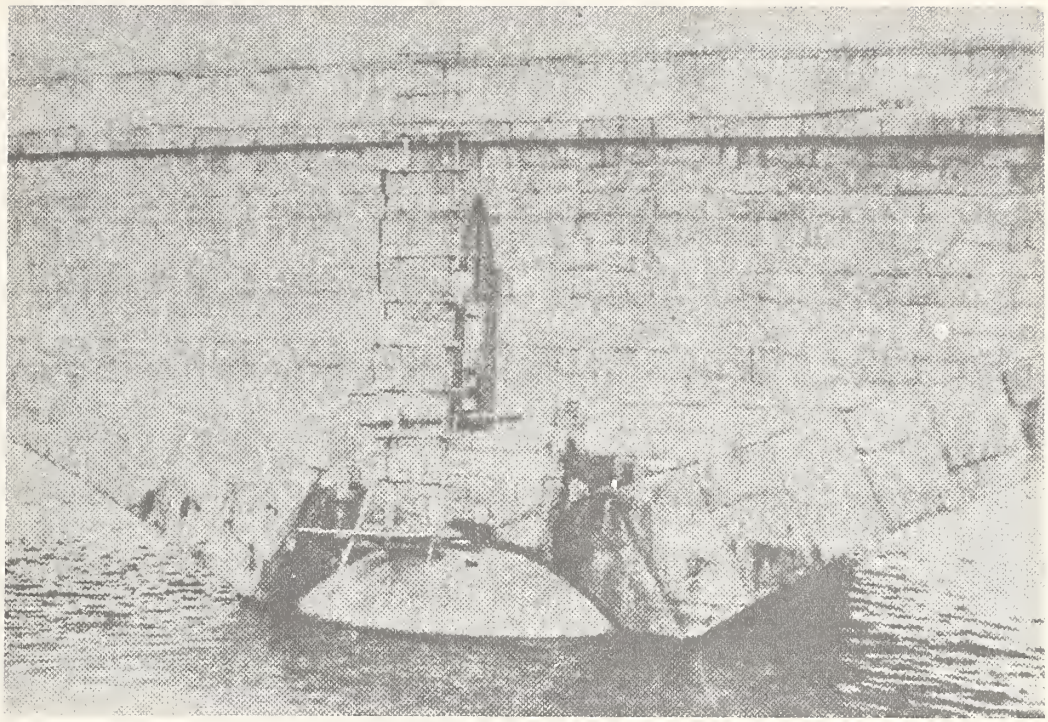

Photo. 2.41 Damage to the Bandai bridge

Photo. 2.42 Damage to the Showa bridge

Photo. 2.43 Damage to the Showa bridge (settlement of the approach road at the left-bank abutment).

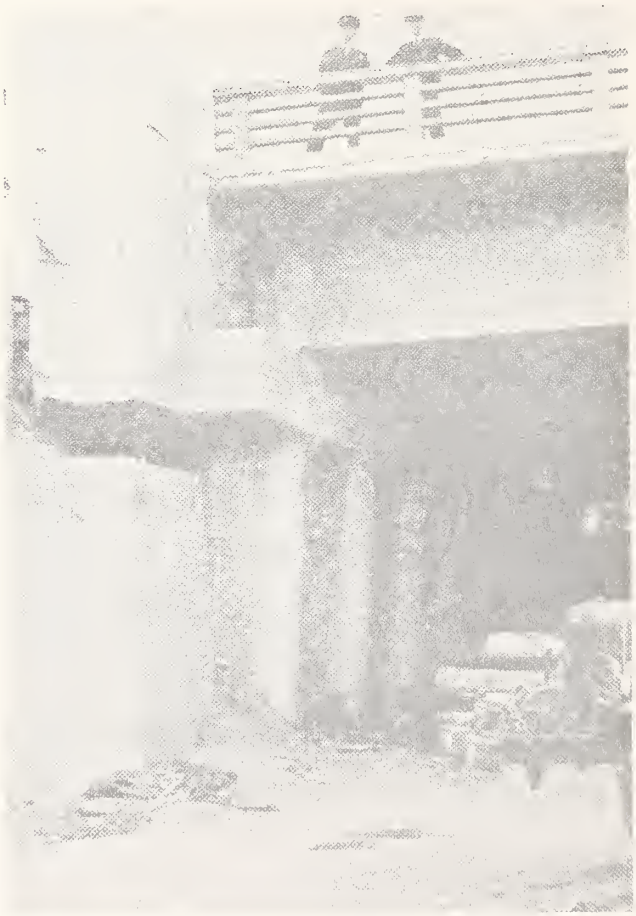

Photo. 2.44 Damage to the left-bank abutment of the Showa bridge

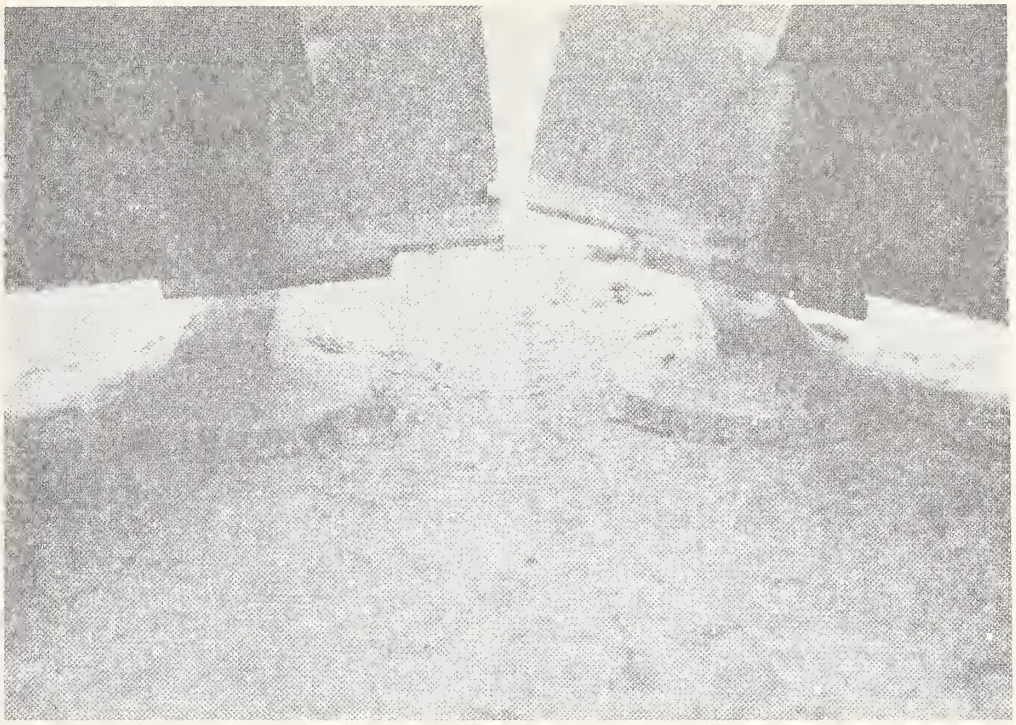

Photo. 2.45 Damage to the girders at the seventh pier of the Showa bridge

Photo. 2.46 Damage to the third girder at the second pier of the Showa bridge.

Photo. 2.47 Damage to a pulled-out pile at the fourth pier of the Showa bridge.

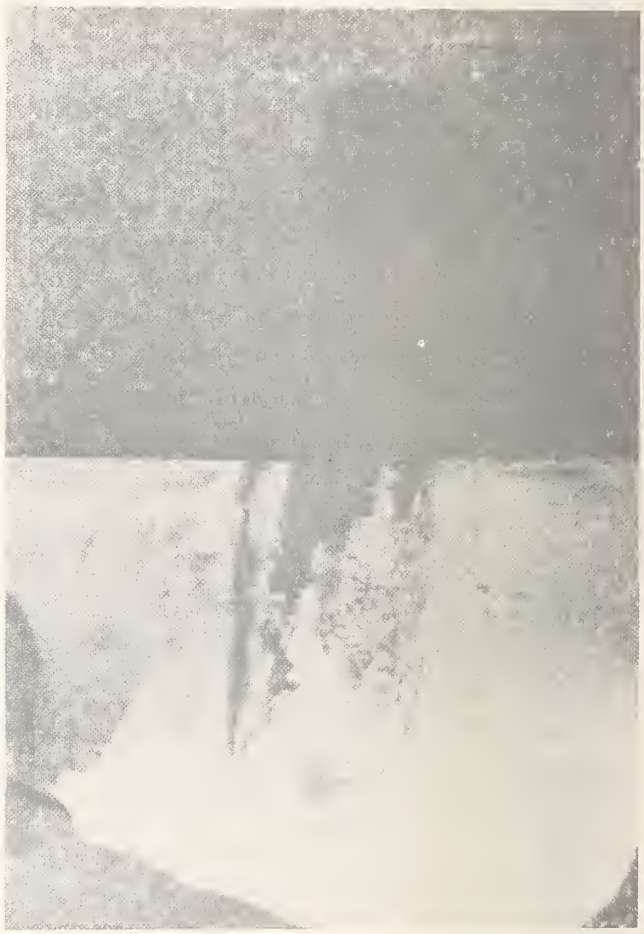

Photo. 2.48 Buckling feature of the pile shown in Photo 2.47.

Photo. 2.49 Damage to the Yachi ɔ bridge.

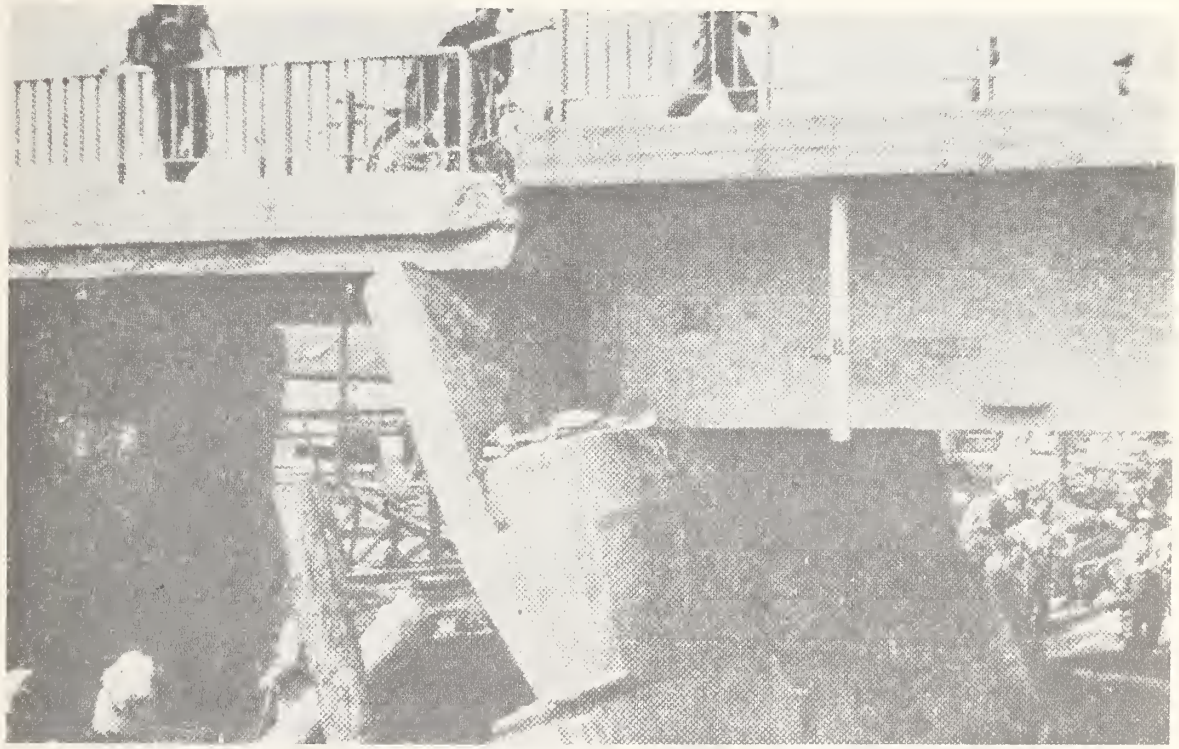

Photo. 2.50 Damage to the second pier of the Yachi ɔ bridge.

Photo. 2.51 Damage to the second pier of the Yachiyo bridge

Photo. 2.52 Damage to the end of the tenth girder at the ninth pier of the Yachiyo bridge

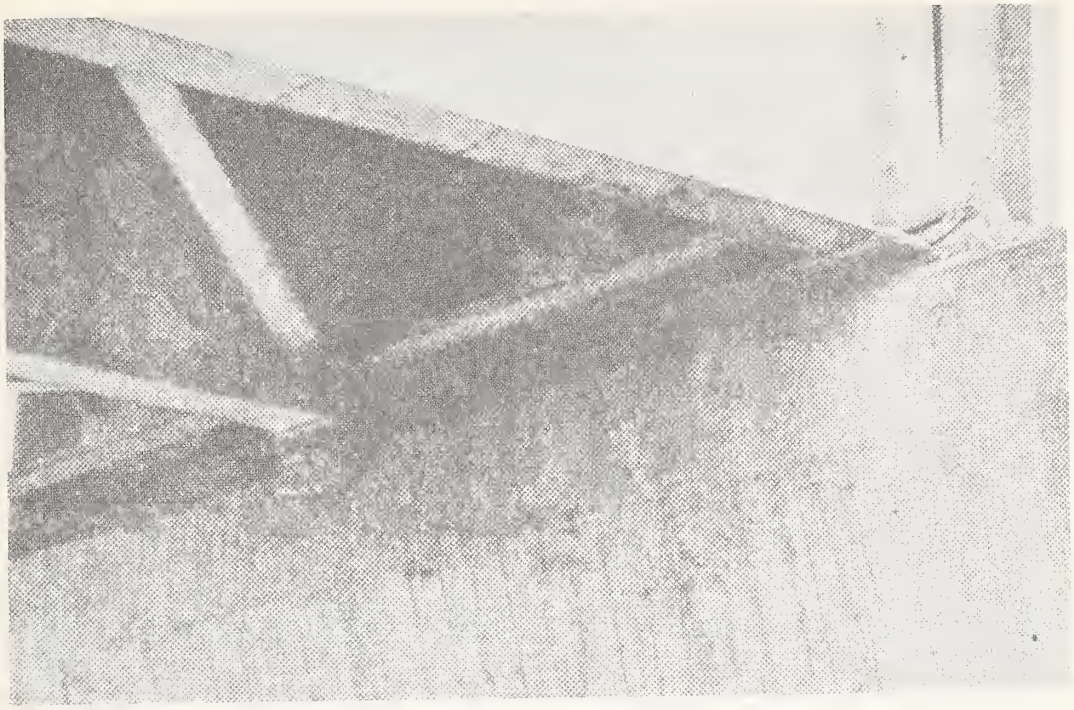

Photo. 2.53 Damage to the end of the tenth girder at the ninth pier of the Yachiyo bridge.

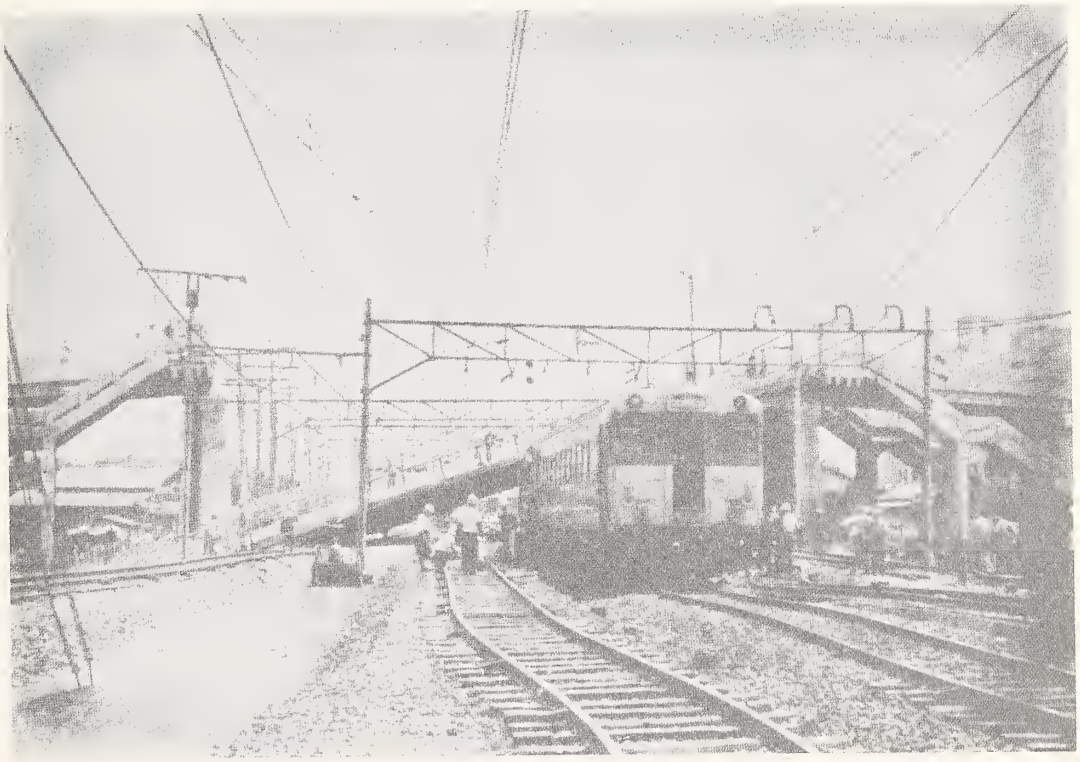

Photo. 2.54 Damage to the Higashi-Kosenkyo bridge

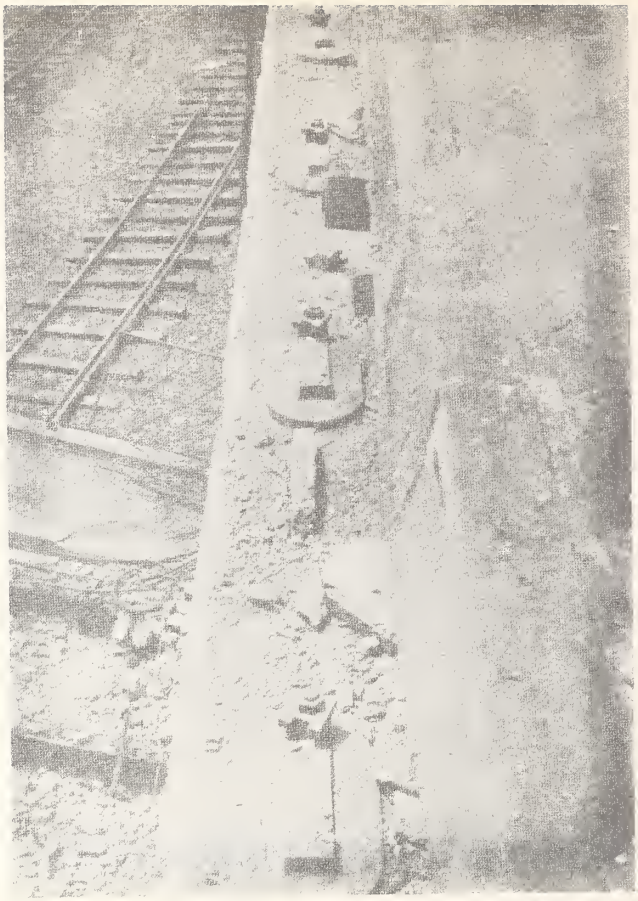

Photo. 2.55 Damage to the pier cap at the ninth pier of the Higashi-Kosenkyo bridge

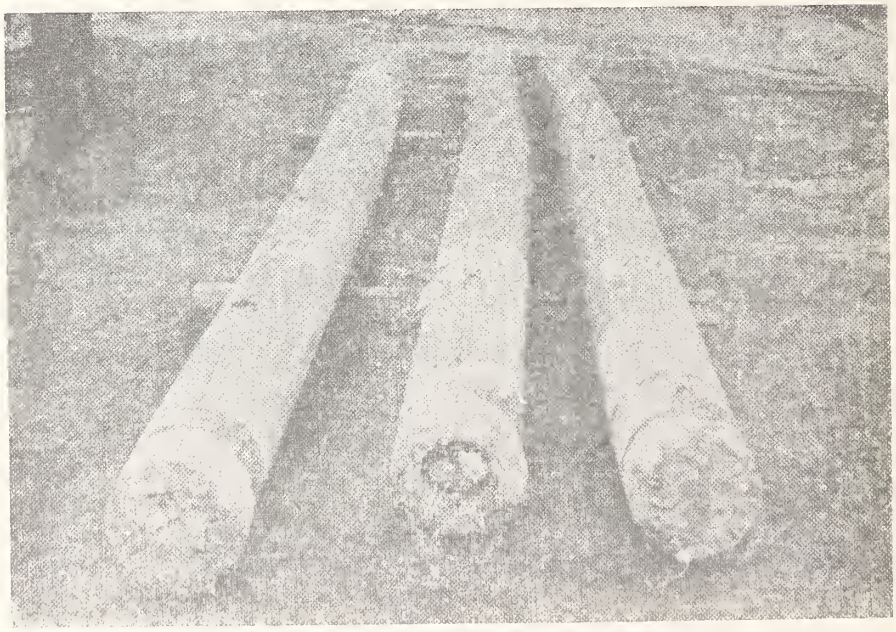

Photo. 2.56 Damaged piles pulled out from the ninth pier of the Higashi-Kosenkyo bridge.

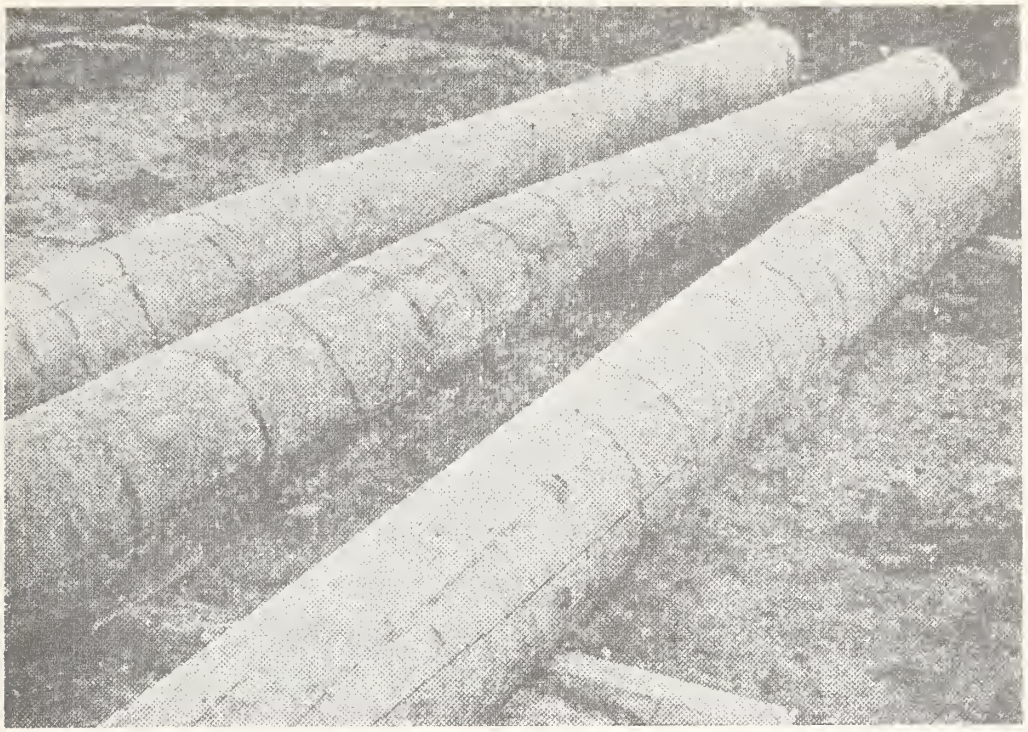

Photo. 2.57 Damaged piles pulled out from the ninth pier of the Higashi-Koshenkyo bridge

Photo. 2.58 Damage to the Matsuhama bridge.

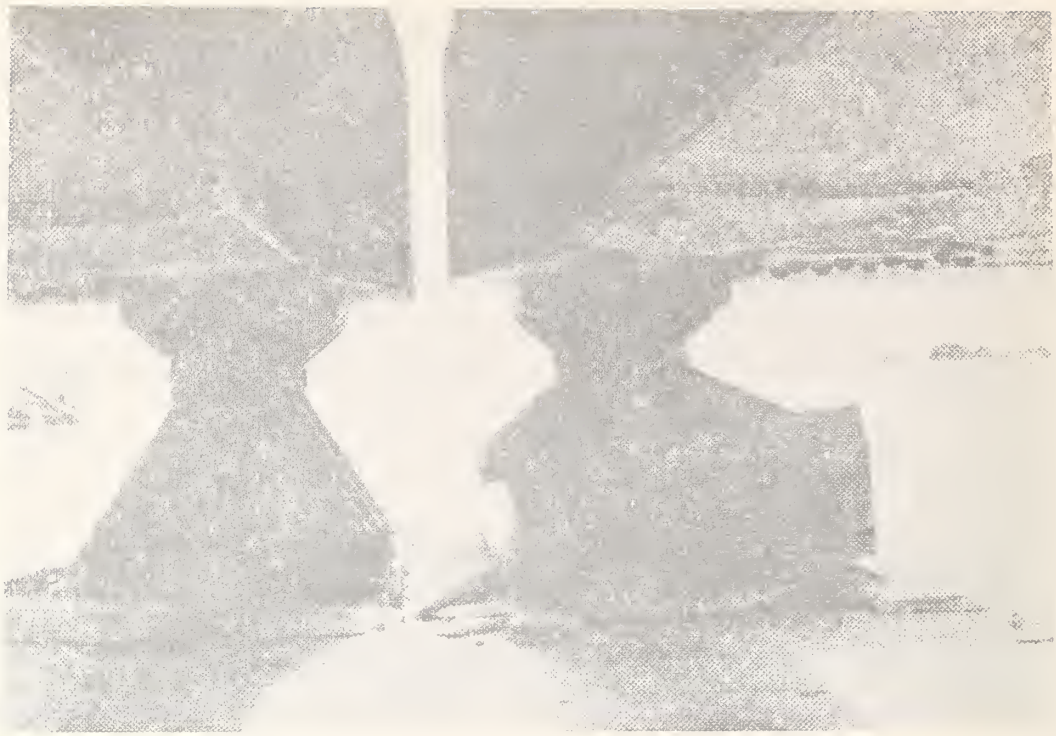

Photo. 2.59 Damage to the support shoe on the thirteenth pier of the Matsuhama bridge

Photo. 2.60 Damage to the PC girder and the abutment of the Kamezawa bridge.

Photo. 2.61 Damage to the Kamimasaki bridge

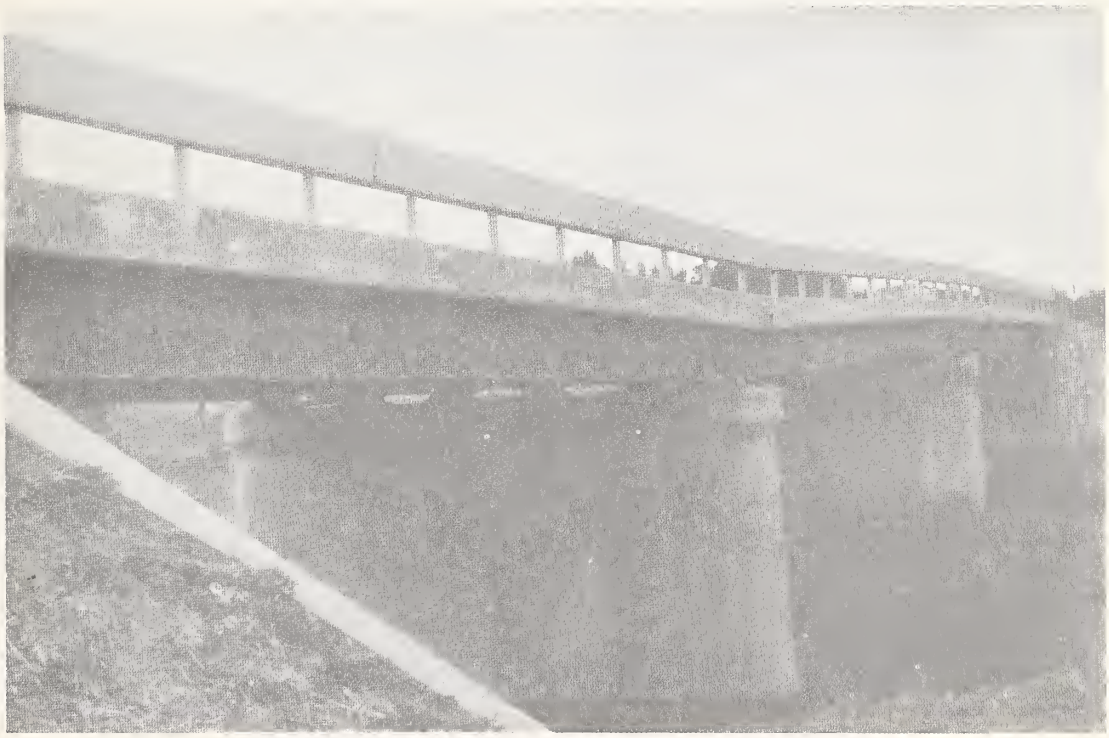

Photo. 2.62 Damage to the Ikejima bridge
(pier settled due to soil liquefaction)

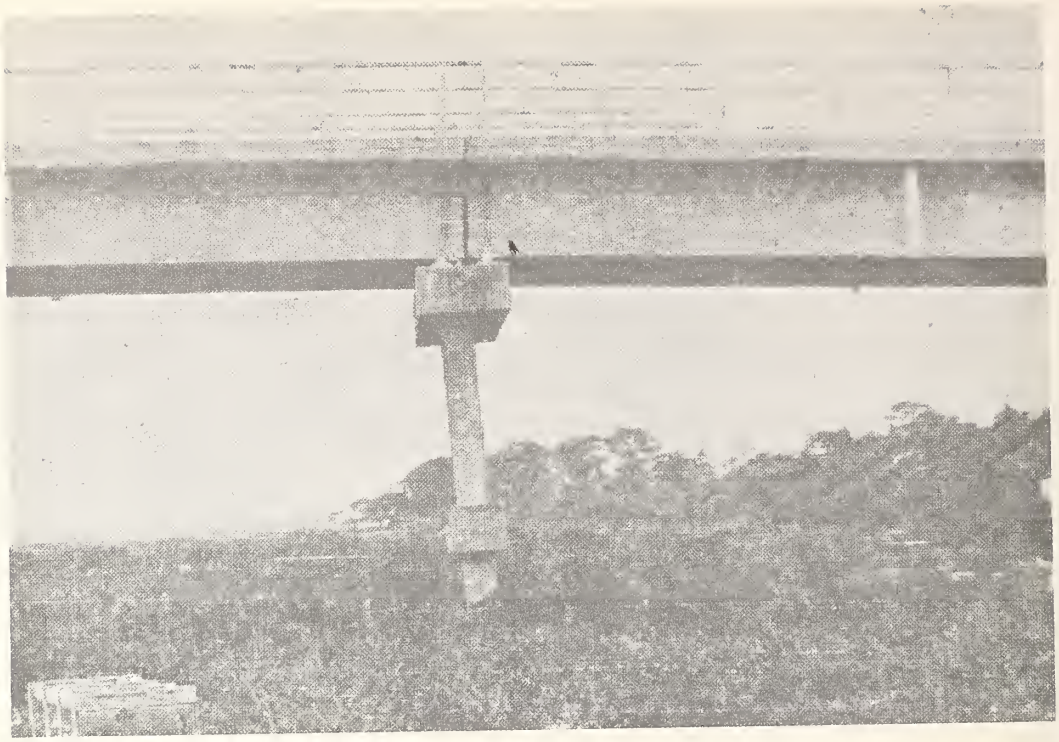

Photo. 2.63 Damage to the pile-bent pier of the Kaimei bridge

Photo. 2.64 Settlement of pier at the Shiriuchi bridge.

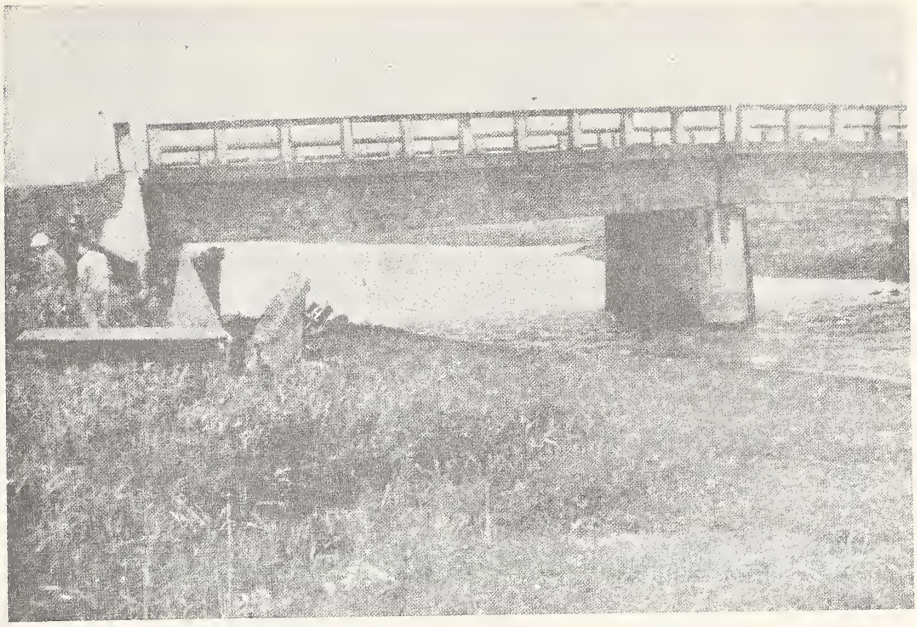

Photo. 2.65 Damage to the abutment of the Noushi bridge

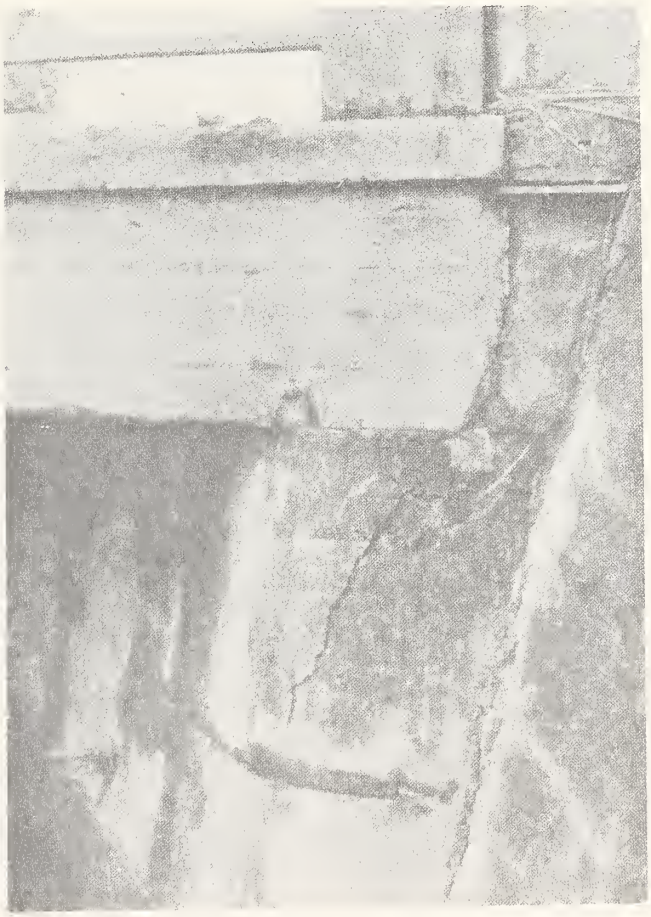

Photo. 2.66 Damage to the abutment of the Deto bridge.

Photo. 2.67 Crack of abutment of the Komagome bridge

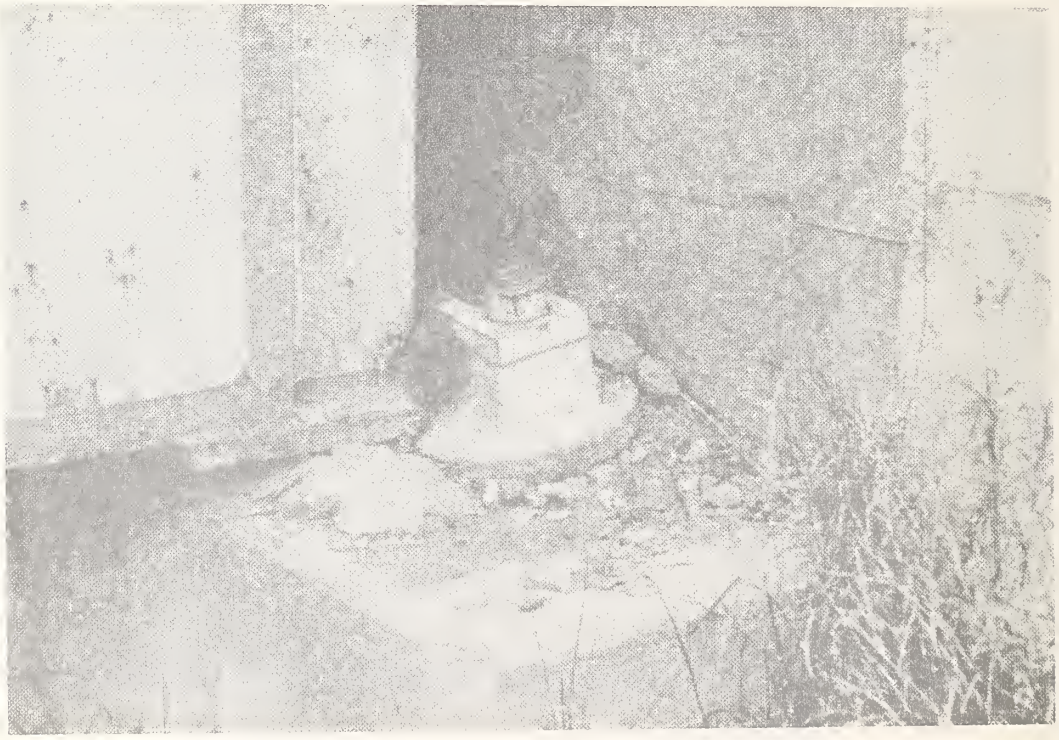

Photo. 2.68 Damage to the support shoe of the Kaimei bridge.

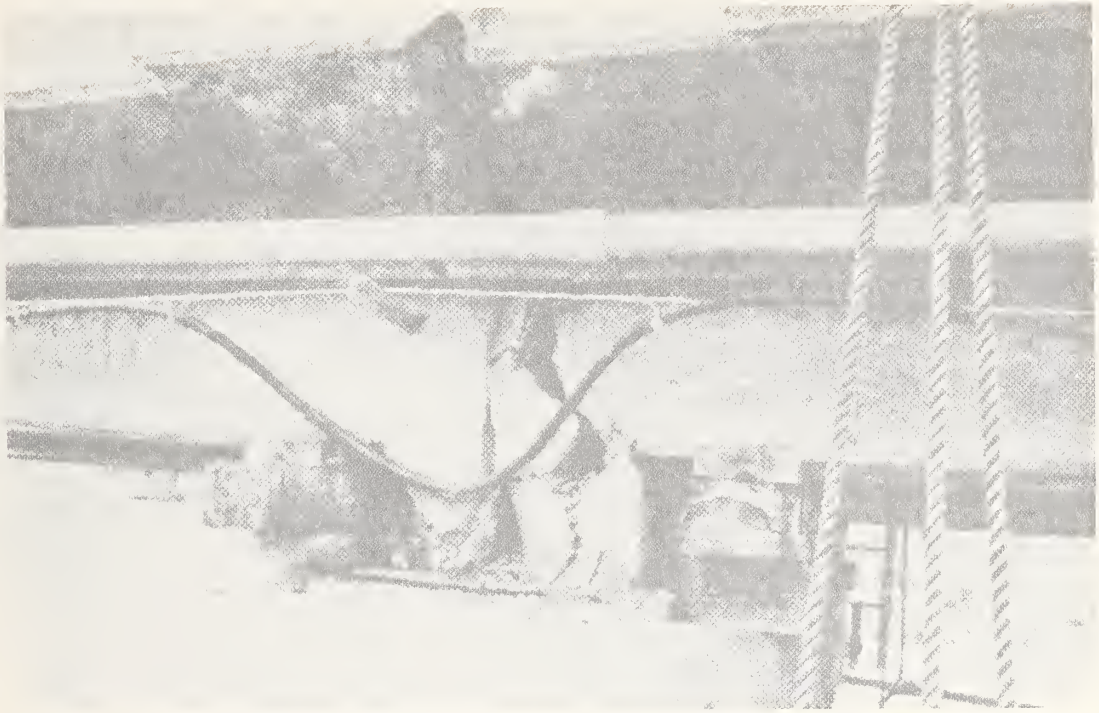

Photo. 2.69 Failure of the concrete girders of the Komoto bridge

Photo. 2.70 North abutment of overcrossing at Golden State Freeway and Foothill Freeway interchange.

Photo. 2.71 South abutment of overcrossing at Golden State Freeway and Foothill Freeway interchange

Photo. 2.72 Damaged San Fernando Road Overhead

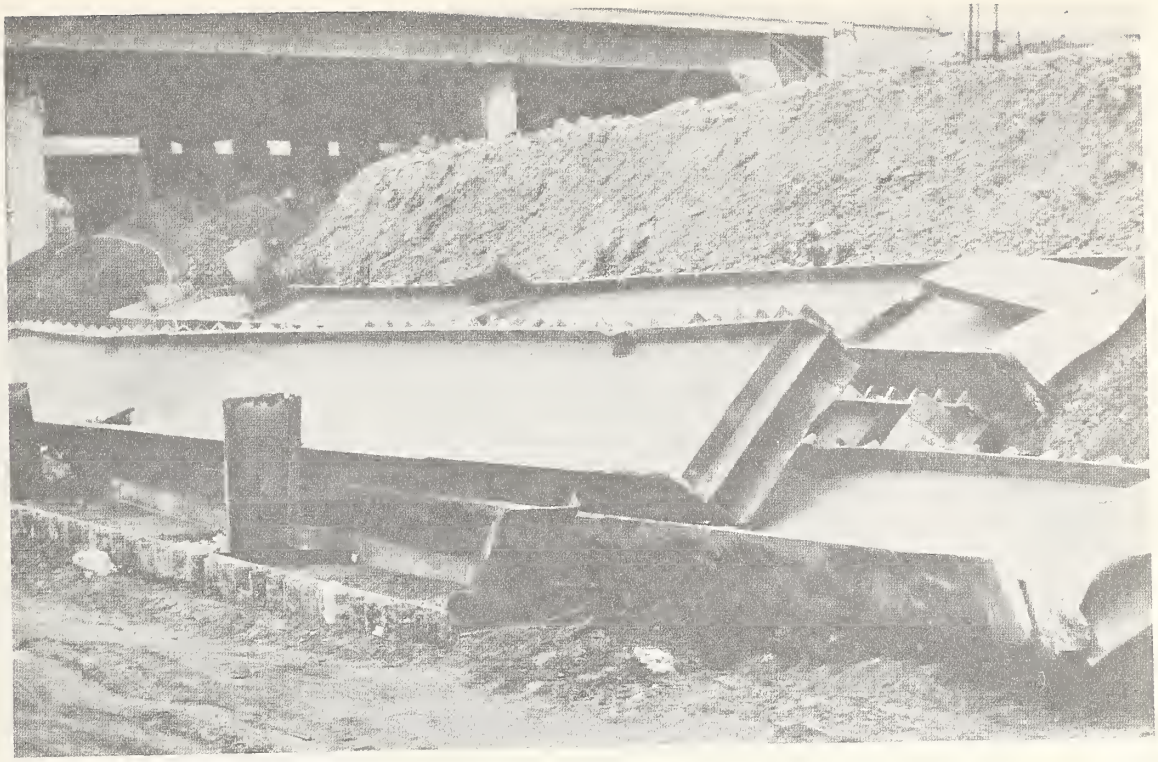

Photo. 2.73 Steel girders taken from San Fernando Road Overhead

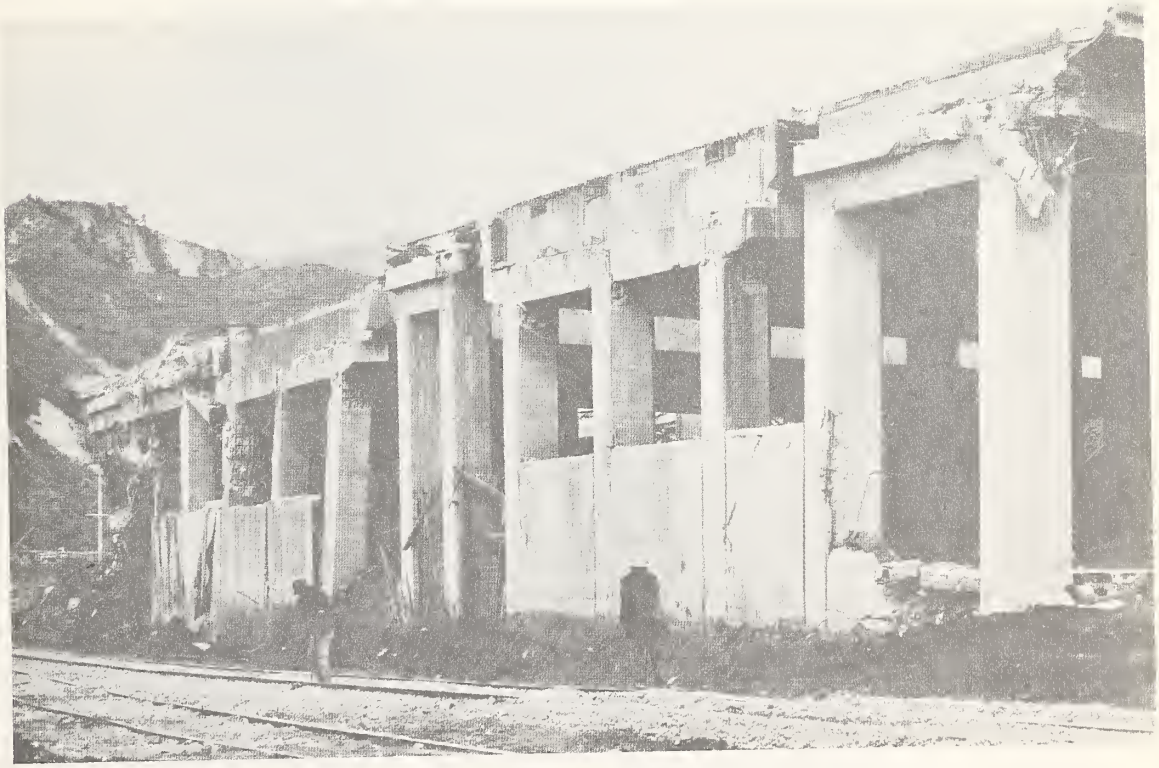

Photo. 2.74 Damaged San Fernando Road Overhead

Photo. 2.75 Southern portion San Fernando Road Overhead

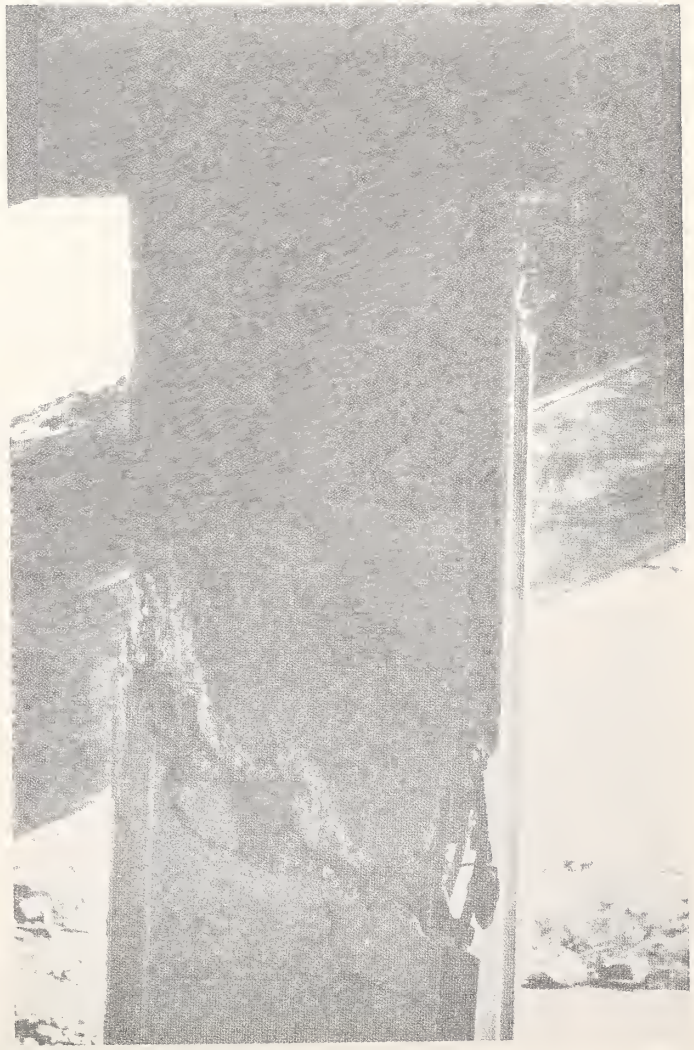

Photo. 2.76 Shear failure in column of San Fernando Road Overhead

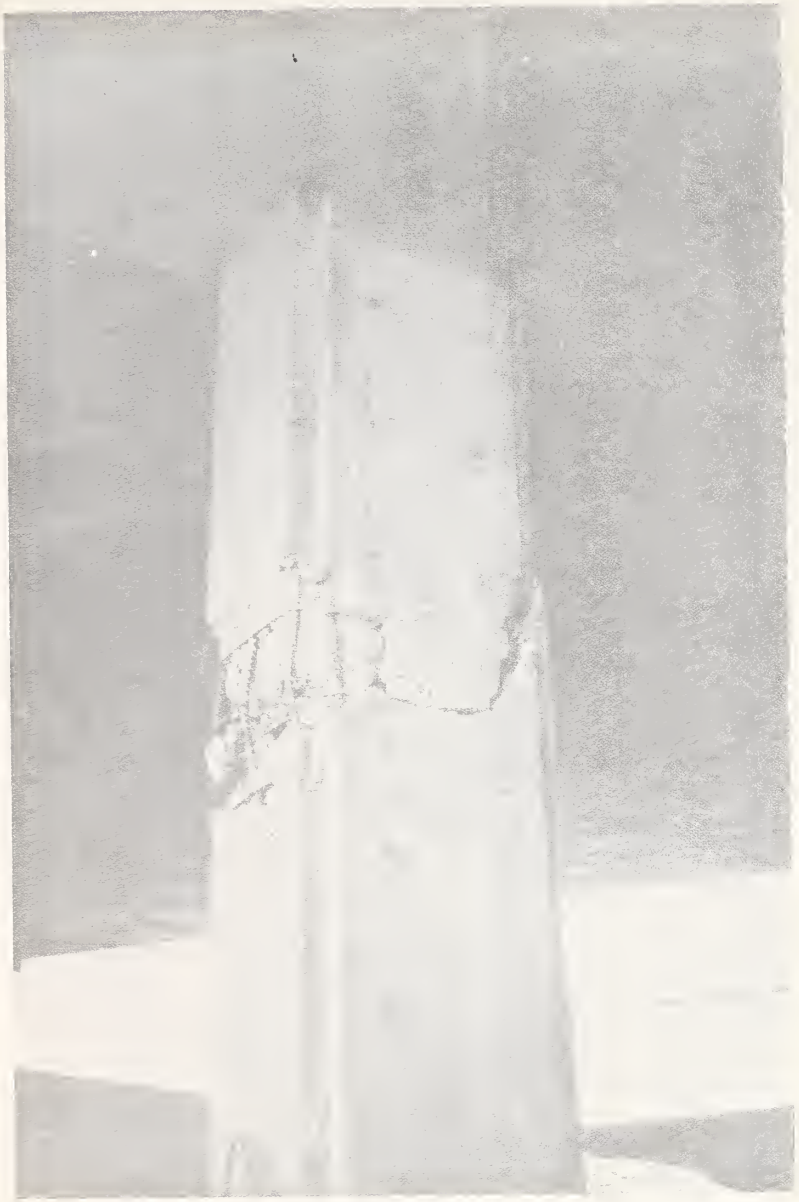

Photo. 2.77 Shear failure in column of San Fernando Road Overhead

Photo. 2.78 Flexural damage in column of San Fernando Road Overhead

Photo. 2.79 Flexural damage in column of San Fernando Road Overhead

Photo. 2.80 Flexural damage in column of San Fernando Road Overhead

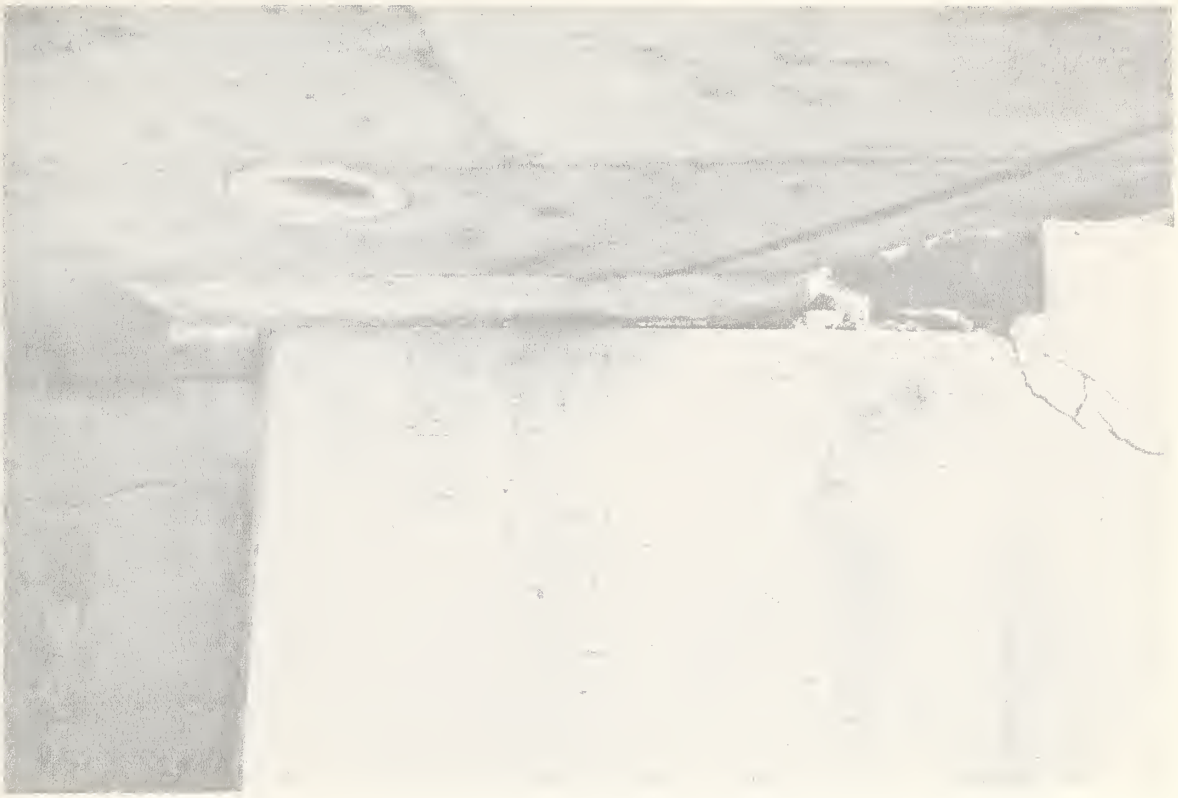

Photo. 2.81 View showing horizontal displacement of bridge deck on its support - San Fernando Road Overhead

Photo. 2.82 Dislodged rocker support - San Fernando Road Overhead

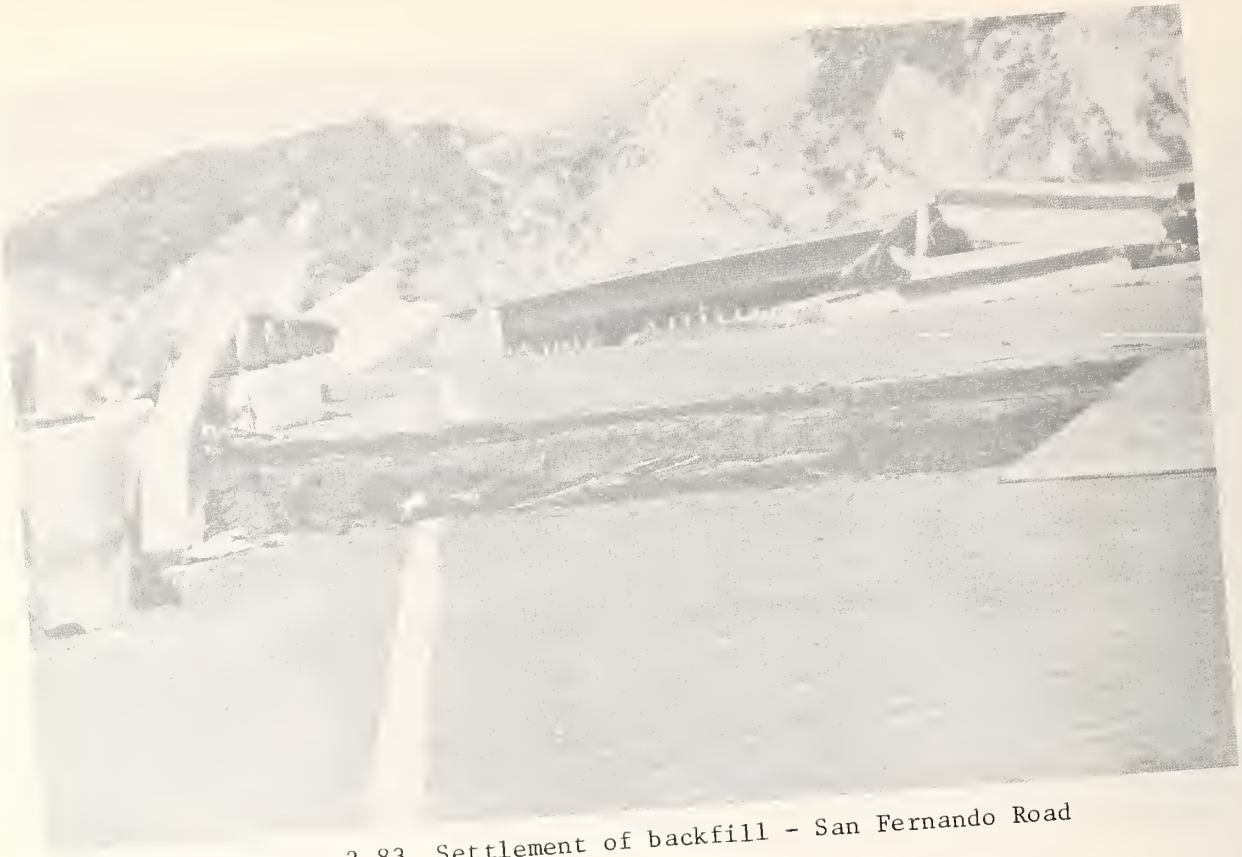

Photo. 2.83 Settlement of backfill - San Fernando Road Overhead

Photo. 2.84 Damaged overcrossing at Golden State Freeway and Foothill Freeway interchange

Photo. 2.85 Damaged overcrossing at Golden State Freeway and Foothill Freeway interchange

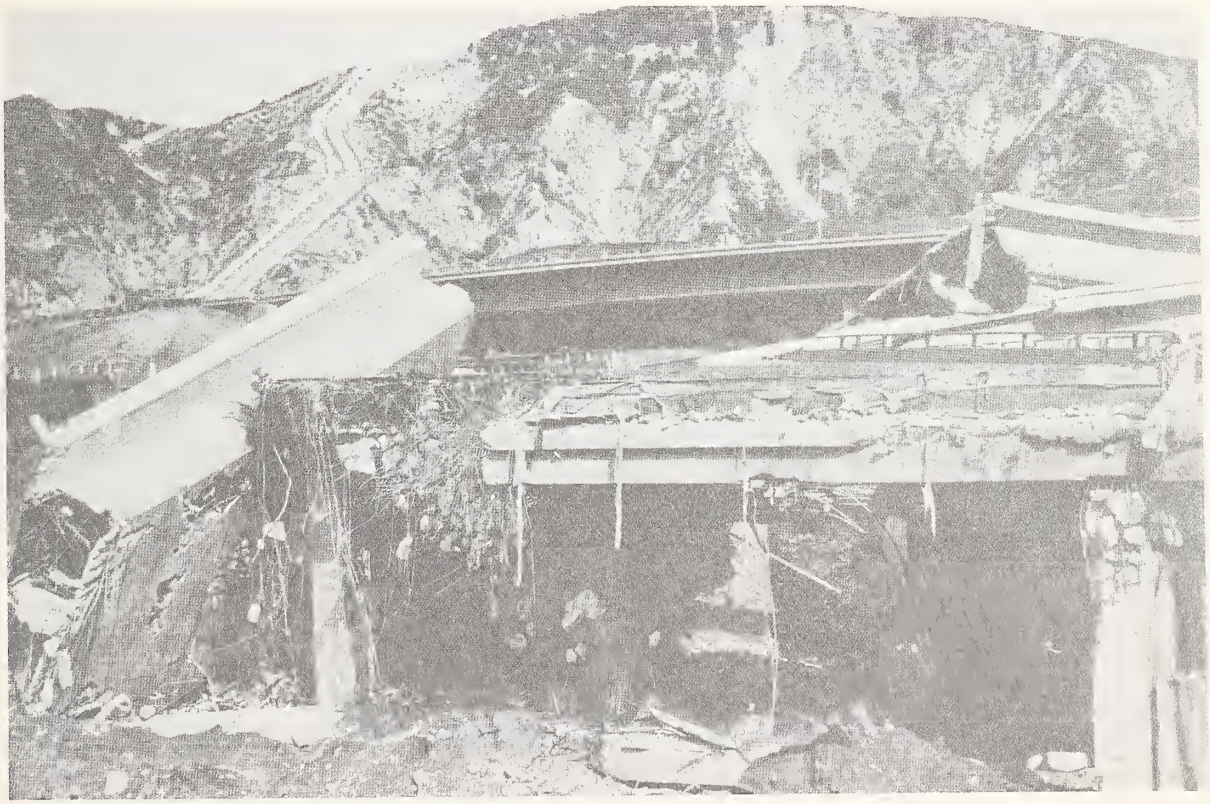

Photo. 2.86 Damaged overcrossing at Golden State Freeway and Foothill Freeway interchange

Photo. 2.87 Damaged overcrossing at Golden State Freeway and Foothill Freeway interchange

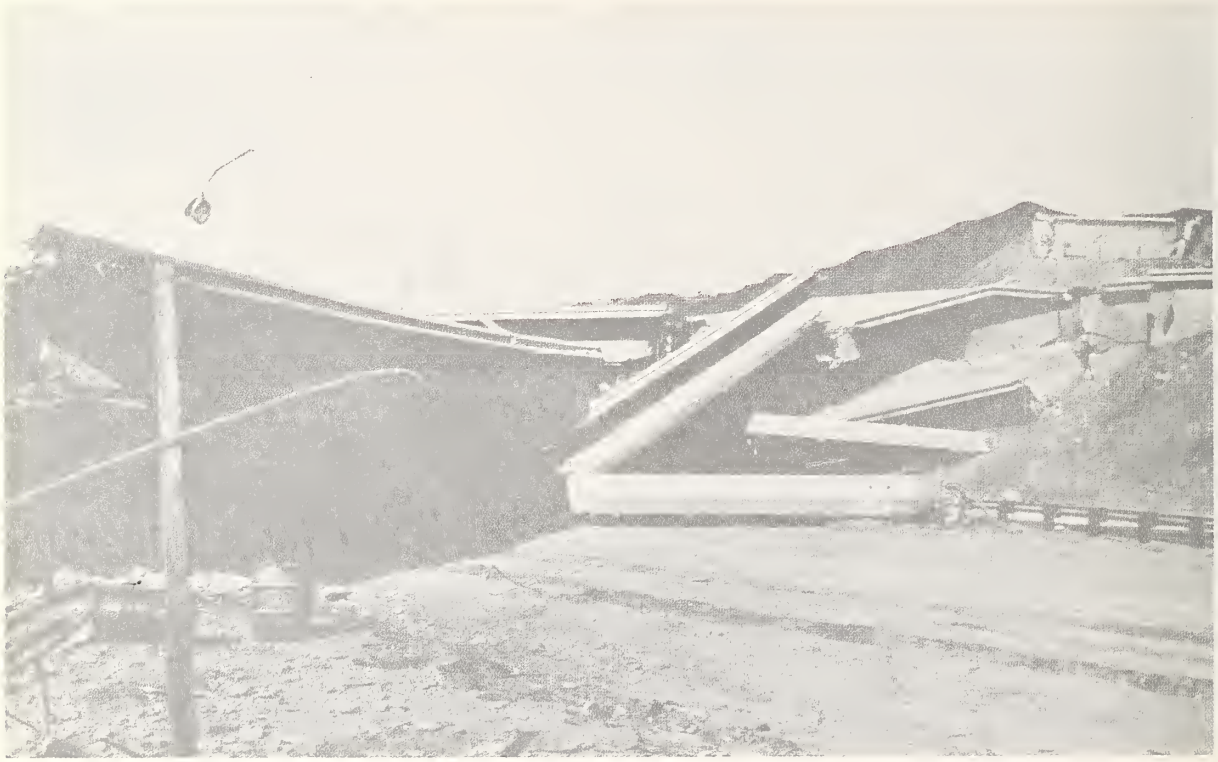

Photo. 2.88 Damaged overcrossing at Golden State Freeway and Foothill Freeway interchange

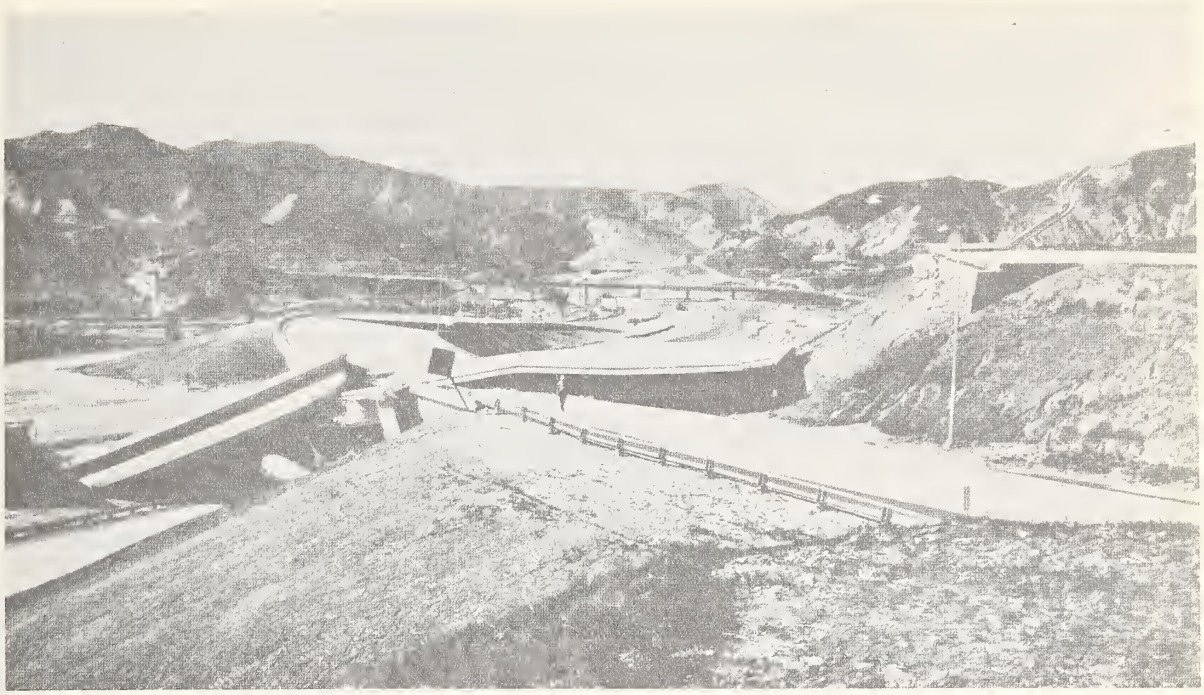

Photo. 2.89 Damaged overcrossing at Golden State Freeway and Foothill Freeway interchange

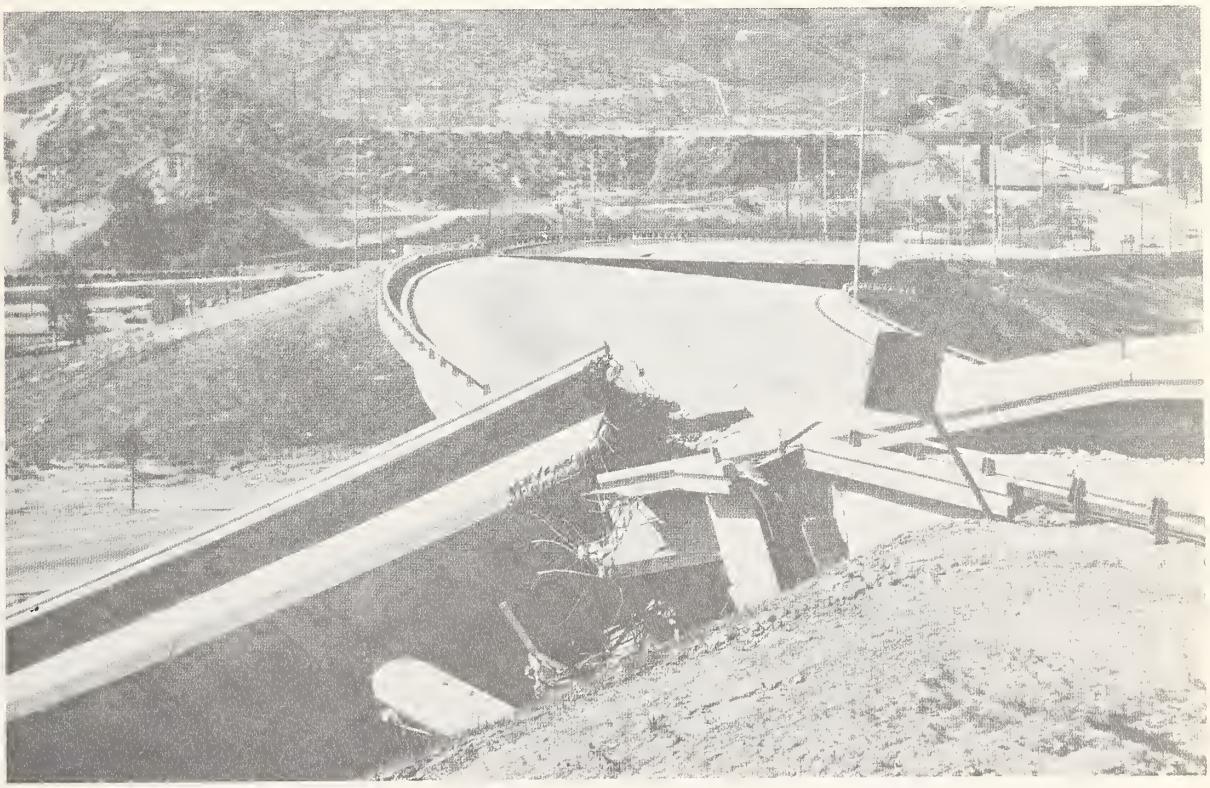

Photo. 2.90 Damaged overcrossing at Golden State Freeway and Foothill Freeway interchange

Photo. 2.91 Damaged overcrossing at Golden State Freeway and Foothill Freeway interchange

Photo. 2.92 Damaged overcrossing at Golden State Freeway and Foothill Freeway interchange

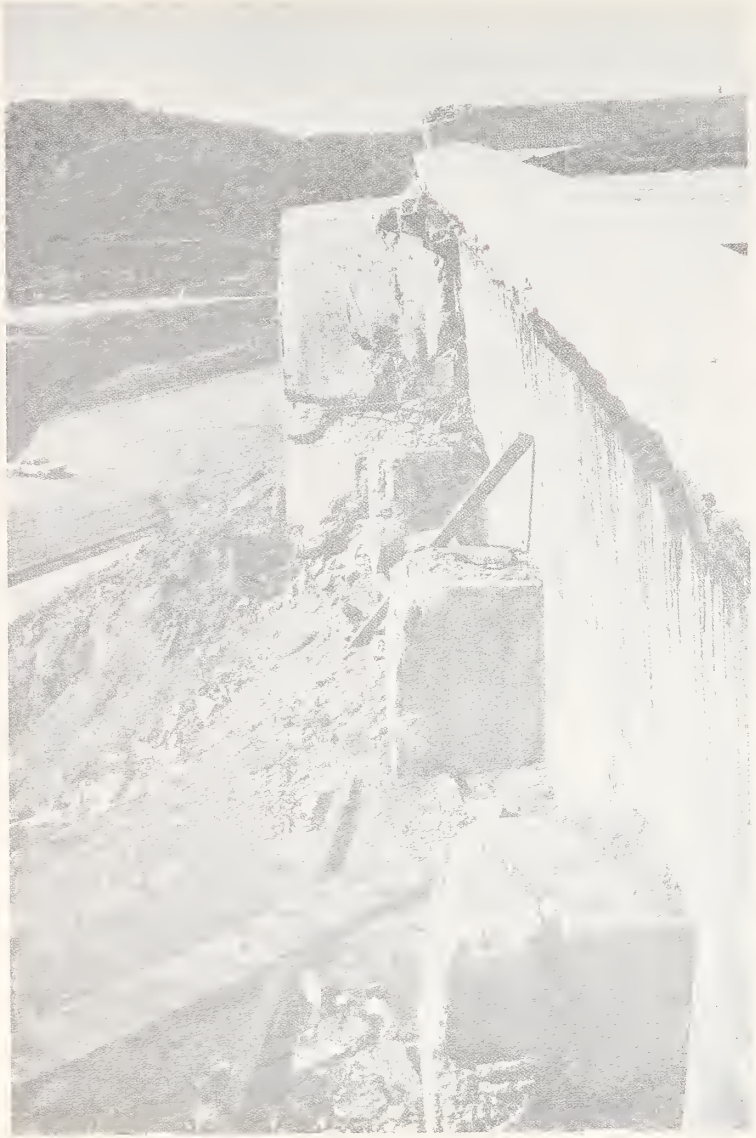

Photo. 2.93 Abutment of overcrossing at Golden State Freeway and Foothill Freeway interchange

Photo. 2.94 Column of overcrossing at Golden State Freeway and Foothill Freeway interchange

Photo. 2.95 Column of overcrossing at Golden State Freeway and Foothill Freeway interchange

Photo. 2.96 Failure at base of column supported on a single 6 foot diameter cast-in-drilled-hole pile - Golden State Freeway and Foothill Freeway interchange

Photo. 2.97 Failure at base of column supported on a single 6 foot diameter cast-in-drilled-hole pile - Golden State Freeway and Foothill Freeway interchange

Photo. 2.98 Failure at base of column supported on spread footing - Golden State Freeway and Foothill Freeway interchange

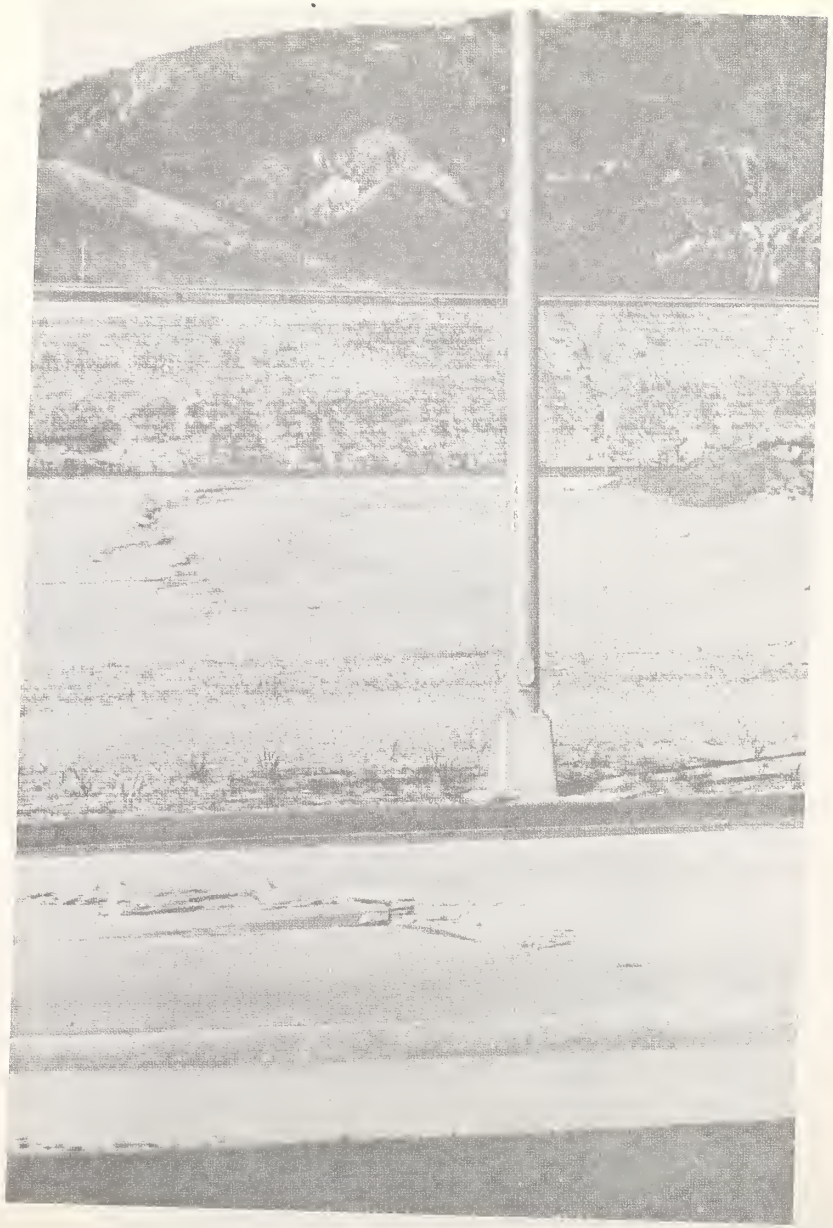

Photo. 2.99 Concentrated ground deformation having appearance of fault trace

Photo. 2.100 Damaged railroad tracks near Golden State Freeway and Foothill Freeway interchange

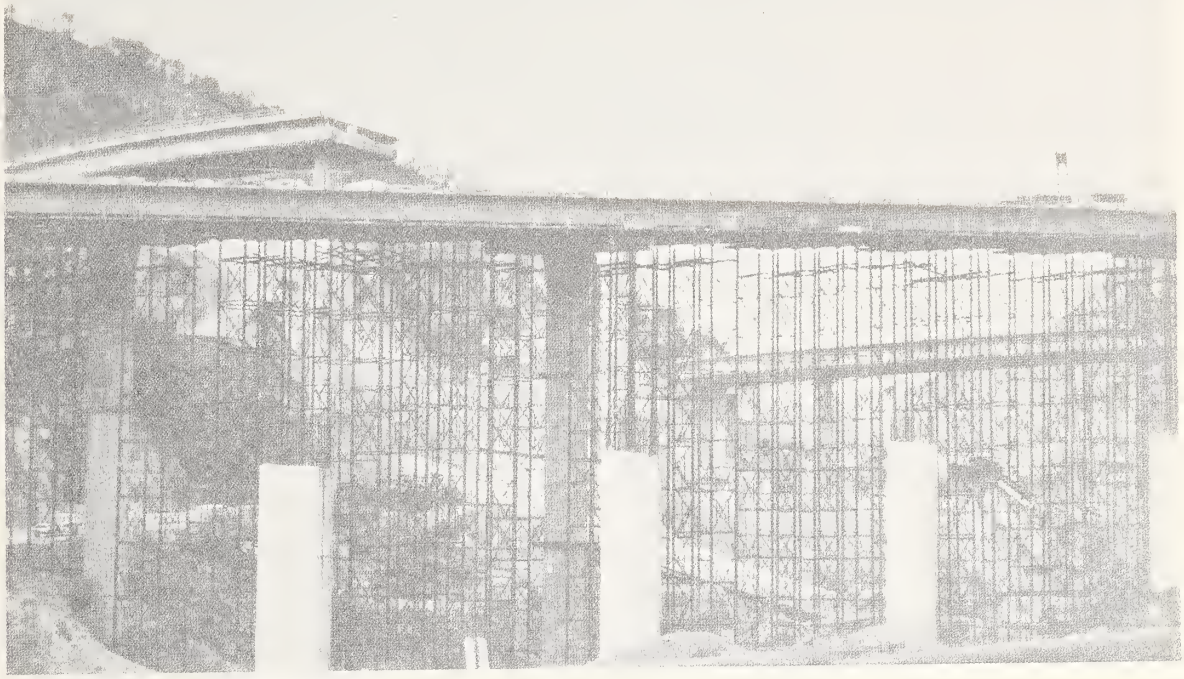

Photo. 2.101 Freeway structures at Golden State Freeway and State Highway 14 interchange

Photo. 2.102 Overcrossing at Golden State Freeway and State Highway 14 interchange

Photo. 2.103 Overcrossing at Golden State Freeway and State Highway 14 interchange

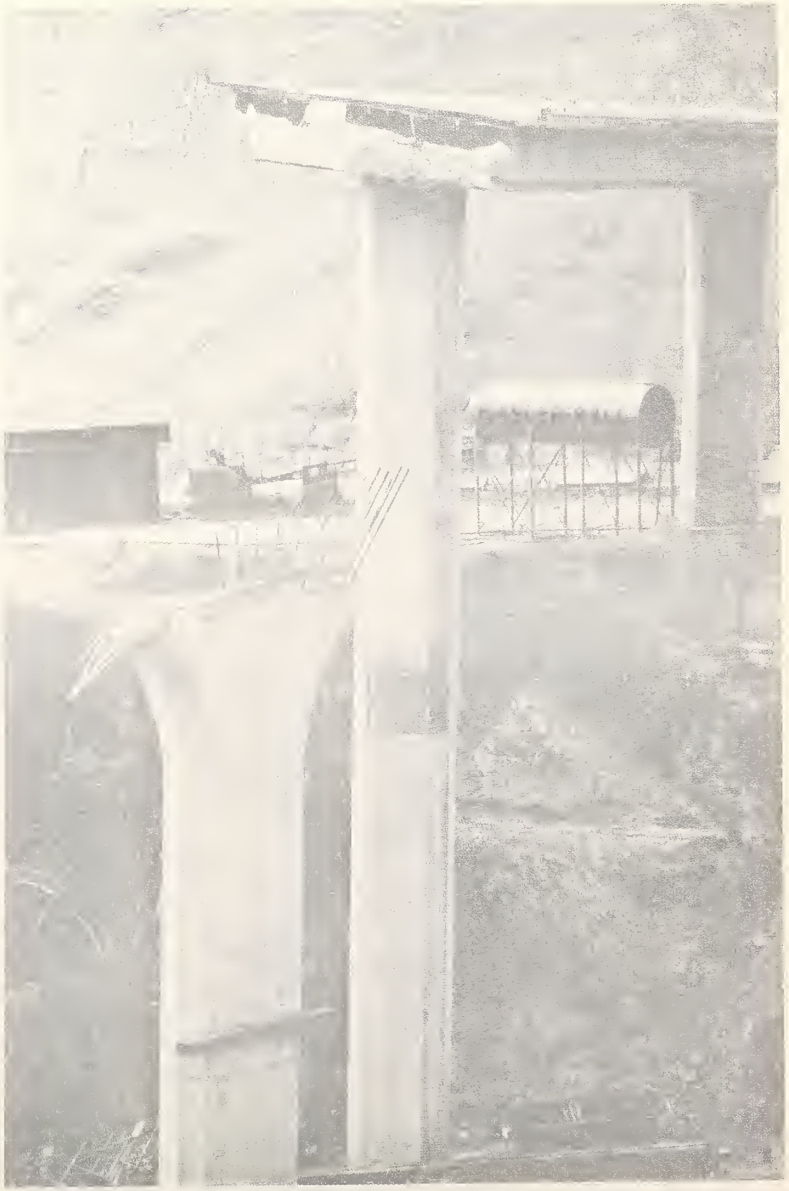

Photo. 2.104 Overcrossing at Golden State Freeway and State Highway 14 interchange

Photo. 2.105 Overcrossing at Golden State Freeway and State Highway 14 interchange

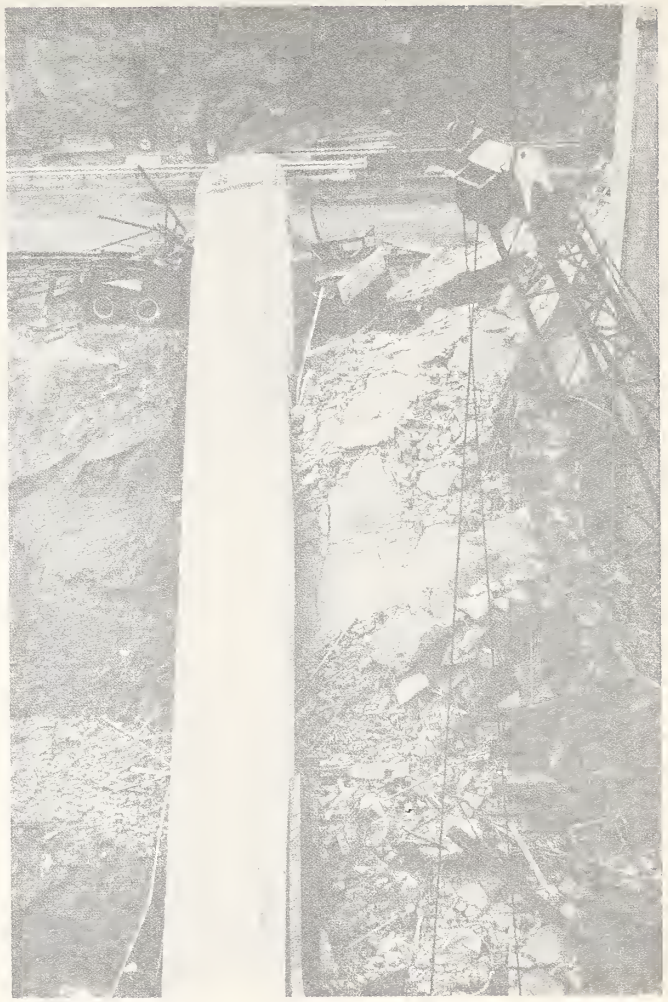

Photo. 2.106 Collapsed span of overcrossing at Golden State Freeway and State Highway 14 interchange

Photo. 2.107 Crane truck crushed by column - Golden State Freeway and State Highway 14 interchange

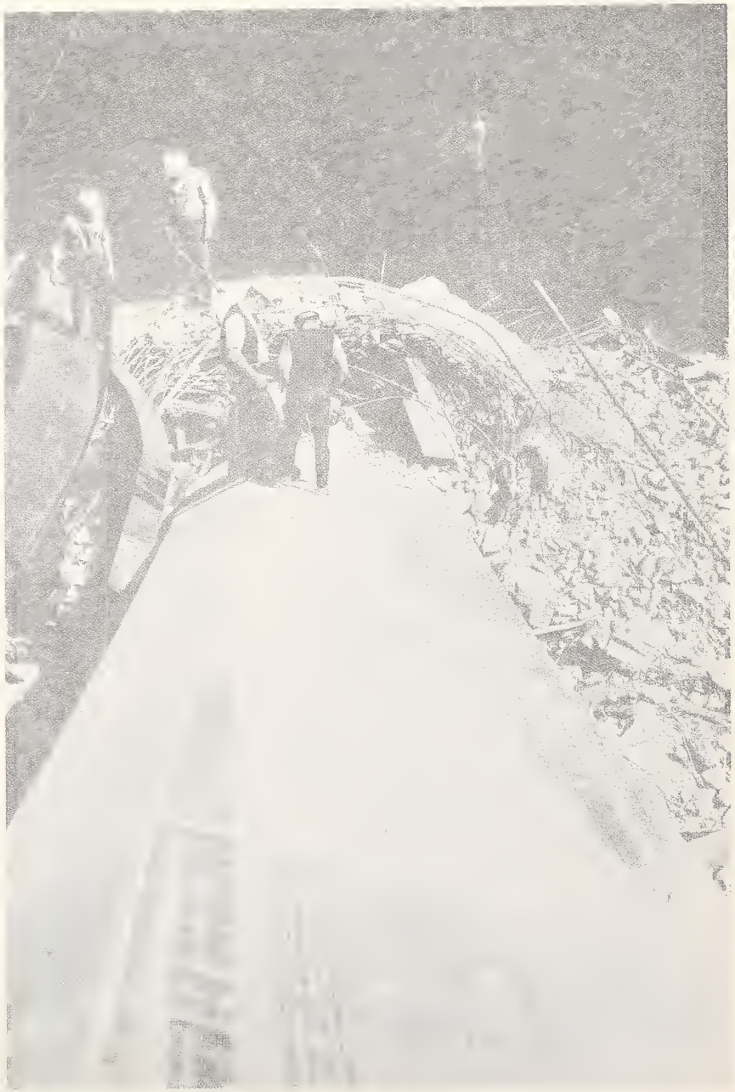

Photo. 2.108 Collapsed column of over-crossing at Golden State Freeway and State Highway 14 interchange

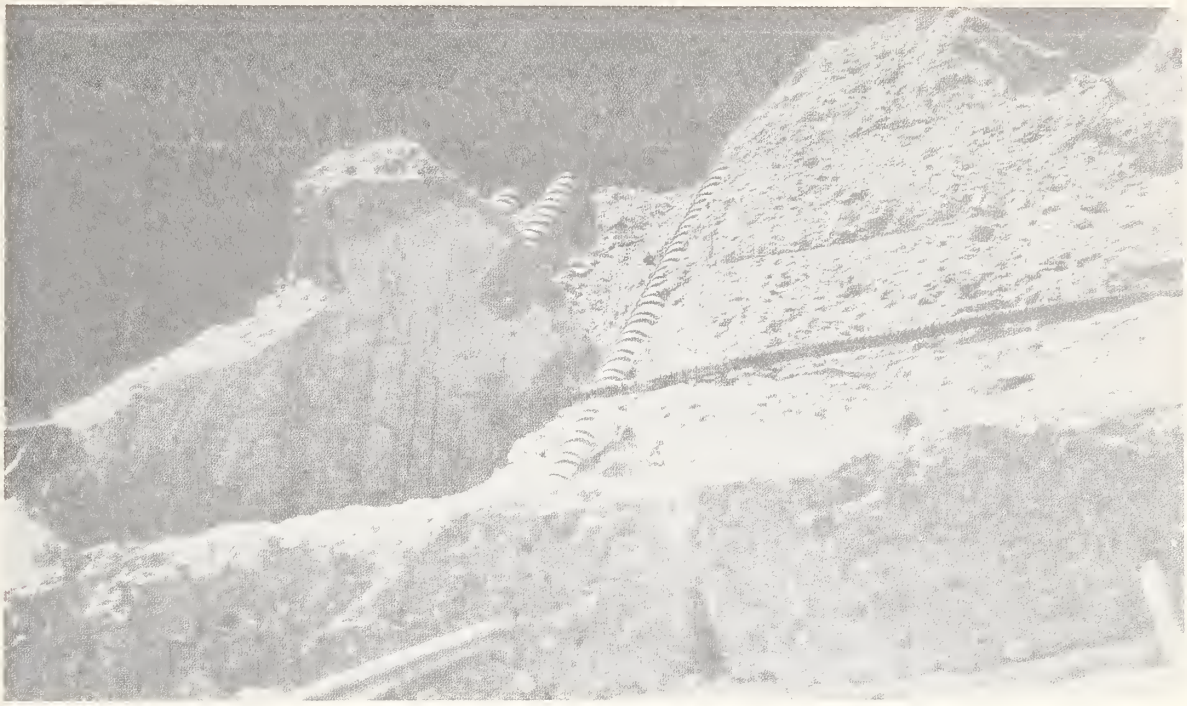

Photo. 2.109 Top end of collapsed column of overcrossing at Golden State Freeway and State Highway 14 interchange

Photo. 2.110 Top end of collapsed column of overcrossing at Golden State Freeway and State Highway 14 interchange

Photo. 2.111 Settlement of backfill at abutment of overcrossing - Golden State Freeway and State Highway 14 interchange

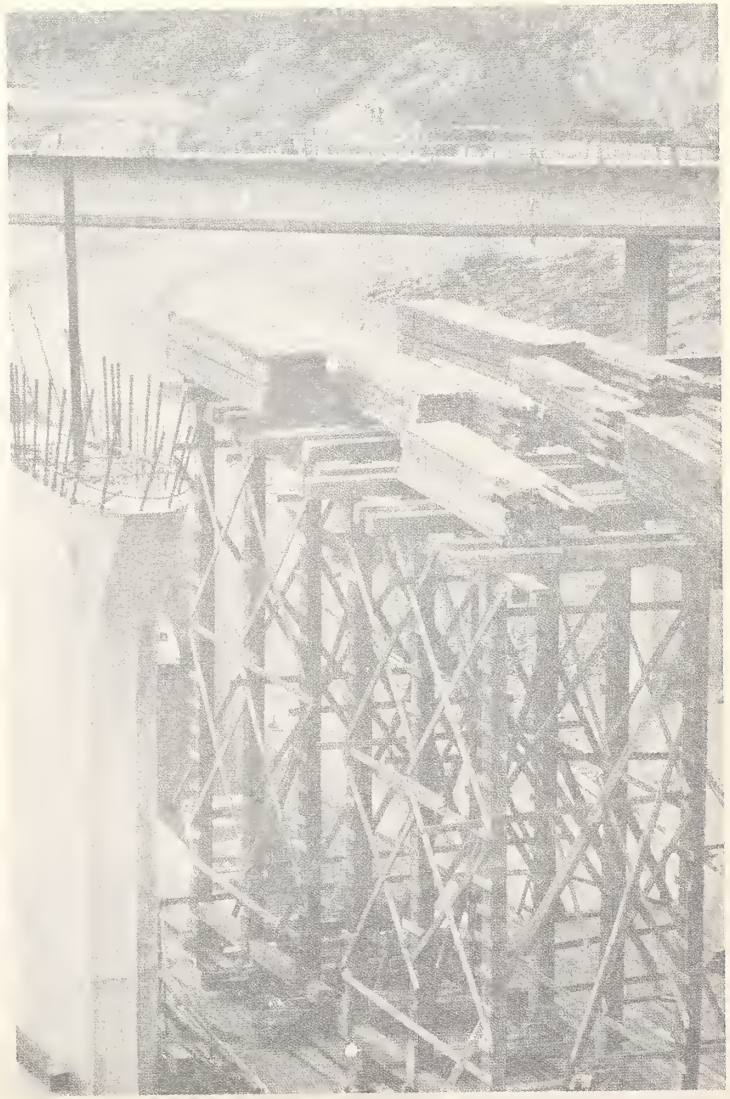

Photo. 2.112 Timber falsework - Golden State Freeway and State Highway 14 interchange

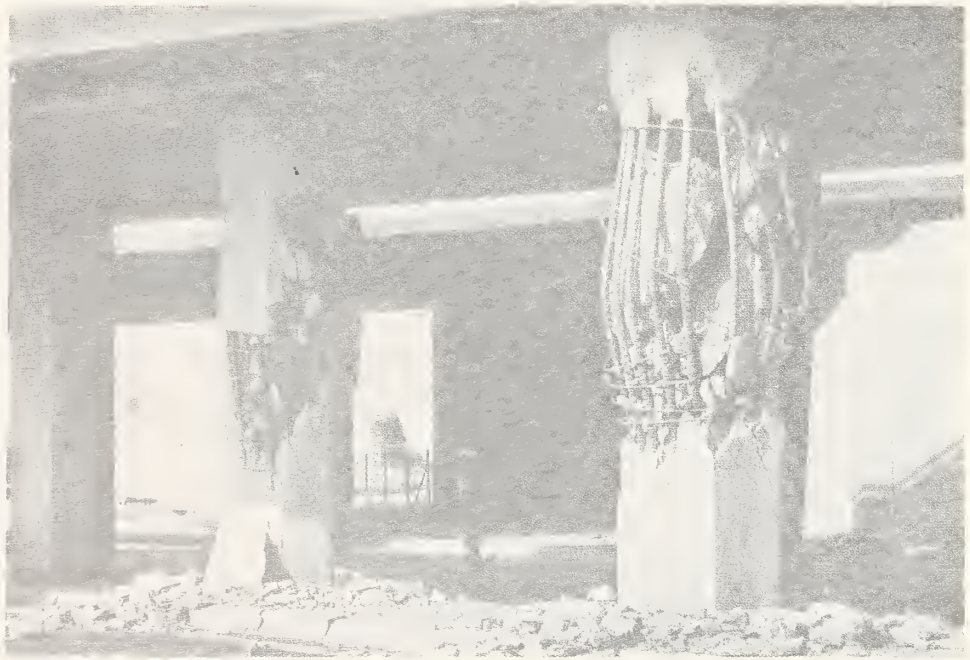

Photo. 2.113 Foothill Boulevard Undercrossing at Foothill Freeway looking in a westerly direction

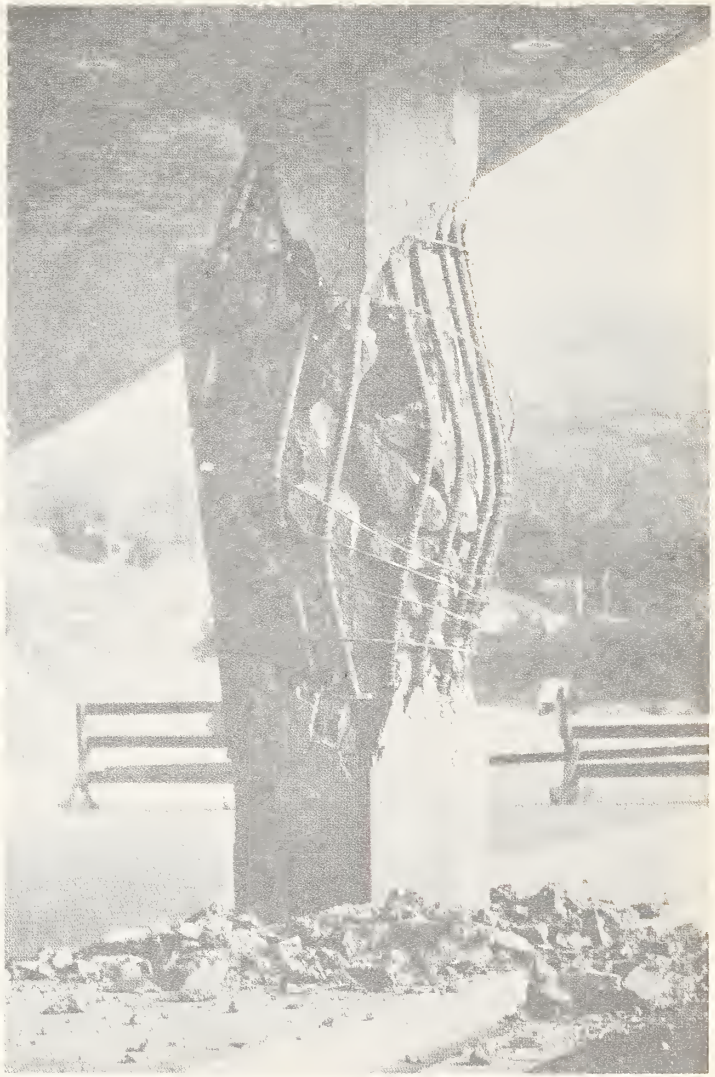

Photo. 2.114 Shear failure of column - Foothill Boulevard Undercrossing at Foothill Freeway

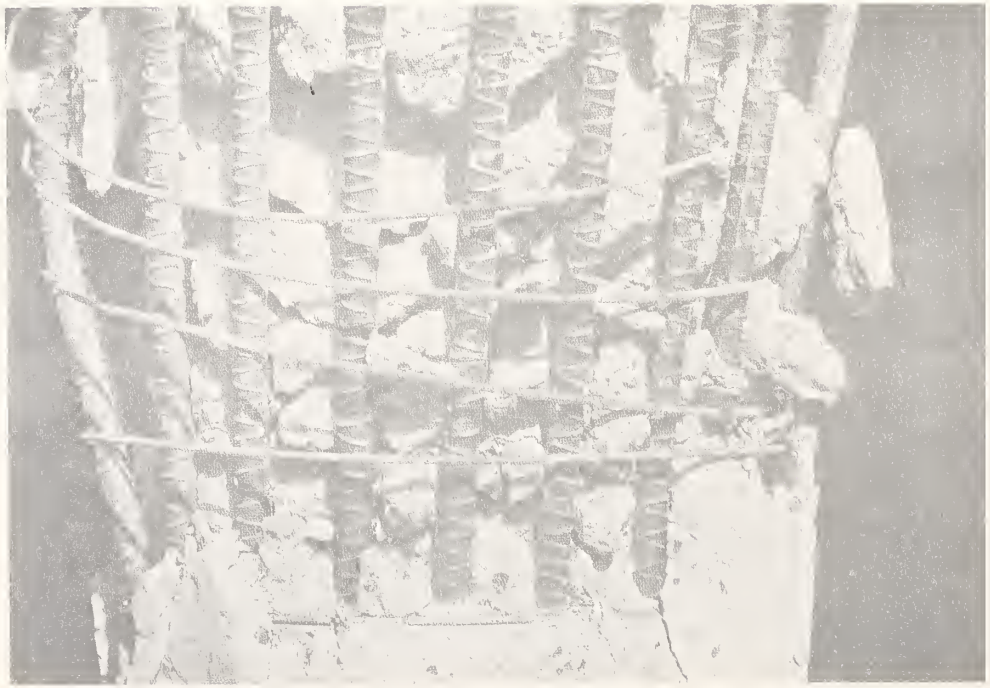

Photo. 2.115 Shear failure of column - Foothill Boulevard Undercrossing at Foothill Freeway

Photo. 2.116 Foothill Boulevard Undercrossing at Foothill Freeway looking in an easterly direction

Photo. 2.117 Damaged wing wall of abutment - Roxford Street Undercrossing at Foothill Freeway

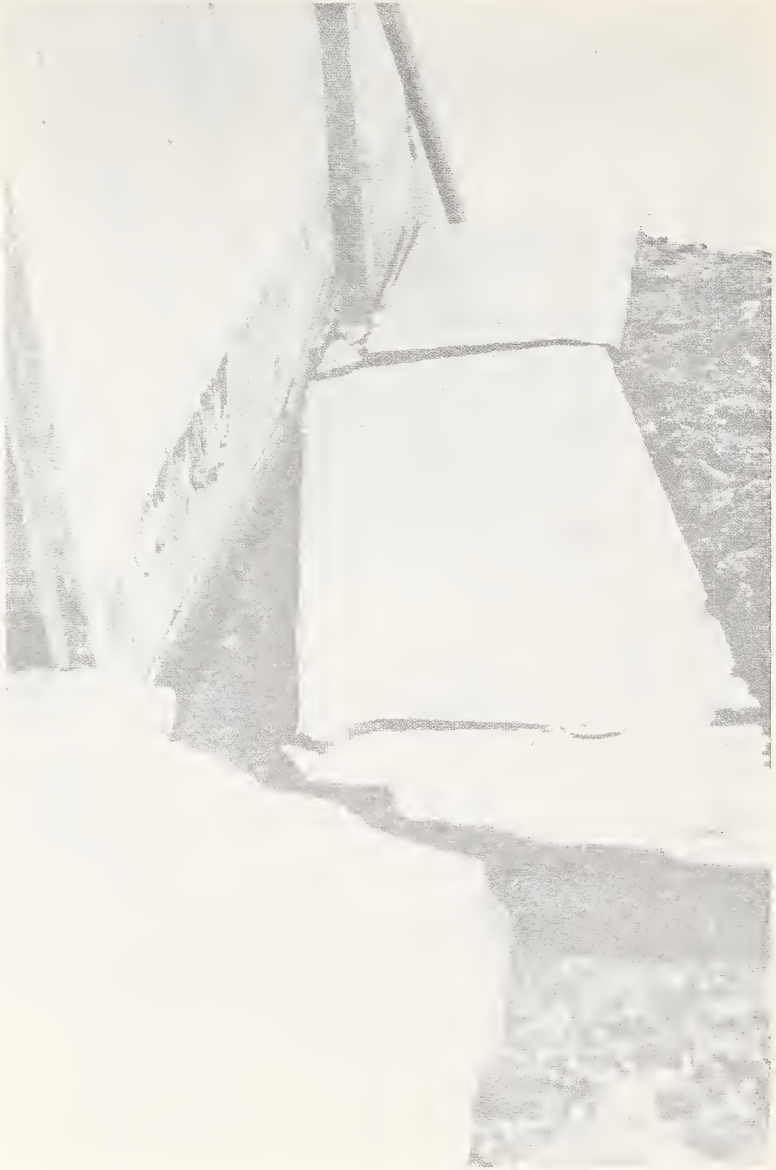

Photo. 2.118 Damaged concrete apron on abutment slope - Roxford Street Undercrossing at Foothill Freeway

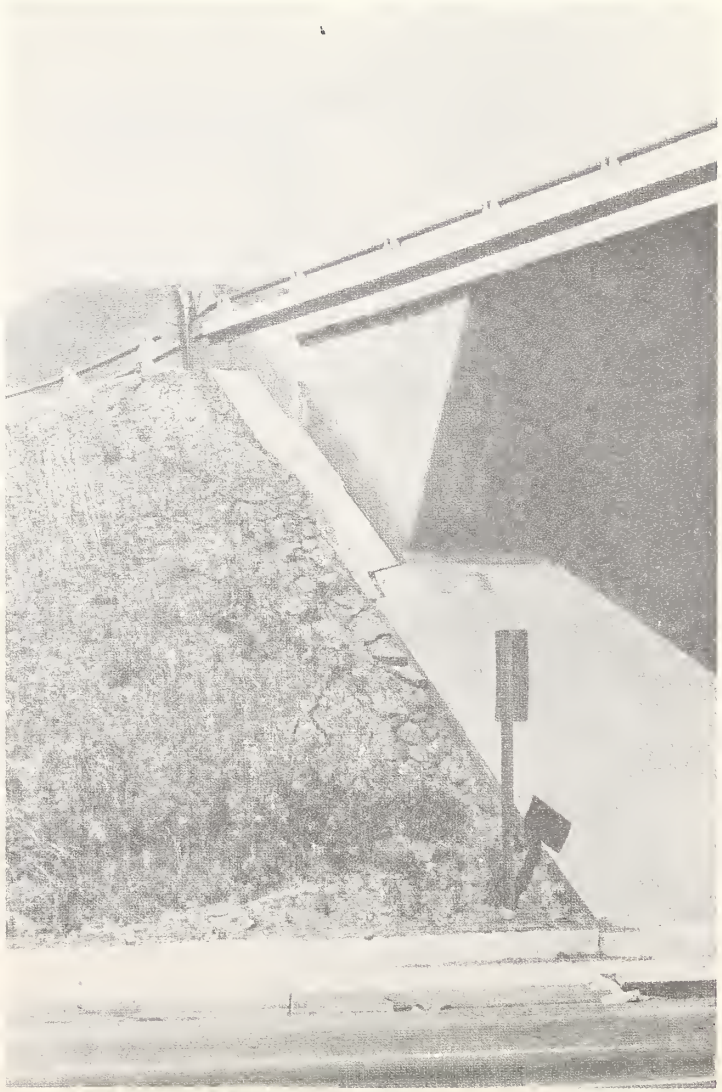

Photo. 2.119 Damaged concrete apron on abutment slope - Roxford Street Undercrossing at Foothill Freeway

Photo. 2.120 Damaged concrete apron on abutment slope - Roxford Street Undercrossing at Foothill Freeway

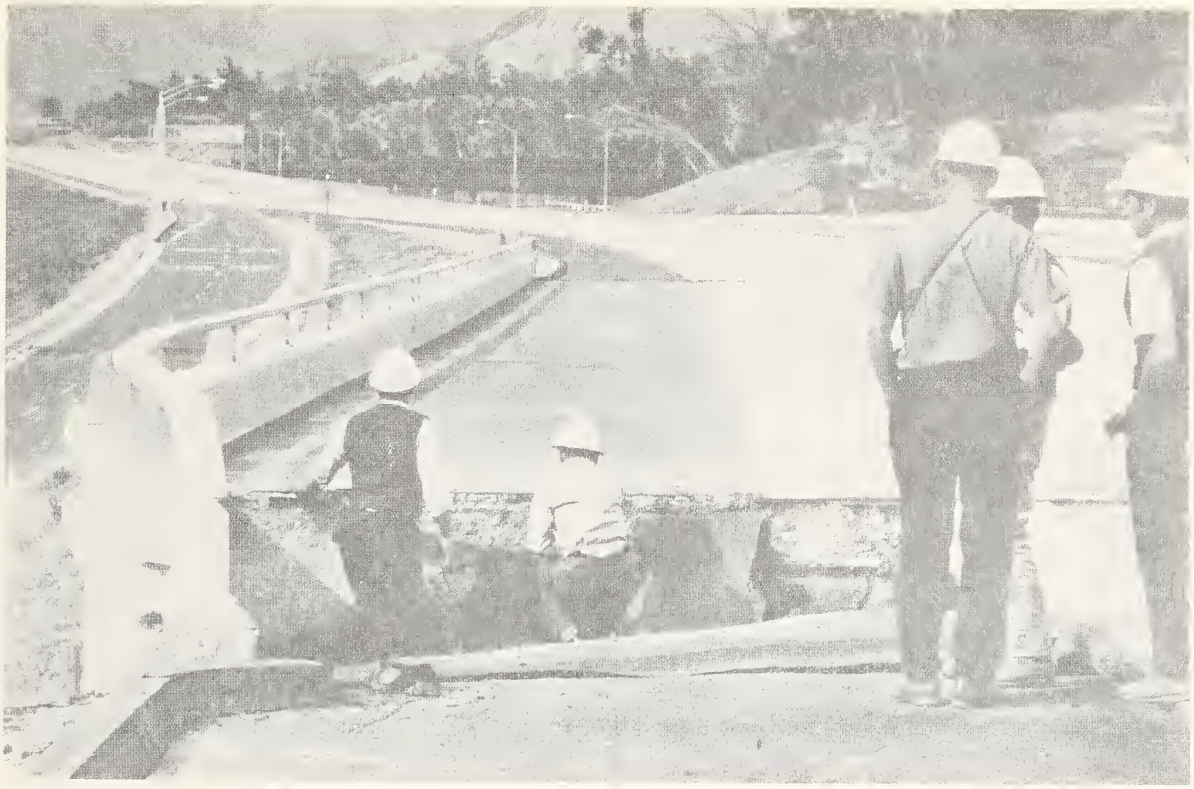

Photo. 2.121 Differential settlement of backfill at abutment - Roxford Street Undercrossing at Foothill Boulevard

Photo. 2.122 Differential settlement of backfill at abutment - Roxford Street Undercrossing at Foothill Boulevard

Photo. 2.123 Differential settlement of backfill at abutment - Polk Street Undercrossing at Foothill Freeway

Photo. 2.124 Differential settlement of backfill at abutment - Polk Street Undercrossing at Foothill Freeway

Photo. 2.125 Differential settlement of backfill at abutment - Polk Street Undercrossing at Foothill Freeway

Photo. 2.126 Differential settlement of backfill at abutment - Polk Street Undercrossing at Foothill Freeway

Photo. 2.127 Differential settlement of backfill at abutment - Polk Street Undercrossing at Foothill Freeway

Photo. 2.128 Buckled asphalt pavement caused by large compressive ground deformations

Photo. 2.129 Differential settlement of backfill at abutment - Hubbard Street Undercrossing at Foothill Freeway

Photo. 2.130 Buckled asphalt pavement caused by large compressive ground deformations

Photo. 2.131 View showing crushed rock forced out of weep hole - Bledsol Street Undercrossing at Foothill Freeway

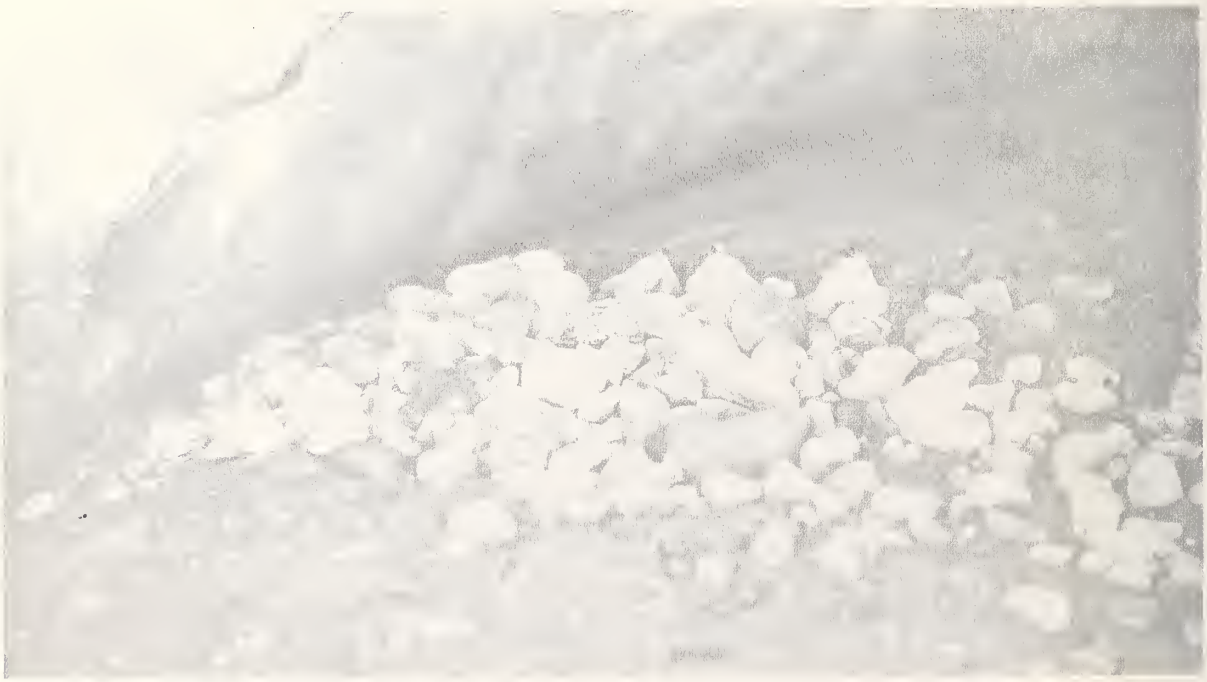

Photo. 2.132 View showing crushed rock forced out of weep hole - Bledsol Street Undercrossing at Foothill Freeway

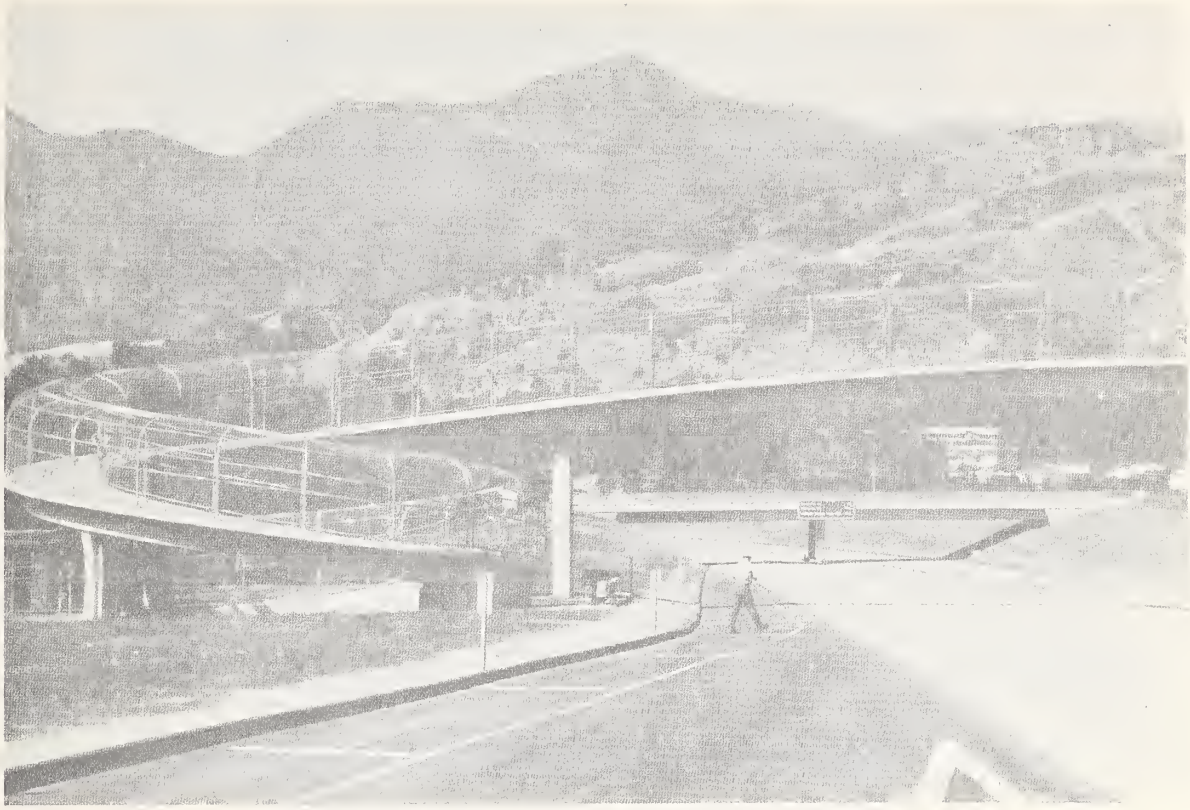

Photo. 2.133 Tyler Street Pedestrian Overcrossing at Foothill Freeway

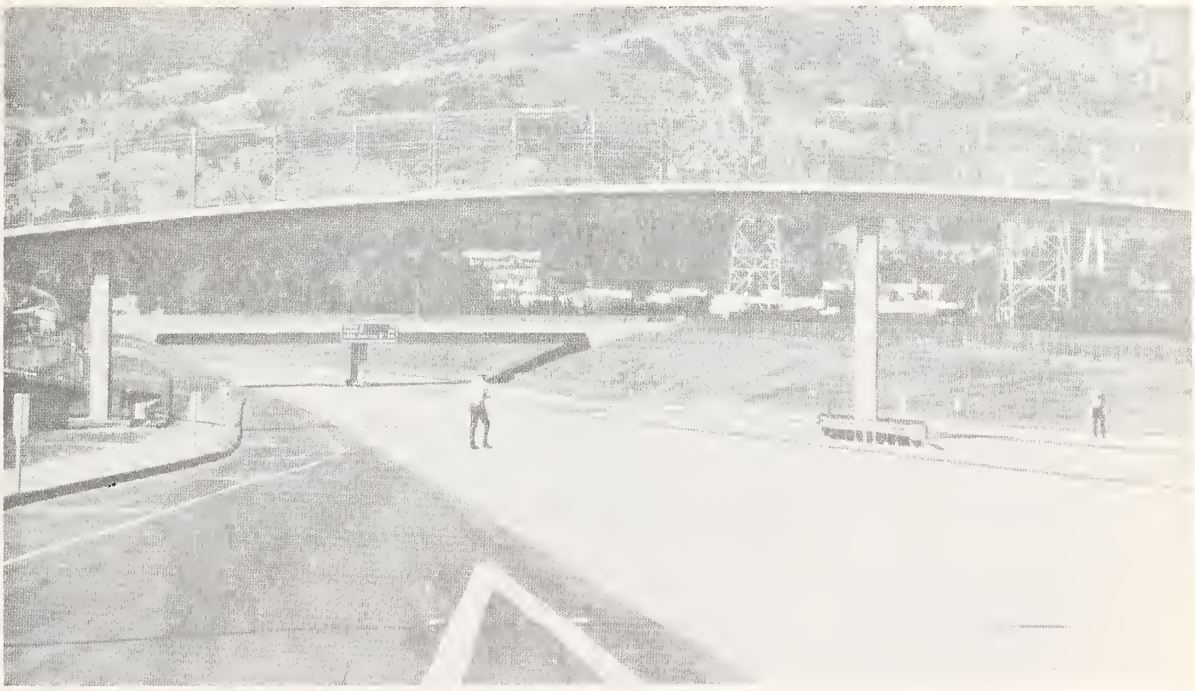

Photo. 2.134 Tyler Street Pedestrian Overcrossing at Foothill Freeway

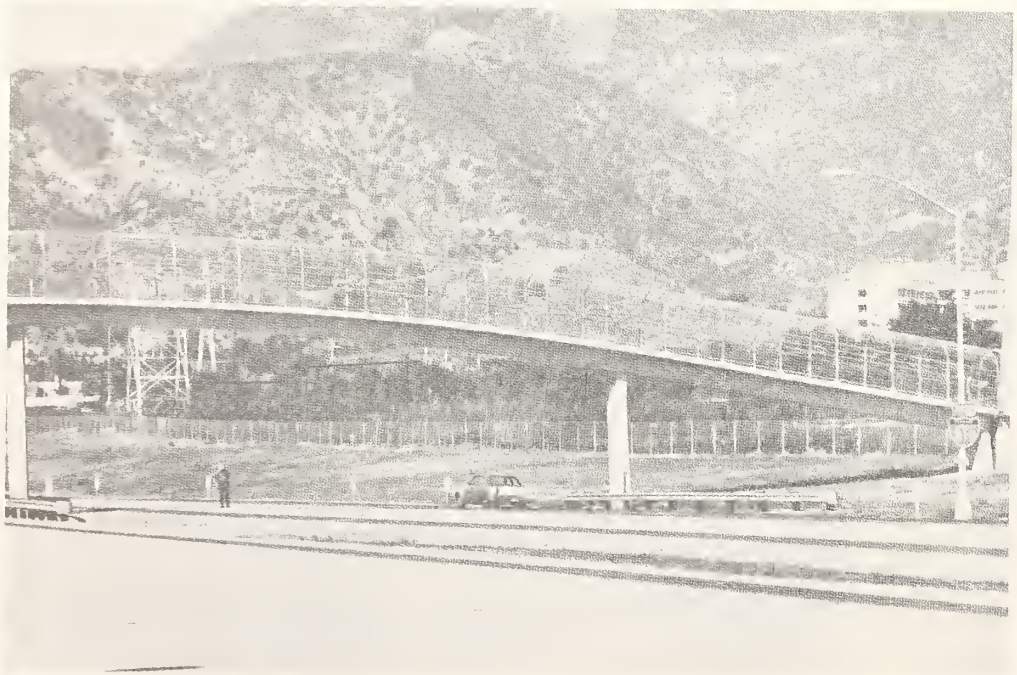

Photo. 2.135 Tyler Street Pedestrian Overcrossing at Foothill Freeway

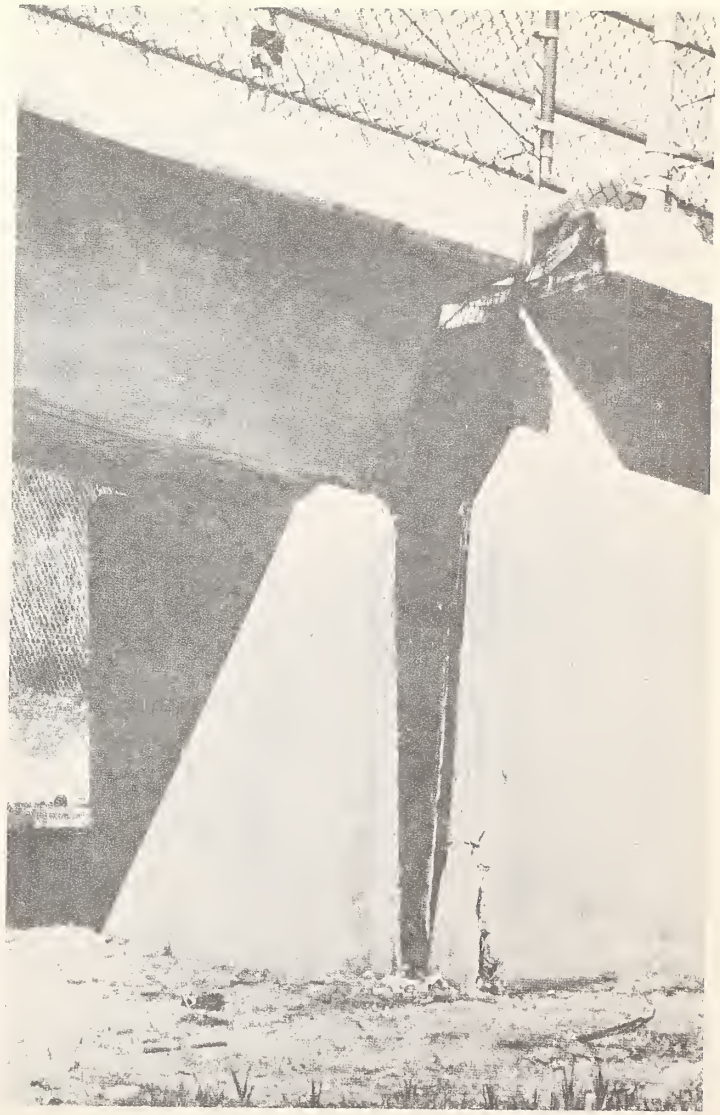

Photo. 2.136 View of permanent support displacement - Tyler Street Pedestrian Overcrossing at Foothill Freeway

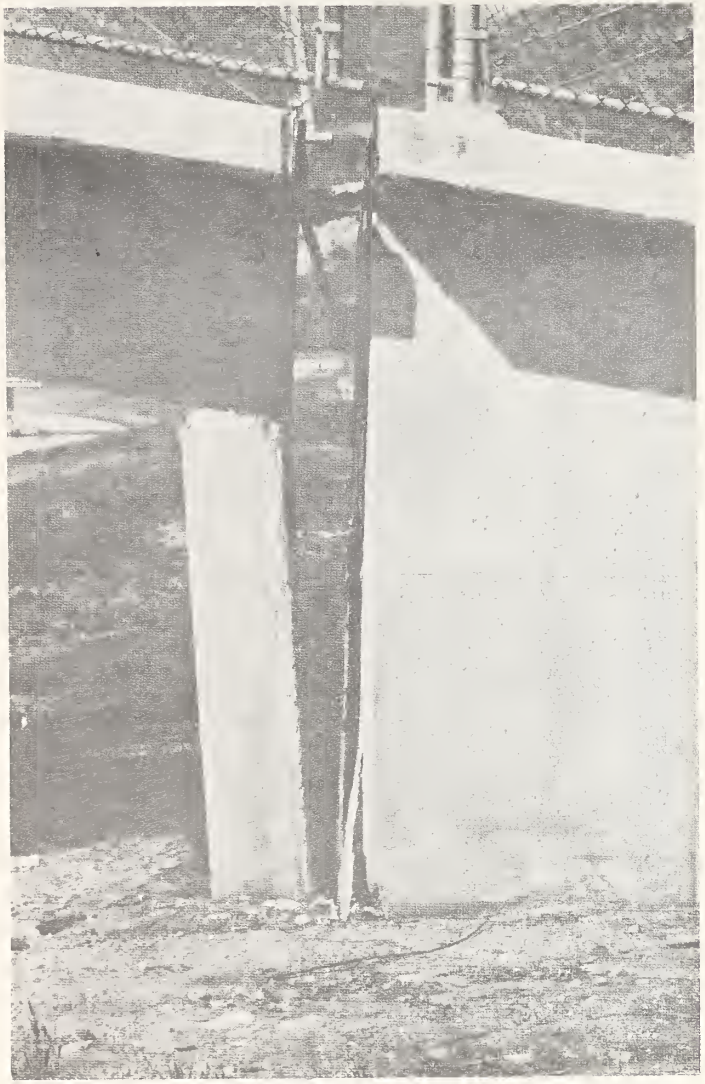

Photo. 2.137 View of permanent support displacement - Tyler Street Pedestrian Overcrossing at Foothill Freeway

Photo. 2.138 Flexural damage at top of column - Tyler Street Pedestrian Overcrossing at Foothill Freeway

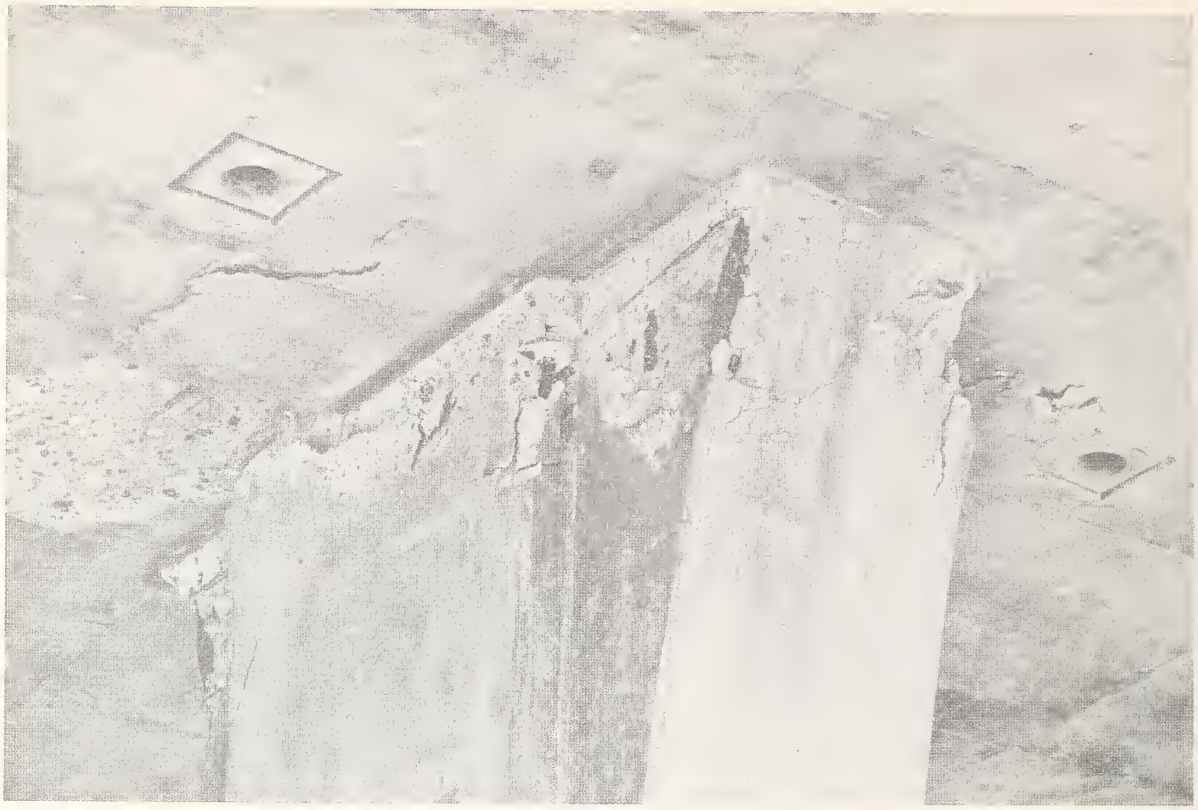

Photo. 2.139 Flexural damage at top of column - Tyler Street Pedestrian Overcrossing at Foothill Freeway

Photo. 2.140 Base of column - Tyler Street Pedestrian Overcrossing at Foothill Freeway

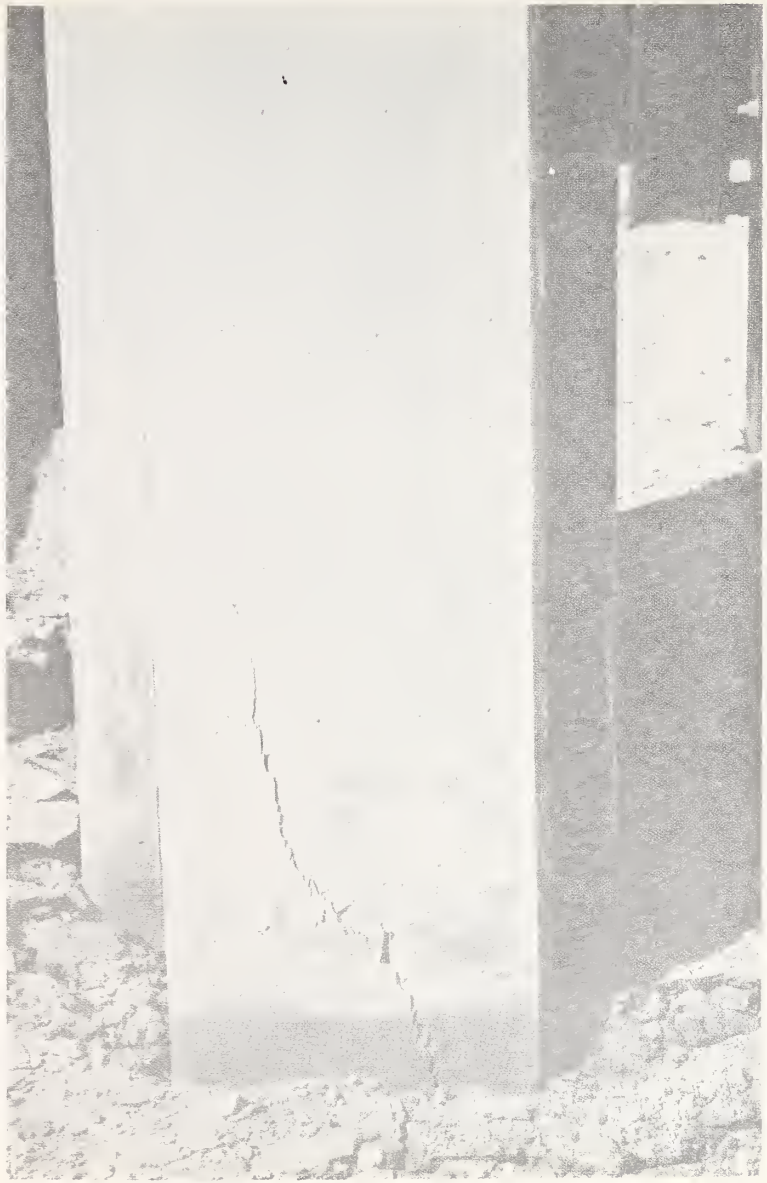

Photo. 2.141 Base of column - Tyler Street Pedestrian Overcrossing at Foothill Freeway

Photo. 2.142 Damaged wing wall of culvert which passes under Foothill Freeway

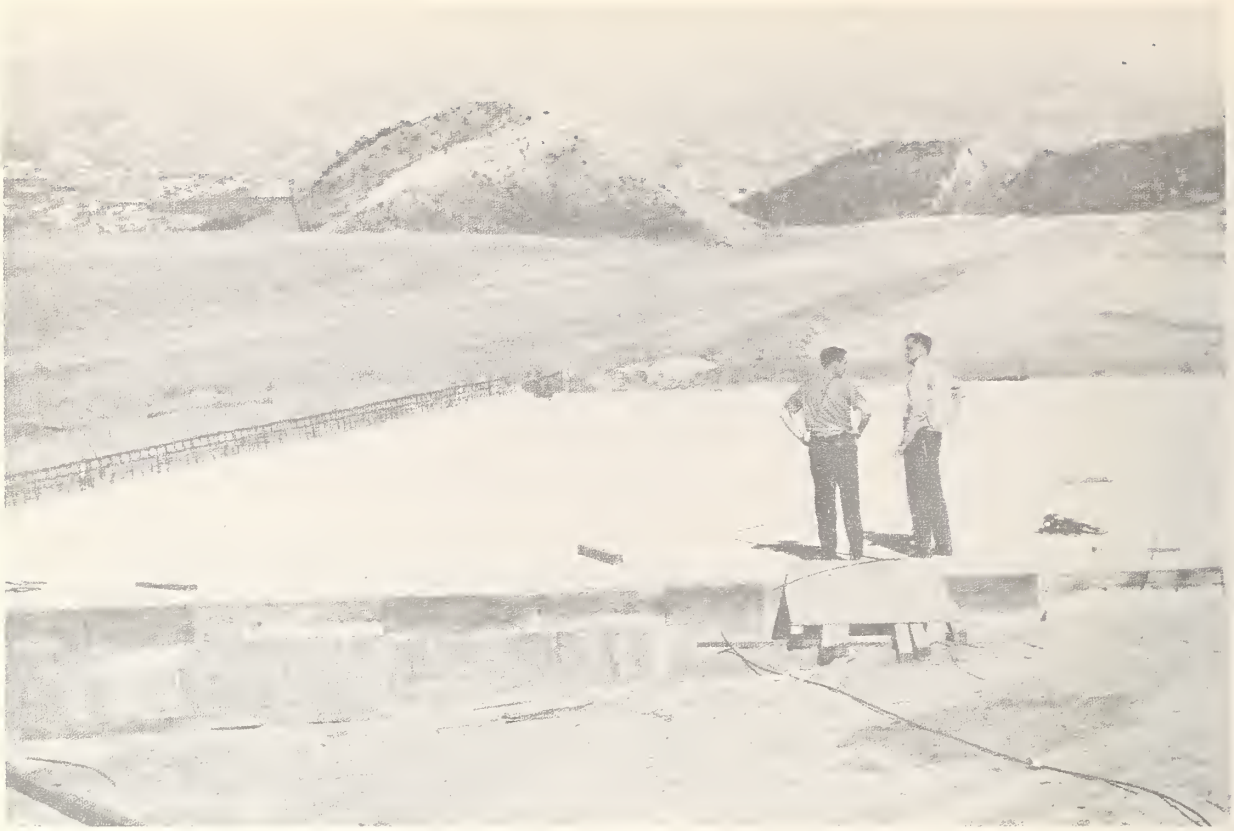

Photo. 2.143 Via Princessa Undercrossing on State Highway 14

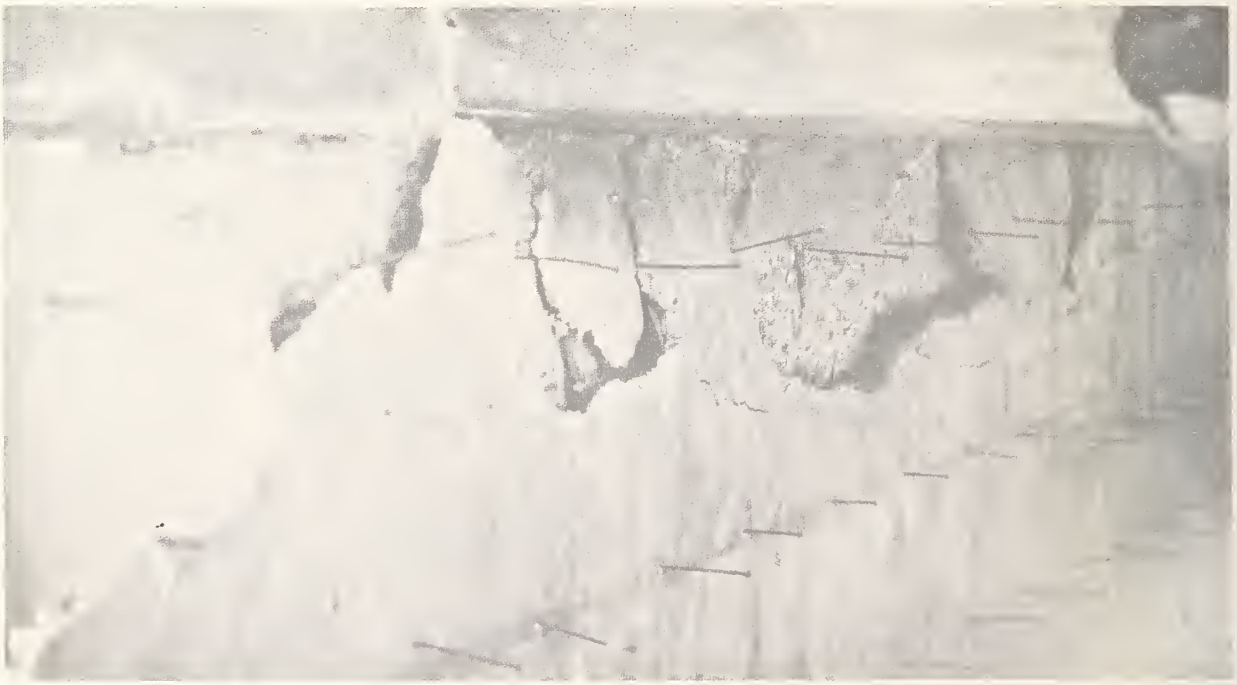

Photo. 2.144 Flexure cracking in diaphragm abutment -
Via Princessa Undercrossing on State Highway 14

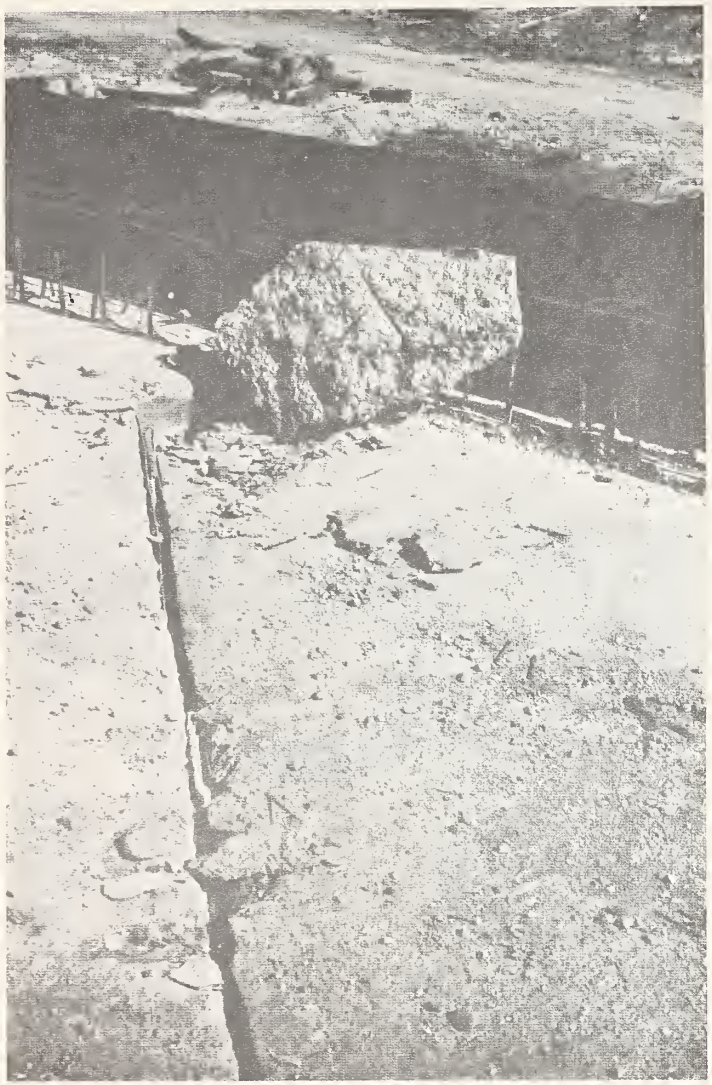

Photo. 2.145 Pounding damage at expansion joint - Santa Clara Overhead Crossing on State Highway 14

Photo. 2.146 Buckled flexible splice in steel conduit - Santa Clara Overhead Crossing on State Highway 14

III RESEARCH ACTIVITIES ON SEISMIC EFFECTS ON BRIDGES

This chapter reviews pertinent research activites related to earthquake-resistant design of bridge structures. Since most of this research has been conducted in Japan, this chapter will be primarily a review of the literature published in that country.

One of the first considerations in any seismic design is to evaluate the seismicity of the site of the proposed structure. This evaluation should consider not only frequency of occurrence of earthquakes but also predictions of intensity and frequency composition of expected ground motions. These predictions are very much related to local soil properties at the structure location. The determination of design seismic forces depends on the predicted ground motions and on the dynamic properties of the structure.

These properties include natural frequencies, mode shapes, damping, and post yield force-deformation characteristics. The dynamic properties of the substructure, as well as the superstructure, are important considerations. These include the effects of surrounding soil and water.

Knowing ground excitation and structural characteristics, analytical capabilities are necessary in predicting accurately dynamic response. Both field and laboratory testing of full scale and model structures can be helpful in developing design criteria.

In the following sections, the above mentioned considerations will be discussed in some detail.

A. SEISMICITY

In Japan, H. Kawasumi performed a study on seismic risk maps for that country and reported his work in 1951 [80]. He listed 342 major earthquakes which occurred in or near Japan between the years 599 and 1945 A.D. Epicenter locations and magnitudes were reported as shown in

Fig. 3.1 and evaluations of expected maximum accelerations throughout the country were given for certain intervals of time. Figure 3.2 shows three maps indicating his contours of expected maximum accelerations for intervals of 75 (A), 100 (B), and 200 (C) years. Although this study was conducted primarily for establishing seismic regulations for buildings, recent seismic regulations for all engineering structures are based on these seismic maps.

In 1968, S. Okamoto published charts of seismic activity in Japan which showed maximum ground displacements occurring during major earthquakes since 1905 [81]. His data were shown graphically in chronological order for 236 locations throughout the country. From these data, he established a relationship giving expected maximum ground displacement at any location in terms of magnitude and epicentral distance.

H. Goto and H. Kameda published a statistical study in 1968 which presented predictions of maximum ground motions during earthquakes [82, 83]. Figures 3.3 and 3.4 show results of their analyses giving maximum ground accelerations and velocities expected during an interval of 75 years.

Later in 1970, T. Okubo and T. Terashima proposed new zoning maps of earthquake risk based on Kawasumi's maps and on the distribution of seismic intensities measured by the Japan Meteorological Agency (JMA) for major earthquakes occurring since 1923 [85], (Fig. 3.5).

Seismicity studies such as those described above are invaluable in determining appropriate seismic forces to be used in structural design. Other factors such as social, economical, and engineering judgement, should also be considered when establishing design loads [162].

B. CHARACTERISTICS OF STRONG GROUND MOTIONS

Earthquake response spectral curves for a linear viscously damped single degree of freedom system are often used as an index for representing dynamic effects of ground motions on structures. M. A. Biot introduced this method [86] in 1943 and later G. W. Housner, R. R. Martel, and

J. L. Alford greatly advanced its acceptance by publishing many response spectrum curves of strong motion earthquakes recorded in the United States [87]. In 1959 Housner proposed using average response spectrum curves as shown in Fig. 3.6(A). Figure 3.6(B) indicates spectrum curves of magnification factors (ratios of response absolute acceleration to the maximum ground acceleration) obtained from Housner's average spectrum curves by assuming the maximum ground acceleration to be 4 ft/sec^2.

In 1965, T. Takata, T. Okubo, and E. Kuribayashi also proposed average response spectrum curves based on an analysis of 20 components of strong motion records in Japan, including one component recorded during the Niigata earthquake of 1964. These average spectrum curves are shown in Fig. 3.7 plotted in terms of amplification factor. It is significant to note that the amplification factors in this figure are generally greater than corresponding values shown in Fig. 3.6(B) for systems with non-zero damping. These factors (Fig. 3.7) have been applied to dynamic analyses of several highway bridges in Japan and also to the specifications for earthquake-resistant design of the proposed Honshu-Shikoku suspension bridges [9].

T. Katayama published in 1969 the results of his analysis of 70 components of strong ground motions recorded in Japan. The objective of this study was to clarify the effects of earthquake magnitude and peak ground acceleration on the characteristics of the response spectrum curves [90]. Later in 1970, S. Hayashi, H. Tsuchida, and E. Kurata published the results of their study of 61 components of strong ground motion recorded for 21 stations during the 1968 Tokachi-oki earthquake and its aftershocks [91]. This study investigated the effects of ground conditions on the characteristics of the response spectrum curves.

In a paper published in 1971 by E. Kuribayashi, T. Iwasaki, and K. Tuji, the authors discussed the effects of such factors as earthquake magnitude, peak ground acceleration, epicentral distance, and ground conditions on the characteristics of response spectrum curves [92]. They proposed four different spectral curves as shown in Fig. 3.8 for various kinds of subsoil conditions ranging from rock to soft alluvium.

C. SUBSOIL FAILURES

Bridge superstructures are supported on substructures which rest on foundations surrounded by subsoil. As pointed out in Chapt. II, ground failures such as faulting, sliding, liquefaction, etc. often cause severe damage to bridge structures. Therefore to design a safe structure it is important to know the possibility of occurrence of these failures. A sound prediction of this type requires careful consideration of geological and engineering information. Should this prediction indicate a high probability of occurrence of a catastrophic subsoil failure, any important structure proposed should not be constructed. Particular attention must however be given to those structures which are inevitably built on such sites.

Since lack of bearing capacity of subsoils seems to be a cause of severe damage to bridge structures, bridge foundations should be designed with full consideration of estimated bearing capacities of subsoils using sound principles of soil mechanics and foundation engineering. It should be recognized that bearing capacities for dynamic loads during earthquakes may be quite different than for static loads. A very large decrease in bearing capacity is often observed for soft saturated sandy soils due to liquefaction during earthquakes. Once liquefaction occurs, the liquefied soils may exert large pressures on substructures during the latter part of a long duration earthquake. In some cases, the ground may slide carrying with it foundations and substructures.

For a complete discussion of the phenomenon of liquefaction and its effects on structures, it is recommended that reference be made to the many excellent papers and reports recently published on this topic.

D. EARTH PRESSURES ON ABUTMENTS

1. Static Earth Pressures - For cohesionless soils, the static earth pressures acting on abutments or retaining walls are given approximately by the well-known Coulomb's formulas [207]. The active

earth pressure p_a at depth x acting on the wall (Fig. 3.9) is given by the equation

$$p_a = [\gamma x + \frac{q \cos \theta}{\cos (\theta - \alpha)}] C_a \tag{1}$$

where C_a is the coefficient of active earth pressure expressed by

$$C_a = \frac{\cos^2 (\phi-\theta)}{\cos^2\theta \cos(\theta+\delta) [1 + \sqrt{\frac{\sin(\phi+\delta) \sin(\phi-\alpha)}{\cos(\theta+\delta) \cos(\theta-\alpha)}}]^2} \tag{2}$$

and where

γ = unit weight of soil

q = uniform vertical surcharge on back fill

θ = angle between the vertical line and the wall surface.

α = angle between the horizontal line and the surface of the backfill.

ϕ = angle of internal friction for the soil

δ = angle of friction between the wall and the soil, usually assumed as $|\delta| = (\frac{1}{2} \sim \frac{3}{4})\phi < 15°$

The passive earth pressure p_p at depth x acting on the wall (Fig. 3.9) is given by the relation

$$p_p = (\gamma x + \frac{q \cos \theta}{\cos(\theta - \alpha)}) C_p \tag{3}$$

where C_p is the coefficient of passive earth pressure expressed by

$$C_p = \frac{\cos^2 (\phi+\theta)}{\cos^2\theta \cos(\theta - \delta) [1 - \sqrt{\frac{\sin(\phi+\delta) \sin(\phi+\alpha)}{\cos(\theta-\delta) \cos(\theta-\alpha)}}]^2} \tag{4}$$

Figures 3.10 and 3.11 indicate the values of coefficients C_a and C_p for various values of ϕ and δ for the case where $\theta = 0$ (vertical wall), $\alpha = 0$ (horizontal backfill), and $q = 0$ (no surcharge).

2. Dynamic Earth Pressures - N. Mononobe [206] and S. Okabe [93] developed two quasi-static methods for predicting approximate earth-pressures acting on walls during earthquakes. One method is based on Rankin's theory of earth pressures and the other is based on Coulomb's theories by simply assuming that the wall together with the backfill statically inclines toward the front of the wall for evaluating active pressures during earthquakes and toward the back of the wall for evaluating passive pressures. The angle of inclination θ_o may be expressed by Eq. (5), when both horizontal and vertical accelerations are taken into consideration simultaneously (Fig. 3.12).

$$\theta_o = \tan^{-1} \frac{k_h}{(1-k_v)} \equiv \tan^{-1} k \tag{5}$$

where

θ_o = angle of inclination of wall and backfill
k_h = horizontal seismic coefficient
k_v = vertical seismic coefficient
k = combined or resultant seismic coefficient

Figure 3.13 indicates the values of k and θ_o for various values of k_h and k_v.

After both wall and backfill rotate by an amount θ_o, the horizontal and vertical lines will tilt by the same amount and the apparent acceleration of gravity may be assumed as $g(1-k_v) \sec \theta_o$ instead of the normal acceleration of gravity g. Based on the assumptions made, the seismic earth pressures acting on the wall (Fig. 3.9) at depth x when subjected to horizontal acceleration $k_h g$ and upward vertical acceleration $k_v g$, simultaneously, can be expressed by the Mononobe-Okabe relations

$$p_{ea} = (1-k_v)\left[\gamma x + \frac{q \cos \theta}{\cos(\theta-\alpha)}\right] C_{ea} \tag{6}$$

$$p_{ep} = (1-k_v)\left[\gamma x + \frac{q \cos \theta}{\cos(\theta-\alpha)}\right] C_{ep} \tag{7}$$

where C_{ea} and C_{ep} are the coefficients of earth pressures during earthquakes as given by

$$C_{ea} = \frac{\cos^2(\phi-\theta_o-\theta)}{\cos\theta_o \cos^2\theta \cos(\delta+\theta+\theta_o)\left[1+\sqrt{\frac{\sin(\phi+\delta)\sin(\phi-\theta_o-\alpha)}{\cos(\delta+\theta+\theta_o)\cos(\alpha-\theta)}}\right]^2} \tag{8}$$

$$C_{ep} = \frac{\cos^2(\phi-\theta_o+\theta)}{\cos\theta_o \cos^2\theta \cos(\delta+\theta-\theta_o)\left[1-\sqrt{\frac{\sin(\phi-\delta)\sin(\phi-\theta_o+\alpha)}{\cos(\delta+\theta-\theta_o)\cos(\alpha-\theta)}}\right]^2} \tag{9}$$

It should be noted that the earthpressures given by Eqs. (6) and (7), are total pressures, i.e. the sum of the ordinary pressures and the increased pressures during earthquakes.

Although the inclination θ_o of both wall and backfill is intentionally assumed for calculation of earthpressures during earthquakes, it does not mean that they actually tilt by that amount. The direction of earth pressures during an earthquake, is therefore still the same as that of ordinary earth pressures as expressed by Eqs. (1) and (2).

Figures 3.14 and 3.15 indicate the values of the coefficients C_{ea} and C_{ep} for various values of k and ϕ for the case where $\theta = 0$, $\alpha = 0$, $q = 0$, and $\delta = 0$(zero friction between wall and soil). Values for $\delta = \pm 15°$ are also given [15]. From these figures, one will note that the magnitudes of seismic earth pressures for the case of $k = 0.2$ are about 1.5 times the ordinary active pressures and about 90 percent of the ordinary passive earth pressures.

In 1933, N. Mononobe reported results of an experiment to determine seismic earth pressures using a container placed on top of a harmonic shaking table [206]. The results he obtained agree quite satisfactorily with the formulas described above. Figure 3.16 gives the basic results of this experiment. Similar experiments were later reported by H. Matsuo and S. Ohara [94], S. Niwa [95], Y. Ishii,

H. Arai, and H. Tsuchida [96], and others.

Y. Ishii, H. Tsuchida, and T. Furube reported in 1963 the results of an experiment on dynamic earth pressures and dynamic pore water pressures in saturated sands considering the behavior of the saturated sands after the occurrence of liquefaction [97].

Regarding the dynamic earth pressures for cohesive soils, very little information is available. When designing structures for these soils, it is often assumed that earth pressures during earthquakes are equal to the static pressures. However, in some cases increased earth pressures are used to account for seismic forces.

E. HYDRODYNAMIC PRESSURES ON SUBSTRUCTURES

To determine the hydrodynamic pressures acting on dams during earthquakes, H. M. Westergaard developed the following simplified formula which assumes the dam as a two-dimensional vertical wall [98].

$$p = \frac{7}{8} k_h \gamma_w \sqrt{hx} \tag{10}$$

where

p = hydrodynamic pressure at depth x

k_h = horizontal seismic coefficient

γ_w = unit weight of water

h = depth of reservoir

This formula has been used widely in the design of gravity dams.

Considerable research has been conducted to determine the dynamic effects of reservoirs on columns such as bridge piers. As reported in 1939, J. L. Savage attempted to evaluate the dynamic effects of a reservoir on the piers of the Pit River Bridge [99]. R. W. Clough conducted extensive experiments on the dynamic effects of water on rigid and flexible columns [100]. A. Sakurai performed three-dimensional analysis and experiments on the hydrodynamic pressures acting on vertical

circular columns [101]. H. Goto and K. Toki also conducted three-dimensional analyses and experiments and suggested the following formulas for computing hydrodynamic pressures on columns when subjected to seismic motions, Fig. 3.18 [103].

$$p = \alpha\, k_h\, \gamma_w\, A\, \frac{b}{a}\left(1 - \frac{b}{4h}\right)\sqrt[3]{\frac{x}{h}} \qquad \frac{b}{h} \leqslant 2$$

$$p = \alpha\, k_h\, \gamma_w\, A\, \frac{b}{a}\left(0.7 - \frac{b}{10h}\right)\sqrt[3]{\frac{x}{h}} \qquad 2 < \frac{b}{h} \leqslant 4 \tag{11}$$

where

p = hydrodynamic loading acting on column per unit length at depth x.

A = cross-sectional area

α = a coefficient depending on vibrational mode of column ($\alpha = 1$ for translational motion)

These formulas are commonly used in Japan for use in the design of bridge piers.

S. Kotsubo and T. Iwasaki also conducted theoretical analyses and experiments on hydrodynamic effects on bridge piers [102, 104].

F. DYNAMIC PROPERTIES OF HIGHWAY BRIDGES

Extensive investigations have been carried out primarily in Japan to determine the dynamic properties of bridge structures such as natural periods, mode shapes, and damping characteristics. Numerous dynamic tests have been conducted on actual bridges usually with excitations small in comparison with those caused by major earthquakes.

In the following sections, the results of some typical dynamic tests on actual bridge structures will be described.

1. Shinkatsushika Bridge [116] - This bridge crosses the Edo River on National Highway No. 6 between Tokyo and Chiba. It was constructed

by the Ministry of Construction in 1965 (Figs. 3.19 - 3.24; Table 3.1 - 3.3).

Figure 3.19 gives a general view of the bridge, a typical cross-section of the superstructures (steel box girders), and the subsoil conditions near the site of pier No. 5 including the results of standard penetration tests. The bridge consists of 8 equal spans having a total length of 442 m and a width of 17.7 m. Figures 3.20 and 3.21 give brief information on piers Nos. 4 and 5 in which several transducers (accelerometers, earth pressure meters, and pore-water pressure meters) were installed during construction to measure their dynamic characteristics. The soil conditions at the bridge site are generally very dense sandy layers. Both abutments are reinforced concrete buttress types supported on steel pipe piles. The seven piers are of reinforced concrete construction with open caisson foundations. The static seismic coefficients used in design of the bridge were 0.25 in a horizontal direction and 0.10 in the vertical direction. Components of force in both directions were assumed to act simultaneously.

Employing a centrifugal-type mechanical exciter capable of exerting dynamic horizontal forces up to 40 tons with a frequency range 1-13 Hertz, the Public Works Research Institute of the Ministry of Construction conducted comprehensive dynamic tests on two piers (Nos. 4 and 5) in 1963 and on the overall structure immediately after completion of the bridge in 1965. The object of these tests was primarily to obtain the dynamic properties of the substructures and the whole structure in the longitudinal direction.

The test results for pier No. 4 are briefly summarized in Table 3.1 and Fig. 3.22 which include resonance curves for the motions at the pier cap, damping ratios, and distribution of dynamic earth pressures for various magnitudes of exciting forces. Similar results are shown in Table 3.2 and Fig. 3.23 for pier No. 5. The results for the whole structure are summarized in Table 3.3 and Fig. 3.24. Based on these results, the following conditions have been deduced:

(a) The fundamental resonant frequencies were between 4.9 - 5.8

Hertz and 5.0 - 6.0 Hertz for piers Nos. 4 and 5, respectively. These frequencies varied appreciably with magnitude of the exciting force indicating non-linear behavior. Maximum accelerations at the caps of the piers during the various tests were about 60 - 220 gals (1000 gals $\doteq$ 1 g) for pier No. 4 and 20 - 110 gals for pier No. 5. The damping ratios were 5 - 7 percent of critical for pier No. 4 and 8 - 12 percent for pier No. 5. In neither case was there a clear relationship between amount of damping and amplitude of oscillation. The shapes of deformation during vibration were primarily rocking motion with the centers of rotation about one-third height from the bottom of the caisson foundations and simple bending of the columns. The dynamic earth pressures acting on the sides of the caisson foundations were approximately proportional of the dynamic amplitudes of displacement and the dynamic coefficient of subgrade reaction (ratio of earth pressure to amplitude) was approximately 4 kg/cm^3.

(b) Regarding the whole structure, its fundamental frequency was about 2.8 Hertz in the longitudinal direction with damping ratios of about 6.6 percent of critical. The maximum acceleration at the level of the superstructure was about 14 gals. for an exciting force amplitude of 9.1 tons. Pier No. 5, supporting the fixed bridge supports, vibrated together with the superstructure. However, the other substructures (P4, P6, P7, and A2) having movable bridge supports moved a negligible amount. The shape of deformation of pier No. 5 was similar to that of the pier itself without the superstructure being present.

The dynamic behavior of the Shinkatsushika bridge during actual earthquakes have been measured by six transducers (three accelerometers and three earth pressure meters) installed for the dynamic tests in the caisson foundation of pier No. 5, and two strong-motion accelerographs permanently installed after completion of the bridge on the crest of pier No. 5 and on the ground surface nearby. Some results obtained by these instruments will be discussed subsequently.

2. Torii Bridge [116] - This bridge, constructed by the Ministry of Construction in 1968, is located on National Highway No. 49 at the boundary between Fukushima and Niigata Prefectures (Figs. 3.25 - 3.29). A side view of this bridge is shown in Fig. 3.26 and several brief drawings of the caisson foundation of Pier No. 1 are presented in Fig. 3.26. Several transducers (ten accelerometers and eleven earth pressure meters) were installed in this pier during construction for use during dynamic testing.

Both abutments are L-shaped reinforced concrete buttress-type structures with projections to resist horizontal forces. The two piers are solid reinforced concrete columns (cross-sections pier No. 1, 3.0 m x 10.2 m bottom, 1.5 m x 10.2 m crest) with caisson foundations (cross-section pier No. 1, 8 m x 13.5 m with depth 8 m). The design seismic coefficients used were 0.25 horizontally and 0.1 vertically. The foundations of all four substructures rest on tuff and the two caisson foundations are surrounded by tuffy clay with gravel.

The superstructure of length 115 m and width 7 m consists of 3 continuous curved spans using steel plate girders. The supports are fixed at the left abutment, pinned at the piers, and movable at the right abutment.

The dynamic field tests were performed in two stages. In 1967, the caisson foundation of pier No. 1 was excited with a mechanical shaker capable of producing force amplitudes up to 10 tons within the frequency range 0.5 - 20 Hertz. During this same year, the overall bridge structure was excited in the transverse direction using a larger shaker (20 tons maximum force) placed on the deck slab between the two piers.

The results of the first series of tests on the foundation of pier No. 1 are shown in Figs. 3.27 and 3.28 for longitudinal and transverse excitation, respectively. Figure 3.29 presents the results for the second test series on the overall structure with excitation in the transverse direction. These results show typical response curves, natural frequencies, damping ratios, and mode shapes from which the following conclusions may be deduced:

(a) The fundamental frequencies of the caisson foundation are

12.0 and 13.0 Hertz in the longitudinal and transverse directions, respectively, and the damping ratios are about 15 percent in both directions. The mode shape is a combination of rocking motion and translation with the center of rotation being near the base of the foundation for longitudinal motion and being approximately 10 m below the base for transverse motion. The coefficient of subgrade reaction at the base was found to be about 15 kg/cm^3.

(b) The three lowest resonant frequencies for vibration of the complete structure in the transverse direction was 3.26, 4.12, and 5.70 Hertz. The damping ratios for these modes were all about 2.8 percent of critical.

Following the vibration tests, extensive analytical studies were conducted to establish better mathematical models for both the superstructure and substructure to be used in dynamic analyses.

3. Sokozawa Bridge [116] - This bridge was constructed in 1968 by the Japan Highway Public Corporation. It is located on the Chuo Expressway about 50 km west of Tokyo at a point where the expressway crosses a deep creek. A general view of the bridge and the dimensions of pier No. 3 are shown in Figs. 3.30 and 3.31, respectively. Both abutments are gravity-type reinforced concrete structures and the four piers are I-shaped steel framed reinforced concrete construction with spread footings. Piers 1 and 4 use cast-in-place concrete pile foundations resting on hard rock to support the footings. The columns of two piers (Nos. 2 and 3) are about 50 m high while the other two are about 30 m high.

The superstructures consist of two separate continuous steel truss girders. One is continuous over two spans and the other is continuous over three spans. The superstructures are hinged to the pier caps so that the longitudinal seismic forces of the superstructures and parts of the piers are carried by the two rigid gravity-type abutments.

The bridge was designed in accordance with specifications proposed by the Subcommittee on Highrise Piers, Expressway Research Foundation. These specifications are presented subsequently in Chapter IV. The basic seismic coefficients used in design were 0.2 horizontally and 0.1 vertically. The design seismic coefficients for the piers in the transverse direction were increased by factors of 1.00 to 1.66 with the magnitude of increase changing with pier height.

Two series of field dynamic tests were conducted on this bridge. The first series in 1967 were carried out on pier No. 3 just before erection of the superstructure and the second series were carried out on the overall structure immediately after completion of the bridge in 1967.

The first series of experiments on pier No. 3 consisted of steady state forced vibration tests in the longitudinal direction using a 15-ton exciter and in the transverse direction using a 40-ton exciter and impulse free vibration tests utilizing the propulsion of a rocket in the longitudinal direction. Since the fundamental period of vibration of the pier was estimated to be relatively long (about 1.4 sec) in the longitudinal direction, a rocket engine capable of yielding a thrust of 2 tons with a duration of 1 second was mounted on the pier cap. The short duration impulsive load initiated the dynamic response and the free vibration response which followed was monitored. While this method of excitation is now commonly used in Japan, the Sokozawa bridge tests were the first of its kind to utilize this method. The results of these tests are tabulated in Table 3.4 along with calculated values. Resonant frequencies of 0.77 and 4.62 Hertz were found in the longitudinal direction and a resonant frequency of 2.38 Hertz was found in the transverse direction. The damping ratios were found to be in the range 0.6 - 1.0 percent of critical.

The second series were steady state forced vibration tests of the whole structure. Excitation was in the transverse direction using a mechanical exciter. Twenty transducers were used to monitor the dynamic response (Fig. 3.32). Resonance curves for the motion

measured at midpoint of the center span are shown in Fig. 3.33(A). The three lowest resonant frequencies measured were 1.53, 2.38, and 2.63 Hertz. Damping ratios for the corresponding modes were 1.3, 1.7, and 1.7 percent of critical, respectively. The shapes of these modes are given in Fig. 3.33(B).

Following the field tests, extensive analytical studies were carried out to evaluate dynamic properties and predict dynamic response (see Section H).

4. Other Japanese Bridges - A number of field dynamic tests were conducted on other bridges located along the Chuo and Tomei Expressways which were constructed by the Japan Highway Public Corporation. These include the Yokobuki, Tsuru-kawa, and the Sakawa-gawa bridges which are similar in construction to the Sokozawa bridge.

5. Observed Dynamic Properties of Japanese Highway Bridges - During the period 1958 to 1969, twenty six highway bridges in Japan, including those described above, have been tested dynamically. A summary of some of the more pertinent results of these tests, especially the relationship between natural periods and damping ratios, has been published by E. Kuribayashi and T. Iwasaki [116].

Figure 3.34 indicates the relationship found between natural periods and corresponding damping ratios. In this figure, Group A denotes results of fundamental modes for ordinary bridges, while Group B denotes results for the 1st, 2nd, and 3rd modes of vibration for bridges supported on piers of heights greater than 25 meters above the crests of foundations. The results in Fig. 3.34 have been obtained for foundations alone, piers on foundations and for overall bridge structures. The data presented are classified on the basis of structural type (foundation, substructure, overall structure) and kind of foundation (footings, piles, caissons).

The natural period - damping ratio relation found for Group A structures are shown in Fig. 3.35. In this figure, the numerals indicate mode numbers and the data for one structure are linked by a solid line. Figure 3.36 indicates the relationship between height

of piers and fundamental periods of vibration for overall structures together with corresponding results of isolated piers. From these results the following conclusions may be deduced:

(a) The fundamental natural periods of horizontal motions are about 0.07 to 1.0 seconds for foundations, and about 0.1 to 1.3 seconds for overall structures. The fundamental periods get noticeably longer as pier heights increase.

(b) Damping ratios of bridge structures for horizontal vibrations are approximately 0.02/T for ordinary bridge structures including foundations, piers, and superstructures (T denotes fundamental period in seconds) and are about 0.013 for highrise piers alone and for bridges with highrise piers.

(c) The results obtained from field tests are for small amplitude vibration. Based on the results of the Shinkatsushika bridge it appears that the dynamic properties vary significantly with even small changes in amplitude. Therefore, dynamic properties for large amplitude oscillation can be expected to differ appreciably from those described above. The natural periods tend to get longer and the damping ratios become higher as the amplitude of oscillation increases.

6. Waiau River Bridge [228] - This bridge, located at Tuatapere in the South Island of New Zealand was tested at several stages of construction with steady-state forced vibration excitation to determine the dynamic properties of the substructure. The bridge consists of six continuous spans (62 ft.+ 4 @ 85 ft. + 62 ft.) built with post-tensioned prestressed beams and a reinforced concrete deck slab. The piers are of reinforced concrete construction and are supported on H-piles. The bed of the river is firm mudstone. One abutment has been designed as a "fixed abutment" to carry all of the longitudinal seismic forces while the other abutment is designed so that the superstructure is free to move longitudinal without significant resistance.

The results of the test confirm that the bridge behaves in a manner reasonably consistent with the design assumptions. Mode shapes and frequencies were obtained from the tests and damping for low amplitude response was found to be about 4 percent of critical.

7. Other New Zealand Bridges [229] - Other bridges in New Zealand have been tested under steady state harmonic excitation using mechanical vibrators. These bridges include the Kowai, Kaiapoi, and Cam river bridges. The particular bridges are all sited on reasonably cohesionless material ranging from silty sands to rounded river gravel.

These tests show significant reductions in natural frequencies due to soil flexibilities in the foundations. They also show that frequencies usually decrease considerably with amplitude of oscillation. Further, it was found that the effective mass of soil vibrating with the substructure can in some cases have a significant influence on the natural frequencies. Within the range of amplitudes used in testing, the values of damping were found to be almost random and varied between 6 and 23 percent of critical for substructures and between 2 and 5 percent for whole structures.

G. MEASURED DYNAMIC RESPONSE OF BRIDGES TO STRONG MOTION EARTHQUAKES

1. Strong Motion Measurements at Highway Bridges - Observation of the dynamic response of engineering structures during strong motion earthquakes was initiated in Japan after development of the SMAC-type accelerograph was completed in 1953. As of March 1969, the number of strong-motion accelerographs installed on engineering structures totalled 510; see Fig. 3.5 [65]. Of this total, 106 had been placed on highway bridges and on the ground near these bridges. By March 1970, this number had increased to 119 [72]. Figure 3.37 shows the network of accelerograph locations for 57 highway bridges at that time.

Sixty one of these locations are on the bridge structures while fifty eight are on the ground surface near the bridges. The installation of these instruments is generally done by individual organizations such as the Ministry of Construction, the Hokkaido Development Agency, and Prefectures and Highway Public Corporations which are in charge of construction and maintenance of the structures.

In addition to strong-motion accelerographs, electro-magnetic-type seismographs have been placed on seven bridges (three of the 57 mentioned above plus four others) to measure their dynamic response. Two of these bridges also have earth pressure meters and accelerometers mounted in their foundations.

In addition, extensive field measurements are being made for proposed bridges such as the Honshu-Shikoku bridge and others to be located on Tokyo Bay Loop Highways. These measurements include subsoil measurements using downhole seismometers (some at depths greater than 100 m) as well as the standard seismometer and SMAC accelerograph measurements on the surface. These measurements will provide pertinent information for seismic design of these and other major bridges now under consideration.

Records obtained from the above described field measurement programs have been published annually since 1966 by the Public Works Research Institute along with similar records obtained for other structures such as highway tunnels, dams, river and coastal embankments, etc. [57, 58, 60, 64, 72].

In the following sections, the general features of field measurements on bridges are described and the results of strong-motion measurements on several bridges are summarized [63, 67, 68].

2. <u>General Features of Earthquake Response of Japanese Highway Bridges</u> - To determine the dynamic characteristics of highway bridges, 119 SMAC-type accelerographs at 57 bridges and electro-magnetic-type seismographs at 7 bridges had been installed as of March 1970. Most of these bridges have two or three sets of accelerographs. Usually one on the ground surface near the bridge and one or two at

the crests of representative substructures. The ground locations are chosen after careful consideration of topography and subsoil conditions at the bridge site.

Accelerographs at 28 bridges have already triggered yielding meaningful records of dynamic response (Table 3.6). The subsoil conditions at these bridges range from soft clayey soils to hard rock. Various types of foundations are represented, i.e., spread footings, pneumatic and open caissons, and piles. The dimensions of these bridges are quite common for bridges in Japan. The heights of substructures above ground level are less than 20 m and the superstructures, consisting of girders or trusses, have spans less than 100 m except for two bridges. Both of these exceptional cases have substructure heights of 42 m and one case has a span length of 150 m. The fundamental natural periods of these bridges in a horizontal direction are estimated to be in the range of 0.2 - 1.0 seconds.

Table 3.7 gives descriptions of earthquakes and compares maximum ground accelerations with maximum accelerations measured at pier crests. Figure 3.38 compares maximum horizontal accelerations at ground level measured away from substructures with those measured at the substructure. Based on these results, the following observations can be made: (a) In most cases, maximum accelerations at pier crests are greater than those measured on ground surface, (b) ratios of pier to ground accelerations tend to decrease with intensity level of the ground acceleration, (c) accelerations at crests of abutments are usually less than the ground accelerations.

Figure 3.39 gives certain data on maximum vertical accelerations. From these data and the data of Table 3.7, it is noted that the vertical ground accelerations range from $\frac{1}{3}$ to $\frac{1}{2}$ the intensity of the horizontal accelerations. Also it can be observed that the response accelerations at crests of substructures are $\frac{1}{2}$ to 2 times the ground accelerations.

3. Highrise Bridges [63] - Among the 28 bridges covered by Table 3.6, eight bridges have substructures higher than 10 m above ground surface. Thirteen strong-motion records are available for

these bridges. Figure 3.40 gives a relationship between maximum ground acceleration (a_G) and maximum response acceleration at crests of substructures (a_R) and Fig. 3.41 gives a relationship between height of substructure (H) and the ratio (β) of response acceleration to ground acceleration. Based on these results, the following observations can be made: (a) ratios of response acceleration to ground acceleration are in the approximate range 2 - 4 and are nearly independent of substructure height, i.e. no distinct relation appears to exist between substructure height and their response, (b) intensities of ground accelerations have greater significance on bridge response than does substructure height, (c) when subjected to ground accelerations less than 100 gals (no records obtained for ground motions greater than 100 gals), the ratios of response acceleration to ground acceleration for highrise bridges are usually in the range 1 - 4, and (d) highrise bridges are expected to respond as linear structures for moderate ground motions.

4. Ochiai Bridge [54, 55, 58, 59, 63, 68] - This bridge, completed in 1966, is one of the Nagano Prefectural roads located near the confluence of two rivers (Chikuma and Sai) in Wakaho, Nagamo City. A general view of this bridge and an outline of a typical pier (No. 11) are shown in Figs. 3.42 and 3.43, respectively. The subsoil near the bridge is an alluvial layer of consolidated coarse granular sediment (Fig. 3.43).

The right and left abutments are reinforced concrete structures resting on a caisson foundation and a pile foundation, respectively. Fifteen piers (P1 - P15) are reinforced concrete structures with caisson foundations. The remaining six piers near the left bank are of similar construction but rest on pile foundations. The superstructures having a total length of 948 m and a width of 6 m consist of Gerber steel girders over 12 spans and simple steel girders over 10 spans (Fig. 3.42).

This bridge is located about 7 km north of the town of Matsushiro where numerous earthquakes have occurred since midyear of 1965. The peak rate of occurrence was in April 1966 when over a period of one month more than one hundred thousand earthquakes were recorded of which some twelve thousand were of high enough intensity to be felt by humans.

These earthquakes can be characterized by the fact that they had very shallow hypocenters and very short durations of shaking. Fortunately, the magnitudes were not too great; however, several registered 5.0 to 5.2 on the Richter scale.

Although these earthquakes caused no significant damage to modern engineering structures including highway bridges, a number of strong motion records were obtained by seismographs located on the ground surface, in downholes, and at various locations on structures. In late 1965, the Public Works Research Institute installed three accelerographs (SMAC-B2); one at the Ochiai bridge on top of pier No. 11, one on the river bed nearby (Fig. 3.43), and one on the ground surface in the vicinity of the central part of Nagano City. These instruments were installed specifically for the purpose of obtaining quantitative information on seismic effects on engineering structures, including the Ochiai bridge.

By the end of 1969, these three accelerographs produced 786 strong-motion records (see Fig. 3.44). The Ochiai bridge suffered no significant damage eventhough the ground accelerations exceeded 200 gals on seven different occasions. The records obtained indicate high accelerations with short periods of vibration. Figure 3.45 shows a relationship between maximum values of acceleration at the crest of pier No. 11 and the ground level acceleration nearby. In this figure, a_R and a_G denote maximum values of accelerations in the longitudinal direction at pier crest and on the ground, respectively. From these results, it appears that a_R is greater than a_G for the smaller intensities of ground shaking but gradually becomes less as the intensity of shaking increases. This relationship is given approximately by the emperical formula

$$\beta \equiv \frac{a_R}{a_G} = 8.33\ a_G^{-0.5} \tag{12}$$

where a_R and a_G are measured in gals. This equation suggests that the bridge responds as a nonlinear structure

Table 3.8 gives maximum accelerations measured on the ground surface at the bridge location with respect to six representative

earthquakes between 12 February and 28 May 1966. This table also shows the results of dynamic analyses for three analytical models including nonlinear ones. In addition to these analyses, extensive studies were conducted using strong-motion records obtained at the Ochiai bridge [63].

5. Itajima Bridge [63, 68] - This bridge, completed in 1965, is one of the prefectural roads in Uwajima City, Ehime Prefecture, Shikoku Island. A general view of this bridge is illustrated in Fig. 3.46.

The ground at the site of this bridge is a comparatively soft alluvial layer of clayey loam or silt. Both abutments are reinforced concrete structures with steel pile foundations (length 18 m). The four piers are also reinforced concrete structures having open caisson foundations (depth 16 m). The superstructures having a total length of 125 m and a width of 6 m consists of simple composite girders over 5 spans (19.5 m + 3 @ 28.4 m + 19.7 m).

Immediately after completion of this bridge, a pair of accelerographs (SMAC-B2) were installed. One was located on the crest of pier No. 3 and the other was located on the ground surface about 200 m away.

This bridge has experienced several severe earthquakes. The Hyuganada earthquake, which registered 7.5 on the Richter scale occurred on April 1, 1968, and was located under the sea about 101 km south of the bridge site. A major aftershock was experienced following this earthquake. Figure 3.47 gives acceleration records obtained during the main shock at two locations. The maximum horizontal accelerations recorded were 186 gals on the ground surface and 375 gals at the crest of the bridge pier.

The Bungosuido earthquake which occurred on August 6, 1968 registered 6.6 on the Richter scale and was located only 11 km from the bridge site. The depth of hypocenter was 46 km. Figure 3.48 shows two accelerograph records obtained during the main shock. The maximum horizontal accelerations were 438 gals on the ground and 233 gals at the crest of

the bridge pier. Six major aftershocks followed the main shock. Data for two of these aftershocks were given in Table 3.7, along with the 3-component acceleration data for the main shock. The other four major aftershocks had magnitudes of 4.9, 5.3, 4.2, and 4.4 on the Richter scale and maximum values of horizontal acceleration of 130, 280, 80, and 88 gals, respectively.

The relationship between maximum values of ground accelerations (a_G) and response accelerations (a_R) at the crest of the bridge pier is given in Fig. 3.49. This figure also shows some results of dynamic response analyses using four major records. Single-degree-of-freedom response spectra were determined for the strong motions recorded at ground level. Using these spectra, response accelerations (Fig. 3.49) of the bridge were determined assuming the bridge as an idealized simple system having a natural period of 0.55 seconds and a damping ratio of 10% of critical.

Comparing measured response accelerations with their corresponding calculated values, Fig. 3.49, good agreement is observed for moderate ground accelerations (200 gals or less). However, for severe ground accelerations (greater than 300 gals), calculated values are greater than measured values. It should be noted that the Itajima bridge sustained no damage even though it experienced several severe earthquakes.

6. Shinkatsushika Bridge [63, 68] - This bridge , which was described previously (Section F), was instrumented with two strong-motion accelerographs (SMAC-B2). One accelerograph was placed on the crest of pier No. 5 and the other was placed on the ground surface nearby. In addition, four accelerometers and four earthpressure meters were installed in the foundation (21 m depth) of pier No. 5.

Table 3.9 summarizes the results of measurements at this bridge. A relationship between maximum horizontal accelerations measured at ground surface and at the crest of pier No. 5 is shown in Fig. 3.50. Figures 3.51 and 3.52 show two accelerograph records obtained during the Higashi Matsuyama earthquake of July 1, 1968. The distribution of maximum values of accelerations and earth pressures in the longitudinal

direction of the bridge is shown in Fig. 3.53. Based on these results, it may be noted that (a) during earthquakes with maximum ground accelerations of 40 gals or less, accelerations at the crest of the pier were greater (1.1 to 3.3 times) than ground accelerations while accelerations below ground level in the caisson foundation were less, and (b) although the dynamic tests in the longitudinal direction showed a fundamental period of 0.36 seconds and a subgrade reaction coefficient of about 4 kg/cm^3, the structure responded during the earthquake with a fundamental period of 0.50 seconds and a subgrade reaction coefficient of about 2 kg/cm^3. The displacement amplitudes of the well foundation near its crest were about 0.1 mm during the dynamic tests and about 2 mm during the earthquake. It may therefore be concluded that the rigidity of ground soils tend to decrease with amplitude of vibration.

7. Other Japanese Bridges [63, 68] - The results of strong-motion measurements at Chiyoda bridge, Hirai bridge, and Soka viaduct are shown in Figs. 3.54, 3.55, and 3.56, respectively. The maximum ground accelerations are about 50 to 100 gals for these structures. It may be noted, that the ratios of response to ground accelerations are independent of the intensity of ground motion for moderate ground accelerations less than 100 gals.

H. DYNAMIC ANALYSES

1. Present Status - In assessing the earthquake resistance of major highway bridges, dynamic analyses are now frequently conducted particularly in Japan eventhough designs are normally carried out using the conventional seismic coefficient method or a modified seismic coefficient method. Several factors are responsible for this trend in Japan. First, the heavy damages sustained by bridges during the 1964 Niigata earthquake emphasized the importance of dynamic effects during earthquakes and second, several highrise bridges have been erected on Japan Highway Public Corporation expressways since about 1965. This trend was also

expedited by the new bridge specifications for earthquake-resistant design which stipulate that response analyses shall be adopted for those bridges requiring detailed investigation (see Chapter IV). Two methods of analysis are commonly used, namely, the response spectrum method and the time history method. By the response spectrum method, maximum values of structural response are determined using appropriate response spectrum curves. The time history method generates complete time histories of response using selected accelerograms as the input excitation. In applying either of these methods in the design process, it is important to (a) establish accurate mathematical models for the overall structure, including substructures, foundations, and surrounding soils, (b) select appropriate seismic excitation for the bridge site, and (c) properly interpret the results of analysis in terms of prototype behavior.

Table 3.10 indicates a number of Japanese highway bridges for which dynamic analyses have been conducted. In the following sections, the analyses of several of these bridges (Showa, Yoneyama, Sokozawa, Honshu-Shikoku, Otani) and a few bridges in other countries are briefly described.

2. Showa Bridge [35] - As described earlier in this report, this bridge sustained severe damage during the Niigata earthquake of June 16, 1964. To clarify the causes of damage to this bridge, extensive dynamic analyses were carried out. In preparing the computer program, the substructure was treated as shown in Fig. 3.57 in order to generalize the program for use on bridges having pile foundations. For dynamic response in the longitudinal direction, the prototype structure was modelled as shown in Fig. 3.58 and the following assumptions were made: (a) the bridge can be idealized as a four-degree-of-freedom system representing a pier with a concentrated mass of the substructure resting on the crest of the pier and with a spread footing and piles, (b) piers and piles deform elastically, (c) relative displacements of tips of piles with respect to the surrounding soils are zero, (d) the vertical spring constant of piles can be determined considering elastic deformation

with fixed end conditions at their tips, (e) the horizontal spring constant for piles can be determined by treating them as beams supported by an elastic foundation, (f) the superstructure may be treated as a concentrated mass located at the crest of the pier, (g) the mass of a pier may be concentrated at two locations, namely, the crest and at the level of the footing, and (h) based on field measurements the coefficient of subgrade reaction is 1.0 kg/cm^3 and the damping ratio for the structural system is 2 percent of critical.

To define the excitation, response spectrum curves for the strong-motion record obtained in the basement for an apartment house in Niigata were employed. The maximum ground accelerations for the E-W and N-S components were approximately 0.15 g and 0.14 g, respectively. Based on the dynamic analysis, it was predicted that the maximum displacement at pier crest level would be 1.3 m or more provided no horizontal soil resistance was present to a depth of 10 m below the surface due to liquefaction of the saturated sands. Forces acting on the substructure were calculated to be larger than allowable.

It seemed highly probable that the girders would fall from their supports if the relative displacement between two adjacent piers reached 50 cm. This prediction is based on the fact that the width of the crest of each pier supporting a fixed shoe and a movable shoe was 50 cm and also due to the fact that no devices were present to prevent falling of the girders.

In addition to the above described spectral analysis, other dynamic analyses were conducted on this bridge using the time history approach. These analyses also assisted in correlating the damages of the Showa bridge.

3. Yoneyama Bridge [123] - This bridge, completed by the Ministry of Construction in 1956, is located on Highway No. 8 in Yoneyama, Niigata Prefecture, about 80 km southwest of Niigata City. It is slightly curved and has pier heights of about 43 m (Fig. 3.59).

The substructures are steel rigid frames with reinforced concrete spread footings on rocky ground. The superstructures consist of

continuous steel box girders with steel slabs over 3 spans (lengths 67 m, 93 m, 67 m) and continuous steel plate girders with concrete slabs over 2 spans (lengths 25 m, 25 m).

A conventional earthquake-resistant design of this bridge was carried out using a static horizontal seismic coefficient of 0.2. However, because of its high piers, a dynamic analysis was also conducted. In the dynamic analysis, seismic effects were evaluated using average response spectrum curves, Fig. 3.7, as proposed by PWRI in 1964 [89]. Seismic excitation was applied separately in both the longitudinal and transverse directions. The maximum ground acceleration was taken as 0.2 g.

Transverse excitation was found to be critical for this bridge. Therefore, only this case will be described here.

The bridge was idealized using the model shown in Fig. 3.60. Both girders and piers were assumed to be uniform members with the properties shown in Table 3.11. Referring to Fig. 3.60, the girders between nodal points 0 and 3, and between 3 and 5, are continuous. At nodal point 3, shearing forces and bending moments can be transmitted to pier No. 3. At nodal points 1, 2, and 4, connections between girders and piers consist of fixed shoes. Points 0, 5, 6, 7, 8, and 9 move simultaneously in phase during an earthquake. The base of the four piers are fixed to the footings at nodal points 6, 7, 8, and 9.

At nodal points 0 and 6, three different end conditions were considered, namely, perfectly fixed, 90 percent fixed (when subjected to a bending moment, the end rotation is 10 percent of the corresponding rotation for a free end), and 50 percent fixed. The effects of twisting of girders and piers were considered negligible and were ignored in the analysis. Two damping ratios were assumed in the dynamic analysis, i.e. 2 and 5 percent of critical.

Superposition of modal response values to obtain maximum response was accomplished using two methods. One method simply summed the absolute values of modal maximum response while the other method weighted the modal maximum response values by taking the square root of the sum of their squared values.

The results of the dynamic analysis for this bridge are shown in Figs. 3.61 - 3.64. Figure 3.61 shows the shapes of the first five normal modes while Figs. 3.62, 3.63, and 3.64 show maximum displacements, bending moments, and shearing forces, respectively. The dotted lines in the figures indicate the initial design values using the static seismic coefficient of 0.2 applied to the superstructures. The design of the bridge was revised as a result of the dynamic analysis.

After completion of the bridge in 1966, three SMAC accelerographs were installed to measure the dynamic response of the bridge to earthquakes.

4. Sokozawa Bridge [122, 124] - As discussed previously, the dynamic properties of the Sokozawa bridge were evaluated by field dynamic tests. Dynamic analyses were also conducted. Figure 3.65 shows the analytical model used in the analysis for excitation in the transverse direction. Six cases were analyzed as shown in Table 3.12 which had varying beam-column connection conditions and different moments of inertia for the concrete sections. Calculated natural frequencies and mode shapes for the first four modes are indicated in Table 3.13 and Fig. 3.66, respectively. Also indicated are the corresponding results of field tests. Case 6 shows comparatively good agreement for low amplitudes between calculated and field results.

For the case where a ground motion having 0.2 g peak acceleration is applied to the model with 2 percent of critical damping (Case 3, Table 3.12), the maximum bending moments at the bases of piers Nos. 1, 2, 3, and 4 are 22,500, 49,000, 57,000, and 28,000 ton meters, respectively and the absolute maximum displacement is 20 cm. This particular case is considered most realistic of all six cases.

Besides the Sokozawa bridge, several other highrise bridges built by the Japan Highway Public Corporation on the Chuo and Tomei expressways have been studied extensively by dynamic analyses. These bridges include the Sakai-gawa, Yokobuki, and Sakawa-gawa bridges.

5. Proposed Honshu-Shikoku Suspension Bridge [123, 140, 149] -

Extensive dynamic analyses of the proposed Honshu-Shikoku suspension bridge connecting Honshu and Shikoku Islands have been carried out to determine its response to strong-motion earthquakes. The following description will treat only one example case.

Table 3.14 summarizes a preliminary design of this bridge using a center span of 1500 m. As indicated in this table, 4 cases of ground conditions are considered in the analysis by varying Young's modulus for the foundation rock. Coordinates for several sections and dimension symbols are shown in Fig. 3.67. The analytical mass-spring model used in the analysis is presented in Fig. 3.68. It has a total of 94 lumped masses. Symbols A, B, C, F, P, and T in this figure denote anchor block, bent pier, cable, stiffening girder, main pier, and tower, respectively, while symbols L, M, and R represent left span, midspan, and right span, respectively. The definitions of other symbols are as follows:

b: width (m)

E: Young's Modulus (t/m^2)

G: shear modulus (t/m^2)

h: height (m)

I: moment of inertia (m^4)

J: moment of gyration ($tm\ sec^2$)

K_u: horizontal spring constant (t/m)

K_v: vertical spring constant (t/m)

l: span length (m)

u: horizontal displacement (m)

v: vertical displacement (m)

w: dead weight per unit length (t/m)

ϕ: rotation angle (radian)

The equations of motion for this bridge are initially established for the analytical model shown in Fig. 3.67. They are then replaced by finite-difference equations for the discrete model shown in Fig. 3.68. Mode shapes and frequencies are obtained for this model. Maximum combined response for displacements and forces are obtained by superimposing each

modal response using average response spectra, Fig. 3.7, proposed by PWRI in 1964 [89].

From this analysis, maximum bending moments for the main tower and the main pier have been determined as shown in Fig. 3.69.

6. Otani Interchange Bridge [115] - This bridge was constructed in 1970 by the Japan Highway Public Corporation as the rampway at the Otani Interchange of the Kita-Kyushu Bypass in northern Kyushu. The main portion of the bridge, between piers Nos. 2 and 8, consists of a continuous curved steel box girder over six spans (Fig. 3.70). This portion has seven reinforced concrete hollow cylindrical piers (height 20 - 30 m; inner and outer diameters 2.5 m and 3.5 m, respectively) supported by very rigid spread foundations on open caissons founded on bed rock. The total length of the above mentioned six spans is about 204 m (30 m + 4 @ 36 m + 30 m). Five approaching spans at both ends of the bridge are simple composite girders. Their total length is about 126 m (each span length 20 to 29 m) and their effective width is 8.0 to 8.8 m.

S. Yamaguchi, et. al. extensively studied the seismic resistance of this bridge since it has relatively high piers and a radius of curvature which is very small (40 m). Their studies included a field test on an isolated pier (No. 7) prior to erection of the superstructures, a field test on the overall structure after construction was completed and dynamic analyses of the main six spans when subjected to seismic excitation.

For the field test of pier No. 7, an exciter capable of generating sinusoidal forces up to 20 tons was placed on top of the pier and horizontal forces were generated in the frequency range 1.0 to 4.0 Hertz. From this test, it was disclosed that the pier had a fundamental frequency of 1.58 Hertz and a damping ratio of 2.5 percent of critical (Fig. 3.72).

During testing of the whole structure, the same exciter was mounted at three different locations on the deck slab, i.e. above pier No. 3, between piers Nos. 4 and 5, and above pier No. 7 (Fig. 3.70). The

bridge was excited in both horizontal directions (x and y coordinates, Fig. 3.70) separately with harmonic forces having frequencies in the range 1.0 to 3.0 Hertz.

Resonance curves, natural frequencies and mode shapes were obtained as shown in Fig. 3.71, Table 3.15, and Fig. 3.73, respectively. The damping ratios were found to be about 2.2 and 1.8 percent of critical for the first and second modes, respectively.

In the dynamic analysis investigation, natural frequencies and mode shapes were determined as indicated in Table 3.15 and Fig. 3.73 where they may be compared with the experimental results. Figure 3.74 and Table 3.16 give results of the dynamic analysis when the N-S component of the 1940 El Centro, California, earthquake record normalized to a maximum acceleration of 165 gals is used as the excitation. In Table 3.16, the analytical results are compared with corresponding design values using a static horizontal coefficient of 0.165. It is significant to note that these comparisons are not consistent.

7. Kaiapoi and Cam River Bridges [229] - Extensive dynamic analyses were carried out on these bridges using two computer programs. One program, developed by C. D. Matthewson, was used to find insitu soil properties by utilizing results from laterally loaded pile tests and the other, developed by A. J. Carr, enabled dynamic analyses to be performed on soil-substructure systems which were simulated using the finite element technique. Mode shapes and frequencies were determined for the combined soil-structural system.

8. Tied Cantilever Bridge [230] - A. S. Arya and S. K. Thakkar carried out dynamic analyses for a tied cantilever-type bridge. A discrete parameter mathematical model was used which simulated the complete bridge structure including the towers, ties, deck, and substructures. The deformations in the buried portion of the well foundation were accounted for by introducing linear and rotational springs at the level of maximum scour. The Holzer's method was used for calculating mode shapes and frequencies. The response of the whole structure was obtained

using the root-mean-square superposition of the maximum response in the first three normal modes. The results of the analyses are compared with corresponding code values obtained by use of the static seismic coefficient. A $\frac{1}{40}$ scale model of this bridge was constructed and tested and the results obtained therefrom were compared with theoretical values.

9. Proposed Elkhorn Slough Bridge [231] - In 1968, the California State Division of Highways considered building a bridge approximately 3000 ft. in length across the Elkhorn Slough which is located near Monterey, California. At this bridge site, a surface layer of saturated soft to firm gray silty clay is present that varies in depth from approximately 50 ft. at the proposed bridge abutment locations to about 120 ft. midway between these locations. A very shallow layer of water covers the clay layer, and a well-compacted sand lies below the clay layer. To aid the State Division of Highways in carrying out a rational design of a bridge-pile structural system for this site, an analytical investigation was undertaken at the University of California, Berkeley, to determine the interaction effects between the bridge structure and its supporting piles and between the supporting piles and the clay medium when subjected to strong-motion earthquake excitation. The analysis was separated into two parts (1) the determination of the dynamic response of the clay medium alone when excited through its lower boundary by a prescribed horizontal seismic motion and (2) the determination of the interaction of the entire structural system, including the piles, with the moving clay medium. Each analysis used discrete parameter models and appropriate theories were developed to determine the properties of these models. This investigation produced results on which the following conclusions and recommendations were based:

(a) A deep clay layer can be expected to greatly filter the higher frequency components of a typical earthquake acceleration input at its base before such accelerations reach the surface.

However, the lower frequency components that are near the fundamental shear mode frequency of the clay layer are likely to be amplified if the clay system has sufficient strength. In such cases structures built on the surface and having fundamental frequencies that match or nearly match the fundamental frequency of the clay layer will experience greater peak response than if excited directly by the earthquake acceleration. The proposed Elkhorn Slough bridge shows a somewhat greater peak response in this respect when the N-S component of El Centro Earthquake acceleration is the prescribed input, i.e., the peak bridge deck acceleration is approximately 1.2 g when considering the entire clay-pile-bridge superstructure system and is approximately 0.9 g when considering only the bridge superstructure system.

(b) The bridge superstructure, including attachments to piles, should be designed with full recognition of the importance of providing ductility so that large amounts of energy can be absorbed during the period of a very strong earthquake.

(c) The deformations that could be expected in the clay medium at the Elkhorn Slough site, if subjected at its base to an earthquake similar to that recorded at El Centro, would produce curvatures in the piles of the same order of magnitude as their yield curvatures. Such piles therefore should be designed so that they can withstand a considerable amount of inelastic deformation without losing their vertical load-carrying capacity.

(d) It is quite apparent that standard size piles will never "cut" their way through a moving clay medium of the Elkhorn Slouth type. Rather, such piles will be forced to deform essentially with the clay medium and will be given only relatively small relief by the interaction displacements. This type of behavior means that considerably more control is placed on pile curvatures than on pile moments. Therefore, standard or possibly somewhat smaller than standard diameter piles would have an advantage over the larger diameter

piles as far as flexural stresses are concerned. Of course, one must use a larger number of smaller size piles than larger size piles because of their lower vertical load-carrying capacities.

(e) If the piles are driven to a considerable depth in the highly compacted sand layer just below the clay medium, very large curvatures should be expected to develop in the piles at the interface of these two layers during a strong earthquake. In such a case the piles should be designed with the necessary ductility in this region so that their vertical load-carrying capacities are maintained.

(f) Further investigation is recommended to establish the existing "permanent elastic" moduli for the Elkhorn Slough clay medium that can be used to study the lateral stability of the piles under static conditions. Lateral stability of the piles is, of course, not a problem during the short period of transient excitation produced by an earthquake.

(g) Since the phase relations of the dynamic response of the bridge deck will differ from one section to the next, adequate separation should be provided in the expansion joints so that one section of bridge deck will not "pound" against the adjacent sections during the period of a strong earthquake.

I. MODEL EXPERIMENTS

To study the dynamic behavior of bridges, investigations have been conducted in Japan using laboratory models and subjecting them to dynamic excitation using shaking tables and exciters.

1. Viaduct [128] - E. Kuribayashi, K. Takada, and K. Kimura performed model experiments on a viaduct made of four reinforced concrete columns and a prestressed concrete girder which was constructed

on one of the Tokyo expressways. The principle objectives of the model experiments were to determine its dynamic characteristics and to observe the degree of generation of cracks and failures in the columns. The experiments were carried out by considering similarity relations between prototype and model. Two different models were constructed. One a 1/3.75 model (Model I) made of similar materials to the prototype and a second one (Model II) made of plastics at 1/20 scale.

A mechanical exciter (maximum force amplitude 10 tons) was placed on Model I as shown in Fig. 3.75. Generation of cracks and failures of the concrete columns was observed for relatively strong motions and the variations of dynamic characteristics were investigated with respect to the degree of cracking produced. This experiment revealed many cracks in the reinforced concrete columns when the model was subjected to an acceleration of about 0.2 g. However, no crack could be observed in the prestressed girder.

The small scale plastic model was placed on a shaking table as shown in Fig. 3.75 and its dynamic response was measured when subjected to sinusoidal excitation of relatively small amplitude. The model material appeared to have remained in the elastic range during the tests.

2. Pile Foundations [129] - N. Ogata and S. Kotsubo studied theoretically and tested experimentally the horizontal resistance of a pile foundation. The experimental setup used is shown in Fig. 3.77. Bakelite tubes as piles were imbedded in dry sand within a box which was placed on a shaking table. Dynamic strains produced in the piles and accelerations at several locations were measured during testing. From these experiments and the theoretical investigations, it was concluded that deformations of surface soil layers during earthquakes can have significant effects on the horizontal resistance of piles.

3. Tower-Pier System of Suspension Bridge [130, 134, 137, 138] - I. Konishi and Y. Yamada, et. al., conducted extensive studies on the seismic response characteristics of suspension bridges [130, 134, 137, 138]. These investigations included an experiment on the tower-pier system to evaluate the effects of inelasticity of the foundation and structural

damping on response [130].

A model of the tower-pier system was tested on a shaking table as shown in Fig. 3.78. From this experiment, several observations were made. First, the tower-pier system has a significant influence on the dynamic response of the whole structure and the rotational deformation of the pier is also important. Second, it was found that the inelastic properties of the foundations considerably reduce the dynamic response of the whole structure. Therefore, these properties should be considered in predicting overall response.

4. Structure on Pile Foundation [131] - K. Kubo conducted a model experiment on a large shaking table to determine the dynamic behavior of a liquid gas tank structure supported on a pile foundation, Fig. 3.79. The shaking table supported a box 10 m long, 4 m deep, and 2 m wide, capable of containing soil materials weighing up to about 170 tons. The shaking table is excited in one horizontal direction by an actuator having an electro-hydraulic servo system. Periods of vibration produced by this system are in the range 0.1 to 1.0 seconds. The maximum displacement amplitude possible is 10 cm while the maximum acceleration provided is 400 gals. From this experiment, it was found that the surrounding soils exert significant forces on the piles.

5. Three-Span Suspension Bridge [132] - E. Kuribayashi, Y. Oyamada, and Y. Iida investigated the response of a model of a three-span suspension bridge proposed to connect Honshu and Shikoku Islands. In this experimental investigation, a 1/100 scale model was supported on a synchronized electro-magnetic earthquake simulator system having four separate shaking tables as shown in Fig. 3.80. The results of an experiment, during which the model was excited at the base of the tower only, are given in Fig. 3.81. The results obtained from the experimental investigation were compared with design values and with the results of a dynamic analysis.

Table 3.1 Results of Vibration Test for Pier 4 of the Shinkatsushika Bridge

Test No.	Resonant Frequency f_r (Hz)	Damping Ratio* h	Maximum Amplitude during Resonance			Maximum Earth Pressure during Resonance		Coefficient of Subgrade Reaction K (kg/cm^3)	Acting Force during Resonance F (t)
			Location	Acceleration α (gals)	Displacement a (cm)	Location	Earth Pressure p (kg/cm^2)		
1	5.78	0.0599	Crest of Pier	65.3	0.0496	E-6	0.039	---	4.1
2	5.58	0.0504	Crest of Pier	148.0	0.1200	E-6	0.060	7.0	9.0
3	5.31	0.0689	Crest of Pier	164.0	0.1470	E-6	0.080	3.4	13.0
4	5.09	0.0485	Crest of Pier	225.0	0.2200	E-6	0.095	7.3	21.0
5	4.86	---	Crest of Pier	211.0	0.2260	E-6	---	---	27.0
6	5.62	0.0640	Crest of Pier	60.5	0.0486	E-6	0.025	2.0	3.7
Average	5.55	0.0583	---	---	---	---	---	4.7	---

*Damping ratios are obtained from the shape of resonance curves.

Table 3.2 Results of Vibration Test for Pier 5 of the Shinkatsushika Bridge

Test No.	Resonant Frequency f_r (Hz)	Damping Ratio* h	Maximum Amplitude during Resonance			Maximum Earth Pressure during Resonance		Coefficient of Subgrade Reaction K (kg/cm^3)	Acting Force during Resonance F (t)
			Location	Acceleration α (gals)	Displacement a (cm)	Location	Earth Pressure p (kg/cm^2)		
1	6.12	0.118	K_2	17.6	0.0119	E_2	0.0083	3.0	4.5
2	5.98	0.109	K_2	41.0	0.0290	E_2	0.0186	2.5	10.4
3	5.91	0.080	K_2	62.9	0.0456	E_2	0.0290	3.6	16.1
4	5.63	0.100	K_2	94.2	0.0752	E_2	0.0450	2.5	25.4
5	5.26	0.099	K_2	108.0	0.0990	E_2	0.093	4.9	31.7
6	6.00	0.103	K_2	15.6	0.0110	---	---	---	4.3
Average	5.80	0.111	---	---	---	---	---	---	---

*Damping ratios are obtained from the shape of resonance curves.

Table 3.3 Results of Vibration Test for the Overall Structure of the Shinkatsushika Bridge

Test No.	Resonant Frequency f_r (Hz)	Damping Ratio* h	Maximum Amplitude during Resonance			Maximum Earth Pressure during Resonance		Coefficient of Subgrade Reaction K (kg/cm^3)	Acting Force during Resonance F (t)
			Location	Acceleration α (gals)	Displacement a (cm)	Location	Earth Pressure p (kg/cm^2)		
1-1	2.79	0.0728	K-55	8.66	0.0295	E_2	0.0125	4.1	6.24
1-2	2.69	0.0787	K-21	9.52	0.0346	E_2	0.0194	4.4	8.28
1-3	2.77	0.0642	K-52	12.57	0.0401	---	---	---	8.78
1-4	2.77	0.0584	K-52	11.35	0.0380	E_2	0.0179	3.6	8.78
2-1	2.78	0.0675	K-55	14.28	0.0458	E_2	0.0179	4.5	9.84
2-2	2.82	0.0455	K-22	9.76	0.0315	---	---	---	9.10
Average	2.77	0.0660	---	---	---	---	---	4.2	---

*Damping ratios are obtained from the shape of resonance curves.

Table 3.4 Test Results for Pier 3 at the Sokozawa Bridge

Outline of Experiment	Direction		Longitudinal	Transverse			Remarks
	Excitor		40t-Excitor	15t-Excitor	2t-Rocket		
	Date		Oct. 11, 1967	Oct. 12, 13, 1967	Oct. 14, 1967		
Results Experimented	Order of Modes		1st	1st	1st	2nd	
	Resonant Frequency		2.38 Hz	0.77 Hz	0.77 Hz	4.62 Hz	
	Period		0.42 sec	1.30 sec	1.30 sec	0.62 sec	
	Damping Ratio		1.0%	0.7%	0.6%	0.7%	From Free Damped Oscillation
			less than 2%	0.6%	---	---	From Resonance Curve
	Mode Shape		Bending Deformation of Cantilever	Bending Deformation of Cantilever	Bending Deformation of Cantilever		
	Maximum Amplitude	Acceleration	190 gal	7.0 gal	3.45 gal	2.8 gal	Maximum Amplitude at the Crest of Pier
		Displacement	0.95 cm	0.30 cm	0.15 cm	0.0033 cm	
Results Calculated	Natural Frequency		2.58 Hz	0.710 Hz		4.45 Hz	
	Natural Period		0.388 sec	1.41 sec		0.225 sec	

Table 3.5 Numbers of Strong-Motion Accelerographs

(As of March 31, 1969)

Number of Accelerographs / Installed at	At Structures	On Grounds	TOTAL
Building	192	10	202
Bridge	55	51	106
Railway	20	36	56
Harbor	3	43	46
Telephone Office	37	0	37
Power Plant	12	1	13
Atomic Power Plant	5	14	19
Dam	11	7	18
River	2	4	6
Road	0	7	7
TOTAL	337	173	510

Table 3.6 Outline of Twenty-Eight Bridges where Seismic Records are Available

Bridge No.	Name of Bridge	Structural Features					Numbers of Accelerographs			Dynamic Properties in the Longitudinal Direction		Number of Structural Location	Remarks
		Total Length	Width	Superstructure	Foundation	Soil	On Ground	At Bridge: Pier*	At Bridge: Abutment*	Period (sec)	Damping Ratio		
1	Ajigawa	1,368.00m	33.00m	Box Girder	Caisson	Silt	1	1 (8.1m) 1 (12.6)		0.50 0.80	0.10 0.10	1-1 1-2	Pier 1 Pier 1
2	Amagasaki	280.00	28.30	Plate Girder	Caisson	Silt	1	1 (4.2)		0.60	0.10	2	Viaduct
3	Chiyoda	706.00	6.00	Warren Truss RC Girder	Caisson Spread	Sand	1	1 (9.5)	1 (4.0m)			3-1 3-2	
4	Date	288.00	7.00	Warren Truss	Caisson	Gravel	1	1 (9.7)		0.50	0.10	4	
5	Fumimaki	144.00	7.60	RC Girder	Caisson	Sand	1	1 (5.8)				5	
6	Hirai	622.00	20.00	Gerber Box Girder	Caisson	Silt	1	1 (8.8) 1 (8.8)				6-1 6-2	Pier 5 Pier 6
7	Horoman	140.00	7.50	RC Girder	Caisson	Gravel	1	1 (4.8)				7	
8	Ichinohashi	--	8.80	Plate Girder	Cast-in-place RC Pile	Siltstone	1	1 (16.0)				8	Viaduct
9	Ishiseto	82.00	6.00	Howe Truss	Spread	Sand	1	1 (12.2)				9	
10	Ishizuchi	211.55	6.00	PC Girder	Caisson	Gravel	1	1 (5.5)				10	
11	Itajima	125.20	6.00	Plate Girder	Caisson	Silt	1	1 (5.0)		0.55	0.10	11	
12	Kinokawa	747.35	10.50	Box Girder	Caisson	Sand	1	1 (16.0)				12	
13	Myoken	237.70	8.00	Composite Girder	Steel Pile	Clay	1	1 (5.0)				13	
14	Nishiarai	444.60	15.00	Gerber Plate Girder	Caisson Steel Pile	Sand	1	1 (6.7) 1 (7.4)				14-1 14-2	Pier 7 Pier 9
15	Ochiai	948.00	6.00	Gerber Plate Girder	Caisson	Gravel	2	1 (6.5)		0.35	0.10	15	
16	Otanoshike	220.80	11.80	Composite Girder	Steel Pile	Sand	1	1 (4.5)				16	
17	Otome	275.00	6.00	Plate Girder	Caisson	Gravel	1	1 (4.8)				17	
18	Sakaigawa	227.10	10.45	Warren Truss	Spread	Rock	1	1 (42.0)				18	
19	Shinkatsushika	442.00	17.70	Box Girder	Caisson	Medium Sand	1	1 (8.3)		0.36	0.07	19	
20	Shintonegawa	654.00	10.85	Plate Girder	Steel Pile	Sand	1	1 (7.5)				20	
21	Shitoku	101.00	7.00	Trussed Langer	Spread	Rock	1	1 (42.0)				21	
22	Soka	--	8.20	Composite Girder	Steel Pile	Clayey Silt	1	1 (6.5)				22	
23	Taira	141.60	19.30	Plate Girder	Steel Pile	Silt	1		1 (6.0)			23	
24	Takatsu	325.60	10.20	Composite Girder	Caisson	Fine Sand	1	1 (6.0)				24	
25	Toyohama	561.00	6.80	Composite Girder	Steel Pile	Gravel	1	1 (6.6)				25	
26	Yokoshi	481.79	25.50	Plate Girder	Cast-in-place RC Pile	Gravel	1	1 (18.0)				26	
27	Yorima	205.60	7.00	Plate Girder	Caisson	Gravel	1	1 (13.4)		0.20	0.10	27	
28	Yoshica	270.20	22.00	Box Girder	Caisson	Sand	1	1 (7.8) 1 (7.8)		0.20 0.30	0.10 0.10	28-1 28-2	Pier 1 Pier 2

*Values in the parentheses indicate the height of substructure above the ground surface.

Table 3.7 Comparison of Ground Accelerations (a_G) and Response Accelerations (a_R) at Bridges from Measurements during Earthquakes

Bridge No.	Name of Bridge	Date of Occurrence of Earthquake	Magnitude	Depth of Hypocenter (km)	At Bridge Site I	At Bridge Site Epicentral Distance (km)	Maximum Accelerations (gals) Longitudinal a_G	Longitudinal a_R	Transverse a_G	Transverse a_R	Vertical a_G	Vertical a_R	No. of Structural Location	Data No.
1	Ajigawa	Mar. 27, 1963	6.9	0	4	121	21.9	67.0 28.0	34.0	25.0 25.0	14.0	6.0 --	1-1 1-2	1 2
2	Amagasaki	Mar. 27, 1963	6.9	0	4	121	28.0	46.0	37.6	50.0	13.5	9.0	2	3
3	Chiyoda	Mar. 12, 1967	4.5	10	3	35	32.5	31.3 33.8	25.0	41.3 23.8	5.3	7.5 10.6	3-1 3-2	4 5
		July 5, 1967	4.1	170	3	71	33.8	58.8 42.5	28.8	27.5 25.0	5.3	13.8 15.0	3-1 3-2	6 7
		Sept. 19, 1967	--	90	3	195	23.8	36.5 20.0	26.3	33.8 27.5	5.3	6.3 6.3	3-1 3-2	8 9
		May 16, 1968	7.9	20	4	241	87.5	131.3 91.3	72.5	112.5 75.0	25.0	25.0 31.3	3-1 3-2	10 11
		May 16, 1968	7.5	40	3	172	37.5	77.5 43.8	31.3	50.0 36.3	18.8	17.5 18.8	3-1 3-2	12 13
4	Date	Jan. 17, 1967	6.3	30	3	151	22.1	28.8	19.1	43.8	—	8.8	4	14
		July 5, 1968	6.4	50	4	169	23.0	20.0	18.0	30.0	5.0	5.0	4	15
5	Fumimaki	Dec. 24, 1963	--	—	—	--	37.0	43.9	27.5	22.4	--	--	5	16
6	Hirai	Mar. 19, 1967	—	80	3	41	15.6	25.0	17.5	16.3	10.0	—	6-1	17
		Mar. 6, 1968	5.2	50	3	39	30.0	20.0 58.0	25.0	18.0 13.0	8.0	8.0 8.0	6-1 6-2	18 19
		July 1, 1968	6.1	50	4	52	58.1	108.0 128.0	48.8	63.0 60.0	25.0	30.0 30.0	6-1 6-2	20 21
		Oct. 8, 1968	--	70	3	34	30.0	48.0 65.0	35.0	35.0 28.0	5.0	15.0 15.0	6-1 6-2	22 23
7	Horoman	May 16, 1968	7.9	20	5	157	68.8	72.5	51.3	90.0	23.8	36.3	7	24
		May 16, 1968	7.5	40	5	74	56.3	68.8	43.8	87.5	18.8	25.0	7	25
8	Ichinohashi	Mar. 6, 1968	5.2	50	3	46	20.0	40.0	20.0	50.0	5.0	10.0	8	26
		July 1, 1968	6.1	50	4	46	38.0	140.0	48.0	173.0	18.0	25.0	8	27
		Oct. 8, 1968	--	70	3	39	55.0	120.0	55.0	125.0	13.0	28.0	8	28
9	Ishiseto	Feb. 21, 1968	6.1	0	4	39	22.5	50.0	20.0	25.0	10.0	5.0	9	29
		Mar. 25, 1968	5.7	0	3	39	22.5	50.0	22.5	35.0	10.0	5.0	9	30
		Apr. 1, 1968	7.5	30	4	131	25.0	70.0	30.0	35.0	15.0	10.0	9	31
10	Ishizuchi	Apr. 1, 1968	7.5	30	4	182	35.0	83.0	55.0	65.0	10.0	23.0	10	32
		Aug. 6, 1968	6.6	40	4	89	63.0	75.0	63.0	78.0	20.0	23.0	10	33
11	Itajima	Jan. 1, 1967	4.6	10	2	248	27.5	18.8	17.5	28.8	--	--	11	34
		Apr. 1, 1968	7.5	30	4	101	169.9	213.0	186.2	375.0	43.0	55.0	11	35
		Apr. 1, 1968	6.3	0	3	99	34.0	35.0	36.0	65.0	10.0	13.0	11	36
		Aug. 6, 1968	6.6	40	5	11	437.5	200.0	360.9	233.0	140.0	100.0	11	37
		Aug. 6, 1968	4.1	30	3	19	55.0	30.0	55.0	65.0	10.0	8.0	11	38
		Aug. 6, 1968	4.8	40	3	18	50.0	100.0	60.0	65.0	8.0	20.0	11	39
12	Kinokawa	Mar. 30, 1968	5.0	0	4	6	80.0	115.0	70.0	55.0	85.0	30.0	12	40
13	Myoken	Apr. 1, 1968	7.5	30	3	337	35.0	45.0	48.0	48.0	20.0	8.0	13	41
		Aug. 6, 1968	6.6	40	3	226	18.0	25.0	18.0	25.0	5.0	20.0	13	42

Table 3.7 -continued-

14	Nishiarai	July 1, 1968	6.1	50	4	41	80.0	95.0	48.0	33.0	15.0	10.0	14-1	43
		Oct. 8, 1968	--	70	3	42	40.0	40.0 33.0	50.0	38.0 50.0	8.0	5.0 10.0	14-1 14-2	44 45
16	Otanoshike	May 16, 1968	7.9	0	4	257	31.3	45.0	41.3	43.8	12.5	12.5	16	46
17	Otome	Nov. 28, 1967	--	130	2	68	16.1	23.7	10.0	8.7	--	--	17	47
18	Sakaigawa	July 1, 1968	6.1	50	4	45	25.0	85.0	55.0	125.0	10.0	15.0	18	48
19	Shinkatsushika	Mar. 2, 1967	--	85	3	36	15.0	38.8	21.3	28.7	--	--	19	49
		Nov. 10, 1967	--	80	3	42	18.9	43.8	14.4	48.8	--	6.0	19	50
		July 1, 1968	6.1	50	4	47	37.0	50.0	38.6	55.0	10.0	10.0	19	51
		Oct. 8, 1968	--	70	3	37	35.0	38.0	28.0	45.0	5.0	10.0	19	52
20	Shintonegawa	July 1, 1968	6.1	50	4	31	75.0	90.0	65.0	53.0	25.0	13.0	20	53
21	Shitoku	July 1, 1968	6.1			136	30.0	40.0	25.0	98.0	18.0	13.0	21	54
22	Soka	Mar. 7, 1968	5.1			42	18.0	60.0	25.0	35.0	5.0	5.0	22	55
		July 1, 1968	6.1			38	50.0	75.0	50.0	65.0	15.0	8.0	22	56
		Oct. 8, 1968	--			45	35.0	45.0	48.0	63.0	10.0	5.0	22	57
23	Taira	Feb. 26, 1968	5.4			64	50.0	23.0	40.0	35.0	20.0	10.0	23	58
		May 16, 1968	7.9			473	23.0	8.0	25.0	15.0	8.0	5.0	23	59
24	Takatsu	Apr. 1, 1968	7.5			271	20.0	118.0	25.0	75.0	5.0	20.0	24	60
		Aug. 6, 1968	6.6			159	25.0	95.0	33.0	83.0	8.0	20.0	24	61
25	Toyohama	May 9, 1968	5.6			58	30.0	60.0	23.0	85.0	8.0	10.0	25	62
26	Ubakubo	July 1, 1968	6.1	50	4	32	35.0	48.0	45.0	178.0	15.0	15.0	26	63
27	Uonuma	Jan. 9, 1966	5.2			42	28.0	65.0	32.5	27.5	--	--	27	64
		Sept. 8, 1966	5.1			5	50.0	63.0	45.0	63.0	14.0	13.0	27	65
28	Yoshida	Aug. 19, 1961	7.0			135	15.8	38.0 43.2	19.0	-- --	--	-- --	28-1 28-2	66 67

Note) Data for the Ochiai Bridge (No. 15) are shown in Table 3.8.

Table 3.8 Observed Accelerations and Analyzed Responses at the Ochiai Bridge (Longitudinal Direction)

Earthquake		Observed Max. Acc.		Analyzed Response Acc.			Percentages of Analyzed Acc. to Observed Acc.		
No.	Date Time (Magnitude)	Ground	Top of Pier	Linear	Nonlinear Case 1	Nonlinear Case 2			
		a_G (gal)	a_R (gal)	a_R^L (gal)	a_R^{N1} (gal)	a_R^{N2} (gal)	$\frac{a_R^L}{a_R} \times 100$ (%)	$\frac{a_R^{N1}}{a_R} \times 100$ (%)	$\frac{a_R^{N2}}{a_R} \times 100$ (%)
I	Apr. 5, '66 17:52	30.0	51.3	43.7	43.7	43.7	85.2	85.2	85.2
II	Feb. 12, '66 04:05	60.0	43.8	55.1	55.1	54.0	125.8	125.8	123.3
III	May 6, '66 19:08	70.0	100.0	97.1	97.1	80.5	97.1	97.1	80.5
IV	May 28, '66 14:21	102.5	107.5	156.4	128.1	106.6	145.5	119.2	99.2
V	Apr. 5, '66 17:51	212.5	190.0	325.8	187.0	195.5	171.5	98.4	102.9
VI	Apr. 17, '66 10:21	302.5	145.0	303.4	202.7	211.8	209.2	139.8	146.1

Note: Linear: Linear System; $T = 0.35$ sec, $h = 0.1$

Nonlinear Case 1: Bi-linear System; $T = 0.35$ sec, $h = 0.1$, $\eta = 0.6$, $X_y = 0.3$ cm

Nonlinear Case 2: Bi-linear System; $T = 0.35$ sec, $h = 0.1$, $\eta = 0.4$, $X_y = 0.15$ cm

Table 3.9 Results of Earthquake Observation at the Shinkatsushika Bridge

Date of Earthquake	Magnitude	At Bridge Site		Strong-Motion Accelerographs						Transducers Equipped in the Caisson Foundation of Pier 5						Data No.	Remarks
				Maximum Accelerations (gals)						Max. Accelerations (gals)			Max. Earth Pressures (kg/cm^2)				
		JMA Intensity	Epicentral Distance (km)	On Ground			At Crest of Pier 5			A-1	A-2	A-3	E-1	E-3	E-4		
				L	T	V	L	T	V	L	L	L	L	L	L		
Mar. 2, 1967	---	3	36	15.0	21.3	---	38.8	28.7	---	---	---	---	---	---	---	50	
Nov. 10, 1967	---	3	42	18.9	14.4	---	43.8	48.8	6.0	17.4	27.9	8.2	0.199	0.046	0.034	51	
July 1, 1968 (Higashi-Matsuyama Eq.)	6.1	4	47	37.0	38.6	10.0	50.0	55.0	10.0	32.1	25.0	21.8	1.295	0.218	0.108	52	See Figs. 3.50 - 3.53
Oct. 8, 1968	---	3	37	35.0	28.0	5.0	38.0	45.0	10.0	23.6	17.9	12.7	---	0.112	---	53	

Notes: L : Longitudinal Direction

T : Transverse Direction

V : Vertical Direction

Data numbers correspond to Table 3.7.

Table 3.10 Some Examples of Highway Bridges on Which Dynamic Analyses were Conducted

Name of Bridges (Location)	Horizontal Design Seismic Coefficient	Analytical Model, Damping Ratio (h) (Direction Analyzed)	Method of Analysis	Organizations Administrated	Organizations Analyzed (Year)	Remarks
Amakusa No. 4 (Kumamoto, Kyshu)	0.150	34-mass spring system h = 1 or 2% for Superstr. h = 3 or 5% for Substr. (Transverse)	Direct Integration Method (Taft - 1952, a_G = 150 gals)	Japan Highway Public Corporation	JHPC and PWRI (Ministry of Construction) (1967)	Field Experiment
Hirai (Tokyo, Honshu)	0.300	Elastic Continuum h = 5% (Longitudinal and T)	Response Spectrum Method (PWRI - 1964, a_G = 300 gals)	Tokyo Metropolitan Government	Tokyo M. G. and PWRI (MOC) (1966)	•Field Experiment on Substructures •Observation of Strong-Motion Earthquake
Honshu-Shikoku (Honshu-Shikoku)	0.200	94-mass spring system h = 2 or 5% (L, T, and Vertical)	Response Spectrum Method (PWRI - 1964, a_G = 200 gals)	Kinki Regional Construction Bureau (MOC)	PWRI (MOC) (1966)	Model Experiment
Otani (Kitakyushu, Kyushu)	0.165	35-mass spring system h = 2 or 5% (L and T)	Direct Integration Method (El Centro - 1940, a_G = 165 gals)	JHPC	JHPC (1970)	Field Experiment
Sakai-gawa (Kanagawa, Honshu)	0.200	Elastic Continuum h = 2, 5, 10% (T)	Response Spectrum Method (PWRI - 1964, a_G = 200 gals)	JHPC	JHPC (1965)	Observation of Strong-Motion Earthquake
		41-mass spring system h = 2, 5, 10% (T)	Direct Integration System (El Centro - 1940, a_G = 200 gals)			
Showa (Niigata, Honshu)	0.200	Elastic Continuum h = 5% (L)	Response Spectrum Method (PWRI - 1964, Niigata - 1964, a_G = 200 gals)	Niigata Prefectural Government	PWRI (MOC) (1964)	•Damage Experience •Observation of Strong-Motion Earthquake
		One-mass bi-linear system h = 2% (L)	Direct Integration Method (Niigata - 1964, a_G = 157 gals)			
Sakozawa (Kanagawa, Honshu)	0.200	Elastic Continuum h = 2% (T)	Response Spectrum Method (PWRI - 1964, a_G = 200 gals)	JHPC	JHPC (1968)	Field Experiment
Yachiyo (Niigata, Honshu)	0.200	Elastic Continuum h = 5% (L)	Response Spectrum Method (PWRI - 1964, Niigata - 1964, a_R = 200 gals)	Niigata Municipal Government	PWRI (MOC) (1964)	Seismic Damage Experience
Yoneyama (Niigata, Honshu)	0.200	Elastic Continuum h = 2, 5% (L and T)	Response Spectrum Method (PWRI - 1964, a_R = 200 gals)	Hokuriku Regional Construction Bureau (MOC)	Hokuriku Regional Construction Bureau (MOC) (1965)	Observation of Strong-Motion Earthquake

Notes: a_G : Maximum accelerations considered in dynamic analyses.

h : Damping ratios to critical damping considered in analyses.

Table 3.11 Dimensions of Girders and Pier Columns of the Yoneyama Bridge

Girder	0-1	1-2	2-3	3-4	4-5
Span Length, l (m)	67.0	93.0	67.0	25.0	25.0
Moment of Inertia, I (m^4)	1.016	1.016	1.016	0.800	0.800
Unit Weight, w (t/m)	5.70	5.60	5.70	7.39	7.39
Column	**1-6**	**2-7**	**3-8**	**4-9**	**Remarks**
Height, l (m)	43.452	43.452	30.625	17.628	Height above the crest of Foundation
Moment of Inertia, I (m^4)	1.0100	1.0100	0.2030	0.0838	
Unit Weight, w (t/m)	4.4300	4.4300	1.1370	0.7918	

Table 3.12 Six Cases Considered in the Analysis of the Sokozawa Bridge

Case No.	Bases of Columns	Connections at Crest of Pier 2		Evaluation of Moment of Inertia	
		Girder	Column		
1	Fixed	Hinged		Girder Column	Consider all cross-section of concrete Consider all cross-section of concrete
2	Fixed	Hinged		Girder Column	Neglect tensile area of concrete Consider all cross-section of concrete
3	Fixed	Hinged		Girder Column	Neglect tensile area of concrete Neglect tensile area of concrete
4	Fixed	Fixed		Girder Column	Neglect tensile area of concrete Consider all cross-section of concrete
5	Fixed	Fixed	Consider Twisting	Girder Column	Neglect tensile area of concrete Consider all cross-section of concrete
6	Fixed	Hinged		Girder Column	Consider all cross-section of concrete and end bracing Consider all cross-section of concrete

Table 3.13 Natural Frequencies Analyzed and Resonant Frequencies from the Field Experiment

Order of Modes		1st	2nd	3rd	4th
Experiment		1.53 Hz	---	2.38 Hz	2.64 Hz
Dynamic Analysis	Case 1	1.68	1.94 Hz	3.09	3.41
	Case 2	1.50	2.22	2.48	3.00
	Case 3	0.93	1.05	1.47	1.66
	Case 4	1.50	1.59	2.26	2.55
	Case 5	1.50	1.59	2.29	2.55
	Case 6	1.60	1.82	2.35	2.82

Table 3.14 Preliminary Design of the Proposed Honshu-Shikoku Suspension Bridge Analyzed

(A) Superstructure

Definition	Symbol	Dimension	Value
Central Span Length	l_M	m	1,500.0
Side Span Length	l_L, l_R	m	750.0
Cable Sag at Central Span	f_M	m	136.4
Cable Sag at Side Span	f_L, f_R	m	34.1
Height of Main Tower		m	210.0
Distance between Shafts at Main Tower		m	36.0
Height of Stiffening Truss		m	12.0
Cross-sectional Area of Cable		m^2	2 x 0.689
Unit Weight of Cable		t/m	11.0
Unit Weight of Suspended Structure		t/m	20.0
Weight of Main Tower		t	24,300.0
Total Weight of Superstructure		t	117,400.0

Table 3.14 Preliminary Design of the Proposed Honshu-Shikoku Suspension Bridge Analyzed (Continued)

(B) Substructure

(a) Common Quantities

Sub-structure	h_a (m)	a (m)		b (m)	w_c (t/m^2)	h_b (m)	W_b (t)	W_c (t)	W_{ad} L_g (t)	W_{ad} T_r (t)	W_G L_g (t)	W_G T_r (t)	V Dry (t)	V Sat (t)
Main Pier	75	L_g	50	80	2.0	21.5	0	6×10^5	281,000 ~ 250,000	165,000 ~ 166,000	884,000 ~ 850,000	765,000 ~ 766,000	657,600	417,600
		T_r	80	50										
Anchor Pier	65	L_g	100	70	2.0	21.5	1.7×10^5	9.1×10^5	171,000 ~ 152,000	267,000 ~ 264,000	1,251,000 ~ 1,232,000	1,347,000 ~ 1,344,000	1,082,000	732,000
		T_r	70	100										

(b) Quantities for Four Cases

Case No.	h_s (m)	E_{RO} (t/m^2)	E_s (t/m^2)	M.P. h_w (m)	M.P. T L_g (sec)	M.P. T T_r (sec)	M.P. h_g (m)	A.P. h_w (m)	A.P. T L_g (sec)	A.P. T T_r (sec)	A.P. h_g (m)
1	10	10^{14}	10^{14}	50	0.09	0.08	36.2	40	0.03	0.04	38.82
2	10	600,000	16,000	50	0.51	0.41	36.2	40	0.46	0.54	38.82
3	10	80,000	10,000	50	1.28	1.32	36.2	40	1.21	1.43	38.82
4	10	40,000	5,000	50	2.02	2.32	36.2	40	1.64	2.03	38.82

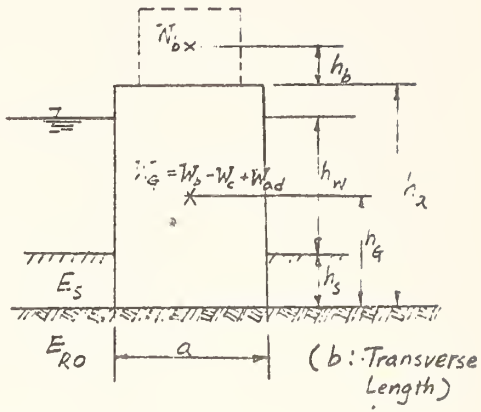

Notes: W_{ad} --- Added weight due to water and soils

V --- Effective reaction at the base of foundation

L_g --- Longitudinal, T_r --- Transverse

Dry --- No buoyancy, Sat --- Full buoyancy

Table 3.15 Natural Frequencies in Hertz from Test and Analysis for the Otani Interchange Bridge (After S. Yamaguchi, et al. [115])

Mode		1st	2nd	3rd	4th
Test		1.18	1.41	1.65	2.00
Computed	Case 1	(0.81) 0.96	(0.90) 1.06	(0.89) 1.26	1.64
	Case 2	(0.88) 1.04	(0.95) 1.34	1.96	2.27

Values in parentheses refer to ratios of computed frequency to tested frequency.

Table 3.16 Results of Dynamic Analysis for the Otani Interchange Bridge (After S. Yamaguchi, et al. [115])

(A) Maximum Displacement by Earthquake

Wave in Direction x unit: cm

Displacement / Point	δ_x Method of Analysis: Seismic Coefficient Method	δ_x Modal Analysis h = 0.02	δ_x Modal Analysis h = 0.05	δ_y Method of Analysis: Seismic Coefficient Method	δ_y Modal Analysis h = 0.02	δ_y Modal Analysis h = 0.05
1	6.35	0	0	0.24	3.20	2.66
6	6.36	0.36	0.30	0.49	2.00	1.56
12	6.02	0.72	0.55	0.06	2.11	1.65
18	4.35	2.70	2.24	0.76	1.42	1.12
24	2.86	2.07	1.80	0.06	1.45	1.30
30	2.42	1.52	1.84	0.59	2.49	1.63
35	1.74	0	0	0.30	1.90	1.41

(B) Maximum Displacement by Earthquake

Wave in Direction y unit: cm

Displacement / Point	δ_x Method of Analysis: Seismic Coefficient Method	δ_x Modal Analysis h = 0.02	δ_x Modal Analysis h = 0.05	δ_y Method of Analysis: Seismic Coefficient Method	δ_y Modal Analysis h = 0.02	δ_y Modal Analysis h = 0.05
1	0.39	0	0	6.76	12.24	8.30
6	0.36	0.37	0.25	6.56	7.75	5.69
12	0.23	2.27	1.53	5.22	4.71	3.45
18	0.48	2.63	1.80	5.00	4.45	3.46
24	0.06	1.46	0.90	4.69	3.72	3.16
30	0.42	1.44	1.29	2.22	2.71	2.24
35	0.13	0	0	1.22	2.93	2.34

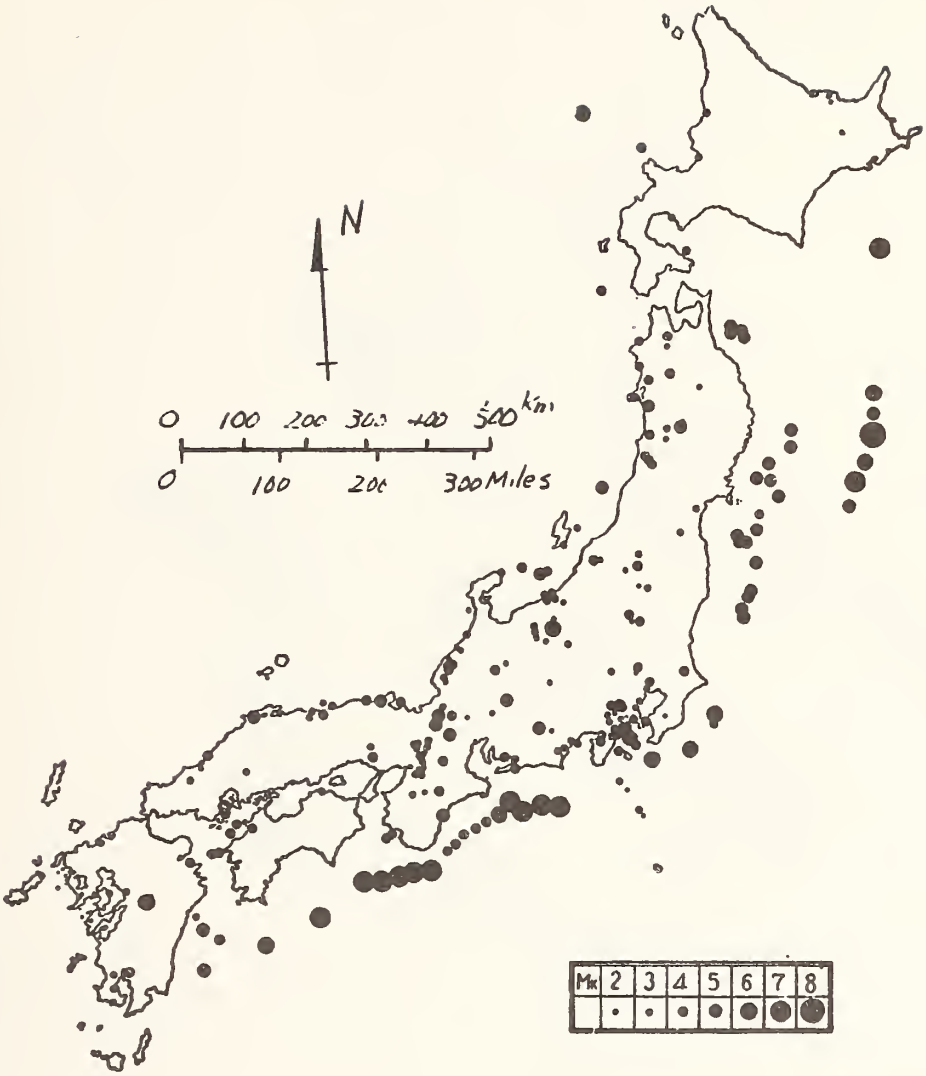

Fig. 3.1 Distribution of epicenter and magnitude of major historical earthquakes in Japan (after H. Kawasumi [80])

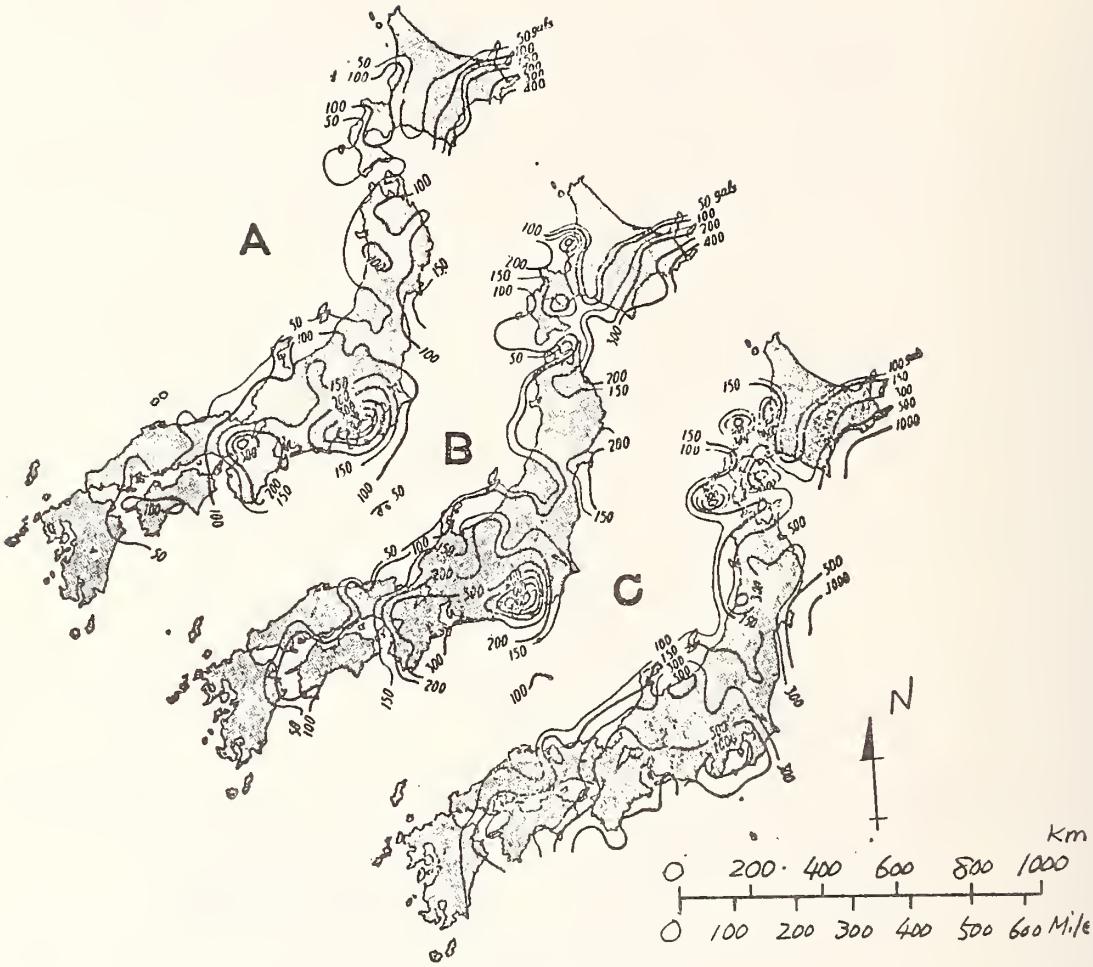

Fig. 3.2 Contours of maximum earthquake accelerations expected in Japan within periods of (A) 75, (B) 100, and (C) 200 years (after H. Kawasumi [80])

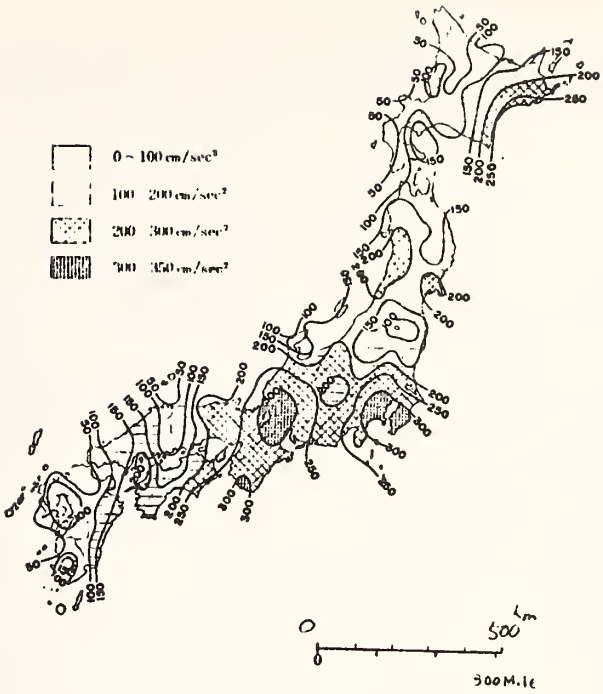

Fig. 3.3 Contours of maximum seismic accelerations expected within a period of 75 years (after H. Goto and H. Kameda [82])

Fig. 3.4 Contours of maximum seismic velocities expected within a period of 75 years (after H. Goto and H. Kameda [82])

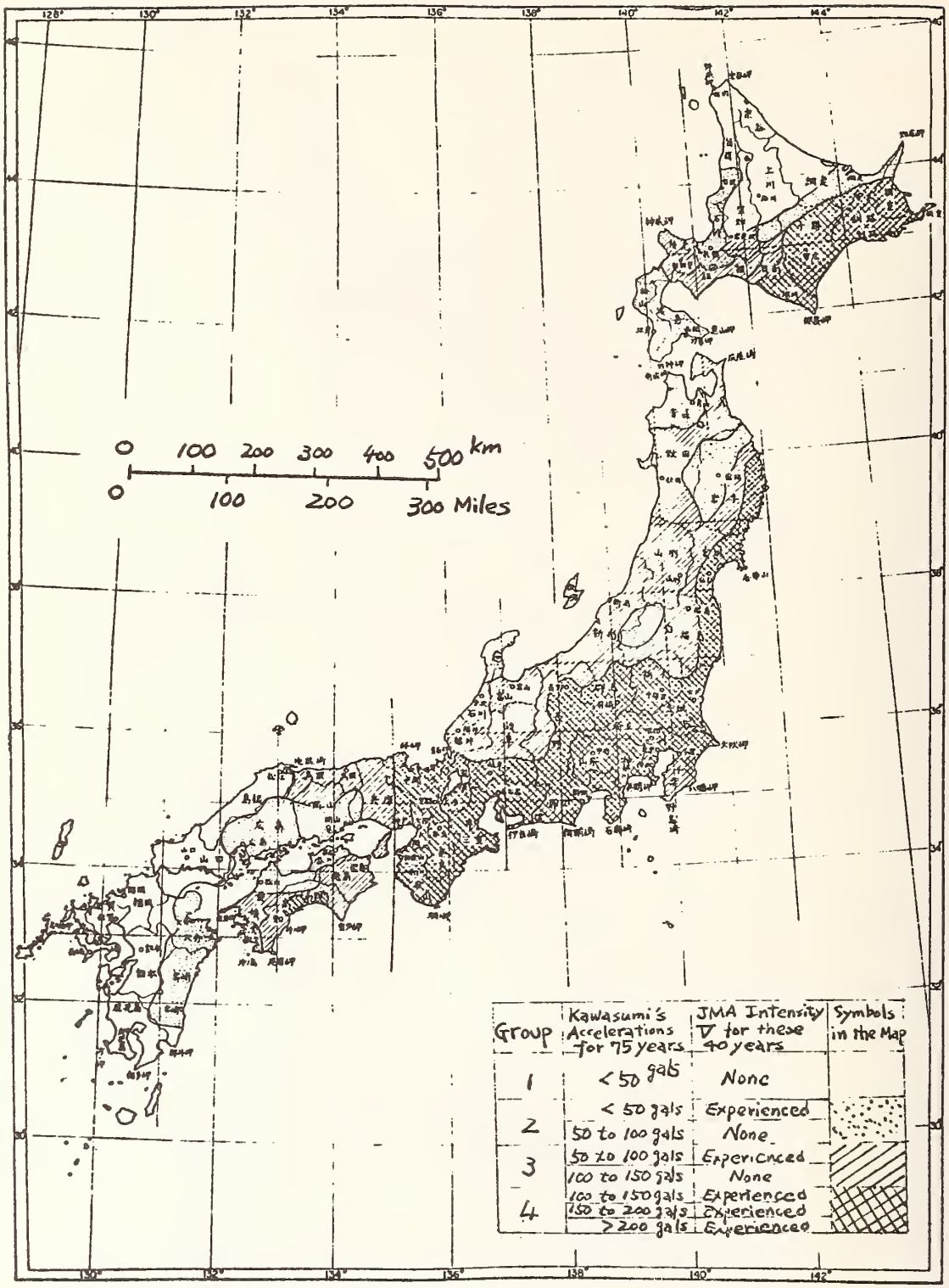

Fig. 3.5 Seismic risk map (after T. Okubo and T. Terashima [85])

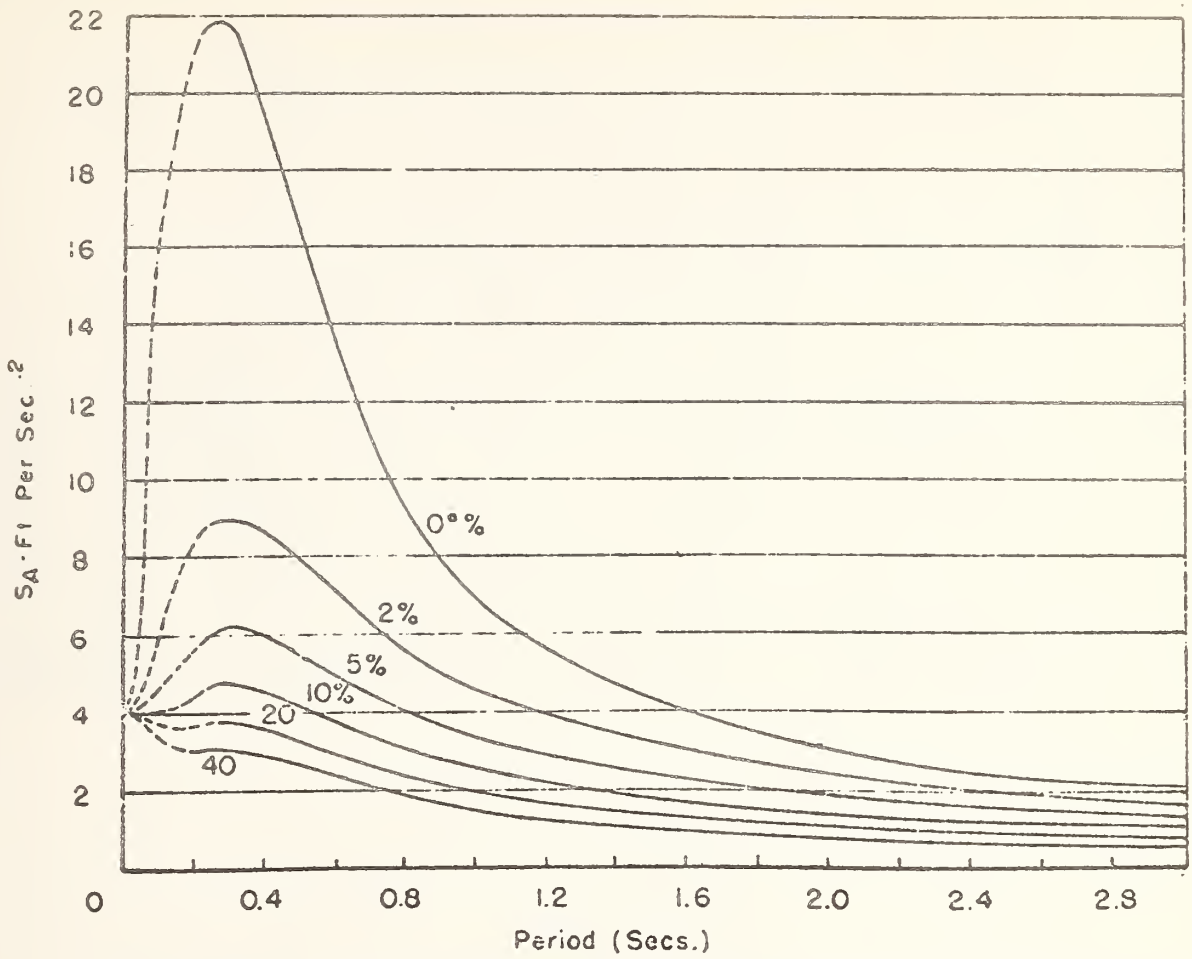

Fig. 3.6(A) Average acceleration spectrum (after G. W. Housner [88])

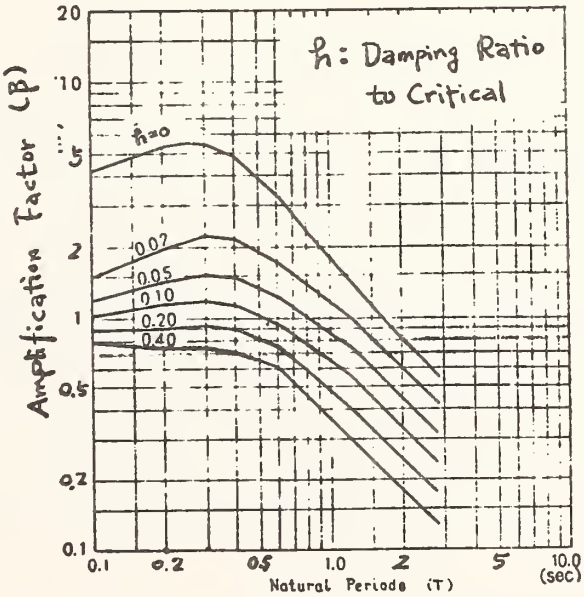

Fig. 3.6(B) Amplification factor spectrum obtained from Fig. 3.6(A)

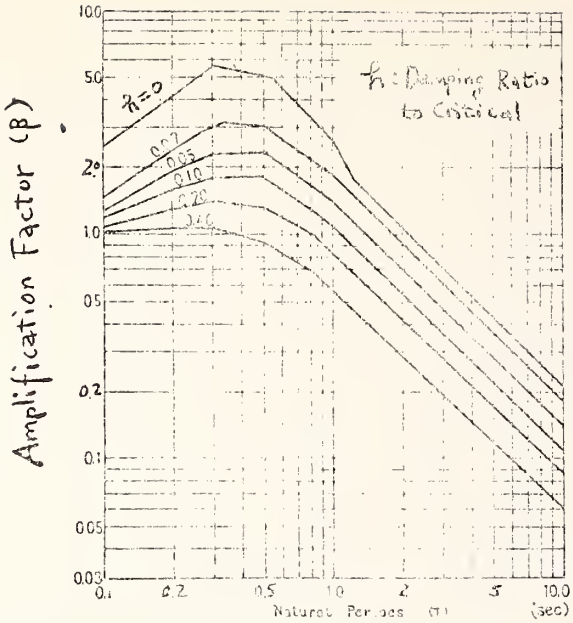

Fig. 3.7 Amplification factor spectrum (after T. Takata, T. Okubo, E. Kuribayashi [89])

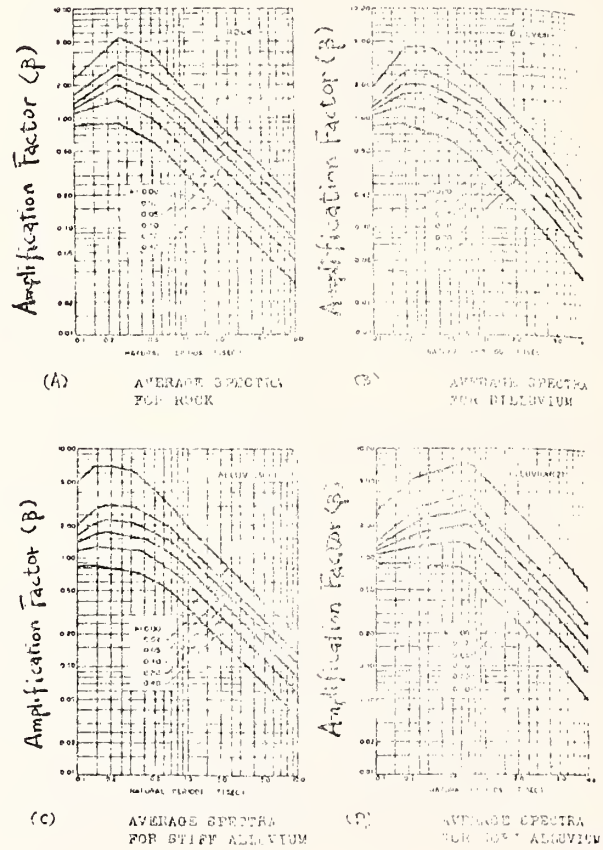

Fig. 3.8 Amplification factor spectrum for four kinds of ground condition (after E. Kuribayashi, T. Iwasaki, K. Tuji [92])

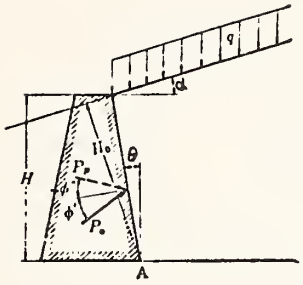

Fig. 3.9 Earth pressure acting on wall

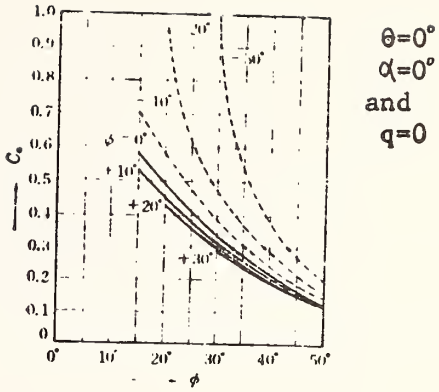

Fig. 3.10 Coefficient of active earth pressure

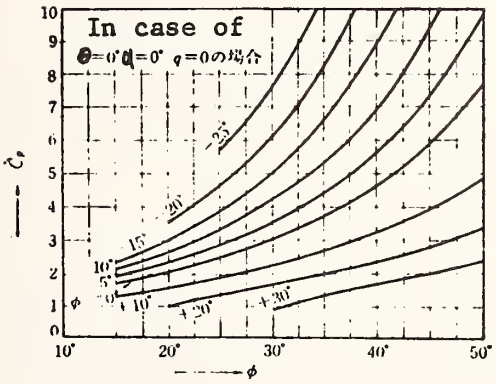

Fig. 3.11 Coefficient of passive earth pressure

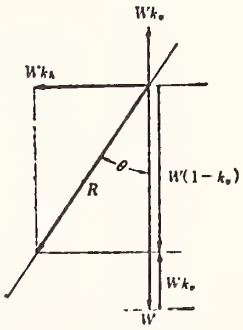

Fig. 3.12 Resultant seismic coefficient

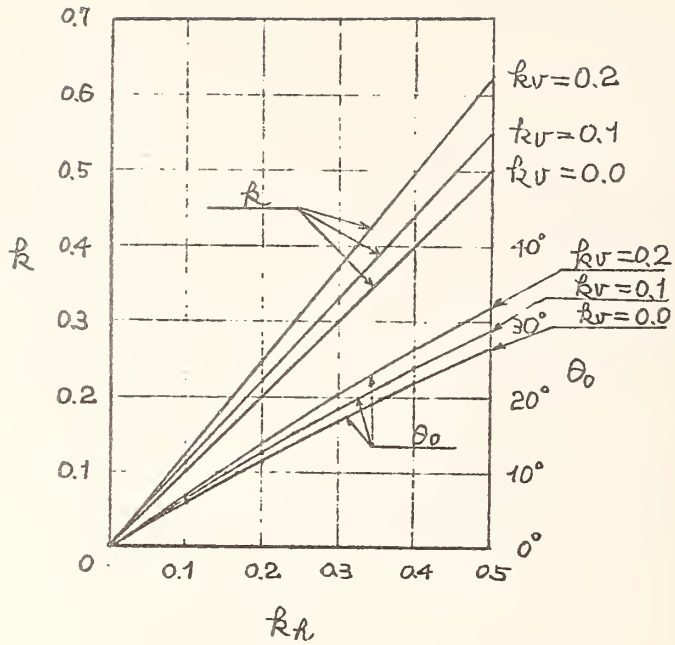

Fig. 3.13 k and θ_o values for various k_h and k_v

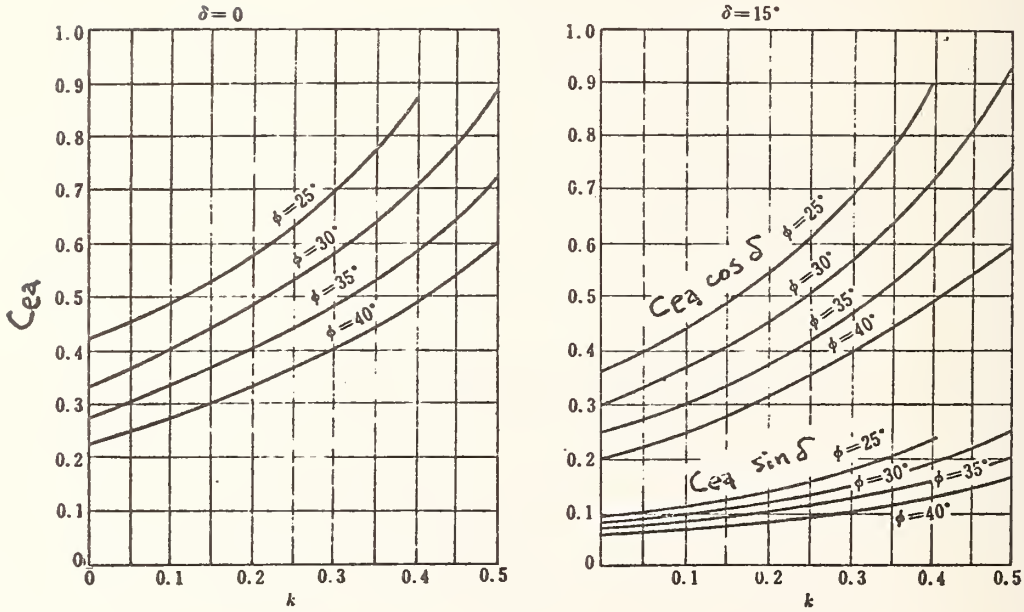

Fig. 3.14 Coefficient of active earth pressure during earthquakes

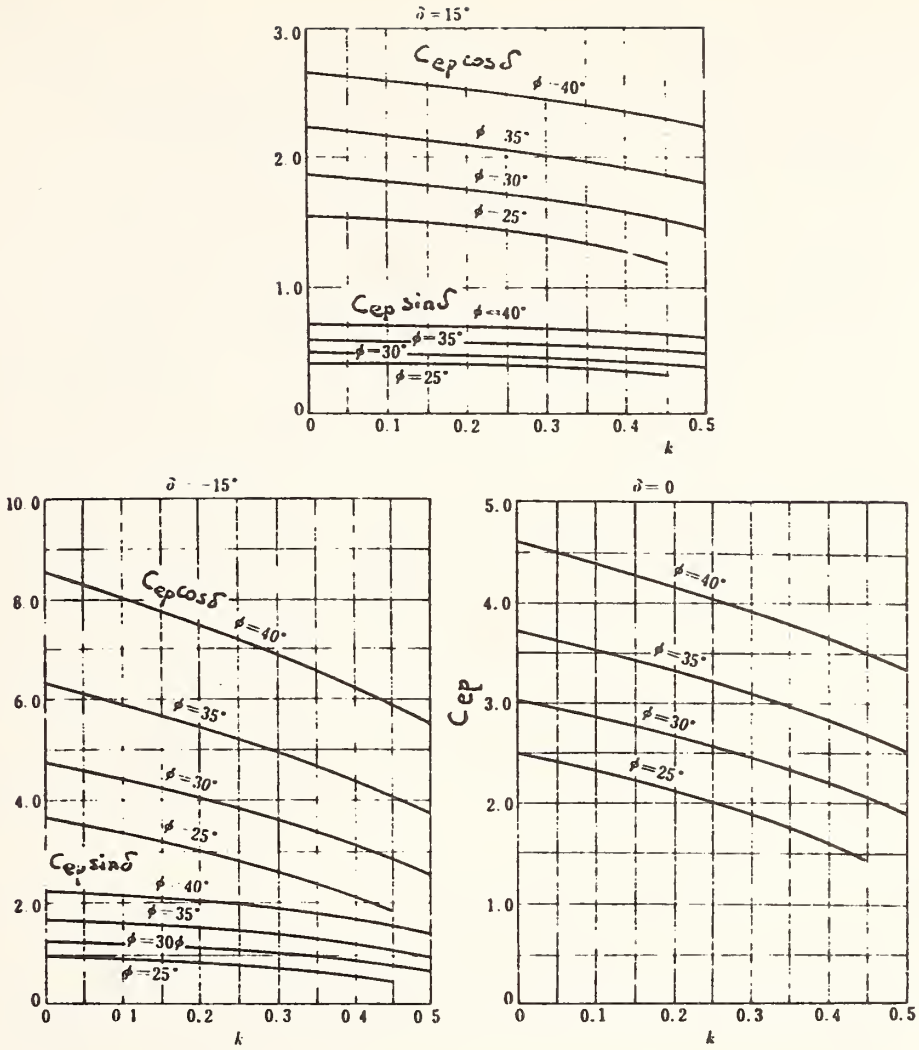

Fig. 3.15 Coefficient of passive earth pressure during earthquakes

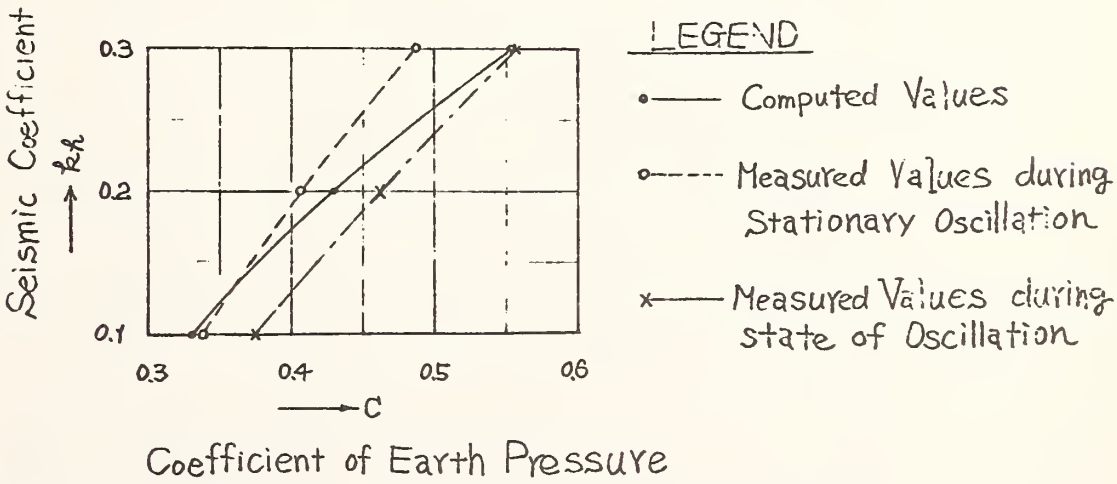

Fig. 3.16 Experimental results of earth pressure during harmonic excitation (after N. Mononobe [206])

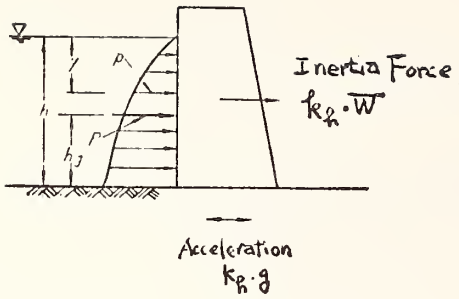

Fig. 3.17 Hydrodynamic pressure on vertical wall

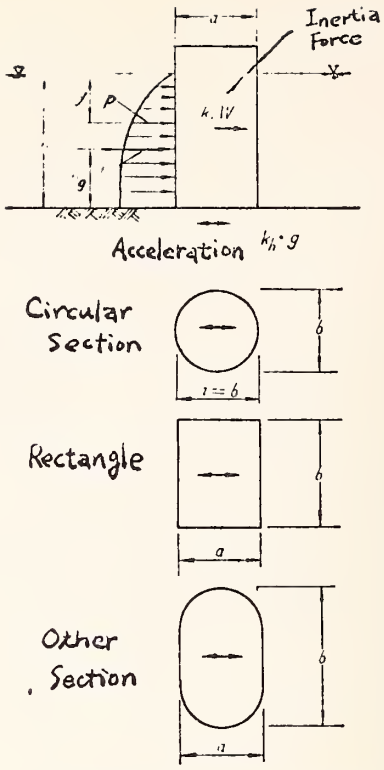

Fig. 3.18 Hydrodynamic pressure on column

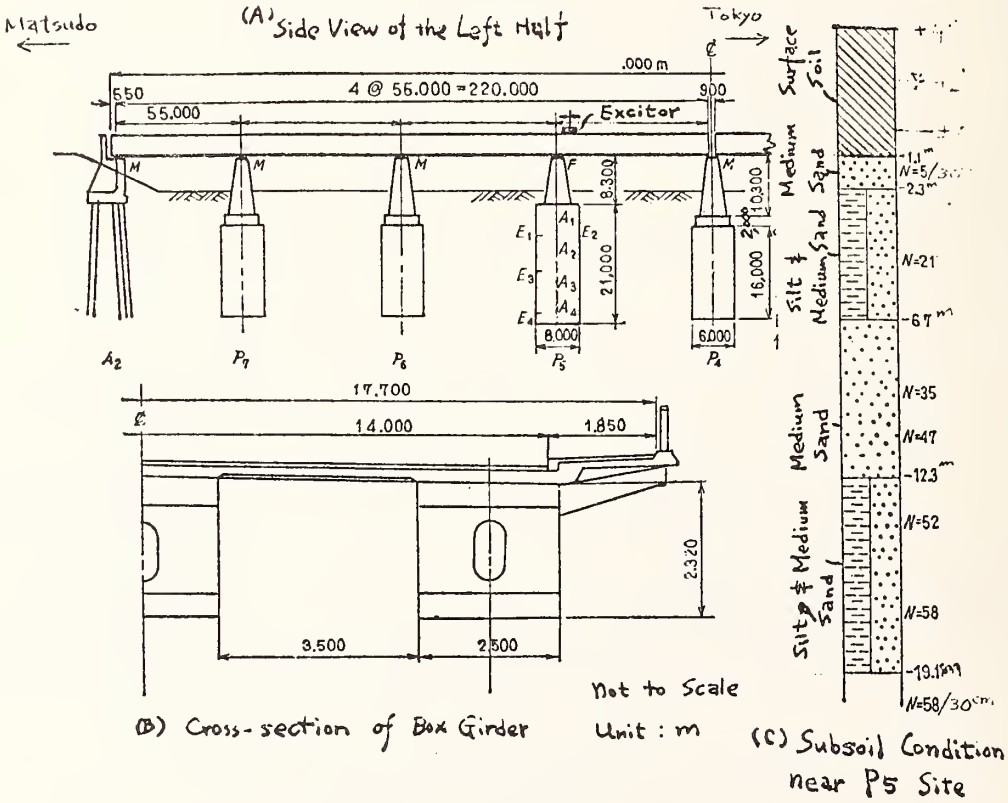

Fig. 3.19 General view of the Shinkatsushika bridge

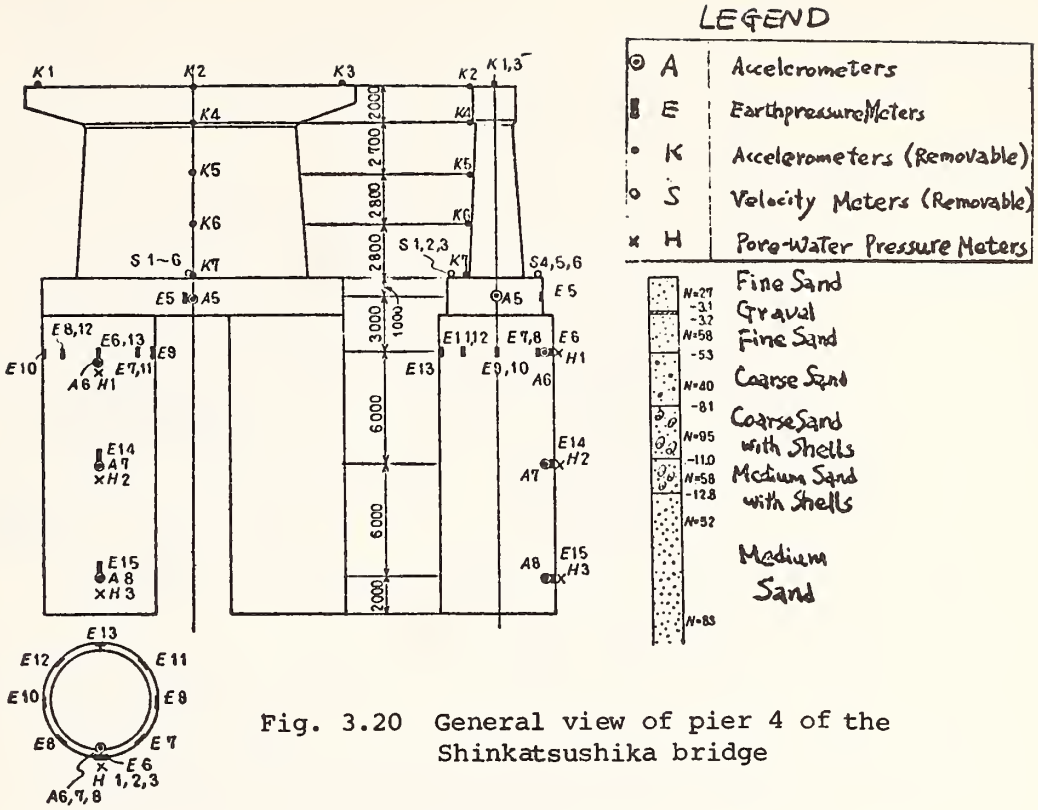

Fig. 3.20 General view of pier 4 of the Shinkatsushika bridge

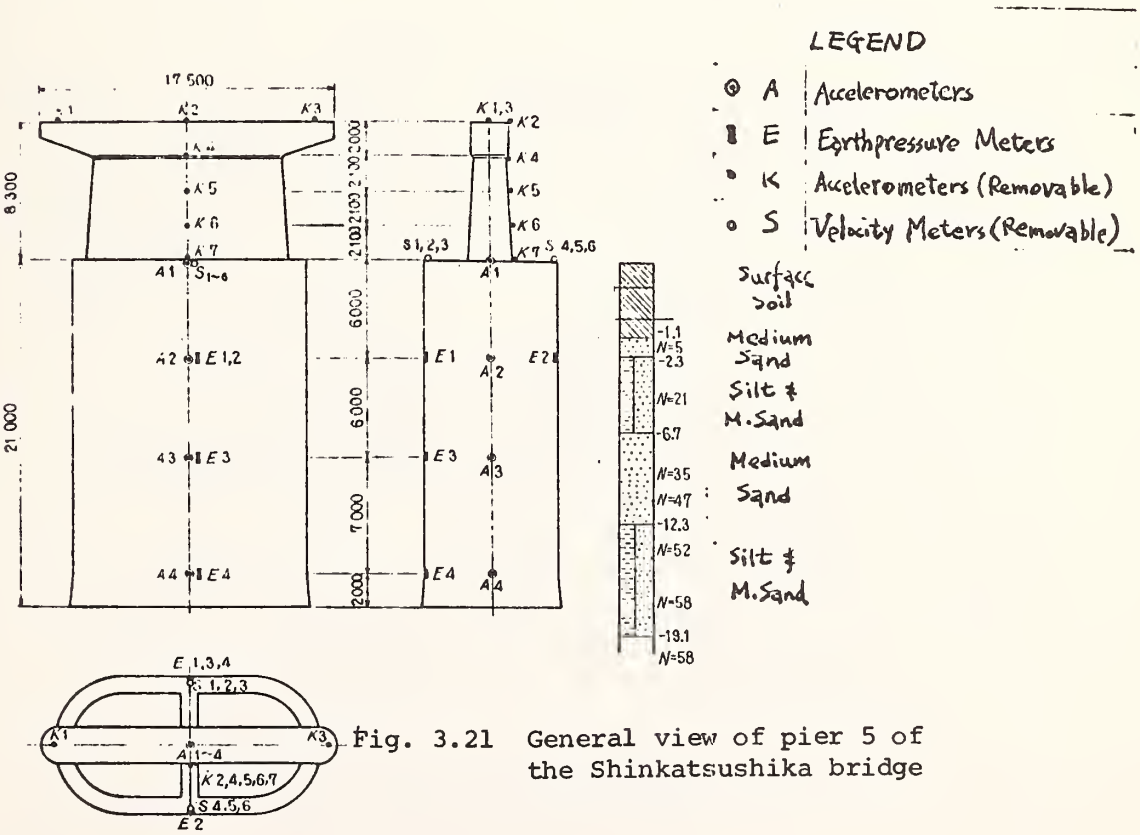

Fig. 3.21 General view of pier 5 of the Shinkatsushika bridge

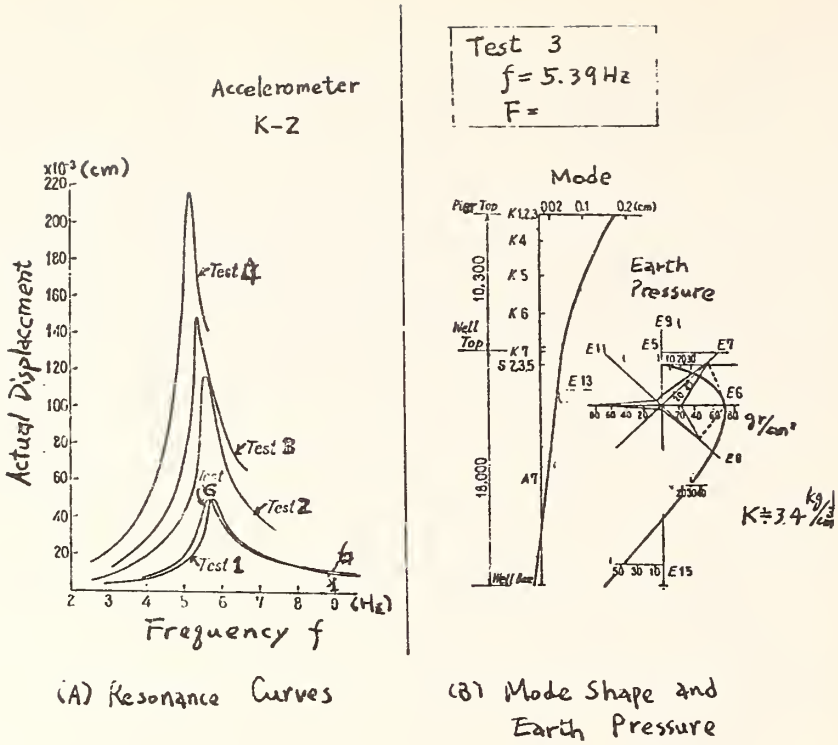

(A) Resonance Curves (B) Mode Shape and Earth Pressure

Fig. 3.22 Vibration test results for pier 4 of the Shinkatsushika bridge

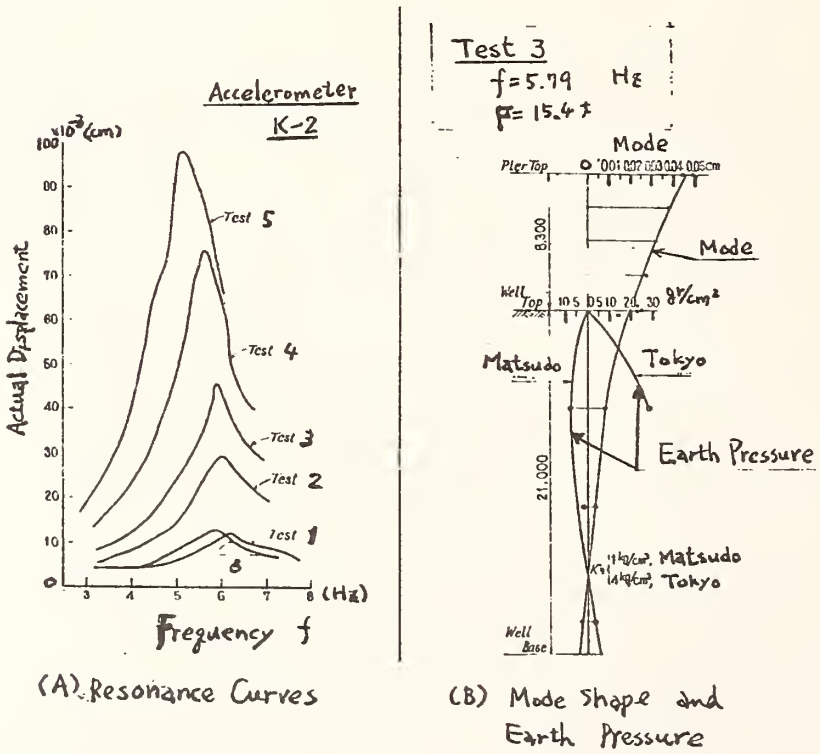

(A) Resonance Curves (B) Mode Shape and Earth Pressure

Fig. 3.23 Vibration test results for pier 5 of the Shinkatsushika bridge

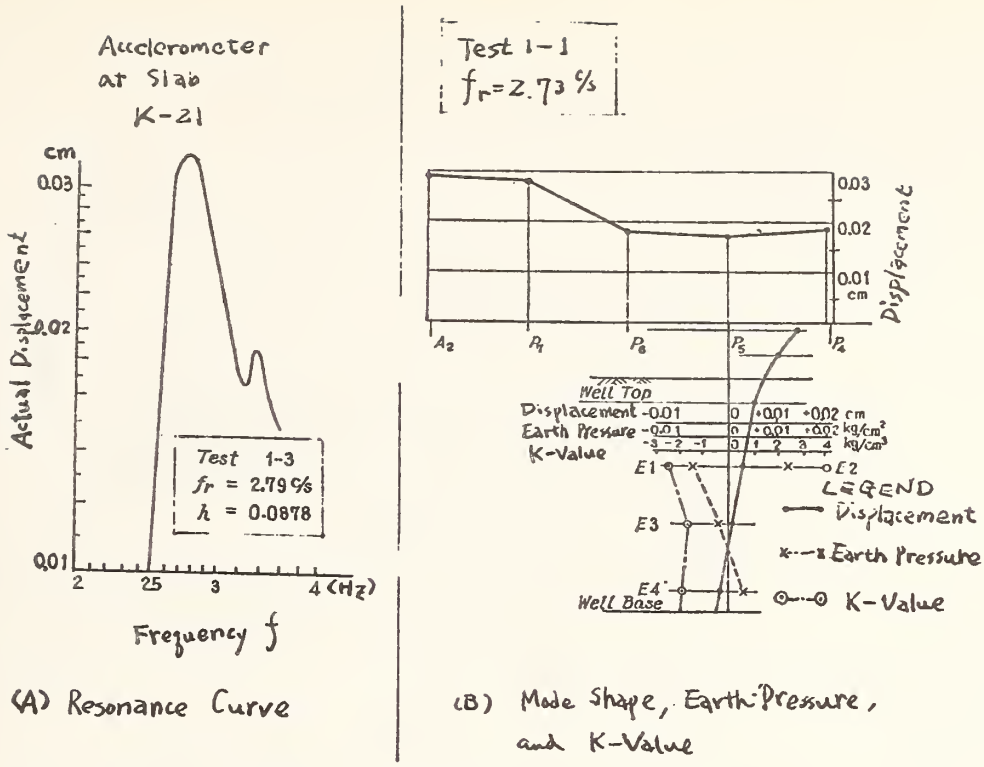

Fig. 3.24 Vibration test results for the whole bridge structure of the Shinkatsushika bridge

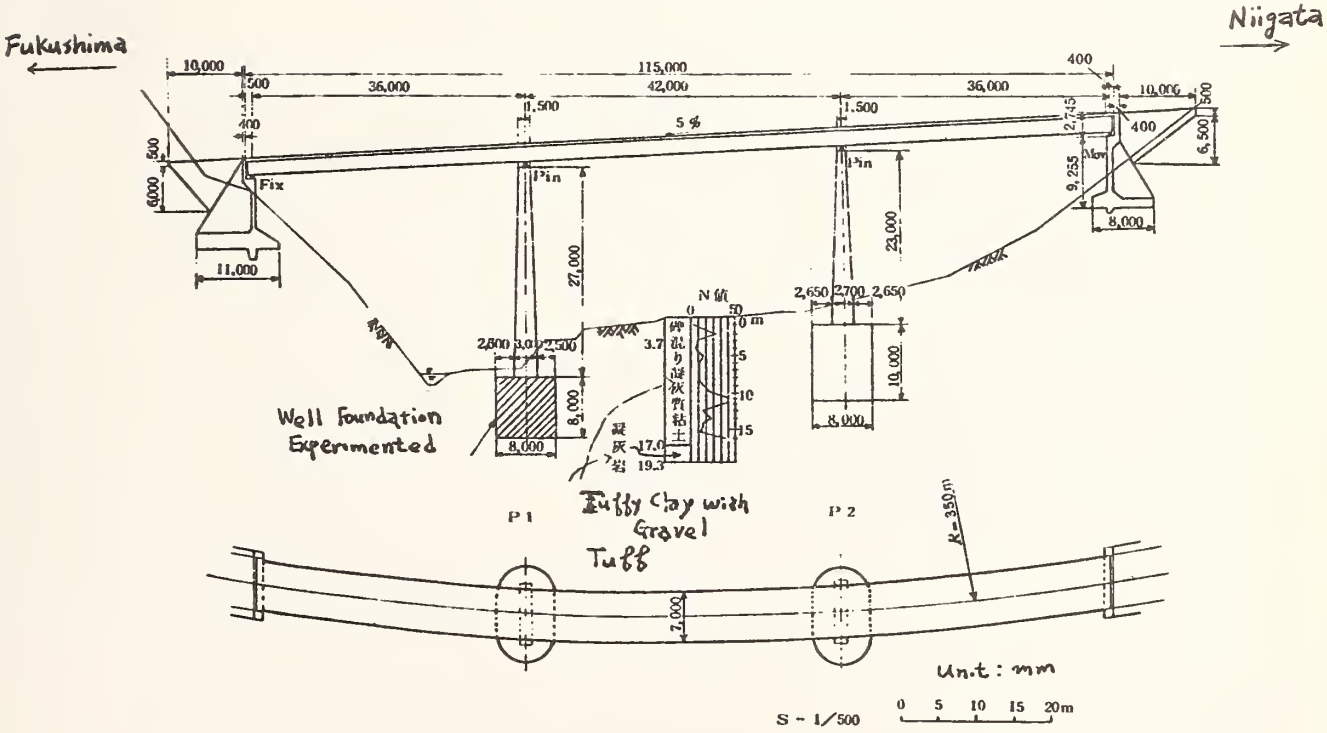

Fig. 3.25 General view of the Torii bridge

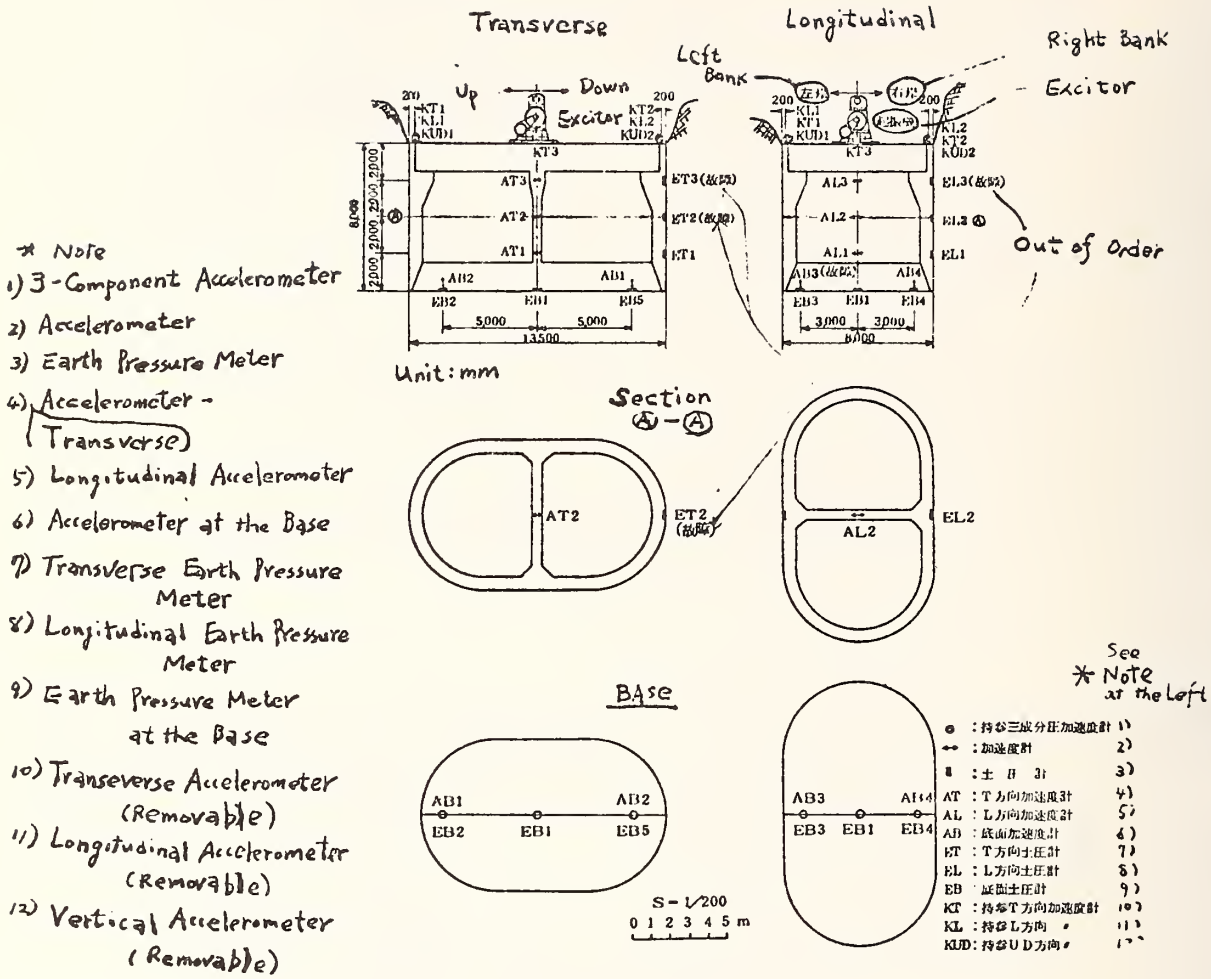

Fig. 3.26 Open caisson foundation of pier 1 of the Torii bridge

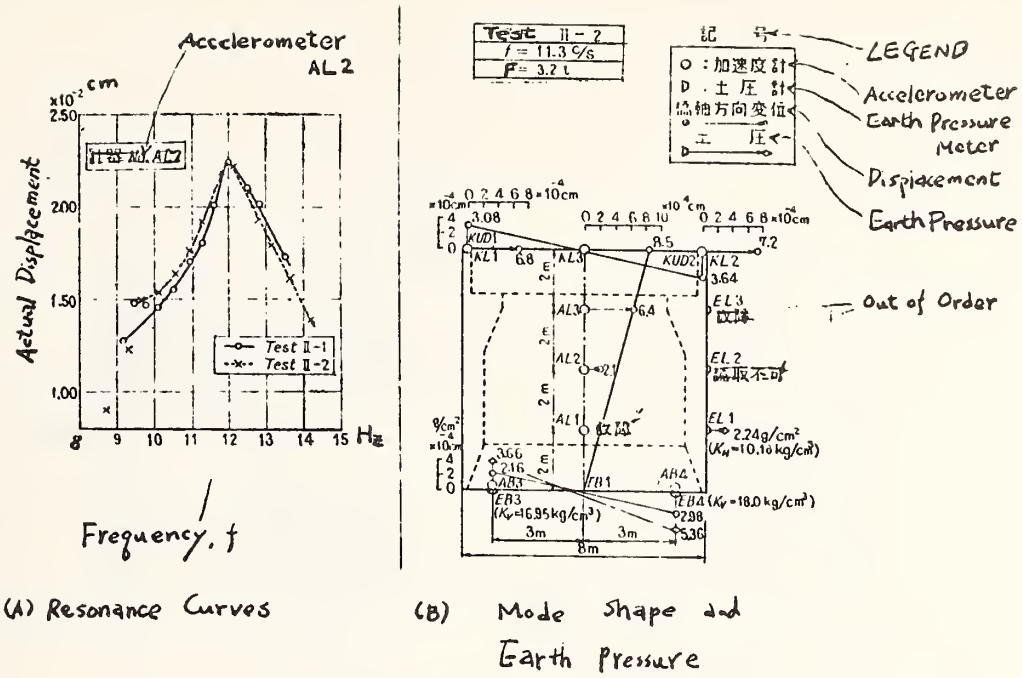

(A) Resonance Curves (B) Mode Shape and Earth Pressure

Fig. 3.27 Test results for the foundation of pier 1 of the Torii bridge (longitudinal direction)

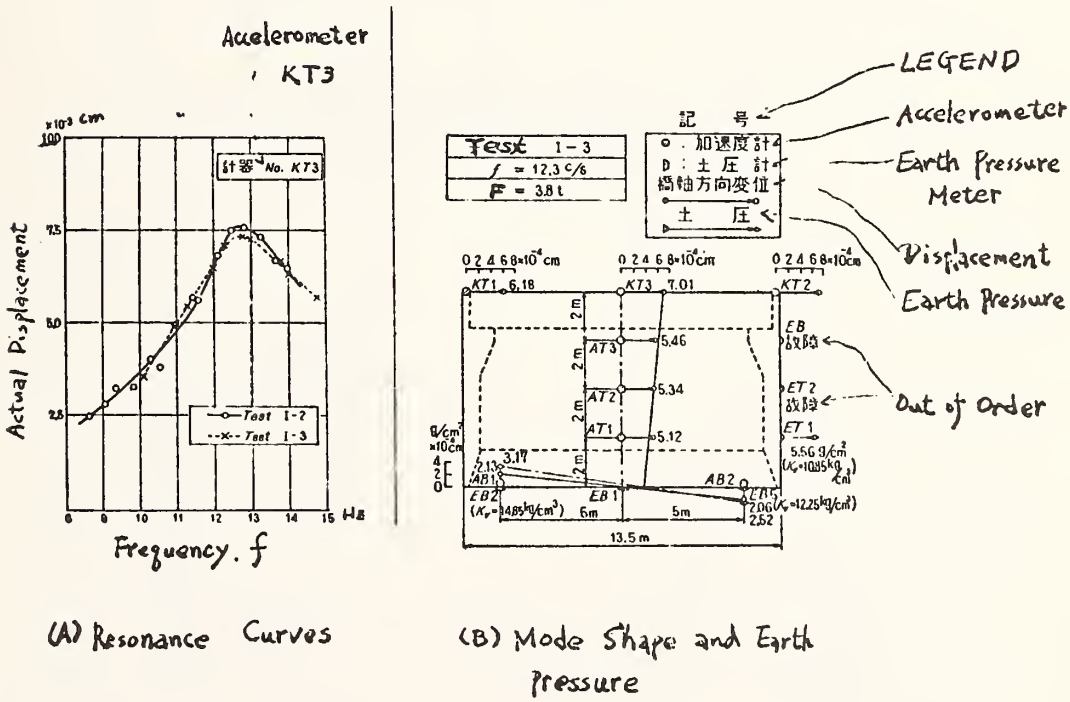

(A) Resonance Curves (B) Mode Shape and Earth Pressure

Fig. 3.28 Test results for the foundation of pier 1 of the Torii bridge (transverse direction)

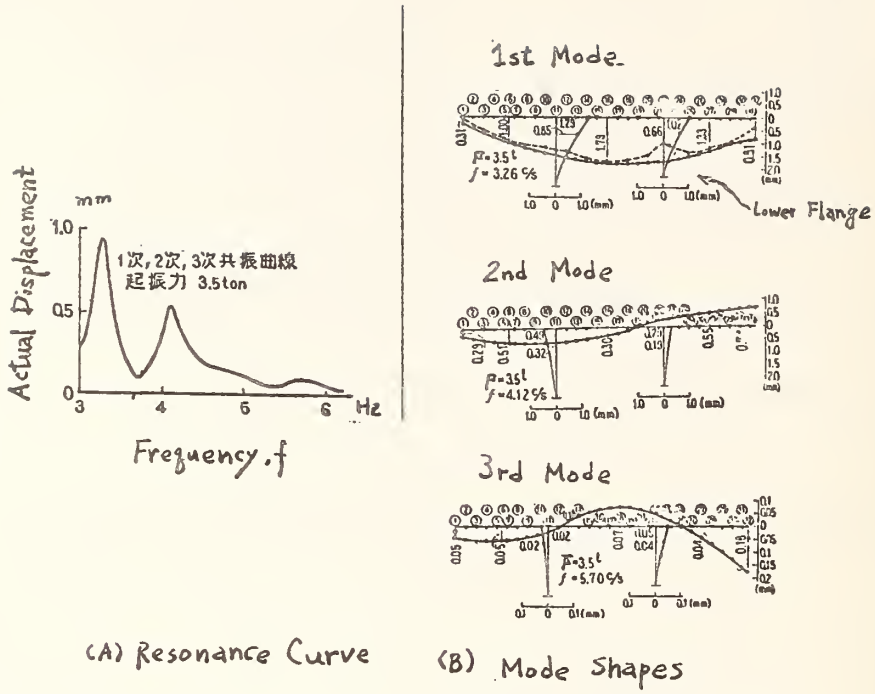

Fig. 3.29 Test results for the whole bridge structure of the Torii bridge (transverse direction)

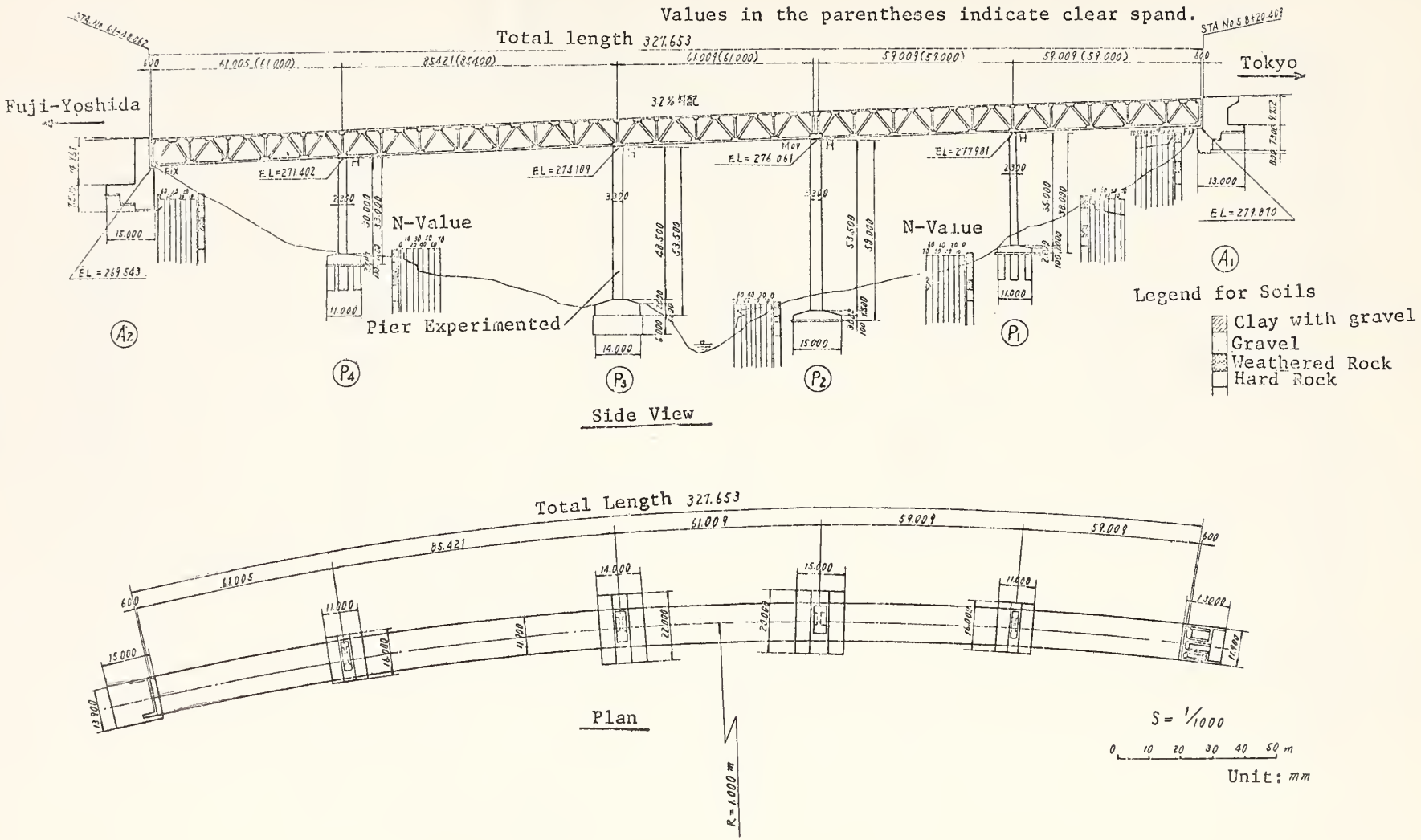

Fig. 3.30 General view of the Sokozawa bridge.

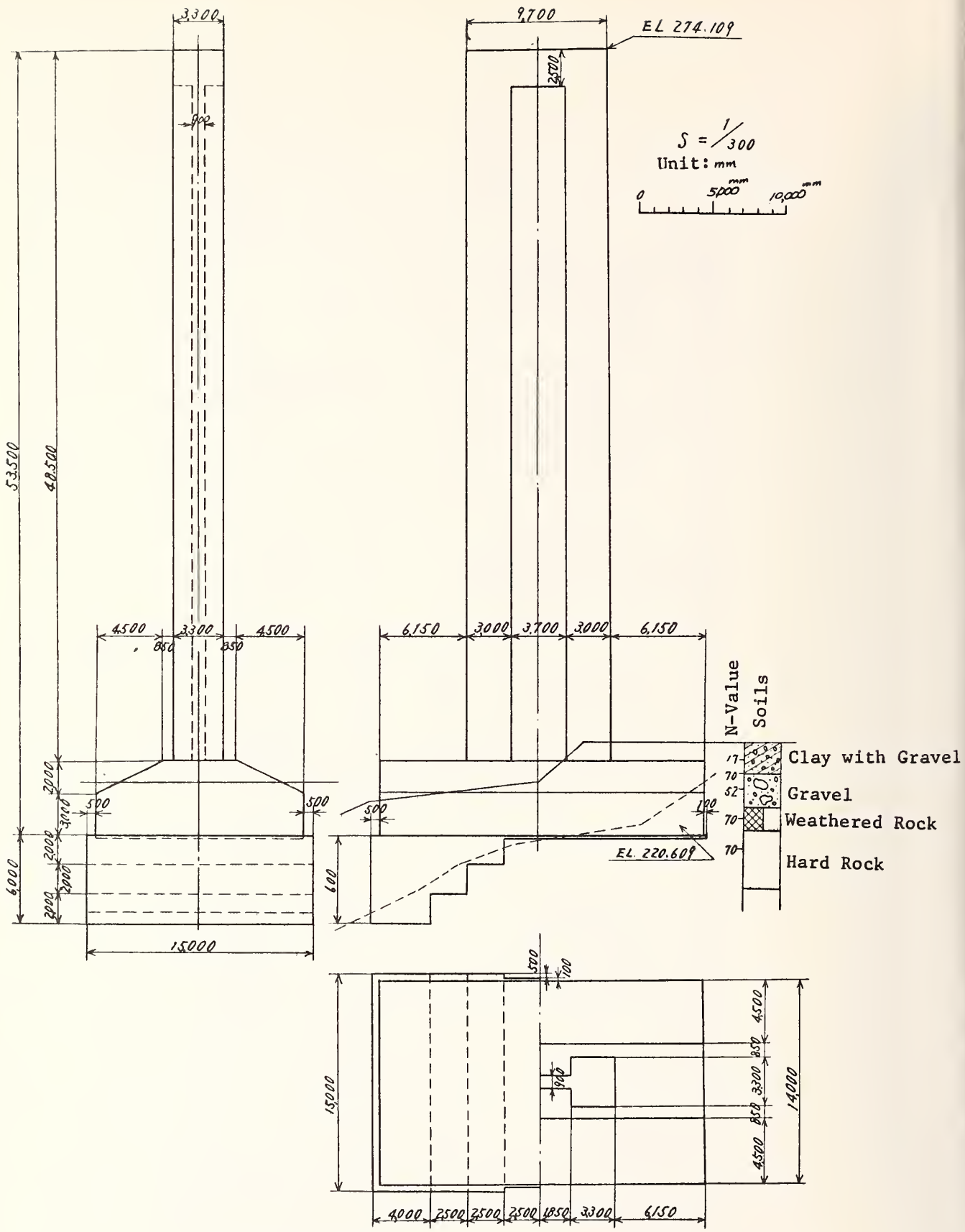

Fig.3.31 Pier 3 at the Sokozawa bridge

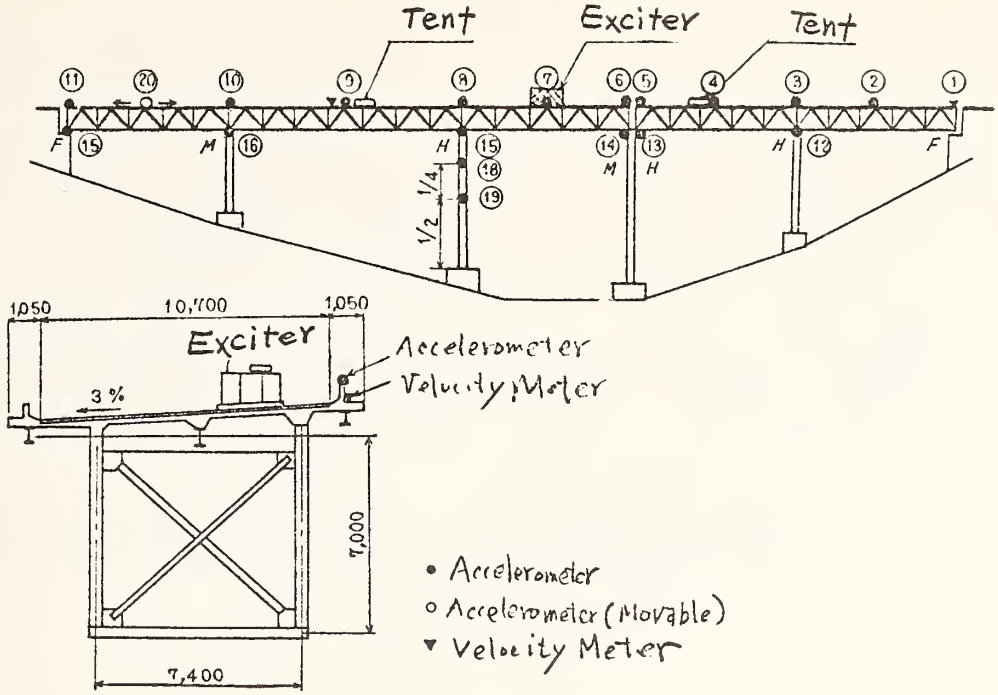

Fig. 3.32 Locations of exciter and pick-ups

	Resonant Frequency	Damping Ratio	Exciting Force
1st	1.53 Hz	1.3 %	1.5 t
2nd			
3rd	2.38	1.7	3.5 t
4th	2.64	1.7	3.5 t

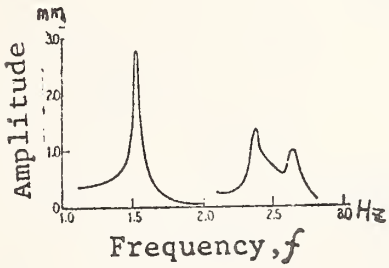

(A) Resonance Curve

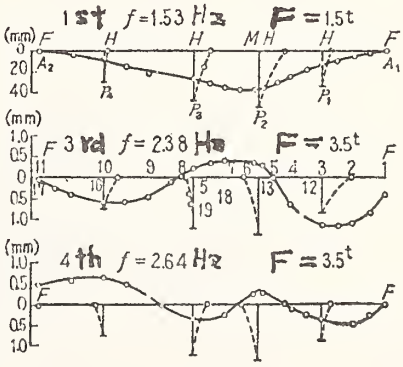

(B) Mode shape

Fig. 3.33 Test results for the whole bridge structure of the Sokozawa bridge (transverse direction)

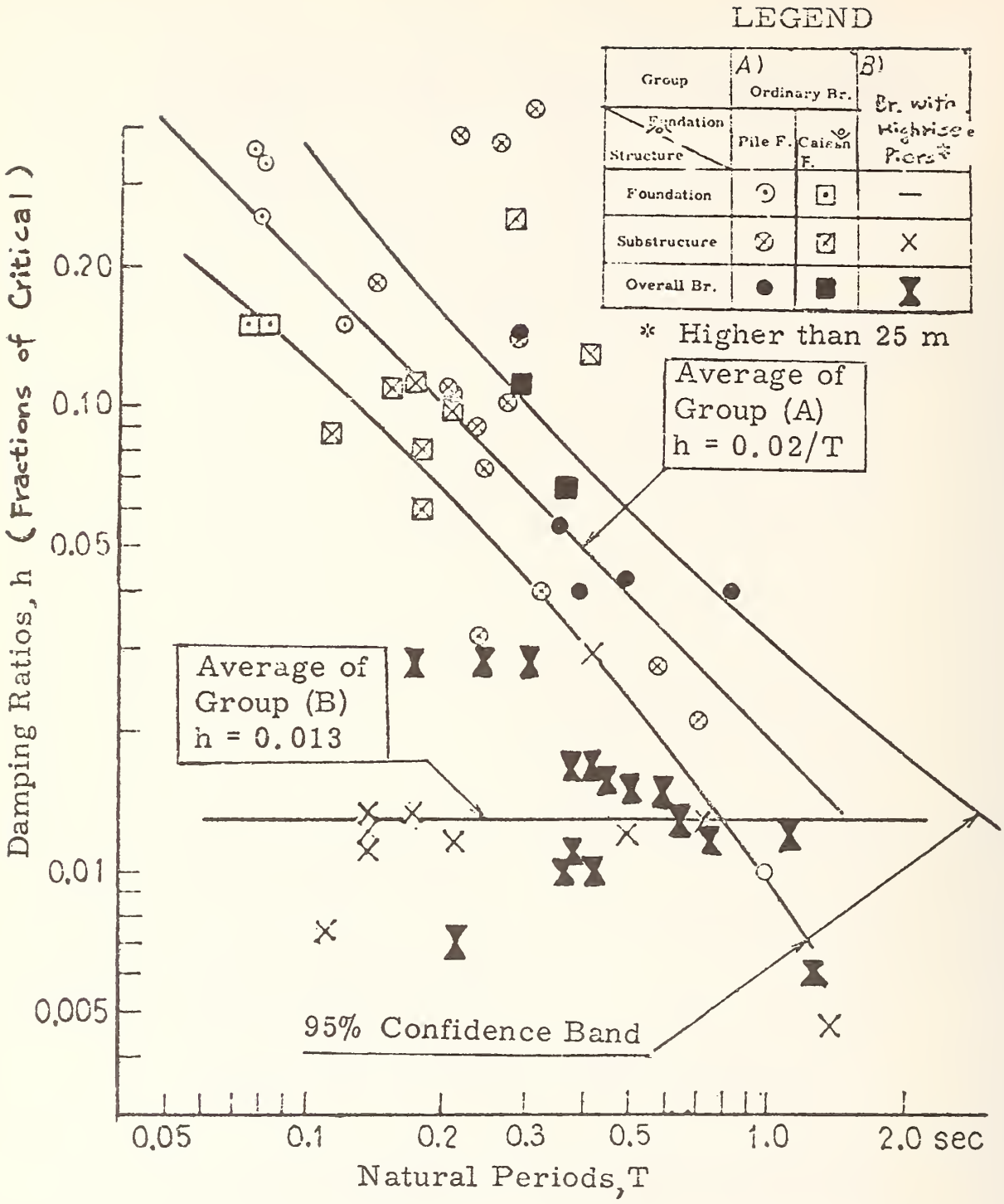

Fig. 3.34 Relationship between natural period and damping ratio for bridge structures

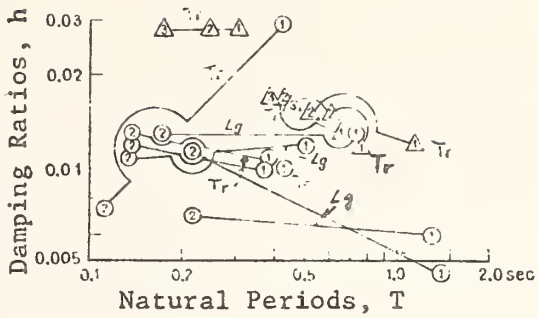

Legend

O : Isolated Pier

Δ : Overall Bridge

L_g : Vibration in the Longitudinal Direction of Bridge Axis

T_r : Vibration in the Transverse Direction

Numerals indicate order of vibration Modes

Fig. 3.35 Relationship between natural period and damping ratio for bridges with highrise piers

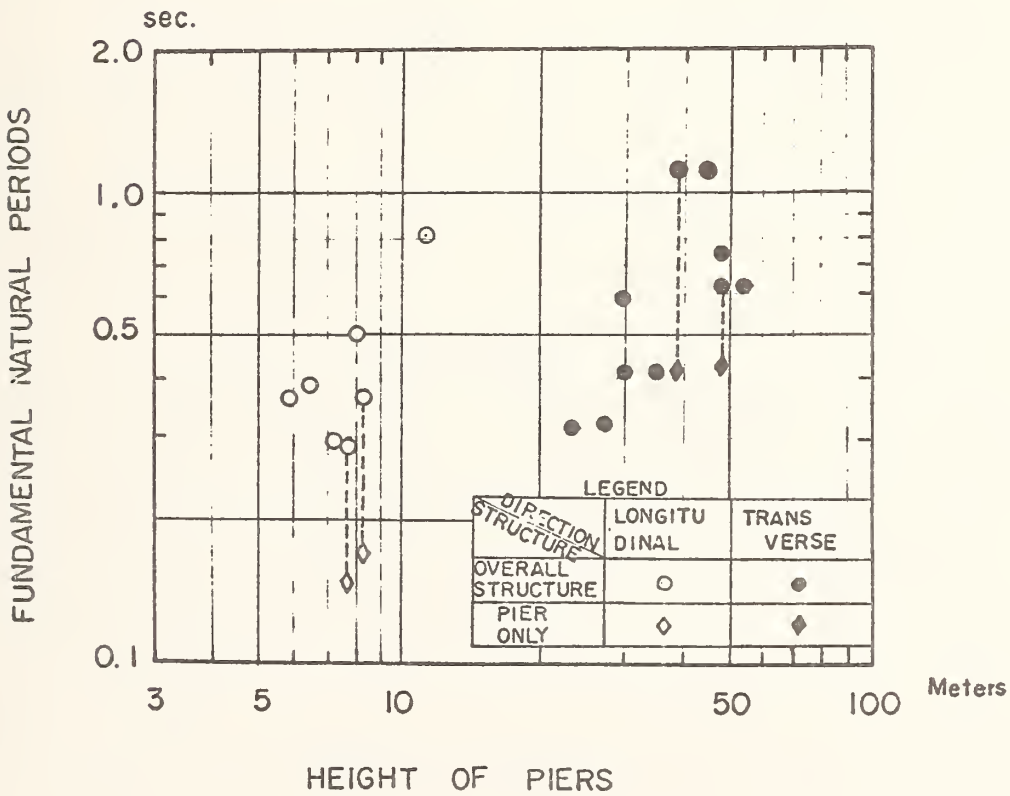

Fig. 3.36 Relationship between height of pier and fundamental natural period

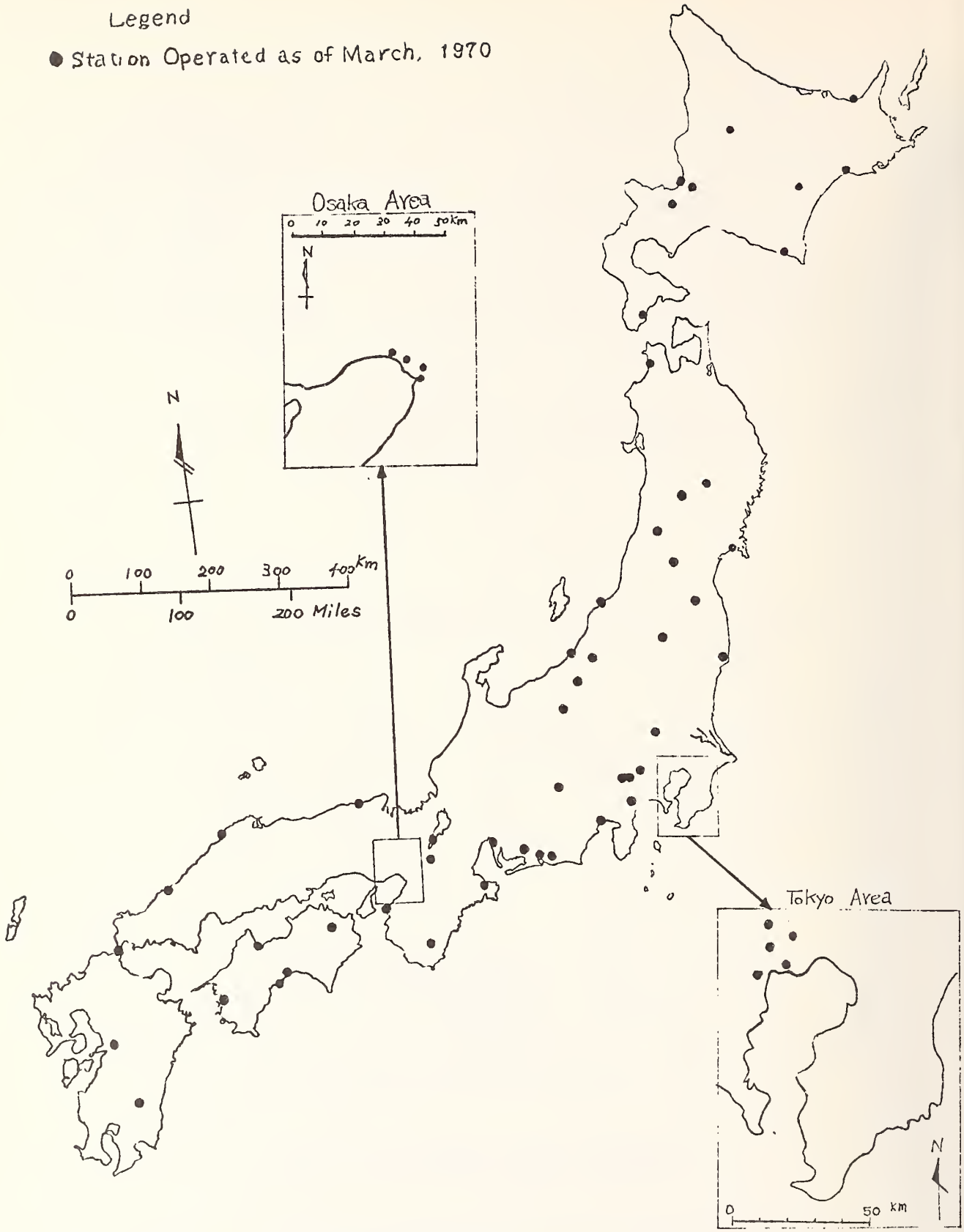

Fig. 3.37 Network of strong-motion accelerographs at highway bridges

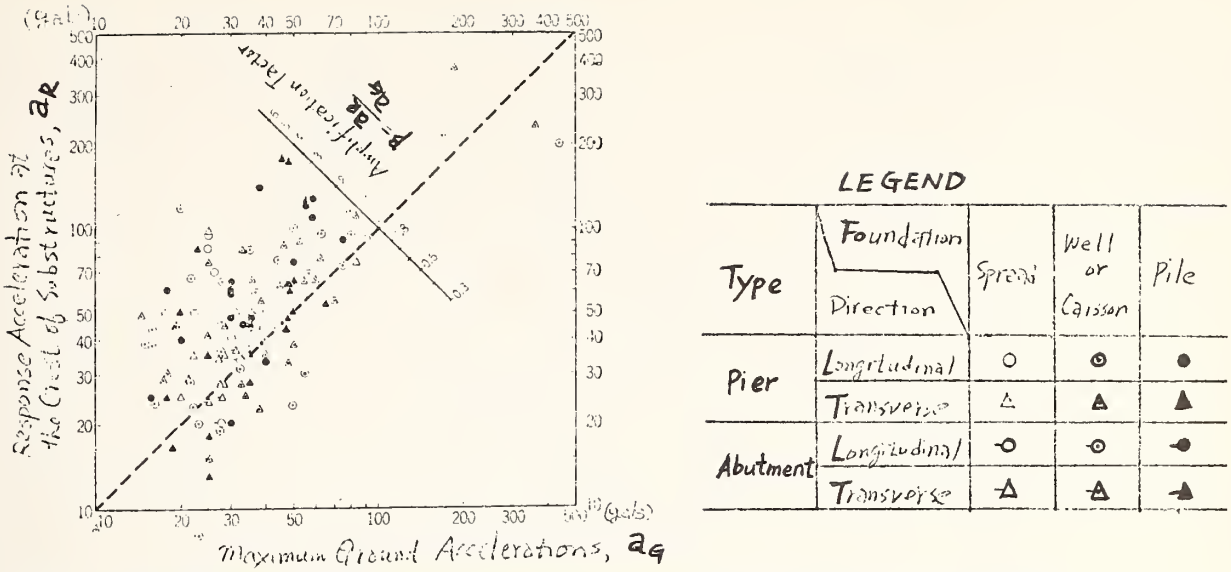

Fig. 3.38 Results of earthquake measurements at twenty seven bridges

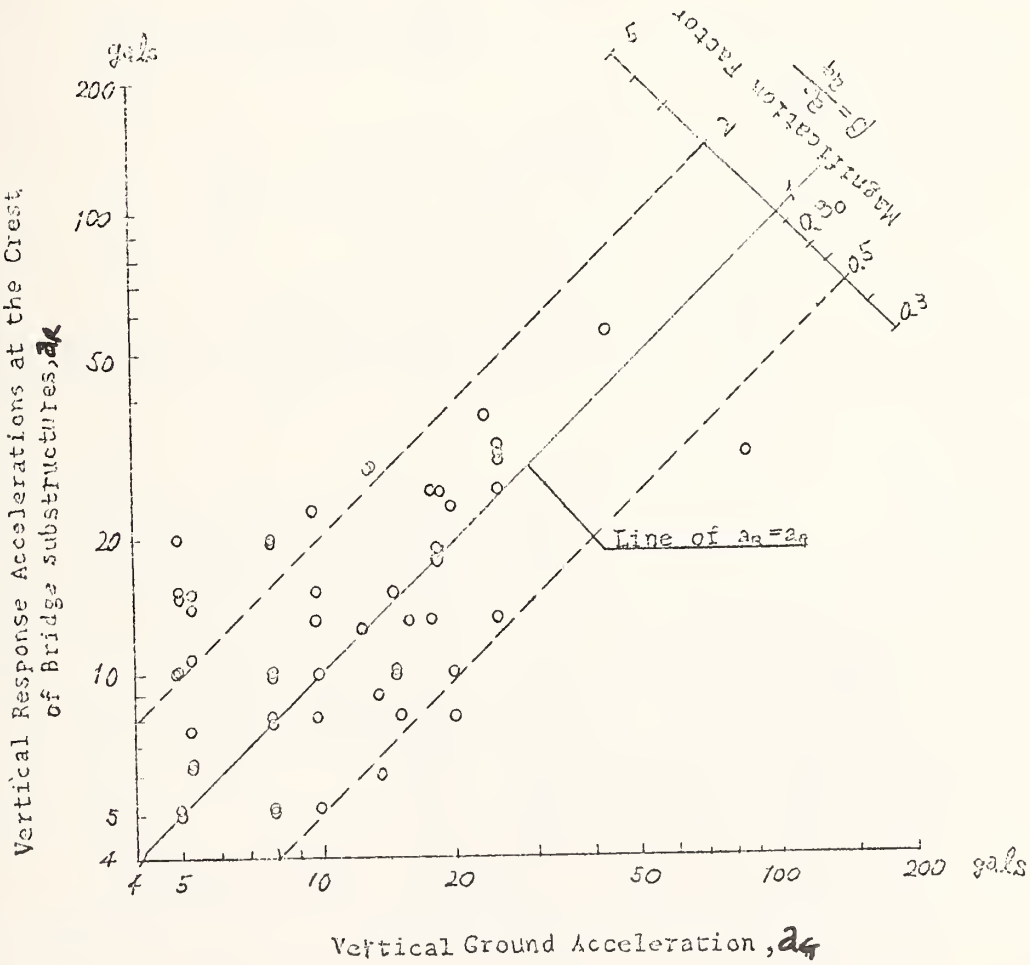

Fig. 3.39 Relation between ground acceleration and response acceleration at the crest of bridge structures in the vertical direction

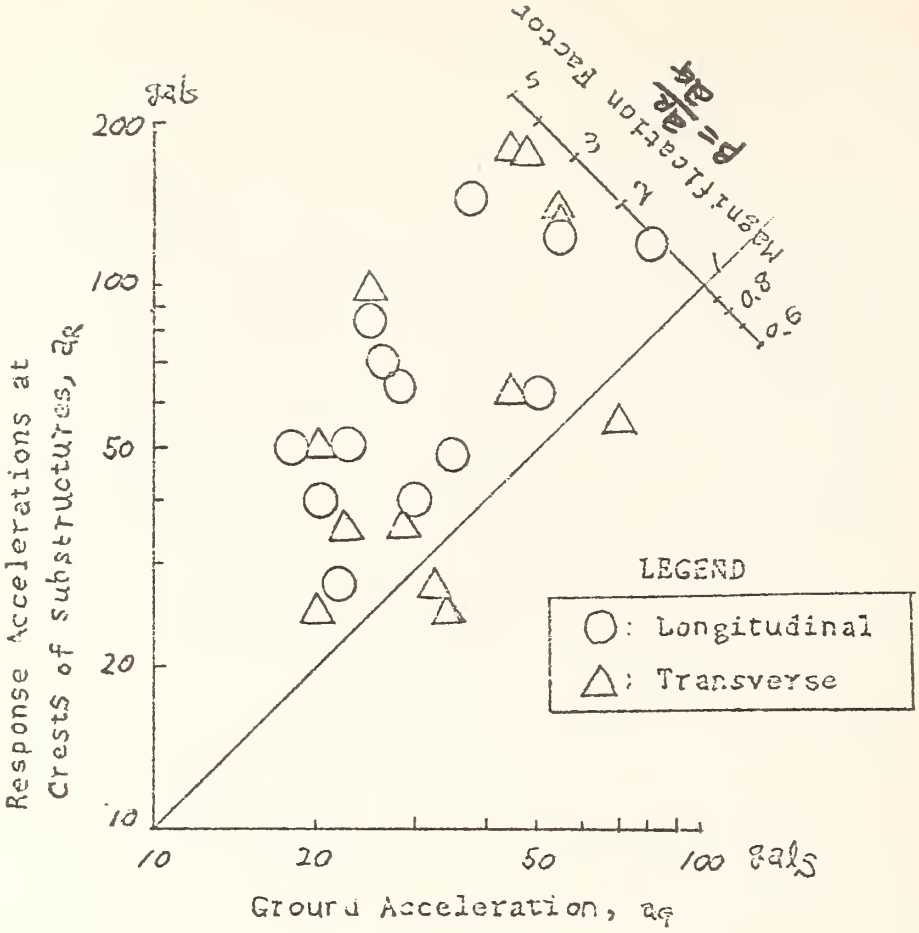

Fig. 3.40 Results of earthquake measurements at light bridges with highrise piers (over 10 m above ground surface)

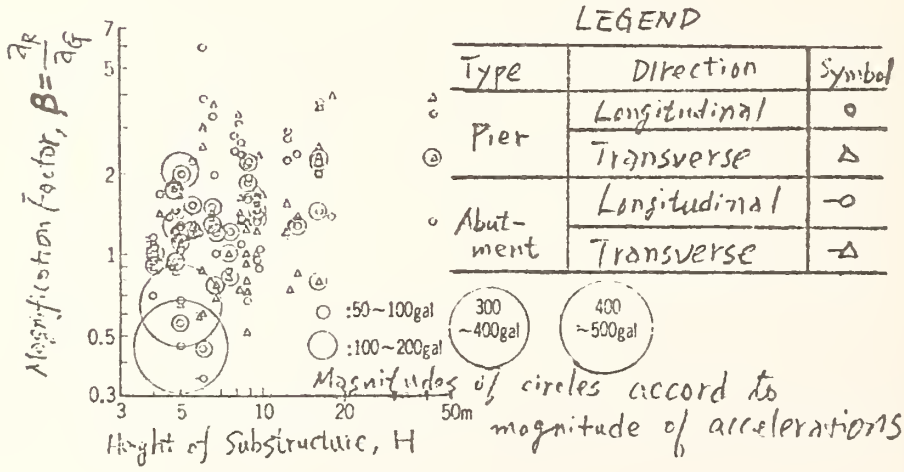

Fig. 3.41 Magnification factors measured vs. height of bridge structures

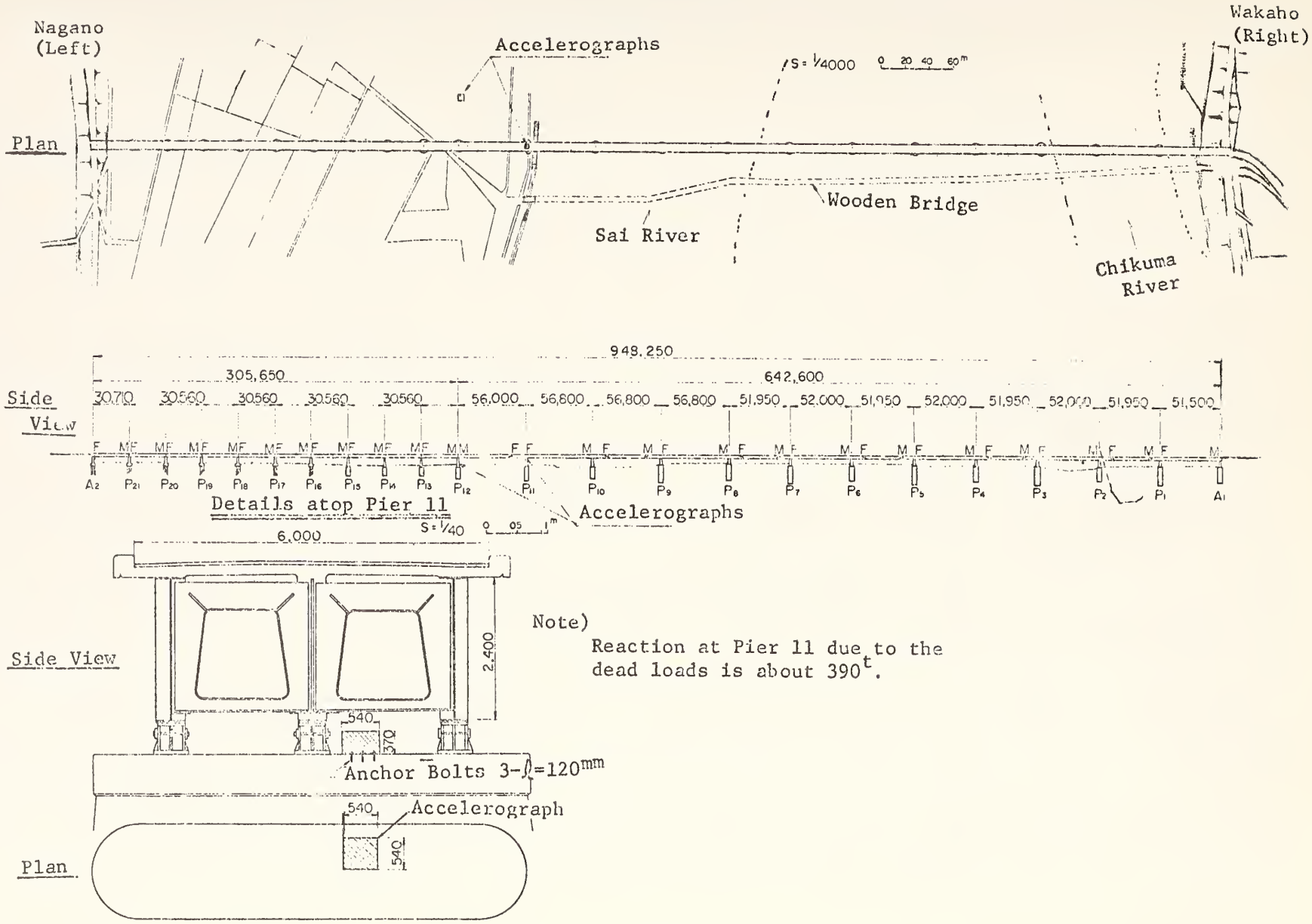

Note)
Reaction at Pier 11 due to the dead loads is about 390^{t}.

Fig. 3.42 General view of the Ochiai bridge

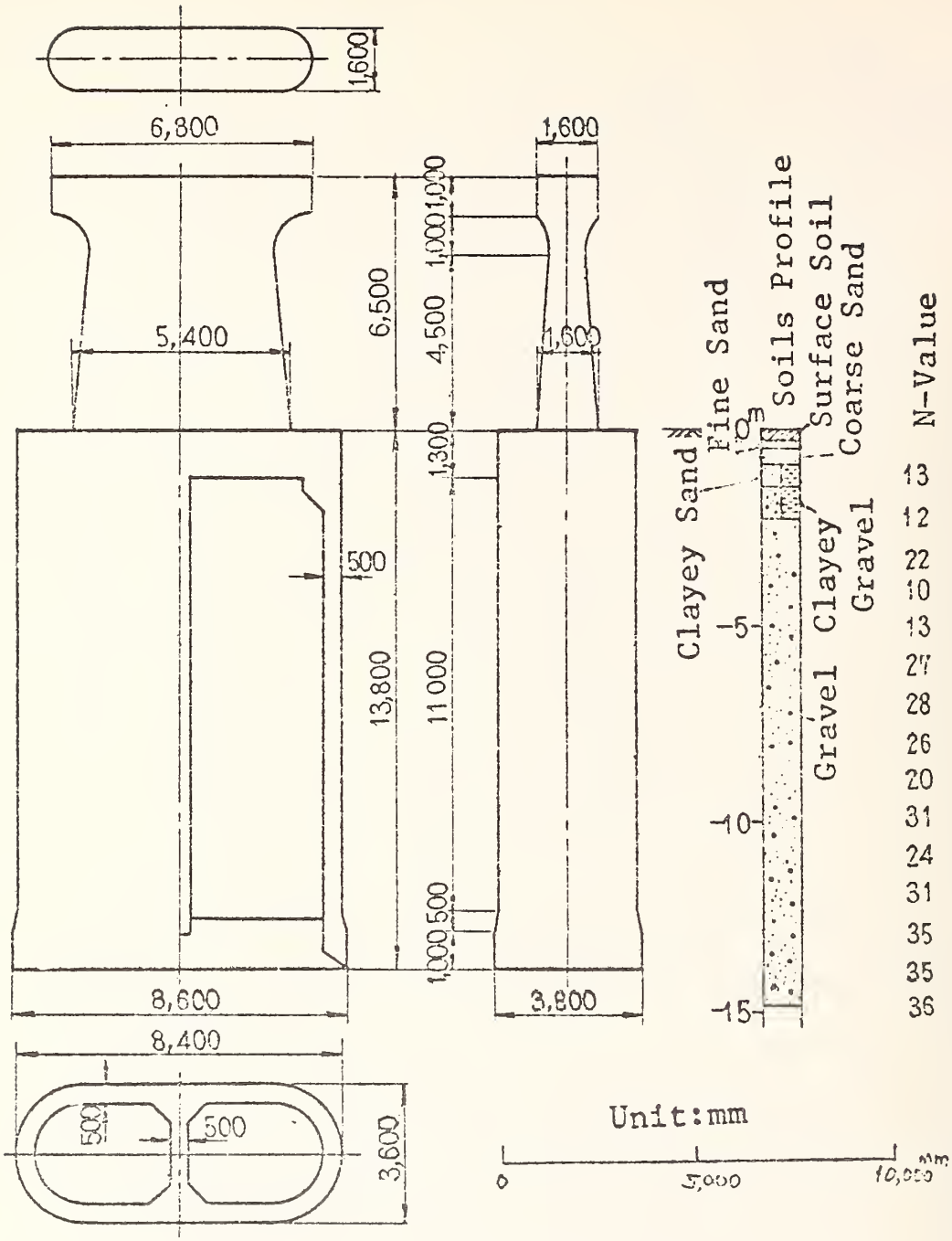

Fig. 3.43 Outline of pier 11 of the Ochiai bridge

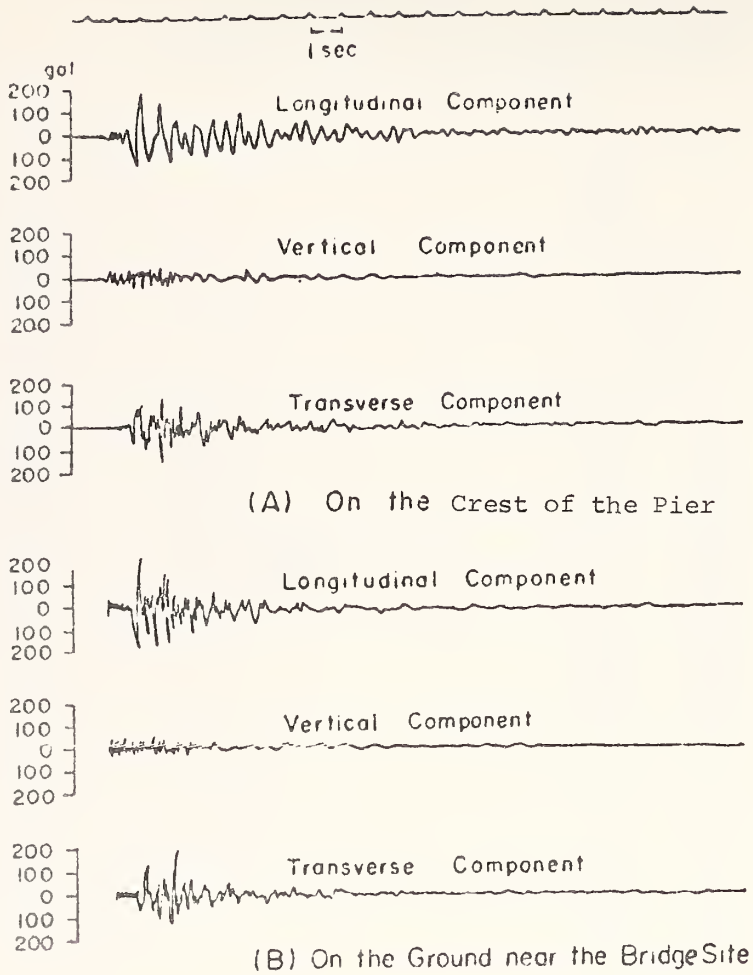

Fig. 3.44 Examples of acceleration records observed at the Ochiai bridge station

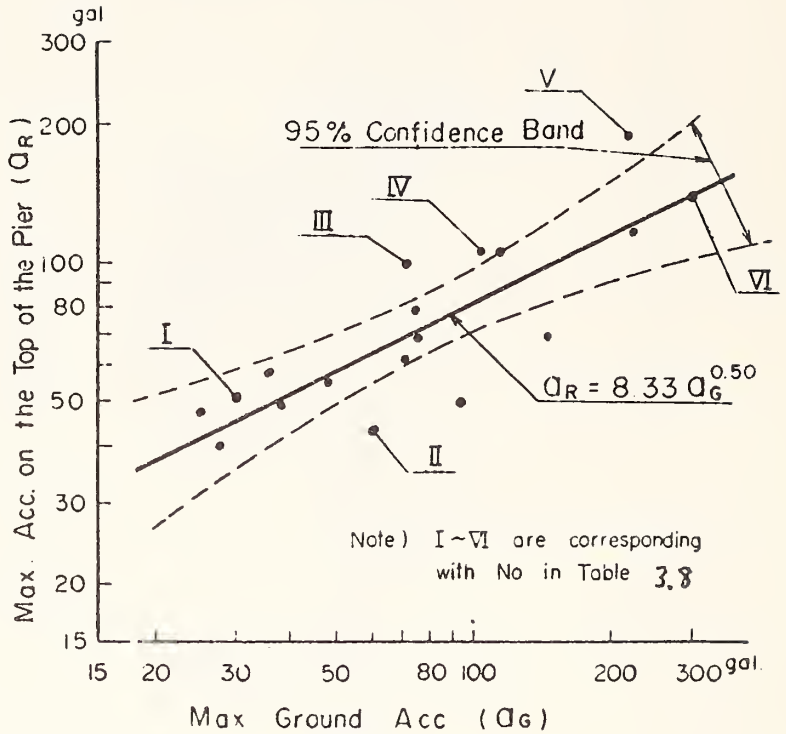

Fig. 3.45 Relation between ground acceleration and response acceleration observed at the Ochiai bridge in the longitudinal direction

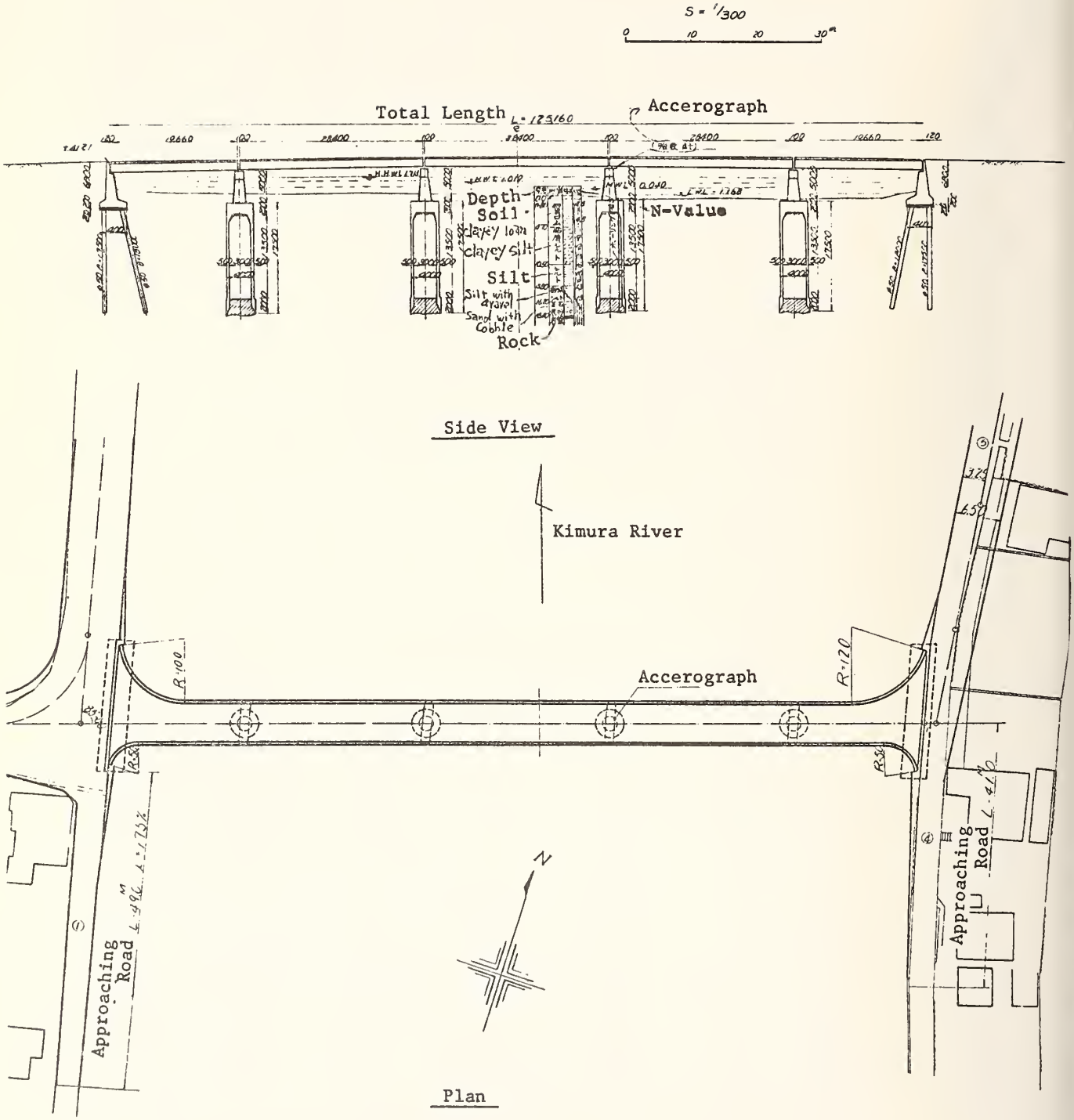

Fig. 3.46 General view of the Itajima bridge

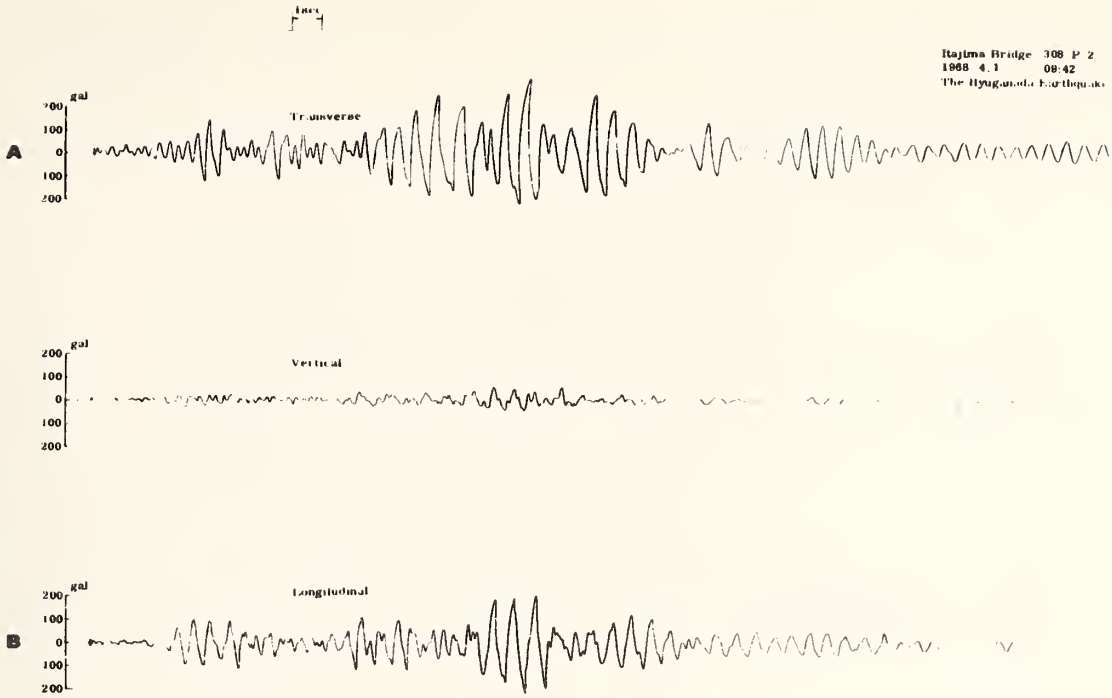

(A) at the Crest of Pier 3 (Record no. 308-P-2)

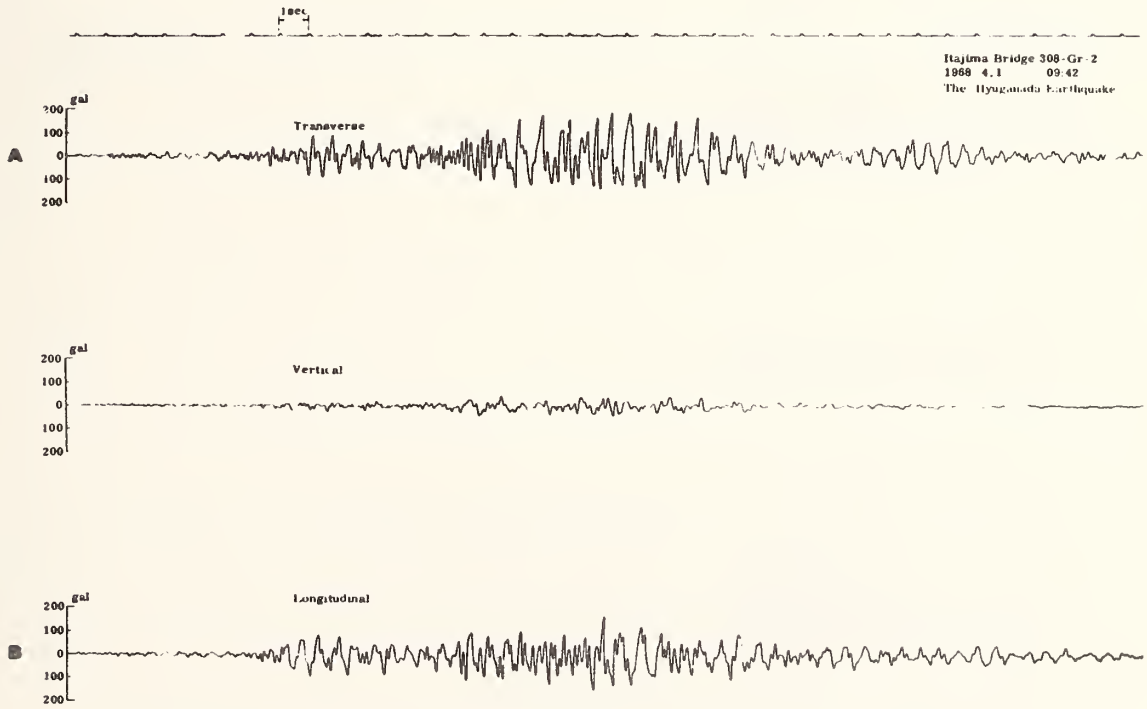

(B) On the Ground Surface nearby (Record no. 308-Gr-2)

Fig. 3.47 Acceleration records at the Itajima bridge during the Hyuganada Earthquake of April 1, 1968 [64]

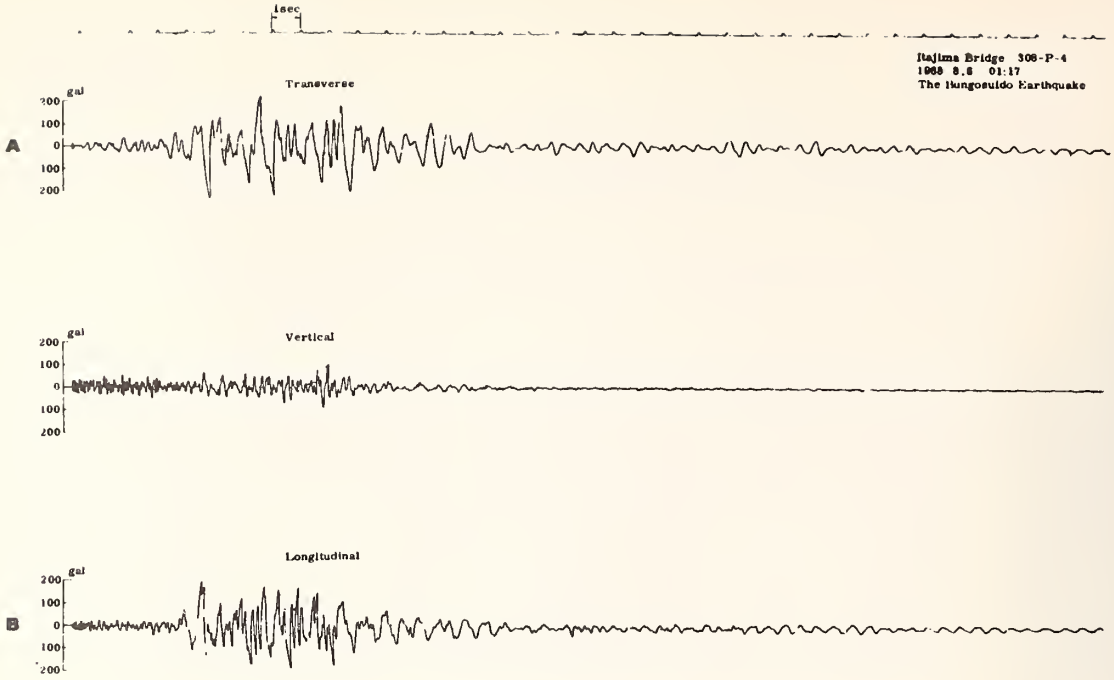

(A) At the Crest of Pier 3 (Record no. 308-P-4)

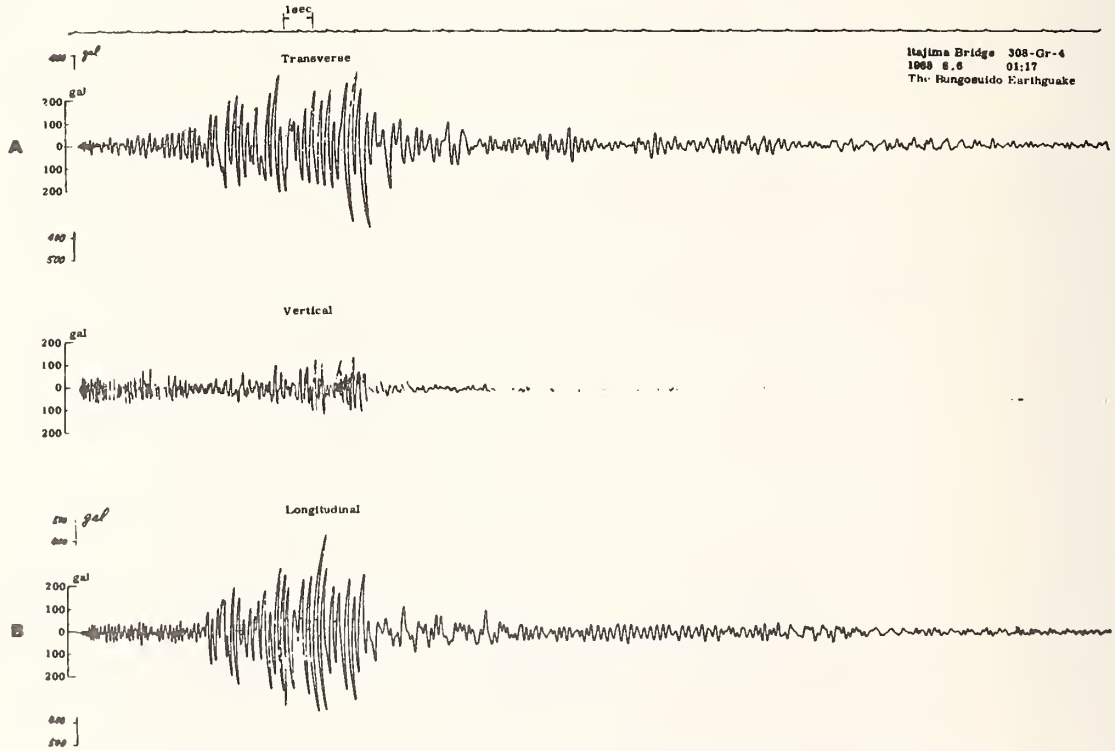

(B) On the Ground Surface nearby (Record no. 308-Gr-4)

Fig. 3.48 Acceleration records at the Itajima bridge during the Bungosuido Earthquake of August 6, 1968 [64]

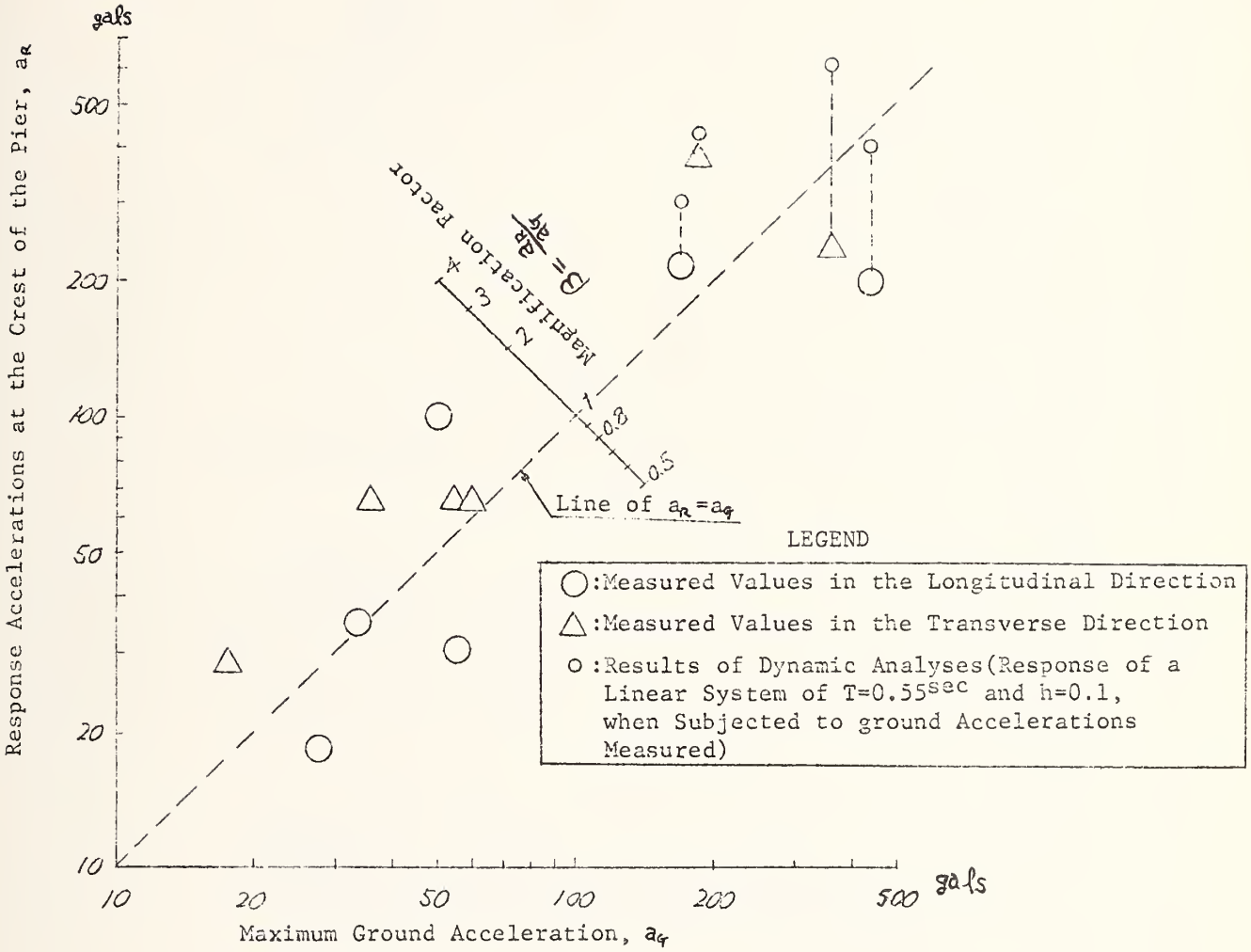

Fig. 3.49 Results of measurements and dynamic analyses at the Itajima bridge.

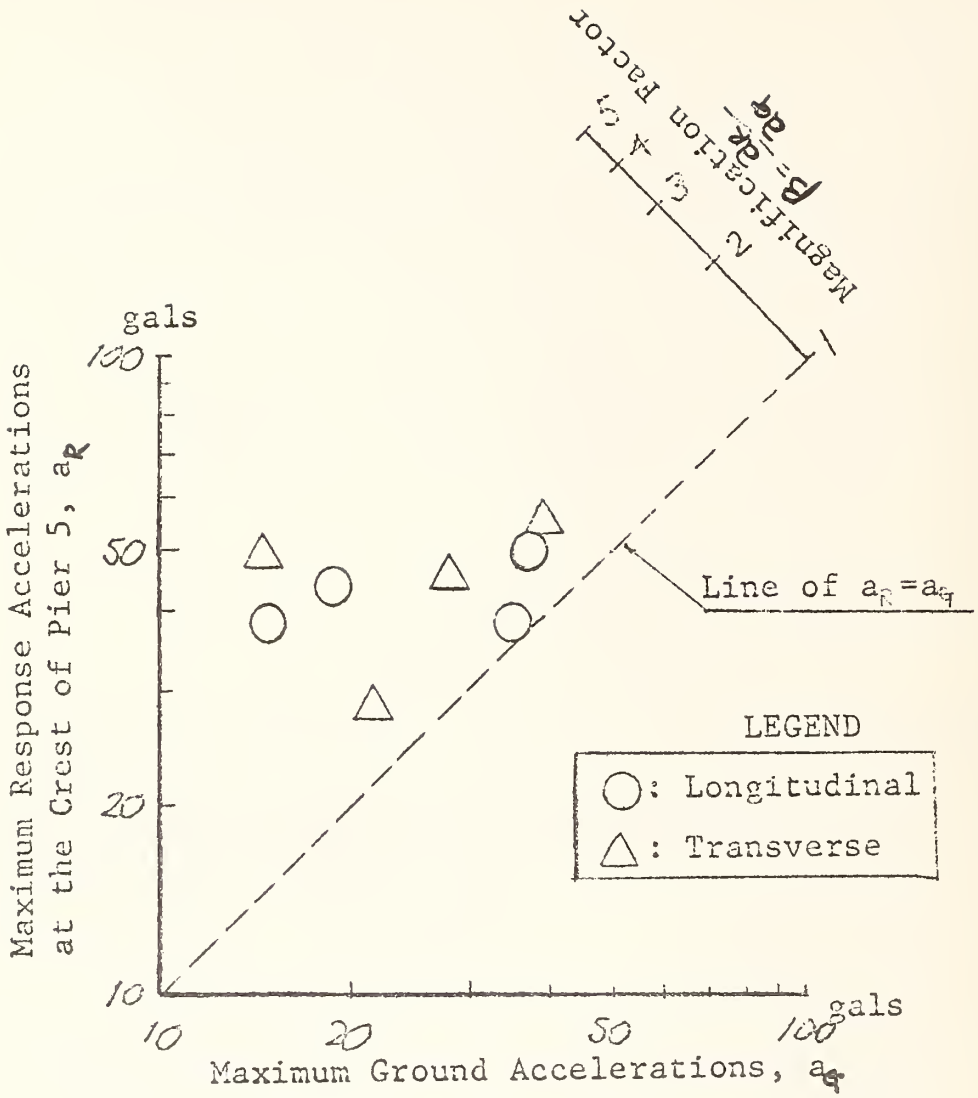

Fig. 3.50 Results of earthquake measurements at the Shinkatsushika bridge.

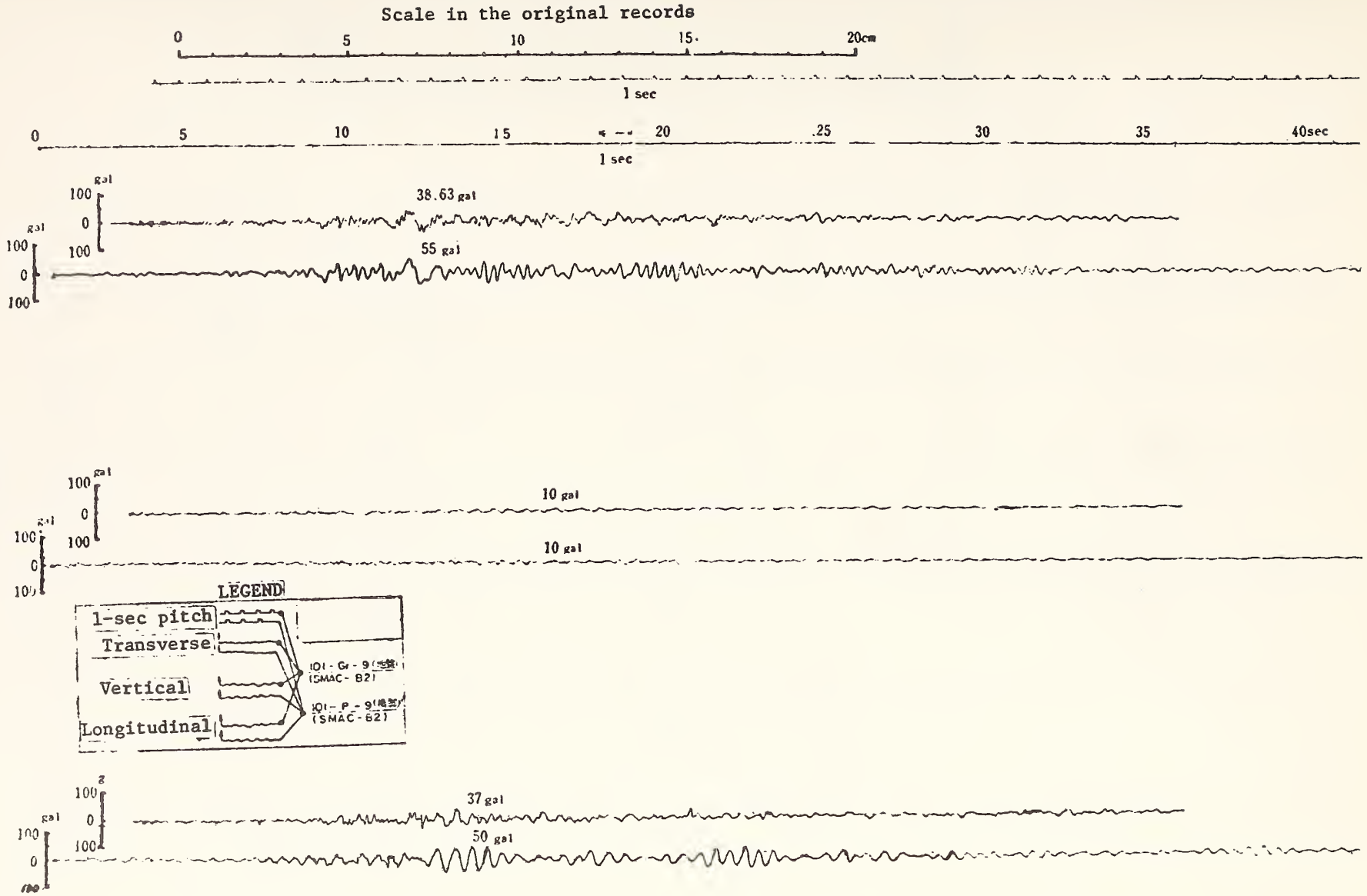

Fig. 3.51 Acceleration records at the Shinkatsushika bridge during the Higashi-Matsuyama Earthquake of July 1, 1968 (recorded by strong-motion accelerographs on the ground surface and at the crest of pier 5)

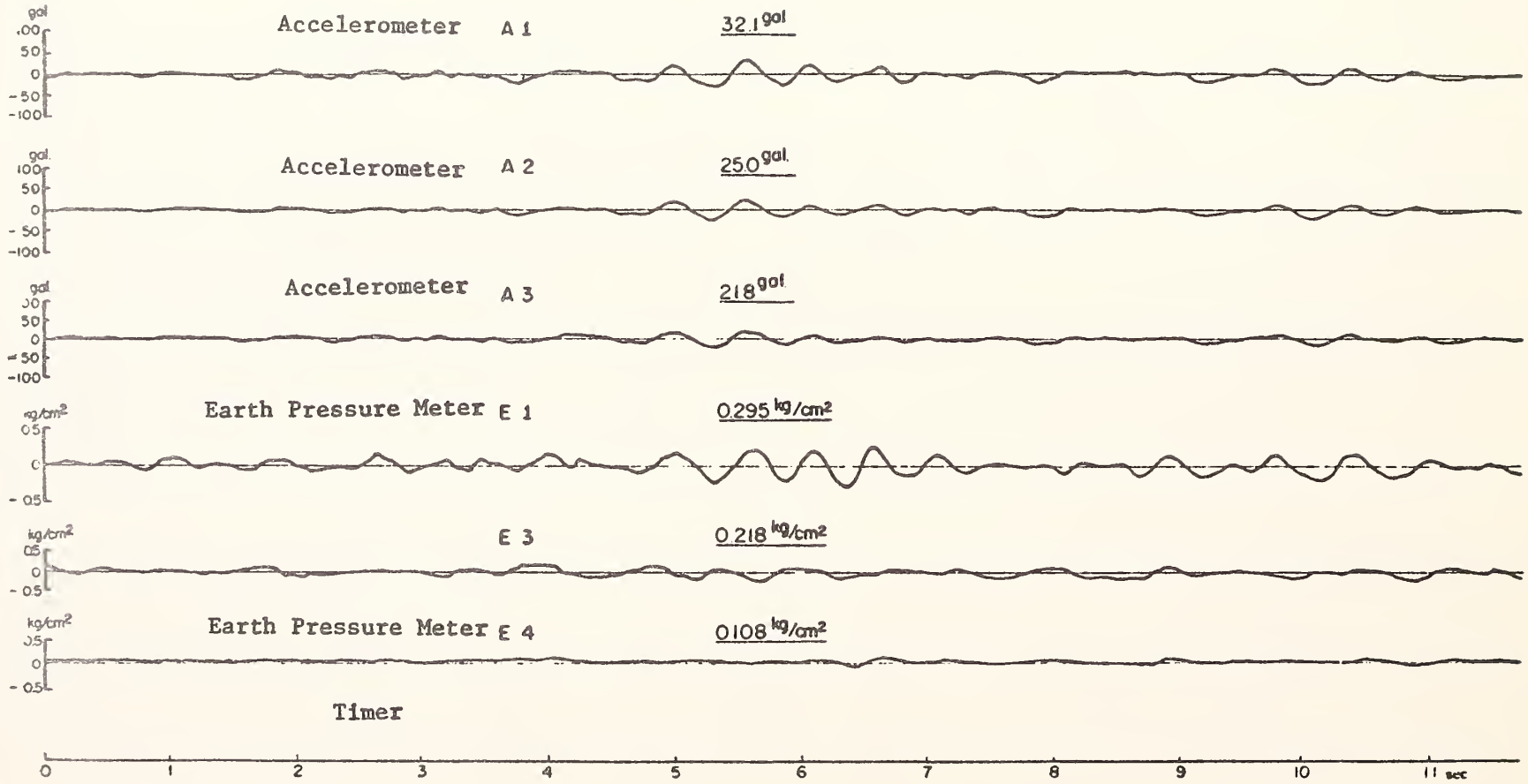

Fig. 3.52 Earthquake records at the Shinkatsushika bridge during the Higashi-Matsuyama Earthquake of July 1, 1968 (records of accelerations and earth pressures at the foundation of pier 5)

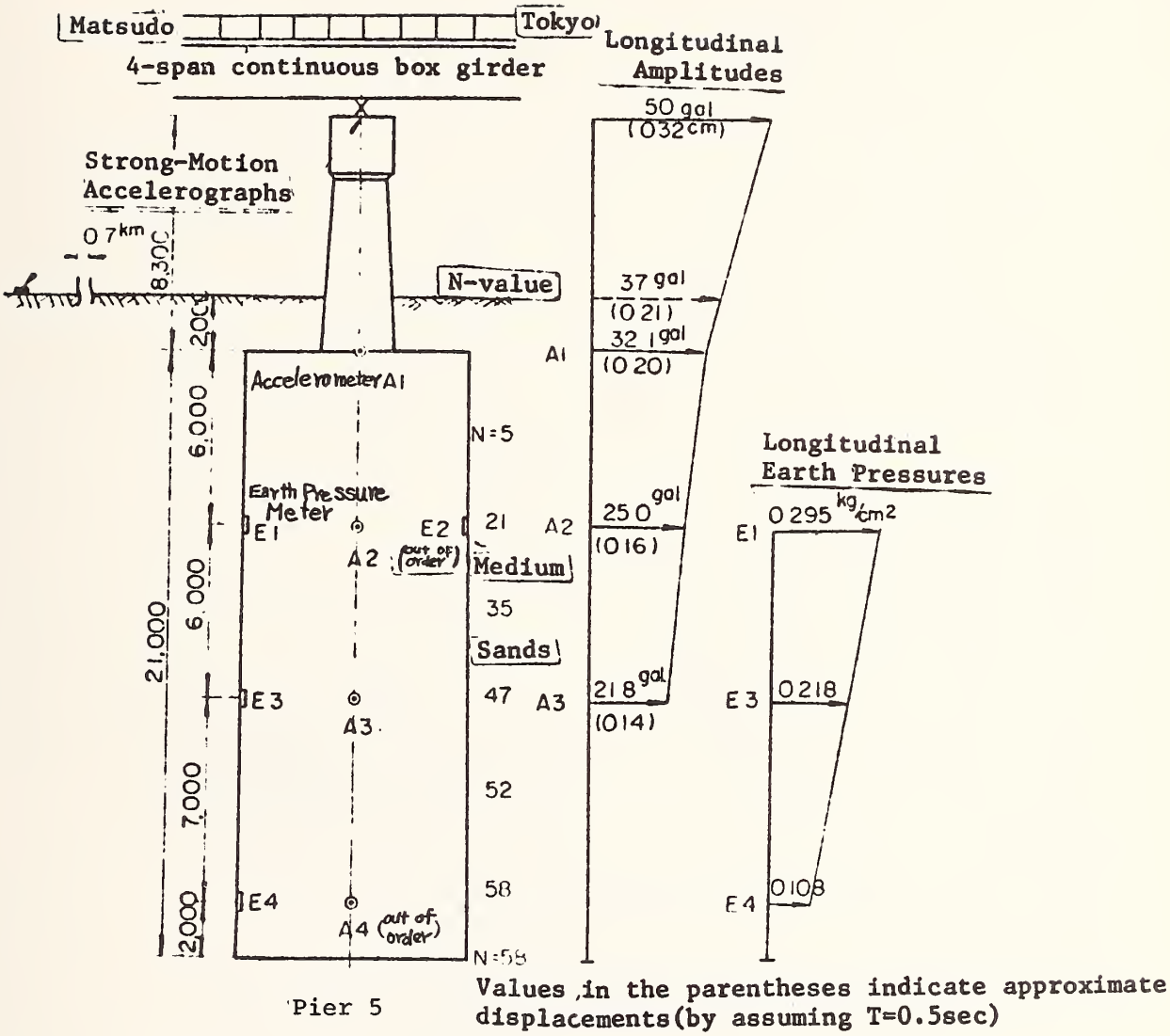

Fig. 3.53 Results of earthquake measurements at the Shinkatsushika bridge during the Higashi-Matsuyama Earthquake of July 1, 1968.

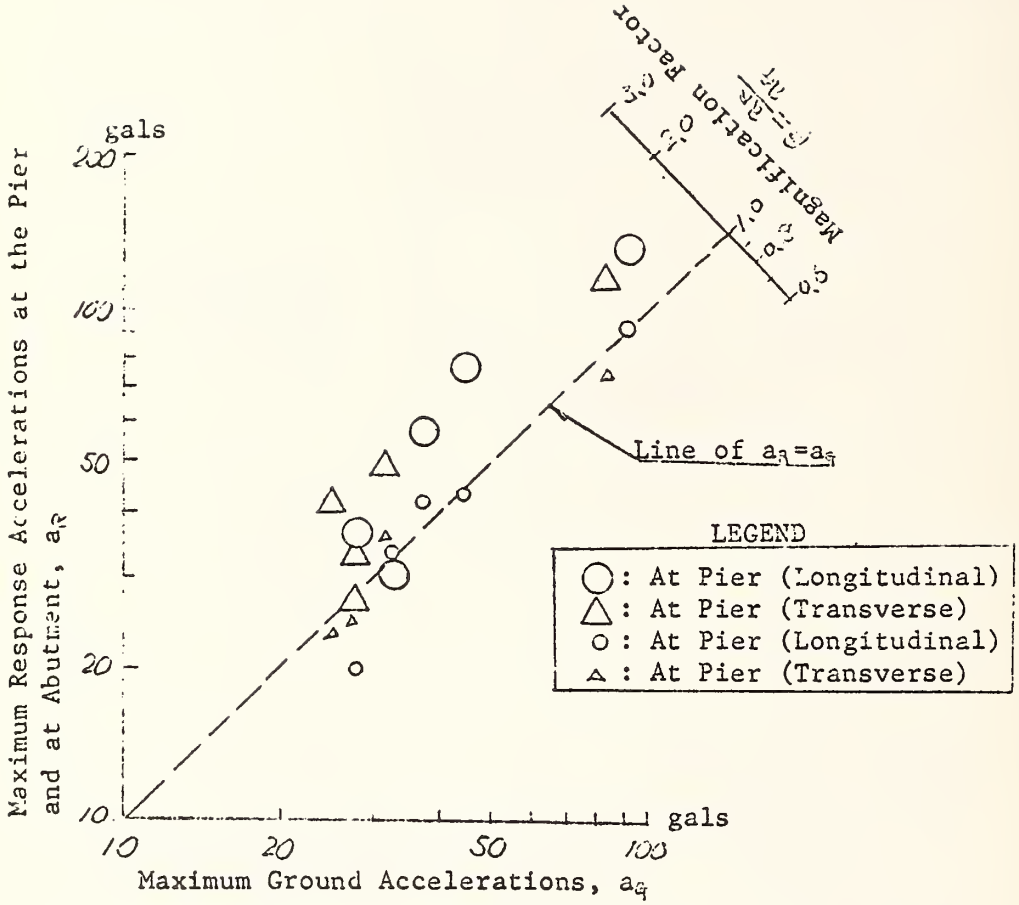

Fig. 3.54 Results of earthquake measurements at the Chiyoda bridge

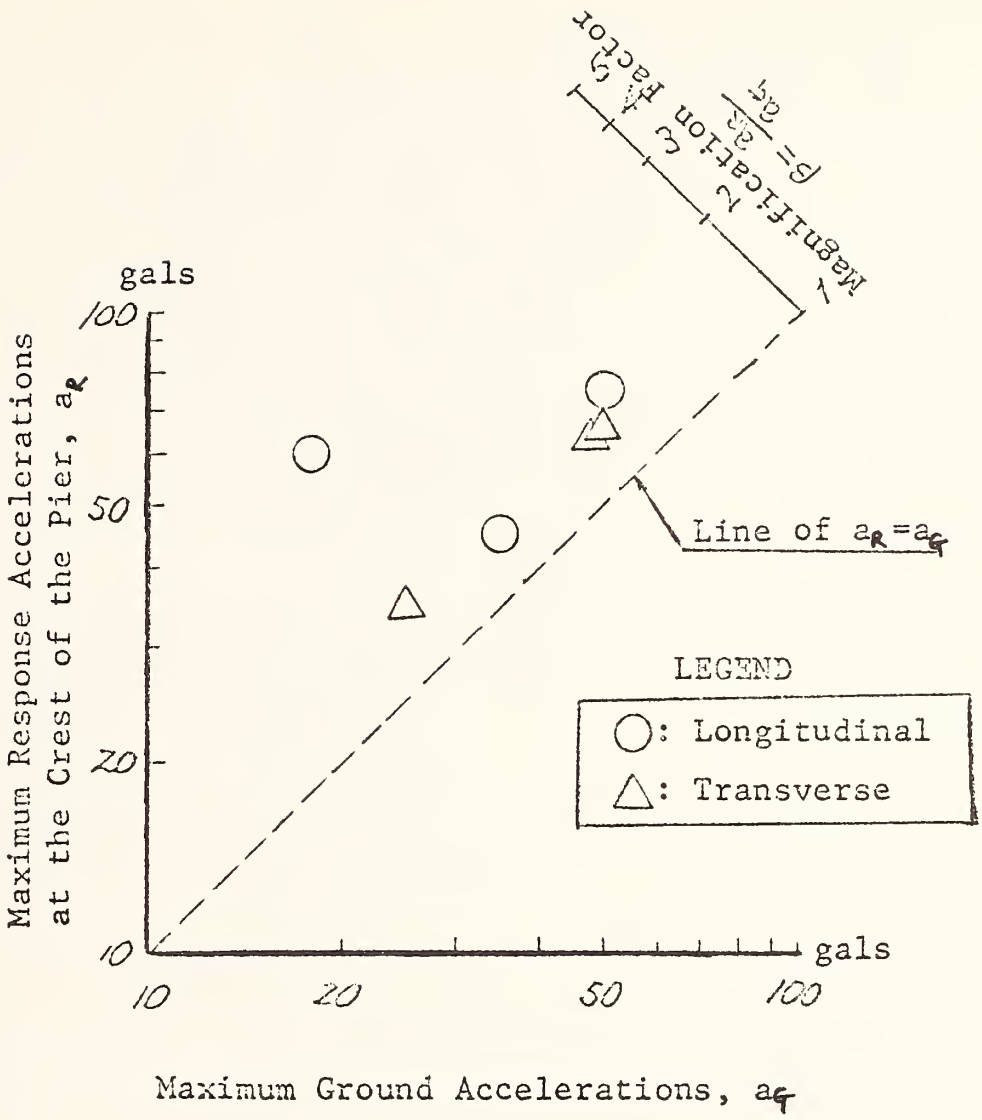

Fig. 3.55 Results of earthquake measurements at the Hinai bridge

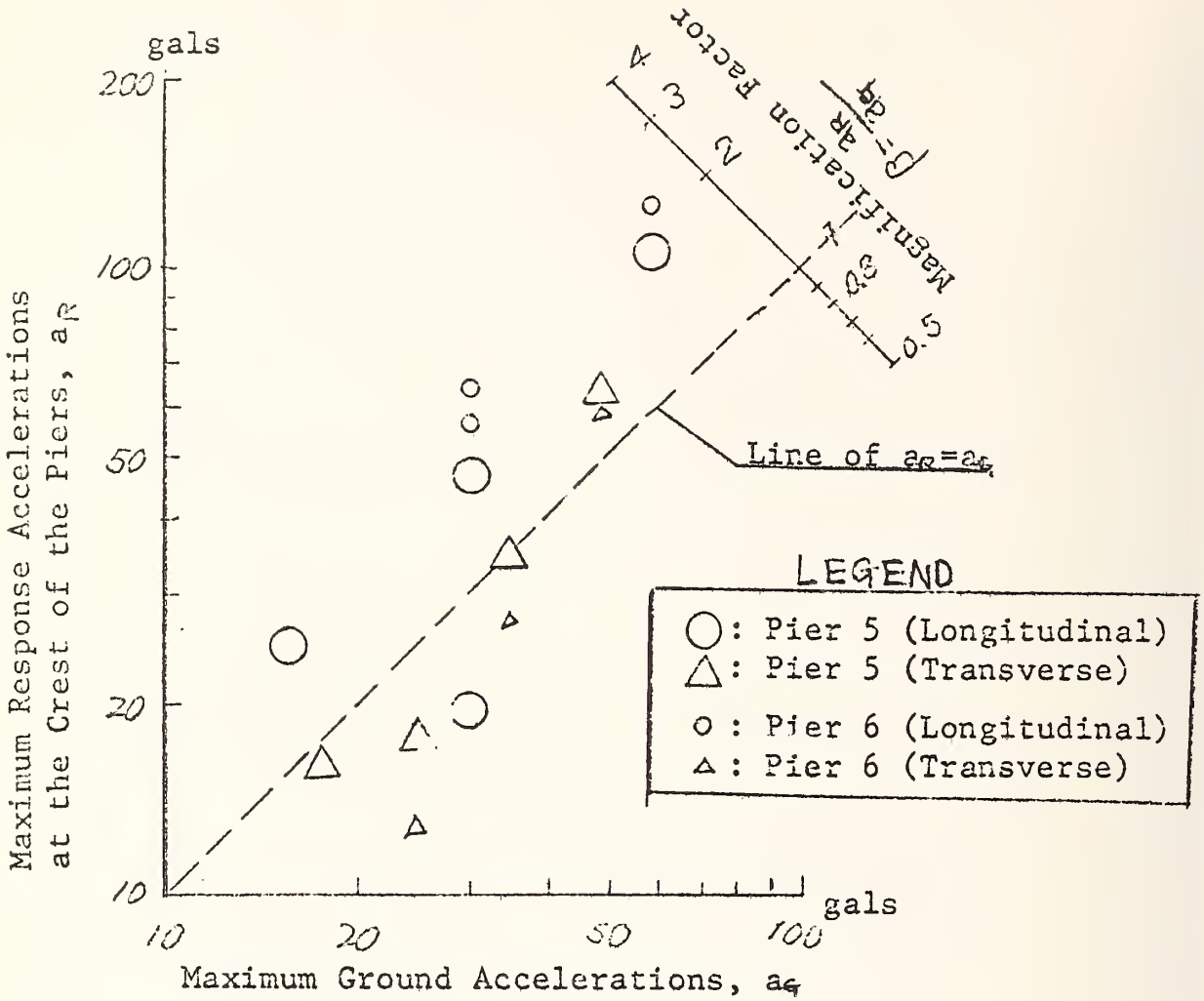

Fig. 3.56 Results of earthquake measurements at the Soka viaduct

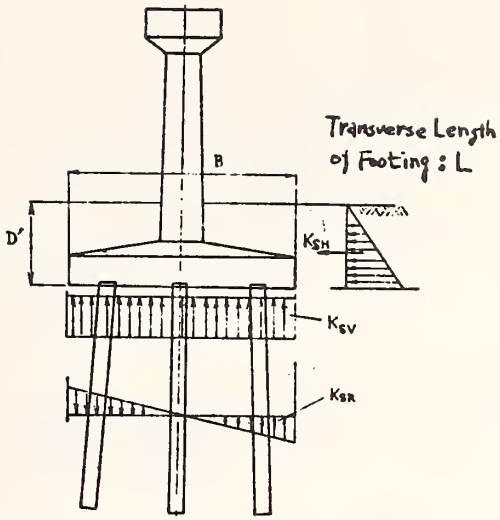

Fig. 3.57 General bridge substructure with pile foundation

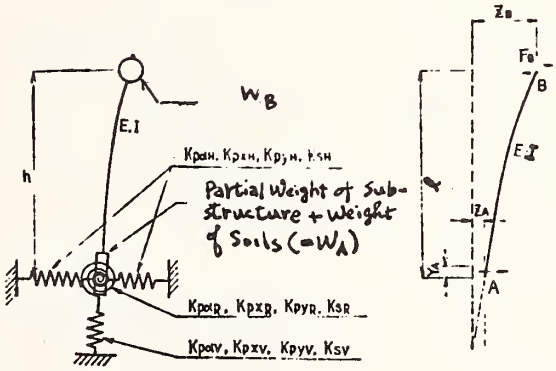

W_B = Weight of superstr. + partial weight of substructure.

Fig. 3.58 Analytical model for bridge substructure with pile foundation

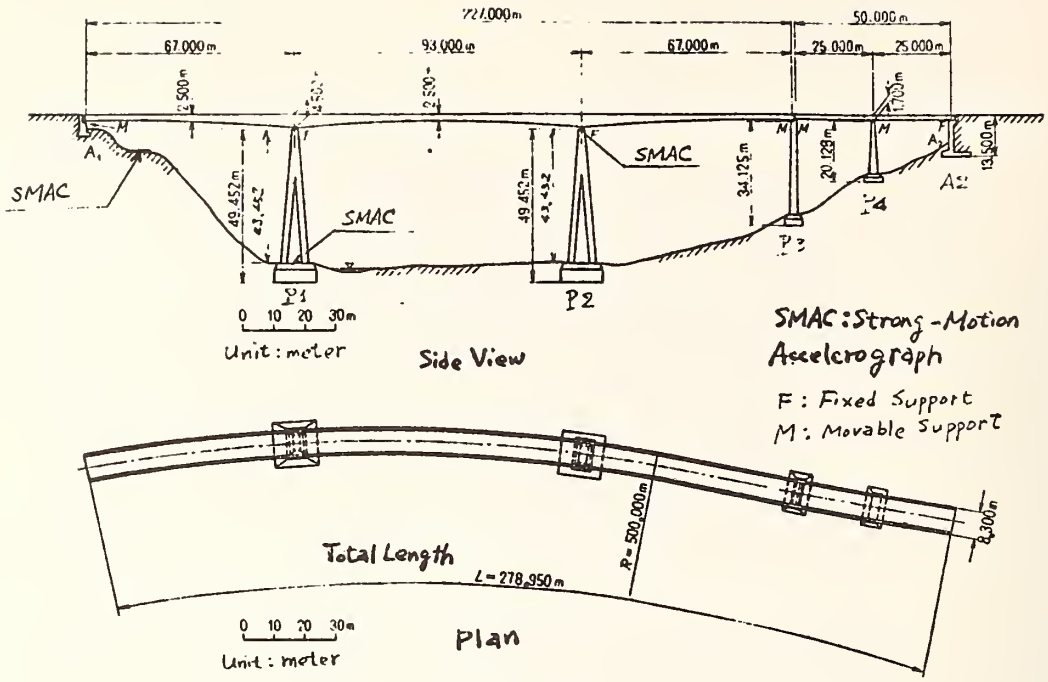

Fig. 3.59 General view of the Yoneyama bridge

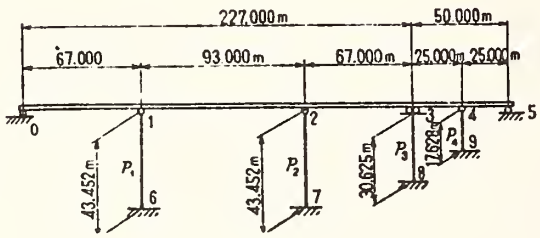

Fig. 3.60 Analytical model for the Yoneyama bridge

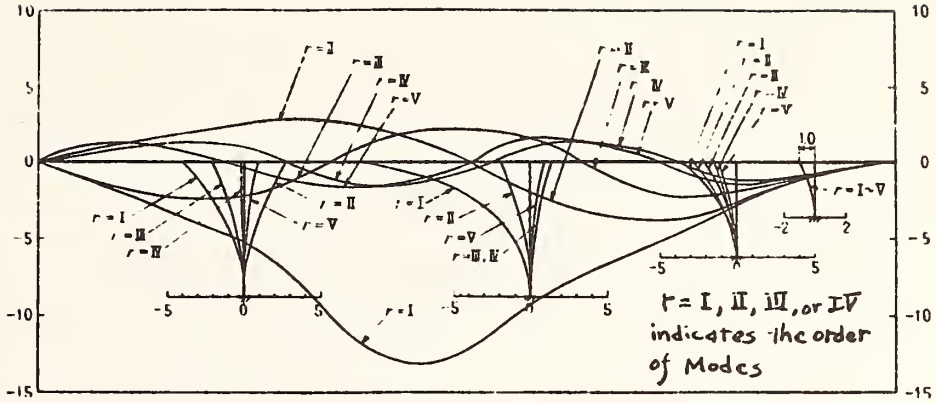

Fig. 3.61 Results of dynamic analysis - 1st to 4th mode shapes of the Yoneyama bridge in the transverse direction

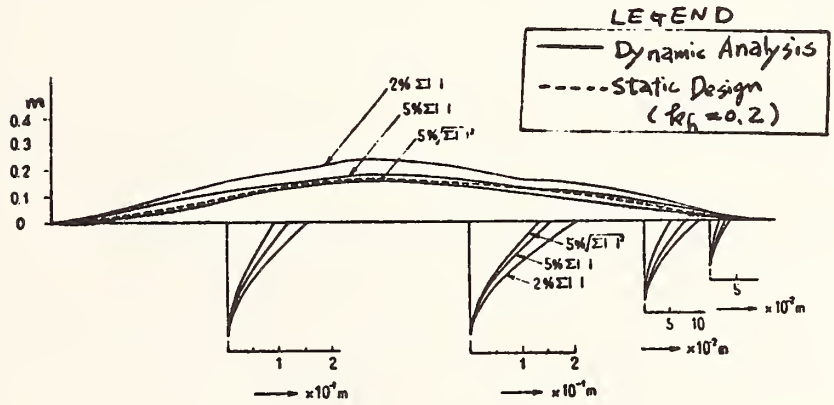

Fig. 3.62 Results of dynamic analysis - displacement

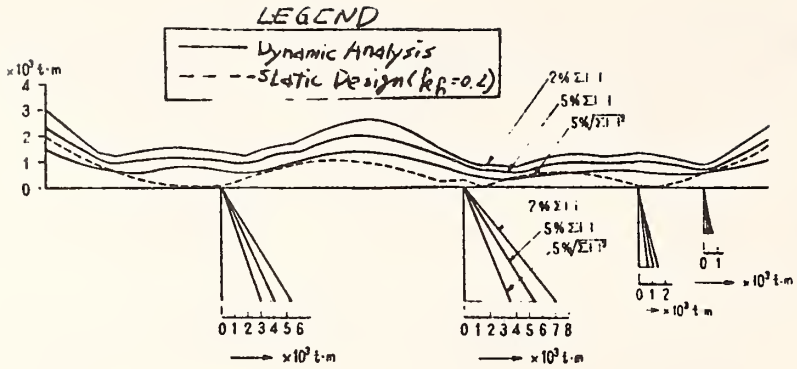

Fig. 3.63 Results of dynamic analysis - bending moment

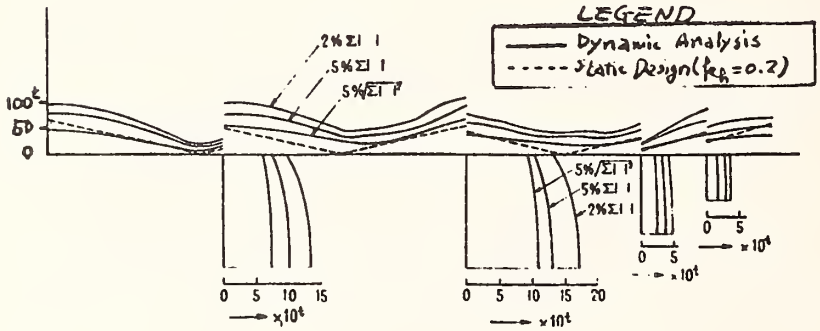

Fig. 3.64 Results of dynamic analysis - shearing force

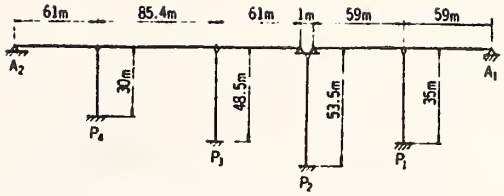

Fig. 3.65 Analytical model for the Sokozawa bridge (T. Suruga, et. al [114])

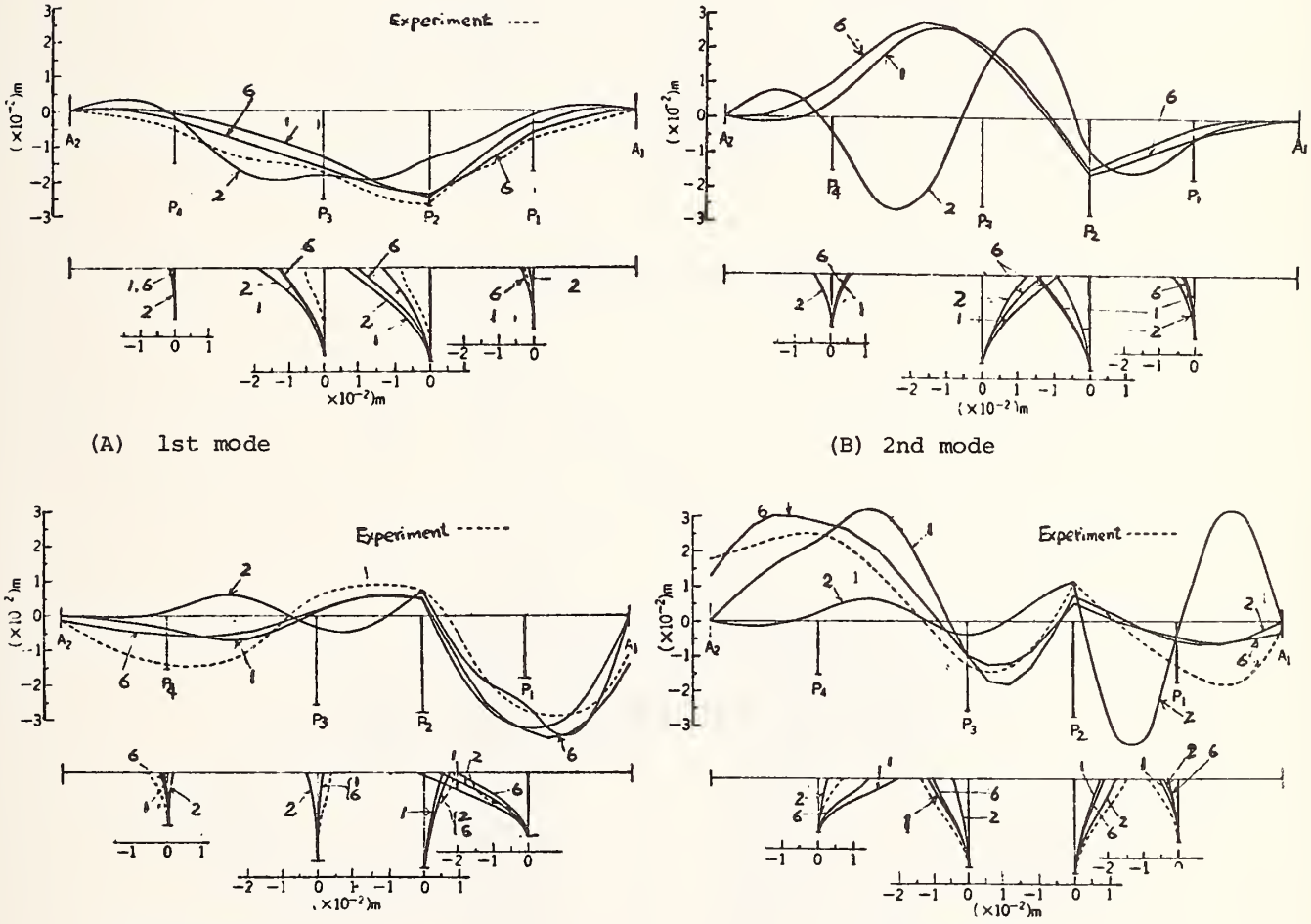

(A) 1st mode

(B) 2nd mode

(C) 3rd mode

(D) 4th mode

Note: numbers 1 to 6 indicate case numbers,cf.Table 3.12

Fig. 3.66 Comparison of mode shapes by analysis and by experiment for the Sokozawa bridge (after T. Suruga, et. al [114])

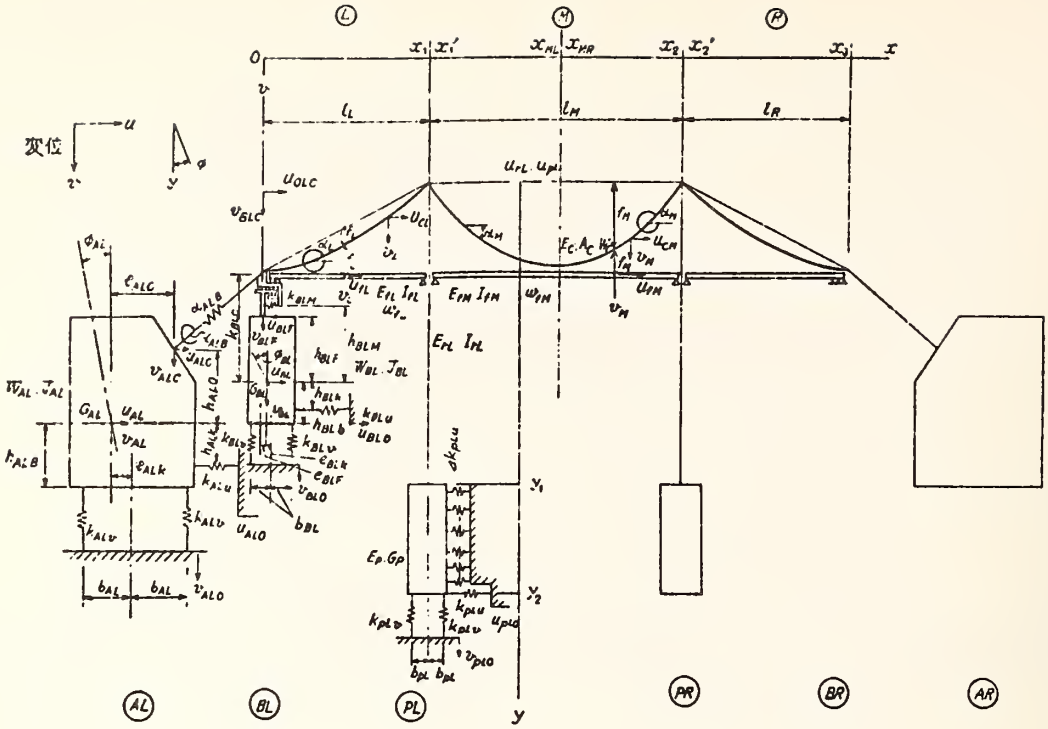

Fig. 3.67 Coordinates of a suspension bridge

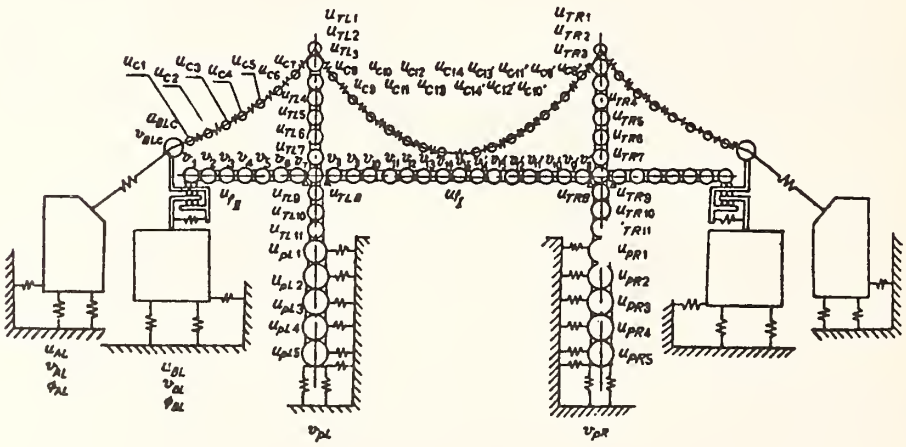

Fig. 3.68 An analytical model for dynamic analysis

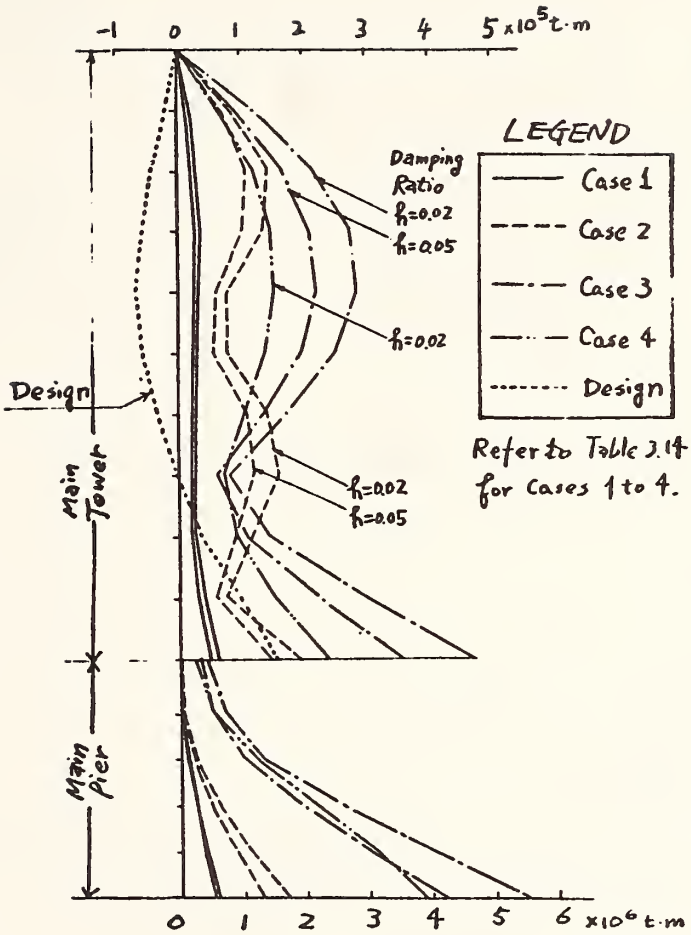

Fig. 3.69 Maximum bending moments for the main tower including pier in the longitudinal direction

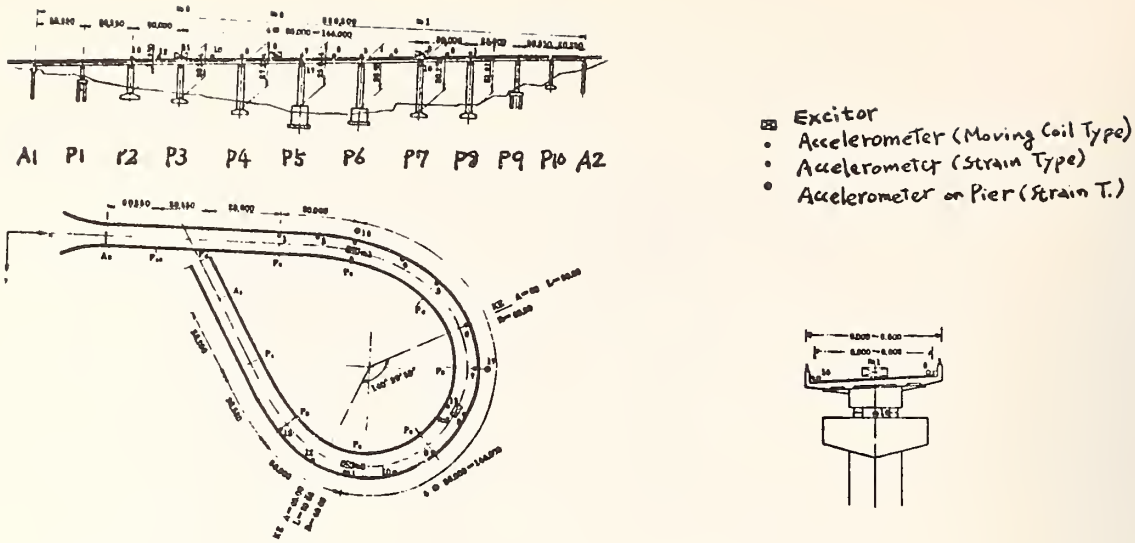

Fig. 3.70 General view of the Otani interchange bridge (after S. Yamaguchi, et al [115])

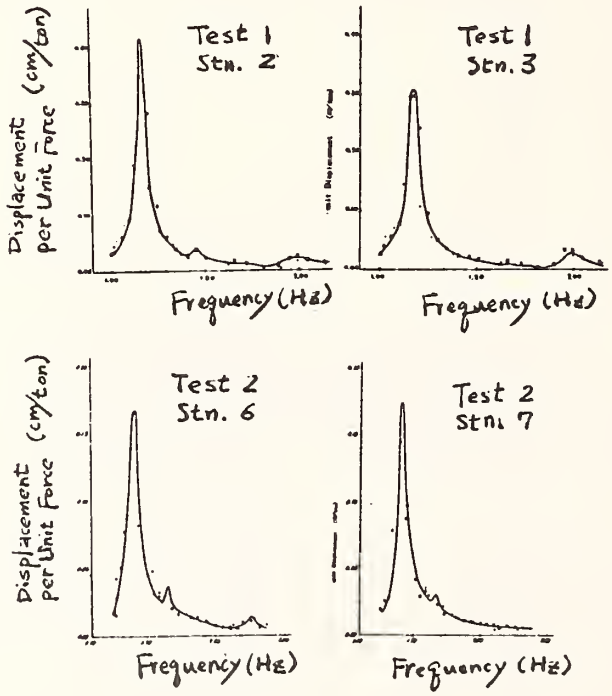

Fig. 3.71 Resonance curves for the overall bridge structure of the Otani interchange bridge (after S. Yamaguchi, et al [115])

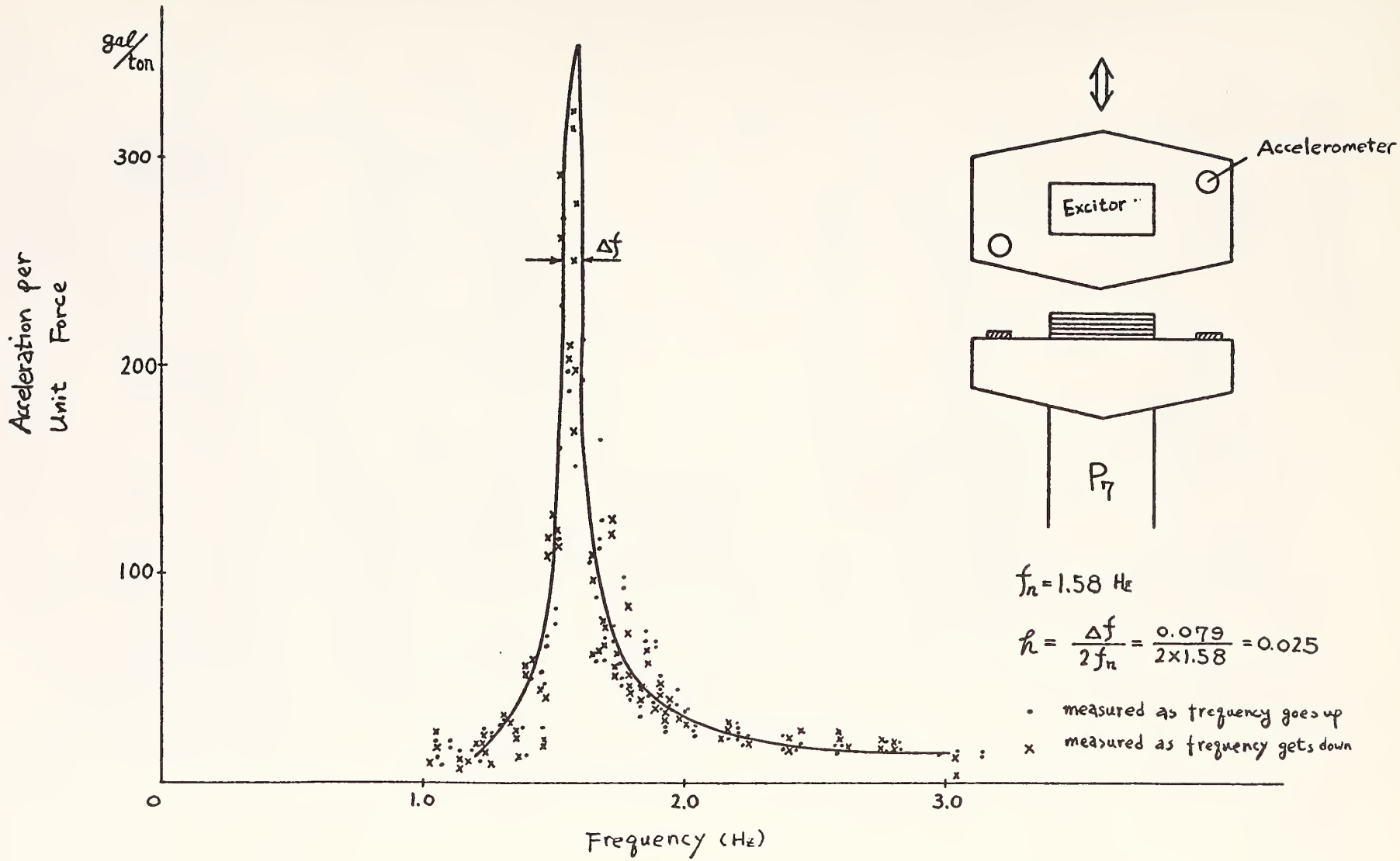

Fig. 3.72 Resonance curve for pier 7 of the Otani interchange bridge (after S. Yamaguchi, et al [115])

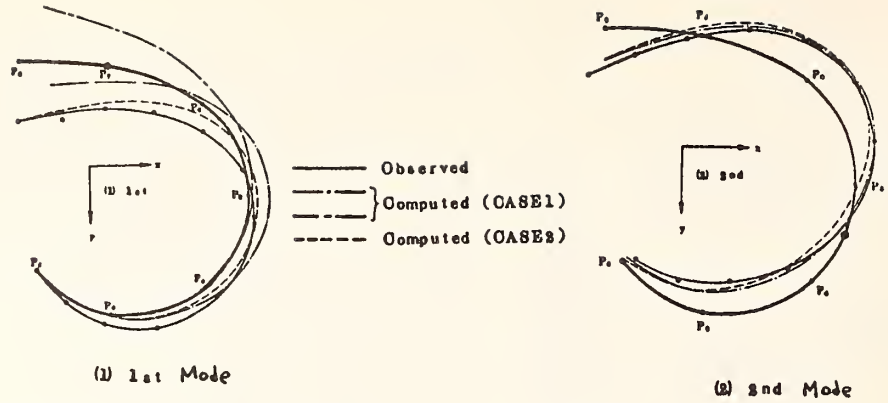

Fig. 3.73 1st to 3rd modes of the Otani interchange bridge - observed and computed (after S. Yamaguchi, et al [115])

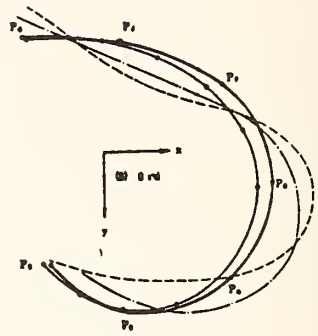

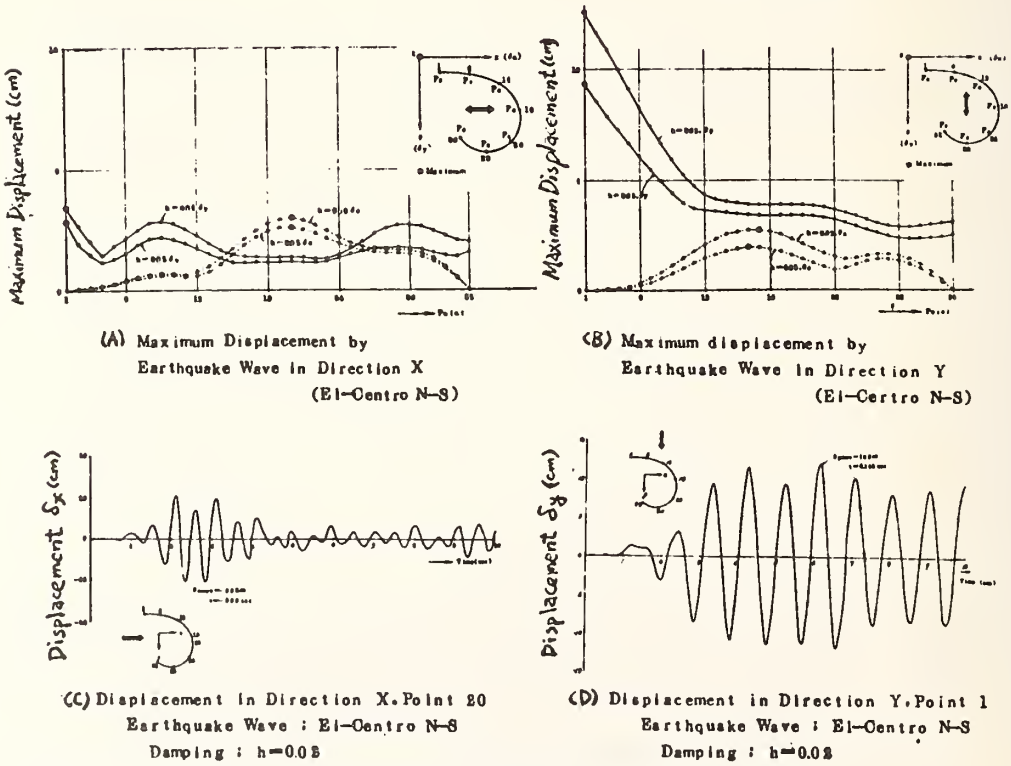

(A) Maximum Displacement by Earthquake Wave in Direction X (El-Centro N-S)

(B) Maximum displacement by Earthquake Wave in Direction Y (El-Centro N-S)

(C) Displacement in Direction X. Point 20 Earthquake Wave : El-Centro N-S Damping : h=0.03

(D) Displacement in Direction Y. Point 1 Earthquake Wave : El-Centro N-S Damping : h=0.03

Fig. 3.74 Results of dynamic analysis for the Otani interchange bridge (after S. Yamaguchi, et al [115])

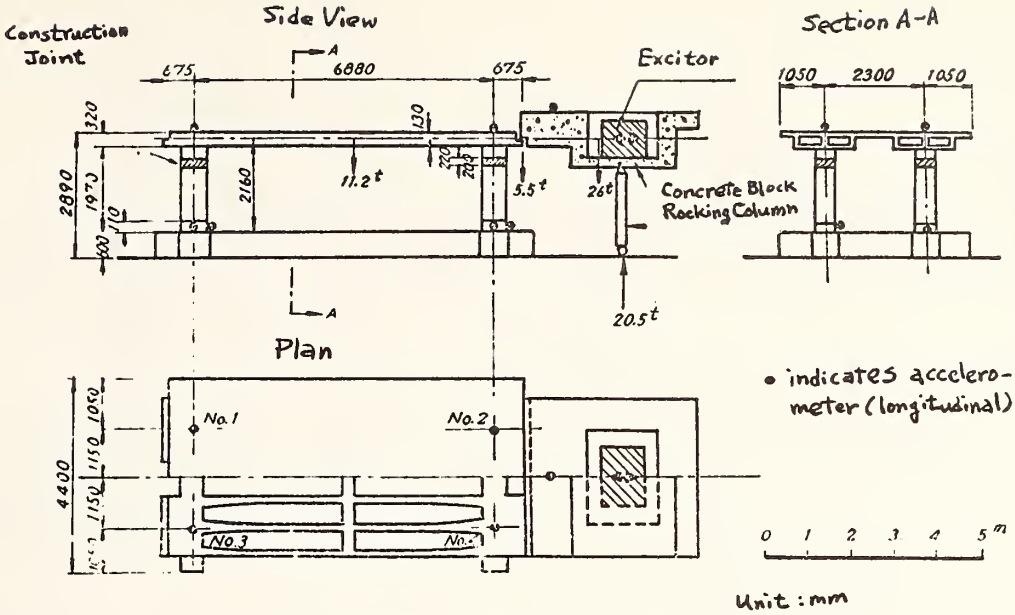

Fig. 3.75 Model I for dynamic tests of a viaduct (after E. Kuribayashi, et al [128])

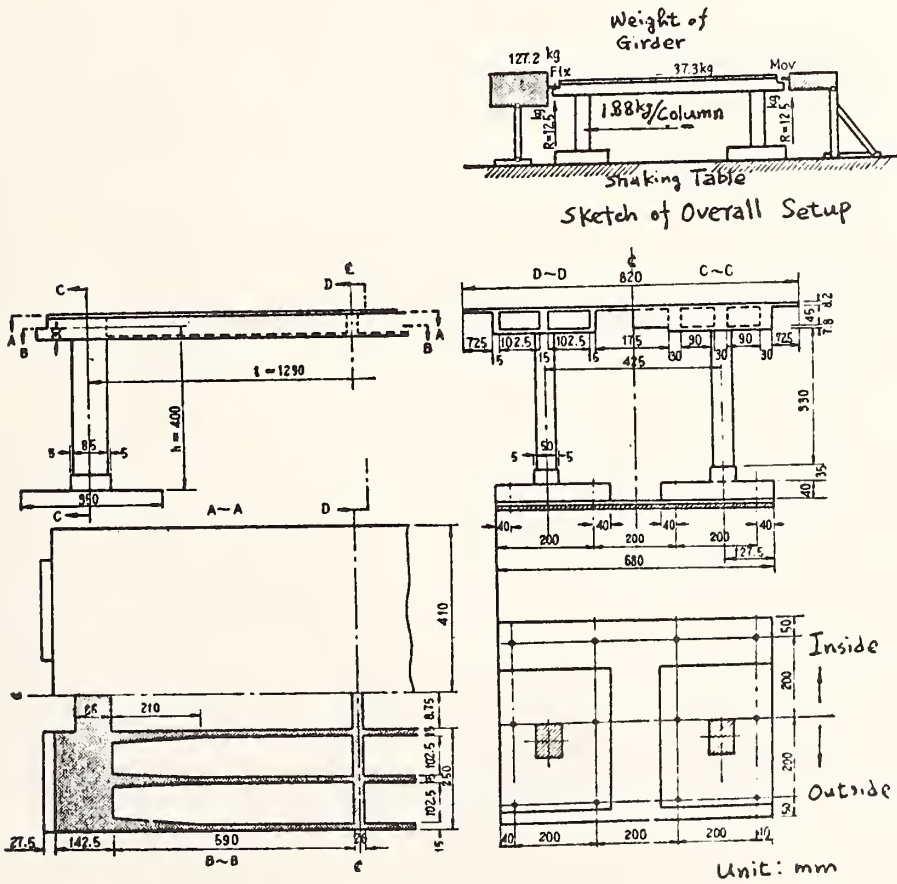

Fig. 3.76 Model II for dynamic tests of a viaduct (after E. Kuribayashi, et al [128])

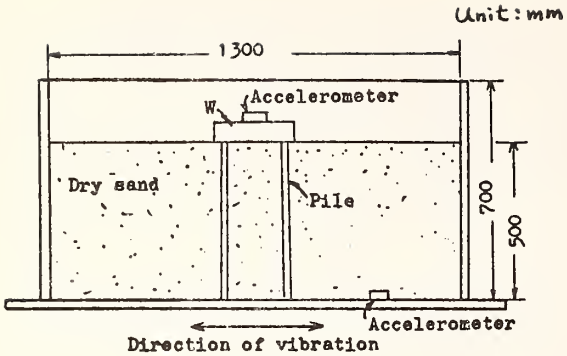

Fig. 3.77 Setup of a dynamic test for seismic effects of pile foundation. (N. Ogata, S. Kotsubo [129])

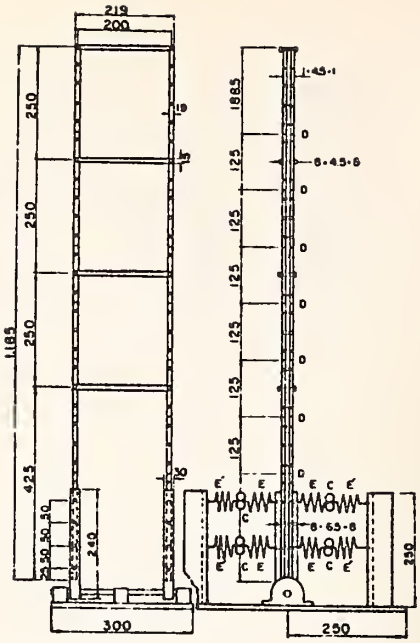

Fig. 3.78 A model of tower-pier system for suspension bridges (I. Konishi, et al. [130])

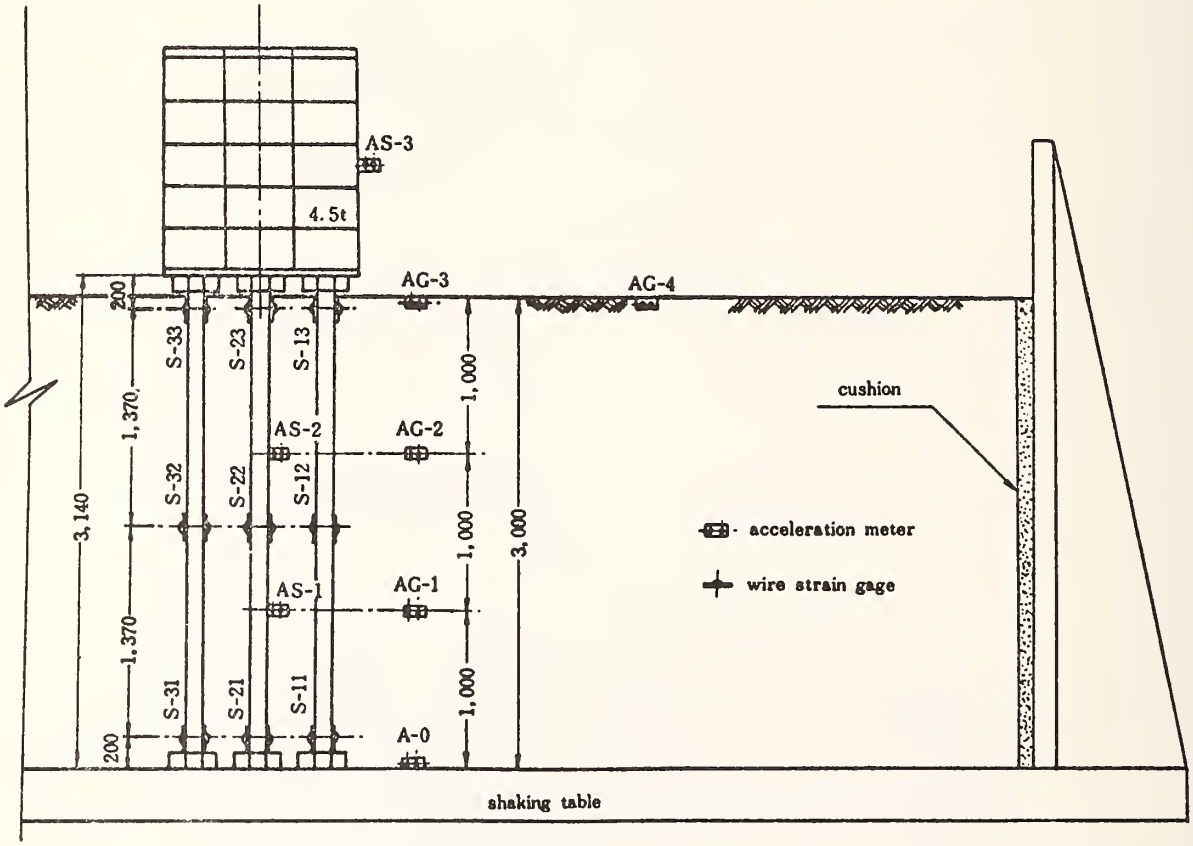

Fig. 3.79 Sketch of a model structure supported on piles for dynamic tests (after K. Kubo [131])

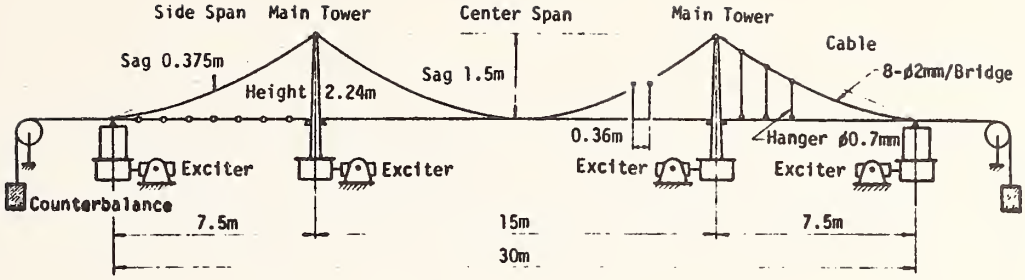

Fig. 3.80 General view of a model for a suspension bridge subjected to earthquake excitation (E. Kuribayashi, et al [132])

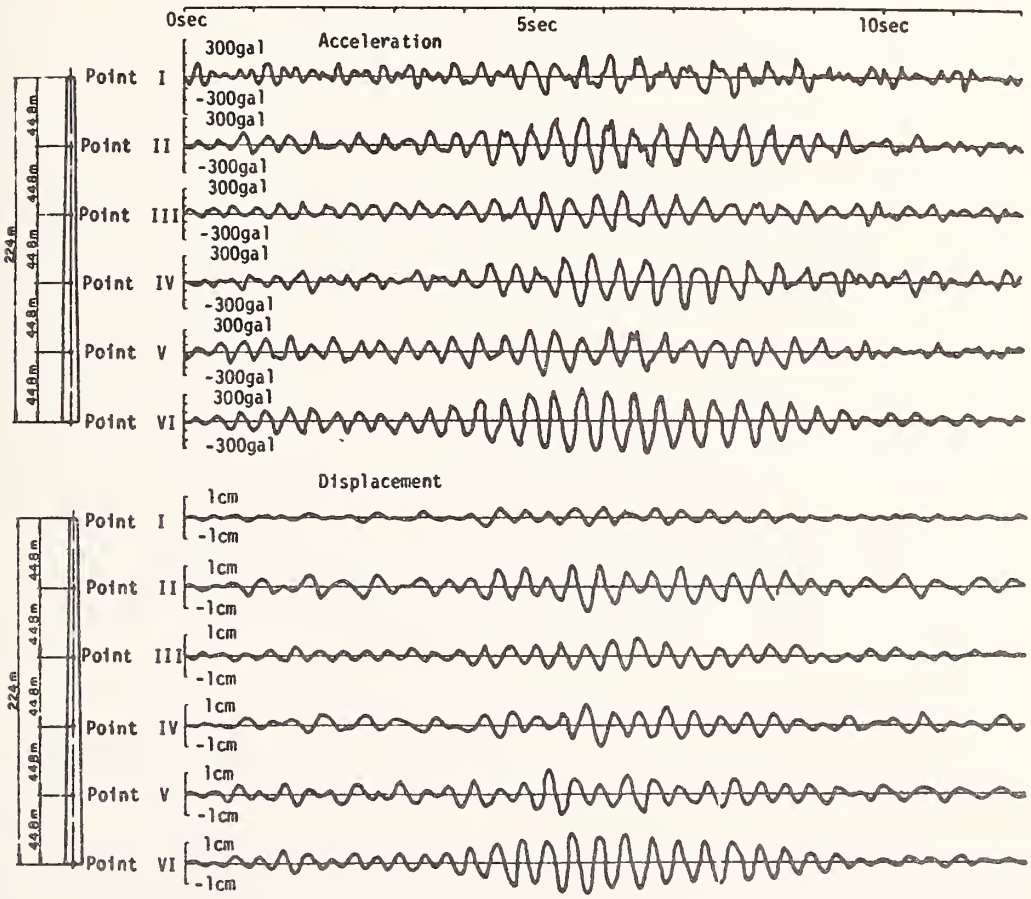

Fig. 3.81 Records of model response to the Kushiro Earthquake ground motion, E-W component (after E. Kuribayashi, et al. [132])

IV EARTHQUAKE-RESISTANT DESIGN CRITERIA

From the previous chapters, it is quite evident that Japan has been the world's leading country in its efforts to understand the dynamic response characteristics of bridge structures during strong-motion earthquakes. It is understandable, therefore, that this country would make similar efforts to develop rational design criteria specifically for earthquake-resistant bridges. Because of this advanced state, this chapter is devoted primarily to a presentation of current Japanese bridge design criteria. Earthquake regulations for other countries are only briefly mentioned.

A. HISTORY OF EARTHQUAKE-RESISTANT DESIGN CRITERIA IN JAPAN

During the 1923 Kanto earthquake several highway bridges sustained substantial damage. As a result of this experience, the Ministry of Home Affairs put into effect in 1926 "Specifications for Design of Roads" which formed a part of "Road Laws". These specifications required, for the first time, that seismic forces be taken into account in the design of highway bridges. To be more specific, these specifications had the provision that highway bridges shall be designed in accordance with the static seismic coefficient method using coefficients ranging from 0.1 to 0.4. The specific value of coefficient to be used depended upon location of bridge site and ground conditions at the site. For bridges to be constructed in Tokyo and Yokohama where bridges suffered damage during the Kanto earthquake, seismic coefficients of 0.3 or more were recommended.

In 1939, the Ministry of Home Affairs issued "Specifications for Design of Steel Highway Bridges" which replaced the earlier specifications. These specifications stipulated that seismic forces should be taken into account using the seismic coefficient method. A horizontal coefficient of 0.2 and a vertical coefficient of 0.1 were to be applied simultaneously. These specifications were revised in 1964 by the Japan Road Association along with a commission from the Ministry of Construction. The revised specifications

required that a horizontal coefficient of 0.1 to 0.35, depending on site location and soil conditions, and a vertical coefficient of 0.1 be considered simultaneously in the design.

In view of later technological advances in bridge and earthquake engineering, the Japan Road Association in 1971, again with a commission from the Ministry of Construction, prepared the current specifications which are used exclusively for earthquake-resistant design of highway bridges. In these specifications, two methods are provided for seismic design. One is the conventional seismic coefficient method to be used for rigid structures with coefficients ranging between 0.1 and 0.24 depending on site location, ground conditions, and importance. The other method is a modified seismic coefficient method to be used for relatively flexible structures. This method applies a horizontal seismic coefficient ranging from 0.05 to 0.30 depending upon the fundamental natural period of vibration in addition to the above mentioned three factors.

Specifications for seismic design of highway bridges have been tentatively proposed during the period 1966-1967, by the Japan Highway Public Corporation (JHPC), the Tokyo Expressway Public Corporation (TEPC), the Hanshin Expressway Public Corporation (HEPC), and the Honshu-Shikoku Bridge Authority (HSBA) for bridges under their administrative control. In addition, the Japanese National Railways stipulated its own design criteria for railway bridges in 1968.

The above mentioned brief history of seismic design loads for highway bridges in Japan is summarized in Table 4.1. Table 4.2 gives brief information on certain technical fields of the highway administrations and research in Japan. It should be noted that the information provided in Table 4.2 is not official; therefore, it may not be correct in every respect at the time of this writing.

B. EARTHQUAKE-RESISTANT DESIGN CRITERIA JRA-1971 [22]

Since 1956, the earthquake-resistant design of highway bridges has been conducted in accordance with the provisions of Section 13 (Section 2.9 in the English version) of "Specifications for Design of Steel Highway Bridges"

which were issued originally in 1956 by the Japan Road Association and revised in 1964 [4]. The English version of these specifications was issued in 1968. Section 13 contains the following provisions: 1) the horizontal design seismic coefficient shall be determined in accordance with Table 4.3, 2) the vertical design seismic coefficient shall be taken as 0.10, and 3) increases in allowable stresses for seismic forces alone or for dead loads plus seismic loads shall be taken as 70 percent for steel structures and 50 percent for concrete and reinforced concrete structures.

Since the provisions of Section 13 were not sufficiently comprehensive, it was found necessary to draw up new detailed specifications to be used exclusively for seismic design of highway bridges. As a result, the current "Specifications for Earthquake-Resistant Design of Highway Bridges" were issued in January 1971 by the Japan Road Association. These specifications apply to the design of bridges with spans not exceeding 200 meters to be constructed on expressways, national highways, prefectural highways and principal municipal highways. The specifications stipulate the use of seismic coefficient methods and provide two methods for determining the seismic coefficients. One is the conventional method which applies to the design of relatively rigid structures. The other is a modified coefficient method to be applied to relatively flexible structures. The main features of these specifications are the following (See Appendices B and C for detailed specifications):

(1) The horizontal design seismic coefficient for a rigid structure depends on geographical location, ground conditions at the site, and the importance of the bridge. The horizontal design coefficient for a flexible structure depends on its fundamental natural period.

(a) For a rigid structure, the horizontal design seismic coefficient (k_h) shall be determined by the relation

$$k_h = v_1 \, v_2 \, v_3 \, k_0 \tag{13}$$

where

k_0: standard horizontal design seismic coefficient is equal to 0.20

v_1: seismic zone factor

v_2: ground condition factor

v_3: importance factor

The values of v_1, v_2, and v_3 are shown in Tables 4.4, 4.5, and 4.6, respectively. The definitions of the classifications are given in the specifications. The minimum value of k_h shall be considered as 0.10.

(b) For a relatively flexible structure, the modified seismic coefficient method shall be used. Bridge structures with pier heights greater than 25 m, or with fundamental periods longer than 0.5 seconds fall into this classification. The horizontal design seismic coefficient (k_{hm}) shall be determined by

$$k_{hm} = \beta\, k_h \tag{14}$$

where k_h is given by Eq. (13) and where β is a factor depending upon the fundamental period of the bridge, Fig. 4.1. For structures having fundamental periods less than 0.5 seconds, β may be considered as 1.0. The minimum value of k_{hm} shall be 0.05.

(2) The vertical design seismic coefficient may generally be considered as zero, except for special components such as bearing supports.

(3) The horizontal design seismic coefficient for structural components, soils, and water below ground surface may be considered as zero.

(4) Hydrodynamic pressures must be considered as given in the specifications. Earth pressures are given in related specifications.

(5) Special attention must be given to very soft soils vulnerable to liquefaction during an earthquake.

(6) Special attention must also be given to the design of structural details with full consideration given to knowledge gained in damage evaluations for previous earthquakes. Certain provisions are made for preventing bridge girders falling from their supports.

(7) When considering earthquake loading, increases in combined allowable stresses are permitted as follows:

concrete in reinforced concrete structures	:	50%
steel reinforcing in reinforced concrete structures	:	50%
structural steel for superstructures	:	70%
structural steel for substructures	:	50%
concrete compressive stresses in prestressed concrete structures	:	65%
foundation soils	:	50%

C. EARTHQUAKE-RESISTANT DESIGN CRITERIA JHPC-1970 [18]

The Japan Highway Public Corporation provided comprehensive "Specifications for Design of Highways" in January 1970 consisting of three volumes issued by the Expressway Research Foundation. Section 6.2 of Part 5, Vol. 2, gives specifications related to seismic effects which may be summarized as follows:

(1) General - The earthquake-resistant design of a highway bridge shall provide sufficient stability against seismic disturbances for the structure as a unit and also for all parts thereof including superstructures, substructures, and surrounding soils, with full consideration of topographical and geological conditions at the site.

(2) Design Seismic Coefficients - The horizontal design seismic coefficient shall be determined after considering a survey of previously experienced seismic effects on bridges, geological features, microtremor characteristics at the site, and relevant specifications for earthquake-

resistant design of engineering structures. The vertical design seismic coefficient shall generally be assumed as 0.10. The vertical and horizontal coefficients for structural portions underground and lower than 15 m above ground surface shall be the basic coefficients mentioned above.

(3) Increase in Horizontal Design Seismic Coefficient for Highrise Structures - The horizontal design seismic coefficient for structural portions above 15 m from the ground surface shall be determined by increasing the basic coefficient by 5 percent for each 5 m increase in height. The vertical coefficient does not have a corresponding increase.

For bridges having a continuous steel superstructure with a reinforced concrete slab, each span having a length in the approximate range 50 to 90 m and having either reinforced concrete or steel frame reinforced concrete substructures (solid section) should be designed with an increased seismic coefficient in the transverse direction. The horizontal design seismic coefficient for these bridges varies with height (H) of the structure above ground as follows: a) use basic coefficient for $0 < H < 15$ m, b) use 5 percent increase for each 5 m increase in height within the range $15 \leq H \leq 25$ m, c) use 14 percent increase for each 5 m increase in height within the range $25 \leq H \leq 40$ m, and d) use the same value of coefficient for $H \geq 40$ m.

The horizontal design seismic coeffocient in the longitudinal direction shall be selected in accordance with the same specifications regulating selection for the transverse direction.

It should be noted that Section 6.2, Part 5, Vol. 2, of the 1970 JHPC "Specifications for Design of Highways" became invalid upon adoption of the 1971 JRA "Specifications for Earthquake-Resistant Design of Highway Bridges".

D. SEISMIC DESIGN STANDARDS TEPC-1967 [10]

The Tokyo Expressway Public Corporation issued its own tentative standards for seismic design of bridges in July 1967. The main features of these standards are the following:

(1) Design Seismic Coefficients - These coefficients are selected in accordance with Table 4.7. Ground conditions in this table shall be decided as indicated in Table 4.8. Structures that are constructed on very soft soil and structures whose fundamental frequencies may coincide approximately with the predominant ground frequencies shall receive particular attention by conducting dynamic analyses. The parentheses in Table 4.8 denote those structures having rigid foundation depth to diameter (or the shorter length if non-circular in cross-section) ratios of 3 or less. In cases where the depth of alluvial (or loam) layer is between 0 and 3 m, and a firm layer exists below, the thin layer shall be removed before construction of the bridge. In such cases, the ground condition shall be considered as class 1.

(2) Combination of Applied Loads and Allowable Stresses - These loads and stresses as used in earthquake-resistant design are tabulated in Table 4.9. The individual loads are designated as dead loads, earth pressures, hydraulic pressures, buoyancy forces, and uplift forces. Foundations implied are spread footings, piles, and caissons. Piers denote parts of substructures above crests of foundations.

E. SEISMIC DESIGN STANDARDS HEPC-1968 [16]

The Hanshin (Osaka-Kobe) Expressway Public Corporation also has its own tentative standards for earthquake-resistant design of engineering structures to be built on its expressways. The standards issued by HEPC in December 1968 are summarized as follows:

All civil engineering structures shall generally be designed by the seismic coefficient method. The horizontal design seismic coefficient (k_h) shall be determined by the relation

$$k_h = m\, k_0 \tag{15}$$

where k_0 is the basic seismic coefficient equal to 0.20 and m is a

modification factor dependent upon depth of embedment of foundation and upon the average N value (N = no. of blows of standard penetration test) obtained for the site, see Table 4.10. Seismic coefficients for structural portions higher than 10 m above ground surface shall be increased by 1 percent for each 1 m increase in height above 10 m. The vertical seismic coefficient shall be one-half of the horizontal coefficient. Seismic coefficients for retaining walls shall be taken as 0.2 in the horizontal direction and 0.1 in the vertical direction, simultaneously. Earth pressures during earthquakes shall be estimated by the Mononobe-Okabe method previously described. Provisions on stability of structure and on allowable stresses are specified.

F. SPECIFICATIONS FOR HONSHU-SHIKOKU BRIDGES JSCE-1967 [9]

The Japan Society of Civil Engineers along with a joint commission of the Ministry of Construction and the Japanese National Railways issued "Specifications for Earthquake-Resistant Design of Honshu-Shikoku Bridges" in May 1967. These specifications have been written primarily for long-span suspension bridges having large foundations under the sea. The primary features of these specifications are the following:

The basic design shall be made using the conventional seismic coefficient method or the modified seismic coefficient method. The basic design should be checked by dynamic analysis when considered desirable.

When applying the conventional seismic coefficient method, the horizontal seismic coefficient (k_h) and the vertical coefficient (k_v) shall be determined using the relations

$$k_h = S\,C_0$$
$$k_v = \tfrac{1}{2}\,k_h \qquad (16)$$

where S is a modification factor depending on ground conditions and is

selected in accordance with Table 4.11, and where C_0 is the basic seismic coefficient equal to 0.20 (this basic coefficient was changed to 0.18 in the 1971 JSCE report, Ref. 150). The value of k_h shall be increased with height of structure in accordance with Fig. 4.2.

When applying the modified seismic coefficient method, a design seismic coefficient (k) shall be determined by the relation

$$k = m_1 \; m_2 \; C \tag{17}$$

where m_1 is a dynamic magnification factor based on the response of a single-degree-of-freedom system to the earthquake excitation (depends on fundamental period, damping, nonlinearities, etc. as shown in Fig. 4.3), m_2 is a factor required to correct for the simple single-degree-of-freedom assumption used for determining m_1, and where C is the basic coefficient C_0 equal to 0.20 horizontally and 0.10 vertically (changed to 0.18 horizontally and 0.09 vertically by JSCE-1971 [150] for substructures). The values of C shall be the coefficient k_T at the top of corresponding main piers for main towers and shall be the coefficient k_T at the top of abutment for suspended structures and cables as shown in Fig. 4.4. It should be pointed out that the modified design seismic coefficient method is normally adopted in practice for suspension bridges.

To evaluate the seismic response of the specific suspension bridge under consideration, dynamic analyses shall be carried out for the complete structural system including both superstructures and substructures. Either the response spectrum or the time history methods may be employed in these analyses. In carrying out the dynamic analyses, sufficient considerations should be given to establish appropriate dynamic properties of the structures. According to the 1971 JSCE report [150], the damping ratios should be taken as 10, 5, and 2 percent of critical for rigid substructures, flexible concrete substructures and steel structures, respectively.

The effects of earth and hydraulic pressures on substructures during earthquakes shall be taken into account in the design of the overall structure and in carrying out the dynamic analyses. Formulas for calculating hydrodynamic pressures were previously given by Eq. 11.

In designing the superstructures, dead, live, thermal, and seismic loads shall be combined. Likewise in designing the substructures, all loads imposed by superstructures, dead loads of substructures, hydrodynamic forces, and buoyancy forces shall be combined with the seismic loads.

When designing for seismic loads, the allowable bearing capacity of foundation soils may be taken as 1.5 times the capacity for ordinary loads. The increased capacity shall, however, be less than 3/4 yield capacity. The resultant force acting on the base of the foundation shall fall within the center 2/3 of the base area. The factor of safety against sliding of substructure shall be greater than 1.5.

Stresses in steel structures such as towers, cables, stiffening girders and hangers shall remain within the elastic range. Stresses in some local members may, however, be permitted to exceed yield levels provided the structure as a whole does not suffer severely. Stresses permitted in concrete structures shall meet the provisions of the JSCE "Standard Specifications for Concrete" [8].

Displacements and deformations of superstructures and substructures shall be held within allowable limits as determined by the response of the structure as a whole.

G. SEISMIC DESIGN CRITERIA FOR RAILWAY BRIDGES JSCE-1968 [1.5]

In 1968, the Japan Society of Civil Engineers along with a commission from the Japanese National Railways issued a "Report On The Seismic Design Of The Substructures Of Railway Bridges". The main features of this report are the following:

(1) Horizontal Seismic Coefficient - The horizontal seismic coefficient (k_h) shall be determined by

$$k_h = m_S \, m_I \, k_0 \tag{18}$$

where k_0 is the basic seismic coefficient equal to 0.20 and 0.15 for zones A and B, respectively, m_S is a soil condition factor equal to 1.2, 1.0, and 0.8 for soft, medium, and hard soils, respectively, and where m_I is an

importance factor equal to 1.1, 1.0, and 0.9 for high, ordinary, and low importance structures, respectively. Soft soil classification is designated when the surface layer is either a) 2 to 5 m depth with N-value (standard penetration test) equal to zero, b) 5 to 10 m depth with N-value less than 2, or c) greater than 10 m depth with N-value less than 4. Medium soil classification is used when the surface soil layers consist of diluvial or alluvial materials not falling in the soft soil classification. Hard soil classification is used when surface layers consist of rock formed in the Tertiary Age, or before. See Table 4.12 for values of k_h.

(2) Vertical Seismic Coefficient - The vertical seismic coefficient shall be taken as one-half the vertical coefficient in those cases where it is required in the design process.

(3) Highrise Bridges - The design seismic coefficients for portions of structures higher than 10 m above ground surface shall be those values taken from Table 4.12, but increased 1 percent for each 1 m increase in height above 10 m.

(4) Underground Structures - The design seismic coefficient for underground portions of structures and underground structures shall be determined by considering values of m_S as shown in Fig. 4.5 for various soil conditions.

(5) Earth Pressures - Earth pressures used in seismic design shall be obtained by the Mononobe-Okabe method.

(6) Hydrodynamic Pressures - Hydrodynamic pressures shall be added to static pressures and shall be determined by Eq. 3.11.

H. SEISMIC DESIGN FORCES - CALIFORNIA STATE DIVISION OF HIGHWAYS [227]

The seismic design forces used in bridge design by the California State Division of Highways prior to the San Fernando earthquake of February 9, 1971,

are stated in "Bridge Planning and Design Manual", California State Division of Highways, Vol. I - Design Specifications, Section 2-25, as follows:

2-25 Seismic Forces

All structures except underground structures and retaining walls shall be designed to resist earthquake forces (EQ) in accordance with the following equations. A nomograph is available on Page 5-65 of Vol. III of the Bridge Planning and Design Manual for solving equation (2).

(1) $EQ = KCD$

EQ = The force applied horizontally at the center of gravity of the structure. This force shall be distributed to supports according to their relative stiffnesses.

K = Numerical coefficient representing energy absorption of the structure:

K = 1.33 For bridges where a wall with a height to length ratio of 2.5 or less resists horizontal forces applied along the wall.

K = 1.00 For bridges where single columns or piers with a height to length ratio greater than 2.5 resist the horizontal forces.

K = 0.67 For bridges where continuous frames resist horizontal forces applied along the frame.

(2) $C = \frac{0.05}{\sqrt[3]{T}}$ (Maximum value of C = 0.10)

C = Numerical coefficient representing structure stiffness.

(3) $T = 0.32\sqrt{\frac{D}{P}}$ for single story structures only.

T = Period of vibration of structure.

D = Dead load reaction of structure.

P = Force required for one inch horizontal deflection of structure.

The EQ forces calculated above shall never be less than 0.02D. Special consideration shall be given to structures founded in soft materials capable of large earthquake movements, and to large structures having massive piers.

Following the San Fernando earthquake, the California State Division of Highways adopted new Interim Criteria For Earthquake Design [232] requiring bridge columns to be designed for seismic forces as follows:

EQ = 2 KCD for frames on spread footings

EQ = 2.5 KCD for frames on pile footings

(No change in allowable 33% overstress)

I. SEISMIC RESISTANCE OF NEW ZEALAND BRIDGES

Some relevent remarks regarding certain published information in New Zealand on seismic resistance features of New Zealand bridges, were transmitted to the authors on 1 May 1972, by Mr. R. J. P. Garden, as follows:

1. P. L. Laing Reinforced Concrete Bridges Proc. N.Z.I.E. Jan. 1943 Vol 28 No. 4.

   Old bridges with bearing surfaces of pairs of steel plates with no anchorages were found to slide and cut the bearing surfaces, and monolithic construction at supports became prevalent after 1938 e.g. Mesnager hinges.

   0.10 (D.L.) = C.W. = Horiz. Seismic Force

   Discussed sharing of resistance by piers of varying sizes.

2. C. W. O. Turner Railway Bridges of Reinforced Concrete Proc. N.Z.I.E. Vol XXXI 1945.

   P. 312 et seq. discusses continuously connected spans and having piers slender enough to accept deck-shortening effects and choice of a strategic point for a single anchor against longitudinal earthquakes.

   C = 0.10

3. V. A. Murphy New Zealand Earthquake Problem in Relation to Engineering Structures Proc. N.Z.I.E. Vol XXXII 1946.

4. G. A. Toynbee Collingwood Street Bridge N.Z. Engineering Vol 13 No. 1 1958.

   C = 0.25 Deadman anchor for longitudinal seismic forces; rockers at distant piers.

5. A. N. Grigg The New Melling Bridge N.Z. Engineering Vol 14 No. 7 1959.

   5 spans of 90 feet: width 42 feet. Longitudinal seismic forces taken at abutment against soil at pile cap level, some 25 feet below road level, each abutment structure being a row of open A frames.

   (Comment for 1972 review: the restraining frames seem to lack flexibility).

6. R. G. Norman Tauranga Harbour Bridge N.Z. Engineering Vol 15 No. 2 1960.

   33 spans of 30 feet each. Each pier consists of 5 - 18" square prestressed piles of 60 feet length. These resist lateral seismic forces in flexure and the designers preferred this to having rigid propping from raked piles.

   Each abutment is to resist longitudinal seismic forces from a half of the 1040 feet long bridge, and they are described as gravity boxes in the rock fill of the approach embankment. The description states that dowels and linkage bars at piers are encased in rubber and that this 1040 feet long superstructure should be able to accommodate itself to long term changes in length while having good instantaneous shear transfer and damping properties.

   Loc. cit Vol 15 No. 5 Discussion on above; C.W.O. Turner and C.R. Davis reported that they also preferred vertical piles to raking piles for resisting seismic forces.

7. A. G. Stirrat and J. B. S. Huizing Trends in Highway Bridging N.Z. Engineering Vol 16 No. 11 1961.

   Recommends vertical rather than raking piles to resist seismic forces, and recommends that the designer should consider the effects of acceleration and deceleration of the soil around the substructure.

8. C. P. O. Turner Mohaka Bridge Submergence Effect on Bridge Piers Under Earthquake. N.Z. Engineering Vol 17 No. 1 1962.

   Virtual mass of pier and displaced water, and the damping effects of submergence are taken into account.

9. Unpublished criterion 1962.

   Displacement of abutments out of phase with each other is an aspect

for whcih allowance is made. e.g. 1" differential was allowed for between the abutments of the Kawarau Bridge which spans across a rock gorge.

10. A. W. Smith The Newmarket Viaduct N.Z. Engineering Vol 20 No. 12 1965.

Consideration given, to statistical interpretation of recorded seismicity. Housner's spectrum values were used, and natural periods determined for successive jointed sections of this viaduct of 16 spans.

Examples of calculated values of period, acceleration and deflection for different sections, using 5% damping:

1.5S	0.07g	± 1.4 in.
1.0S	0.09g	± 0.74 in.
0.7S	0.12g	± 0.55 in.

11. Discussion on Ref. 10; N.Z. Engineering Vol 21 No. 8 1966. The above responses were based on an El Centroquake centered 50 miles from the site.

12. J. B. S. Huizing and others. Design of the Thornton Overbridge N.Z. Engineering Vol 23 No. 12 1968.

A seismic factor of 0.3 was used for ultimate strength design. Ductility was incorporated in places. Important local details were designed for seismic factors of "0.5 to 1.0 at yield stress".

13. A. K. Lewis Design of Superstructure of Ramp B Flyover - Dominion Road Interchange.

N.Z. Engineering Vol 25k No. 3 1970.

Seismic Coefficient 0.10. He explains sharing of seismic forces between the piers of this 10 span structure which is curved 70° in plan.

14. J. B. Wilson, Notes on Bridges and Earthquakes, Bulletin of the New Zealand Society for Earthquake Engineering, Vol. 1, No. 2, Dec. 1968.

Gives summary of New Zealand practices.

15. R. J. P. Garden, Timaru Port Access Overbridge, Unpublished, Address given to a Branch of New Zealand Institution of Engineers. Section 5.4 of the script in the third paragraph mentions prestressing cables carried from end to end of the bridge. In carrying these through the hinged articulations at the junctions of lengths of superstructure, consideration was required of the fatigue life of the tensioned cables under the effects of hinge rotations caused by temperature hogging and by deflections from live loads. This bridge design was by E. R. Garden & Partners, Consulting Engineers.

16. Allanton Bridge - Design being completed by E. R. Garden & Partners in cooperation with the County Engineer, for the Taieri County, New Zealand.

DATA OF STRUCTURE

Length	1296 feet - 18 spans of 72 feet
Width	30 feet (2 lanes of 12 feet)
Superstructure	Precast, prestressed I beams and R.C. deck.
Live Load	H20.S16.T16
Substructure	R.C. piers on piles, bottoming in medium stiff clay-silts.

SEISMIC RESISTANCE

Coefficient in Seismic Zone C. 0.08.

Factor for Cantilevered pier 2.0; giving F = 2 x 0.08 x Wt.

Pier design for seismic load was based on $\frac{U}{\emptyset} = 1.1\ D + 1.4\ EQ$

The undercapacity factor Ø, of value 0.7 for the rectangular pier.

The cumulative effects of using Building Code coefficients for a Bridge, and of undercapacity factors for a bridge situated in the country's lowest rated zone of seismicity, seems a relatively conservative provision. The designers were, however, not unwilling to accept a conservative approach when using a static-coefficient design for a structure of this type. The structure may be described as a loosely linked succession of simple spans having piled supports in soft lacustrine deposits of some depth, and its dynamic response to earthquakes must be expected to be somewhat irregular and uncertain.

STRUCTURAL DETAILS

Some design details related to seismic resistance are mentioned in the following.

As dowels and vertical holding down bolts between pier caps and superstructure are suspected by the designers of being sources of likely trouble, these were not used. The spans meeting at a pier-top have horizontal link bolts to prevent separation at the pier seating, and stub members rising above the pier seating level act in combination with the link bolts as shear keys. Slack is left for deck-shortening movements, and rubber packing used under washers of the link bolts.

Clause 10.11.5.1 of ACI 318-71 was used when assessing slenderness ratios for the succession of seventeen piers of varying height. The average height to deck is about 25 feet. A ductility factor

of 4 was provided at the bottom of the cantilevering pier shafts; as P is less than 0.4 of Pu, the confining steel etc. was provided as required as for flexural members.

J. SUMMARY OF WORLD'S EARTHQUAKE REGULATIONS

A summary of earthquake regulations for twenty one countries is given by Table 4.13. The information provided in this table has been taken from an available world list of regulations [21] and from specifications in effect in Japan and the United States. It should be pointed out that due to language difficulties, certain regulations in the world list have been omitted from Table 4.13

Table 4.13 gives approximate ranges of horizontal design seismic coefficients for the zone of greatest seismicity in each country. Factors affecting these coefficients and increases in allowable material stresses for seismic conditions are shown. It should be noted that most of these regulations are primarily for the design of buildings as only four out of the twenty-one countries represented have regulations in the world listing specifically for highway bridges.

Regarding values of horizontal seismic coefficients in Table 4.13, five countries use values in the range 0 to 0.1, ten countries in the range 0 to 0.2, four countries in the range 0 to 0.3, and two countries in the range 0 to 0.4.

As indicated by Table 4.13, most regulations use seismic zone factors and soil condition factors. Also many countries have importance factors and make coefficients dependent upon fundamental natural period of vibration. Some countries also take into account mode shapes in determining values of seismic coefficients.

Table 4.1 History of Design Loads for Highway Bridges in Japan (Primarily Seismic Loads)

YEAR	NAME OF REGULATIONS	CLASS	DESIGN LIVE LOADS: Truck Roller LOADS Streetcar	DESIGN LIVE LOADS: Uniform LOADS	DESIGN LIVE LOADS: Line LOADS	IMPACT LOADS	SEISMIC LOADS k: HORIZONTAL SEISMIC COEFFICIENT	OTHER SEISMIC REGULATIONS (k: Seismic Coef.)	MAJOR EARTHQUAKES
1) 1886	Order No. 13 Ministry of Home Affairs (MHA)			U-454kg/m	---	not considered	not considered	1924. Building Law ($k \geq 0.1$) 1950. Kawasumi's Seismic Map. 1950. New Building Law ($k = 0.2$, $H \leq 16$m increase 0.01 per an increase of 4m above 16m) 1964. Highrise Building. ($H \geq 45$m) $k = (0.18 \sim 0.36)/T$ (T: period) ($0.05 \leq k \leq 0.2$) 1965. Report of JSCE on Civil Earthquake-Resistant Design of Engineering Structures. 1968. Report of JSCE on Earthquake-Resistant Design of Substructures of Railway Bridges.	($M \geq 7$) after Rika Nenpyo (1971) 1923. Kanto ($M = 7.9$) 1946. Nankai ($M = 8.1$) 1948. Fukui ($M = 7.3$) 1952. Tokachi-oki ($M = 8.2$) 1964. Niigata ($M = 7.5$) 1968. Tokachi-oki ($M = 7.9$)
2) 1906	Order MHA		R-13.6t S-12.7	U-400 600kg/m (carriage way) U-270 400kg/m (footway)	---	not considered	not considered		
3) 1919	Road Laws MHA		R-13.6t T-11.2t S-30t	Same as 2)	---	not considered	not considered		
4) 1926	Specifications for Design of Roads, Road Laws, MHA	1st	T-12t	U-600kg/m	---	considered	Seismic Coefficient Method $k = 0.15 \sim 0.4$ depending on location and ground condition $k \geq 0.3$ advised in Tokyo, Yokohama		
		2nd	T-8t	U-500kg/m					
		3rd	T-6t	U-500kg/m					
5) 1939	Specifications for Design of Steel Highway Bridges, MHA	1st	T-13t	U-500kg/m	---	considered	Seismic Coefficient Method $k_h = 0.2$, $k_v = 0.1$		
		2nd	T-9t	U-400kg/m					
6) 1956 (and 1964)	Revision of Specifications for Design of Steel Highway Bridges, JRA	1st	T-20t	---	L-20(5t/m)	considered	Seismic Coefficient Method $k = 0.1 \sim 0.35$ depending on location and ground conditions		
		2nd	T-14t	---	L-14(3.5t/m)				
7) 1964 to 1971	Specifications for Design of Substructures of Highway Bridges, JRA	same as 6)					same k as 6) Detailed calculation methods		
8)*1966 (and 1970)	Design Standards, JHPC	same as 6)					Design Code for Highrise Bridges, (Increase in k with the height of the piers.)		
9)*1967	Specifications for Earthquake-Resistant Design of Honshu-Shikoku Bridges, JSCE	Special Live Loads and Impact Loads for Suspension Bridges are considered					Modified Seismic Coefficient Method (Basic Coefficient $k_o = 0.2$)		
10)*1967	Specifications for Earthquake-Resistant Design of Tokyo Expressways, TEPC	same as 6)					Seismic Coefficient Method $k = 0.2 \sim 0.3$		
11)*1968	Aseismic Design Standards, HEPC	same as 6)					Seismic Coefficient Method $k = 0.2 \sim 0.28$		
12) 1971	Specifications for Earthquake-Resistant Design of Highway Bridges, JRA	same as 6)					Seismic Coefficient Method $k = 0.1 \sim 0.24$ (Rigid) Modified Seismic Coefficient Method $k = 0.05 \sim 0.3$ (Flexible)		

*Note: Regulations in 8) to 11) are relating to special projects.

TABLE 4.2 HIGHWAY ADMINISTRATION IN JAPAN (Technical Field)

(ORGANIZATION)			(IN CHARGE OF)
Ministry of Construction	Council of Roads		
	(D) Road Bureau ※	(D) Regional Construction Bureaus (8)	National Highways (Free)
		(I) Hokkaido Development Bureau (Hokkaido Development Agency)	National Highways (Free)
		(I) Prefectural Public Works Divisions (52) (Prefectural Governments)	Prefectural Roads (Free); General Toll Roads (Toll)
		(I) Municipal Public Works Divisions (-) (Municipal Governments)	Municipal Roads (Free); General Toll Roads (Toll)
		(S) JHPC (Japan Highway Public Corporation)	National Expressways (Toll) (Limited-Access); General Toll Roads (Toll) (Limited-Access)
		(S) HSBA (Honshu-Shikoku Bridge Authority)	Honshu -Shikoku Bridges (Toll) (Limited-Access)
	(D) City Bureau	(S) TEPC (Tokyo Expressways Public Corporation)	Tokyo Expressways (Toll) (Limited-Access)
		(S) HEPC (Hanshin (Osaka-Kobe) Expressways Public Corporation)	Hanshin Expressways (Toll) (Limited-Access)
	Auxiliary Organs	(A) GSI (Geology Survey Institute)	
		(A) PWRI (Public Works Research Institute)	Survey and Research Work on Public Works (Fundamental)
		(A) BRI (Building Research Institute)	
		(A) CC (College of Construction)	
※ Related Organs		(R) JRA (Japan Road Association)	Survey and Research Work on Roads (Applied Field, Specifications)
		(R) JHUC (Japan Highway Users Conference)	
		(R) ERF (Expressway Research Foundation)	

Abbreviation

A : Auxiliary Organs of the Ministry of Construction
D : Directly Controlled by the Ministry of Construction (or Organs of the Ministry)
I : Indirectly Controlled by the Ministry of Construction
R : Related Organs
S : Supervised by the Ministry of Construction

(Notes) 1. The above information may not be complete.
2. JSCE (Japan Society of Civil Engineers) is doing survey and research work in the academic field.

Table 4.3 Horizontal Design Seismic Coefficient (Out of Date)

Regions* \ Ground Conditions*	Weak	Ordinary	Firm
Where severe earthquakes have been frequently experienced	0.35 ~ 0.30	0.30 ~ 0.20	0.20 ~ 0.15
Where severe earthquakes have occurred	0.30 ~ 0.20	0.20 ~ 0.15	0.15 ~ 0.10
Other regions	0.20	0.15	0.10

*No further description on regions and ground conditions.

Table 4.4 Seismic Zone Factor ν_1 for General Highway Bridges

Zone	Value of ν_1
A	1.00
B	0.85
C	0.70

Table 4.5 Ground Condition Factor ν_2 for General Highway Bridges

Group	Definitions[1)]	Value of ν_2
1	(1) Ground of the Tertiary era or older (defined as bedrock hereafter) (2) Diluvial layer[2)] with depth less than 10 meters above bedrock	0.9
2	(1) Diluvial layer[2)] with depth greater than 10 meters above bedrock (2) Alluvial layer[3)] with depth less than 10 meters above bedrock	1.0
3	Alluvial layer[3)] with depth less than 25 meters, which has soft layer[4)] with depth less than 5 meters	1.1
4	Other than the above	1.2

Notes: 1) Since these definitions are not very comprehensive, the classification of ground conditions shall be made with adequate consideration of the bridge site.

Depth of layer indicated here shall be measured from the actual ground surface.

2) Diluvial layer implies a dense alluvial layer such as a dense sandy layer, gravel layer, or cobble layer.

3) Alluvial layer implies a new sedimentary layer made by a landslide.

4) Soft layer is defined in Section 3.7 "Soil Layer Whose Bearing Capacities are Neglected in Earthquake Resistant Design."

Table 4.6 Importance Factor ν_3
for General Highway Bridges

Group	Definitions	Value of ν_3
1	Bridges on expressways (limited-access highways), general national highways and principal prefectural highways. Important bridges on general prefectural highways and municipal highways.	1.0
2	Other than the above	0.8

Note: The value of ν_3 may be increased up to 1.25 for special cases in Group 1.

Table 4.7 Design Seismic Coefficient for Tokyo Expressways

Classification of Ground Conditions		1	2	3	4
Horizontal Seismic Coefficient k_h	Above Ground	0.20	0.24	0.27	0.30
	Underground	0.15	0.18	0.20	0.23
Vertical Seismic Coefficient, k_v		0.10	0.10	0.10	0.10

Table 4.8 Classification of Ground Conditions* for Tokyo Expressways

Properties of Alluvial Layer and Loam Layer** / Depth of Alluvial Layer and Loam Layer	Gravel	Sand, Clay, and Loam ($N \geqq 5$)	Soft Soil	
			$N = 2 \sim 5$	$N < 2$
0 ~ 3 m	See Note (c)			
3 ~ 10 m	3 (2)	3 (2)	4 (3)	4 (3)
10 ~ 25 m	3 (2)	4 (3)	4 (3)	4 (4)
25 m or more	4 (3)	4 (3)	4 (4)	4 (4)

*See the report.

**N indicates number of blows per 30 cm by the standard penetration test.

Table 4.9 Combination of Loads and Allowable Stresses in the Earthquake-Resistant Design of Tokyo Expressways

Type of Structures		Combination of Loads	Increases in Allowable Stresses (%)	Allowable Stress of Concrete
Foundations or Retaining Walls	Reinforced Concrete Structures	Principal Loads + Seismic Loads	50	$\frac{\sigma_{28}}{3}$ or 100 kg/cm^2
	Reinforced Concrete Structures	Principal Loads + Temperature + Humidity + Seismic Loads	65	
	Steel Structures	Principal Loads + Seismic Loads	50	
Superstructures or Piers	Reinforced Concrete Structures	Dead Loads + Seismic Loads	50	$\frac{\sigma_{28}}{3}$
	Reinforced Concrete Structures	Dead Loads + Temperature + Humidity + Seismic Loads	65	
	Steel Structures	Dead Loads + Seismic Loads	70	

Table 4.10 Values of Factor m for Hanshin Expressways

N-Values of Sandy Soils / N-Values of Cohesive Soils / Depth of Embedment of Foundation	$N \geqq 30$	$30 \geqq N \geqq 10$	$N < 10$
	$N \geqq 8$	$8 \geqq N \geqq 4$	$N < 4$
less than 10 m	1.00	1.00	1.10
10 m ~ 25 m	1.00	1.10	1.25
25 m or more	1.10	1.25	1.40

Table 4.11 Value of Factor S for Honshu-Shikoku Suspension Bridges

Soil Condition	Factor S
Rock (Tertiary or older)	1.0
Diluvium	1.1
Alluvium	1.2

Table 4.12 Design Horizontal Seismic Coefficient ($k_h = m_S \cdot m_I \cdot k_o$) for JNR Bridges

Zone			A (k_o = 0.2)			B (k_o = 0.15)		
Soil Condition			Soft m_S = 1.2	Medium m_S = 1.0	Hard m_S = 0.8	Soft m_S = 1.2	Medium m_S = 1.0	Hard m_S = 0.8
Degree of Importance of Structure	Important	m_I = 1.1	0.25	0.20	0.20	0.20	0.15	0.15
	Ordinary	m_I = 1.0	0.25	0.20	0.15	0.20	0.15	0.10
	Less important	m_I = 0.9	0.20	0.20	0.15	0.15	0.15	0.10

k_o : Basic seismic coefficient

TABLE 4.13 DESIGN SEISMIC COEFFICIENTS IN VARIOUS COUNTRIES

COUNTRY	APPROXIMATE RANGE OF HORIZONTAL DESIGN SEISMIC COEFFICIENTS IN VARIOUS COUNTRIES (IN THE HIGHEST SEISMIC ZONE FOR EACH COUNTRY) 0 0.1 0.2 0.3 0.4	FACTORS AFFECTING DESIGN SEISMIC COEFFICIENTS[1]						INCREASE IN ALLOWABLE STRESSES FOR EARTHQUAKE RESISTANT DESIGN[2]	STRUCTURES TO WHICH THE REGULATIONS APPLY PRIMARILY
		ZONE	GROUND CONDITIONS OR TYPE OF FOUNDATIONS	PERIOD, HEIGHT OR NO. OF STORIES	IMPORTANCE OR USAGE	STRUCTURAL MEMBER OR STRUCTURAL POPERTIES	MODE SHAPE		
ARGENTINA		○	○	○	○	○	×		BUILDINGS
BULGARIA		○	○	○	○	○	○	50%	〃
CANADA		○	○	○	○	○	×		〃
CHILE		×	△	○	○	○	×		〃
CUBA STATIC		×	○	×	○	○	×	W,SS,B : 50%	〃
CUBA DYNAMIC		×	×	○	×	○	○	ME,C,MA,G : 33%	
EL SALVADOR		○	×	×	○	○	×	W,SS,B : 50% ME,C,MA : 33%	〃
GREECE		○	○	×	×	×	×	C,S : 20%	〃
INDIA		○	○	×	×	○	×	G : 30～50%	BUILDINGS AND BRIDGES
IRAN LOW		○	○	×	○	×	×	33%	BUILDINGS
IRAN HIGH-RISE		○	○	○	×	○	×		
ISRAEL		○	○	○	×	○	×	33%	〃
ITALY		○	×	×	×	×	×	SS ; 1400kg/cm² HS : 2000kg/cm²	〃
JAPAN RIGID		○	○	×	○	○	×	SS : 70%	HIGHWAY BRIDGES (Japan Road Assoc.)
JAPAN FLEXIBLE		○	○	○	○	△	×	B,C : 50%	
MEXICO		○	○	×	○	○	×	W,SS,B : 50% ME,C,MA : 33%	BUILDINGS
NEW ZEALAND		○	×	○	○	×	×		〃
PERU		○	×	○	○	○	×	SS,C : 33%	〃
PHILIPPINES		○	○	○	×	○	×		〃
PORTUGAL		○	○	×	×	○	×	SS : 2400kg/cm² C : 100%	〃
RUMANIA		○	○	○	×	○	○		〃
TURKEY		○	○	○	×	○	×	50%	BUILDINGS AND BRIDGES
USA AASHO		×	○	×	×	×	×	33%	HIGHWAY BRIDGES
USA CALIFORNIA		△		○	×	○	×		
VENEZUELA		○	○	×	○	○	×	33%	BUILDINGS

NOTES: 1) Factors with circles are considered, and factors with triangles are considered partially or indirectly.

2) B : Bars for reinforcement, C : Concrete, G : Ground, HS : High-tension steel, MA : Masonry ME : Metals other than steel, SS : Structural Steel, W : Wood

3) Mostly by 「A World List of Seismic Regulations (1970)」, 4) See Appendix B for further details.

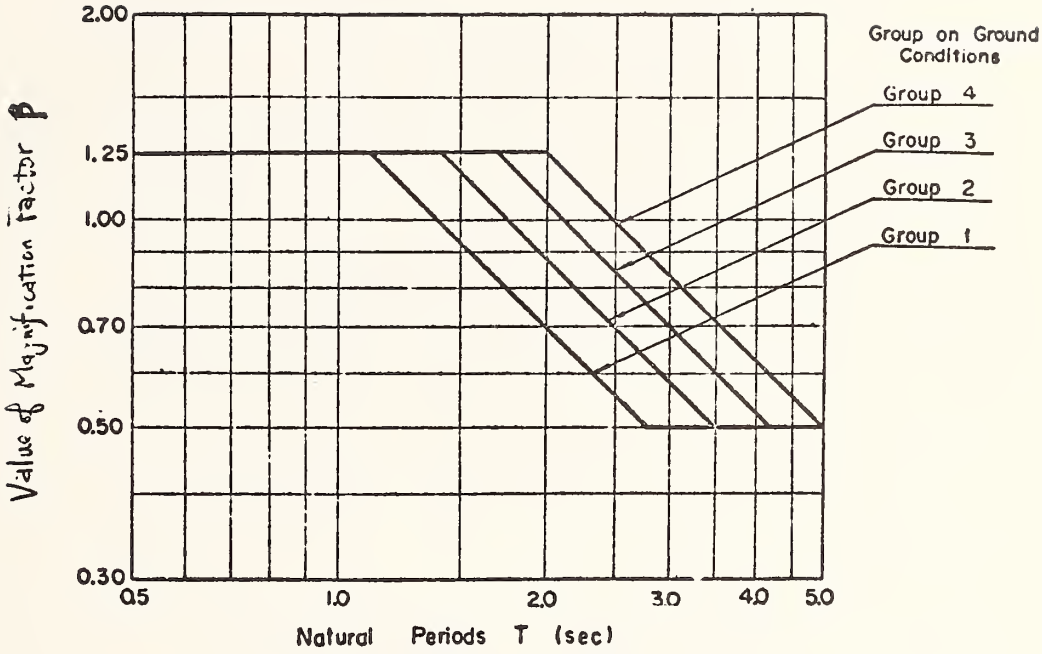

Fig. 4.1 Magnification factor (β) for general highway bridges

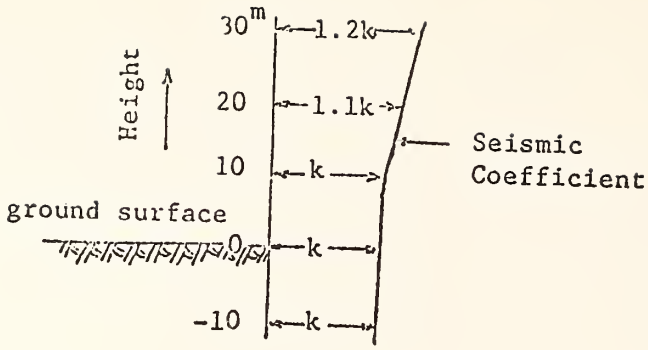

Fig. 4.2 Seismic coefficient for higher parts of structures

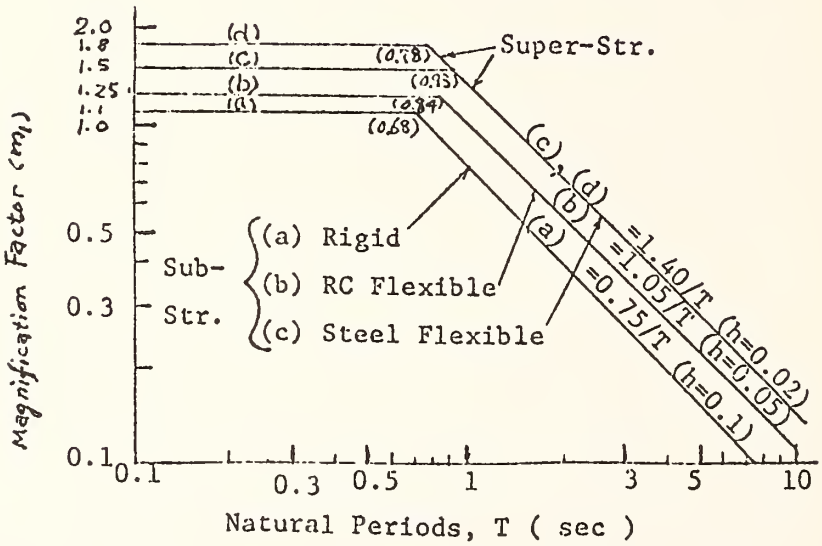

Fig. 4.3 Magnification factor β

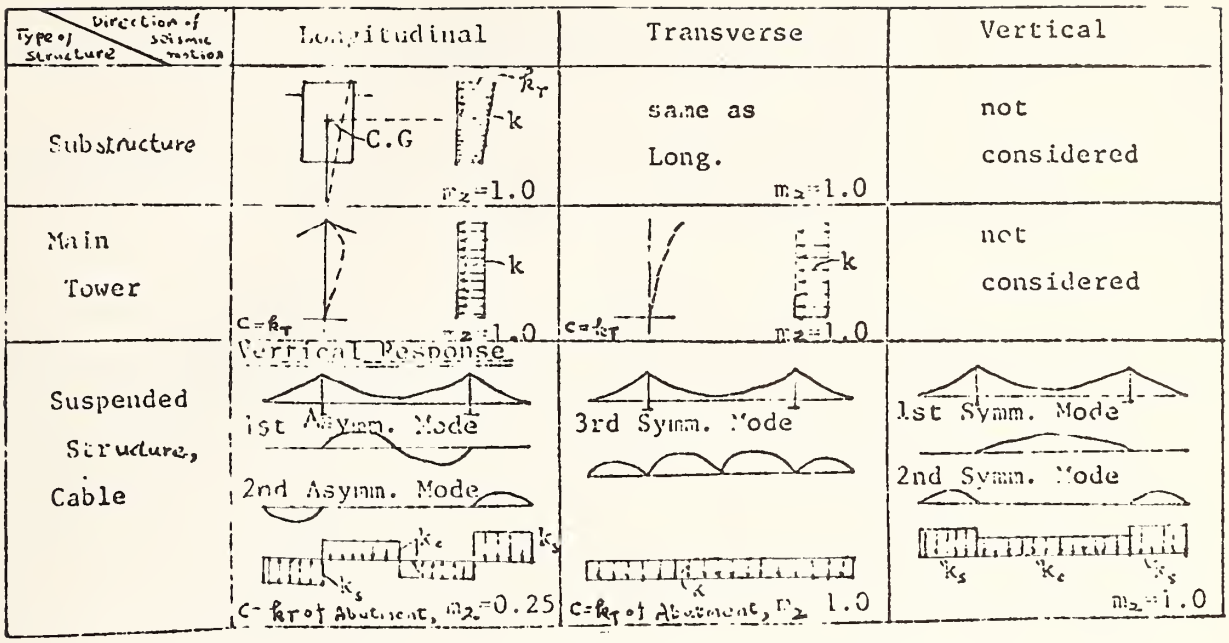

Fig. 4.4 Distribution of design seismic loads and valve of m_2

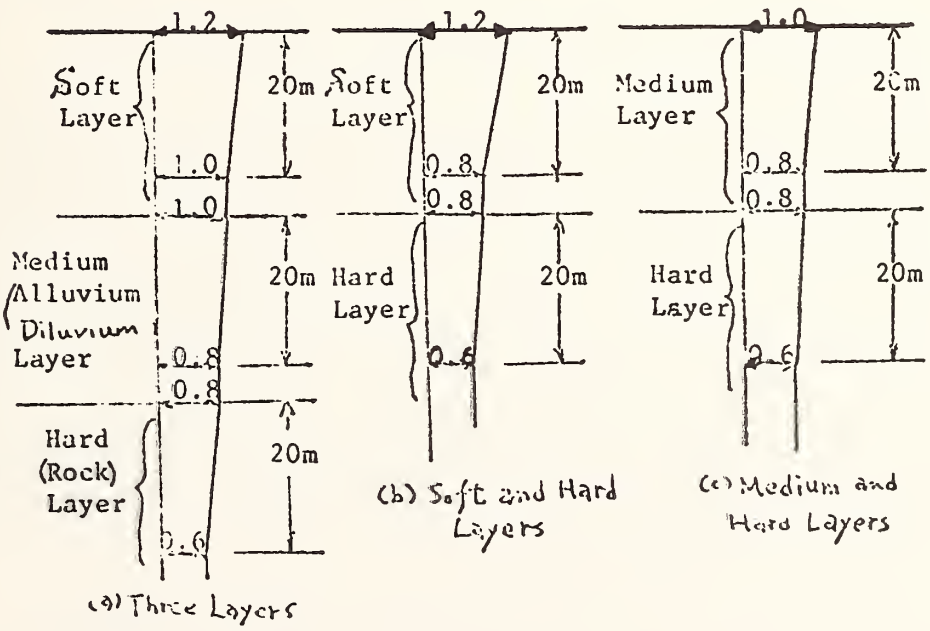

Fig. 4.5 Valve of m_2 for underground layers

V CONCLUSIONS AND RECOMMENDATIONS

Based on the damage surveys reported herein, several general conclusions may be deduced as follows:

(1) Seismic damages, particularly to low bridges, are most commonly caused by foundation failures resulting from excessive ground deformation and/or loss of stability and bearing capacity of the foundation soils. As a result, substructures often tilt, settle, slide, or even overturn, thus, experiencing severe cracking or complete failure. These large displacements may cause relative shifting of and damage to the superstructures, and may induce failures within the bearing supports.

(2) Backfills exert large forces on abutments which can at certain times be in-phase with the seismic inertia forces developed in the superstructures. These forces in combination may cause severe failures, often of a brittle nature, in the substructures. It is common for wing walls to break loose from their abutments due to excessive backfill forces. Settlement of backfills resulting from compaction is often observed.

(3) Seismic damages due to vibration effects are much less common than damages due to other effects; however, they may occur in higher bridge structures which lack sufficient strength, stiffness, and toughness.

(4) To minimize damages, bridge structures should be designed with proper recognition of the stability and bearing capacities of foundation soils, force-deformation and energy absorption characteristics of substructure, superstructure and connecting elements, the dynamic nature of structural response, and the dynamic characteristics of all forces acting on the complete soil-structure system.

To improve seismic design methodology of bridge structures, further investigations are required in the following areas:

(1) Seismicity and Ground Motion Characteristics - Statistical studies should be made to establish probable frequencies of occurrence and intensities for expected strong motion earthquakes at bridge sites. Predictions should be made of the characteristics of ground motions, particularly with respect to local ground conditions. Strong motion measurements should be made to provide basic data for these studies.

(2) Subsoil and Backfill Dynamic Characteristics - To evaluate realistic earth pressures on substructures, the stability, bearing capacities and other pertinent characteristics of subsoils should be carefully examined and predictions should be made of the possibility of experiencing ground failures such as surface faulting, sliding, liquefaction, and relative settlements. Magnitudes of dynamic backfill forces on substructures should be carefully investigated.

(3) Structural Types - In designing for seismic resistance, selection of structural types should be made with full consideration of seismicity, geological and soil conditions at the site, and dynamic response characteristics of structural systems.

(4) Seismic Design of Substructures - Rational design methods should be established for substructures consisting of piers and abutments together with various foundations such as spread footings, caissons, and piles. Structural detailing should be carried out in a manner consistent with good force deformation and failure characteristics of individual components. If the static seismic coefficient method is used, damage surveys of ordinary bridges indicate that the horizontal coefficient should not be less than 0.1.

(5) Seismic Design of Superstructures - Experience shows that special attention should be given to the design details of bearing supports, hinges, and devices for preventing spans from falling off their supports.

(6) Dynamic Analyses - Methods of dynamic analysis should be established using realistic mathematical models for combined soil-structural

systems. These models should reflect appropriate mass, force-deformation, and failure characteristics of the combined system. Two basic types need immediate attention, namely, the taller, more flexible structures where vibration effects are important, and the shorter, stiff structures where soil-structure interaction effects are important.

(7) Field Dynamic Tests - Field vibration tests should be conducted on a variety of bridge structural types to determine their dynamic characteristics, i.e., mode shapes, frequencies, and damping ratios. These should include tests on substructural systems such as piers, abutments, and footings where soil-structure interaction effects are important. Further, selected bridge types should be instrumented so that input excitations and dynamic response time histories will be measured during future strong motion earthquakes.

(8) Laboratory Experiments - Selected components of bridge structural systems should be tested in the laboratory to determine their force-deformation and failure characteristics under large deformation reversed loading conditions, e.g., reinforced concrete piers and columns. Appropriate model tests should be conducted on a shaking table to observe and correlate overall gross behavior with analytical results and field measurements recorded on prototype structures during real earthquakes.

(9) Damage Surveys - Thorough damage surveys should be conducted for bridges immediately following each moderate to severe earthquake. The results of these investigations should be correlated with the results of previous surveys, analytical studies, and laboratory experiments.

APPENDIX A

BIBLIOGRAPHY ON SEISMIC EFFECTS ON BRIDGES

1. Japan Society of Civil Engineers (JSCE), "Specifications for Design and Construction of Prestressed Concrete Structures," August, 1961, pp. 1-124. (J)

2. Japan Road Association (JRA), "Specifications for Design of Substructures of Highway Bridges -- Volume for Design of Pile Foundations," March, 1964, pp. 1-72. (J)

3. JRA, "Specifications for Welded Highway Bridges," May, 1964, pp. 1-225. (J)

4. JRA, "Specifications for Design of Steel Highway Bridges," June, 1964, pp. 1-301 (J); pp. 1-117 (E).

5. JRA, "Specifications for Design of Reinforced Concrete Highway Bridges," June, 1964, pp. 1-59. (J)

6. JRA, "Specifications for Design and Construction of Composite Beams for Steel Highway Bridges," July, 1965, pp. 1-57. (J)

7. JRA, "Specifications for Design of Substructures of Highway Bridges -- Volume for General Provisions for Survey and Design," November, 1966, pp. 1-53. (J)

8. JSCE, "Standard Specifications for Concrete (1967)," May, 1967, pp. 1-438. (J)

9. JSCE, "The Specifications for Earthquake-Resistant Design of the Honshu-Shikoku Bridges (1967)," July, 1967, pp. 1-194. (J)

10. Tokyo Expressway Public Corporation, "Seismic Design Standards," Doro, July, 1967, pp. 16-18. (J)

11. Government of Japan, International Engineering Consultants Association, "Specifications for Earthquake-Resistant Design of the Bosphorus Bridge," November, 1967, pp. 1-79. (E)

Notes: (J): written in Japanese, (E): written in English

12. JRA, "Specifications for Prestressed Concrete Highway Bridges," March, 1968, pp. 1-139. (J)

13. JRA, "Specifications for Design of Substructures of Highway Bridges -- Volume for Design of Abutments and Piers, and -- Volume for Design of Spread Foundations," March, 1968, pp. 1-59. (J)

14. JRA, "Specifications for Design of Substructures of Highway Bridges -- Volume for Construction of Pile Foundations," October, 1968, pp. 1-83. (J)

15. JSCE, "Earthquake-Resistant Design for Civil Engineering Structures, Earth Structures and Foundations in Japan," November, 1968, pp. 1-139. (E)

16. Hanshin (Osaka-kobe) Expressway Public Corporation, "Seismic Design Standards," December, 1968, pp. 1-28. (J)

17. Tada, Y., "Specifications for Wind and Earthquake-Resistant Design of Highway Bridges in Japan," 1st Joint Meeting of U.S.-Japan Panel on Wind and Seismic Effects, UJNR, April, 1969, pp. 139-181 (E); also Journal of Research, PWRI, Vol. 12, Part I, 1971, pp. 269-314 (E).

18. Expressway Research Foundation, "Specifications for Design of Highways at Japan Highway Public Corporation," January, 1970, Vols. I, II, and III. (J)

19. JRA, "Specifications for Design of Substructures of Highway Bridges -- Volume for Design of Caisson Foundations," March, 1970, pp. 1-94. (J)

20. Tada, Y., "Trends on a Revision of the Specifications for the Earthquake-Resistant Design of Highway Bridges," 2nd Joint Meeting of U.S.-Japan Panel on Wind and Seismic Effects, UJNR, May, 1970, pp. 1-9 (E); also Journal of Research, PWRI, Vol. 12, Part V, 1971, pp. 521-529 (E).

21. International Association For Earthquake Engineering (IAEE), "Earthquake-Resistant Regulations, A World List 1970," November, 1970, pp. 1-465. (E) (Some Other)

22. JRA, "Specifications for Earthquake-Resistant Design of Highway Bridges," January, 1971, pp. 1-32 (J); pp. 1-42 (E).

23. JSCE and Bureau of Reconstruction, "The Kanto Earthquake of 1923, Report on Damage -- Part III Bridges, Buildings and Highways," 1926, pp. 1-59 (for Bridges). (J)

24. Public Works Research Institute (PWRI), "The Nankai Earthquake of 1946, Report on Damage," June, 1948, pp. 1-322. (J)

25. PWRI, "The Fukui Earthquake of 1948, Report on Damage," Report of PWRI, No. 78, March, 1949, pp. 1-172. (J)

26. Inose, S., "Earthquakes and Bridges," Doro, Vol. 25-11, November, 1950, pp. 328-332. (J)

27. Okamoto, S. and Kubo, K., "Damage to Civil Engineering Structures Caused by the Imaichi Earthquake," Transactions, JSCE, No. 10, December, 1951, pp. 1-14. (J)

28. Committee for Survey of the Tokachi-oki Earthquake of 1952, "Report of Survey on the Tokachi-oki Earthquake of 1952," 1954. (J)

29. Kuribayashi, E., "Earthquake-Resistance of Bridge Piers, Parts I and II," Doboku-Gijitsu-Shiryo (Technical Record in Civil Engineering), Vol. 3-5 (May, 1961), pp. 1-5; Vol. 4-1 (January, 1962), pp. 2-10. (J)

30. Tada, Y., Matsuno, S., Yamamura, K., and Kuribayashi, E., "The Tohoku Earthquake of 1962, Report on Damage, Parts I and II," Doboku-Gijitsu-Shiryo (Technical Record in Civil Engineering), Vol. 4-10 (October), pp. 27-38; Vol. 4-11 (November), pp. 26-30, 1962. (J)

31. Kodera, G., "Seismic Damage to Bridge Foundations and Soils, Parts I to V," Soils and Foundations, Vol. 12-3 (March), pp. 11-18; Vol. 12-4 (April), pp. 9-16; Vol. 12-5 (May), pp. 17-26; Vol. 12-6 (June), pp. 26-33; Vol. 12-8 (August), pp. 27-32, 1964. (J)

32. Komaki, S., "Observation of Aftershocks of the Niigata Earthquakes on the Showa Bridge and the Yachiyo Bridge -- Preliminary Report on the Niigata Earthquake," Earthquake Research Institute, University of Tokyo, September, 1964, pp. 123-129. (J)

33. JSCE, "Bridge on Earthquake Engineering -- Earthquake Resistant Design for Civil Engineering Structures, Earth Structures and Foundations in Japan," Compiled by JSCE, December, 1964, pp. 89-122. (E)

34. JNR Technical Research Institute, "Report on Damage to Bridges and Tunnels Caused by the Niigata Earthquake," March, 1965, pp. 1-94. (J)

35. PWRI, "Report on Niigata Earthquake, Chapter 5. Damages to Highway Bridges," Report of PWRI, No. 125, June, 1965, pp. 1-148. (J)

36. Fukuoka, M., "On the Earthquake at Niigata," Annual Report of Roads, JRA, July, 1965, pp. 136-148. (E)

37. Yoshida, I., "On the Damage to Reinforced Concrete Pile Foundations of Bridges Caused by the Niigata Earthquakes," Proceedings, 8th Meeting on Earthquake Engineering, JSCE, October, 1965, pp. 11-12. (J)

38. JSCE, "Report on Damage Due to the Niigata Earthquake," June, 1966, pp. 1-904. (J)

39. Tada, Y., Yoshida, I., and Kuribayashi, E., "On the Damage to Bridges Caused by the Niigata Earthquake," Proceedings, JEES, October, 1966, pp. 385-390. (J)

40. Fukuoka, M., "Base Ground Disasters Due to Earthquake," Journal of Research, PWRI, Vol. 11, 1966, pp. 1-32. (E)

41. Yoshida, I., "The Fall of the Showa Bridge Due to the Niigata Earthquake," The Bridge and Foundation Engineering, Vol. 1-10, October, 1967, pp. 24-27. (J)

42. Katayama, S. and Yamada, T., "Reconstruction of Bridges Damaged by the Niigata Earthquake," Annual Report of Roads, JRA, October, 1967, pp. 73-85. (E)

43. PWRI, "The Ebino Earthquakes of 1968, Report on Damage," Report of PWRI (1968), December, 1969, pp. 129-150. (J)

44. Architectural Institute of Japan (AIJ), "Report on Damage Due to the Tokachi-oki Earthquake of 1968," December, 1968, pp. 1-773. (J)

45. Kanai, et al., "Kushiro Strong-Motion Records and Damage to Structures Due to the Hiroo-oki Earthquake," March, 1969, pp. 1-130. (J)

46. Design Center for Long-Span Bridges, "Seismic Damage to Bridge Structures," A Report to the Public Works Research Institute, March, 1969, pp. 1-29. (J)

47. Hayashi, S., "Damage to Harbour Structures by the 1968 Tokachi-oki Earthquake," 2nd Joint Meeting of U.S.-Japan Panel on Wind and Seismic Effects, UJNR, May, 1970, pp. 1-37. (E)

48. Fukuoka, M. and Kuribayashi, E., "Survey on the Disaster Due to the Tokachi-oki Earthquake, 1968, Roads, Rivers and Highway Bridges," 2nd Joint Meeting of U.S.-Japan Panel on Wind and Seismic Effects, UJNR, May, 1970 (E); also Journal of Research, PWRI, Vol. 12, Part II, 1971, pp. 481-520 (E).

49. PWRI, "Damage to Roads, Dikes and Highway Bridges During the Tokachi-oki Earthquake," Soils and Foundations, Vol. X, No. 2, Japanese Society of Soil Mechanics and Foundation Engineering, June, 1970, pp. 15-38. (E)

50. PWRI, "Survey on Disaster Due to the Tokachi-oki Earthquake of 1968," Report of PWRI, No. 141, November, 1970, pp. 1-126. (J)

51. Tokyo Astronomical Observatory, "Rika Nenpyo (Annual Report of Science)," Maruzen, 1971, pp. 134-229 (in Chapter of Geography). (J)

52. Takahashi, R. and Hirano, K., "Present Status of the Strong-Motion Earthquake Observation in Japan and Some Analyses of the Observation Results," Proceedings, JEES, November, 1962, pp. 1-6. (J) (Summary in English)

53. PWRI, "Manual for Strong-Motion Earthquake Measurements on Public Works," Technical Memorandum of PWRI, No. 61, June, 1965, pp. 1-18. (J)

54. Kuribayashi, E. and Iwasaki, T., "Strong-Motion Earthquake Records from Public Works in Japan (the Matsushiro Quake Swarm, 9th December, 1965-28th February, 1966, the Ochiai Bridge)," Technical Memorandum of PWRI, No. 163, April 1, 1966, pp. 1-5. (J)

55. Kuribayashi, E. and Iwasaki, T., "Strong-Motion Earthquake Records from Public Works in Japan (the Matsushiro Quake Swarm, 1st March-22nd June, 1966, the Ochiai Bridge)," Technical Memorandum of PWRI, No. 194, July, 1966, pp. 1-28. (J)

56. Okubo, T., "Observation of Earthquake Response of Civil Engineering Structures," Proceedings, JEES, October, 1966, pp. 463-469. (J) (Summary in English)

57. Kuribayashi, E. and Iwasaki, T., "Strong-Motion Earthquake Records from Public Works in Japan (1961-1966)," Technical Memorandum of PWRI, No. 217, December, 1966, pp. 1-108. (J)

58. Kuribayashi, E. and Iwasaki, T., "Strong-Motion Earthquake Records from Public Works in Japan (the Matsushiro Quake Swarm, 25th June-1st December, 1966, the Ochiai Bridge)," Technical Memorandum of PWRI, No. 254, March, 1967, pp. 1-38. (J)

59. Kuribayashi, E. and Iwasaki, T., "Results of Strong-Motion Observation at the Ochiai Bridge During the Matsushiro Earthquakes," Proceedings, 9th Meeting on Earthquake Engineering, JSCE, October, 1967, pp. 5-8. (J)

60. Kuribayashi, E., Iwasaki, T., Wakabayashi, S., and Mimaki, T., "Strong-Motion Earthquake Records from Public Works in Japan (1967)," Technical Memorandum of PWRI, No. 341, February, 1968, pp. 1-159. (J)

61. PWRI, "Digitized Data of Strong-Motion Earthquake Records (No. 1)," Technical Memorandum of PWRI, No. 317, March, 1968, pp. 1-105. (J)

62. PWRI, "Digitized Data of Strong-Motion Earthquake Records (No. 2)," Technical Memorandum of PWRI, No. 318, March, 1968, pp. 1-148. (J)

63. Kuribayashi, E. and Iwasaki, T., "Observed Earthquake Responses of Bridges," Proceedings, 4th WCEE, January, 1969, pp. (B-1) 44-60 (E); also Journal of Research, PWRI, Vol. 12, Part I, 1971, pp. 213-229 (E).

64. Kuribayashi, E., Iwasaki, T., Wakabayashi, S., and Wakatsuki, T., "Strong-Motion Earthquake Records from Public Works in Japan (1968)," Technical Memorandum of PWRI, No. 430, April, 1969, pp. 1-190. (E)

65. Ariga, T., "Present Status of the Observations of Strong-Motion Earthquakes in Japan," 1st Joint Meeting of U.S.-Japan Panel on Wind and Seismic Effects, UJNR, Compiled by PWRI, April, 1969, pp. 23-43. (E)

66. PWRI, "Digitized Data of Strong-Motion Earthquake Records (No. 3)," Technical Memorandum of PWRI, No. 461, May, 1969, pp. 1-162. (J)

67. Kuribayashi, E. and Iwasaki, T., "Measurements and Analyses on Earthquake Response of Highway Bridges," Proceedings, 10th Meeting on Earthquake Engineering, JSCE, July, 1969, pp. 41-44. (J)

68. Iwasaki, T., "An Investigation on Earthquake-Resistant Design of Bridge Foundations Considering Dynamic Effects," The Bridge and Foundation Engineering, Vol. 3-10, October, 1969, pp. 144-150. (J)

69. Ariga, T., Hirono, T., and Tada, Y., "Notes on Some Important Results Obtained from Recent SMAC Records in Japan," 2nd Joint Meeting of U.S.-Japan Panel on Wind and Seismic Effects, UJNR, May, 1970. (E)

70. PWRI, "Descriptions of Strong-Motion Seismograph Installations on Structures," Vol. I, January, 1971. (J)

71. PWRI, "Descriptions of Strong-Motion Seismograph Installations on Structures," Vol. II, January, 1971. (J)

72. Kuribayashi, E., Iwasaki, T., Wakabayashi, S., and Wakatsuki, T., "Strong-Motion Earthquake Records From Public Works in Japan (1969)," Technical Memorandum of PWRI, No. 641, March, 1971, pp. 1-69. (E)

73. Shibata, N., "Analysis of Foundation Reactions," Kashima Publishing Co., January, 1959, pp. 1-114. (J)

74. Yokoyama, Y., "Design and Construction of Steel Piles," Sankaido, 1963, pp. 1-319. (J)

75. Tamano, H. and Yahagi, K., "Calculation Method of Pile Foundations (1) to (4)," The Bridge and Foundation Engineering, Vol. 1, Nos. 2-5, February to May, 1967, pp. 3-7, pp. 4-8, pp. 12-15, and pp. 15-19. (J)

76. Shimokawa, H. and Tanabe, S., "Comments on Design and Construction of Highway Bridges," The Bridge and Foundation Engineering, Vol. 1-9, September, 1967, pp. 1-5. (J)

77. JSCE, "Examples of Designing of Reinforced Concrete Structures Using Deformed Bars," Concrete Library No. 3, July, 1968, pp. 1-92. (J)

78. Horii, S., et al., "Planning, Surveying and Designing of Bridge Foundations," The Bridge and Foundation Engineering, Vol. 3, No. 10, October, 1969, pp. 66-143. (J)

79. Adachi, Y. and Izumi, T., "An Example of Design Calculation of Caisson Foundations," The Bridge and Foundation Engineering, Vol. 5, No. 3, March, 1971, pp. 7-12. (J)

80. Kawasumi, H., "Measures of Earthquake Danger and Expectancy of Maximum Intensity throughout Japan as Inferred from the Seismic Activity in Historical Times," Bulletin of ERI, University of Tokyo, Vol. 29, Part 3, 1951, pp. 469-482. (E)

81. Okamoto, S., "Chart of Seismic Activity in Japan," Ohm-sha, 1968, pp. 1-244. (J) and (E)

82. Goto, H. and Kameda, H., "A Statistical Study of the Maximum Ground Motion in Strong Earthquakes," Transactions, JSCE, Vol. 159, November, 1968, pp. 1-12. (J)

83. Goto, H. and Kameda, H., "Statistical Inference of the Future Earthquake Ground Motion," Proceedings, 4th WCEE, January, 1969, pp. (A-1) 39-54. (E)

84. Omote, S., "Seismicity of Japan," 1st Joint Meeting of U.S.-Japan Panel on Wind and Seismic Effects, UJNR, Compiled by PWRI, April, 1969, pp. 183-202. (E)

85. Okubo, T. and Terashima, T., "The Zoning Map of Earthquake Risk," Report of PWRI, January, 1970, pp. 1-18. (J)

86. Biot, M. A., "Analytical and Experimental Methods in Engineering Seismology," Transactions of ASCE, 1943, Paper No. 2183, pp. 365-408. (E)

87. Housner, G. W., Martel, R. R., and Alford, J. L., "Spectrum Analysis of Strong-Motion Earthquakes," Bulletin of SSA, Vol. 43, No. 2, April, 1953, pp. 97-119. (E)

88. Housner, G. W., "Behaviors of Structures During Earthquakes," Journal of EM Division, Proceedings of ASCE, October, 1959, pp. 109-129. (E)

89. Takata, T., Okubo, T., and Kuribayashi, E., "Earthquake Response Spectra - 1964 -- Studies on Earthquake-Resistant Design of Bridges, Part I," Report of PWRI, Vol. 128, April, 1966, pp. 1-51 (J); also Journal of Research, PWRI, Vol. 11, 1966, pp. 213-257 (E).

90. Katayama, T., "A Note on the Acceleration Ratio Spectrum of Seventy Japanese Strong-Motion Earthquake Records," Bulletin, Faculty of Science and Engineering, Chuo University, Vol. 12, December, 1969, pp. 7-18. (E)

91. Hayashi, S., Tsuchida, H., and Kurata, E., "Acceleration Response Spectra on Various Site Conditions," Proceedings, 3rd JEES, November, 1970, pp. 207-214 (E); also "Average Response Spectra for Various Subsoil Conditions," 3rd Joint Meeting of U.S.-Japan Panel on Wind and Seismic Effects, UJNR, May, 1971, pp. 1-17 (E).

92. Kuribayashi, E., Iwasaki, T., and Tuji, K., "Factors Affecting Earthquake Response Spectra," Proceedings, 11th Meeting on Earthquake Engineering, JSCE, July, 1971, pp. 71-74. (J)

93. Okabe, S., "General Theory on Earth Pressure and Seismic Stability of Retaining Walls and Dams," Journal of JSCE, Vol. 10, No. 6, 1924. (J)

94. Matsuo, H. and Ohara, S., "Lateral Earth Pressure and Stability of Quay Walls During Earthquakes," Proceedings, 2nd WCEE, Vol. I, 1960, pp. 165-181. (E)

95. Niwa, S., "An E..perimental Study of Oscillating Earth Pressures Acting on a Quay Wall," Proceedings, 2nd WCEE, Vol. I, 1960, pp. 281-296. (E)

96. Ishii, Y., Arai, H., and Tsuchida, H., "Lateral Earth Pressure in an Earthquake," Proceedings, 2nd WCEE, Vol. I, 1960, pp. 211-230. (E)

97. Ishii, Y., Tsuchida, H., and Furube, T., "Studies on Lateral Earth Pressure and Dynamic Pore Water Pressure of Water Saturated Sand During Vibration," Report of Port and Harbor Technical Research Institute, Vol. 2, No. 2, 1963.

98. Westergaard, H. M., "Water Pressure on Dams During Earthquakes," Transactions, ASCE, Vol. 98, 1933, pp. 1303-1318. (E)

99. Savage, J. L., "Earthquake Investigation for the Pit River Bridge," Civil Engineering, Vol. 9, 1939, pp. 470-472. (E)

100. Clough, R. W., "Effects of Earthquakes on Under-water Structures," Proceedings, 2nd WCEE, Vol. II, 1960, pp. 815-832. (E)

101. Sakurai, A., "Vibrational Problems of Underwater Column Structures," Doboku Gijitsu (Civil Engineering Technics), Vol. 16-6, June, 1961, pp. 11-17. (J)

102. Kotsubo, S., "External Forces on Submerged Bridge Piers with Elliptic Cross Section and Their Vibration During Earthquakes -- A Study on the Seismic Design of Underwater Structures," Transactions, JSCE, Vol. 120, April, 1965, pp. 14-24. (J)

103. Goto, H. and Toki, K., "Vibrational Characteristics and Aseismic Design of Submerged Bridge Piers," Proceedings, 3rd WCEE, January, 1966, Vol. V, pp. 107-125. (E)

104. Iwasaki, T., "Model Tests on Hydrodynamic Pressures on Submerged Caissons During Vibration," Technical Memorandum of PWRI, No. 202, October, 1966, pp. 1-51. (J)

105. Kubo, K., "Damping and Vibrational Characteristics of Bridge Piers," Proceedings, JEES, November, 1962, pp. 135-140. (J) (Summary in English)

106. Kuribayashi, E., "On Elastic and Damping Characteristics in Vibration of Pile-Foundation in Bridges," Proceedings, JEES, November, 1962, pp. 225-230. (J) (Summary in English)

107. Takata, T. and Narita, N., "A Dynamic Test on Ajigawa Bridge Pier," Proceedings, JEES, 1962, pp. 277-282. (J) (Summary in English)

108. Ito, M. and Katayama, T., "Damping of Bridge Structures," Transactions, JSCE, Vol. 117, May, 1965, pp. 12-22. (J)

109. Hatanaka, M., "Seismic Tests on Civil Engineering Structures," Proceedings, JEES, October, 1966, pp. 421-490. (J)

110. Sasado, M., Sato, T., and Akai, K., "Steel-Pipe Pile Loading Test in Tokyo-Nagoya Expressway," Annual Report of Roads, JRA, October, 1967, pp. 37-56. (E)

111. Sakamoto, Y. and Fujita, K., "Pier Foundation Steel Pile Anchored with Prestressing Strand to Rock," Annual Report of Roads, JRA, 1968, pp. 3-14. (E)

112. Hakuno, M. and Nojiri, Y., "An Experiment on Dynamical Properties of a Wall Foundation," Transactions, JSCE, Vol. 1, Part 2, 1969, pp. 301-317. (E)

113. Okubo, T. and Iwasaki, T., "Vibration Tests of a High Rise Bridge Pier Using Rocket Propulsion Method," Annual Report of Roads, 1969, JRA, November, 1969, pp. 44-50. (E)

114. Suruga, T., Tsuchimochi, H., Ichikawa, M., and Igarashi, K., "Sokozawa Bridge on Chuo Expressway," The Bridge and Foundation, Vol. 4, No. 2, February, 1970, pp. 20-27. (J)

115. Yamaguchi, S., Kawamoto, S., Fukuyama, T., Sato, S., Miyajima, N., Tawaraya, Y., and Yamada, T., "Studies on Vibrational Characteristics of the Continuous Curved Steel Box Girder Bridge," Proceedings, JEES, November, 1970, pp. 635-642. (J) (Summary in English)

116. Kuribayashi, E. and Iwasaki, T., "Experimental Studies on Vibrational Damping of Bridges -- Studies on Earthquake-Resistant Design of Bridges, Part III," Report of PWRI, No. 139, May, 1970, pp. 63-165. (J) (Summary in English)

117. Kuribayashi, E., Iwasaki, T., and Iida, Y., "Vibrational Characteristics of a Huge Foundation Structure," 3rd Joint Meeting of U.S.-Japan Panel on Wind and Seismic Effects, UJNR, May, 1971, pp. 1-18. (E)

118. Goto, H. and Kaneta, K., "Analysis with an Application to Aseismic Design of Bridge Piers," Proceedings, 2nd WCEE, Vol. II, March, 1961, pp. 1449-1465. (E)

119. Expressway Research Foundation, "Research on Bridges with Highrise Piers," February, 1966, pp. 1-48. (J)

120. Takata, T., Kurihara, T., and Kunihiro, T., "An Investigation on Vibrational Behaviors and Seismicity of Multispan Dywidag-type Prestressed Concrete Bridge -- Case of Amakusa Connecting 4th Highway Bridge," Report of PWRI, No. 128, April, 1966, pp. 121-146. (J)

121. Tajimi, H., "Dynamic Analysis of Structures Supported on Deep Foundations," Proceedings, JEES, October, 1966, pp. 255-260. (J) (Summary in English)

122. Otofuji, K., Kubo, K., Sasado, S., and Muto, T., "The Vibration Characteristics and Response of High Pier Bridges Due to An Earthquake," Proceedings, JEES, October, 1966, pp. 291-296. (J) (Summary in English)

123. Kuribayashi, E., Iwasaki, T., and Oyamada, Y., "Methods for Analyzing Earthquake Response of Structures, (1) - (7)," Doboku-Gijitsu-Shiryo (Technical Record in Civil Engineering), Vol. 8-11 - Vol. 9-5, November, 1966 - May, 1967. (J)

124. Expressway Research Foundation, "Research on Seismic Design (2)," February, 1970, pp. 1-98. (J)

125. Kuribayashi, E., Iwasaki, T., Oyamada, Y., and Tuji, K., "Effects of Ground Stiffness on Structures During Vibration," Proceedings, JEES, November, 1970, pp. 81-88. (J) (Summary in English)

126. Kotsubo, S., Harada, J., and Uno, K., "Transient Earthquake Response of Long-Span Bridges," Proceedings, JEES, November, 1970, pp. 421-428. (J) (Summary in English)

127. Ozaka, Y. and Kodera, J., "Dynamic Response of Railway Bridges and Its Application to the Design," Proceedings, JEES, November, 1970, pp. 747-754. (J) (Summary in English)

128. Kuribayashi, E., Takada, K., and Kimura, K., "Model Tests on Earthquake Resistance of a Prestressed Concrete Viaduct, (I) and (II)," Doboku-Gijitsu-Shiryo (Technical Record in Civil Engineering), Vols. 5-2, 3, February, March, 1963, pp. 11-16 and pp. 13-15. (J)

129. Ogata, N. and Kotsubo, S., "Seismic Force Effect on Pile Foundation," Proceedings, JEES, October, 1966, pp. 55-60. (J) (Summary in English)

130. Konishi, I., Yamada, Y., Takaku, T., Ikumi, H., and Isa, T., "Experimental Studies on Effects of Structural Damping and Foundation Conditions to Earthquake Responses of Suspension Bridge Tower Pier Systems," Proceedings, JEES, October, 1966, pp. 285-290. (E)

131. Kubo, K., "Vibration Test of a Structure Supported by Pile Foundation," Proceedings, 4th WCEE, January, 1969, Vol. III, pp. (A-6) 1-12. (E)

132. Kuribayashi, E., Oyamada, Y., and Iida, Y., "Earthquake Responses of the Honshu-Shikoku Suspension Bridge," Proceedings, JEES, November, 1970, pp. 627-634. (J) (Summary in English)

133. Okamoto, S. and Kubo, K., "Damping Coefficients Measured at Suspension Bridges," Seisan Kenkyu, University of Tokyo, Vol. 9-12, 1957. (J)

134. Konishi, I. and Yamada, Y., "Earthquake Responses of a Long Span Suspension Bridge," Proceedings, 2nd WCEE, July, 1960, Vol. II, pp. 863-878. (E)

135. Kubo, K., "Aseismicity of Suspension Bridges Forced to Vibrate Longitudinally," Proceedings, 2nd WCEE, July, 1960, Vol. II, pp. 913-929. (E)

136. Kubo, K., "Vibration of Suspension Bridge Due to Vertical Ground Motion," Transactions, JSCE, No. 75, July, 1961, pp. 69-76. (J) (Summary in English)

137. Konishi, I., Yamada, Y., and Takaoka, N., "Earthquake-Resistant Design of Long Span Suspension Bridges," Proceedings, JEES, November, 1962, pp. 87-92. (E)

138. Konishi, I., Yamada, Y., Takaku, T., Ikumi, H., and Isa, T., "Experimental Studies on Effects of Structural Damping and Foundation Conditions to Earthquake Responses of Suspension Bridge Tower Pier Systems," Proceedings, JEES, October, 1966, pp. 285-290. (E)

139. Kuribayashi, E., "Seismic Design Method Taking into Account Dynamic Response for the Honshu-Shikoku Suspension Bridge," Proceedings, JEES, October, 1966, pp. 397-402. (J) (Summary in English)

140. Kuribayashi, E., Iwasaki, T., and Oyamada, Y., "Research on Earthquake-Resistant Design of the Honshu-Shikoku Suspension Bridges," Technical Memorandum of PWRI, October, 1966, pp. 171-239. (J)

141. Takata, T., Kuribayashi, E., and Narita, N., "Field Tests and Notes on Aseismic Design of Suspension Bridges," International Symposium on Suspension Bridges, November, 1966 (E); also Journal of Research, PWRI, Vol. 11, Part I, 1971, pp. 47-53. (E)

142. Takata, T., Okubo, T., and Kuribayashi, E., "Earthquake Load in the Trans-Seto Inland Sea Suspension Bridge," PWRI, June, 1967, pp. 31-46. (E)

143. Konishi, I. and Yamada, Y., "Studies on the Earthquake-Resistant Design of Suspension Bridge Tower and Pier System," Proceedings, 4th WCEE, January, 1969, Vol. II, pp. (B-4) 107-118. (E)

144. Kuribayashi, E., "Application of Earthquake Forces Taking into Account Dynamic Structural Responses to Earthquake-Resistant Design of Long-Span and Deep-Foundation Suspension Bridges -- Studies on Earthquake-Resistant Design of Bridges, Part II," Report of PWRI, No. 136, July, 1969, pp. 13-45. (J) (Summary in English)

145. Yamada, Y. and Takemiya, H., "Studies on the Responses of Multi-Degree-of-Freedom Systems Subjected to Random Excitation with Applications to the Tower and Pier Systems of Long Span Suspension Bridges," Transactions, JSCE, Vol. 1, Part 1, 1969, pp. 59-74. (E)

146. Takaoka, N. and Sato, Y., "Influence of Rocking Motion of Tower Piers on the Earthquake Response of Long Span Suspension Bridge Towers," Transactions, JSCE, Vol. 1, Part 2, 1969, pp. 435-444. (E)

147. Kurata, M., Okamura, H., Tada, H., and Shindo, Y., "Three-Dimensional Vibrations of Tower and Multi-Column Pier Foundations," Proceedings, JEES, November, 1970, pp. 397-404. (J) (Summary in English)

148. Yamada, Y. and Takemiya, H., "Earthquake Response Analysis and Earthquake-Resistant Design of Multi-Degree-of-Freedom Systems," Proceedings, JEES, November, 1970, pp. 413-420. (E)

149. Kuribayashi, E., Oyamada, Y., and Iida, Y., "Earthquake Responses of the Honshu-Shikoku Suspension Bridge," Proceedings, JEES, November, 1970, pp. 627-634. (J) (Summary in English)

150. JSCE, "Report of Research for Improving the Earthquake-Resistant Design Criteria for the Honshu-Shikoku Bridges," June, 1971, pp. 1-18. (J)

151. Okamoto, S., "On Designed Seismic Safety Factor of Bridges," Annual Report of Roads, JRA, 1961, pp. 18-28. (E)

152. Uemae, Y., "A Proposal for Aseismatic Bridge Structure by Damper Method," Annual Report of Roads, JRA, September, 1962, pp. 13-21. (E)

153. Kodera, J., "How to Apply the Experience of the Earthquake Failures to the Design of the Piers," Proceedings, JEES, November, 1962, pp. 129-134. (J) (Summary in English)

154. Goto, H. and Watabe, T., "Studies on Earthquake Resistance of Single Pedestal-Type Bridge Piers Arranged under Elevated Highway," Proceedings, JEES, November, 1962, pp. 141-146. (J) (Summary in English)

155. Okamoto, S., "Seismicity and Earthquake-Resistant Design of Civil Engineering Structures," Proceedings, JEES, November, 1962, pp. 289-293. (J)

156. Kodera, J., "On Dynamic Methods in Designing Bridge Superstructures," Proceedings, JEES, November, 1962, pp. 297-301. (J)

157. Kubo, K., "Earthquake-Resistant Design of Substructures of Civil Engineering Structures," Proceedings, JEES, November, 1962, pp. 323-327. (J)

158. Tajimi, H., "An Approximate Method of Determining the Optimum Lateral Strength of Structures for Seismic Design," Proceedings JEES, November, 1962, pp. 75-80. (J) (Summary in English)

159. Ogata, N. and Kotsubo, S., "Seismic Force Effect on Pile Foundation," Proceedings, JEES, October, 1966, pp. 55-60. (J) (Summary in English)

160. Tamura, K., "An Earthquake-Resistant Design for Caissons in Cohesive Soil," Proceedings, JEES, October, 1966, pp. 403-408. (J) (Summary in English)

161. Hachioji Construction Bureau, Japan Highway Public Corporation, "On Seismic Design of Bridges on the Chuo Expressway," September, 1968, pp. 1-57. (J)

162. Kuribayashi, E., "A Study on Optimum Resistibility to Earthquakes -- Evaluation of Economic and Social Conditions," Technical Memorandum of PWRI, No. 522, July, 1969, pp. 1-9. (J)

163. Kuribayashi, E., Iwasaki, T., Oyamada, Y., and Iida, Y., "Design Seismic Coefficients for Bridges with Highrise Piers -- Modified Seismic Coefficients Considering Dynamic Response in the Transverse Direction," Technical Memorandum of PWRI, No. 548, December, 1969, pp. 1-22. (J)

164. Yamada, Y. and Takemiya, H., "Studies on the Statistical Aseismic Safety of Relatively Long Period Structures," Transactions, JSCE, Vol. 1, Part 2, 1969, pp. 445-460. (E)

165. Kodera, J., "On Earthquake-Resistant Design of Bridges, (1) - (3)," Doboku Gijitsu (Civil Engineering Technics), Vols. 26-3, 4, 5, March to May, 1971, pp. 37-44, pp. 32-39, and pp. 34-40. (J)

166. Omote, S., et al., "Lectures on Earthquake Engineering, (1) - (7)," Journal, JSCE, Vols. 48-6 to 12, June to December, 1963, pp. 64-70, pp. 112-119, pp. 86-93, pp. 57-63, pp. 65-73, pp. 78-82, and pp. 98-104. (J)

167. PWRI, "Literature Survey on Earthquake Resistance of Soils, Grounds and Fill Type Structures," Bulletin, PWRI, No. 26, October, 1966, pp. 1-28. (J)

168. PWRI, "Earthquake Damage to Fill Type Structures," Bulletin, PWRI, No. 27, October, 1966, pp. 1-43. (J)

169. Murakami, E. and Okubo, T., "Recent Trends of Highway Bridges and Aseismic Design of Them," PWRI, February, 1967, pp. 1-12. (E)

170. Japan National Committee of IAEE, "Some Recent Earthquake Engineering Research and Practice in Japan," December, 1968, pp. 1-171. (E)

171. PWRI, "Summarized Note on the Survey of the Damage of Engineering Structures Caused by Recent Earthquakes," Technical Memorandum of PWRI, No. 531, July, 1969, pp. 1-21. (J) (E)

172. PWRI, "Review of Recent Studies on Earthquake Engineering at the Public Works Research Institute," Technical Memorandum of PWRI, No. 532, July, 1969, pp. 1-20. (J) (E)

173. Iseda, T., "The Present Status of Study and Research in the Public Works Research Institute," PWRI, August, 1969, pp. 1-16 (E); also Journal of Research, PWRI, Vol. 12, Part II, 1971, pp. 343-359 (E).

174. Kuribayashi, E., "Lectures on Earthquake Engineering, (1) - (15)," The Bridge and Foundation Engineering, Vol. 3-2 (February, 1969) - Vol. 4-5 (May, 1970), pp. 35-39, pp. 34-38, pp. 37-41, pp. 38-41, pp. 31-36, pp. 41-44, pp. 37-40, pp. 37-41, pp. 43-46, pp. 34-39, pp. 38-42, pp. 40-43, pp. 41-46, pp. 51-54, and pp. 41-44. (J)

175. JRA, "Annual Report of Roads, 1962," September, 1962, pp. 1-123. (E)

176. JRA, "Annual Report of Roads, 1963," December, 1963, pp. 1-136. (E)

177. JRA, "Annual Report of Roads, 1964," August, 1964, pp. 1-143. (E)

178. JRA, "Annual Report of Roads, 1965," July, 1965, pp. 1-178. (E)

179. Ministry of Construction, Japan, "Ministry of Construction, Its Organization and Function," 1966, pp. 1-42. (E)

180. PWRI, "Facilities and Instruments for Earthquake Engineering at PWRI," Technical Memorandum of PWRI, No. 218, December, 1966, pp. 1-50. (J)

181. JRA, "Annual Report of Roads, 1967," October, 1967, pp. 1-156. (E)

182. Yoshida, K., "Characteristics of Tokyo-Fujiyoshida Route of Chuo Expressway," Annual Report of Roads, 1968, JRA, 1968, pp. 50-70. (E)

183. JRA, "Annual Report of Roads, 1969," November, 1969, pp. 1-79. (E)

184. JRA, "Roads in Japan, 1969," Published by JRA and Edited by Road Bureau, Ministry of Construction, 1969, pp. 1-72. (E)

185. National Disaster Prevention Research Center, Science and Technology Agency, "Large-Size Earthquake Engineering Experimental Apparatus," March, 1970. (J)

186. JSCE, "Civil Engineering in Japan, Vol. 9, 1970," JSCE, 1970, pp. 1-181. (E)

187. JSCE, "Bridges in Japan, 1969-1970," February, 1971, pp. 1-94. (J)

188. Road Bureau, Ministry of Construction, "Pocket Book on Roads, 1971," April, 1971, pp. 1-72. (J)

189. JSCE, "Proceedings of the 1st Meeting on Earthquake Engineering," September, 1957, pp. 1-54. (J)

190. JSCE, "Proceedings of the 2nd Meeting on Earthquake Engineering," September, 1958, pp. 1-46. (J)

191. JSCE, "Proceedings of the 3rd Meeting on Earthquake Engineering," September, 1959, pp. 1-68. (J)

192. JSCE, "Proceedings of the 4th Meeting on Earthquake Engineering," November, 1960, pp. 1-66. (J) (Partially E)

193. JSCE, "Proceedings of the 5th Meeting on Earthquake Engineering," October, 1961, pp. 1-65. (J) (Partially E)

194. AIJ, JSCE, JSSMFE, and SSJ, "Proceedings of Japan National Symposium on Earthquake Engineering," November, 1962, pp. 1-327. (J) (Summary in English)

195. JSCE, "Proceedings of the 6th Meeting on Earthquake Engineering," October, 1963, pp. 1-41. (J)

196. JSCE, "Proceedings of the 7th Meeting on Earthquake Engineering," October, 1964, pp. 1-48. (J)

197. JSCE, "Proceedings of the 8th Meeting on Earthquake Engineering," October, 1965, pp. 1-51. (J)

198. AIJ, JSCE, JSSMFE, and SSJ, "Proceedings of Japan Earthquake Engineering Symposium, 1966," October, 1966, pp. 1-496. (J) (Summary in English)

199. JSCE, "Proceedings of the 9th Meeting on Earthquake Engineering," October, 1967, pp. 1-103. (J)

200. U.S.-Japan Cooperative Program in Natural Resources (UJNR), "Presentations by Japanese Members to the 1st Joint Meeting of U.S.-Japan Panel on Wind and Seismic Effects," Edited by PWRI, April, 1969, pp. 1-230 (Paper 5 of Japan Side). (E)

201. JSCE, "Proceedings of the 10th Meeting on Earthquake Engineering," July, 1969, pp. 1-116. (J)

202. UJNR, "Preprints for the 2nd Joint Meeting of U.S.-Japan Panel on Wind and Seismic Effects," May, 1970. (E)

203. AIJ, JSCE, JSSMFE, and SSJ, "Proceedings of the 3rd Japan Earthquake Engineering Symposium, 1970," November, 1970, pp. 1-826. (J) (Summary in English)

204. UJNR, "Preprints for the 3rd Joint Meeting of U.S.-Japan Panel on Wind and Seismic Effects," May, 1971. (E)

205. JSCE, "Proceedings of the 11th Meeting on Earthquake Engineering," July, 1971, pp. 1-145. (J)

206. Monanobe, N."Earthquake-Resistant Design of Civil Engineering Structures," Riko-Tosho, 1933, 1952 (Revised), pp. 1-283. (J)

207. Goto, H., et al., "Handbook for Disaster Prevention," Giho-Do, December, 1964, pp. 93-204. (J)

208. Yamada, Y., et al., "A Text on Dynamic Behaviors of Bridges," JSSC, December, 1969, pp. 1-401. (J)

209. Okamoto, S., et al., "New Design Method of Civil Engineering Structures," Kanto Branch of JSCE, December, 1970, pp. I-1 - IX-28. (J)

210. Okamoto, S., "Earthquake Engineering," Ohm-sha, September, 1971, pp. 1-473. (J)

211. Ministry of Education, "Japanese Scientific Terms in Civil Engineering," Published by JSCE, 1954, pp. 1-395. (J) (E)

212. Japanese Society of Soil Mechanics and Foundation Engineering (JSSMFE), "Terminology in Soil Engineering," Giho-Do, July, 1957, pp. 1-75. (J) (E)

213. Ministry of Education, "Terminology in Seismology," November, 1966, pp. 1-71. (J) (E)

214. Takeuchi, H., et al., "Terminology in Geoscience, Vols. I and II," Kokin-Shoin, December, 1970, pp. 1-483, pp. 1-656. (J) (Terms in English)

215. JSCE, "Terminology in Civil Engineering," 1971, pp. 1-1421. (E)

216. Sturman, G. G., "The Alaska Highway System," The Great Alaska Earthquake of 1964: Engineering, National Academy of Sciences (to be published). (E)

217. Ross, G. A., Seed, H. B., and Migliaccio, R. R., "Performance of Highway Bridge Foundations," The Great Alaska Earthquake of 1964: Engineering, National Academy of Sciences (to be published). (E)

218. Golub, H., Bridge damage report, March 27, 1964, earthquake, Anchorage: Alaska Department of Highways, April 24, 1964. (E)

219. Sherman, R. G. and Shumway, R. D., Foundation study report, Snow River Bridge No. 605, center channel. Project No. F-031-(6)., Anchorage: Alaska Department of Highways, May, 1962. (E)

220. Smith, C. P., Highway destruction in Alaska: Part I, Alaska bridges experience an earthquake, Transport-Communications Monthly Review, August, 1965. (E)

221. Migliaccio, R., Earthquake damage to highways in the Valdez District, Alaska, Anchorage: Alaska Department of Highways, January, 1965. (E)

222. Alaska Department of Highways, Report of damage caused by March 27, 1964, earthquake to Alaska's federal-aid highway system, Juneau: Alaska Department of Highways, 1964. (E)

223. Ellison, B. K., "Earthquake Damage to Roads and Bridges, Madang, R.P.N.G. -- Nov. 1970," Bulletin of the New Zealand Society for Earthquake Engineering, Vol. 4, No. 2, April, 1971. (E)

224. Eisenberg, A., Husid, R., and Luco, J. E., "A Preliminary Report -- The July 8, 1971 Chilean Earthquake," Bulletin of the Seismological Society of America, Vol. 62, No. 1, February, 1972. (E)

225. California Division of Highways, "San Fernando Earthquake of February 9, 1971," EERI-NOAA Report, Section on Bridges, by Bridge Department (to be published). (E)

226. Allen, C. R., et al., "Main Shock and Larger Aftershocks of the San Fernando Earthquake, 9 February through 1 March 1971 -- A Preliminary Report," Seismological Laboratory, California Institute of Technology, Pasadena, California. (E)

227. California Division of Highways, "Bridge Planning and Design Manual," Vol. 1 - Design Specifications, March, 1968, pp. 2-24. (E)

228. Shepherd, R. and Charleson, A. W., "Experimental Determination of the Dynamic Properties of A Bridge Substructure," Bulletin of the Seismological Society of America, Vol. 61, No. 6, December, 1971, pp. 1529-1548. (E)

229. Charleson, A. W., "The Dynamic Behaviour of Bridge Substructures," A Report to The National Roads Board, University of Canterbury, New Zealand, 1970. (E)

230. Arya, A. S. and Thakkar, S. K., "Response of the Substructure of A Major Bridge to Earthquake Motions," Journal of the Indian Roads Congress, Vol. XXXIII-2, September, 1970. (E)

231. Penzien, J., "Soil-Pile Foundation Interaction," Earthquake Engineering (R. L. Wiegel, coordinating editor), Prentice-Hall, Inc., 1970. (E)

232. California Division of Highways, "Report on Evaluation and Modification of Earthquake-Resistant Design Criteria," Internal Report of the Bridge Department, March 16, 1971. (E)

233. Joshi, R. N. and Apte, M. P., "Aseismic Design of Bridges," Paper No. 235, Indian Roads Congress. (E)

234. Krishna, J., "Basic Principles Underlying Seismic Design of Bridges," Third Symposium on Earthquake Engineering, SRTEE, University of Roorkee, Roorkee, India, November, 1966. (E)

235. Arya, A. S. and Prakash, A., "Behaviour of Cellular Bridge Piers under Dynamic Loads," Bulletin of the Indian Society of Earthquake Technology, Vol. VI, No. 3, September, 1969. (E)

236. Arya, A. S. and Thakkar, S. K., "Earthquake Response of a Tied Cantilever Bridge," Proceedings, Third European Symposium on Earthquake Engineering, Sofia, Bulgaria, September, 1970. (E)

237. Chandrasekaran, A. R., "Behavior of Simply Supported Bridges Under Earthquakes," Journal of Institution of Engineers (India), Vol. 50, No. 7, March, 1970. (E)

238. Troitsky, M. S., "Aseismic Design of Bridges," Proceedings, 1st Canadian Conference on Earthquake Engineering, Vancouver, Canada, May, 1971. (E)

239. Tezcan, S. S. and Cherry, S., "Earthquake Analysis of Suspension Bridges," Proceedings, 4th WCEE, Santiago, Chile, 1969. (E)

240. Kodera, J., "Some Tendencies in the Failures of Bridges and Their Foundations During Earthquakes," Proceedings, 3rd WCEE, New Zealand, 1965. (E)

241. Lium, R. G., "Earthquake-Resistant Design Details for Concrete Bridges," American Concrete Institute First International Symposium on Concrete Bridge Design, Committee 443, 1970. (E)

APPENDIX B

BRIEF SUMMARY OF SEISMIC DESIGN CODES IN VARIOUS COUNTRIES

		Page
1.	Argentina	B-2
2.	Bulgaria	B-3
3.	Canada	B-4
4.	Chile	B-5
5.	Cuba	B-6
6.	El Salvador	B-7
7.	Greece	B-8
8.	India	B-9
9.	Iran	B-10
10.	Israel	B-11
11.	Italy	B-12
12.	Japan (JRA, TEPC, JSCE(Honshu-Shikoku), JSCE (JNR))	B-13
13.	Mexico	B-17
14.	New Zealand	B-18
15.	Peru	B-19
16.	Philippines	B-20
17.	Portugal	B-21
18.	Rumania	B-22
19.	Turkey	B-23
20.	U.S.A.	B-24
21.	Venezuela	B-25

COUNTRY	SPECIFICATIONS	Seismic Coefficient, k (k in V = kW)	Increase in Allowable Stresses	Remarks
ARGENTINA	Centro Para Estudio De Normas Estructurales Del Holmigon (CINEH)	$k = \gamma_e \gamma_d S C_o$		Regulation on Instrumentation

zone	Basic Coefficient Co
3	0.1
2	0.07
1	0.04
0	0

σ_a : Allowable Bearing Power of the Ground

S (Magnification Factor)

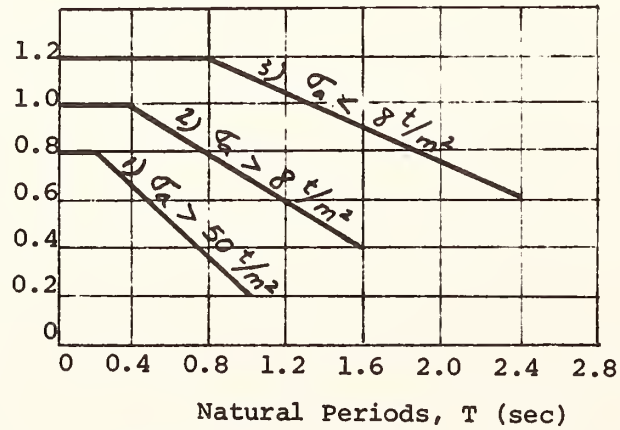

Usage	γ_d
Group A) Specially Important	1.3
B) Ordinary	1.0
C) less important	0.8

Type of Structure	γ_e
Type I) strong	1.0
II) medium	1.3
III) weak	1.8

COUNTRY	SPECIFICATIONS	Seismic Coefficient, k	Increase in allow stresses	Remarks
BULGARIA	State committee for Building and Architecture, Ministry of Construction, Bulgaria. Code for Buildings in Earthquake Region (1964)	$k = \Psi\beta\eta k_c$	50%	

Basic Seismic Coef. kc

Soil Condition	Seismic Intensity VII	VIII	IX
1. Rock	-	-	0.05
2. Semi-rock, coarse gravel, rigid clay	-	0.033	0.067
3. Medium	0.025	0.050	0.1
4. Soft	0.033	0.067	0.133

η: Coef. of Mode shape (1.35 for first mode)

β: dynamic coef. of one-degree-of-freedom system $\beta = 0.9/T$. $0.6 \leq \beta \leq 3$.

Ψ: coef. accounting damping capacity of structures
= 1.0 - ordinary structures,
= 1.5 - flexible structures with small damping.

Usage	Region of Seismic Intensity in (M.M.) VII	VIII	IX
A. Especially Important	VII	IX	X*
B. Important	VII	VIII	IV
C. Ordinary	VII	VII	VIII
D. Less Important	not considered		

* Seismic Force for X = 1.3 X (IX)

COUNTRY	SPECIFICATIONS	Seismic Coefficient, k	Increases in Allowable Stresses	Remarks
CANADA	National Building Code of Canada, 1970	$k = (\frac{1}{4})\ R \cdot K \cdot C \cdot I \cdot F$ R = Seismic Regionalization Factor depending on Climate Data K = 0.67 - 3.00 (on structure) C = 0.10 for 1 and 2 - storey building $C = 0.05 / \sqrt[3]{T}$ (max. = 0.1) I = 1.3 (post disaster service, school) or = 1.0 (other) F = 1.5 (soils of low dynamic shear modulus) or = 1.0 (other soils)		

COUNTRY	SPECIFICATIONS	Seismic Coefficient, k (k in V = k W)	Increases in Allowable Stresses	Remarks
CHILE	Institute Nacional De Investigaciones Technologicasy Normalizacion (INDITECNOR)	$k = K_1 K_2 C$		Regulations on Instrumentation, Dynamic Analysis

Usage	K_1
a) Specially Important	1.2
b) Ordinary	1.0
c) Less Important	0.8

Type of Structure	K_2
d) weak	1.2
e) Moderate	1.0
f) Strong	0.8

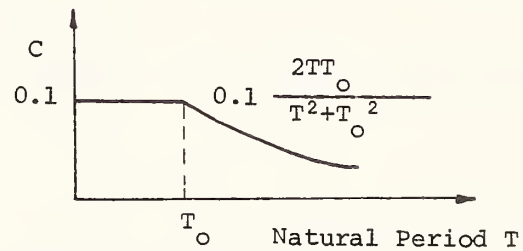

T; Natural Fundamental Period

Ground Condition	T_o (sec)
Rock, Dense gravel	0.2
Dense Soil	0.3
Soft	0.9

COUNTRY	SPECIFICATIONS	Seismic Coefficient, k				Increase in Allowable Stresses	Remarks
CUBA	NOCAE NO. 1 Standards for Structural Design	1) Static Method (For Mercalli 8 zone)				a) Wood and structural or reinforcing steel, 50% b) Other metals, Concrete and masonry, 33% c) Soil, 33%	Regulation on Limit for Horizontal Displacement
		Importance	Type of Structure	High Compressibility zone	Low Compressibility zone		
		A (Specially)	1 Strong	0.08	0.05		
			2 Medium	0.1	0.1		
			3 Weak	0.2	0.13		
		B (Ordinary)	1 Strong	0.06	0.04		
			2 Medium	0.08	0.08		
			3 Weak	0.15	0.10		
		C (Less)	1 Strong	0	0		
			2 Medium	0	0		
			3 Weak	0	0		
		2) Dynamic Method $k = K_c \beta \eta$ $K_c = 0.05$ (For Mercalli 8 zone) β = dynamic Factor For shear deformation structures : $0.6 < \beta = \frac{0.9}{T} < 3$ For flexure deformation structures (of small damping) : $1 < \beta = \frac{1.5}{T} < 5$ η : coef. varying with mode shape Dynamic Method > (60%) Static One					

COUNTRY	SPECIFICATIONS	Seismic Coefficient, k	Increase in Allowable Stresses	Remarks
EL SALVADOR	Regulations for Seismic Design, Republic of El Salvador, C.A. 21, January, 1966	k = C or CD Values of C Group (A): 1.3 Times Group (B) Group (B): Type of Str. / Seismic Zone / Seismic Zone 1 / 0.12 / 0.06 2 / 0.24 / 0.12 3 / 0.30 / 0.15 Group (C): 0 Group and type of str. see Mexican Regulation (p. B-17) Reduction Factor $D=\sqrt{C/X_e}$ $(0.6<D<1.0)$ X_e = displacement of Center of gravity of body due to seismic coef. C (cm)	a) Timber, Structural or Reinforcing Steel, 50% b) Other metals, concrete, masonry 33% c) Soils: Study	Regulations on Dynamic Analysis, Instrumentation

COUNTRY	SPECIFICATIONS	Seismic Coef. k	Increase in Allowable Stresses	Remarks
GREECE	Royal Decree About Anti-Seismic Regulation for Building Construction, June 1959		Concrete - 20% Steel - 20%	

Seismicity of areas	Soil Condition (a)	(b)	(c)	(d)
I slight	0.04	0.06	0.08	*
II Moderate	0.06	0.08	0.12	
III Strong	0.08	0.12	0.16	

Soil Conditions:

(a) good
(b) moderate
(c) poor
(d) worst

Definitions are defined

* Construction of permanent building must be avoided except there is no possibility to confront eventual risk of land slide or settling.

COUNTRY	SPECIFICATIONS	Seismic Coefficient, k	Increase in Allowable Stresses	Remarks
INDIA	Indian Standard Criteria for Earthquake Resistant Design of Structures (1966)		Permissible Increase Soil I 50% " II 30% " III 30%	Vertical Coef = 1/2 (Horiz.) Regulations on Hydro-Dynamic Pressure, Earth pressure on Retaining Walls. Regulation on Details for the Design of Bridges

Zone No.	Horiz. Seis. Coef. k: Soil Type I	Soil Type II	Soil Type III
VI	0.08	0.1	0.12
V	0.06	0.08	0.10
IV	0.05	0.06	0.08
III	0.04	0.05	0.06
II	0.02	0.03	0.04
I	0	0.01	0.02
0	0	0	0

Soil Type I : $\sigma_a > 45t/m^2$
" II : $\sigma_a > 20t/m^2$
" III: $\sigma_a > 10t/m^2$ (N > 10)

(σ_a: allowable bearing power of the soil)

Loose sands with N < 10 may liquefy: In important project, need special investigations. k: consider only above scour depth: For portions below the scour depth, k = 0
Seismic force shall be calculated on the basis of depth of scour caused by mean annual flood.

COUNTRY	SPECIFICATIONS	Seismic Coefficient, k	Increase in Allowable Stresses	Remarks
IRAN	Iranian Antiseismic Code for <u>Building</u> Construction	$k = K \cdot C$ $K = 1$ (Seismicity Coef.) $C = 0.1$ (for soil with normal bearing capacity less than 10 t/m^2) $C = 0.08$ (for soil with normal bearing capacity more than 10 t/m^2) For public bldg.: 25% increase. For bldg. having 5 story or more structures higher than 18m, C shall be determined by $C = \frac{0.025}{T} \geqq 0.04$ T : fundamental period (sec.) $C = \frac{0.05}{T}$: for chimney, towers, reservoirs.	1/3	

COUNTRY	SPECIFICATIONS	Seismic Coefficient, k			Increase in Allowable Stresses	Remarks
		Seismicity / Building and Soil	Value of k REGION A	Value of k REGION B		
ISRAEL	Proposed Israel Standard Loads in Buildings: Earthquakes	Whole Buildings			1/3	Regulation on Seismic Coefficient for Structural Parts
		1.1 Multi-Story Buildings founded on good soil ($\sigma_a \geq 15t/m^2$)	0.1 / m + 4.5	0.2 / m + 4.5		
		1.2 Multi-Story Buildings founded on bad soil ($\sigma_a < 15t/m^2$)	0.2 / m + 4.5	0.4 / m + 4.5		
		1.3 Various Structures such as reservoirs, connected building, etc. founded on good soil ($\sigma_a \geq 15t/m^2$)	0.02	0.04		
		1.4 Various Structures shown in 1.3, founded on bad soil ($\sigma_a < 15t/m^2$)	0.04	0.08		
		1.5 Slender Structures (water towers, chimneys)	0.04	0.08		
		m : number of stories above one under consideration and assuming that the floor panels or other structural stiffness elements transmit the forces in their plane. Region A : up to Intensity VII Region B : up to Intensity IX				

COUNTRY	SPECIFICATIONS	Design Seismic Coefficient k	Allowable Stresses	Remarks
ITALY	Italian Standard Specifications for Buildings in Seismic Zones	k zone a / zone b Basic k: 0.1g / 0.05g F_H: 0.1(D + 1/3.L) / 0.05(D + 1/3.L) F_V: 1.4(D + 1/3.L) / 1.25(D + 1/3.L) $F_V > D + L$ D : Dead Load L : Live Load F_H: Horizontal Force F_V: Vertical Force	mild steel f_s = 1,400 kg/cm^2 medium steel f_s = 2,000 kg/cm^2	not simultaneous Horizontal and Vertical

COUNTRY	JAPAN	CODE	Japan Road Association, "Specifications for Earthquake-Resistant Design of Highway Bridges (1971)," and Related Specifications.

DESIGN SEISMIC COEFFICIENT

(1) Conventional Seismic Coefficient Method (for relatively rigid structures; T < 0.5 sec)

$k_h = \nu_1 \cdot \nu_2 \cdot \nu_3 \cdot k_o > 0.1$

$k_o = 0.2$

Table 1

Zone	ν_1
A) Active	1.0
B) Moderate	0.85
C) Mild	0.7

Table 2

Ground Conditions	ν_2
1. Rock	0.9
2. Diluvium	1.0
3. Alluvium	1.1
4. Soft	1.2

Table 3

Importance	ν_3 *	Remarks
Important	1.0	General
Less important	0.8	

* When exceptionally important, ν_3 can be up to 1.25.

(2) Modified Seismic Coefficient Method Considering Structural Response (for relatively flexible structures such as ones with high-rise piers higher than 25m or ones with fundamental natural periods longer than 0.5 sec)

$k_{hm} = \beta k_h > 0.05$ (k_h: CSCM in (1))

β is shown in Fig. 1 ($0.5 < \beta < 1.25$), $\beta = 1.0$ for $T < 0.5$ sec.

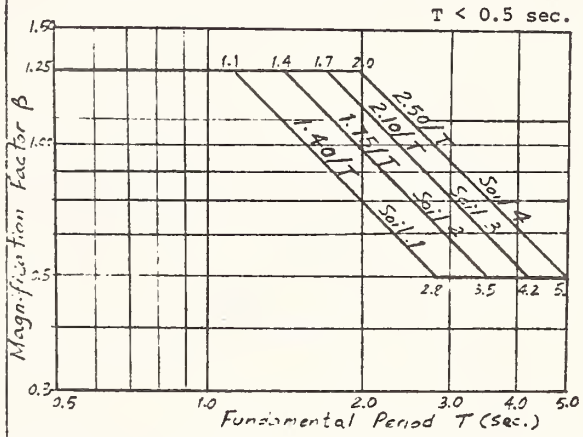

Notes for both (1) and (2):

1) Vertical Coefficient $k_v = 0$ except for special parts like supports

2) $k_h = 0$ for structural parts under the ground (except underground structures)

Fig. 1 The Value of Factor β

Increases in Allowable Stresses

Concrete and Reinforcements in RC Structures: 50%, Prestressed Concrete: 65% for Compression Zone

Steel: 70% for Superstructures and 50% for Substructures, Foundation Soils: 50%

Remarks

Provisions on the followings are specified.

1) Earth and water pressures during earthquakes,

2) Soils which have no resistance during earthquakes (due to liquefaction of sands)

3) Special attention to prevent fall of superstructures from substructures.

COUNTRY	JAPAN	CODE	Specifications for Earthquake Resistant Design in Tokyo Expressways Public Corporation (July, 1967).

DESIGN SEISMIC COEFFICIENT

Table 1. Seismic Coefficients (see Note (a) below)

Classification of Soil Condition		1	2	3	4
Horizontal Coefficients, k_h	Above ground	0.2	0.24	0.27	0.3
	Under-ground	0.15	0.18	0.20	0.23
Vertical Coefficients, k_v		0.1	0.1	0.1	0.1

Table 2. Classification of Soil Condition (see Note (b) below

Property of Alluvial Layer or Loam Layer / Depth of Alluvial layer or Loam Layer	Gravel	Sand, Clay and Loam (N > 5)	Soft Soil	
			N=2-5	N < 2
0-3m	See Note (c) below			
3-10m	3(2)	3(2)	4(3)	4(3)
10-25m	3(2)	4(3)	4(3)	4(4)
25 or more	4(3)	4(3)	4(4)	4(4)

Notes

(a) For those structures which will be constructed in very soft soils, and whose natural periods may coincide with predominate periods of the ground, special attention should be drawn by dynamic analysis method.

(b) Values in the parentheses in Table 2 are for those structures which have rigid foundations, such as caisson or well foundations with depth to diameter (or shorter length of bases) ratios of three or less. N indicates number of blow per 30 cm by the standard penetration test.

(c) In cases where depth of alluvium layer or loam layer is between 0 and 3m, and a firm layer is under this thin layer, the surface alluvium or loam layer should be removed. In the cases Soil Condition will be classified into 1.

Combination of Loads and Allowable Stresses

Type of Structures		Combination of Loads	Increases in Allowable Stresses (%)	Allowable Stresses of Concrete
Foundations or Retaining Walls	Reinforced Concrete Structures	Principal Loads + Seismic Loads	50	$\frac{\sigma_{28}}{3}$ or 100kg/cm^2
	Reinforced Concrete Structures	Principal Loads + Temperature + Humidity + Seismic Loads	65	
	Steel Structures	Principal Loads + Seismic Loads	50	
Superstructures or Substructures	Reinforced Concrete Structures	Dead Loads + Seismic Loads	50	$\frac{\sigma_{28}}{3}$
	Reinforced Concrete Structures	Dead Loads + Temperature + Humidity + Seismic Loads	65	
	Steel Structures	Dead Loads + Seismic Loads	70	

Notes

(1) Principal Loads = Dead Loads + Earth Pressures + Water Pressures + Buoyancy + Uplift,

(2) Foundations imply spread footings, pile foundations, and caisson foundations,

(3) Substructures mean the part of substructures above the top of foundations.

COUNTRY	JAPAN	CODE	JSCE: "Specifications for Earthquake Resistant Design of the Honshu-Shikoku Suspension Bridges (1967)" July, 1967 JSCE: "Revision of Specifications (1967)" June, 1971

DESIGN SEISMIC COEFFICIENTS

[1] Seismic Coefficient Method (out of use)

Horizontal: $k = S.C_o$; Vertical: $k_v = (1/2)k_h$

($C_o = 0.18$)

Table 1

Soil Condition	Value of S
Rock (Tertiary or older)	1.0
Diluvium	1.1
Alluvium	1.25

Increase seismic coefficient for higher part (Fig. 1)

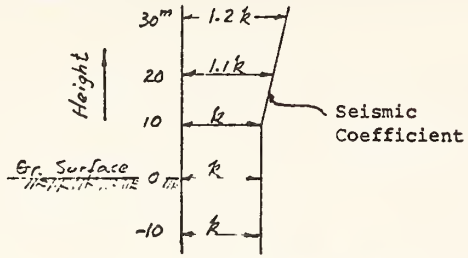

Fig. 1 Seismic Coefficient for Higher Part of Structures

[2] Modified Seismic Coefficient Method Considering Structural Response (employed)

Design Seismic Coefficient, $k=m_1\ m_2\ C_o$ ($C_o = 0.18$ in Horizontal, 0.09 in Vertical)

m_1 = Magnification factor for simple one-degree-of-freedom system (depends on type of structure, periods, damping, non-linearity, etc.) (Fig. 2).

m_2 = A factor used when actual structures are considered to be simple systems to which simplified distributed seismic loads are applied (Fig. 3).

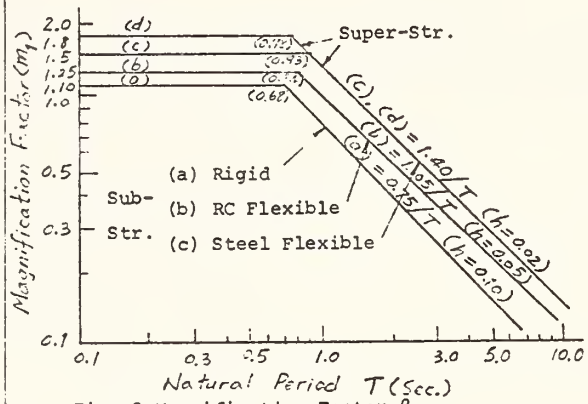

Fig. 2 Magnification Factor, β

Direction of Seismic Motion	Longitudinal	Transverse	Vertical
Substructure	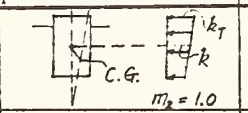	same as long. $m_2 = 1.0$	not considered
Main Tower		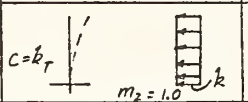	not considered
Suspended Structure, Cable	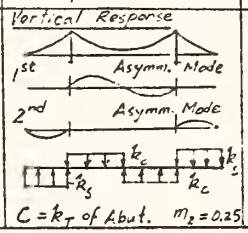	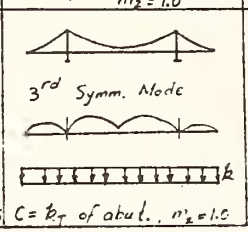	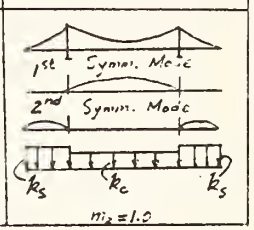

Fig. 3 Distribution of Design Seismic Loads and Value of m_2

REMARKS

Provisions on the following subjects are specified:

Dynamic Analysis, Earth Pressures, Hydrodynamic Pressures, Safety Factor, Other Considerations.

COUNTRY	JAPAN	CODE	JSCE (Commissioned from the Japanese National Railways): "Report on the Aseismic Design of Sub-Structures of Railway Bridges (1968),"

DESIGN SEISMIC COEFFICIENTS

Table 1. Design Horizontal Seismic Coefficients. $k_h = m_s\, m_x\, k_o$

Zone			A (k_o = 0.2)			B (k_o = 0.15)		
Soil Condition			Soft m_s = 1.2	Medium m_s = 1.0	Hard m_s = 0.8	Soft m_s = 1.2	Medium m_s = 1.0	Hard m_s = 0.8
Degree of Importance of Structure	Important	m_x=1.1	0.25	0.2	0.2	0.2	0.15	0.15
	Ordinary	m_x=1.0	0.25	0.2	0.15	0.2	0.15	0.1
	Less Important	m_x=0.9	0.2	0.2	0.15	0.15	0.15	0.1

k_o: Basic Seismic Coefficient

Definition of Soil Condition

Soft: Alluvial Layers which have
depth of 2 - 5m with N=0,
depth of 5 - 10m with N≦2, or
depth of 10 or more with N≦4

Medium: Alluvium (except Soft Layer) and Diluvium

Hard: Rock Layer older than Tertiary

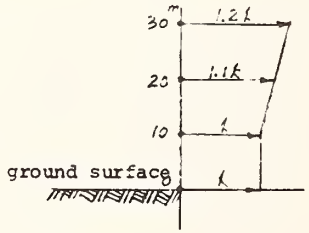

Fig. 1 Seismic Coefficient for Higher Portion

Notes

(1) Seismic Coefficients for Higher Portion of Structures (Fig. 1): For the part of structures higher than 10m above ground surface, the design seismic coefficient shall be obtained by increasing by 1% per an increase of 1m in height.

(2) Seismic Coefficients below Ground Surface (Fig. 2): Seismic coefficients for underground portion of structures, underground structures, caisson foundations, etc. are obtained by multiplying m_s (shown in Fig. 2 for various ground conditions and depth) by $m_x k_o$ given in Table 1.

(3) Vertical Seismic Coefficients, k_v shall be one half of the horizontal, when needed.

(4) These specifications shall apply to bridges and retaining walls.

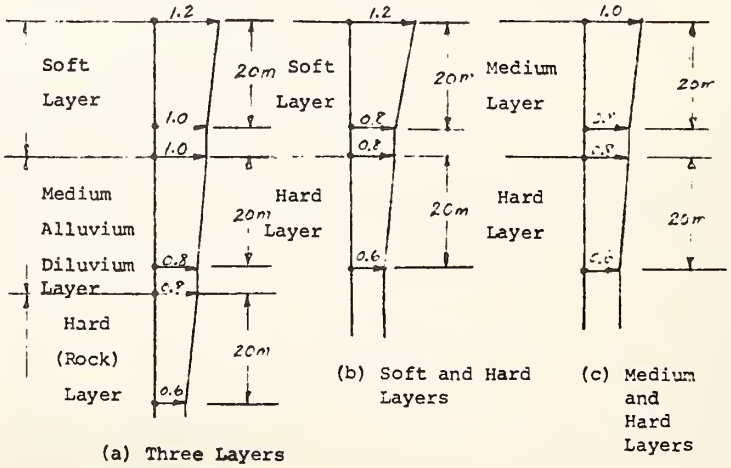

(a) Three Layers

(b) Soft and Hard Layers

(c) Medium and Hard Layers

Fig. 2 Values of m_s for Underground

COUNTRY	SPECIFICATIONS	Seismic Coefficient, k (k in V = kW)					Increase in Allowable Stresses	Remarks
		Group A	Group B			Group C		
			Type of Structure	Zone 1	Zone 2			
MEXICO	Provisions for Earthquake Resistant Design in the Federal District, Mexico. February, 1966 (For Building)	1.3Times Group B	1	0.06	0.04	0	Timer, structural or reinforcing steel: 50% Other metals, Concrete, masonry: 33% Soils: according to the chapter on foundations.	Regulations on Repairing, Instrumentation, Dynamic Analyses, Maximum relative displacements.
			2	0.08	0.08	0		
			3	0.15	0.1	0		

Group A: specially important
" B: important
" C: less important
Type 1: strong structure
" 2: moderate structure
" 3: weak structure
Zone 1: Zone of High Compressibility
2: Zone of Low Compressibility

COUNTRY	SPECIFICATIONS	Seismic Coefficient k	Increase in Allowable Stresses	Remarks
NEW ZEALAND	New Zealand Standard Mode Building Bylaw (NZSS1900), Chapter 8 Basic Design Loads, Earthquake Provisions. (1965)	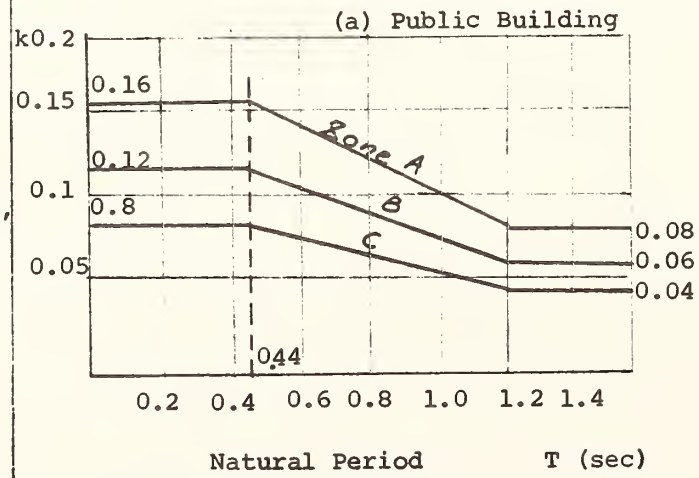 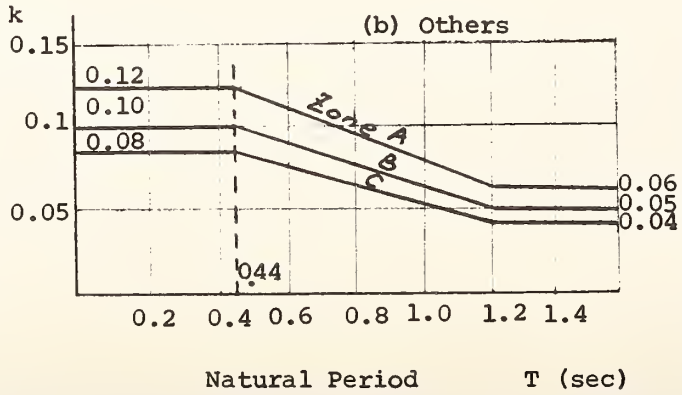		

COUNTRY	SPECIFICATIONS	Seismic Coefficient k	Increase in Allowable Stresses	Remarks
PERU	Peruvian Standards for Antiseismic Design. September 30, 1968	k = UKC U: Factor depending on the use of building and on the region Region / Usage: 1, 2, 3, Remarks A). Rural: Special Recommendations B). Ordi: 1, 0.8, 0.6 C). Public: 1.2, 1.0, 0.7 D). Special: Special Consideration, Bigger than C K = 1.33 = 1.0 = 0.80 = 0.67 modifying factor used to take into account structural response to aseismic action, according to its energy absorption capacity. $C = 0.05/\sqrt[3]{T}$ Soil Classification I : Hard Soil - rocks, rocky soils, dense soils II : Soft Soil - soil with low bearing capacity, high water content, and high watertable. III: Undesirable Soil - Very soft soil. Notes: 1) For soils II and III, foundations should be designed in such a way that effects of differential settlement and disorderly vibration will be minimarized. 2) On soils III, type D should not be built, and seismic forces should be increased for type A to C. 3) In urban planning, soils III should be used as green areas, recreation areas, and avenues.	Elastic Method: 33% for steel 33% for concrete Ultimate-Resistant Method : load factor 1.33	Vertical Seismic Forces: It will be necessary to verify the effect of the vertical seismic force in the following cases: A) In cantilever element and heavily loaded tie roads, etc. B) Elements of great lengths, especially cantilever, bracings, and bridges. Regulations on Dynamic analysis for non-conventional structures, Instrumentation.

COUNTRY	SPECIFICATIONS	Seismic Coefficient k	Increase in Allowable Stresses	Remarks
PHILIPPINES	Draft of the National Building Code of Philippines	$k = Z \cdot C \cdot K$		Regulation on Instrumentation

Values of Z

Zone \ Found	A	B	C
1	0.8	1.0	1.2
2	0.6	0.8	1.0
3	0.4	0.6	0.8

$$C = \frac{2.05}{\sqrt[3]{T}} \leq 0.1$$

C = 0.1 - one and two-story buildings

K: Horizontal Force Factor

(0.67 - 3)

Found: Foundation Conditions

COUNTRY	SPECIFICATIONS	Seismic Coefficient, k							Allowable Stresses
				Zone A		Zone B		Zone C	
				(1)	(2)	(1)	(2)		
PORTUGAL	Portuguese Codes on Earthquake-Resistant Structures	Construction as a Whole	Construction with a reserve of strength due to non-structural bracing members	0.1	0.15	0.05	0.075	0	limit design mild steel: 2400kg/cm^2 other steel: 0.8 x (ultimate stress) Concrete: 2/3 (rupture stress)=120kg/cm^2 (minimum rupture stress 180kg/cm^2) Elastic Design mild steel: 2400kg/cm^2 (tensile, bending, or non-buckling compressive) For other type of loads: 1.7X (permissible stress for ordinary loads) Concrete: 2 X (permissible stress for ordinary loads)
			Construction without a reserve of strength due to non-structural bracing members	0.15	0.2	0.075	0.1	0	
		Building Members	Walls and Similar Members	0.20		0.10		0	
			Balconies, chimneys and other members projecting from the outer walls and from the roofing.	0.30		0.15		0	

(1) : Usual cases of foundation ground

(2) : foundation ground with particularly unfavourable seismic characteristics, like the case with mud, soft clay, silt and recent embankments, for layers at least about ten meters thick, even when the foundation structure goes through these layers are rests on harder ones.

COUNTRY	SPECIFICATION	Seismic Coefficient, k	Increase in Allowable Stresses	Remarks
RUMANIA	Earthquake Regulations	$k = K_s \beta \varepsilon \Psi$ $k > 0.02$		

Design seismic degree	K_s
7	0.025
8	0.05
9	0.1

β: dynamic factor (σ_a: allowable bearing power)

soil	β
(a) $\sigma_a > 20t/m^2$	$0.6 < \beta = \frac{0.9}{T} < 3$
(b) $\sigma_a < 20t/m^2$	$0.75 < \beta = \frac{1.125}{T} < 3$
(c) soft	$0.9 < \beta = \frac{1.35}{T} < 3$

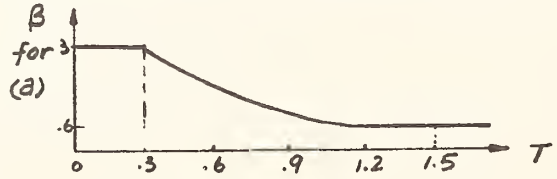

ε : mode participation factor

Ψ : = 1.0 = usual building

= 1.2 = frame structure building of RC, building with hinged roofs or RC strut,

= 1.5 = flexible structure such as chimneys, water tanks, towers, etc.

COUNTRY	SPECIFICATIONS	Seismic Coefficient, k	Increase in Allowable Stresses	Remarks
TURKEY	Regulation For Buildings in Disaster Areas Highways	$k = C_o \cdot n_1 \cdot n_2$ C_o 40m: 0.1, 0.09, 0.08, 0.07, 0.06 6m, 6m, 6m, 6m, 16m Above 40m C_o will be increased by 0.01 per 3.0 meters.	50%	not considered for embankments of highways. Regulations on Earthpressure.

n_1

soil	steel	RC
I Hard rock	0.6	0.8
II Compact soils	0.8	0.9
III Soft	1.0	1.0

Earthquake Region	n_2
1 st Degree	1.0
2 nd Degree	0.6
3 rd Degree	0.6

COUNTRY	SPECIFICATIONS	Method	Horizontal Seismic Coefficient k in V=kW (V= Horizontal Force, W= Total Weight)		Increase in Allowable Stresses
U. S. A.	Standard Specifications for Highway Bridges AASHO (1965)	simple quasi-static formula	Structures on spread footing on soil of allowable bearing pressure > $37t/m^2$	k = 0.02	1/3 (Dead Load + primary forces except live load)
			Structures on spread footing on soil of allowable bearing pressure < $37t/m^2$	k = 0.04	
			Structures on piles	k = 0.06	
	State of California Division of Highways. SEAOC (1959) "Recommended Force Requirements"	Modified Seismic Coefficient Method	k = KC K: Horizontal Force Factor = 1.33 for systems where the lateral forces are restricted by diaphragm = 1.00 for columns or piers which have a height/length ratio greater than 2.5 = 0.67 where lateral loads are resisted by rigid frame action $C = 0.05/T^{\frac{1}{3}}$ T: natural fundamental period (sec) $= 0.32 \left(\frac{D}{P}\right)^{\frac{1}{2}}$ D: Dead load of vibrating part (lb) P: force to produce one inch of lateral deflection (lb/in) k > 0.02		

COUNTRY	SPECIFICATIONS	Seismic Coefficient k	Increase in Allowable Stresses	Remarks
VENEZUELA	Venezuela Building Regulations		33%	

k for zone 3

Type of Structure	Alluvial Deposit (1)		Bedrock (2)	
	Usage of Building		Usage of Building	
	Group 1	Group 2	Group 1	Group 2
I	0.075	0.06	0.06	0.045
II	0.09	0.07	0.11	0.085
III	0.15	0.12	0.13	0.10

Group 1: Specially Important

Group 2: Important

Group 3: Less Important (k = 0)

k for zone 2: 1/2 X (zone 3)

k for zone 3: 1/4 X (zone 3)

k for zone 0: 0

I : bending frame

II : shear, axial force

III: one column, one line of resisting

Soil Classification

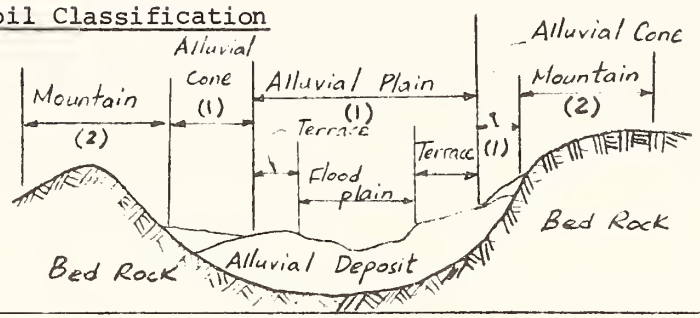

APPENDIX C

SPECIFICATIONS FOR EARTHQUAKE-RESISTANT DESIGN

OF

HIGHWAY BRIDGES

JAPAN ROAD ASSOCIATION

JANUARY, 1971

FOREWORD

The earthquake resistant design of highway bridges is currently being conducted in accordance with the provisions of Section 13 (Section 2.9 in the English version) of the Specifications for Design of Steel Highway Bridges. Since the provisions concerning earthquake resistant design are not very comprehensive as stated in the preface of the Specifications, the design is in many respects dependent on the designer's interpretation. Accordingly the results of the various designs were not always consistent. To alleviate this problem it was necessary to revise the Section 13 of the Specifications and to draw up new detailed Specifications exclusively for earthquake resistant design of highway bridges.

In response to the need for revisions, the Japan Road Association established the Earthquake Resistant Design Subcommittee under the Highway Bridge Committee in 1966. Between 1966 and 1968 a preliminary draft was prepared. The task was taken over by the Earthquake Resistant Design Branch-Committee of the Specifications Subcommittee in 1968, when the Highway Bridge Committee was reorganized.

The Subcommittee and the Branch-Committee have seriously attempted to draw up the revision through surveys of the available research work, discussions with specialists from universities and other organizations, and trial calculations and bridge designs at several stages in accordance with the interim drafts, and finally completed the revision of the Specifications in 1971.

The new Specifications are completed basically in accordance with the provisions of Section 13 of the Specifications for Design of Steel Highway Bridges, and also by extensively referring to the results of recent investigations on earthquake engineering. Therefore the design methodology of Section 13 of the current Specifications was generally traced in establishing the new Specifications.

In determining the design seismic coefficient the importance factor is newly considered in addition to the traditional factors such as zone factor and ground condition factor. Moreover, for bridges which have longer natural periods the factor on the natural periods of the structures are considered.

Although the design horizontal seismic coefficient used to be 0.1 to 0.35 in the Section 13 of the current Specifications, the value is reduced to 0.1 to 0.3 and over 0.3 only for rare occasions in the new Specifications. This is based on the results of recent investigations that it seems more essential to pay attention to soil conditions rather than to the magnitude of seismic coefficients in design of bridges against seismic forces.

Since design seismic forces in the new Specifications were determined by referring to the seismic risk map expected for 75 years presented by Dr. Kawasumi and by reflecting the results of a recent study on the meteolorogical data since the Kanto Earthquake in 1923, seismic forces considered in the new Specifications would cover the severest earthquakes experienced in individual regions in Japan.

The seismic forces would also correspond to those due to the greatest earthquakes in the seismological point of view.

In the new Specifications the following aspects differ from the previous method.

(1) The design seismic coefficients of a bridge are determined systematically dependent on geographical location of the bridge site, the ground conditions at each substructure site, and the importance of the bridge.

(2) The vertical design seismic coefficients are generally neglected.

(3) The design seismic coefficients for structural parts, soils and water below the ground surface are neglected.

(4) Special attention is paid to very soft soil layers and soil layers vulnerable to liquefaction during earthquakes. The bearing capacities of these layers are neglected in the design in order to assure high earthquake-resistance for those structures which are constructed in these layers.

(5) The design seismic coefficients for bridges with high-rize piers are determined in accordance with the modified seismic coefficient method considering structural response, instead of the conventional way in which the design seismic coefficients increase with the height of the piers.

(6) Special attention is also paid to the design of structural details in view of earthquake damage previously experienced to bridge structures. To this end provisions are specified for bearing supports and devices for preventing superstructures from falling.

Although the Specifications were developed through extensive studies and discussions of research reports on earthquake engineering from throughout the world as well as Japan, some unexpected problems may arise when they are applied to actual structures. Because of this and the fact that technological improvements take place very rapidly, another revision will be required in the future. Everyone is urged to indicate any insufficient points or to make any suggestions for the present Specifications, so that they may be improved in subsequent revisions.

The present publication is limited to the provisions which are considered to be sufficient for the design of bridges. Comments which dedscribe the basis and the application methods of the provisions will be issued immediately after their completion. They will be indispensable when it is necessary to revise the present Specifications again or when any parts of the provisions are found to be uncertain in their application.

Dr. Hiroshi Kawasumi, Dr. Tsutomu Terashima, and Mr. Tsutomu Tomita participated in the discussions on special matters as special members of the Committee. Their cooperation is greatly appreciated.

January, 1971

Earthquake Resistant Design Branch-Committee
Specifications Subcommittee
Highway Bridge Committee
Japan Road Association

3-3-3 Kasumigaseki
Chiyoda-ku, Tokyo

LIST OF MEMBERS

HIGHWAY BRIDGE COMMITTEE

Chairman:	Aoki, Kusuo	
Members:	Arie, Yoshiharu	Fukuda, Takeo
	Fukuoka, Masami	Hirai, Atsushi
	Hiura, Taizo	Inomata, Shunji
	Kokubu, Masatane	Konishi, Ichiro
	Kono, Michiyuki	Matsuzaki, Akimaro
	Murakami, Eiichi	Murakami, Tadashi
	Nakajima, Takeshi	Nakano, Takayuki
	Naniwa, Hayato	Naruse, Katsutake
	Okamoto, Shunzo	Okubo, Tadayoshi
	Okumura, Toshie	Ozaki, Hisashi
	Suzuki, Toshio	Tahara, Yasuji
	Tanaka, Goro	Tomonaga, Kazuo
	Uemae, Yukitaka	Yokomichi, Hideo
Secretaries:	Komada, Keiichi	Kutsukake, Tetsuo
	Miyazaki, Shoji	Okada, Tetsuo
	Sawai, Hiroyuki	

LIST OF MEMBERS

SPECIFICATIONS SUBCOMMITTEE

Chairman: Murakami, Eiichi

Members:

Adachi, Ko	Asama, Tatsuo
Fuse, Yoichi	Horii, Kenichiro
Ikeda, Tetsuo	Inoue, Hirosato
Ito, Manabu	Kato, Masaharu
Komada, Keiichi	Kunihiro, Tetsuo
Kutsukake, Tetsuo	Maeda, Kunio
Miyazaki, Shoji	Nakamura, Shohei
Narita, Nobuyuki	Nishiyama, Hironobu
Nishiwaki, Takeo	Okada, Tetsuo
Okinaka, Koichiro	Okubo, Tadayoshi
Saiki, Saburo	Samukawa, Shigeomi
Sasado, Shoji	Sawai, Hiroyuki
Tada, Yasuo	Takata, Takanobu
Tamano, Mitsuharu	Tanabe, Suenobu
Yoshida, Iwao	

Secretaries:

Kato, Hiroshi	Mori, Hiroaki
Numata, Shoichiro	Sato, Nobuhiko
Yamaki, Takashi	

LIST OF MEMBERS

EARTHQUAKE RESISTANT DESIGN BRANCH-COMMITTEE

Chairman: Tada, Yasuo

Members:

Adachi, Ko	Adachi, Yoshio*
Arakawa, Tadashi *	Asama, Tatsuo
Hakuno, Motohiko	Iida, Yutaka*
Ishihara, Kenji	Iwamatsu, Yukio
Iwasaki, Toshio*	Keto, Hideyuki
Komada, Keiichi	Kunihiro, Tetsuo
Kuribayashi, Eiichi*	Muto, Hayahiko
Nakagawa, Kyoji	Nakamura, Hiroaki
Nakano, Seiji	Nishiyama, Hironobu
Okada, Tetsuo	Okubo, Tadayoshi
Okubo, Teiji	Oyamada, Yoshihiro*
Saeki, Shoichi	Shimokawa, Hiroshi
Tamura, Koichi	Tsuchida, Hajime
Tsuji, Katsunari *	Yahagi, Kaname
Yoshida, Iwao	Yoshinaka, Ryunoshin

Members with * are also secretaries.

CONTENTS

	Page
FOREWORD	C - i
LIST OF MEMBERS	C - V
Chapter 1 General	C -1
1.1 Scope	C- 1
1.2 Definitions of Terms	C- 2
Chapter 2 Basic Principles for Earthquake Resistant Design	C- 5
Chapter 3 Loads and Conditions in Earthquake Resistant Design	C- 6
3.1 General	C- 6
3.2 Seismic Effects	C- 7
3.3 Inertia Forces	C- 7
3.4 Earth Pressures during Earthquakes	C-11
3.5 Hydrodynamic Pressures during Earthquakes	C- 11
3.6 Ground Surface Assumed in Earthquake Resistant Design	C- 14
3.7 Soil Layers Whose Bearing Capacities are Neglected in Earthquake Resistant Design	C- 15
3.8 Buoyancy or Uplifts	C- 16
Chapter 4 Design Seismic Coefficient	C- 17
4.1 General	C- 17
4.2 Design Seismic Coefficient in the Seismic Coefficient Method	C- 17

4.3 Factors for Modifying the Standard Horizontal Design Seismic Coefficient C-18

4.4 Design Seismic Coefficient in the Modified Seismic Coefficient Method Considering Structural Response C-22

Chapter 5 General Provisions for Design of Structural Details C-31

5.1 General C-31

5.2 Devices for Preventing Superstructures from Falling C-32

5.3 Vertical Seismic Forces for Design of Connections between Superstructures and Substructures C-35

5.4 Methods for Transmitting Seismic Forces at Connections between Superstructures and Substructures C-35

5.5 Devices Expected for Decreasing Seismic Forces C-37

Chapter 6 Miscellaneous Provisions C-38

References* C-39

---

* References are provided exclusively in the English version for the convenience of the reader.

Chapter 1 General

1.1 Scope

The provisions in the Specifications apply to earthquake resistant design of highway bridges with spans not longer than 200 meters, to be built on expressways, national highways, prefectural highways and principal municipal highways.

In regard to matters which are not specified herein, the following Specifications shall be conformed to, in accordance with the type of the structure considered.

Specifications for Design of Steel Highway Bridges,	Japan Road Association
Specifications for Design of Welded Highway Bridges,	Japan Road Association
Specifications for Design and Construction of Composite Beams for Steel Highway Bridges,	Japan Road Association
Specifications for Design of Reinforced Concrete Highway Bridges,	Japan Road Association
Specifications for Design and Construction of Friction Type Joints in Steel Highway Bridges Using High Strength Bolts,	Japan Road Association
Specifications for Design of Substructures of Highway Bridges,	Japan Road Association
Specifications for Prestressed Concrete Highway Bridges,	Japan Road Association

1.2 Definitions of Terms

The following definitions apply only to the provisions of these Specifications.

(1) Earthquake: A phenomenon with propagation of vibration due to a sudden naturally occurring movement at a certain portion inside the earth.

(2) Earthquake Ground Motion: Vibration of ground during earthquakes.

(3) Design Seismic Coefficient: A coefficient indicating the magnitude of acceleration to be considered for earthquake resistant disign of structures, and expressed as a fraction of the acceleration of gravity.

(4) Seismic Coefficient Method: A method for earthquake resistant design in which seismic forces are assumed to act on structures as static forces.

(5) Modified Seismic Coefficient Method Considering Structural Response: A method for earthquake resistant design which is developed through modification of the seismic coefficient method by considering characteristics of earthquake ground motions, dynamic properties of structures, etc. for those structures with long fundamental periods of vibration.

(6) Modified Design Seismic Coefficient Considering Structural Response: A design seismic coefficient used in the modified seismic coefficient method considering structural response in which the design seismic coefficient is dependent on the fundamental period of the structure.

(7) Standard Horizontal Design Seismic Coefficient: The Horizontal design seismic coefficient which applies to a bridge which is located in a zone where severe earthquakes have frequently occurred or where severe earthquakes have a high potential of occurance, and which is constructed in soil layers with ground conditions corresponding to group 2 in Table 4.5.

(8) Seismic Zone Factor: A factor to decrease the horizontal design seismic coefficient in accordance with the geographical location of the structural site. The factor has the value of 1.0 for those zones where severe earthquakes have frequently occurred or where severe earthquakes have a high potential of occurance.

(9) Ground Condition Factor: A factor to modify the horizontal design seismic coefficient depending upon the ground conditions of the structural site. The factor is intended to unify the margin of safety against earthquake disturbances among structures constructed in various ground conditions, in consideration of damage previously experienced.

(10) Importance Factor: A factor to modify the horizontal design seismic coefficient depending on the importance of the structure.

(11) Inertia Force: Product of the weight of the structural body and the design seismic coefficient.

(12) Seismic Force: Any forces such as inertia forces, earth pressures, etc. to which structures are subjected during earthquakes.

(13) Coefficient of Subgrade Reaction: A coefficient given by the following formula, which is also shown in Section 3.1 of the Volume

of Spread Foundations, the Specifications for Design of Substructures of Highway Bridges.

$$K = \frac{p}{\delta}$$

where

K : coefficient of subgrade reaction in kg/cm^3

p : loading pressures in kg/cm^2

δ : displacement in cm

(14) Earthquake Response Analysis: An analysis of the dynamic behavior of structures during earthquakes.

Chapter 2 Basic Principles for Earthquake Resistant Design

(1) The earthquake resistant design for a highway bridge shall provide sufficient stability against seismic disturbances for the structure as a unit and also for all parts thereof, including superstructures, substructuctures, and surrounding soils, considering topographical and geological conditions at the site.

(2) The seismic coefficient method basically shall apply to the earthquake resistant design of relatively rigid structures.

(3) The modified seismic coefficient method considering structural response shall apply to the earthquake resistant design of relatively flexible structures which are of long fundamental periods of vibration, such as bridges with high-rise piers.

The earthquake response analysis shall also be adopted for those structures, for which detailed investigations are required.

(4) Particular attention shall be paid to preventing the fall of superstructures from substructures due to the movements during earthquakes.

When the design allowing for partial failures of the whole system or local failures of certain structural members is required on the basis of economical considerations, special attention to preventing the fall of superstructures shall be paid.

Chapter 3 Loads and Conditions in Earthquake Resistant Design

3.1 General

(1) The following loads shall be taken into account in earthquake resistant design. The appropriate loads shall be selected from this list on the basis of the location and the type of the structure.

1. Dead Loads
2. Earth Pressures
3. Hydraulic Pressures
4. Buoyancy or Uplifts
5. Effects of Temperature Change
6. Effects of Shrinkage due to Humidity in Concrete Structures (Including Creep Effects)
7. Seismic Effects
8. Effects of Friction at Bearing Supports
9. Effects of Consolidation and Settlement of Ground
10. Effects of Movements of Supports
11. Other Loads

(2) Combination of Loads

Design conditions shall be determined considering the following four cases. The combination of various loads listed above shall be decided in accordance with the provisions in individual Specifications according to the type of the bridge considered.

Case 1	Maximum stresses will be expected in the members
Case 2	Maximum reactions will be expected in the foundation soils
Case 3	Maximum displacements will be expected at the supports
Case 4	The structure will become critical conditions due to overturning, sliding, etc.

3.2 Seismic Effects

The following seismic forces shall be taken into account to determine seismic effects in design of a bridge structure.

1. Inertia forces due to the dead weight of the structure: The magnitude of the inertia forces shall be the product of the weight of the structure and the design seismic coefficient. The design seismic coefficient shall be obtained in accordance with the provisions in Chapter 4 "Design Seismic Coefficient."

2. Inertia forces due to the superimposed weight: The magnitude of the inertia forces shall be the product of the superimposed weight and the design seismic coefficient. The design seismic coefficient also shall be obtained in accordance with the provisions in Chapter 4 "Design Seismic Coefficient."

3. Earth pressures during earthquakes.

4. Hydrodynamic pressures during earthquakes.

3.3 Inertia Forces

(1) Both for the seismic coefficient method and the modified seismic coefficient method, bridge substructures shall be subjected to the

inertia forces of superstructures during earthquakes as follows (refer to Fig. 3.1):

(a) Horizontal seismic force acting on A_L (left abutment) shall be

$$H_{AL} = R_{AL} \cdot f_{AL} \tag{3.1}$$

where $$H_{AL} \leq \frac{1}{2} k_h W_A \tag{3.2}$$

In other words,

$$H_{AL} = \text{smallest of} \begin{cases} R_{AL} \cdot f_{AL} \\ \text{or} \\ \frac{1}{2} k_h W_A \end{cases}$$

(b) Horizontal seismic force acting on P_1 (Pier 1) shall be

$$H_{AR} + H_{BL} = \text{largest of} \begin{cases} k_h W_A \ (H_{BL} = 0 \text{ in this case}) & (3.3) \\ \text{or} \\ \frac{1}{2} k_h W_A + R_{BL} \cdot f_{BL} & (3.4) \end{cases}$$

In equation (3.4), $R_{BL} \cdot f_{BL}$ shall satisfy

$$R_{BL} \cdot f_{BL} \leq \frac{1}{2} k_h W_B \tag{3.5}$$

(c) Horizontal seismic force acting on A_R (right abutment) shall be

$$H_{BR} = k_h W_B \tag{3.6}$$

where

f_{AL} : Static friction coefficient at movable support A_L ,

f_{BL} : Static friction coefficient at movable support B_L ,

H_{AL} : Horizontal seismic force (inertia force or friction force) acting on A_L due to Girder A

H_{AR} : Horizontal seismic force (inertia force) acting on P_1 due to Girder A ,

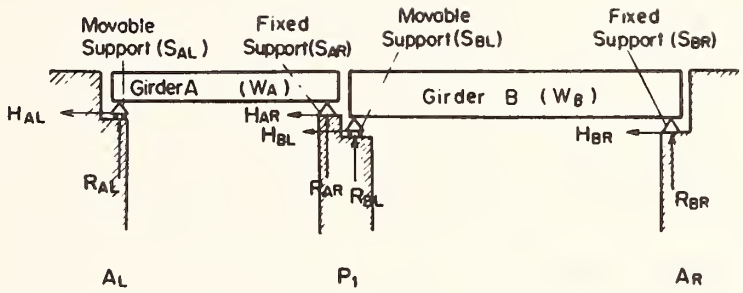

Fig. 3.1 Inertia Forces of Superstructures

H_{BL} : Horizontal seismic force (inertia force or friction force) acting on P_1 due to Girder B

H_{BR} : Horizontal seismic force (inertia force) acting on A_R due to Girder B

k_h : Horizontal design seismic coefficient (in accordance with the provisions in Chapter 4 "Design Seismic Coefficient": k_h in equation (4. 1) for the seismic coefficient method, or k_{hm} in equation (4. 2) for the modified seismic coefficient method, shall be employed),

R_{AL} : Reaction at A_L due to W_A ,

R_{AR} : Reaction at P_1 due to W_A ,

R_{BL} : Reaction at P_1 due to W_B ,

R_{BR} : Reaction at A_R due to W_B ,

W_A : Dead weight of Girder A , and

W_B : Dead weight of Girder B .

(2) Inertia forces shall be assumed to act at the center of gravity of the structure. In designing the substructure, inertia forces exerted from superstructures may be assumed to act at the level of the base of the supports in the longitudinal direction to the bridge axis, and at the level of the center of gravity of the superstructures in the transverse direction.

In the transverse direction the level of the center of gravity of the superstructures may generally be taken as the lower level of the floor slab.

(3) Inertia forces shall be assumed to come from two horizontal directions: longitudinal and transverse to the bridge axis, or parallel and perpendicular to the principal axis of any structural elements of the bridge.

3.4 Earth Pressures during Earthquakes

Earth pressures during earthquakes shall be determined in accordance with the provisions in the Specifications for Design of Substructures of Highway Bridges (See Reference 1 at the end of the English Version). The horizontal seismic coefficient in the calculation of earth pressures shall be in accordance with the provisions in Section 4.2 "Design Seismic Coefficient in the Seismic Coefficient Method."

3.5 Hydrodynamic Pressures during Earthquakes

Hydrodynamic pressures during earthquakes shall be determined by the following formulas. The pressures shall be assumed to act in the same direction as that of the inertia forces given by the provisions in Section 3.3 "Inertia Forces."

(1) Hydrodynamic Pressures on Walls

Hydrodynamic pressures acting on one side of a wall-type structure shall be determined as follows (refer to Fig. 3.2):

$$P = \frac{7}{12} k_h W_o b h^2 \tag{3.7}$$

$$h_e = \frac{1}{2} h \tag{3.8}$$

where

b : Width of the wall in meters in the perpendicular direction to that of the pressure,

h : Depth of water in meters,

h_e : Height of the total hydrodynamic pressure in meters above the bottom of the water,

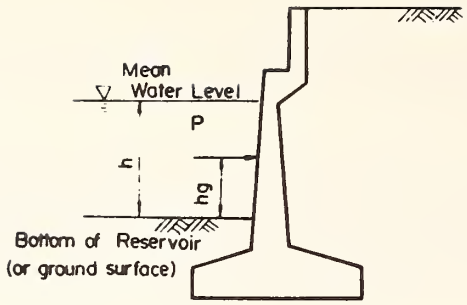

Fig. 3.2 Hydrodynamic Pressures on Wall-Type Structures

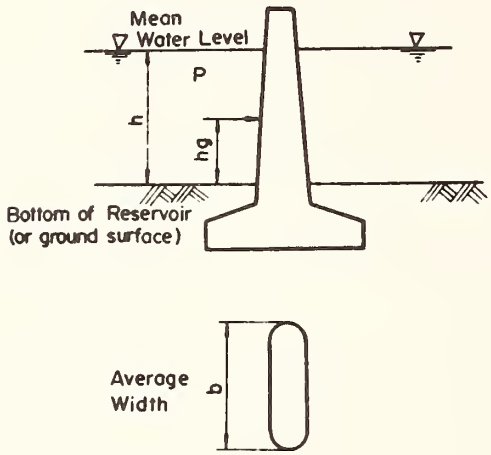

Fig. 3.3 Hydrodynamic Pressures on Column-Type Structures

k_h : Horizontal design seismic coefficient given by the provisions in Section 4.2 " Design Seismic Coefficient in the Seismic Coefficient Method ,"

P : Total hydrodynamic pressure in t, and

W_0 : Unit weight of water in t/m^3.

(2) Hydrodynamic Pressures on Columns

Hydrodynamic pressures acting on a column-type structure surrounding by water shall be determined as follows (refer to Fig. 3.3):

$$P = \frac{3}{4} k_h W_o b^2 h \left(1 - \frac{b}{4h}\right) \qquad \text{for } \frac{b}{h} \leq 2 \qquad (3.9)$$

$$P = \frac{3}{8} k_h W_o b^2 h \qquad \text{for } \frac{b}{h} > 2 \qquad (3.10)$$

$$h_e = \frac{1}{2} h \qquad (3.11)$$

3.6 Ground Surface Assumed in Earthquake Resistant Design

In earthquake resistant design the bearing capacities of soil layers which are specified in Section 3.7 "Soil Layers Whose Bearing Capacities are Neglected in Earthquake Resistant Design" shall be neglected. Ground surface in design shall be assumed to be the level of the lower boundary of the neglected layer, if the layer extends continuously below the actual ground surface.

For this case the neglected layer shall be assumed to have properties of zero cohesion and zero angle of internal friction.

3.7 Soil Layers Whose Bearing Capacities are Neglected in Earthquake Resistant Design

(1) Sandy Soil Layers Vulnerable to Liquefaction

Saturated sandy soil layers which are within 10 meters of the actual ground surface, have a standard penetration test N-value less than 10, have a coefficient of uniformity less than 6, and also have a D_{20}-value on the grain size accumulation curve between 0.04 mm and 0.5 mm, shall have a high potential for liquefaction during earthquakes. Bearing capacities of these layers shall be neglected in design.

Saturated sandy soil layers which have a D_{20}-value between 0.004 and 0.04 mm or between 0.5 mm and 1.2 mm, may liquefy during earthquakes, and shall be given particular attention. Estimation whether or not these layers will liquefy shall be made in accordance with the available information on liquefaction problems.

When a special investigation is performed, the provisions in this item (1) in Section 3.7 may not be required to apply.

(2) Cohesive Soil Layers and Silty Soil Layers

Bearing capacities of cohesive soil layers and silty soil layers, which are within 3 meters of the actual ground surface, and are very soft such as those with the compression strength, determined by unconfined compression tests or field tests, less than 0.2 kg/cm^2, shall be neglected in design.

(3) Weight of Soil Layers Whose Bearing Capacities are Neglected

The weight of soil layers whose bearing capacities are neglected shall have surcharge effects on the lower ground.

3.8 Buoyancy or Uplifts

Buoyancy or uplifts shall be determined in accordance with the provisions in the Specifications for Design of Substructures of Highway Bridges (See Reference 2 at the end of the English Version).

Chapter 4 Design Seismic Coefficient

4.1 General

The design seismic coefficient shall generally be determined in accordance with the provisions in Section 4.2 "Design Seismic Coefficient in the Seismic Coefficient Method." For those bridges, however, which have flexible piers and long fundamental periods, such as those with piers higher than 25 meters above the ground surface, the design seismic coefficient shall be determined in accordance with the provisions in Section 4.4 "Design Seismic Coefficient in the Modified Seismic Coefficient Method Considering Structural Response."

4.2 Design Seismic Coefficient in the Seismic Coefficient Method

(1) The horizontal design seismic coefficient shall be determined by the following formula:

$$k_h = \nu_1 \cdot \nu_2 \cdot \nu_3 \cdot k_0 \qquad (4.1)$$

where

k_h: Horizontal design seismic coefficient,

k_0: The standard horizontal design seismic coefficient (= 0.2),

ν_1: Seismic zone factor,

ν_2: Ground condition factor, and

ν_3: Importance factor.

The value of k_h shall be rounded to two decimals. The minimum value of k_h shall be considered as 0.10. The values of factors ν_1,

ν_2 and ν_3 shall be obtained by the provisions in Section 4.3 "Factors for Modifying the Standard Horizontal Design Coefficient."

(2) The vertical design seismic coefficient, k_v may generally be considered as 0. Vertical seismic forces for design of bearing supports, however, shall be determined in accordance with the provisions in Section 5.3 "Vertical Seismic Forces for Design of Connections between Superstructures and Substructures."

(3) The horizontal design seismic coefficient may be considered as 0 for structural parts, soils and water below the assumed ground surface in design. The assumed ground surface in design shall be determined in accordance with the provisions in Section 3.6 "Ground Surface Assumed in Earthquake Resistant Design."

Item (3), however, shall not apply to underground structures such as culverts.

4.3 Factors for Modifying the Standard Horizontal Design Seismic Coefficient

(1) Seismic Zone Factor

Seismic zone factor shall be determined in accordance with Table 4.1, in which the zone classification shall be determined from Fig. 4.1 or Table 4.2.

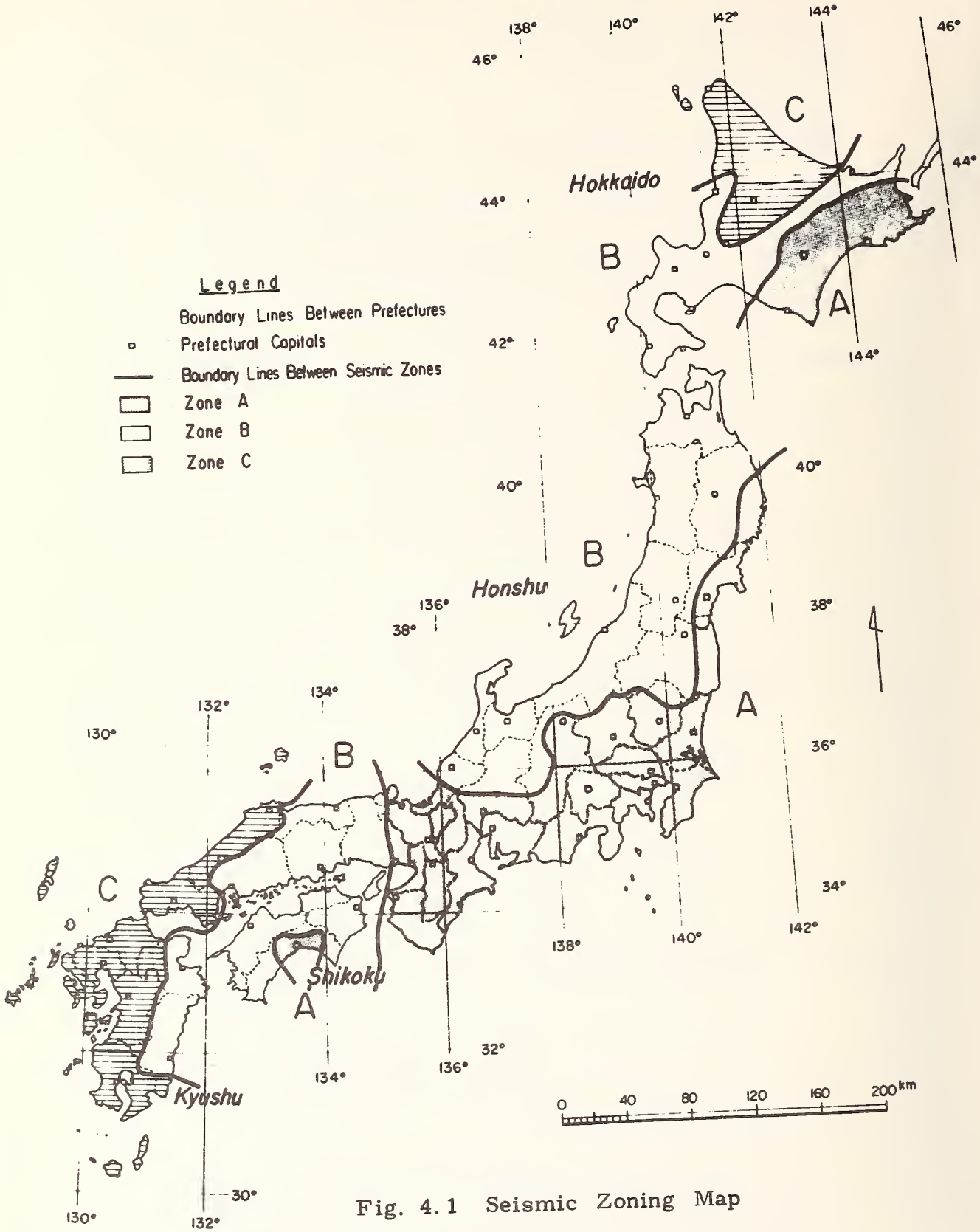

Fig. 4.1 Seismic Zoning Map

Table 4.1 Seismic Zone Factor ν_1

Zone	Value of ν_1
A	1.00
B	0.85
C	0.70

(Note)

Table 4.2, which indicates in detail the seismic zone through the use of place names, is omitted in the English version.

(2) Ground Condition Factor

Ground condition factor shall be determined in accordance with Table 4.3.

Table 4.3 Ground Condition Factor ν_2

Group	Definitions[1)]	Value of ν_2
1	(1) Ground of the Tertiary era or older (defined as bedrock hereafter) (2) Diluvial layer[2)] with depth less than 10 meters above bedrock	0.9
2	(1) Diluvial layer[2)] with depth greater than 10 meters above bedrock (2) Alluvial layer[3)] with depth less than 10 meters above bedrock	1.0
3	Alluvial layer[3)] with depth less than 25 meters, which has soft layer[4)] with depth less than 5 meters	1.1
4	Other than the above	1.2

(Notes) 1) Since these definitions are not very comprehensive, the classification of ground conditions shall be made with adequate consideration of the bridge site. Depth of layer indicated here shall be measured from the actual ground surface.

2) Diluvial layer implies a dense alluvial layer such as a dense sandy layer, gravel layer, or cobble layer.

3) Alluvial layer implies a new sedimentary layer made by a landslide.

4) Soft layer is defined in Section 3.7 "Soil Layer Whose Bearing Capacities are Neglected in Earthquake Resistant Design."

(3) Importance Factor

Importance factor shall be determined in accordance with Table 4.4.

Table 4.4 Importance Factor ν_s

Group	Definitions	Value of ν_s
1	Bridges on expressways (limited-access highways), general national highways and principal prefectural highways. Important Bridges on general prefectural highways and municipal highways.	1.0
2	Other than the above	0.8

Note: The value of ν_s may be increased up to 1.25 for special cases in Group 1.

4.4 Design Seismic Coefficient in the Modified Seismic Coefficient Method Considering Structural Response

The design seismic coefficient specified in this Section shall apply to the design of superstructures and substructures of those bridges which have flexible piers and relatively long fundamental periods, such as ones in which the height of the substructures is 25 meters or more above the ground surface in design.

The above-mentioned ground surface in design shall be specified in Section 3.6 "Ground Surface Assumed in Earthquake Resistant Design."

The Design seismic coefficients in this Section shall be determined by modifying the horizontal design seismic coefficient in Section 4.2 "Design Seismic Coefficient in the Seismic Coefficient Method," on the basis of characteristics of strong earthquake ground motions recorded, and dynamic properties of bridge structures, such as natural periods, mode shapes and damping capacities of bridge substructures.

After obtaining the design seismic coefficient, the method for applying seismic loads for the design shall be the same as specified by the provisions in Chapter 3 "Loads and Conditions in Earthquake Resistant Design."

The provisions in this Section shall not apply to the design of superstructures of those bridges in which superstructures are flexible and have longer periods, such as suspension bridges.

4.4.1 Design Seismic Coefficient

(1) The horizontal design seismic coefficient shall be determined by the following formula:

$$k_{hm} = \beta k_h \tag{4.2}$$

where

k_{hm} : Horizontal design seismic coefficient in the modified seismic coefficient method considering structural response ,

k_h : Horizontal design seismic coefficient given by eq. (4.1) , and

β : A factor dependent on the fundamental period of the bridge, and obtained by Table 4.5 or Fig. 4.2.

For structures whose fundamental periods are shorter than 0.5 sec., β may be considered as 1.0.

The value of k_{hm} shall be rounded to two decimals. The minimum value of k_{hm} shall be considered as 0.05.

(2) The vertical design seismic coefficient shall be provided in accordance with the provisions in Item (2) of Section 4.2.

(3) The horizontal design seismic coefficient for the portions below the assumed ground surface in design, shall be provided in accordance with the provisions in Item (3) of Section 4.2.

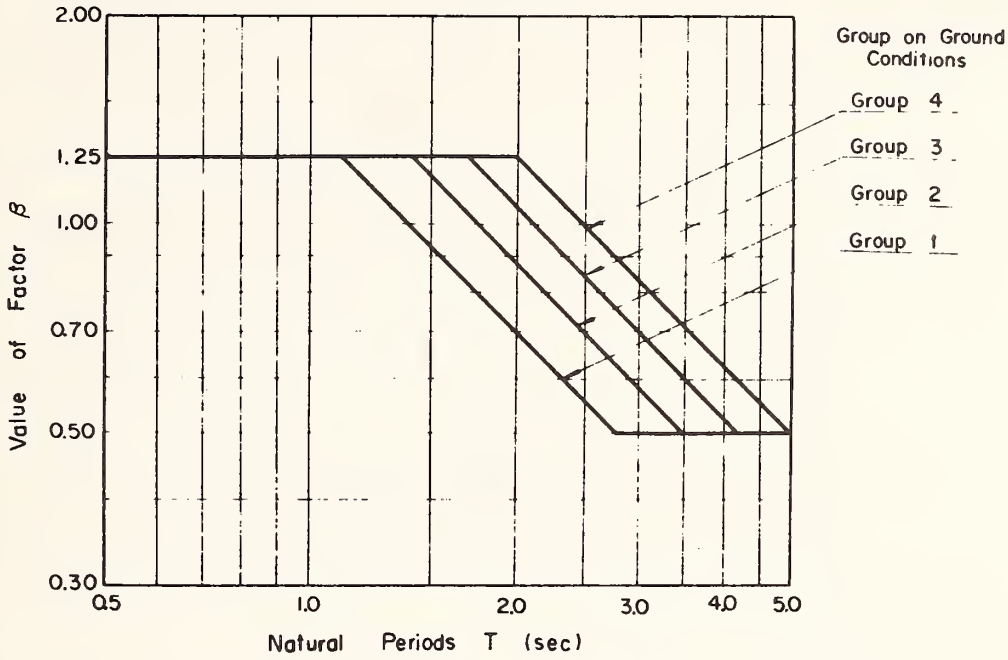

Fig. 4.2 Factor β (For reference of Table 4.5)

Table 4.5 Value of β

Group on Ground Conditions	Value of β for Fundamental Period T (sec.)		
1	$\beta = 1.25$ for $0.5 \leq T \leq 1.1$	$\beta = 1.40/T$ for $1.1 \leq T \leq 2.8$	$\beta = 0.50$ for $T > 2.8$
2	$\beta = 1.25$ for $0.5 \leq T \leq 1.4$	$\beta = 1.75/T$ for $1.4 \leq T \leq 3.5$	$\beta = 0.50$ for $T > 3.5$
3	$\beta = 1.25$ for $0.5 < T \leq 1.7$	$\beta = 2.10/T$ for $1.7 \leq T \leq 4.2$	$\beta = 0.50$ for $T > 4.2$
4	$\beta = 1.25$ for $0.5 < T \leq 2.0$	$\beta = 2.50/T$ for $2.0 \leq T \leq 5.0$	$\beta = 0.50$ for $T > 5.0$

(Notes) 1) Refer to Fig. 4.2.

2) Refer to Table 4.3 regarding groups on ground conditions.

4.4.2 Method for Obtaining Fundamental Periods

Fundamental natural periods of a bridge shall be determined for the individual system consisting of each substructure and the part of superstructures supported by it rather than for the structural system as a whole.

(1) Bridges Supported by Spread Foundations or Pile Foundations

For those bridges which are supported by spread foundations or pile foundations, the foundamental periods may be obtained from Table 4.6.

Any formulas in Table 4.6 shall apply to bridges in which the level of the base of the footing is lower than that of the assumed ground surface in design and the deformation of the substructure is mainly caused by the elastic flexural deformation of the pier which is the upper part of the substructures above the top of the footing. Therefore, they shall not apply to bridges in which the level of the base of the footing is higher than that of the assumed ground surface in design.

Table 4.6 Fundamental Periods of Bridges Supported by Spread Foundations or Pile Foundations

	Type of Structural System	Direction	Formulas for Fundamental Periods	
			Material of Pier	
			Reinforced Concrete	Steel
1	A bridge where most superstructures are continuous, have fixed supports (or movable supports specified in Article 5.2.1) on most substructures, and also have rigid abutments, to one of which the extreme end of the superstructures is connected with a fixed support (See Fig. 4.3)	Transverse	$T=2\pi\sqrt{\frac{0.3W_p+W_s}{3EIg}h^3}$ (4.3)	$T=2\pi\sqrt{\frac{0.3W_p+W_s}{4.5EIg}h^3}$ (4.4)
		Longitudinal	$T=\frac{\pi}{8}\sqrt{\frac{W_p}{EIg}h^3}$ (4.5)	
2	Other than the above: For example, a bridge with simple supports	Longitudinal or Transverse	$T=2\pi\sqrt{\frac{0.3W_p+W_s}{3EIg}h^3}$ (4.6)	

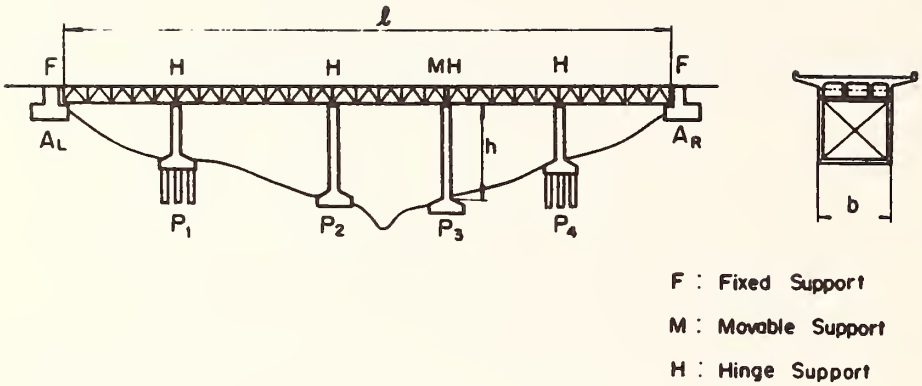

Fig. 4.3 An Example of Type 1 of Structural System in Table 4.6

where

T : Fundamental period in second of the system consisting of a substructure and the section of the superstructures which it supports,

W_p: The weight of the pier in t ,

W_s : The weight of the section of superstructures in t supported by the substructure being considered ,

E : Young's modulus of the pier in t/m^2,

I : Moment of inertia of the pier in m^4 in the direction considered. For piers with varying section with the height, I may be an average value ,

h : The height of the pier in m , and

g : Acceleration of gravity (= 9.8 m/sec^2).

(Note)

Eq. (4.4) shall apply to those bridges which have a ratio of the length between supports on both abutments to the width between outside girders, less than approximately 50 (refer to ℓ/b in Fig. 4.3).

(2) Bridges Supported by Caisson Foundations

For those bridges which are supported by caisson foundations, the fundamental periods may be obtained from Table 4.7.

Table 4.7 Fundamental Periods of Bridges Supported by Caisson Foundations

Type of Structural System		Direction	Formulas for Fundamental Periods
1	Type 1 in Table 4.6	Transverse	one of eqs. (4.3) or (4.4), and (4.7), which gives the largest value of β
		Longitudinal	eq. (4.5)
2	Type 2 in Table 4.6	Transverse Longitudinal	one of eqs. (4.6) and (4.7), which gives the largest value of β

(Note)

$$T=2\pi\sqrt{\frac{\left(h+\frac{2}{3}l\right)^2 W_s+\left(\frac{1}{3}h^2+\frac{2}{3}hl+\frac{4}{9}l^2\right)W_p+\frac{l^2}{9}W_c}{g\left\{K_H\frac{bl^3}{36}+K_s\frac{Al^2}{9}+K_v\,lB\right\}}} \qquad (4.7)$$

where

T : Fundamental period in second of the system consisting of a substructure and the section of the superstructures which it supports,

W_p : The weight of the pier in t,

W_s : The weight of the part of superstructures in t supported by the substructure being considered,

W_c : The weight of the caisson foundation in t,

h : The height of pier in m,

A : Cross-sectional area in m^2 at the base of the caisson foundation,

I_B : Moment of inertia in m^4 at the base of the caisson foundation in the direction considered,

K_H : Horizontal coefficient of subgrade reaction in t/m^3 at the level of the base of the caisson foundation,

K_v : Vertical coefficient of subgrade reaction in t/m^3 at the base of the caisson foundation,

K_s : Horizontal coefficient of subgrade reaction in t/m^3 for shear deformation at the base of the caisson foundation, and

g : Acceleration of gravity (= 9.8 m/sec^2).

Chapter 5 General Provisions for Design of Structural Details

5.1 General

Every bridge structure or every portion thereof shall be designed and constructed to resist seismic forces as provided in Chapter 1 through Chapter 4 and to meet the provisions for design of structural details specified in this Chapter.

Moreover, attention shall be paid to the following respects.

(1) For those abutments which are constructed in soft ground layers, the failure of the ground layer during earthquakes shall be checked.

(2) For those bridges in which any adjacent substructures have different ground conditions, different type of structural systems, or different structural dimensions, special attention shall be paid to the design of structural details, considering that those two substructures may respond differently during earthquakes.

(3) For those portions such as joints between superstructures and substructures, connections between piers and foundations, or connections between footings and piles in pile foundations, where the seismic forces may not be transmitted smoothly and seismic failure have been observed often in the past, particular attention shall be paid to the design of structural details, considering accuracy of evaluation of ground conditions, existance of construction joints, accuracy of construction, etc.

5.2 Devices for Preventing Superstructure from Falling

Movable supports shall have stoppers (special devices for resisting large movements of superstructures during earthquakes) to prevent the superstructures from falling from the substructures, caused by the dislocation of the upper shoes of the supports from the lower shoes during strong earthquakes (refer to 5.2.1).

For the girder ends one of the following methods shall be employed as well as the above-mentioned consideration.

(1) A method extending the length between the end of the support and the edge of the substructure (or widening the width of the crest of the substructure in the longitudinal direction to the bridge axis) in order to prevent the superstructures from falling from the substructure (refer to 5.2.2 or 5.2.3).

(2) A method connecting adjacent girders on the substructure to prevent the superstructures from falling from the substructure even if they become dislodged from the substructure (refer to 5.2.4).

5.2.1 Stoppers at Movable Supports

The allowable movable length in the design of stoppers at movable supports shall be assumed as the sum of the movement due to temperature change, the movement due to the deflection of the girder when subjected to live loads, a margin for covering construction errors, and 20 mm.

The above-mentioned provision need not apply to those stoppers which are not installed near the supports.

The horizontal design seismic coefficients for designing stoppers shall be determined by increasing the horizontal design seismic coefficient given by eq. (4.1) or (4.2) by 50% or more.

5.2.2 Method of Extending the Length between the End of the Support and the Edge of the Substructure

For those substructures which support the ends of girder, the length S(in cm) between the end of the support and the edge of the substructure, shall be equal to or more than the value given by the following formulas:

$$S = 20 + 0.5\ l \qquad \text{for } l < 100 \text{ m}$$

$$S = 30 + 0.4\ l \qquad \text{for } l > 100 \text{ m}$$

where

S: Length between the end of the support and the edge of the substructure in cm , and

l: Span length in meters.

For particularly important bridges consturcted in soft ground layers (Group 4 in Table 4.3), the value of S shall be equal to 35 cm or more.

5.2.3 Suspended Joints

For suspended joints the length between the ends of girders shall be equal to 60 cm or more, as shown in Fig. 5.1. The length for those bridges constructed in soft ground layer (Group 4 in Table 4.3) shall be equal to 70 cm or more.

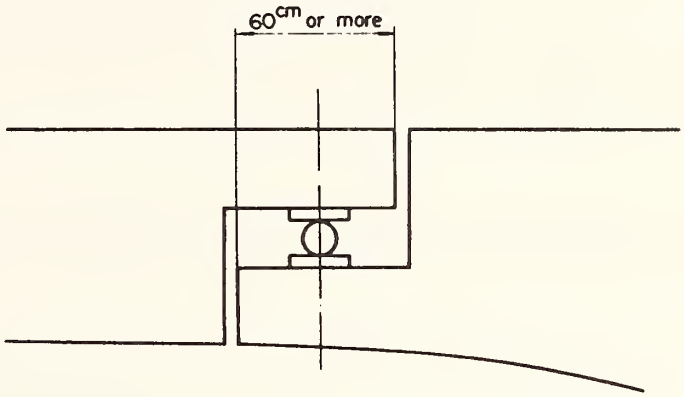

Fig. 5.1 Length between the Ends of both Girders

5.2.4 Method of Connecting Adjacent Girders

Devices for connecting adjacent girders on substructures shall have the movable length specified in Section 5.2.1, for cases in which at least one of two supports is a movable one.

The devices shall be designed to rotate freely to allow the rotation of the girder subjected to live loads, for cases in which both two supports are fixed on one pier.

5.3 Vertical Seismic Forces for Design of Connections between Superstructures and Substructures

The vertical design seismic coefficient for the design of connections between superstructures and substructures shall be assumed as 0.10. When the vertical design seismic coefficient applies upward, only seismic forces shall be considered, neglecting the effects of the dead loads.

The same value of the vertical design seismic coefficient shall be employed for the design of any connections similar to the above.

5.4 Methods for Transmitting Seismic Forces at Connections between Superstructures and Substructures

The method for transmitting seismic forces at connection between superstructures and substructures shall be as follows:

(1) For cast-in-place reinforced concrete bridges, the means of transmission of seismic forces shall be due to the bearing pressure between the swelling at the base of the lower shoe and the concrete at the crest of the substructure. The concrete portion near the

base of the lower shoe shall resist seismic forces as one body together with the pier of the substructure. In the above-mentioned cases, the means of transmission of seismic forces between the upper shoe and the girder shall be due to the anchors fixed on the upper shoe.

For a margin of safety, anchor bolts between the lower shoe and the substructure shall be designed to resist seismic forces alone, in consideration of cases where no resistance between the swelling at the base of the lower shoe and the concrete at the crest of the substructure can be expected.

The above method is recommended not only for cast-in-place concrete bridges, but, if possible, also for prefabricated concrete bridges or steel bridges.

(2) In cases where no bearing resistance of concrete can be expected, anchor bolts shall be employed to transmit the seismic forces. In these cases one of the following two methods shall be considered.

(a) A method in which a steel plate with anchor bolts is fixed firmly on the crest of a substructure while concrete is being placed, and then the lower shoe of the support is welded to the steel plate after the erection of the girders

(b) A method in which a hole is prepared when concrete is placed, a support is set up near the hole, and then anchor bolts are fixed by placing cement mortar into the hole, or a method in which anchor bolts are set up while concrete is being placed, and then the lower shoe is fixed on the anchor bolts.

(3) Anchor bolts used shall be 25 mm or more in diameter, and the depth of the anchor bolts fixed in the concrete shall be 10 times the diameter or more.

5.5 Devices Expected for Decreasing Seismic Forces

When any devices which are expected to decrease seismic force are employed for bridge structures, sufficient investigations shall be conducted on their effectiveness, and special attention shall be paid to preventing the superstructures from falling.

When sufficient reasons exist, these Specifications need not apply to the design of bridges.

Reference

References are provided exclusively in the English version.

[Reference 1]

Specifications for Design of Substructures of Highway Bridges

Volume for Gneral Survey and Design

Part 3 Design, Chapter 2 Loads.

Section 2.5 Earth Pressures

Earth pressures acting on a wall shall be the distributed loads given by the following formulas:

(1) Normal Earth Pressures

(a) Earth pressures acting on a movable wall during normal time shall be determined by the Coulomb's theory as follows:

i) For Sandy Soils

$$P_A = \gamma \cdot K_A x + K_A q$$

$$P_P = \gamma \cdot K_P x + K_P q$$

ii) For Cohesive Soils

$$P_A = \gamma \cdot K_A x - 2C\sqrt{K_A} + K_A q$$

$$P_P \quad \gamma \cdot K_P x + 2C\sqrt{K_P} + K_A q$$

(b) Earth pressures on a fixed wall during normal time shall be determined by

$$P_A = \gamma \cdot K_S \cdot x + K_S q$$

(2) Earth pressures during earthquakes shall be determined by the Mononobe-Okabe method.

$$P_A = (1 - k_v)\gamma \cdot x \cdot K_{EA}$$

$$P_P = (1 - k_v)\gamma \cdot x \cdot K_{EP}$$

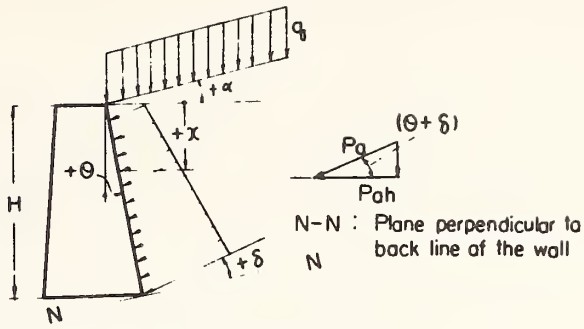

Active Earth Pressure

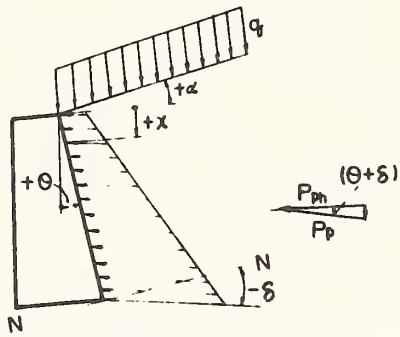

Passive Earth Pressure

Fig. 1 Earth Pressure

where

C : Cohesion of the soil in t/m^2 ,

K_A : Active earth pressure coefficient for Coulomb's theory ,

K_P : Passive earth pressure coefficient for Coulomb's theory ,

K_{EA} : Active earth pressure coefficient during earthquakes ,

K_{EP} : Passive earth pressure coefficient during earthquakes ,

K_0 : Earth pressure coefficient at rest ,

k_v : Vertical seismic coefficient ,

P_A : Active earth pressure in t/m^2 at depth of x meters ,

P_P : Passive earth pressure in t/m^2 at depth of x meters ,

q : Surcharge in t/m^2 on ground surface ,

x : Arbitary depth in meters ,

α : Angle between the ground surface line and the horizontal line ,

γ : Unit weight of the soil in t/m^3 ,

δ : Angle of friction between the wall and the soil ,

ϕ : Angle of internal friction of the soil , and

θ : Angle between the back line of the wall and the vertical line .

(Comments)

K_A , K_P , K_{EA} and K_{EP} are expressed as follows:

$$K_A = \frac{\cos^2(\phi - \theta)}{\cos^2\theta \cdot \cos(\theta + \delta)\left[1 + \sqrt{\frac{\sin(\phi + \delta) \cdot \sin(\phi - \alpha)}{\cos(\theta + \delta) \cdot \cos(\theta - \alpha)}}\right]^2}$$

$$K_P = \frac{\cos^2(\phi + \theta)}{\cos^2\theta \cdot \cos(\theta + \delta)\left[1 - \sqrt{\frac{\sin(\phi - \delta) \cdot \sin(\phi + \alpha)}{\cos(\theta + \delta) \cdot \cos(\theta - \alpha)}}\right]^2}$$

$$K_{EA} \quad \frac{\cos^2(\phi - \theta_0 - \theta)}{\cos\theta_0 \cdot \cos^2\theta \cdot \cos(\theta + \theta_0)\left[1 + \sqrt{\frac{\sin\phi \cdot \sin(\phi - \alpha - \theta_0)}{\cos(\theta - \theta_0) \cdot \cos(\theta - \alpha)}}\right]^2}$$

$$K_{EP} \quad \frac{\cos^2(\phi - \theta_0 + \theta)}{\cos\theta_0 \cdot \cos^2\theta \cdot \cos(\theta - \theta_0)\left[1 - \sqrt{\frac{\sin\phi \cdot \sin(\phi + \alpha - \theta_0)}{\cos(\theta - \theta_0) \cdot \cos(\theta - \alpha)}}\right]^2}$$

where $\sin(\phi \pm \alpha - \theta_0) = 0$ when $\phi \pm \alpha - \theta_0 < 0$

and δ is assumed to be zero during earthquakes.

where

$$\theta_0 = \tan^{-1}\frac{k_h}{1 - k_v}$$

k_h : Horizontal seismic coefficient

k_v : Vertical seismic coefficient

[Reference 2]

Specifications for Design of Substructures of Highway Bridges

Volume for General Survey and Design

Part 3 Design, Chapter 2 Loads

Section 2.7 Buoyancy or Uplifts

When it is apparent that buoyancy forces or uplifts act on structures, they shall be taken into account in the design.

(Comments)

When it is unknown whether they act or not, both cases shall be taken into account in the design.

☆ U. S. GOVERNMENT PRINTING OFFICE : 1973 O - 726-211 (399)

TE 622
.A3 no.
FHWA-RD-73-13
BORROWER
Form DOT F 17
FORMERLY FORM D

DOT LIBRARY
00363023

FHWA

R&D